

Copyright
by
William Laurence Montgomery
2016

**The Dissertation Committee for William Laurence Montgomery Certifies that this is
the approved version of the following dissertation:**

**Synthesis of *aza*-Spirocyclic Dienones and Their Application Toward
Natural Product Synthesis
and
Synthesis and Evaluation of Anticancer Tetracyclic Indole Containing
Compounds**

Committee:

Stephen F. Martin, Supervisor

Jonathan L. Sessler

Emily Que

Hung-wen (Ben) Liu

John D. DiGiovanni

**Synthesis of *aza*-Spirocyclic Dienones and Their Application Toward
Natural Product Synthesis
and
Synthesis and Evaluation of Anticancer Tetracyclic Indole Containing
Compounds**

by

William Laurence Montgomery A.B.

Dissertation

Presented to the Faculty of the Graduate School of
The University of Texas at Austin
in Partial Fulfillment
of the Requirements
for the Degree of

Doctor of Philosophy

**The University of Texas at Austin
August 2016**

Acknowledgements

It's difficult to believe that my time here at the University of Texas come to an end, and there are so many people that I would like to thank. First and foremost, I have to thank my advisor, Stephen Martin. His guidance over that last several years has been invaluable, but it is your generosity and kindness for which I am most grateful. When I approached Steve in my third year about switching to his group, he embraced me as though I had been there the entire time. He could have told me no, and he would have had any number valid reasons to do so, but he did not. For that, I will be forever thankful.

In a similar vein, I need to thank my undergraduate advisor Gordon Gribble. Were it not for you, I never would have discovered my love of indole chemistry. Thank you for mentoring me at Dartmouth and giving me the freedom to make my own mistakes.

There are so many other people that have made these last five years bearable. Charlie, I would have never survived those early days in the Magnus lab without you. Zach, Rachel, and Mike, thanks for putting up me in lab 4; it's been a joy working alongside you guys. I also have to thank Ian and Angela, you two ran a lot of samples for me and performed numerous favors that made my dissertation possible. I also need to thank Dr. Jon Sessler for serving on my committee and allowing me to work in his bio lab. I am also very appreciative of the financial support provided to me by CPRIT and Welch Foundation, without funding these last five years would not have happened.

Lastly and most importantly, I need to thank the love of life, Paloma. I would not have survived these last five years without you. Your unending support and countless trips down I-35 were not in vain.

**Synthesis of *aza*-Spirocyclic Dienones and Their Application Toward
Natural Product Synthesis
and
Synthesis and Evaluation of Anticancer Tetracyclic Indole Containing
Compounds**

William Laurence Montgomery, Ph. D.

The University of Texas at Austin, 2016

Supervisor: Stephen F. Martin

A novel route to access the *aza*-spirocyclic cross-conjugated dienone motif was developed utilizing an intramolecular phenolic *C*-alkylation and Suzuki coupling to form the key quaternary carbon center. A chemoselective addition of crotyl silane to the *aza*-spirocyclic dienone motif was developed in an effort to synthesize the *spiro*-bicyclononane core of (±)-aspernomine and (±)-sespenine.

The structure-activity-relationship of anticancer tetracyclic indole containing compounds was developed via the synthesis and biological evaluation of 48 novel derivatives. Additionally, tool compounds containing a biotin and photoaffinity crosslinker were synthesized for use in future target identification studies.

Table of Contents

List of Tables	xii
List of Figures	xvi
List of Schemes	xxi
Chapter 1: Base Catalyzed Phenolic <i>C</i> -Alkylation as a Alternative to Oxidative Phenolic Coupling.....	1
1.1 The Spirocyclic Dienone Motif and Its Utility in Alkaloid Synthesis...	1
1.1.1 The Spirocyclic Dienone Motif in Alkaloid Biosynthesis	1
1.1.2 Alkaloid Synthesis Via Biomimetic Spirocyclic Dienone Formation	3
1.1.2.1 Biomimetic Synthesis of (\pm)-Galanthamine by Barton et al	3
1.1.2.2 Biomimetic Syntheses of Galanthamine by Node et al	4
1.1.2.3 Biomimetic Synthesis of Salutaridine.....	4
1.1.3 The <i>aza</i> - Spirocyclic Dienone Motif in Alkaloid Synthesis	5
1.1.4 Synthesis of <i>aza</i> -Spirocyclic Dienones.....	10
1.1.4.1 Hypervalent Iodide Based Methods	10
1.1.4.2 Radical Based Methods.....	14
1.1.4.3 Other Oxidative Approaches.....	17
1.1.4.4 Non-oxidative Approaches	19
1.2 Magnus Approach to Alkaloid Synthesis	22
1.2.1 Bond Formation Strategy	22
1.2.2 The Phenolic <i>C</i> -Alkylation Reaction	23
1.2.2.1 Discovery of the Phenolic <i>C</i> -Alkylation.....	23
1.2.2.2 Early Use of the Phenolic <i>C</i> -Alkylation in Natural Product Synthesis	24
1.2.3 Successful Application of the Phenolic <i>C</i> -Alkylation to Alkaloid Synthesis	27
1.2.3.1 Synthesis of Galanthamine and Codeine	27
1.2.3.2 Synthesis of Dihydrosalutaridine	29

1.2.3.3 Synthesis of Cepharatine A.....	31
1.2.3.4 Synthesis of Homoaporphine and Aporphine Alkaloids	32
1.2.3.5 Attempted Synthesis of Crinine	34
1.2.3.6 Attempted Synthesis of Fargenone Alkaloids.....	35
1.3 Conclusion	37
Chapter 2: Synthesis and Utilization of <i>aza</i> -Spirocyclic Dienones	40
2.1 Synthesis of <i>aza</i> -Spirocyclic Dienones Via an Intramolecular Phenolic C-Alkylation	40
2.1.1 Introduction.....	40
2.1.2 <i>para</i> -Phenolic C-Alkylation of Aniline Derived Systems	41
2.1.2.1 First Generation Model System for <i>para</i> -Phenolic C-Alkylation	41
2.1.2.2 Second Generation Model System for <i>para</i> -Phenolic C-Alkylation	44
2.1.2.3 Exploration of Reaction Scope for <i>para</i> -Phenolic C-Alkylation	46
2.1.2.4 Synthesis of Naphthol Derived Dienones	52
2.1.3 Attempted <i>ortho</i> - Phenolic C-Alkylation of Aniline Derived Systems	54
2.2. Chemoselective Addition of Oxygen Nucleophiles to <i>N</i> -Tosyl Hemiaminal Ethers in the Presence of a Dienone	58
2.2.1 Introduction.....	58
2.2.2 Addition of Peroxyacids to <i>N</i> -Tosyl Hemiaminal Ethers in the Presence of a Dienone.....	59
2.2.3 Solvolysis of <i>N</i> -Tosyl Hemiaminal Ethers in the Presence of a Dienone	61
2.3 Studies Towards the Synthesis of the <i>spiro</i> -Bicyclononane Core of Aspernomine and Sespenine	64
2.3.1 Introduction.....	64
2.3.2 Biosynthesis and Previous Synthetic Efforts Towards the <i>spiro</i> -Bicyclononane Core.....	64
2.3.2.1 Proposed Biosynthesis of <i>spiro</i> -Bicyclononane Core.....	64
2.3.2.2 Bioinspired Total Synthesis of Sespenine.....	67

2.3.3 Synthetic Efforts Towards the Synthesis of Aspernomine and Sespenine	71
2.3.3.1 Retrosynthetic Analysis of the spiro-Bicyclononane Core	71
2.3.3.2 Initial Strategy for Addition of Acyl Anion Equivalent	72
2.3.3.3 Revised Strategy for Addition of Acyl Anion Equivalent	80
2.3.3.4 Bis Oxidative Cleavage of Terminal Olefin	83
2.3.3.5 Attempted Intramolecular Michael Addition to Synthesize spiro-Bicyclononane Core	87
2.4 Summary	89
Chapter 3: Previous Synthesis of Actinophyllic Acid and Previous Evaluation of Diverted Intermediates for Anticancer Activity	92
3.1 Natural Products and Their Derivatives as Sources of New Chemotherapeutics.....	92
3.1.1 Introduction.....	92
3.1.2 Natural Products as a Source for New Therapeutics	92
3.1.3 Diverted Total Synthesis as a Strategy for Drug Discovery	93
3.2 Isolation and Prior Synthesis of Actinophyllic Acid	96
3.2.1 Isolation and Initial Biological Evaluation of Actinophyllic Acid	96
3.2.1.1 Carboxypeptidase U and Its Role Fibrinolysis	96
3.2.1.2 Implications of CPU in Cancer	97
3.2.2 Martin Synthesis of Actinophyllic Acid	98
3.3 Discovery of a Lead Compound	103
3.3.1 Discovery of Cytotoxic Properties	103
3.3.2 Analysis of Dose-Response-Curves.....	106
3.3.2.1 The Importance of IC_{50} , E_{max} , and Hill Slope	106
3.3.2.2 Actinophyllic Acid Intermediates Show Consistently Steep Hill Slopes and High E_{max}	110
3.3.3 Actinophyllic Acid Intermediates Induce Rapid Cell Death	112
3.3.4 Hemolysis Assays	115
3.3.5 Preliminary <i>in vivo</i> Analysis	116
3.3.5.1 Determination of Maximum Tolerated Dose and Pharmacokinetic Analysis.....	116

3.3.5.2 Evaluation in Mouse Model for Breast Cancer.....	118
3.4 Investigation Into Mode-of-Action	119
3.4.1 Cell Cycle Arrest Assays	120
3.4.2 Annexin V and Propidium Iodide Staining.....	122
3.4.3 Small Molecule Inhibitors.....	124
3.4.3.1 Small Molecule Inhibitors of Apoptosis	124
3.4.3.2 Necrosis and Other inhibitors	128
3.4.3.3 Endoplasmic Reticulum Stress Inhibitors	131
3.4.4 Western Blot Analysis for ER Stress Markers.....	136
3.4.5 Transcript Profiling and Connectivity Map Analysis	137
3.4.5.1 Initial Results and Preliminary Analysis.....	137
3.4.5.2 Connectivity Map Analysis.....	140
3.4.6 Whole Genome shRNA Screening and siRNA Validation.....	144
3.5 Summary of Results and Future Directions	149
3.5.1 Optimization of Lead Compound	149
3.5.2 Mode-of-Action Studies	151
Chapter 4: Synthesis and Biological Evaluation of Novel Tetracyclic Indole Derivatives and Tool Compounds	153
4.1 Introduction.....	153
4.2. Tool Compounds for Mode-of-Action Studies	153
4.2.1. Introduction.....	153
4.2.1.1 Biotinylated Chemical Probes for Target Identification.....	154
4.2.1.2 Photoaffinity Probes and Their Use in Target Identification	156
4.2.2. Synthesis and Evaluation of Tool Compounds	157
4.2.2.1 Synthesis of Biotinylated Tool Compound.....	158
4.2.2.2 Evaluation of Biotinylated Tool Compound.....	163
4.2.3.1 Synthesis of Photoaffinity Probe	165
4.2.3.2 Evaluation of Photoaffinity Probe	170
4.2.4. Evaluation SFM1257 Mode-of-Action With Small Molecule Tool Compounds	171

4.2.4.1 Guanabenz as a Cytoprotectant.....	172
4.2.4.2 Evaluation of Guanabenz	173
4.2.5 Future Studies	174
4.3 Structure Activity Analysis of Novel Tetracyclic Indole Derivatives	175
4.3.1 Introduction	175
4.3.2 Structure Activity Relationship of Lewis Basic Atoms	177
4.3.2.1 Synthesis of Tetracyclic Derivatives	178
4.3.2.2 Evaluation of Tetracyclic Derivatives	182
4.3.2.3 Synthesis of Pentacyclic Derivatives	184
4.3.2.4 Evaluation of Pentacyclic Derivatives	186
4.3.3 Structure Activity Relationship Associated with Indole Ring ..	188
4.3.3.1 Synthesis of 5- and 6-Substituted Indole Derivatives...	188
4.3.3.2 Evaluation	193
4.3.3.3 Synthesis of 7-Azaindole Derivatives.....	195
4.3.3.4 Evaluation of 7-Azaindole Derived Compounds	197
4.3.3.4 Attempted Synthesis of Oxindole Derivatives.....	198
4.3.4 Minimization of 1,3-Diol Moiety	200
4.3.4.1 Attempted Synthesis of Derivatives Lacking the 1,3-Diol Moiety	201
4.3.4.2 Synthesis of gem-Dimethyl Derivative.....	202
4.3.4.4 Evaluation of Derivatives	207
4.3.5 Further Pharmacophore Elucidation	207
4.3.5.1 Synthesis of Dissected Carbon Framework	208
4.3.5.2 Evaluation of Compounds 4.107 and 4.108.....	209
4.3.6 Structure Activity Relationship of 1,3-Diol Moiety	209
4.3.6.1 Synthesis of O-Substituted Derivatives	210
4.3.6.2 Evaluation of O-Substituted Derivatives	216
4.4 Preliminary Efforts Towards the Synthesis of Enantioenriched Derivatives	218
4.4.1 Introduction	218
4.4.2 Strategies For Stereoselective Additions to Carbocations	218

4.4.3 Chiral Boron Enolate Strategy	220
4.4.4 Cycloheptanone Model Study	222
4.4.5 Vinylogous Amide Boron Enolate Formation Using Weak Base.....	224
4.4.6 Future Studies	226
4.5 Conclusion	227
Chapter 5: Experimental Procedures	230
5.1 General Experimental Section	230
5.2 Experimental Procedures and Compound Characterization	232
Chapter 6: Crystallography Data	435
6.1 Crystallography Data for Compound 2.14.....	435
6.2 Crystallographic Data for 2.33g.....	453
6.3 Crystallography Data for Compound 2.81	472
6.4 Crystallography Data for Compound 4.86b.....	496
References	555

List of Tables

Table 1.1. Synthesis of <i>spiro</i> -Cyclohexyldienone Via an Oxidative Radical Process by Curran <i>et al</i>	15
Table 1.2. Synthesis of <i>spiro</i> -Cyclohexyldienone Via an Oxidative Radical Process from Aryl Azides	16
Table 1.3. Dienone Synthesis Via an Oxidative Radical Process Initiated by Allylsulfonyl Degradation	17
Table 1.4. Guillou <i>et al</i> Synthesis of <i>spiro</i> -Cyclohexyldienones Via an Intramolecular Heck Reaction	20
Table 1.5. Knölker <i>et al</i> Synthesis of <i>spiro</i> -Cyclohexyldienes Via Iron Tricarbonyl Dearomatization	21
Table 2.1. Synthesis of Substituted Biaryls from Corresponding Anilines	49
Table 2.2. Synthesis of Substituted Biaryls from Corresponding Nitrobenzenes	50
Table 2.3. Synthesis of Substituted Hemiaminal Ethers	50
Table 2.4. Synthesis of Differentially Substituted Dienones 2.33	51
Table 2.5. Li, Na, and Zn Acetylide Addition to Dienone 2.14	73
Table 2.6. Cu Acetylide Addition to Dienone 2.14	74
Table 2.7. Attempted Addition of Vinyltrimethylsilane	77
Table 2.8. Failed Attempts to Form Alkene Adduct 2.142	78
Table 2.9. Optimization of Crotylsilane Addition	83
Table 2.10. Optimization of Johnson-Lemieux Oxidation	84
Table 2.11. Attempts to Optimize the Formation of Silyl Enol Ether 2.165	86
Table 2.12. Summary of Results for <i>para</i> -Phenolic C-Alkylation of Aniline Derived <i>spiro</i> -Cyclohexyldienones	90

Table 3.1. Further Evaluation of Cytotoxic Compounds ^{95,96}	106
Table 3.2. IC ₅₀ , Hill slope, and E _{max} Values For SFM1257 Versus FDA Approved Anticancer Drugs ⁹⁶	111
Table 3.3. Genes Significantly Up- and Down-regulated by SFM1257 (3.43) ⁹⁵	139
Table 3.4. Compound Identified by Connectivity Map Analysis ⁹⁵	142
Table 3.5. shRNA Constructs and Their Enrichment ⁹⁵	146
Table 4.1. Successful Alkylation with <i>epi</i> -Chlorohydrin.....	169
Table 4.2. Preliminary SAR and Evaluation of Cytotoxicity ^{95,96,120}	176
Table 4.3. Evaluation of Varying Substitution at Lewis Basic Sites	183
Table 4.4. Evaluation of Pentacyclic Derivatives	187
Table 4.5. Evaluation of 5- and 6-Substituted Derivatives	194
Table 4.6. Evaluation of 7-Azaindole Derivatives	198
Table 4.7. Attempted Cascade Reaction on Primary Acetate	202
Table 4.8. Attempted Synthesis of Acetate 4.97	204
Table 4.9. Optimization of Solvolysis Reaction with MeOH	205
Table 4.10. Synthesis of Tetracycle 4.96	206
Table 4.11. Evaluation of <i>gem</i> -Dimethyl Derivatives.....	207
Table 4.12. Evaluation of Compounds 4.107 and 4.108	209
Table 4.13. Evaluation of Differentially Substituted 1,3-Diol Derivatives	217
Table 6.1. Crystal Data and Structure Refinement for 2.14	437
Table 6.2. Atomic Coordinates (x 10 ⁴) and Equivalent Isotropic Displacement Parameters (Å ² x 10 ³) for 2.14	438
Table 6.3. Bond lengths [Å] and angles [°] for 2.14	440
Table 6.4. Anisotropic Displacement parameters (Å ² x 10 ³) for 2.14	447

Table 6.5. Hydrogen coordinates ($\times 10^4$) and isotropic displacement parameters ($\text{\AA}^2 \times 10^3$) for 2.14 .	449
Table 6.6. Torsion angles [$^\circ$] for 2.14 .	450
Table 6.7. Crystal data and structure refinement for 2.33g .	455
Table 6.8. Atomic coordinates ($\times 10^4$) and equivalent isotropic displacement parameters ($\text{\AA}^2 \times 10^3$) for 2.33g .	456
Table 6.9. Bond lengths [\AA] and angles [$^\circ$] for 2.33g .	458
Table 6.10. Anisotropic displacement parameters ($\text{\AA}^2 \times 10^3$) for 2.33g .	465
Table 6.11. Hydrogen coordinates ($\times 10^4$) and isotropic displacement parameters ($\text{\AA}^2 \times 10^3$) for 2.33g .	467
Table 6.12. Torsion angles [$^\circ$] for 2.33g .	469
Table 6.13. Crystal data and structure refinement for 2.81 .	476
Table 6.14. Atomic coordinates ($\times 10^4$) and equivalent isotropic displacement parameters ($\text{\AA}^2 \times 10^3$) for 2.81 .	477
Table 6.15. Bond lengths [\AA] and angles [$^\circ$] for 2.81 .	479
Table 6.16. Anisotropic displacement parameters ($\text{\AA}^2 \times 10^3$) for 2.81 .	487
Table 6.17. Hydrogen coordinates ($\times 10^4$) and isotropic displacement parameters ($\text{\AA}^2 \times 10^3$) for 2.81 .	489
Table 6.18. Torsion angles [$^\circ$] for 2.81 .	490
Table 6.19. Hydrogen bonds for 2.81 [\AA and $^\circ$].	495
Table 6.20. Crystal data and structure refinement for 4.86b .	499
Table 6.21. Atomic coordinates ($\times 10^4$) and equivalent isotropic displacement parameters ($\text{\AA}^2 \times 10^3$) for 4.86b .	500
Table 6.22. Bond lengths [\AA] and angles [$^\circ$] for 4.86b .	505
Table 6.23. Anisotropic displacement parameters ($\text{\AA}^2 \times 10^3$) for 4.86b .	533

Table 6.24. Hydrogen coordinates ($\times 10^4$) and isotropic displacement parameters ($\text{\AA}^2 \times 10^{-3}$) for 4.86b	538
Table 6.25. Torsion angles [$^\circ$] for 4.86b	543
Table 6.26. Hydrogen bonds for 4.86b [\AA and $^\circ$]	554

List of Figures

Figure 1.1. Representative Examples of Alkaloids with Spirocyclic Dienones as a Biosynthetic Intermediate	1
Figure 1.2. The Cytotoxic Sponge Metabolites of the Discorhabdin Family	6
Figure 1.3. Alkaloids Substructures Related to Büchi's Ketone (1.29)	7
Figure 1.4. Key Oxidative Coupling in the Synthesis of Discorhabdin A and C .	12
Figure 1.5. General Example of Phenolic C-Alkylation in Lieu of Oxidative Coupling	23
Figure 1.6. Mapping of the Dienone from Masamune's Intermediate Onto a Diverse Set of Alkaloids	26
Figure 1.7. Failed Application of Phenolic C-Alkylation to the Synthesis of Crinine	35
Figure 1.8. Natural Products Fargenone A, Fargenin, and a Common Structural Motif	36
Figure 1.9. Summary of Known Methods.....	38
Figure 1.10. Application of Magnus Approach to <i>aza</i> -Spirocyclic Dienone Synthesis	39
Figure 2.1. The <i>aza</i> -Spirocyclic Dienone Motif and and Its Revelance to Natural Products Synthesis	40
Figure 2.2. Proposed Synthesis of <i>spiro</i> -Cyclohexyldienone Via an Intramolecular Phenolic C-Alkylation	41
Figure 2.3. Crystal Structure of 2.14	46
Figure 2.4. Crystal Structure of <i>cis</i> - 2.33g Diastereomer	51
Figure 2.5. Precedent for the conversion of Hemiaminal Ether 2.14 to Amide 2.7360	

Figure 2.6. Crystal Structure of Lactol 2.81	63
Figure 2.7. The Indolosesquiterpenes Aspernomine (2.82) and Sespenine (2.83).....	64
Figure 2.8. Proposed Biosynthesis of Sespenine and Aspernomine	65
Figure 2.9. Copper Acetylide Addition to Hemiaminal Ethers and Acetals	74
Figure 2.10. Examples of Inter- and Intramolecular Vinylsilane Additions.....	76
Figure 2.11. Vinyl Borate Addition to Acetals	79
Figure 2.12. Precedent for Addition of Allyltrimethylsilane to Cyclic <i>N</i> -Tosyl Hemiaminal Ether	81
Figure 3.1. The Natural Product Paclitaxel and Derivative Docetaxel	93
Figure 3.2. Graphic Depiction of Diverted Total Synthesis ¹⁰¹	94
Figure 3.3. The Indole Alkaloid Actinophyllic Acid	96
Figure 3.4. Graphical Depiction of Fibrinolysis Signalling Pathways	97
Figure 3.5. The Cell Viability Probe Alamar Blue	104
Figure 3.6. Compounds That Showed No or Minimal Cytotoxicity	104
Figure 3.7. Compounds That Showed Cytotoxicity	105
Figure 3.8. Initial Screen For Cytotoxicity ⁹⁵	106
Figure 3.9. Example Dose Response Curve.....	107
Figure 3.10. Equation Used to Calculate Percent Cell Death ¹²⁹	108
Figure 3.11. Average E_{max} and Hill Slope Values of SFM1257, Doxorubicin, 5- Fluorouracil, and Cisplatin Over All Cell Lines ⁹⁶	111
Figure 3.12. Relative Rate of SFM1257 (3.43) Induced Cell Death Versus Other Known Cytotoxins ⁹⁵	113
Figure 3.13. Cytotoxins Evaluated For Speed of Cell Death.....	114
Figure 3.14. Dose Response Curve for Hemolysis and Cell Death ⁹⁵	116
Figure 3.15. Pharmacokinetic Analysis of SFM1257 (3.43) ¹⁴⁴	117

Figure 3.16. Evaluation of SFM1258 in 4T1 Syngeneic Mouse Model for Breast Cancer ^{96,144}	119
Figure 3.17. The Cell Cycle and its Checkpoints ¹⁵⁴	121
Figure 3.18. The Structure of Nocodazole (3.52)	122
Figure 3.19. Cell Cycle Analysis of SFM1257 (3.43) Induced Cytotoxicity ^{95,120}	122
Figure 3.20. Dot Plots for PI/Annexin V-FITC Staining	123
Figure 3.21. Structures of Apoptosis Inhibitors	124
Figure 3.22. Apoptotic Signaling Pathways and Their Small Molecule Inhibitors ⁹⁵	125
Figure 3.23. Tool Compounds Used to Block Apoptosis ⁹⁵	128
Figure 3.24. Structures of Tool Compounds Used to Block Non-Apoptotic Cell Death	128
Figure 3.25. Tool Compounds Used to Block Non-Apoptotic Cell Death ⁹⁵	130
Figure 3.26. The Unfolded Protein Response Signaling Pathway and Its Small Molecule Inhibitors ⁹⁵	132
Figure 3.27. Structures of Endoplasmic Reticulum Stress Inhibitors	132
Figure 3.28. Tool Compounds Used to Mitigate Endoplasmic Reticulum Stress ⁹⁵	134
Figure 3.29. Schematic Representation of PERK Signalling ¹⁸⁹	135
Figure 3.30. Western Blot Analysis of eIF2 α and IRE1 Levels ⁹⁶	137
Figure 3.31. Heat Map Analysis of Transcript Levels ⁹⁵	138
Figure 3.32. Structures of High Similarity Matches	143
Figure 3.33. Validation of shRNA Results with siRNA ⁹⁵	148
Figure 3.34. siRNA Constructs that Mitigated SFM1257 (3.43) Caused Cell Death ⁹⁶	148
Figure 3.35. Preliminary SAR Analysis.....	149
Figure 3.36. Examples of Iterative Change to be Made to SFM1257 (3.43)	151

Figure 3.37. Chemical Probes Derived From SFM1257 (3.43)	152
Figure 4.1. Structure of SFM1257 (3.43)	153
Figure 4.2. Pictorial Description of Biotin Pull-Down Experiment	154
Figure 4.3. Commonly Used Photoaffinity Cross-Linking Moieties	157
Figure 4.4. Preliminary Structure-Activity Analysis	158
Figure 4.5. Retrosynthetic Analysis for Biotinylated Tool Compound	158
Figure 4.6. Biological Evaluation of Biotinylated Tool Compound ⁹⁶	164
Figure 4.7. Revised Strategy	166
Figure 4.8. Biological Evaluation of Photoaffinity Probe	171
Figure 4.9. The Selective PP1/GADD34 Inhibitor Guanbenz (4.41) ²⁵⁸	171
Figure 4.10. ER Stress and the Inhibitors Salubrinal (3.74) and Guanabenz (4.41) ¹⁸⁹	172
Figure 4.11. Guanabenz (4.41) Protects against SFM1257 (3.43) Induced Cytotoxicity	174
Figure 4.12. SAR Studies of Lewis Basic Atoms	177
Figure 4.13. Synthesis of Derivatives 4.48 , 4.49 and 4.51	180
Figure 4.14. Proposed Intramolecular Palladium Chelate	181
Figure 4.15. Comparison of Pentacyclic 3.25 to Tetracyclic 3.24	185
Figure 4.16. Indole Ring SAR Studies	188
Figure 4.17 Proposed Oxindole Derivative	198
Figure 4.18. X-Ray Structures of Both 4.86b Enantiomers	199
Figure 4.19: Attempted Deprotection of 3-Oxindole Derivative	200
Figure 4.20. Proposed Synthesis of Derivatives Lacking 1,3-Diol Moiety	201
Figure 4.21. Revised Approach to Derivatives Lacking 1,3-Diol Moiety	203
Figure 4.22. Derivatives to Further Minimize Pharmacophore	208

Figure 4.23. Retrosynthetic Analysis for 1,3-Diol Substituted Derivatives	210
Figure 4.24. The Chirality Forming Step in the Synthesis of SFM1257 (3.43)	218
Figure 4.25 Carbocations in Asymmetric Synthesis	219
Figure 4.26. Proposed Strategy for Obtaining Enantioenriched Material.....	220
Figure 4.27. Structure of (IPC) ₂ BH.....	222
Figure 4.28. Observations From ¹ H-NMR Studies of Boron Enolate Formation	225
Figure 4.30. Additional Boron Reagent Capable of Controlling Absolute Stereochemistry.....	227
Figure 4.31. Summary of SAR to Date	229
Figure 6.1. X-ray Structure of 2.14	435
Figure 6.2. X-ray Structure of 2.33g	453
Figure 6.3. X-ray Structure of 2.81	472
Figure 6.4. X-ray Structure of 2.81	473
Figure 6.5. X-ray Structure of 2.81	474
Figure 6.6. X-ray Structure of 4.86b	496
Figure 6.7. X-ray Structure of 4.86b	497

List of Schemes

Scheme 1.1. Putative Biosynthesis of Lycorine, Crinine, and Galanthamine Via Oxidative Coupling	2
Scheme 1.2: The First Total Synthesis of (±)-Galanthamine (1.2)	3
Scheme 1.3: The Most Recently Published Biomimetic Synthesis of (–)- Galanthamine	4
Scheme 1.4: Biomimetic Synthesis of Salutaridine	5
Scheme 1.5. Synthesis of <i>aza</i> -Galanthamine	6
Scheme 1.6. Synthesis of Büchi's Ketone (1.29) from <i>aza</i> -Spirocyclic Dienone 1.26	7
Scheme 1.7. Enantioselective Synthesis of Indolines from <i>aza</i> -Spirocyclic Dienones	8
Scheme 1.8. Synthesis of Indole Alkaloids (+)-Limaspermidine (1.44) and (+)- Deethylbophyllidine (1.41)	9
Scheme 1.9. Model Studies Towards the Synthesis of Discorhabdin Alkaloids...	11
Scheme 1.10. Initial Report By Doris <i>et al</i> Utilizing Hypervalent Iodide	13
Scheme 1.11. Substitution on Aniline Reduces Yields of Oxidative Coupling	13
Scheme 1.12. Attempted Synthesis of Dienone 1.23 by Guillou <i>et al</i>	14
Scheme 1.13. Mechanism for Formation of Benzylic Oxidation By-product.....	16
Scheme 1.14. Alternative Oxidative Approach to Discorhabdin C using Constant Current Electrolysis	18
Scheme 1.16. Rearrangement of Diene 1.95e to Indoline 1.96	21
Scheme 1.17. Alternative Oxidative Approach to the Discorhabdin Alkaloids using η^4 -Tricarbonyliron	22

Scheme 1.18. First Example of Base Catalyzed Phenolic C-Alkylation	24
Scheme 1.19. First Examples of <i>ortho</i> -Phenolic <i>c</i> -Alkylation	24
Scheme 1.20. Masamune Synthesis of Kaurene, Garryine, and Atisine	25
Scheme 1.21. Synthesis of the Aza-Spirobicyclic Core of Discorhabdin C Via an Intramolecular Base-Catalyzed Phenolic C-Alkylation	27
Scheme 1.22. Sythesis of (±)-Codeine and (-)-Galanthamine Via Phenolic C- Alkylation	29
Scheme 1.23. Phenolic C-Alkylation Used in the Synthesis of 8,14- Dihydrosalutaridine.....	30
Scheme 1.24. Putative Biosynthesis of Cepharatine A	31
Scheme 1.25. Phenolic C-Alkylation-Annulation Used in the Synthesis of Cepharatine A	32
Scheme 1.26. Phenolic Alkylation Strategy for the Synthesis of Proaporphine and Homoproaporphine Alkaloids.....	33
Scheme 1.27. Cyclic Carbamate Formation Occur faster that Phenolic C-Alkylation	34
Scheme 1.28. Phenolic Alkylation Strategy Used in Studies Towards the Fargenone/Fargenin Family of Natural Products.....	36
Scheme 2.1. Retrosynthetic Analysis for Initial Biaryl Model System.....	42
Scheme 2.2. Synthesis of Initial Model System	43
Scheme 2.3. Previous Attempt at Phenolic C-Alkylation	43
Scheme 2.4. Retrosynthetic Analysis for Revised Biaryl Model System	44
Scheme 2.5. Synthesis of <i>spiro</i> -Cyclohexyldienone 2.14	45
Scheme 2.6. Synthesis of Nosyl and Mesyl Protected Anilines	46
Scheme 2.7. Synthesis of Dienones with Varying Sulfonamide Protecting Groups	47

Scheme 2.8. SO ₂ Expulsion from Amidine 2.22	48
Scheme 2.9. Proposed Mechanism for Thermal Decomposition of 2.21	48
Scheme 2.10. The <i>ortho</i> -Methoxy Substituted System Failed to Form the Desired Dienone	52
Scheme 2.11. Synthesis of Naphthol Derived Dienone 2.40	53
Scheme 2.12. Attempted Formation of Extended Dienone 2.44	54
Scheme 2.13. Retrosynthetic Analysis for 2.45	55
Scheme 2.14. Synthesis of Model System for Attempted <i>ortho-ortho</i> Phenolic <i>c</i> - Alkylation	56
Scheme 2.15. Attempted <i>ortho</i> -Phenolic <i>C</i> -Alkylation	57
Scheme 2.16. Attempted <i>ortho</i> -Phenolic <i>C</i> -Alkylation by Timothy Hodges	57
Scheme 2.17. Known Rearrangements of Dienone 1.60	58
Scheme 2.18. Potential Reaction Pathways for Dienone 2.14	59
Scheme 2.19. Proposed Mechanism for Formation of Amide 2.73	61
Scheme 2.20. Solvolysis of Hemiaminal Ether with Methanol.....	62
Scheme 2.21. Rearrangement Observed in the Magnus Synthesis of (–)- Galanthamine ³⁹	62
Scheme 2.22. Proposed Mechanism for Hydrolysis and Rearrangement of Dienone 2.14	63
Scheme 2.23. Unexpected Rearrangement Observed of 3-Hydroxyindole Species 2.88	66
Scheme 2.24. Proposed Mechanism of Oxidative Rearrangement	67
Scheme 2.25. Synthesis of Precursor to Oxidative Rearrangement	68
Scheme 2.26. Attempted Oxidative Rearrangement	69
Scheme 2.27. Revised Approach Utilizing Indole Methyl Ester 2.107	69

Scheme 2.28. Successful Oxidative Rearrangement and Completion of the Natural Product	70
Scheme 2.29. Retrosynthetic Analysis of Sespenine and Aspernomine	71
Scheme 2.30. Initial Strategy for Installation of Acyl Anion Equivalent	72
Scheme 2.31. Synthesis of Protected Allylic Alcohol 2.121	75
Scheme 2.32. Protected Allylic Alcohol Undergoes Rapid Degradation	75
Scheme 2.33. General Mechanism for Petasis Borono-Mannich Reaction	77
Scheme 2.34. Attempted Lewis Acid Catalyzed Petasis Reaction	79
Scheme 2.35. Revised Strategy for Installation of Acyl Anion Equivalent	80
Scheme 2.36. Synthesis of (Z)-Crotylsilane 2.158	82
Scheme 2.37. 2,6-Lutidine as an Additive for a Johnson-Lemieux Oxidation	84
Scheme 2.38. Rationalization for the Observation of Phenol 2.164	85
Scheme 2.39. Johnson-Lemieux Oxidation of Silyl Enol Ether 2.165	87
Scheme 2.40. Proposed Route to Tetracycle 2.111	87
Scheme 2.41. Attempts to Stoichiometrically Form the Kinetic Enol Ether	88
Scheme 2.42. Alternative Method to Form Kinetic Enolates	88
Scheme 2.43. Failed Attempts to Form Kinetic Enolate Under General Base Conditions	89
Scheme 2.44. Summary of Synthetic Efforts Towards the <i>spiro</i> -Bicyclic Nonane Core of Aspernomine and Sespenine	91
Scheme 3.1. Synthesis of (+)-Migrastatin and Analogs by Danishefsky <i>et al</i> ¹⁰¹ ..	95
Scheme 3.2. Retrosynthetic Analysis of (±)-Actinophyllic Acid (3.7)	99
Scheme 3.3. Synthesis of π -Nucleophile 3.10	99
Scheme 3.4. Synthesis of Ketone 3.17	100
Scheme 3.5. One Pot Synthesis of Indolo-Acetate 3.11	100

Scheme 3.6. Successful Formation of the Tetracyclic Core of Actinophyllic Acid	101
Scheme 3.7. Completion of the Natural Product	102
Scheme 4.1. Synthesis of Protected Alkyne 4.15	159
Scheme 4.2. Synthesis of Biotin Tether ²⁵⁶	160
Scheme 4.3. Initial Attempt at Formation of Biotinylate Derivative	160
Scheme 4.4. Successful ‘Click’ Reaction	161
Scheme 4.5. Attempted Removal of Allyl Carbamate Group of 4.21	162
Scheme 4.6. Synthesis of Biotinylated Probe 4.10	163
Scheme 4.7. Photoaffinity Tether Published by Li <i>et al</i> ²⁵⁷	165
Scheme 4.8. Initial Attempt to Alkylate Indole Nitrogen	166
Scheme 4.9. Attempted Alkylation With Various Electrophiles	167
Scheme 4.10. Attempted Alkylation with Ethylene Oxide	168
Scheme 4.11. Completion of the Photoaffinity Probe	170
Scheme 4.12. Synthesis of Derivative 4.43	178
Scheme 4.13. Synthesis of Derivatives 4.45a , 4.45b , 4.46a , and 4.46b	179
Scheme 4.14. Alkylation of Indole Nitrogen Atom	180
Scheme 4.15. Reduction of Compound 4.16	182
Scheme 4.16. Synthesis of Derivatives 4.54a and 4.54b	182
Scheme 4.17. Synthesis of Pentacyclic Derivatives 4.56 , 4.57 , 4.58 , and 4.59 ..	186
Scheme 4.18. Synthesis of 5- and 6-Chloro Indole Scaffolds	189
Scheme 4.19. Synthesis of 5- and 6-Chloro Derivative 4.67a-b and 4.68a-b	190
Scheme 4.20. Synthesis of 5- and 6-Chloro Derivatives SFM1257 (3.43)	191
Scheme 4.21. Synthesis of 5- and 6-Substituted Derivatives 4.73a-b and 4.74a-b	192
Scheme 4.22. Synthesis of 5- and 6-Chloro Analogs of SFM1258 (3.44)	192
Scheme 4.23. Synthesis of Suzuki Adducts 4.76a-b	193

Scheme 4.24. Synthesis of Indolo-acetate 4.78	195
Scheme 4.25. Synthesis of 7-Azaindole Derived Tetracycle 4.79	196
Scheme 4.26. Friedel Craft Acylation of 7-Azaindole ²⁶²	196
Scheme 4.27. Synthesis of 7-Azaindole Derivatives 4.83a and 4.83b	197
Scheme 4.28. Synthesis of 3-Oxidole Derivative 4.86a and 4.86b	199
Scheme 4.29. Previous Work in Martin Group ²⁶⁴	202
Scheme 4.31. Reduction and Alkylation of <i>gem</i> -Dimethyl Tetracycle 4.104	206
Scheme 4.32. Synthesis of Derivative 4.105 and 4.106	207
Scheme 4.33. Synthesis of Derivatives 4.107 and 4.108	209
Scheme 4.34. Synthesis of Ketone 4.114a-c	211
Scheme 4.35. Synthesis of Ketone 4.117	211
Scheme 4.36. Synthesis of Differentially Substituted 1,3-Diol Scaffold	212
Scheme 4.37. Synthesis of Derivative 4.121a-d and 4.122	213
Scheme 4.38. Synthesis of Derivative 4.125a-b	214
Scheme 4.39. Synthesis of Derivatives 4.127a-c and 4.128	215
Scheme 4.40. Synthesis of Derivative 4.127c and 4.129	215
Scheme 4.41. Proposed Enantioselective Cascade Reaction.....	221
Scheme 4.42. Initial Attempts with Cycloheptanone Model System	223
Scheme 4.43. Base Can Coordinate to Boron Enolate	223
Scheme 4.44. Cycloheptanone Model System With Lewis Acid Co-catalyst	224
Scheme 4.45. Rationalization for Lack of Boron Enolate Formation with DTBMP ²²⁶	
Scheme 4.46. Proposed Future Attempt at Boron Enolate Formation	227

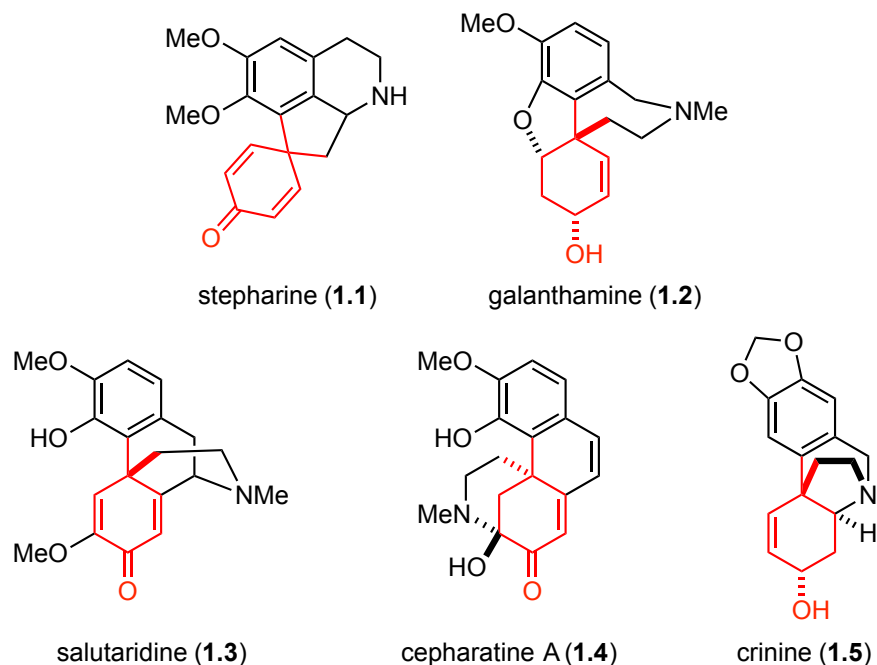
Chapter 1: Base Catalyzed Phenolic C-Alkylation as a Alternative to Oxidative Phenolic Coupling

1.1 THE SPIROCYCLIC DIENONE MOTIF AND ITS UTILITY IN ALKALOID SYNTHESIS

1.1.1 The Spirocyclic Dienone Motif in Alkaloid Biosynthesis

The spirocyclic dienone is a common structural motif found in a large number of natural products and biosynthetic intermediates. In Figure 1.1, examples of alkaloids that contain the spirocyclic dienone motif as a biosynthetic intermediates are shown; the C-C bonds that originate from the dienone motif are highlighted in red.

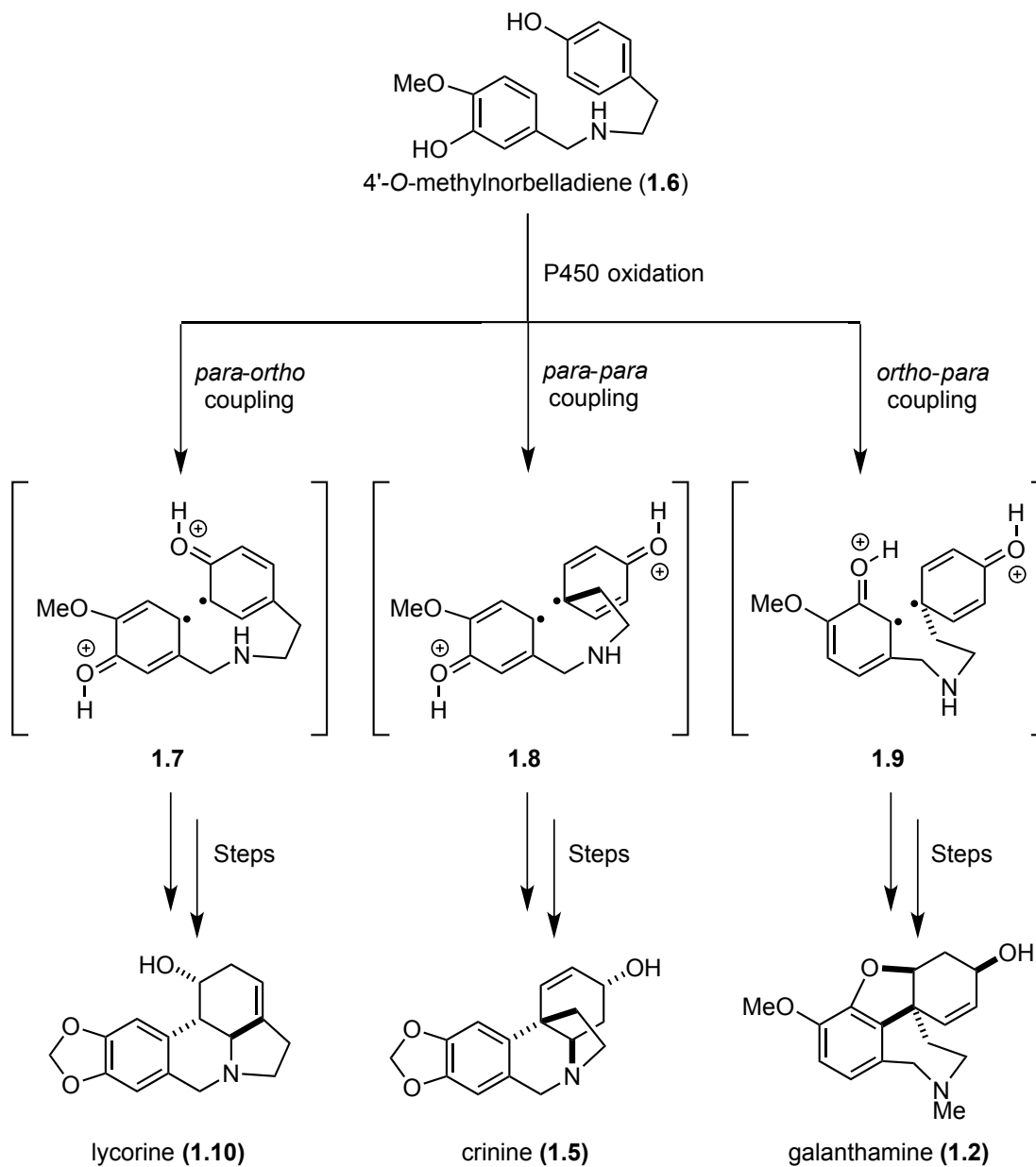
Figure 1.1. Representative Examples of Alkaloids with Spirocyclic Dienones as a Biosynthetic Intermediate



It has been shown that nature synthesizes the cross-conjugated dienone motif via oxidation by cytochrome P450 to form radical cations and then recombination of the radicals produces new C-C bonds. When phenolic radical cations cyclize to form new C-C bonds, the regiochemistry can vary greatly. For example, in the case 4'-O-

methylnorbelladiene (**1.6**), the radicals can combine in a *para-ortho* (**1.7**), *para-para* (**1.8**), or *ortho-para* (**1.9**) fashion to afford the skeletal frameworks of lycorine (**1.10**), crinine (**1.5**), and galanthamine (**1.2**), respectively (Scheme 1.1).¹

Scheme 1.1. Putative Biosynthesis of Lycorine, Crinine, and Galanthamine Via Oxidative Coupling



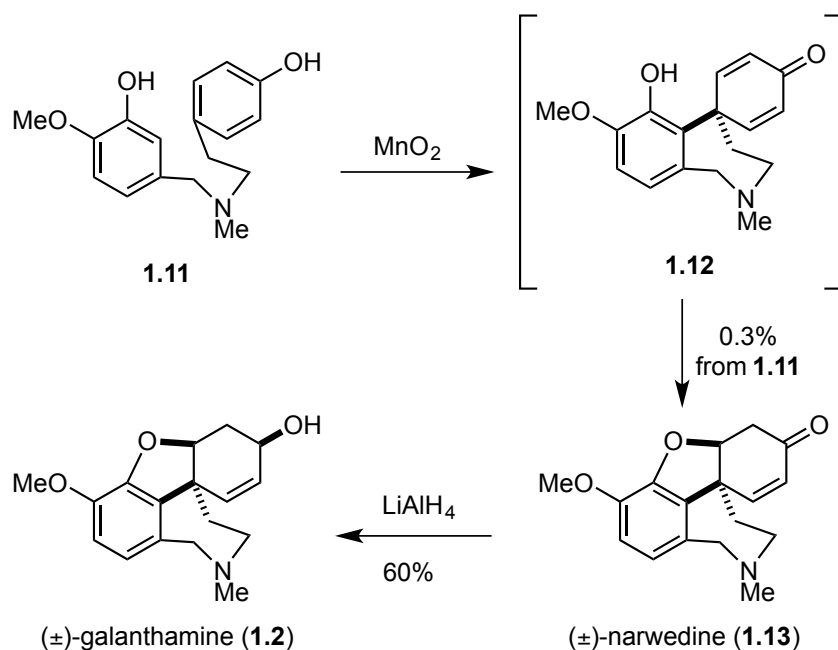
1.1.2 Alkaloid Synthesis Via Biomimetic Spirocyclic Dienone Formation

Although nature performs the oxidative phenolic coupling enzymatically with high efficiency, efforts to replicate this transformation in the laboratory have proven problematic. In the case of galanthamine (**1.2**), issues pertaining to product stability, poor regiocontrol, and over oxidation have plagued attempts at biomimetic syntheses.²⁻¹⁴

1.1.2.1 Biomimetic Synthesis of (±)-Galanthamine by Barton *et al*

In the first total synthesis of (±)-galanthamine (**1.2**), the key biomimetic dienone intermediate **1.12** was formed in 0.3% yield upon exposing phenol **1.11** to MnO₂ (Scheme 1.2). The authors found that polymerization of **1.11** was the major product, yet trace amount of (±)-narwedine (**1.13**) could be isolated, and subsequent reduction of **1.13** with lithium aluminum hydride afforded (±)-galanthamine (**1.2**) in 60% yield.¹³

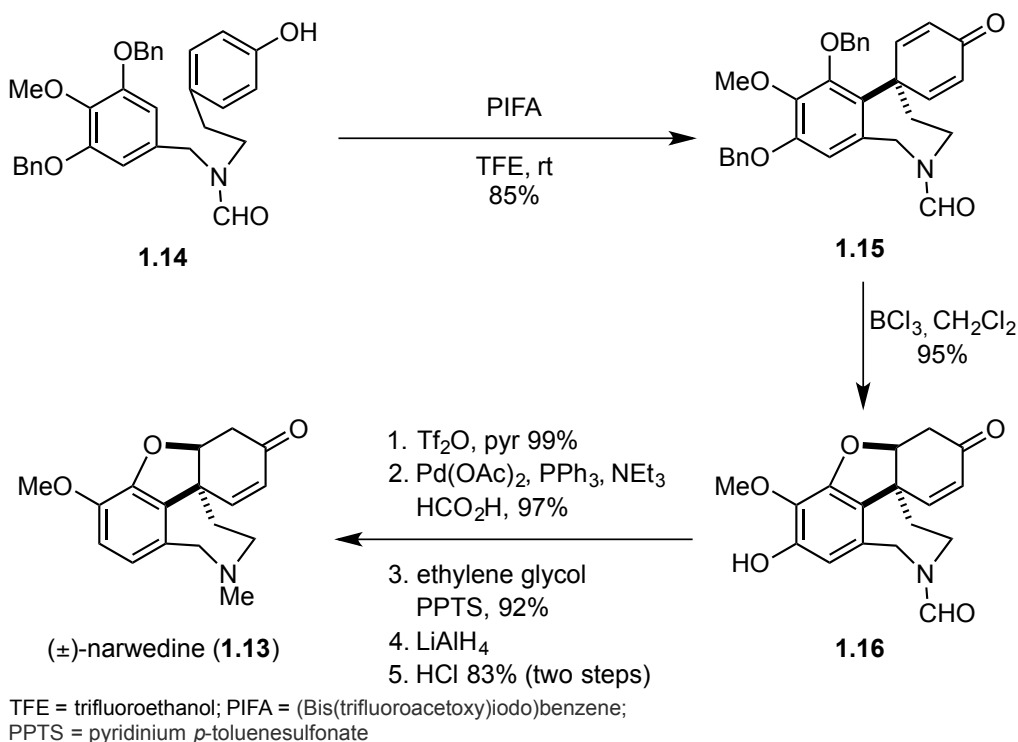
Scheme 1.2: The First Total Synthesis of (±)-Galanthamine (**1.2**)



1.1.2.2 Biomimetic Syntheses of Galanthamine by Node *et al*

In the most recent biomimetic synthesis of (–)-galanthamine (**1.2**), the key oxidative coupling of phenol **1.14** to afford **1.15** proceeded in 85% yield.³ To achieve the desired regioisomer in high yield, several protecting and blocking groups were required (Scheme 1.3). As a result, six additional chemical transformations were needed to convert dienone **1.16** to (±)-narwedine (**1.13**). Since (±)-narwedine (**1.13**) is known to undergo dynamic chiral resolution when recrystallization is seeded with (–)-narwedine,¹⁵ a formal synthesis of (–)-galanthamine was completed.

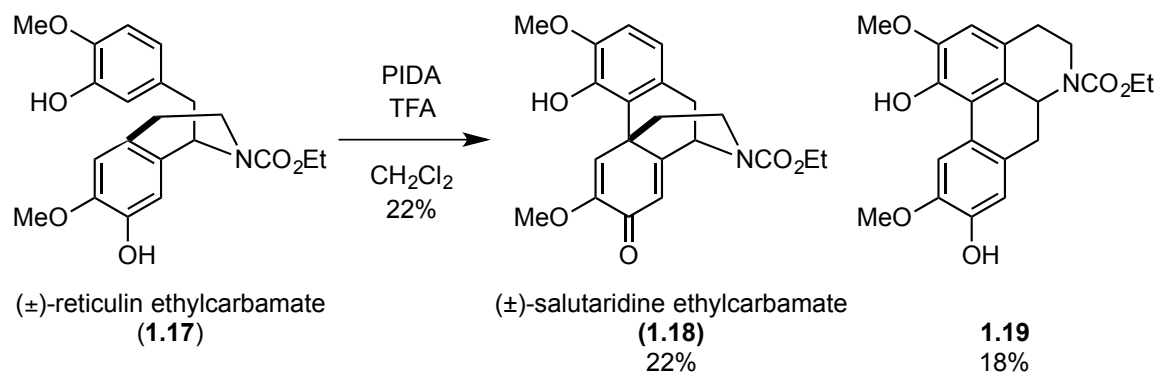
Scheme 1.3: The Most Recently Published Biomimetic Synthesis of (–)-Galanthamine



1.1.2.3 Biomimetic Synthesis of Salutaridine

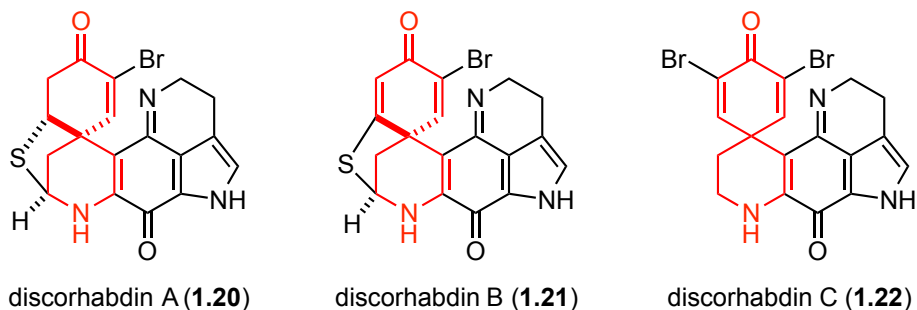
A biomimetic synthesis of (±)-salutaridine (**1.3**) has been published as well. Similar to the biomimetic galanthamine (**1.2**) syntheses by Barton *et al*, this synthesis

also suffered from poor yields of the key oxidative coupling step.¹⁶ Exposure of *N*-protected reticuline **1.17** to periodobenzene diacetate (PIDA) afforded dienone **1.18** in only 22% yield (Scheme 1.4).¹⁶ The major by-product was tetracycle **1.19**, which was isolated in 18% yield and arose due to lack of regiocontrol in the oxidative coupling step.



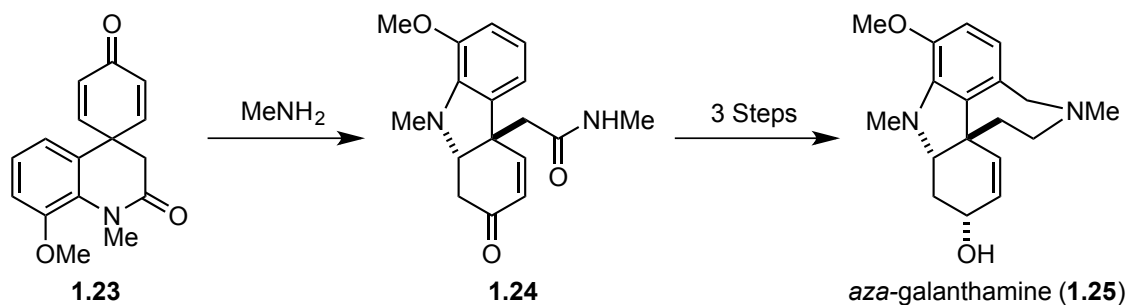
1.1.3 The *aza*- Spirocyclic Dienone Motif in Alkaloid Synthesis

Figure 1.2. The Cytotoxic Sponge Metabolites of the Discorhabdin Family



The *aza*-spirocyclic dienone moiety has also found utility as an intermediate in the synthesis of natural products and natural product-like compounds. For example, the natural product-like compound *aza*-galanthamine (**1.25**) was synthesized from the *aza*-spirocyclic dienone **1.23** (Scheme 1.5). Galanthamine (**1.2**) and the *aza*-derivative **1.25** were both under investigation as a potential therapeutic for Alzheimer's disease through its role as a selective acetylcholinesterase inhibitor.¹⁸

Scheme 1.5. Synthesis of *aza*-Galanthamine



In 2007, Guillou *et al* demonstrated that *aza*-spirocyclic dienone (**1.26**) can be an intermediate in the synthesis of Büchi's ketone (**1.29**) (Scheme 1.6), which is an intermediate in the synthesis of the indole alkaloid vindorosine (**1.30**)¹⁹ and contains the carbon substructure of several *Aspidosperma* alkaloids (Figure 1.3).²⁰ The conversion of dienone **1.26** to indoline **1.28** was believed to occur via nucleophilic attack of an amine to afford intermediate **1.27**, subsequently followed by a double intramolecular Michael

addition to afford indoline **1.28**. Compound **1.28** was converted in five additional steps to Büchi's ketone (**1.29**).

Scheme 1.6. Synthesis of Büchi's Ketone (**1.29**) from *aza*-Spirocyclic Dienone **1.26**

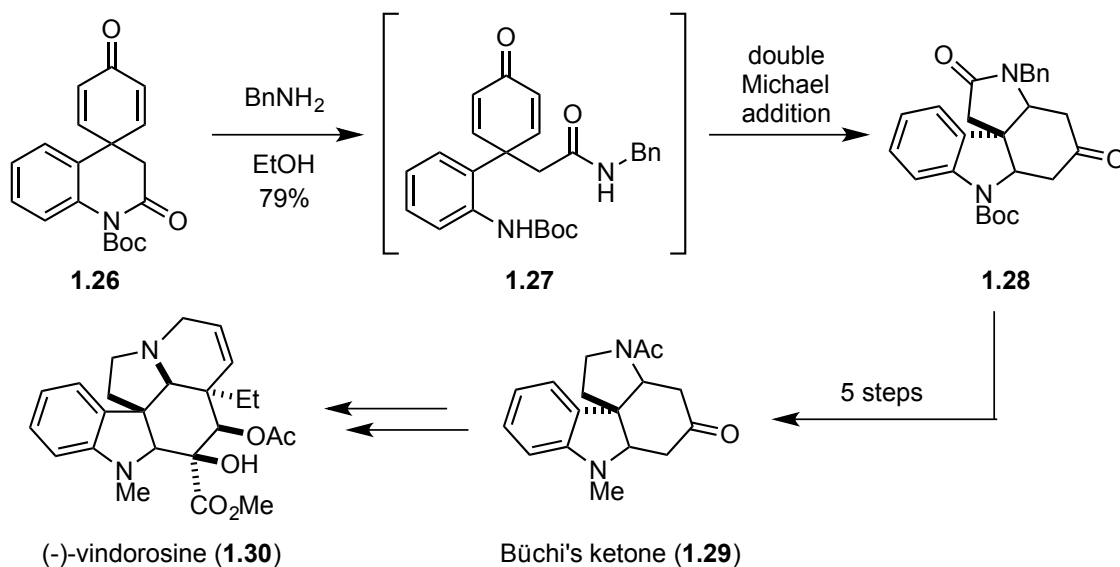
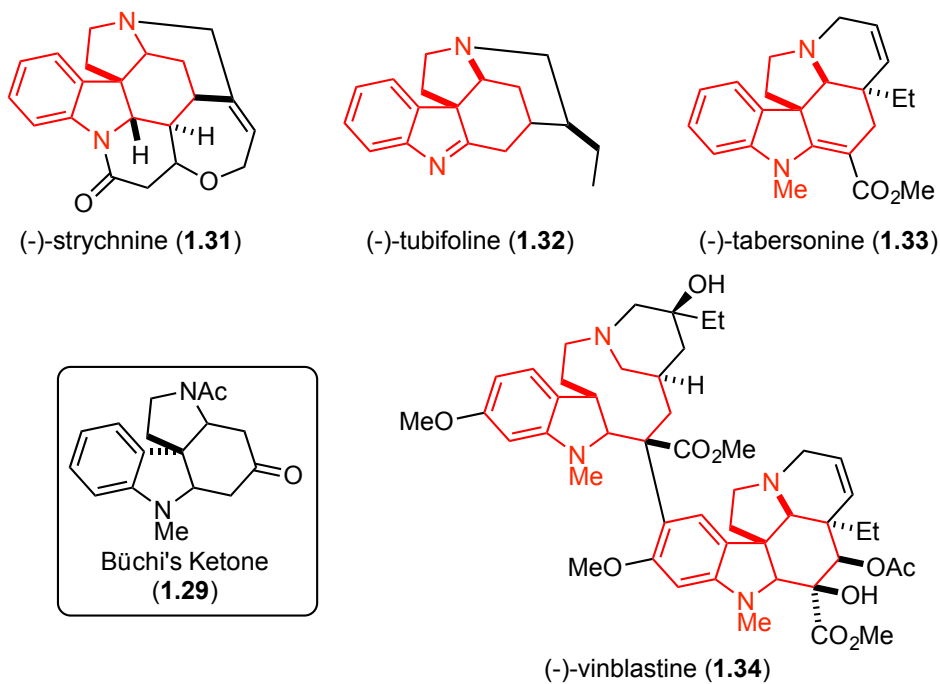
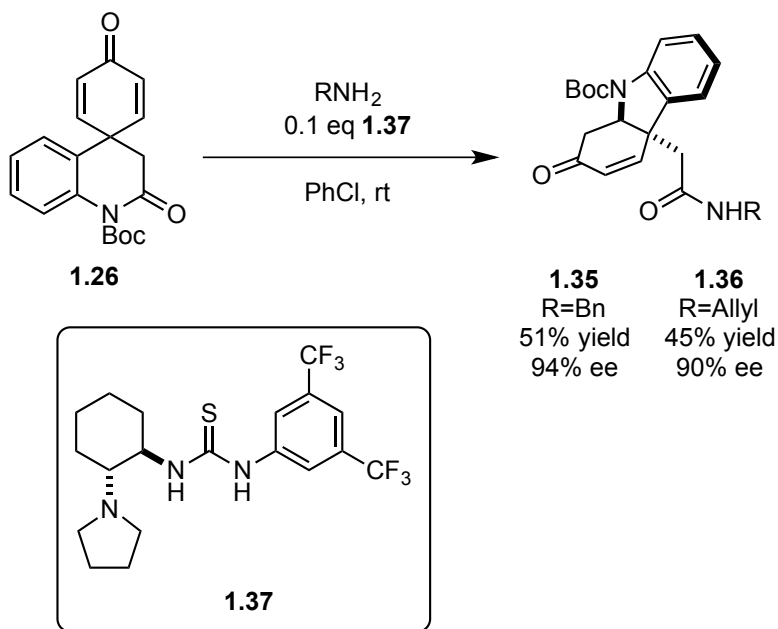


Figure 1.3. Alkaloids Substructures Related to Büchi's Ketone (**1.29**)



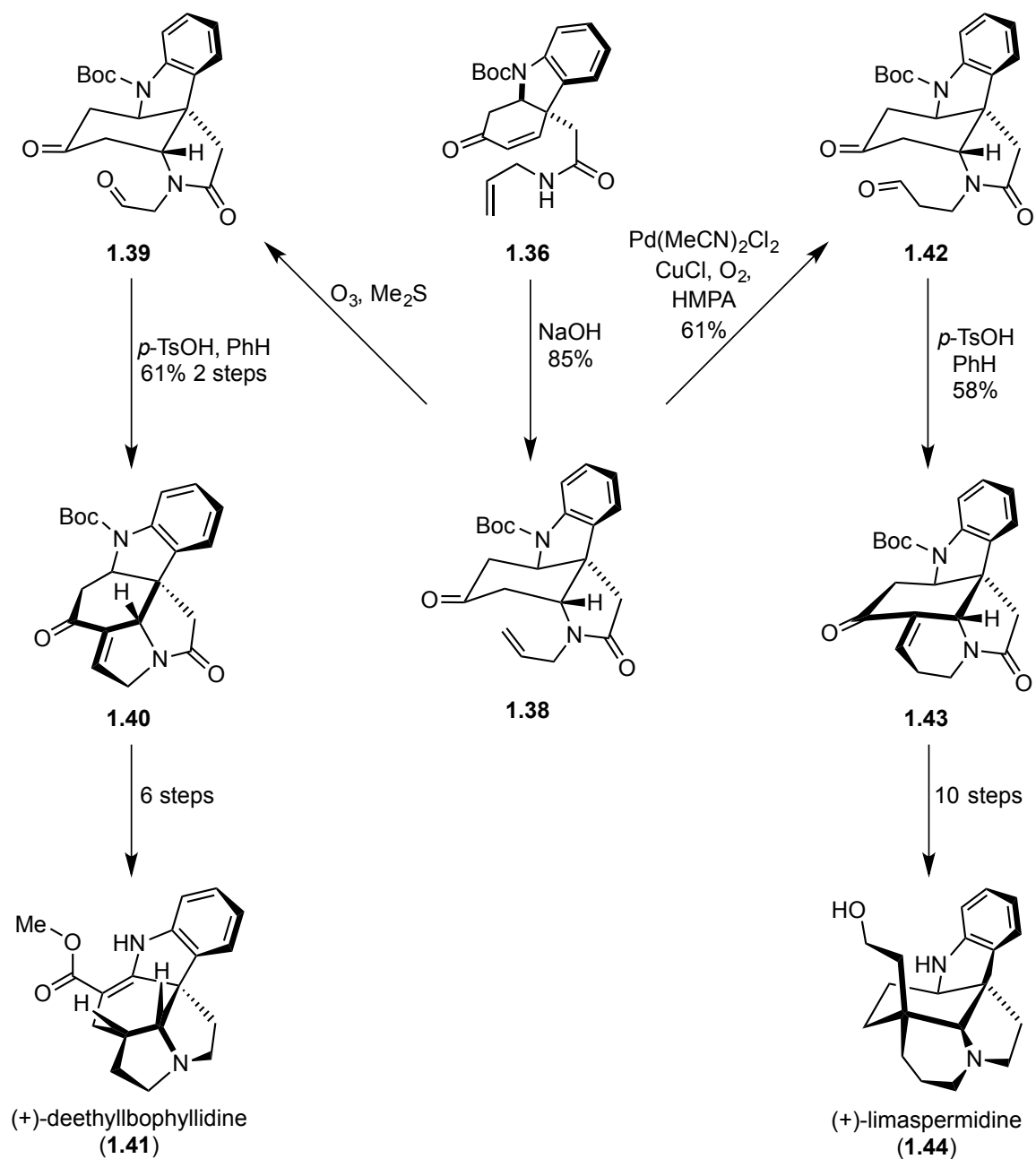
As an expansion of the double Michael addition rearrangement developed to form the indoline skeleton (Scheme 1.6), an enantioselective variant was reported by Fan *et al* that utilizes the chiral thiourea catalyst **1.37** (Scheme 1.7).²¹ The authors found that dienone **1.26** can be converted to indolines **1.35** and **1.36** in 51% yield (94% ee) and 45% yield (90% ee), respectively. The transformation was found to tolerate a wide variety of arene substitution patterns on both the aniline and benzylamine moieties as well as a variety of carbamates on the aniline nitrogen atom.

Scheme 1.7. Enantioselective Synthesis of Indolines from *aza*-Spirocyclic Dienones



With enantiopure indoline **1.36** in hand, the authors were able to rapidly synthesize the indole alkaloids (+)-limaspermidine (**1.44**) and (+)-deethylbophyllidine (**1.41**) in 13 and 9 additional steps, respectively (Scheme 1.8).

Scheme 1.8. Synthesis of Indole Alkaloids (+)-Limaspermidine (**1.44**) and (+)-Deethylbophyllidine (**1.41**)



Given the application of *aza*-spirocyclic dienones in the synthesis of indole alkaloids and natural-product like compounds, it is clear that a methodology to rapidly

and efficiently synthesize these structural motifs would be beneficial to the greater synthetic community.

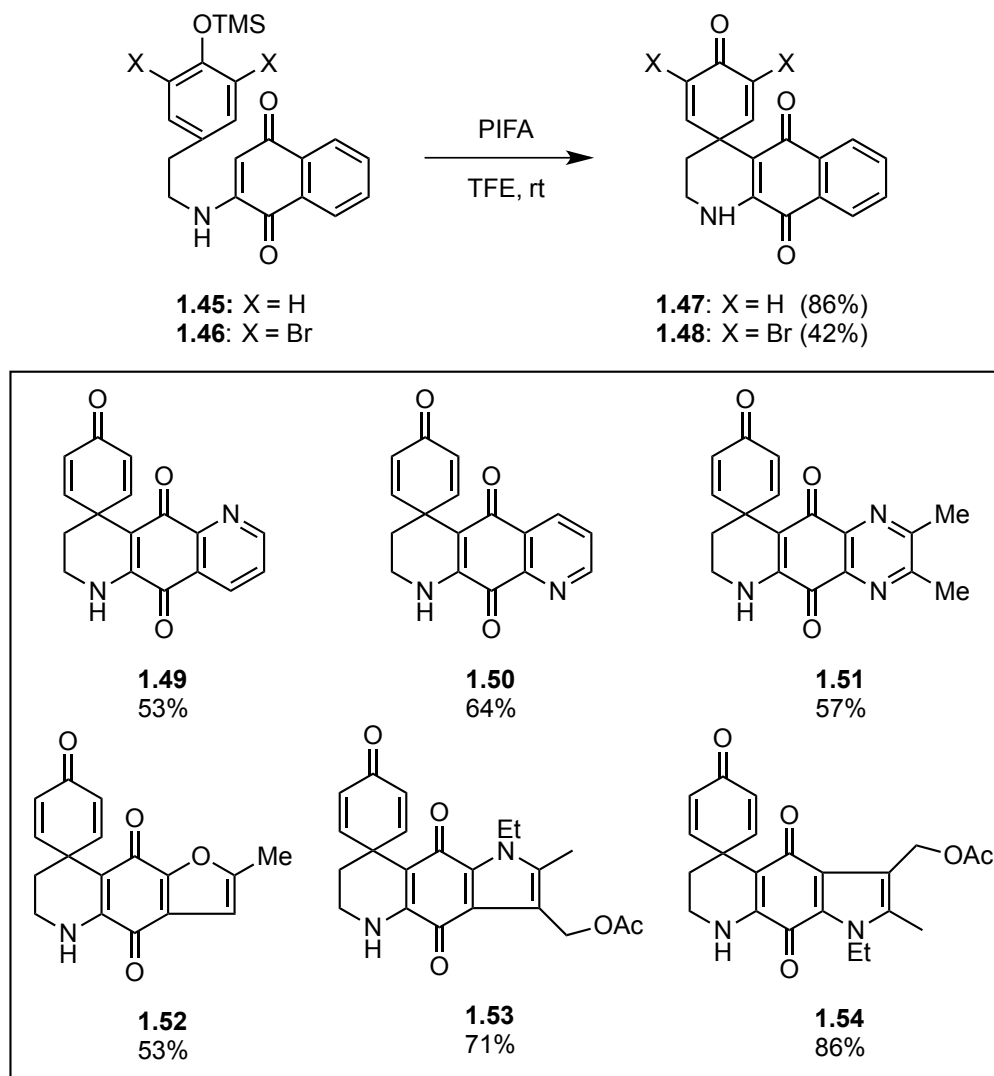
1.1.4 Synthesis of *aza*-Spirocyclic Dienones

There are several known methodologies for the synthesis of *aza*-spirocyclic dienones, and the majority of these rely on oxidative conditions. As such, they suffer from many of the same issues that plagued the oxidative phenolic couplings discussed earlier (Scheme 1.2, Scheme 1.3, and Scheme 1.4).

1.1.4.1 Hypervalent Iodide Based Methods

The earliest example of an oxidative coupling of a phenol to an aniline-like system is shown in Scheme 1.9. In a model study towards the synthesis of the discorhabdin alkaloids, Kita *et al* found that the *aza*-spirocyclic dienones **1.47-54** could be formed from a variety of trimethylsilyl protected phenols in 42-86% yields using the hypervalent iodide reagent PIFA.^{22,23} Unfortunately, the yields of the transformation were highly substrate dependent: for example, the deactivated dibrominated arene **1.46** afforded dienone **1.48** in significantly poorer yield (42%) than the conversion of non-halogenated phenol **1.45** to dienone **1.47** (86%) (Scheme 1.9).

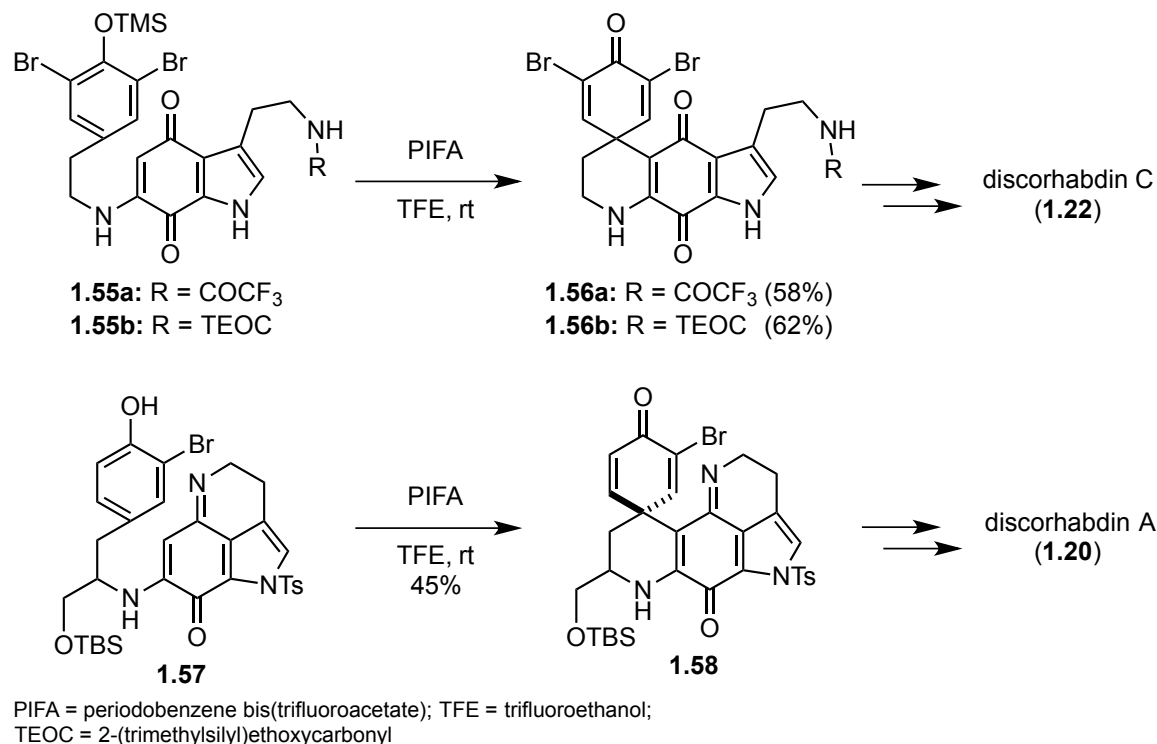
Scheme 1.9. Model Studies Towards the Synthesis of Discorhabdin Alkaloids



PIFA = periodobenzene bis(trifluoroacetate); TFE = trifluoroethanol

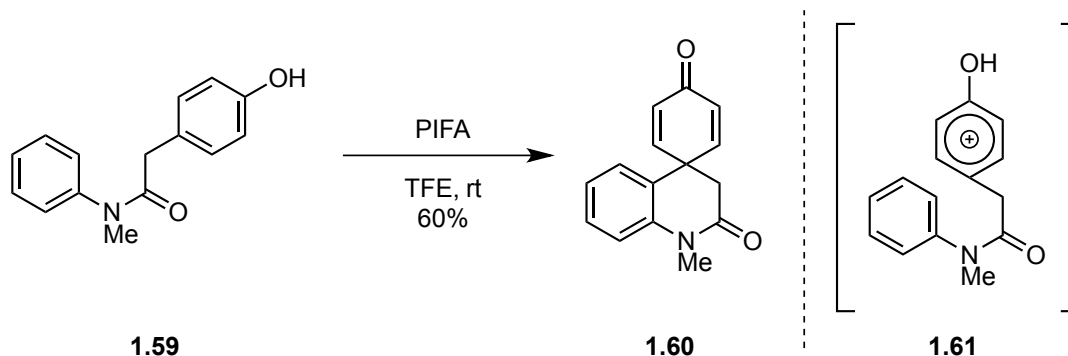
Using the methodology established on their model system, Kita *et al* completed the syntheses of both discorhabdin C (**1.22**) and discorhabdin A (**1.20**).^{24,25} In both cases, the key spirocyclic dienone moiety was formed in modest yield using his oxidative coupling strategy (Figure 1.4).

Figure 1.4. Key Oxidative Coupling in the Synthesis of Discorhabdin A and C



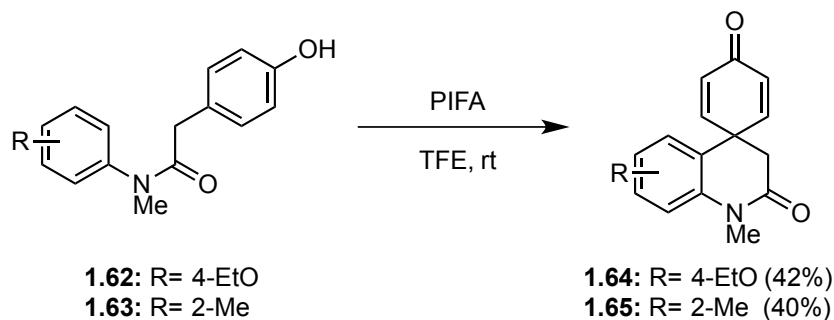
Hypervalent iodide reagents have also been developed to synthesize *aza*-spirocyclic dienones that do not have the indolo-iminoquinone core of the discorhabdin alkaloids. Using oxidative conditions analogous to those used by Kita *et al* the discorhabdin syntheses, Doris *et al* found that spirocyclic **1.60** was obtained in 60% yield from anilide **1.59** (Scheme 1.10).²⁶ The authors propose that the hypervalent iodide oxidant creates intermediate arenium **1.61**, which undergoes electrophilic aromatic substitution with anilide **1.59**. However, the authors reported only one example, and no investigation into the scope of the transformation was performed. Several years later, Yu *et al* extended the substrate scope slightly, demonstrating that the reaction tolerated substitution, albeit in poorer yields (40-42% vs 60%) (Scheme 1.11).²⁷

Scheme 1.10. Initial Report By Doris *et al* Utilizing Hypervalent Iodide



PIFA = periodobenzene bis(trifluoroacetate); TFE = trifluoroethanol

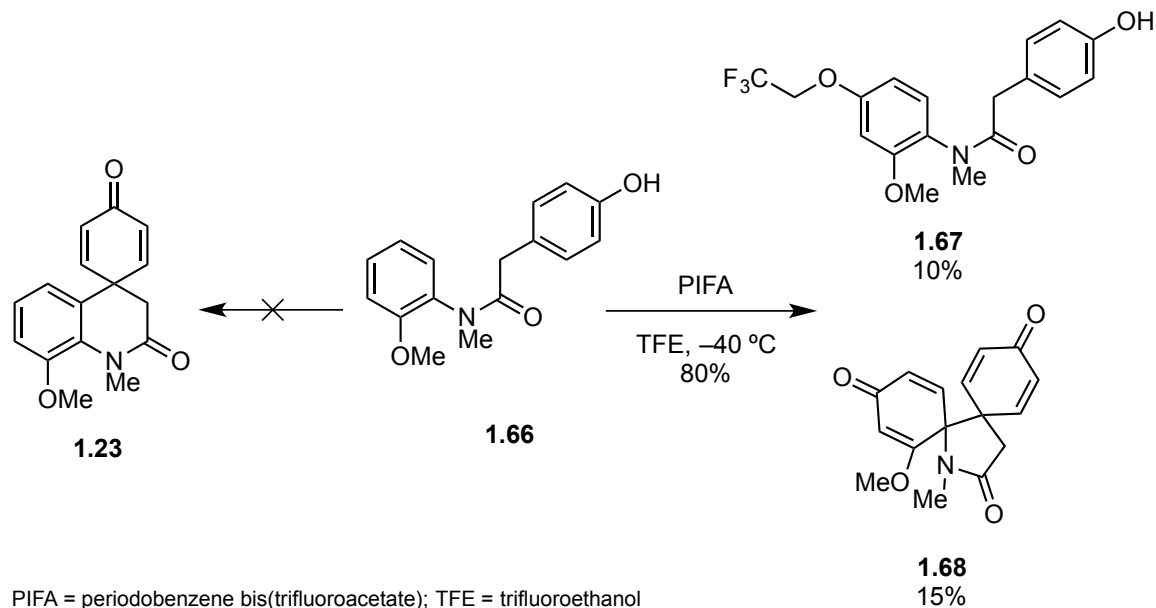
Scheme 1.11. Substitution on Aniline Reduces Yields of Oxidative Coupling



PIFA = periodobenzene bis(trifluoroacetate); TFE = trifluoroethanol

In an attempt to form dienone **1.23** via an oxidative coupling, Guillou *et al* found that oxidation of the *ortho*-methoxy anilide **1.66** did not afford any of the desired dienone **1.23**. Instead, they identified compounds **1.67** and **1.68** as the major products in 10% and 15% yield, respectively (Scheme 1.12).^{28,29} This observation illustrated the sensitivity of these oxidative methodologies to small changes in the electronic character of the system.

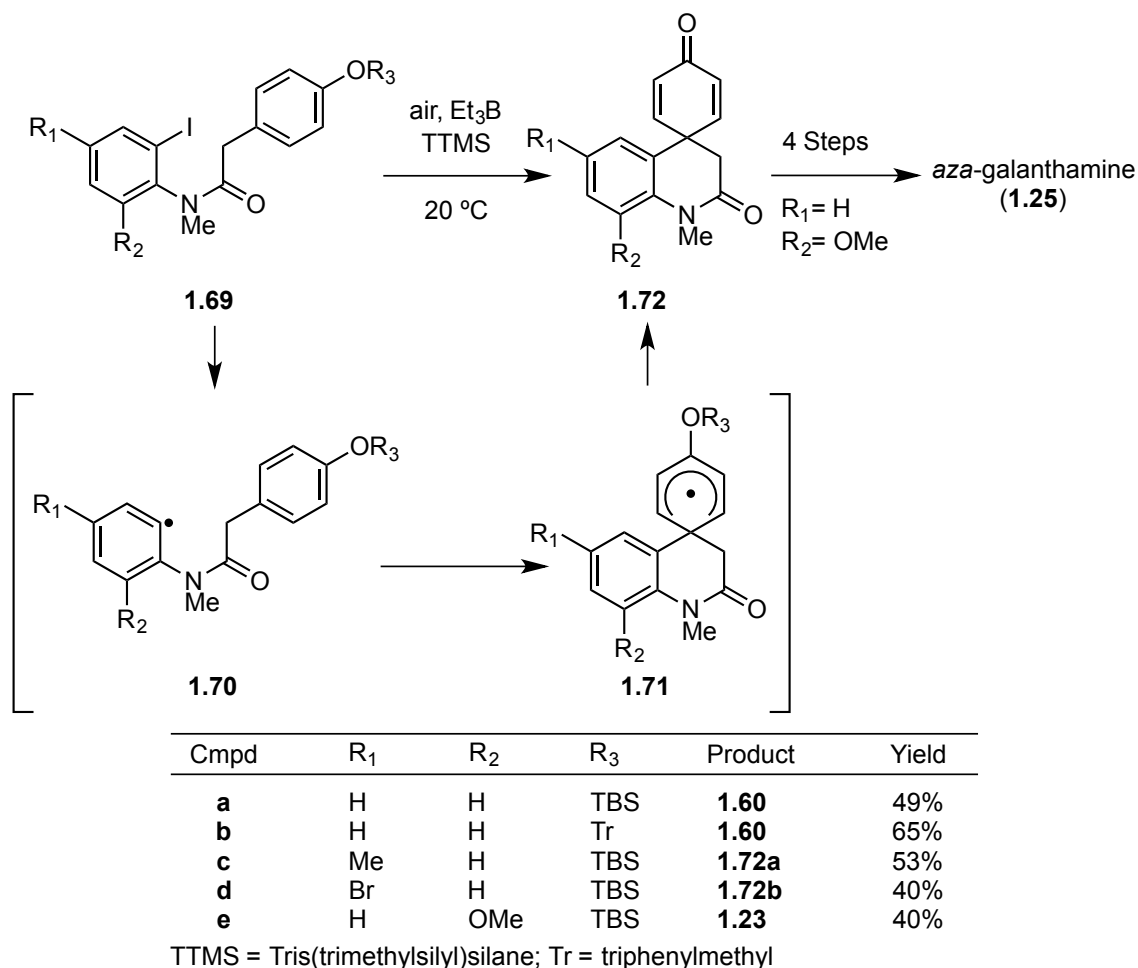
Scheme 1.12. Attempted Synthesis of Dienone **1.23** by Guillou *et al*



1.1.4.2 Radical Based Methods

Other oxidative conditions have been developed in order to overcome some of the limitations of hypervalent iodine reagents. For example, homolytic cleavage of a C-I bond has been used to synthesize *aza*-spirocyclic dienones analogous to **1.60** (Scheme 1.10). Curran *et al* found that iodoanilide **1.69** could be converted to dienone **1.72** in moderate yields using triethylborane/O₂ as a radical initiator in conjunction with TTMS (tris(trimethylsilyl)silane) (Table 1.1).³⁰ Although the yields were comparable to the methods utilizing hypervalent iodide, this strategy provided a broader substrate scope than previous methods. Specifically, the previously inaccessible *ortho*-methoxy derivate **1.23** was formed in 40% yield, culminating in the formal synthesis of aza-galanthamine (**1.25**, Scheme 1.5).

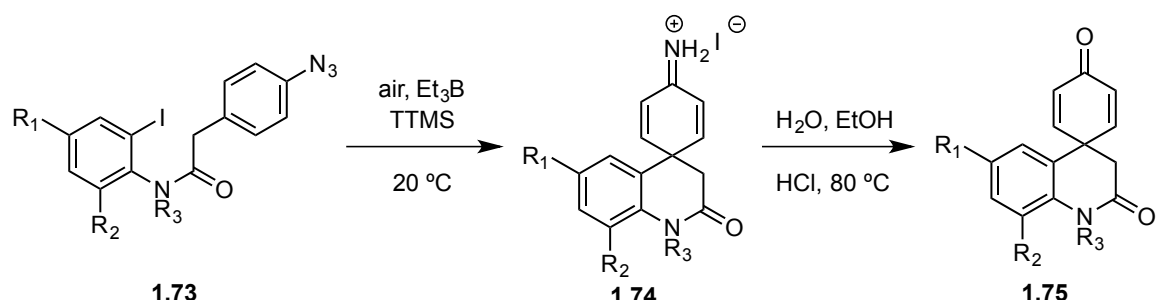
Table 1.1. Synthesis of *spiro*-Cyclohexyldienone Via an Oxidative Radical Process by Curran *et al*



Following the initial efforts by Curran *et al*, Lanza *et al* reported a similar approach utilizing an aryl azide in lieu of a trityl or silyl protected phenol (Table 1.2).^{31,32} The authors reported comparable yields over two steps to that of the Curran group (55-68% vs 40-65%), but they claimed their method was superior because the starting materials were more readily accessible (Table 1.1). The Lanza group also observed a competing reaction pathway in which the benzylic position of the aryl azide was oxidized, affording the benzylic alcohol **1.79** in 10-20% yields (Scheme 1.13). Curiously,

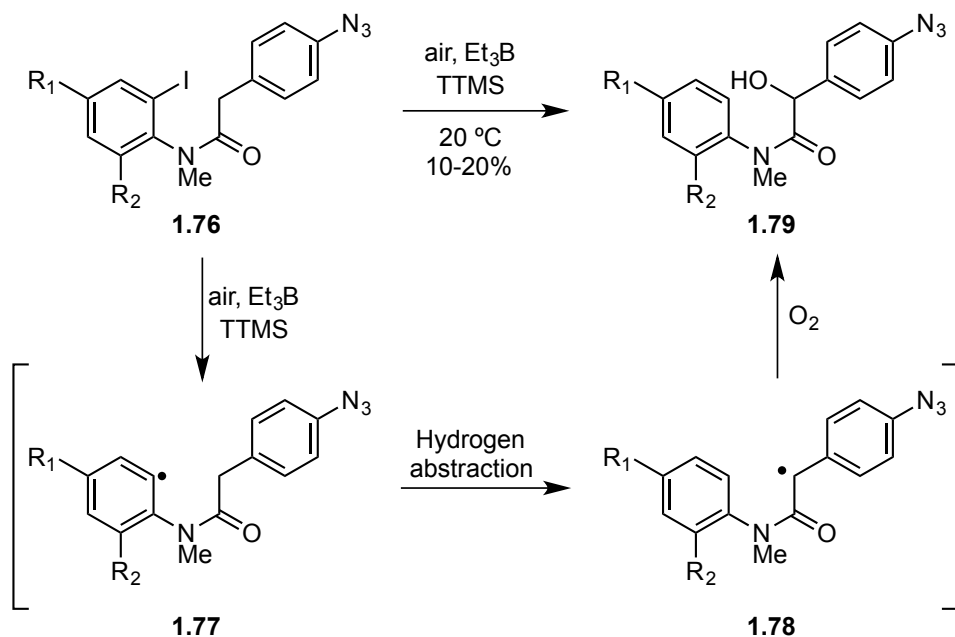
the authors reported that Boc protected anilide **1.73e** did not react under the reaction conditions, and they provided no explanation for the observed lack of reactivity.

Table 1.2. Synthesis of *spiro*-Cyclohexyldienone Via an Oxidative Radical Process from Aryl Azides



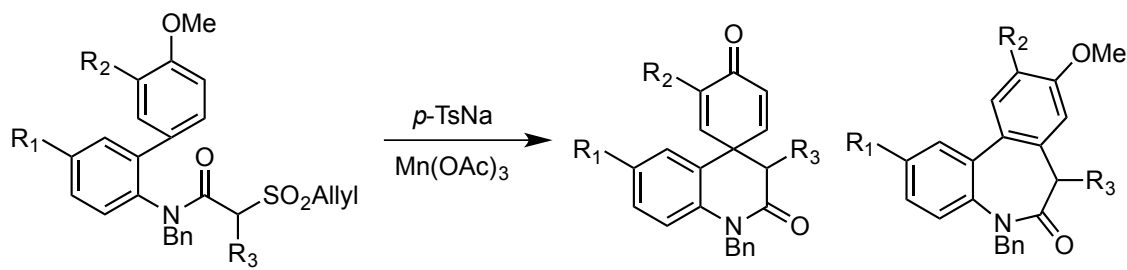
Cmpd	R ₁	R ₂	R ₃	Product	Yield
1.73a	H	H	Me	1.60	55%
1.73b	Me	H	Me	1.75a	58%
1.73c	Br	H	Me	1.75b	55%
1.73d	H	OMe	Me	1.23	54%
1.73e	H	H	Boc	1.26	0%
1.73f	H	H	MOM	1.75c	55-62%
1.73g	Me	H	MOM	1.75d	55-62%
1.73h	Br	H	MOM	1.75e	55-62%

Scheme 1.13. Mechanism for Formation of Benzylic Oxidation By-product



In 2013, Chuang *et al* accessed *aza*-spirocyclic dienones via an oxidative methodology in which the order of bond formation is reversed relative to the Curran and Lanza strategy.³³ In the Chuang *et al* paper, an α -allylsulfonyl amide was treated with sodium *p*-toluenesulfonate and manganese (III) acetate to generate a carbon centered radical that then adds *ipso* to the biaryl affording the desired dienone **1.81** in good yields (72-94%) (Table 1.3). Although this strategy provided that best yields to date, there were some regioselectivity issues as **1.82** was produced in yields as high as 14%. These reactions also required a large amount of manganese (III) acetate (2.5 eq) to proceed, which can complicate purification.

Table 1.3. Dienone Synthesis Via an Oxidative Radical Process Initiated by Allylsulfonyl Degradation



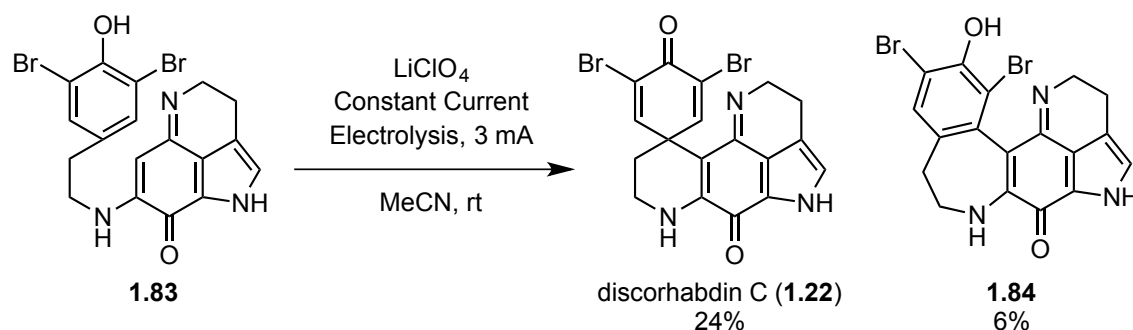
Cmpd	R ₁	R ₂	R ₃	1.81 Yield	1.82 Yield
1.80a	H	H	H	75%	9%
1.80b	Me	H	H	76%	14%
1.80c	Cl	H	H	72%	12%
1.80d	H	Me	H	82%	5%
1.80e	Me	Me	H	83%	6%
1.80f	Cl	Me	H	82%	6%
1.80g	H	H	Me	95%	0%
1.80h	Me	H	Me	96%	0%
1.80i	Cl	H	Me	94%	0%

1.1.4.3 Other Oxidative Approaches

There are two additional oxidative approaches to the *aza*-spirocyclic dienone core of the discorhabdin alkaloids that utilize neither hypervalent iodide reagents nor carbon

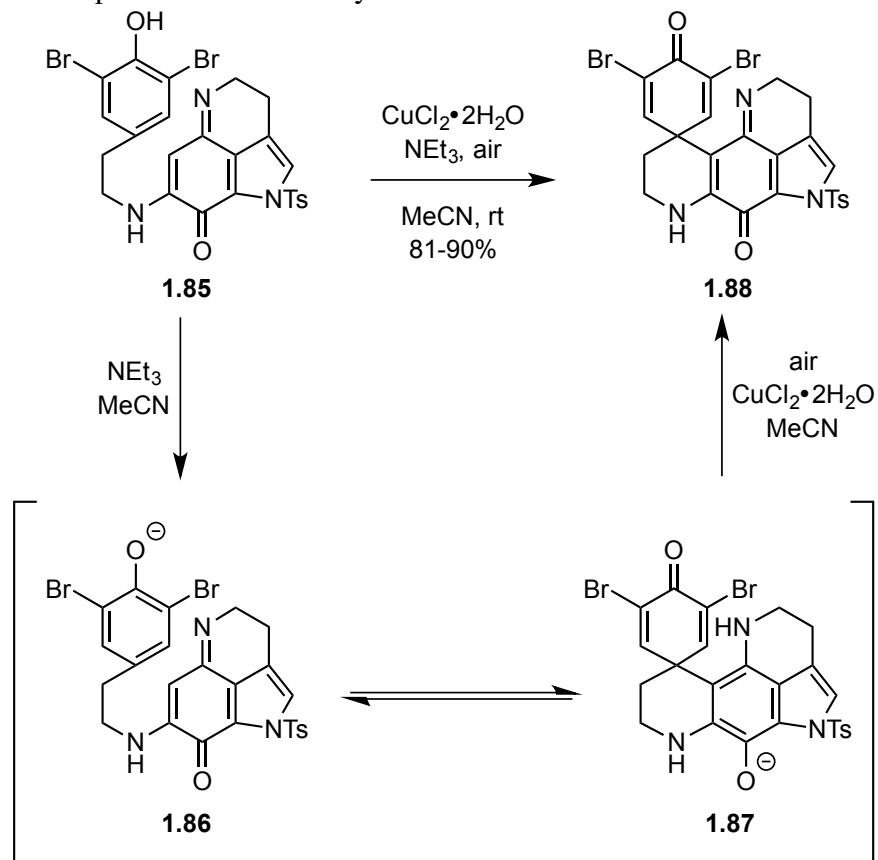
centered radicals to perform the requisite cyclization. Yamamura *et al* explored an approach using constant current electrolysis to synthesize the dienone core of the natural product discorhabdin C (**1.22**).^{34,35} Unfortunately, this electrochemical approach afforded the *aza*-spirocyclic dienone in only 24% yield (Scheme 1.14). In addition, the dienone produced (**1.22**) was shown to decompose under the reaction conditions, affording phenol **1.84** in 6% yield.

Scheme 1.14. Alternative Oxidative Approach to Discorhabdin C using Constant Current Electrolysis



In 1999, Heathcock *et al* published a biomimetic route to discorhabdin C in which he proposed that phenolate **1.86** is in equilibrium with aminohydroquinone **1.87** (Scheme 1.15). Indeed, the authors found that phenol **1.85** proceeded to dienone **1.88** in high yields under slightly basic and mild oxidizing conditions.³⁶ Although this transformation proceeded quite readily, this approach would not be generalizable to scaffolds that do not contain the quinone moiety because the mild oxidant does not oxidize the phenol directly. Rather, the CuCl_2/O_2 system oxidizes aminohydroquinone **1.87** that is formed upon 1,4-addition of the phenolate. Thus, this cyclization reaction would find little utility outside of the synthesis of the discorhabdin alkaloids.

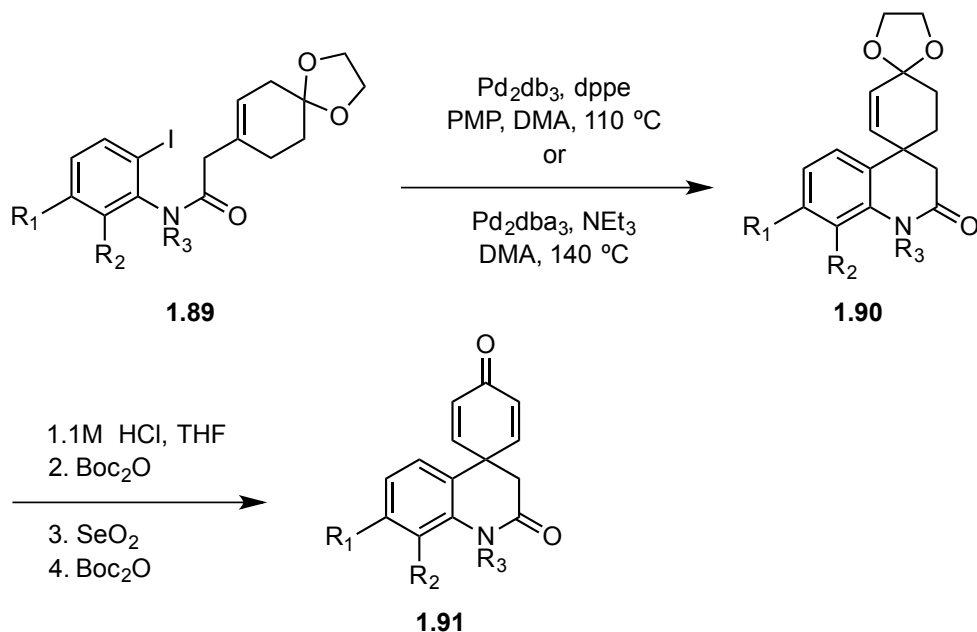
Scheme 1.15. Proposed Biomimetic Synthesis of the Discorhabdin Alkaloids



1.1.4.4 Non-oxidative Approaches

So far, the cyclization strategies shown rely on oxidation of a phenol or aminohydroquinone to form the desired *aza*-spirocyclic dienone moiety. However, there are two published strategies to *aza*-spirocyclic dienones that do not involve oxidation. In 2007, Guillou *et al* utilized an intramolecular Heck reaction followed by selenium dioxide oxidation to form *aza*-spirocyclic dienones (Table 1.4).²⁰ Although this approach was applied to a variety of substituted anilido arenes (Table 1.4, **1.89a-e**), the protracted synthesis of dienone **1.91** (five steps from **1.90**) made this strategy less desirable than others.

Table 1.4. Guillou *et al* Synthesis of *spiro*-Cyclohexyldienones Via an Intramolecular Heck Reaction

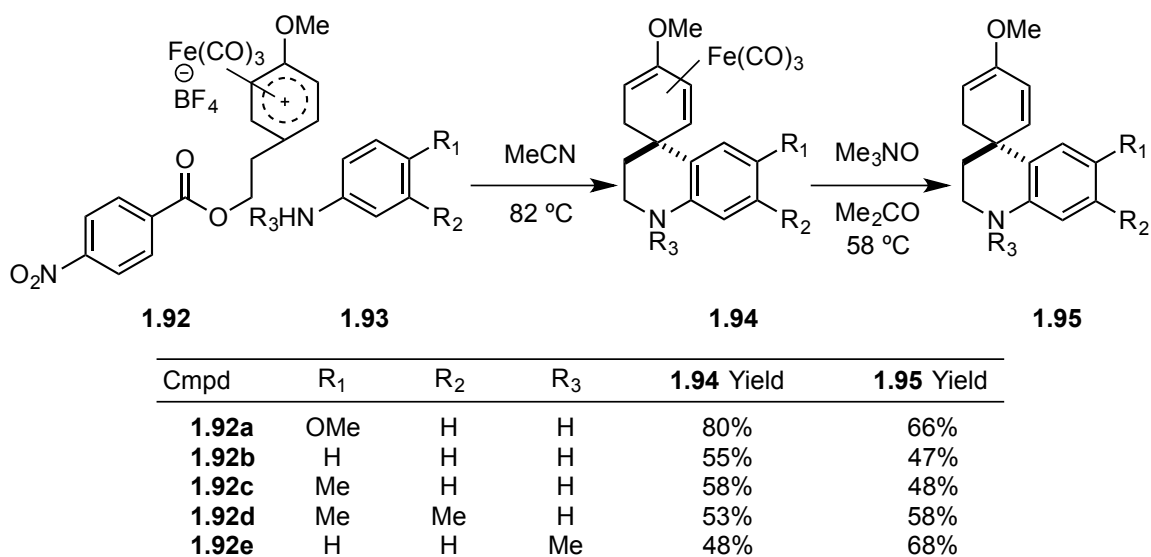


Cmpd	R ₁	R ₂	R ₃	Product	Yield	Cmpd	R ₁	R ₂	R ₃	Product	Yield ^c
1.89a	H	H	H	1.90a	92% ^b	1.90a	H	H	Boc	1.26	62%
1.89b	OMe	H	H	1.90b	87% ^b	1.90b	OMe	H	Boc	1.91a	58%
1.89c	H	OMe	H	1.90c	53% ^b	1.90c	H	OMe	Boc	1.91b	68%
1.89d	H	OMe	Boc	1.90d	40% ^a						
1.89e	H	OMe	Me	1.90e	40% ^a						

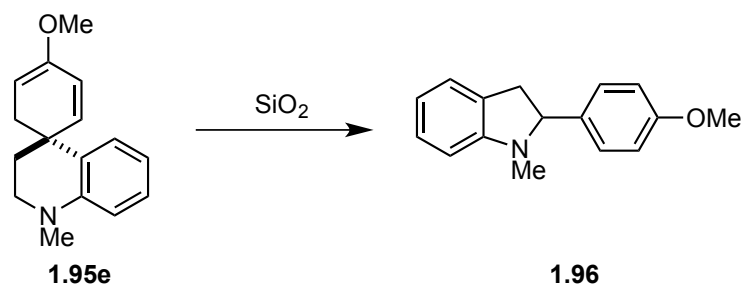
^aHeck reaction with ligand. ^bHeck reaction without ligand. ^cYield over four steps.

In 1989, Knölker *et al* showed that iron tricarbonyl arenium complex **1.92** reacted with anilines **1.93** to synthesize the complexed diene **1.94** (Table 1.5).³⁷ Unfortunately, the de-complexed compounds **1.95** were very unstable, and diene **1.95e** rapidly rearranged to the 2-aryl indoline moiety **1.96** upon contact with SiO₂ (Scheme 1.16).

Table 1.5. Knölker *et al* Synthesis of *spiro*-Cyclohexyldienes Via Iron Tricarbonyl Dearomatization

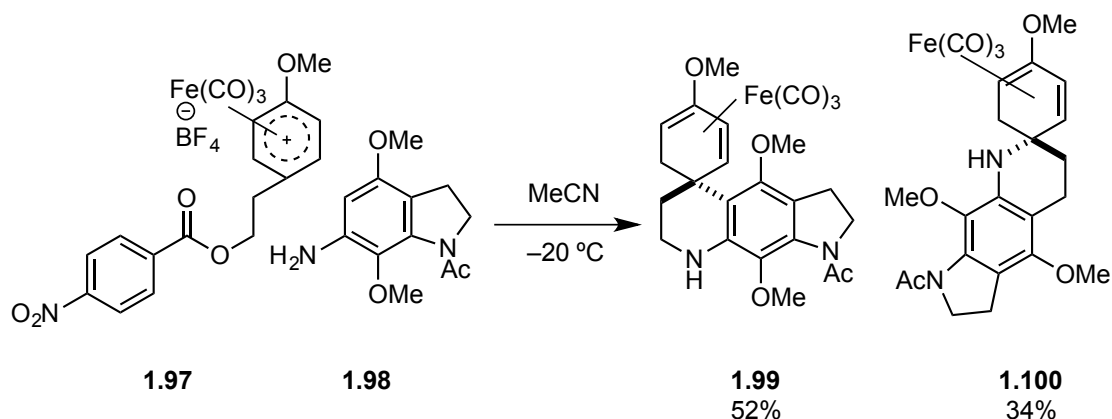


Scheme 1.16. Rearrangement of Diene **1.95e** to Indoline **1.96**



In analogy to their previous work, Knölker *et al* showed that iron tricarbonyl arenium complex **1.97** reacts with indoline **1.98** to access the carbon skeleton of the discorhabdin alkaloids (Scheme 1.17). However, this reaction proceeded with very poor regiocontrol, affording **1.99** and **1.100** as a mixture (3:2) of regioisomers.³⁸

Scheme 1.17. Alternative Oxidative Approach to the Discorhabdin Alkaloids using η^4 -Tricarbonyliron

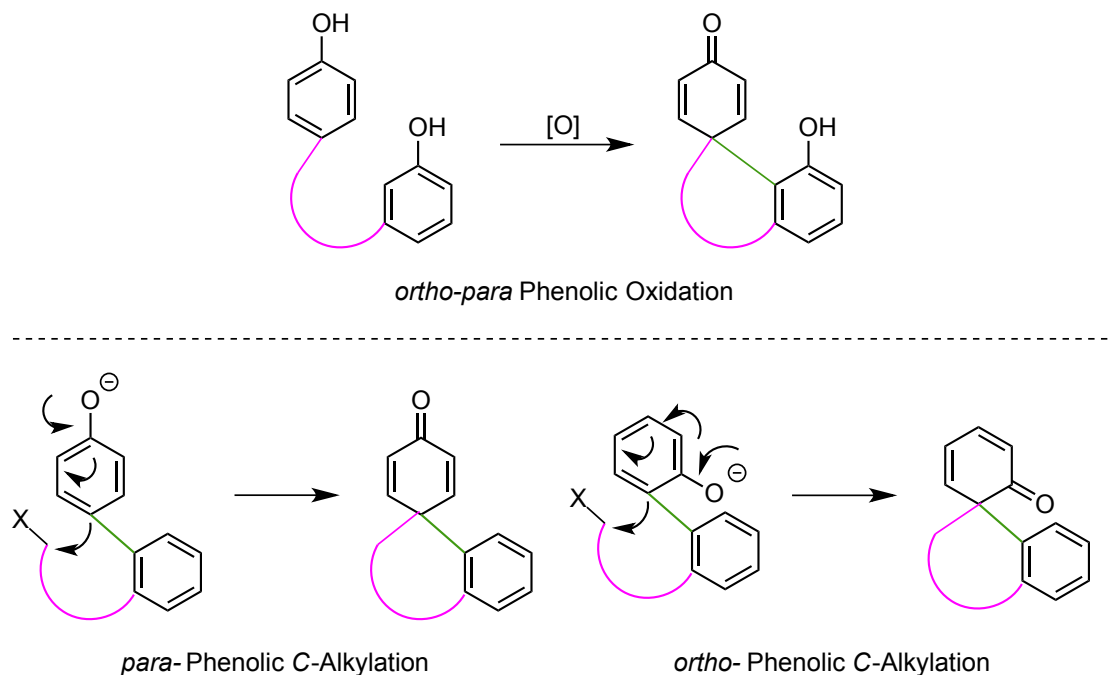


1.2 MAGNUS APPROACH TO ALKALOID SYNTHESIS

1.2.1 Bond Formation Strategy

Given the ubiquitous nature of the spirocyclic cross-conjugated dienone moiety as an intermediate in the biosynthesis of numerous alkaloids, the Magnus lab sought to exploit that structural motif in the synthesis of (\pm)-codeine and (-)-galanthamine.³⁹ In view of the aforementioned limited success by numerous groups to form dienones via biomimetic oxidative methods, Magnus hypothesized that those natural products could be synthesized utilizing a phenolic C-alkylation in lieu of an oxidative coupling. This strategy would allow reversal of the order of bond formation and avoid the poor reaction profiles associated with oxidative couplings, while still utilizing biosynthetically relevant intermediates (Figure 1.5).

Figure 1.5. General Example of Phenolic C-Alkylation in Lieu of Oxidative Coupling

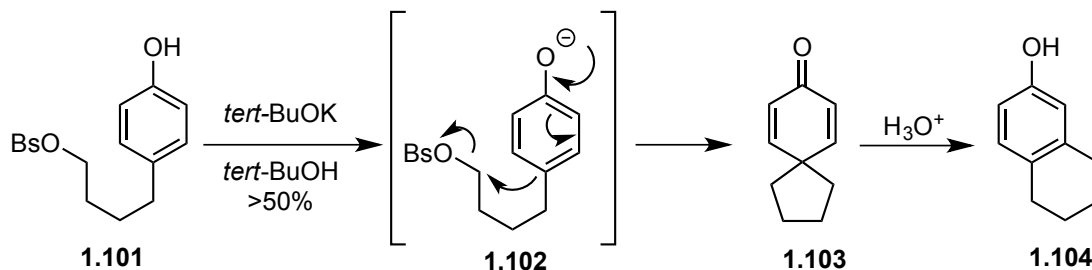


1.2.2 The Phenolic C-Alkylation Reaction

1.2.2.1 Discovery of the Phenolic C-Alkylation

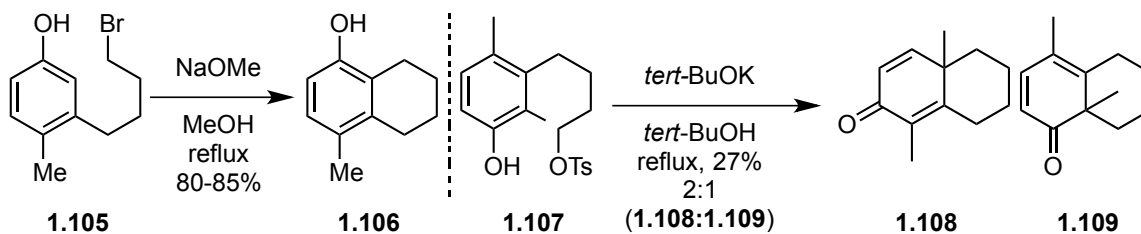
The base induced phenolic C-alkylation was first discovered by Winstein and Baird in 1957.⁴⁰ In their seminal work, phenol **1.101** formed *spiro*-cyclohexyldienone **1.103** upon deprotonation with potassium *tert*-butoxide in anhydrous *tert*-butyl alcohol (Scheme 1.18). They noticed that the product contained a carbonyl group via IR and verified the spirocyclic structural assignment via rearrangement of dienone **1.103** to phenol **1.104** under acidic conditions. After preliminary mechanistic studies, Winstein and Baird further determined that the cyclization occurred via Ar_1 participation of phenolate ion **1.102** and is the dominant pathway over non-anchimerically assisted pathways.⁴¹

Scheme 1.18. First Example of Base Catalyzed Phenolic C-Alkylation



After the initial discovery in 1957, Mandell expanded the methodology to include alkylation at the *ortho* position of a phenol during efforts towards the synthesis of santonin-like compounds.⁴² Mandell found that phenol **1.105** afforded exclusively the *ortho* alkylated product **1.106** after treatment with base, whereas the disubstituted phenol **1.107** afforded a mixture (2:1) of dienones **1.108** and **1.109** (Scheme 1.19).

Scheme 1.19. First Examples of *ortho*-Phenolic *c*-Alkylation

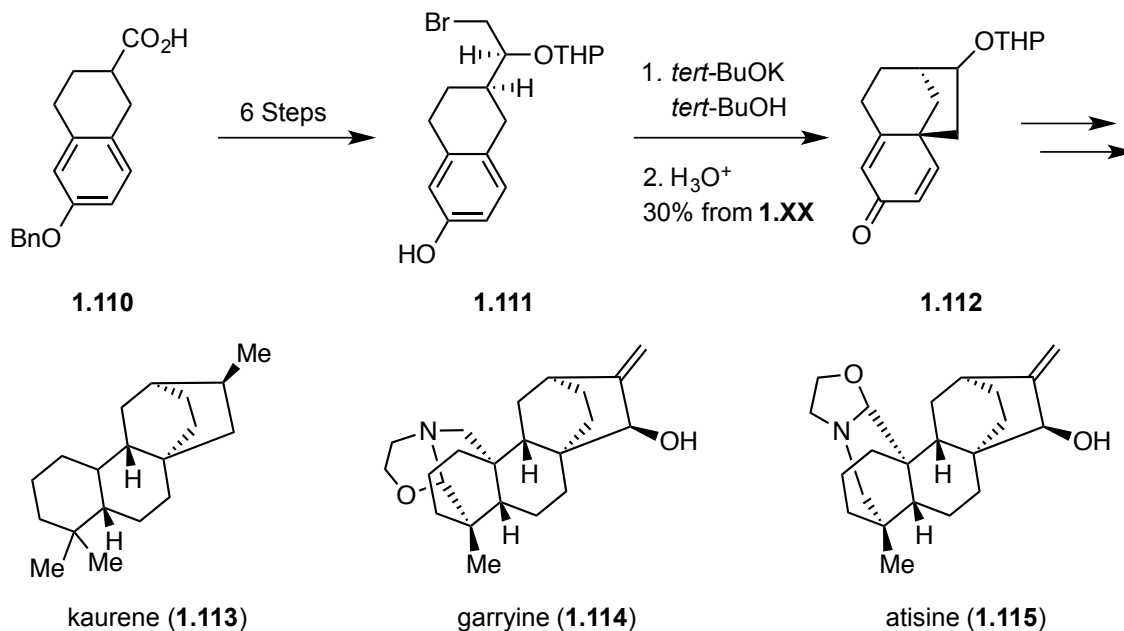


1.2.2.2 Early Use of the Phenolic C-Alkylation in Natural Product Synthesis

In 1963, this methodology proved valuable in the context of natural product total synthesis as a means of generating quaternary carbon centers. Of particular note, Masamune utilized an intramolecular phenolic C-alkylation to synthesize the bicyclo-[3.2.1]octane moiety found in a variety of diterpene natural products.⁴³ The work culminated in back-to-back publications of four articles detailing the syntheses of atisine (**1.115**), garryine (**1.114**), and kaurene (**1.113**) (Scheme 1.20).⁴⁴⁻⁴⁷ Later, the dienone

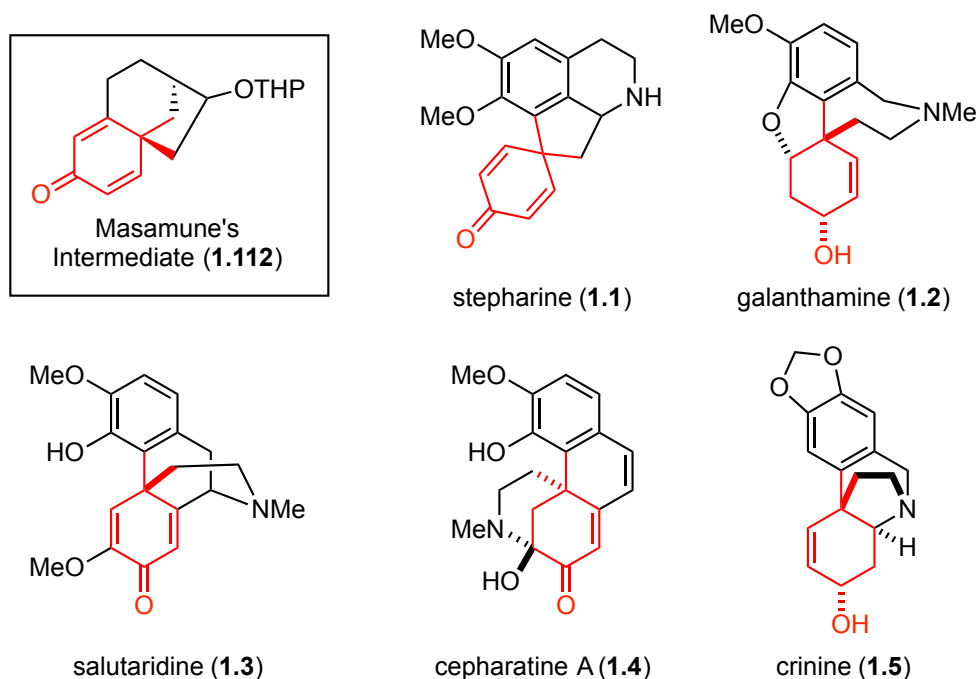
intermediate synthesized by Masamune was utilized by Marshall in the total synthesis of hinesol.⁴⁸

Scheme 1.20. Masamune Synthesis of Kaurene, Garryine, and Atisine



Since the publication of Masamune's work, the base induced phenolic *C*-alkylation has been utilized in the synthesis of terpenes, steroids, and other unique spirocyclic structural motifs.⁴⁹ Given that a wide variety of alkaloid natural products contain a central quaternary carbon center (Figure 1.6), the Magnus lab found it surprising that this C-C bond forming reaction had not been extensively utilized for the synthesis of alkaloids.

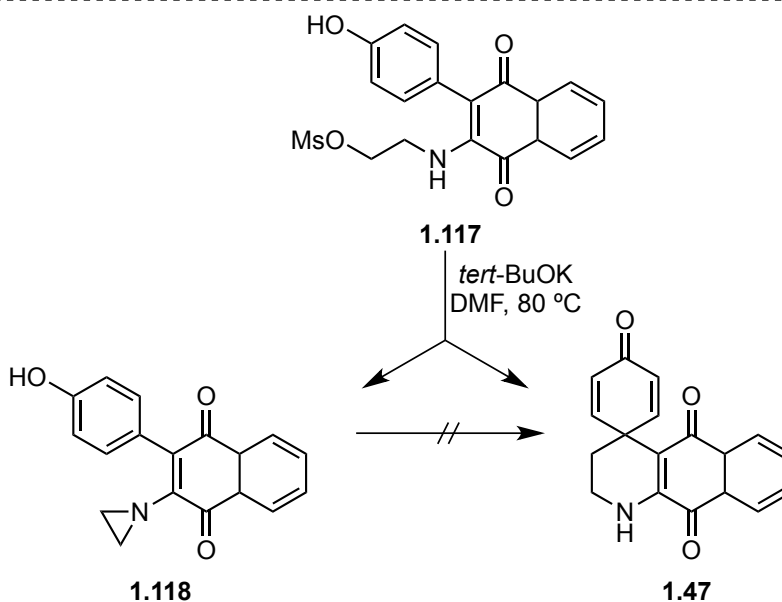
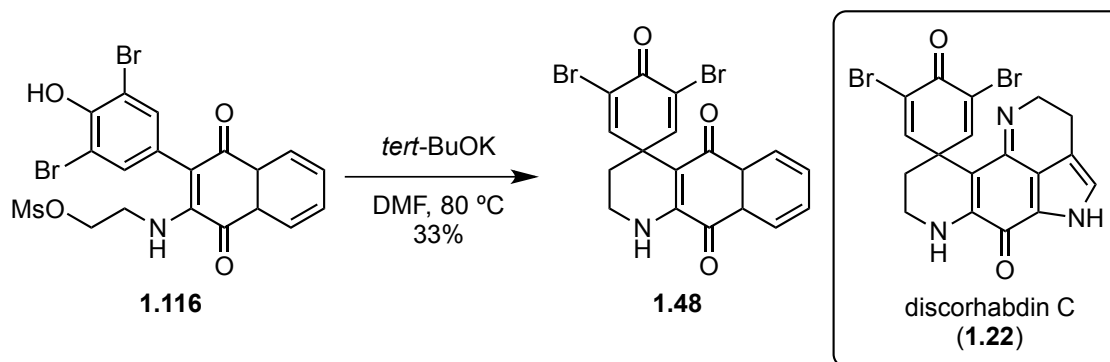
Figure 1.6. Mapping of the Dienone from Masamune's Intermediate Onto a Diverse Set of Alkaloids



Before the Magnus lab investigated the utility of the phenolic *C*-alkylation reaction in 2008, there was only one relevant example of an alkaloid synthesized via a base-induced intramolecular phenolic *C*-alkylation to afford a spirocyclic cross-conjugated dienone.⁵⁰ In 1990, Kublak *et al* published a study towards the synthesis of discorhabdin C (**1.22**). The authors sought to synthesize the unique aza-spirocyclic core via a phenolic *C*-alkylation, but they found that mesylate **1.116** afforded dienone **1.48** in only 33% yield (Scheme 1.21). To further investigate why the reaction proceeded poorly, the authors synthesized model system **1.117**; they discovered that the poor yield in the conversion of **1.117** to **1.47** was due to aziridine **1.118** formation being faster than phenolic *C*-alkylation. In addition, they found that upon resubjecting aziridine **1.118** to the reaction conditions, dienone **1.47** did not form. Thus, the authors speculated that the

σ^* orbital of the aziridine C-N bond could not align with the π system of the phenol, resulting in this unproductive byproduct.

Scheme 1.21. Synthesis of the Aza-Spirobicyclic Core of Discorhabdin C Via an Intramolecular Base-Catalyzed Phenolic C-Alkylation



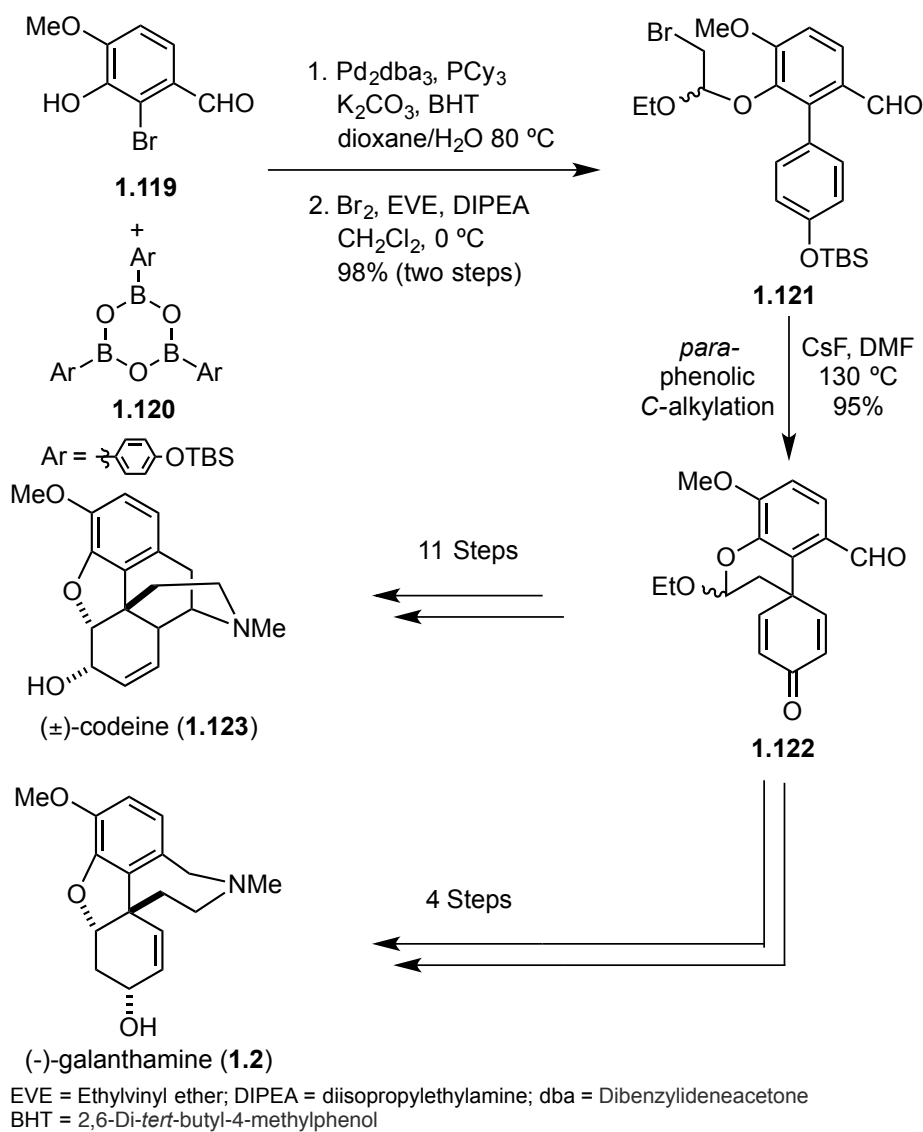
1.2.3 Successful Application of the Phenolic C-Alkylation to Alkaloid Synthesis

1.2.3.1 Synthesis of Galanthamine and Codeine

The Magnus lab hypothesized that an approach employing a phenolic C-alkylation would still be a good strategy for phenol-based systems that cannot form

aziridines. In the syntheses of (-)-galanthamine (**1.2**) and (±)-codeine (**1.123**) in 2009, the spirocyclic dienone **1.122** served as a divergent intermediate for both natural products (Scheme 1.22).³⁹ By first forming the biaryl bond via a Suzuki reaction followed by phenolic C-alkylation, the order of bond formation for the central quaternary carbon was reversed from the biomimetic process (Scheme 1.1), and the key dienone intermediate **1.122** was formed in 95% yield from biaryl **1.121**. This approach proved to be a dramatic improvement over previous syntheses, affording (-)-galanthamine and (±)-codeine in overall yields of 63% and 20%, respectively.

Scheme 1.22. Synthesis of (±)-Codeine and (-)-Galanthamine Via Phenolic C-Alkylation

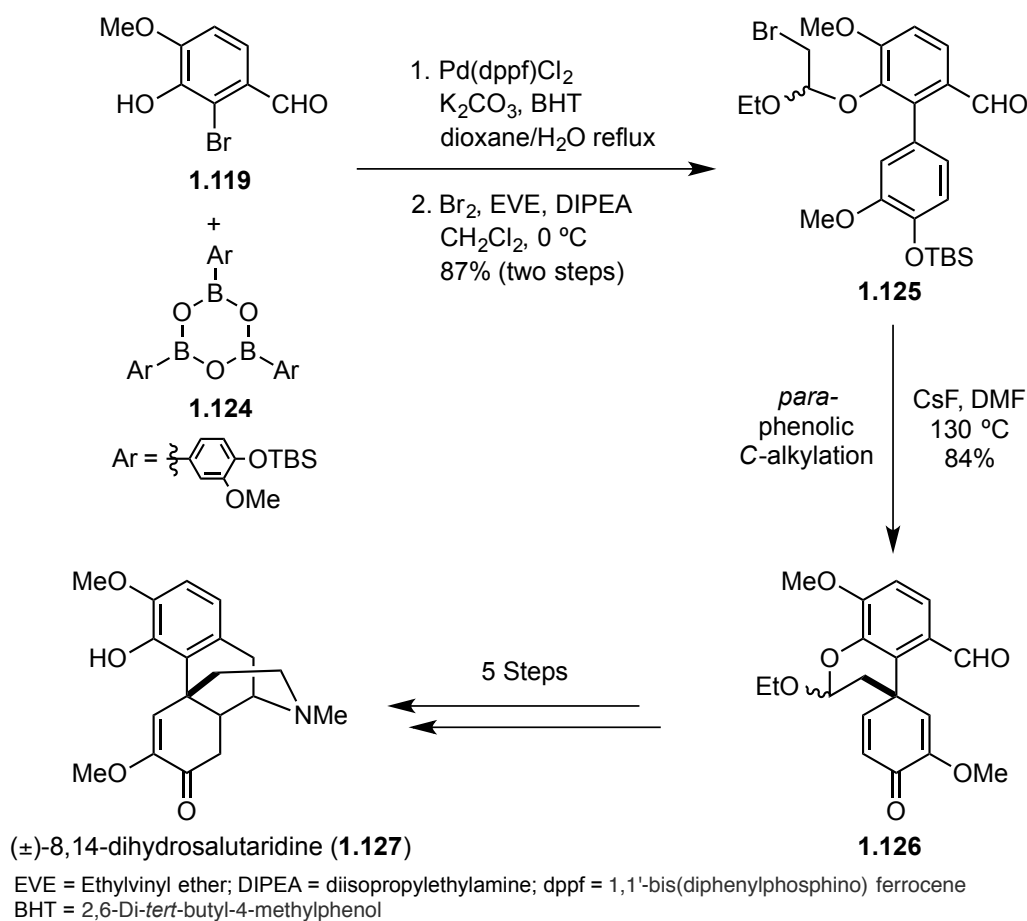


1.2.3.2 Synthesis of Dihydrosalutaridine

After initial success of the phenolic C-alkylation strategy, the Magnus group sought to apply their C-C bond forming strategy to the syntheses of other natural products. The phenolic C-alkylation reaction was next used to synthesize 8,14-dihydrosalutaridine (**1.127**) via dienone (**1.126**), which was obtained from biaryl **1.125** in

87% yield.⁵¹ In addition to rapidly synthesizing **1.127**, this sequence also expanded the phenolic C-alkylation strategy to include the preparation of differentially substituted dienones (Scheme 1.23). This synthesis was a dramatic improvement from the previous biomimetic synthesis of the closely related alkaloid salutaridine (**1.3**), which afforded the key spirocyclic cross-conjugated dienone **1.18** in only 22% yield (Scheme 1.4).¹⁶

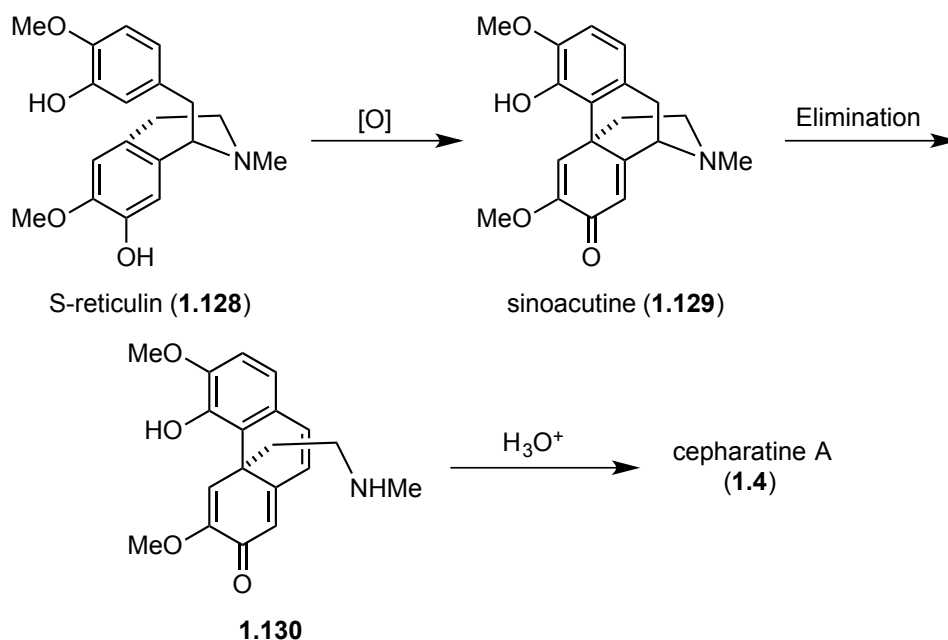
Scheme 1.23. Phenolic C-Alkylation Used in the Synthesis of 8,14-Dihydrosalutaridine



1.2.3.3 Synthesis of Cepharatine A

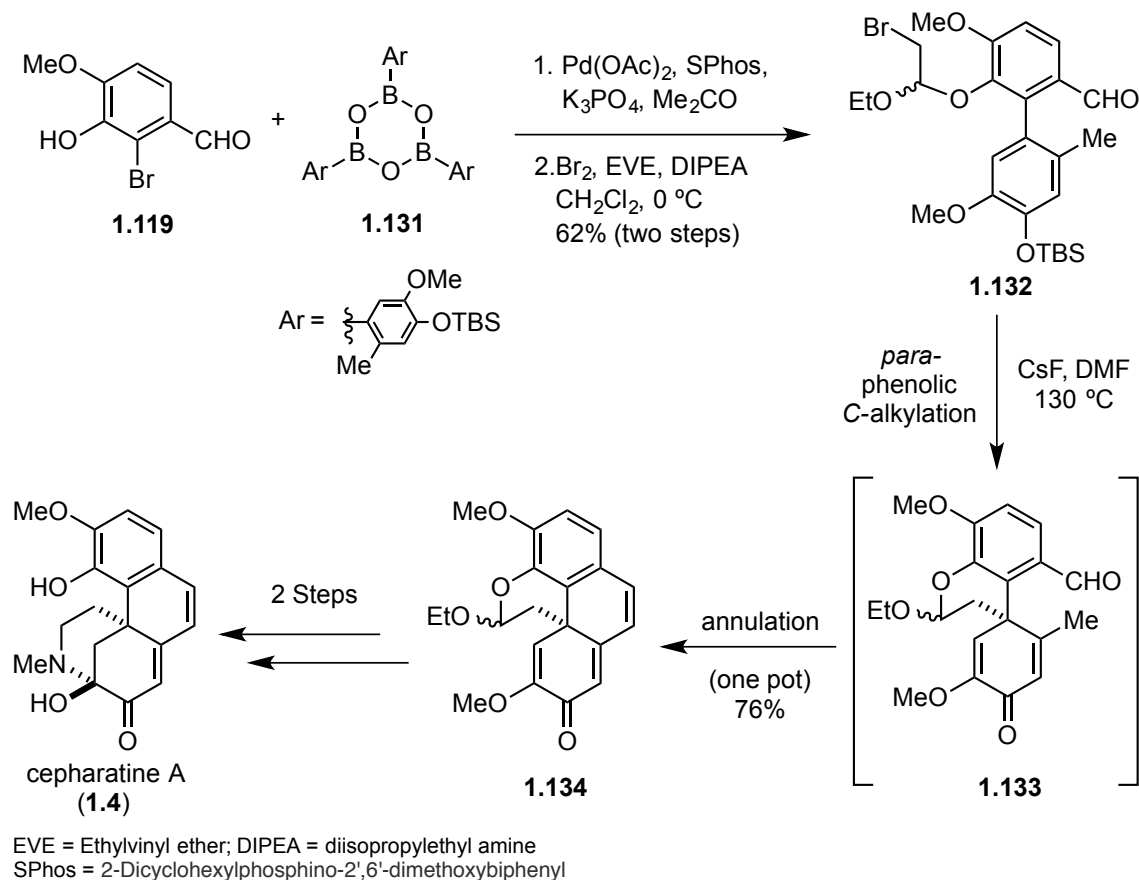
Although there is no biomimetic synthesis for the hasubanan alkaloid cepharatine A (**1.4**), it is believed that the compound arises in nature from sinoacutine (**1.129**), which is synthesized via an oxidative phenolic coupling of (S)-reticulín (**1.128**) (Scheme 1.24).⁵²

Scheme 1.24. Putative Biosynthesis of Cepharatine A



Employing the phenolic alkylation strategy once again, the Magnus lab synthesized tetracyclic dienone **1.134** in one step from biaryl **1.132** via a phenolic alkylation-annulation cascade. The tetracyclic dienone **1.134** was further elaborated into cepharatine A (**1.4**), affording the natural product in seven steps and 16% overall yield (Scheme 1.25).⁵³ This synthesis was an improvement over the previous work done by Reisman *et al* in which (–)-cepharatine A (**1.4**) was synthesized in 10 steps and 10% overall yield.⁵⁴

Scheme 1.25. Phenolic C-Alkylation-Annulation Used in the Synthesis of Cepharatine A

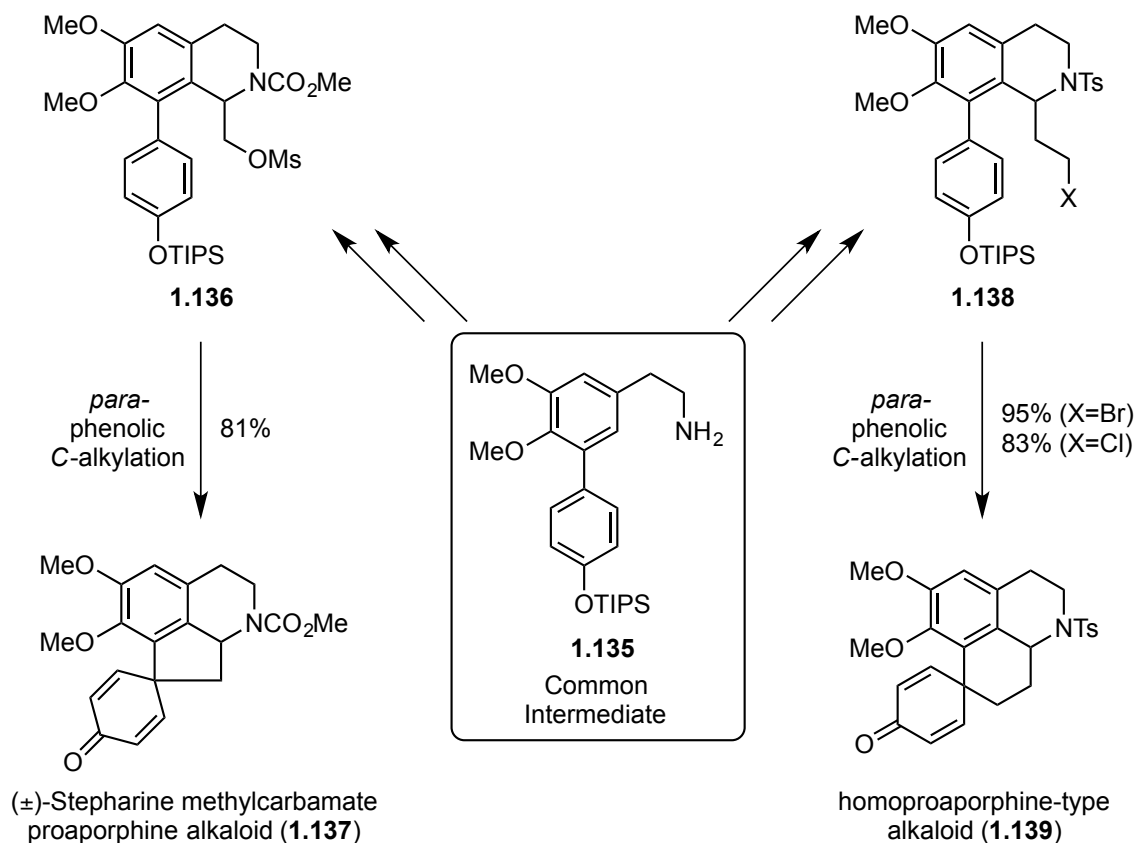


1.2.3.4 Synthesis of Homoaporphine and Aporphine Alkaloids

The Magnus lab has also applied the phenolic C-alkylation strategy to the synthesis of proaporphine and homoproaporphine-type alkaloids.⁵⁵ In this work, the biaryl **1.135** was used as a common divergent intermediate to access tetrahydroisoquinoline moieties **1.136** and **1.138**. It was then shown that mesylate **1.136** afforded dienone **1.137** in 81% yield upon exposure to CsF at elevated temperatures. Under analogous conditions, dienone **1.139** was synthesized in high yields from biaryl **1.138**. The success of those transformations led to a divergent synthesis of the

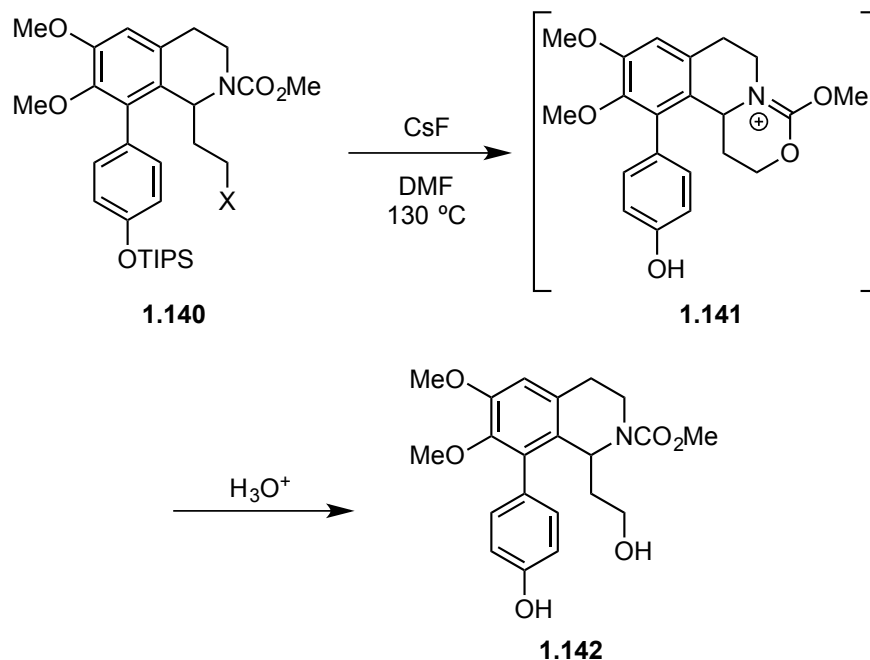
proaporphine alkaloid stepharine (**1.1**) and a general scaffold for homoproaporphine-type alkaloids (**1.139**), respectively (Scheme 1.26).

Scheme 1.26. Phenolic Alkylation Strategy for the Synthesis of Proaporphine and Homoproaporphine Alkaloids



Curiously, the choice in protecting groups for the homoproaporphine systems was paramount to the success of the transformation. When a carbamate protecting group was used instead of a sulfonamide for tetrahydroisoquinoline **1.140**, the nucleophilic oxygen of the carbamate displaced the leaving group affording the cyclic carbamate **1.141**, which, upon work up, hydrolyzed to primary alcohol **1.142** (Scheme 1.27).⁵⁶ This observation provided further insight into the scope and limitations of this reaction.

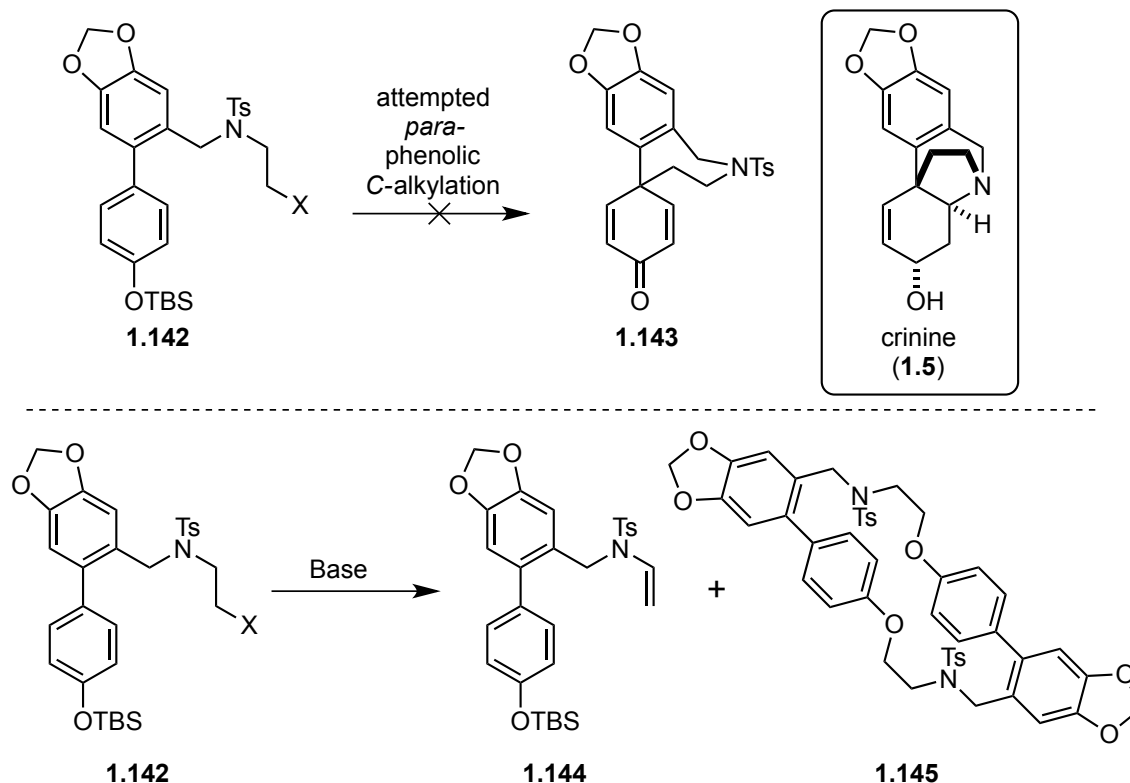
Scheme 1.27. Cyclic Carbamate Formation Occur faster than Phenolic C-Alkylation



1.2.3.5 Attempted Synthesis of Crinine

The phenolic C-alkylation strategy has also been applied to the *Amarylidaceae* alkaloid family in an attempt to prepare crinine (**1.5**), but the cyclization did not proceed as intended. Instead of providing the desired 7-membered ring, products resulting from dimerization (**1.145**) or elimination to the *N*-tosyl enamine (**1.144**) were observed (Figure 1.7).⁵⁷ Although the inability to affect formation of dienone **1.143** was disheartening, the data point was still valuable in establishing the scope and limitation of the strategy because there is a large entropic penalty in the transition state for the formation of seven-membered rings. Thus, if the transition state is too high in energy, the cyclization will not proceed and a non-productive reaction pathway will occur.

Figure 1.7. Failed Application of Phenolic C-Alkylation to the Synthesis of Crinine

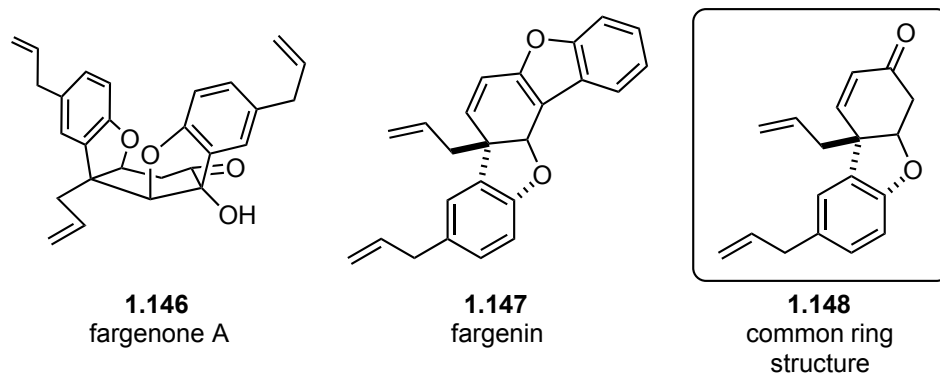


1.2.3.6 Attempted Synthesis of Fargenone Alkaloids

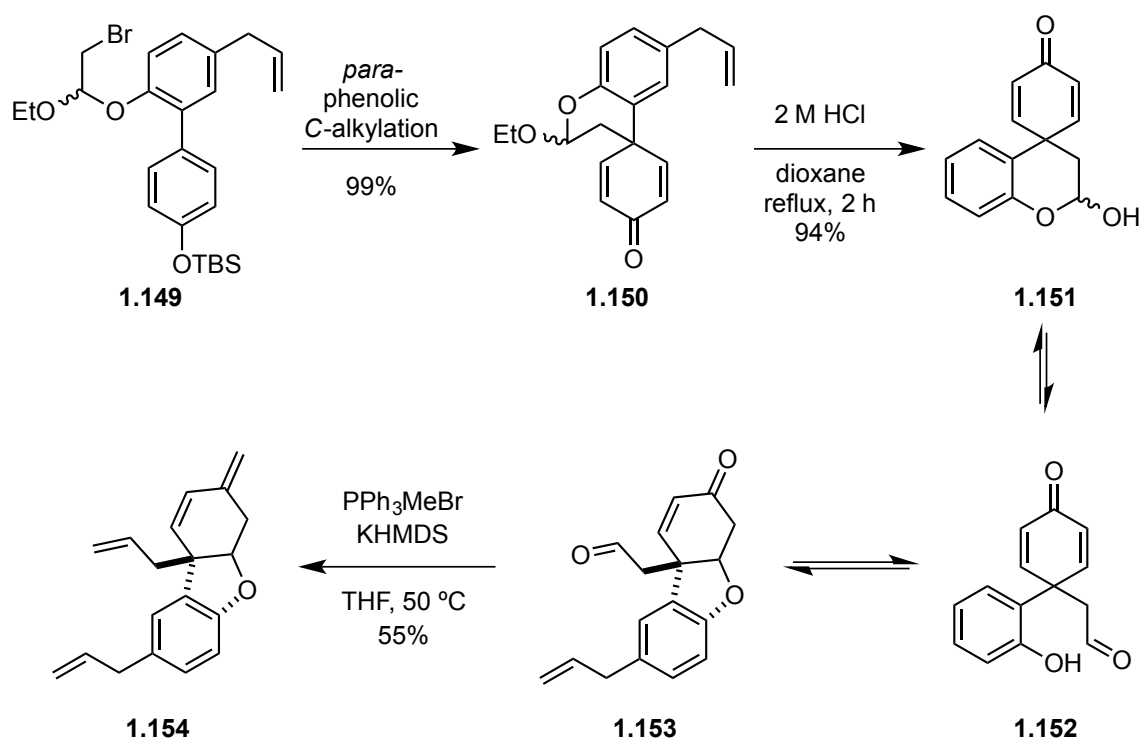
Others outside the Magnus lab have also applied the phenolic alkylation strategy to natural product synthesis. For example, Denton *et al* utilized the phenolic alkylation approach in an attempts to prepare the tricyclic core of the fargenone and fargenin family of natural products, represented by **1.146** and **1.147** (Figure 1.8).⁵⁸ The authors speculated that hemiacetal **1.151** would be in equilibrium with aldehyde **1.153**, and aldehyde **1.153** would react chemoselectively with methyl phosphonium ylide to form alkene **1.148**. Unfortunately, no chemoselectivity was observed. Instead, the double adduct **1.154** was isolated in 55% yield (Scheme 1.28). Although their approach ultimately failed to provide

1.148, they were able to prepare the spirocyclic cross-conjugated dienone **1.150** in 99% yield from biaryl **1.149** (Scheme 1.28).

Figure 1.8. Natural Products Fargenone A, Fargenin, and a Common Structural Motif



Scheme 1.28. Phenolic Alkylation Strategy Used in Studies Towards the Fargenone/Fargenin Family of Natural Products



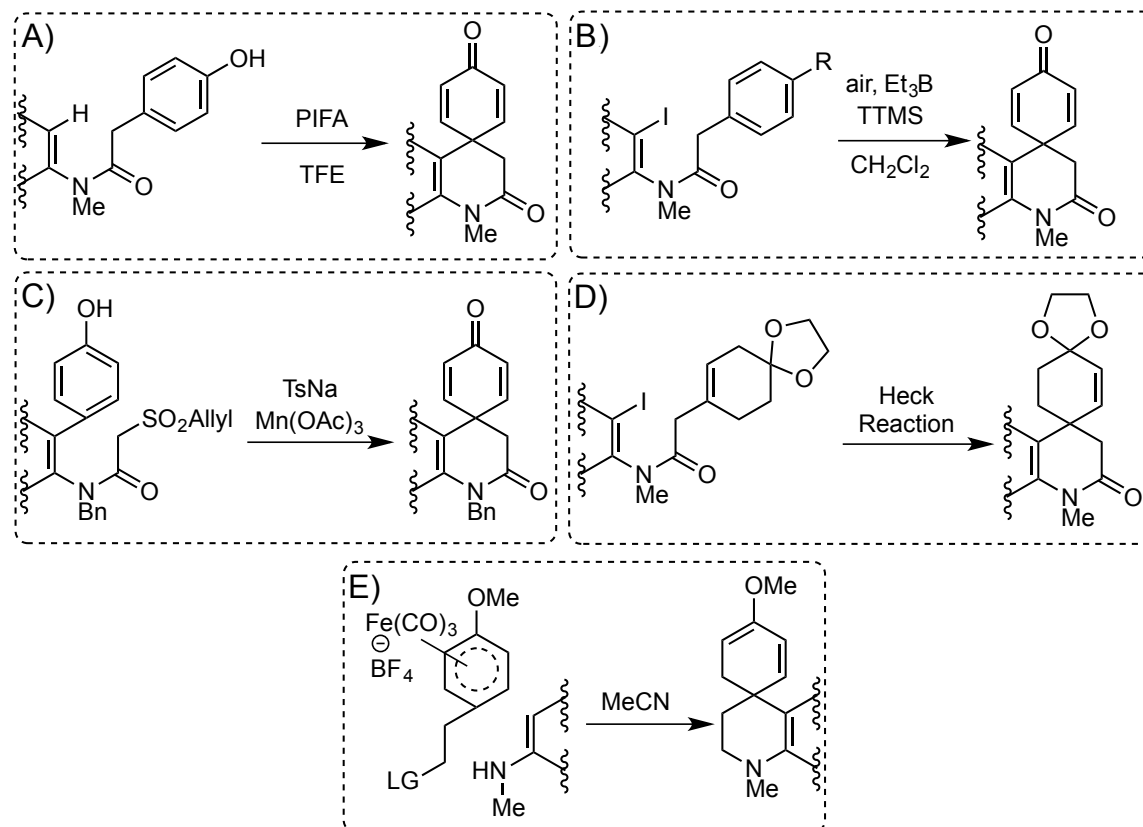
1.3 CONCLUSION

The spirocyclic dienone structural motif is a privileged intermediate that is embedded into the carbon framework of numerous alkaloids (Figure 1.1). Prior to the work done in the Magnus lab, the most efficient way to form these motifs involved using a biomimetic oxidative coupling that often suffered from low yields and poor regiocontrol (Schemes 1.2-4). To overcome these issues, the Magnus lab proposed a different strategy in which the key quaternary carbon is synthesized via a Suzuki coupling followed by an intramolecular phenolic *C*-alkylation (Figure 1.5), and through this bond forming strategy, numerous natural products have been synthesized in high yields (Schemes 1.22-26).

Similarly, the *aza*-spirocyclic dienone is a structural motif found in numerous natural products (Figure 1.2), and it has been used as an intermediate in the synthesis of natural products and natural product-like compounds (Schemes 1.22-26). The current generalizable strategies for synthesizing *aza*-spirocyclic dienones are shown in Figure 1.9, and each of these approaches have various shortcomings that limit the utility of each method. The approach that utilizes the hypervalent iodide reagent PIFA (Figure 1.9a) benefits from the anilide system being very simple and easy to prepare, but yields of the transformation are poor (40-60%) and the substrate scope is very limited (Schemes 1.10-12). The radical based approaches using triethylborane (Figure 1.9b) have a broader substrate scope than the hypervalent iodide method, but the yields (40-60%) are also poor (Tables 1.1 and 1.2). The radical based approach using $\text{Mn}(\text{OAc})_3$ (Figure 1.9c) showed the best yields (70-96%), but the approach encountered regioselectivity issues when substitution was placed on the phenol moiety (Table 1.3). The approach employing a Heck reaction (Figure 1.9d) was able to synthesize the *aza*-spirocyclic dienone moiety, but the overall yield was poor due to the protracted synthesis (Table 1.4). Lastly, the

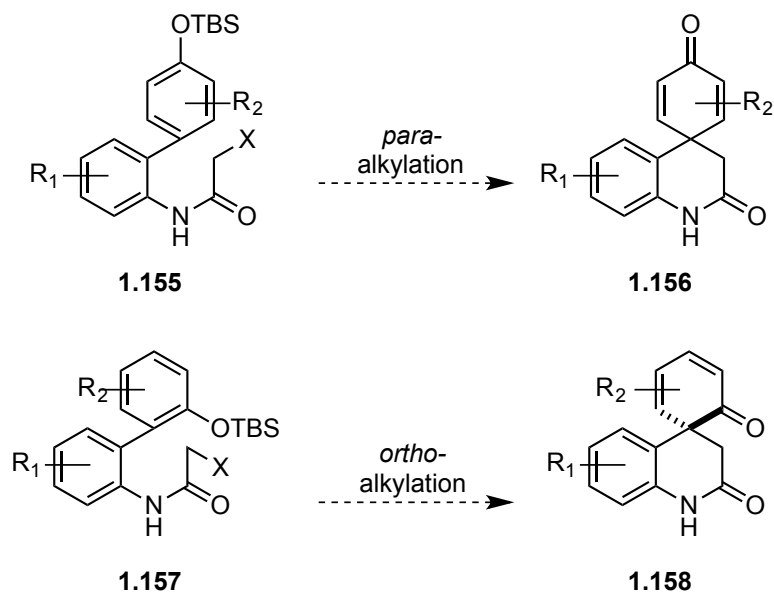
approach that utilizes the iron arenium complex (Figure 1.9e) has nominal utility due to poor regioselectivity and product instability (Table 1.5, Scheme 1.16, and Scheme 1.17).

Figure 1.9. Summary of Known Methods



Because of the glaring deficiencies with the current ways to synthesize the *aza*-spirocyclic dienone structural motif, a new method that is high yielding and function group tolerant would be extremely valuable to the synthetic community. We propose that the Magnus strategy for spirocyclic dienone synthesis could be expanded to aniline based systems, and this approach would be higher yielding and more functional group tolerant than the current methods that are known (Figure 1.10). Additionally, we believe that the Magnus approach could be expanded to include dienones arising from an *ortho*-phenolic C-alkylation as well as dienone arising from a *para*-phenolic C-alkylation.

Figure 1.10. Application of Magnus Approach to *aza*-Spirocyclic Dienone Synthesis



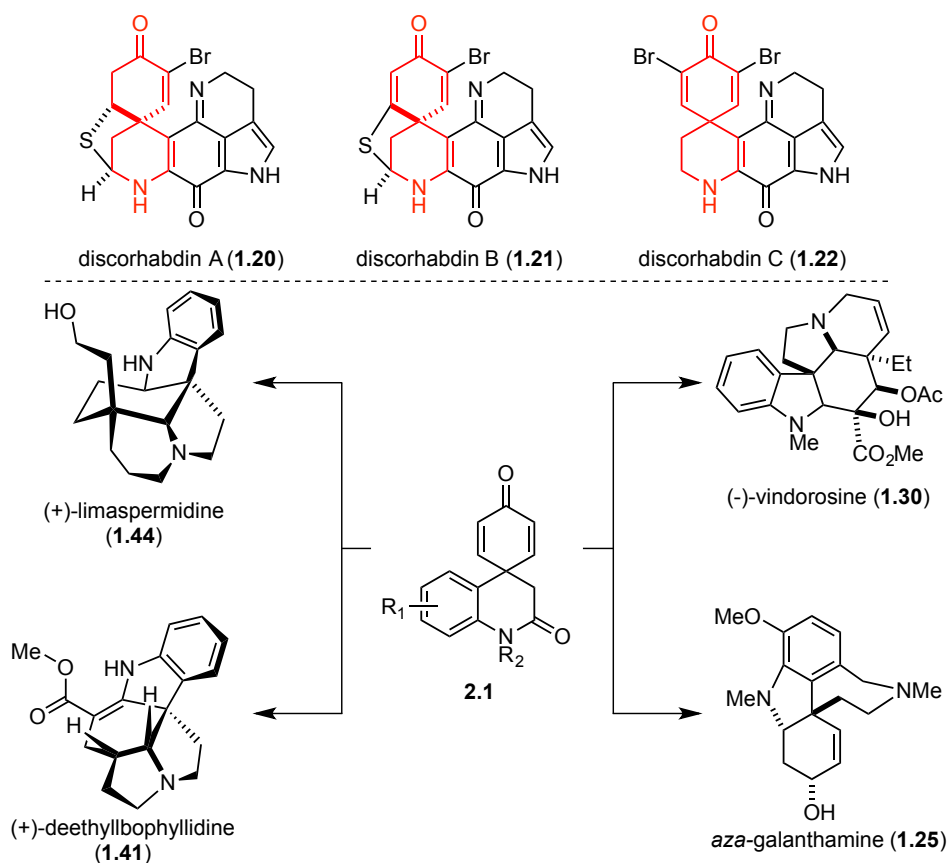
Chapter 2: Synthesis and Utilization of *aza*-Spirocyclic Dienones

2.1 SYNTHESIS OF AZA-SPIROCYCLIC DIENONES VIA AN INTRAMOLECULAR PHENOLIC C-ALKYLATION

2.1.1 Introduction

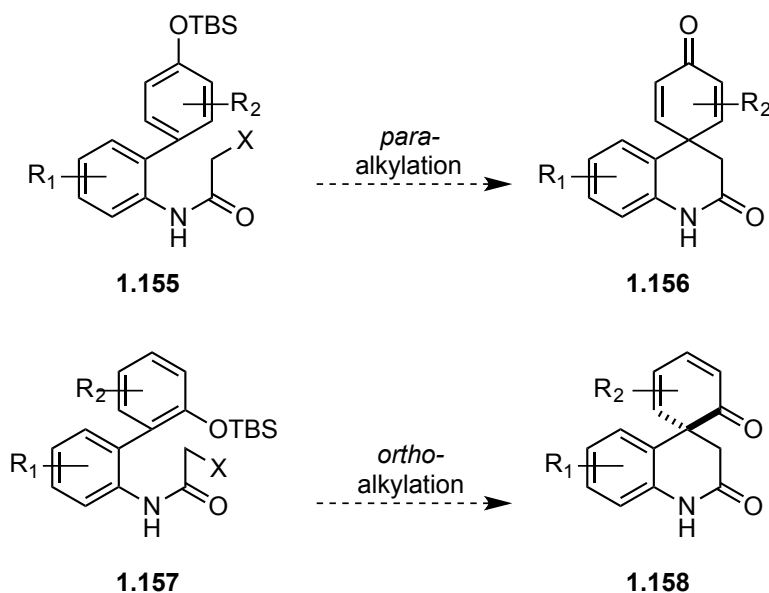
The *aza*-spirocyclic dienone moiety (Figure 2.1, outlined in red) is a structural motif present in the discorhabdin family of indole alkaloids. Additionally, the *aza*-spirocyclic structural moiety has been used as divergent intermediate to access a variety of natural products and natural product-like compounds (Figure 2.1).^{20,21,30}

Figure 2.1. The *aza*-Spirocyclic Dienone Motif and Its Relevance to Natural Products Synthesis



Various strategies have been developed to synthesize the *aza*-spirocyclic dienone motif, and the current approaches have obvious deficiencies, such as low yields and poor scope, that limit their utility and generalizability (Figure 1.9). We hypothesized that the Suzuki coupling/phenolic *C*-alkylation strategy developed in the Magnus lab would be able to synthesize *aza*-spirocyclic dienones in high yields. In addition, we sought to explore whether structures arising from *ortho*- as well as *para*-phenolic *C*-alkylation could be synthesized in order to access novel chemical structures (Figure 2.2).

Figure 2.2. Proposed Synthesis of *spiro*-Cyclohexyldienone Via an Intramolecular Phenolic *C*-Alkylation



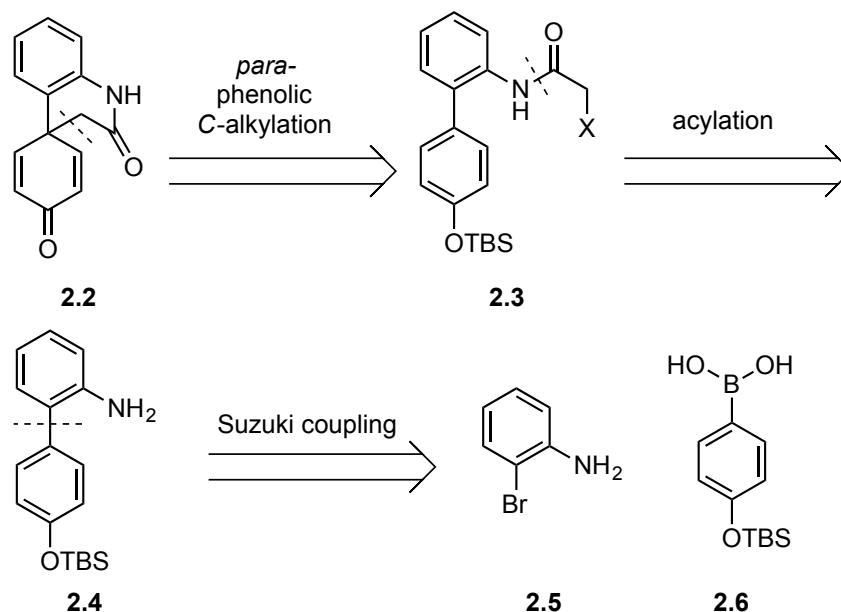
2.1.2 *para*-Phenolic *C*-Alkylation of Aniline Derived Systems

2.1.2.1 First Generation Model System for *para*-Phenolic *C*-Alkylation

To determine the viability of the *para*-phenolic *C*-alkylation strategy for the synthesis of *aza*-spirocyclic dienones, we initially employed the simple model system **2.2** (Scheme 2.1). We envisioned that the alpha halo amide **2.3** could be synthesized via

acylation of biaryl **2.4**, which in turn could be synthesized via a Suzuki cross coupling reaction from known boronic acid **2.6** and commercially available 2-bromoaniline (**2.5**).

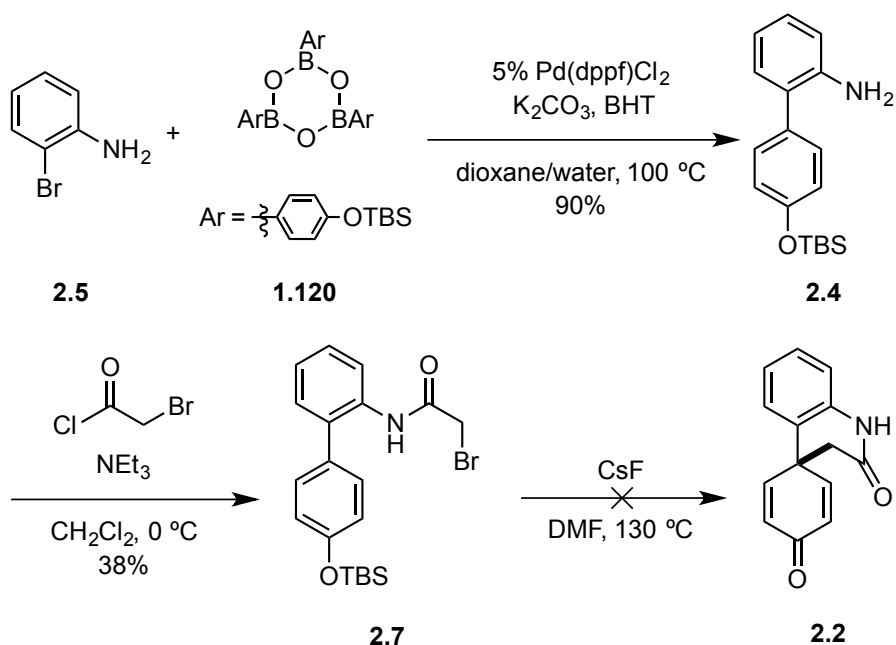
Scheme 2.1. Retrosynthetic Analysis for Initial Biaryl Model System



The metal/ligand complex Pd(dppf)Cl₂ readily catalyzed the coupling of boroxine **1.120** and 2-bromoaniline (**2.5**) to afford biaryl **2.4** in 90% yield (Scheme 2.2). During the course of optimizing the reaction, it was determined that transient oxygen in the reaction flask would react with and degrade the boronic acid generated *in situ*, resulting in highly variable reaction profiles (50-90% yield). Thus, rigorous degassing of the dioxane/water mixture and addition of the oxygen scavenger BHT (2,6-di-*tert*-butyl-4-methylphenol) were key to obtaining consistently high yields of biaryl **2.4**. Acylation of **2.4** with bromoacetylchloride afforded amide **2.7** in 38% yield. Upon subjecting amide **2.7** to the conditions previously optimized by Magnus *et al*³⁹, none of the desired dienone **2.2** was observed. Instead, a mixture of products were obtained, none of which showed the requisite mass for **2.2** on LCMS or ¹H-NMR shifts corresponding to the dienone (**2.2**)

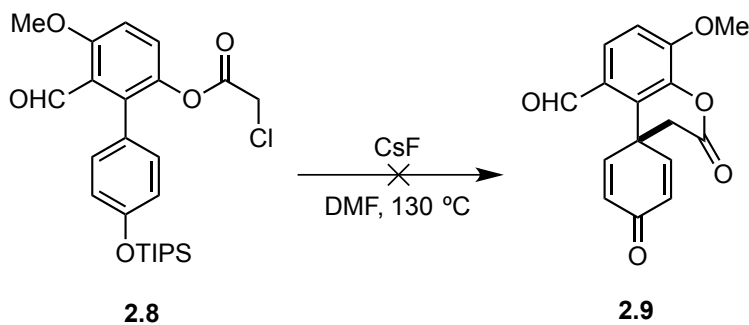
were observed. These results were in alignment with a previous observation in which **2.8** failed to provide dienone **2.9** (Scheme 2.3).⁵⁹ It is hypothesized that the amide resonance rigidified the system by restricting rotation around C-N bond, thus preventing the requisite orbital overlap between the $\sigma^*_{\text{C-Br}}$ and π system required for the reaction to proceed as desired.

Scheme 2.2. Synthesis of Initial Model System



BHT = 2,6-di-*tert*-butyl-4-methylphenol; dppf = 1,1-Bis(diphenylphosphino)ferrocene

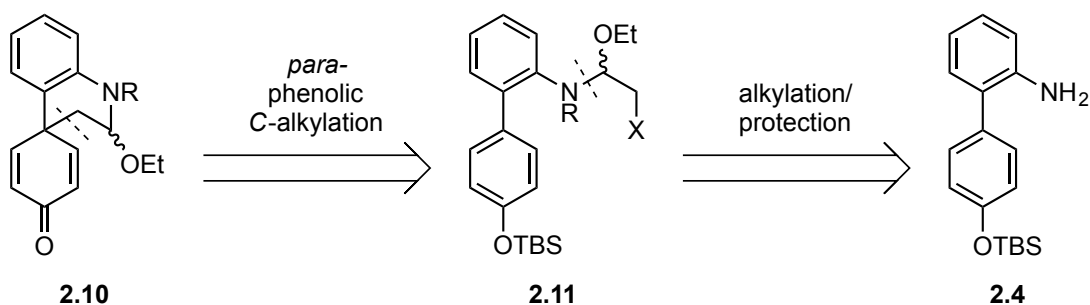
Scheme 2.3. Previous Attempt at Phenolic C-Alkylation



2.1.2.2 Second Generation Model System for *para*-Phenolic C-Alkylation

The model system was then revised to increase the flexibility in the tether to address the proposed issues pertaining to transition state orbital overlap. We envisioned that optimum orbital overlap could be achieved by utilizing the alpha halo hemiaminal ether **2.11** instead of the alpha halo amide **2.7** (Scheme 2.4).

Scheme 2.4. Retrosynthetic Analysis for Revised Biaryl Model System



Before commencing with the synthesis of derivatives of **2.10**, we were aware of several potential issues that needed to be addressed in the model system: 1) hemiaminal ether moieties are known to readily ionize under mild acidic and thermal conditions; and 2) if the nitrogen atom of **2.11** is sufficiently nucleophilic, aziridine formation may occur rapidly and compete with dienone formation. Through previous work, we knew that high temperatures (130 °C, DMF) were needed to induce dienone formation⁵⁹ and that dienone formation does not occur faster than aziridine formation if R = H.⁵⁰ We hypothesized that an inductively withdrawing group appended to the nitrogen atom might mitigate those issues, as long as the protecting group does not allow for additional reaction pathways. Given that amides and carbamates can anchimerically displace alkyl halides, we determined that R = amide or R = carbamate were poor choices. Thus, we decided that R = sulfonamide would meet the stability and reactivity requirements for the model system.

The synthesis of the second generation system commenced with the quantitative protection of biaryl **2.4** with *p*-TsCl to afford **2.12**. The protected biaryl was next alkylated with *in situ* brominated ethyl vinyl ether (**2.15**) to quantitatively afford the hemiaminal ether **2.13**. Upon subjecting hemiaminal ether **2.13** to the conditions developed by Magnus *et al.*,³⁹ the desired dienone **2.14** was obtained in 96% yield (Scheme 2.5). The structure of dienone **2.14** was unambiguously determined by x-ray crystallography (Figure 2.3).

Scheme 2.5. Synthesis of *spiro*-Cyclohexyldienone **2.14**

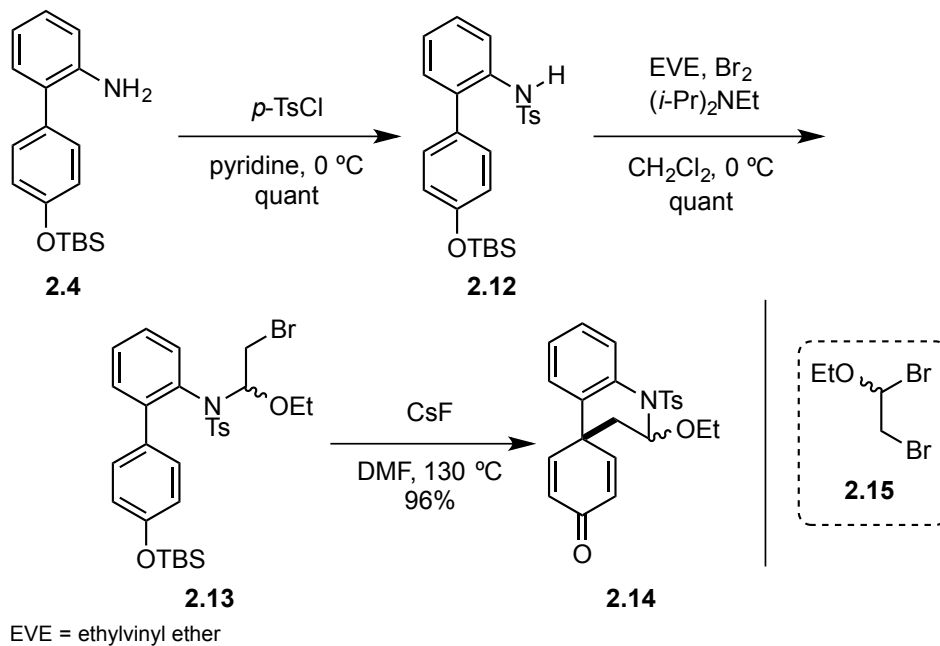
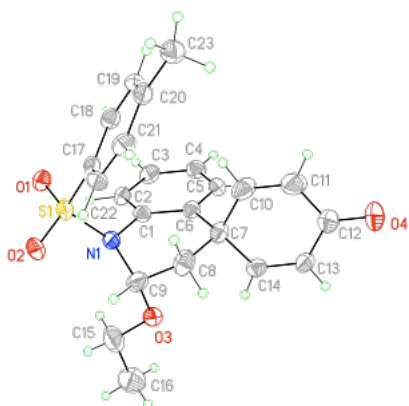


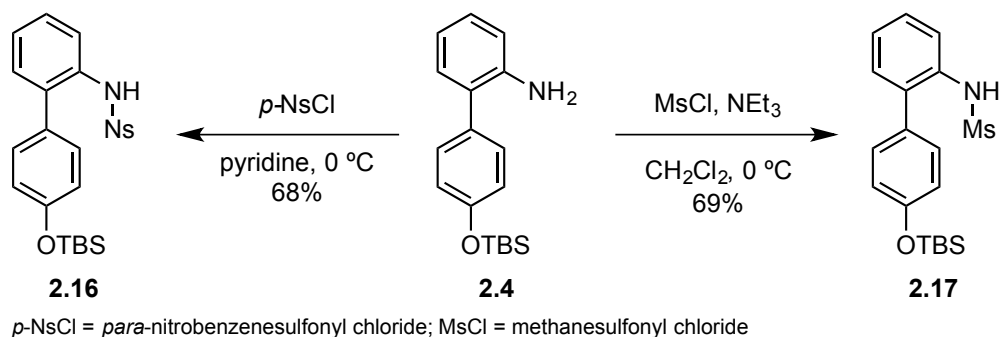
Figure 2.3. Crystal Structure of **2.14**



2.1.2.3 Exploration of Reaction Scope for *para*-Phenolic C-Alkylation

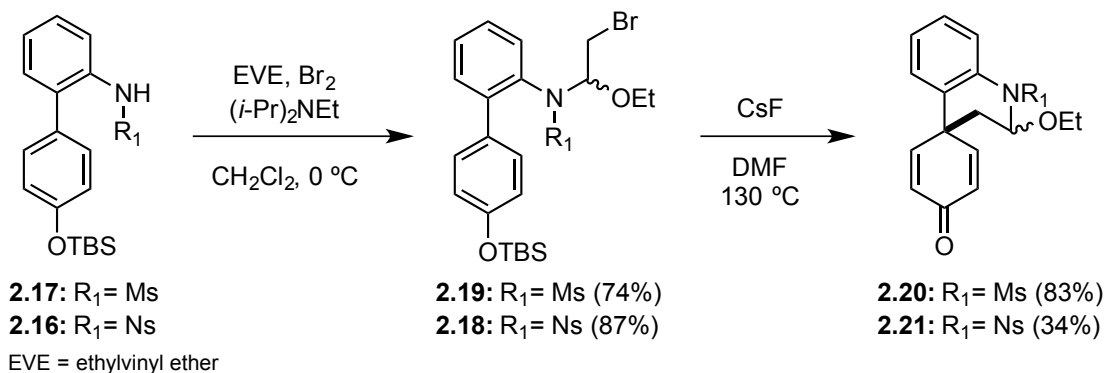
We next sought to explore the scope of the cyclization by exploring other sulfonamide protecting groups. The *para*-nitrobenzenesulfonyl (nosyl) and methanesulfonyl (mesyl) protecting group were appended to biaryl **2.4** to afford **2.16** and **2.17** in 68% and 69% yields, respectively (Scheme 2.6).

Scheme 2.6. Synthesis of Nosyl and Mesyl Protected Anilines



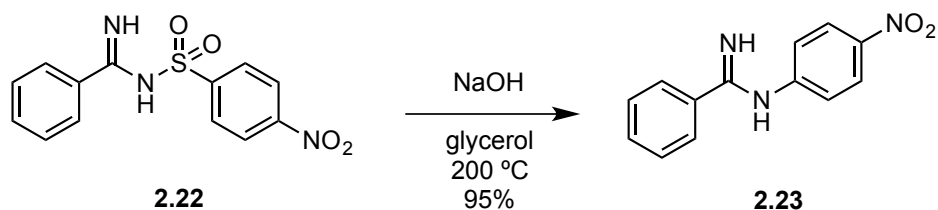
Using our established alkylation conditions, the two sulfonamide protected hemiaminal ethers **2.18** and **2.19** were formed in 87% and 74% yields, respectively (Scheme 2.7). Subjecting compounds **2.18** and **2.19** to CsF/DMF 130 °C afforded dienones **2.21** and **2.20** in 34% and 83% yields, respectively.

Scheme 2.7. Synthesis of Dienones with Varying Sulfonamide Protecting Groups

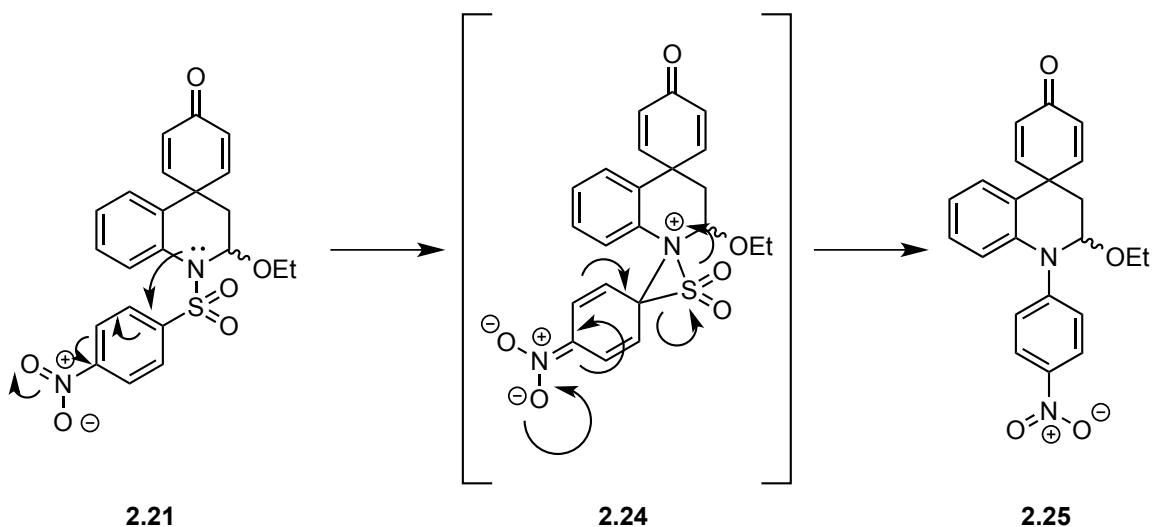


While we were pleased that the mesyl substituted system gave comparable yields to the tosyl substituted system, we were surprised that the nosyl system gave such poor results. Upon LCMS analysis of the crude reaction mixture, masses corresponding to loss of SO₂ were observed. It is known that under basic conditions at elevated temperatures a *para*-nitrobenzenesulfonamide can undergo intramolecular nucleophilic aromatic substitution and decompose to afford the corresponding aniline and an equivalent of SO₂.⁶⁰⁻⁶⁴ For example, Barber reported one of the earliest known examples in which nosyl protected amidine **2.22** could be converted to **2.23** in basic glycerol at 200 °C in 95% yield (Scheme 2.8).⁶⁰ Thus, we hypothesized that dienone **2.21** was not stable to the reaction conditions (CsF, 130 °C DMF), and the poor yield (34%) was due to decomposition of the product. Once the system loses SO₂, the inductively stabilizing effects of the sulfonamide are lost, resulting in further degradation of the system. A proposed mechanism for loss of SO₂ is shown in Scheme 2.9. To test the hypothesis that the product was not stable to the reaction conditions, a small amount of dienone **2.21** was resubjected to the reaction conditions, and rapid loss of SO₂ was observed.

Scheme 2.8. SO₂ Expulsion from Amidine **2.22**

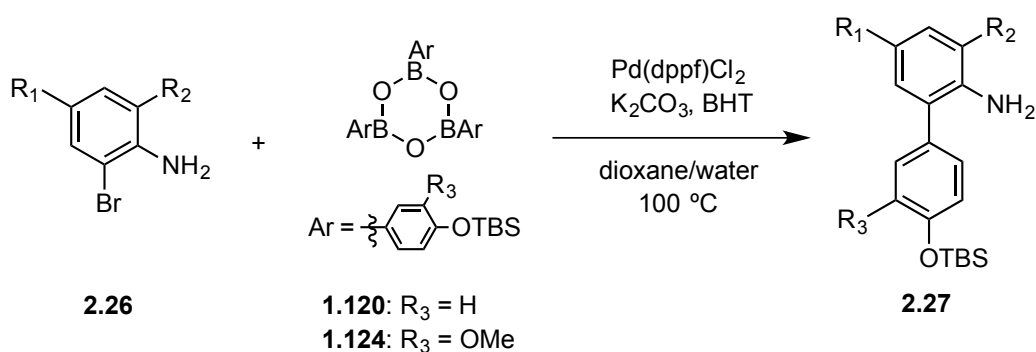


Scheme 2.9. Proposed Mechanism for Thermal Decomposition of **2.21**.



After probing the sensitivity of the reaction to differing sulfonamides, the ability of the system to tolerate substitution on the aniline and phenol moieties was investigated. Starting from the readily available bromoanilines **2.26-d**, the corresponding biaryls **2.27-e** were formed in 59-93% yield employing the same conditions used for substrate **2.4** (Table 2.1).

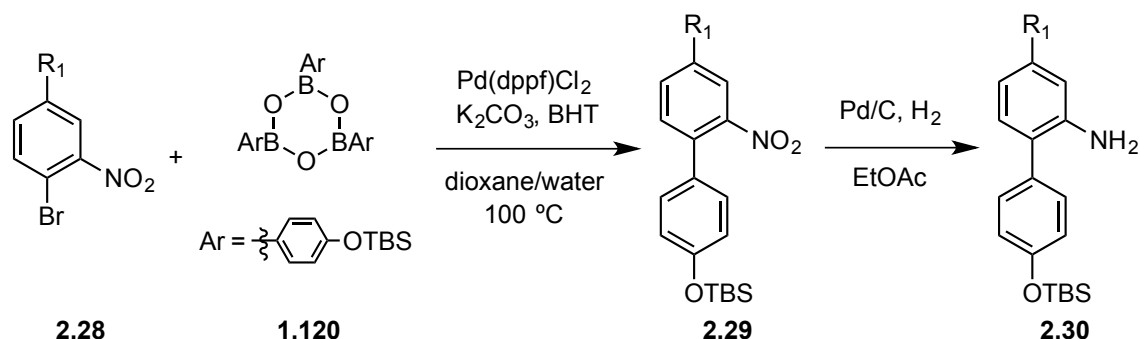
Table 2.1. Synthesis of Substituted Biaryls from Corresponding Anilines



R_1	R_2	R_3	Product	Yield
Me	H	H	2.27a	59%
OMe	H	H	2.27b	93%
Cl	H	H	2.27c	76%
H	OMe	H	2.27d	90%
H	H	OMe	2.27e	80%

BHT = 2,6-di-*tert*-butyl-4-methylphenol
 dppf = 1,1-Bis(diphenylphosphino)ferrocene

Because some of the desired bromoanilines were not readily accessible, bromonitrobenzene derivatives **2.28a** and **2.28b** were used to synthesize biaryls **2.29a** and **2.29b** in 66% and 82% yield, respectively (Table 2.2). During the conversion of **2.28a** to **2.29a**, the corresponding unprotected phenol **2.29c** was isolated in 15% yield. The phenol was subsequently reprotected affording biaryl **2.29a** in quantitative yield. The nitroarenes **2.29a** and **2.29b** were reduced to the corresponding anilines **2.30a** and **2.30b** in 76% and 99% yields, respectively, utilizing catalytic Pd/C under an atmosphere of hydrogen gas.

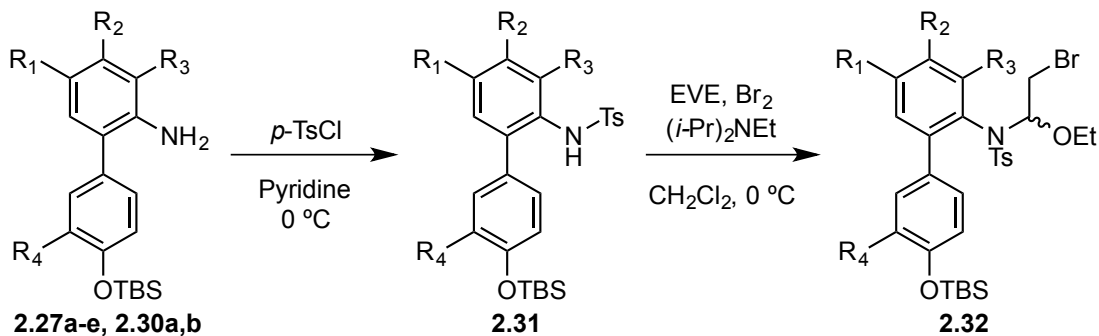
Table 2.2. Synthesis of Substituted Biaryls from Corresponding Nitrobenzenes

R ₁	Product	Yield	R ₁	Product	Yield
Me	2.29a	66% (81%) ^a	Me	2.30a	76%
OMe	2.29b	82%	OMe	2.30b	99%

^aThe free phenol (**2.29c**) was isolated in 15% yield and subsequently quantitatively reprotected

BHT = 2,6-di-*tert*-butyl-4-methylphenol; dppf = 1,1-Bis(diphenylphosphino)ferrocene

The substituted biaryl aniline moieties **2.27a-e** and **2.30a,b** were converted to the tosyl protected hemiaminal ethers **2.31a-g** in high yields over two steps (Table 2.3) with *p*-TsCl/pyridine then EVE/Br₂/*i*-Pr₂NEt.

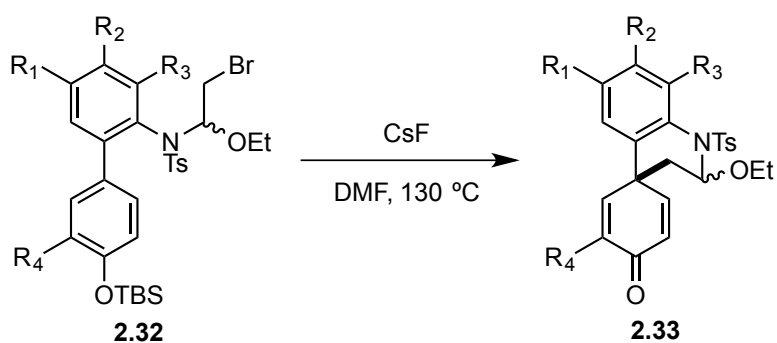
Table 2.3. Synthesis of Substituted Hemiaminal Ethers

R ₁	R ₂	R ₃	R ₄	Product	Yield	R ₁	R ₂	R ₃	R ₄	Product	Yield
Me	H	H	H	2.31a	74%	Me	H	H	H	2.32a	97%
OMe	H	H	H	2.31b	86%	OMe	H	H	H	2.32b	98%
Cl	H	H	H	2.31c	84%	Cl	H	H	H	2.32c	98%
H	OMe	H	H	2.31d	91%	H	OMe	H	H	2.32d	99%
H	Me	H	H	2.31e	96%	H	Me	H	H	2.32e	99%
H	H	OMe	H	2.31f	85%	H	H	OMe	H	2.32f	86%
H	H	H	OMe	2.31g	89%	H	H	H	OMe	2.32g	87%

EVE = ethylvinyl ether

With hemiaminal ethers **2.32a-g** in hand, the desired dienones **2.33a-g** were formed in 89-99% yields upon exposure to CsF at 130 °C, with the exception of hemiaminal ether **2.33f**, which failed to provide dienone **2.33f** (Table 2.4). For dienone **2.33g**, a separable mixture (5:4) of diastereomers was observed, and the relative stereochemistry of the major product was determined via X-ray crystallography.

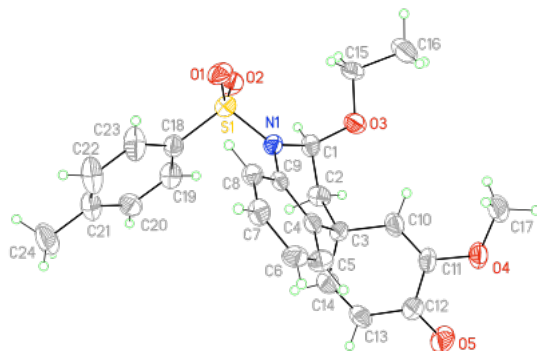
Table 2.4. Synthesis of Differentially Substituted Dienones **2.33**



R ₁	R ₂	R ₃	R ₄	Product	Yield
Me	H	H	H	2.33a	89%
OMe	H	H	H	2.33b	99%
Cl	H	H	H	2.33c	98%
H	OMe	H	H	2.33d	95%
H	Me	H	H	2.33e	98%
H	H	OMe	H	2.33f	0%
H	H	H	OMe	2.33g	91% ^a

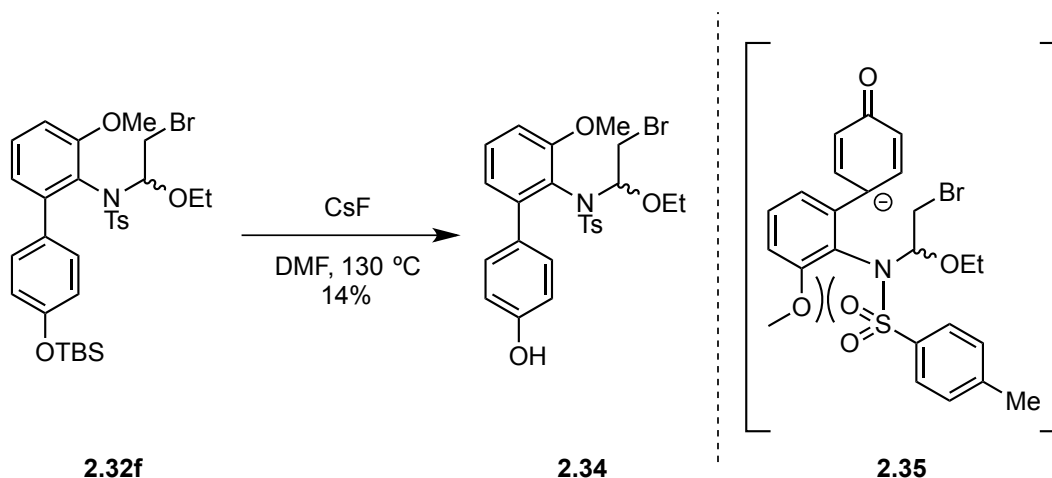
^a5:4 mixture of diastereomers

Figure 2.4. Crystal Structure of *cis*-**2.33g** Diastereomer



We hypothesized that the failure of **2.32f** to form dienone **2.33** was due to an adverse steric interaction in the transition state between the sulfonamide protecting group and the *ortho*-methoxy substituent of the aniline ring (Scheme 2.10). In order for the alkyl bromide to align with the developing negative charge on the phenol, the sulfonamide must eclipse the *ortho*-methoxy substituent, thus increasing the energy of the transition state. All attempts to run the reaction at higher temperatures (CsF/refluxing NMP) afforded only the deprotected phenol **2.34** and unidentified decomposition products.

Scheme 2.10. The *ortho*-Methoxy Substituted System Failed to Form the Desired Dienone

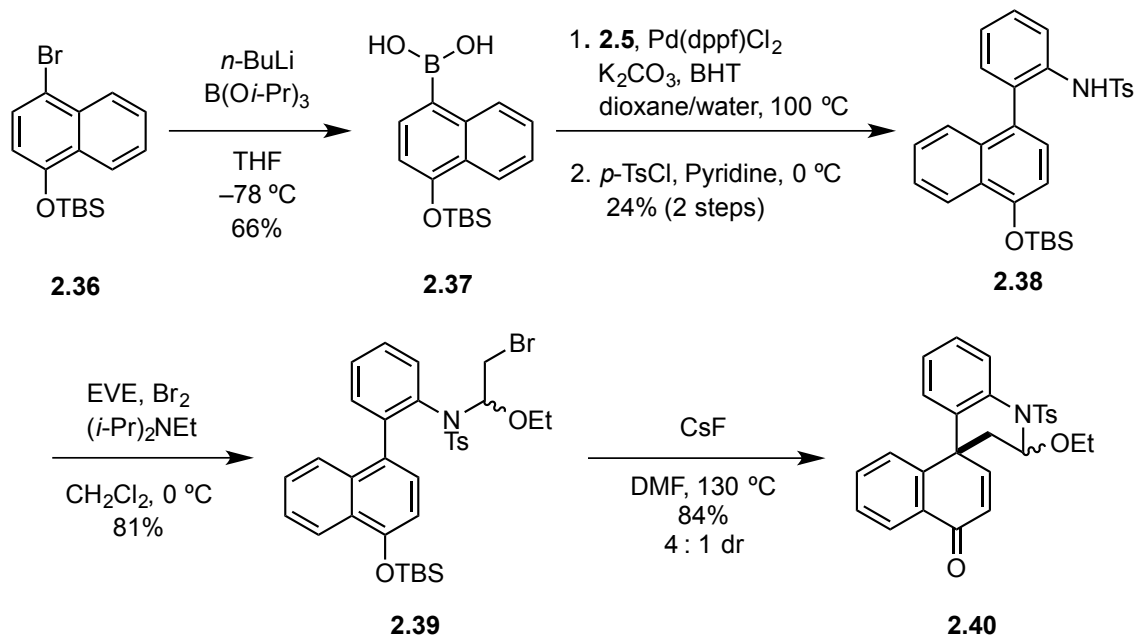


2.1.2.4 Synthesis of Naphthol Derived Dienones

To further investigate the scope of the reaction, derivatives containing a naphthol ring were explored. Beginning with the known silyl protected bromonaphthol **2.36**, the boronic acid was formed in 66% yield via metal-halogen exchange followed by reaction with triisopropyl borate (Scheme 2.11). A Suzuki coupling of **2.37** with 2-bromoaniline (**2.5**) afforded the desired biaryl, yet purification proved to be difficult because the

compound was highly unstable and decomposed readily under ambient conditions. Fortunately, the sulfonamide protected biaryl **2.39** was stable to ambient conditions. Because the biaryl was unstable, the reaction mixture was worked up, and the crude material was used in the next step. By doing so, the protected biaryl **2.38** was isolated in 24% yield over two steps. Alkylation of **2.38** with Br₂/EVE afforded hemiaminal ether **2.39** in 81% yield. Subjecting **2.39** to CsF at 130 °C gave dienone **2.40** in 84% yield as an inseparable mixture (4:1) of diastereomers (Scheme 2.11).

Scheme 2.11. Synthesis of Naphthol Derived Dienone **2.40**

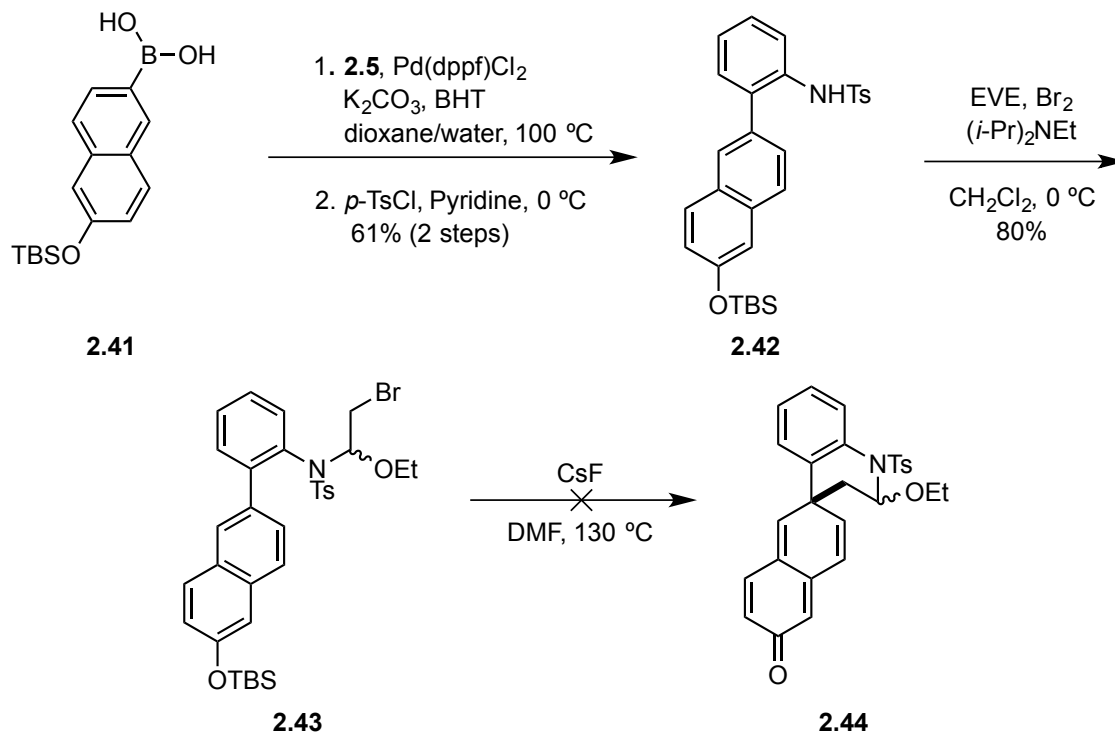


BHT = 2,6-di-*tert*-butyl-4-methylphenol; dppf = 1,1-Bis(diphenylphosphino)ferrocene
 EVE = ethylvinyl ether

Encouraged by the preparation of 1-naphthol derivative **2.40**, efforts were undertaken to perform a *para*-phenolic *C*-alkylation on a 2-naphthol derivative to synthesize the extended dienone **2.44**. A Suzuki coupling of 2-bromoaniline (**2.5**) with the boronic acid **2.41**, followed by sulfonamide formation provided protected biaryl **2.42** in 61% yield over two steps. The hemiaminal ether **2.43** was formed in 80% yield using

the standard alkylation conditions ($\text{Br}_2/\text{EVE}/i\text{-Pr}_2\text{NEt}$). Unfortunately, all attempts to induce cyclization to dienone **2.44** with CsF in DMF at 130 °C afforded an intractable mixture. Lower reaction temperatures resulted in exclusively desilylated starting material, and increased reaction temperatures afforded no observable dienone by LCMS or crude ^1H -NMR analysis. We speculate that the reaction does not proceed as desired because the formation of the requisite anionic intermediate would require completely breaking the aromaticity of the naphthol ring, thus forming a very high-energy transition state.

Scheme 2.12. Attempted Formation of Extended Dienone **2.44**



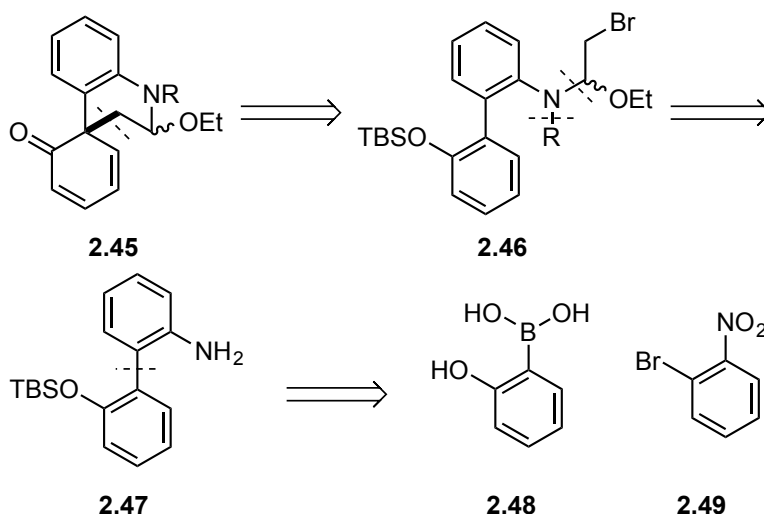
BHT = 2,6-di-*tert*-butyl-4-methylphenol; dppf = 1,1-Bis(diphenylphosphino)ferrocene
 EVE = ethylvinyl ether

2.1.3 Attempted *ortho*- Phenolic C-Alkylation of Aniline Derived Systems

To test whether dienone **2.45** could be synthesized via an *ortho*-phenol C-alkylation, we envisioned employing the system shown in Scheme 2.13. Analogous to the

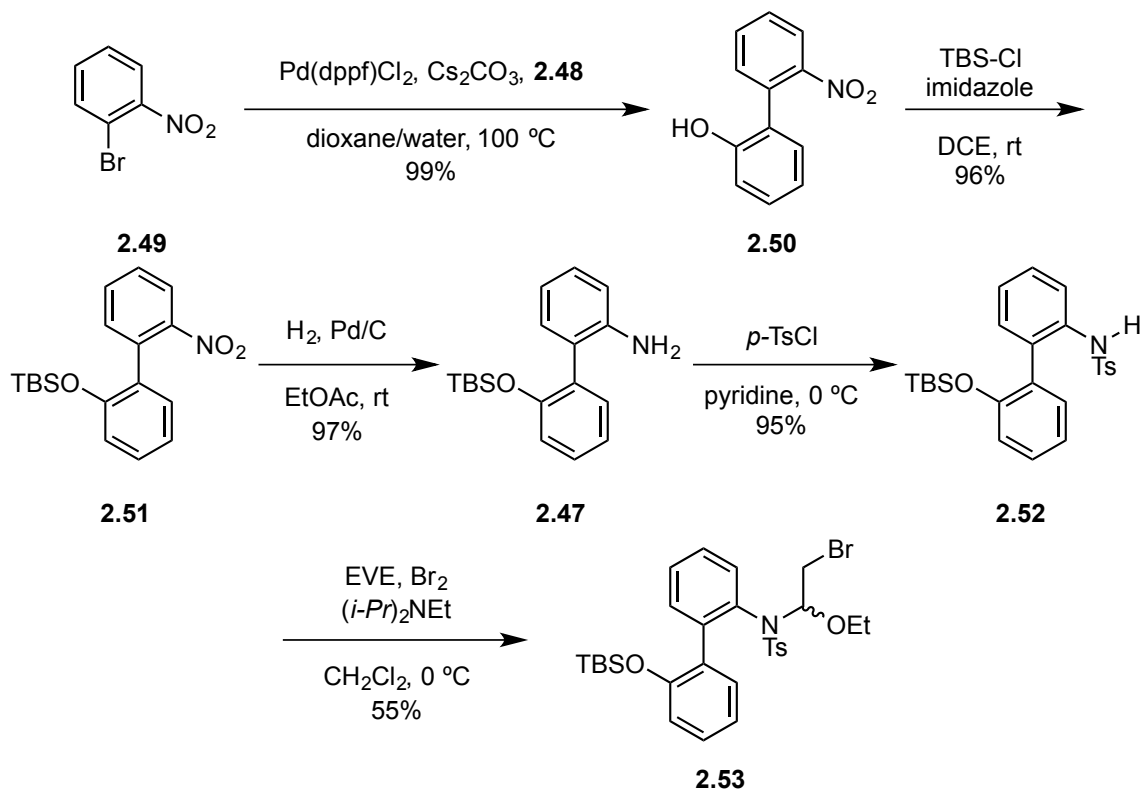
system used for the *para*-phenolic C-alkylation, we believed that commercially available 2-bromonitrobenzene (**2.49**) and 2-hydroxyphenyl boronic acid (**2.48**) would be suitable starting material.

Scheme 2.13. Retrosynthetic Analysis for **2.45**



The synthesis of the **2.45** commenced with a Suzuki coupling between commercially available 2-bromonitrobenzene (**2.49**) and 2-hydroxyphenyl boronic acid (**2.48**) (Scheme 2.14). The previously optimized conditions used to form biaryl **2.4** (Pd(dppf)Cl₂/K₂CO₃) did not work well for this system. Indeed, only ~50% conversion of starting material was observed after 24 h. Fortunately, switching the base from K₂CO₃ to Cs₂CO₃ shortened the reaction time to 6 h and provided the desired biaryl **2.50** in 99% yield. The phenol moiety was then protected as the TBS ether to give **2.51** in 96% yield, which was reduced by catalytic hydrogenation to provide **2.47** in 97% yield. Subsequent sulfonylation of **2.47** afforded sulfonamide **2.52** in 95% yield. The sulfonamide **2.52** was then alkylated with EVE/ Br₂/*i*-Pr₂NEt to give hemiaminal ether **2.53** in 55% yield.

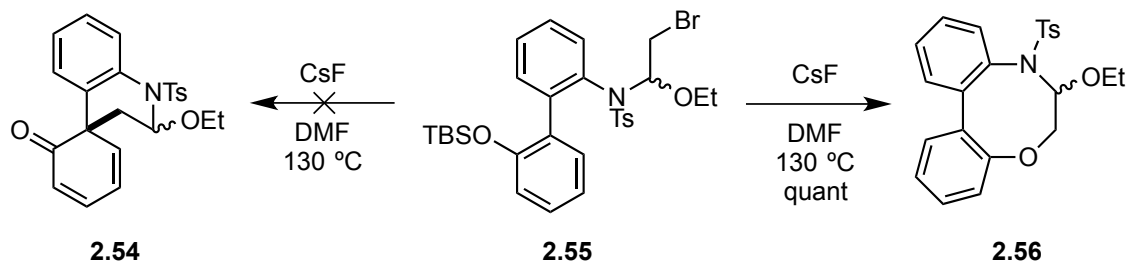
Scheme 2.14. Synthesis of Model System for Attempted *ortho-ortho* Phenolic *c*-Alkylation



EVE = ethylvinyl ether; DCE = 1,2-dichloroethane; dppf = 1,1-Bis(diphenylphosphino)ferrocene

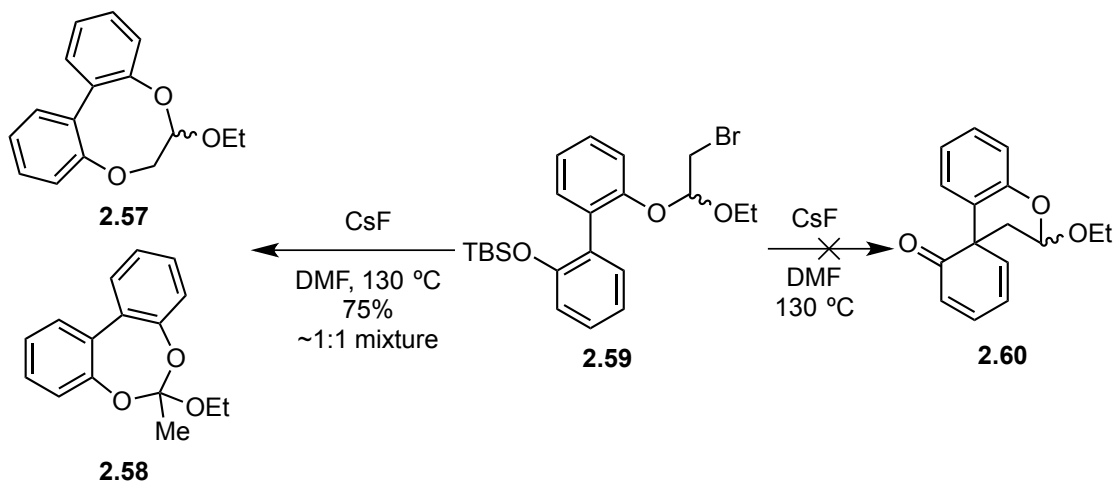
Unfortunately, treatment of **2.53** with CsF at 130 °C failed to afford any of the desired *C*-alkylated product **2.54** (Scheme 2.15). Instead, the *O*-alkylated system **2.56** was isolated in quantitative yield. We hypothesized that the *ortho*-alkylation would require higher energy than the *para*-alkylation, but higher temperatures (CsF/NMP reflux) or classical alkylation conditions (*t*-BuOK/*t*-BuOH) on the phenol failed to provide any of the desired product, as determined by LCMS or NMR analysis of the crude reaction mixtures.

Scheme 2.15. Attempted *ortho*-Phenolic C-Alkylation



While attempts were being made to promote *ortho*-phenolic C-alkylation of an aniline derived system, a colleague, Timothy Hodges, was exploring a similar strategy with a phenol derived model system, and his results were in alignment with mine; none of the desired *ortho*-phenolic C-alkylation was observed (Scheme 2.16).⁵⁷

Scheme 2.16. Attempted *ortho*-Phenolic C-Alkylation by Timothy Hodges

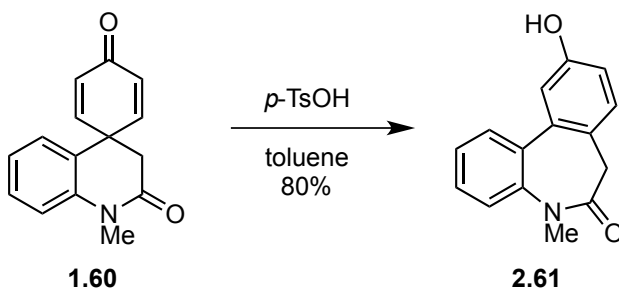


2.2. CHEMOSELECTIVE ADDITION OF OXYGEN NUCLEOPHILES TO *N*-TOSYL HEMIAMINAL ETHERS IN THE PRESENCE OF A DIENONE

2.2.1 Introduction

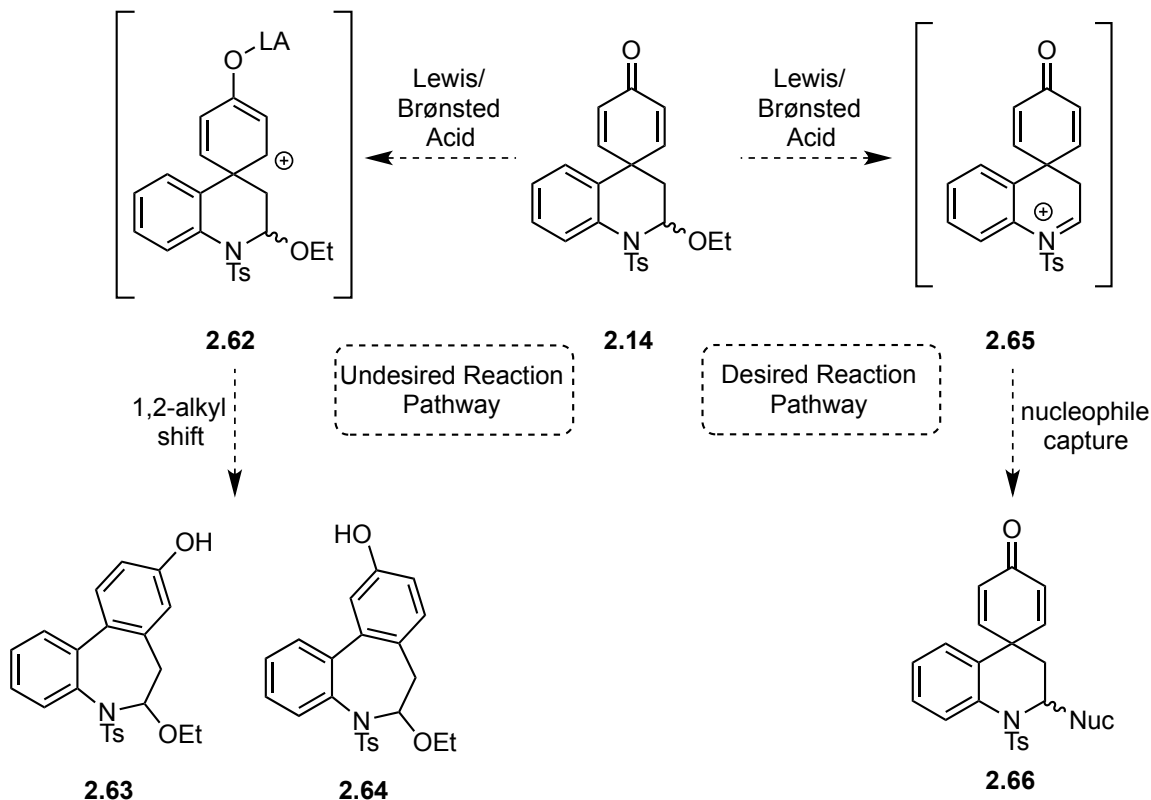
To probe the utility of the *aza*-spirocyclic dienones for the synthesis of natural product and natural product-like compounds, we sought to determine whether the hemiaminal ether moiety of **2.14** could be chemoselectively functionalized in the presence of the dienone moiety. It is well known that cross-conjugated dienones will rearrange to the phenol under acidic conditions.⁶⁵⁻⁶⁸ Indeed, Doris *et al* reported that dienone **1.60** underwent a dienone-phenol rearrangement to give **2.61** under acidic conditions (Scheme 2.17).²⁶

Scheme 2.17. Known Rearrangements of Dienone **1.60**



However, we hypothesized that under mild Lewis or Brønsted acidic conditions hemiaminal ether ionization (Scheme 2.18: **2.14** to **2.65**) would occur more rapidly than dienone phenol rearrangement (Scheme 2.18: **2.14** to **2.63** and **2.64**). If the selective ionization occurred, we further hypothesized that the *N*-tosyliminium species **2.65** would be a more reactive electrophile than the dienone. Thus, we believed various nucleophiles would add chemoselectively into the transiently formed *N*-tosyliminium ion to synthesize compound of the general form **2.66** (Scheme 2.18).

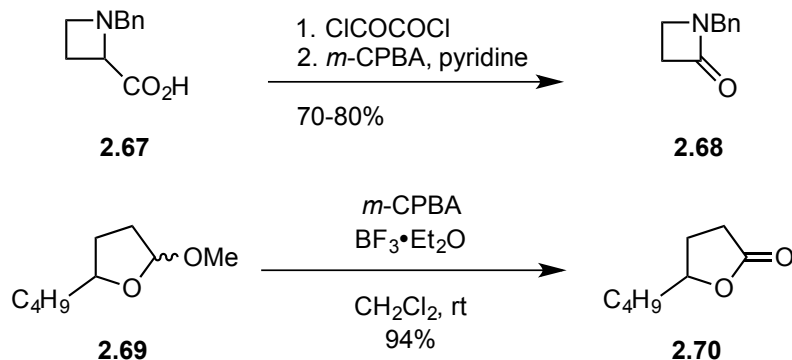
Scheme 2.18. Potential Reaction Pathways for Dienone **2.14**



2.2.2 Addition of Peroxyacids to *N*-Tosyl Hemiaminal Ethers in the Presence of a Dienone

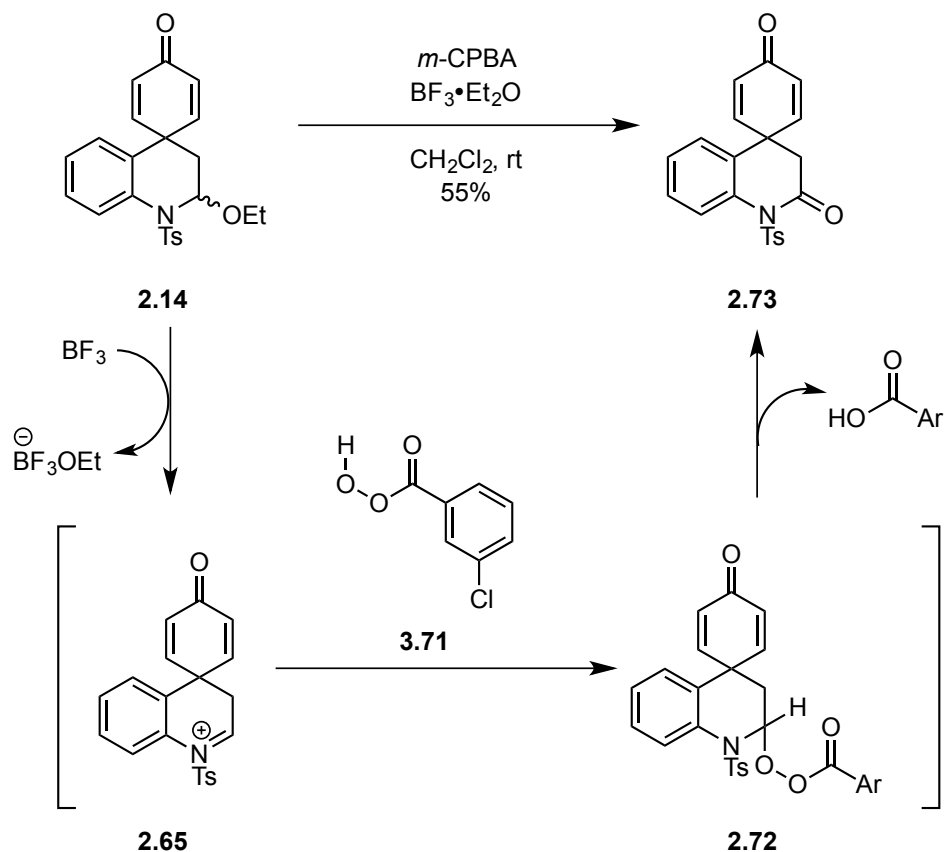
Acetals and iminiums are known to undergo oxidation with *meta*-chloroperoxyacetic acid (*m*-CPBA) to the corresponding lactols and amides.^{69,70} For example, Wasserman *et al* reported that azetidine carboxylic acid **2.67** could be decarboxylated with oxalyl chloride to form an iminium salt, which readily underwent oxidation to the corresponding β -lactam in high yields (Figure 2.5: **2.67** to **2.68**).⁶⁹ Grieco *et al* later reported in 1978 that cyclic acetal **2.69** could be efficiently oxidized to lactone **2.70** in 95% yield (Figure 2.5: **2.69** to **2.70**).

Figure 2.5. Precedent for the conversion of Hemiaminal Ether **2.14** to Amide **2.73**



To test the hypothesis that a nucleophile could add chemoselectively to the transiently formed *N*-tosyliminium ion **2.65**, we sought to oxidize the hemiaminal ether moiety of **2.14** to the corresponding anilide **2.73** (Scheme 2.19). Employing the Lewis acidic conditions published by Grieco *et al*, we found that hemiaminal ether **2.14** underwent facile oxidation to the corresponding anilide **2.73** in 55% yield (Scheme 2.19).⁷⁰ Mechanistically, we envision that BF₃•Et₂O ionized **2.14** to generate *N*-tosyliminium ion **2.65**, and *m*-CPBA (**2.71**) added into **2.65** to form the peroxyaminal **2.72**. Intermediate **2.72** likely undergoes intramolecular deprotonation to afford anilide **2.73** and an equivalent of *meta*-chlorobenzoic acid.

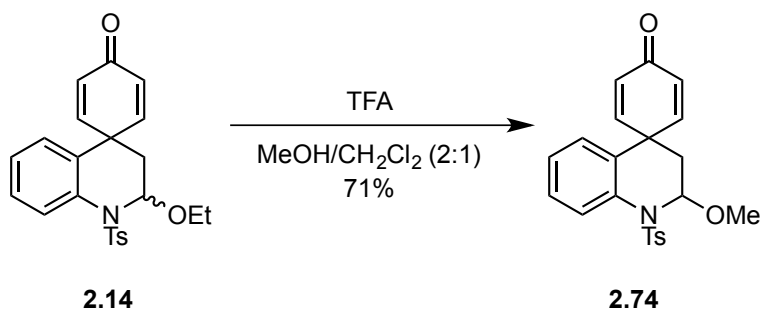
Scheme 2.19. Proposed Mechanism for Formation of Amide **2.73**



2.2.3 Solvolysis of *N*-Tosyl Hemiaminal Ethers in the Presence of a Dienone

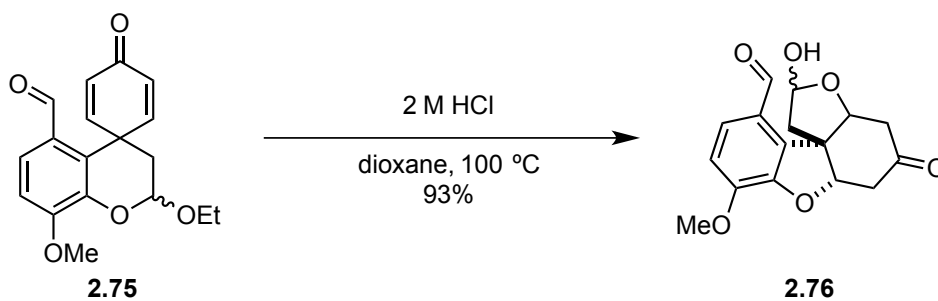
After determining that hemiaminal ether **2.14** could be selectively functionalized under Lewis acidic conditions, several Brønsted acids were screened for their ability to evoke solvolysis of **2.14** with methanol. As expected, mineral acids (H_2SO_4) and *p*-toluenesulphonic acid caused rapid degradation of the dienone to phenolic products, whereas acetic acid returned starting material, even at elevated temperatures. However, trifluoroacetic acid (TFA) afforded the desired product **2.74** in 71% yield (Scheme 2.20).

Scheme 2.20. Solvolysis of Hemiaminal Ether with Methanol



The solvolysis of dienone **2.14** with water was investigated next. In the synthesis of (–)-galanthamine by Magnus *et al*, dienone **2.75** rearranged under aqueous acidic conditions to give lactol **2.76**.³⁹ It was hypothesized that **2.14** would rearrange and hydrate to give a similar lactol.

Scheme 2.21. Rearrangement Observed in the Magnus Synthesis of (–)-Galanthamine³⁹



Dienone **2.14** was subjected to similar conditions to those used by Magnus *et al*, and lactol **2.81** was synthesized in 84% yield (Scheme 2.22). The structure of **2.81** was verified via x-ray crystallography (Figure 2.6). Mechanistically, it is believed that hemiaminal **2.77** is formed first, which would be in equilibrium with aldehyde **2.78**. Compound **2.78** could then undergo an intramolecular conjugate addition to give enone **2.79** that could hydrate to **2.80** and combine with the aldehyde moiety to form **2.81**. We speculate that this rearrangement may prove valuable for the synthesis of indole alkaloids or related compounds.

Scheme 2.22. Proposed Mechanism for Hydrolysis and Rearrangement of Dienone **2.14**

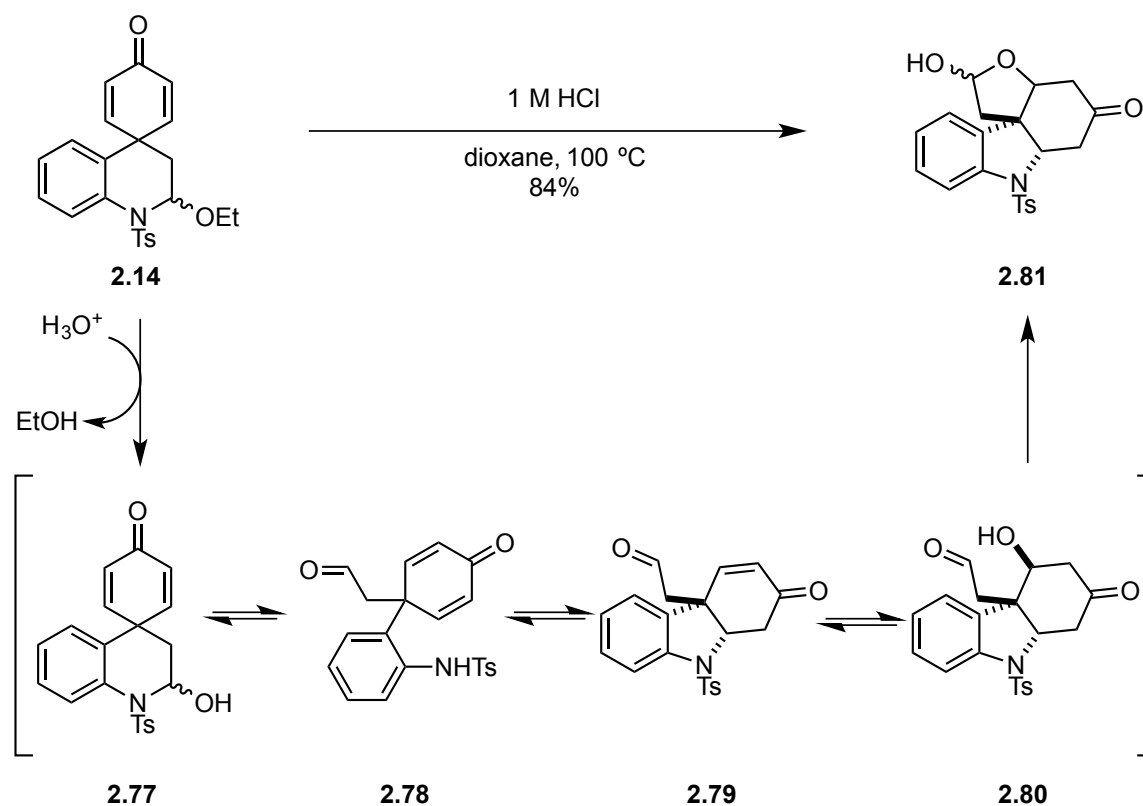
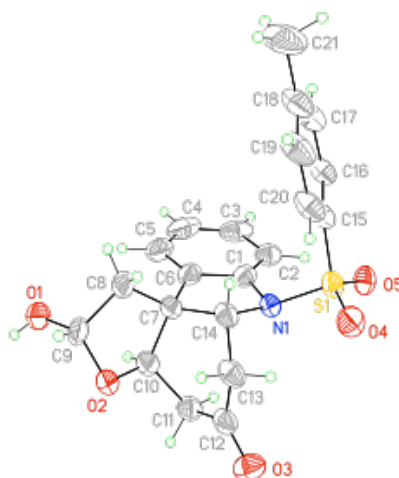


Figure 2.6. Crystal Structure of Lactol **2.81**

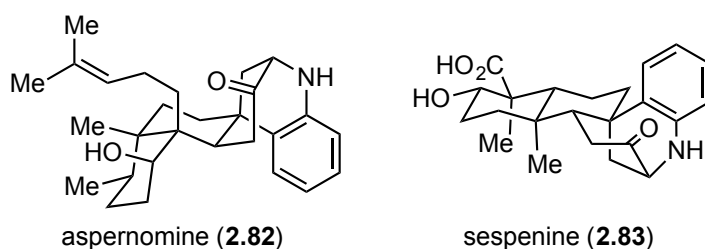


2.3 STUDIES TOWARDS THE SYNTHESIS OF THE *SPIRO*-BICYCLONONANE CORE OF ASPERNOMINE AND SESPENINE

2.3.1 Introduction

The indolosesquiterpenes sespenine (**2.82**) and aspernomine (**2.83**) are secondary metabolites that contain a unique *spiro*-bicyclononane core (Figure 2.7). Aspernomine was first isolated by Staub *et al* in 1992 from the sclerotia of the fungus *Aspergillus nomius* and was found to be cytotoxic against human cancer cell lines and a potent antiinsectan.⁷¹ The related natural product sespenine was first isolated by Ding *et al* in 2011 from a bacterial culture broth of *Streptomyces* sp. HKI0595, an endophyte of the widespread mangrove tree *Kandelia candel*. Sespenine also exhibited potent anti-insectant properties, but it elicited no cytotoxicity in several human cancer cells lines.⁷²

Figure 2.7. The Indolosesquiterpenes Aspernomine (**2.82**) and Sespenine (**2.83**)

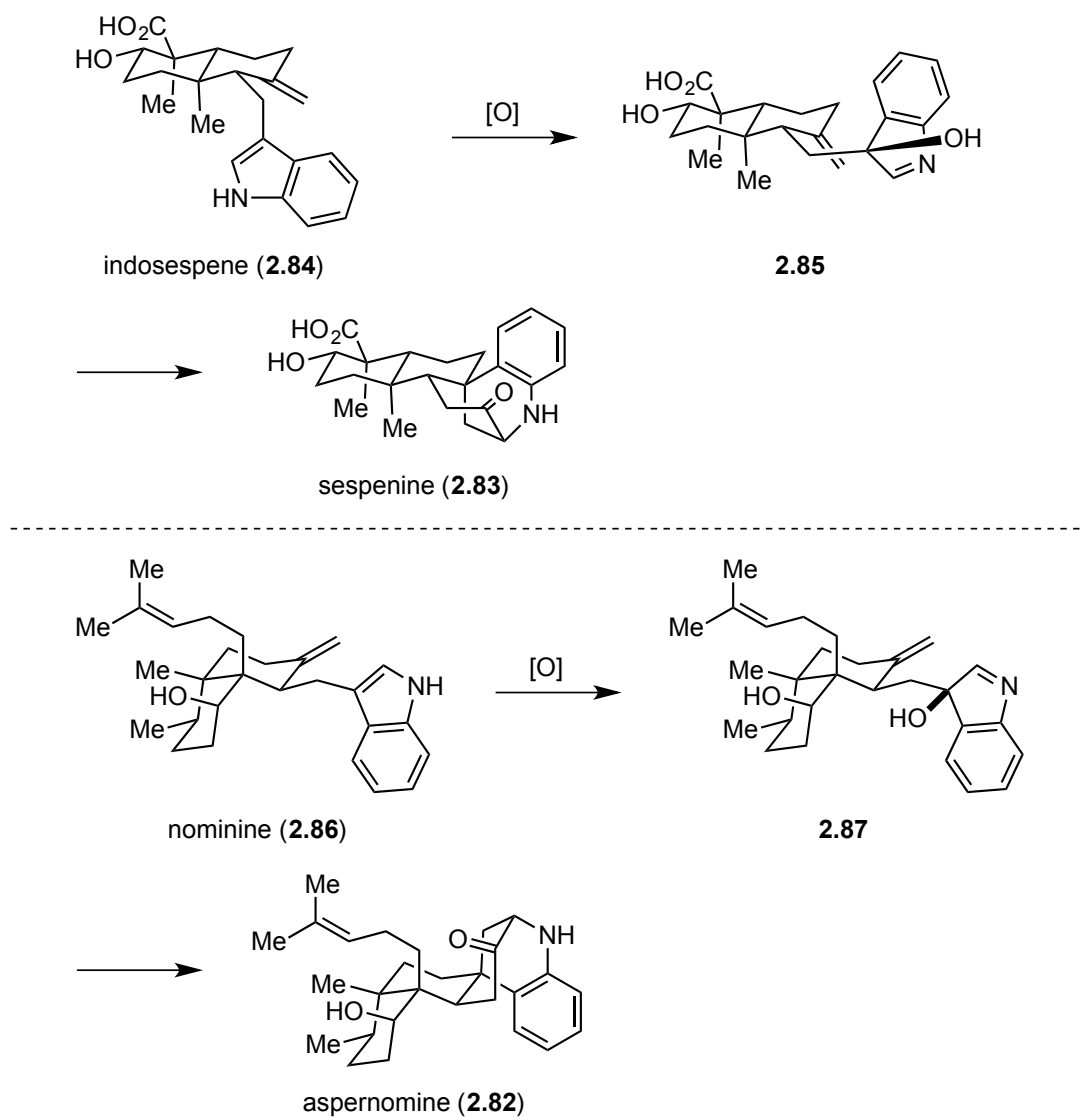


2.3.2 Biosynthesis and Previous Synthetic Efforts Towards the *spiro*-Bicyclononane Core

2.3.2.1 Proposed Biosynthesis of *spiro*-Bicyclononane Core

It has been proposed that the *spiro*-bicyclononane cores of aspernomine and sespenine arise biosynthetically via an oxidative rearrangement of the structurally related indolosesquiterpenes indosespine (**2.84**) and nominine (**2.86**), which were isolated in small quantities from the same fungal and bacterial extracts as aspernomine (**2.82**) and sespenine (**2.83**) (Figure 2.8).^{71,72}

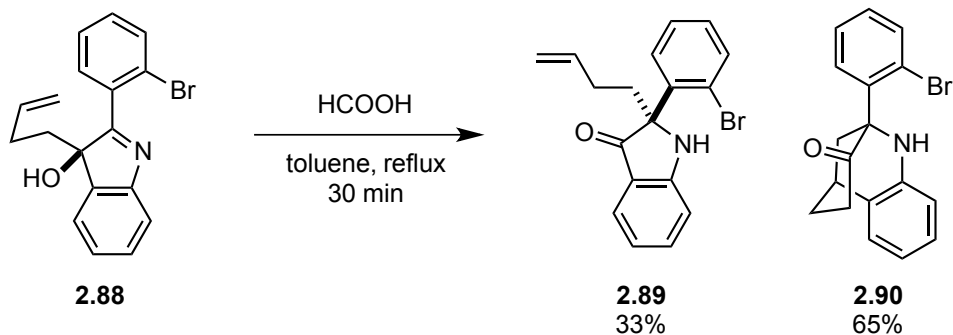
Figure 2.8. Proposed Biosynthesis of Sespentine and Aspernomine



The proposed biosynthesis is supported by both experimental observations and computational studies. In 2003, Liu *et al* observed an unanticipated rearrangement during their synthetic studies towards an unrelated indole alkaloid.⁷³ They found that hydroxyindole **2.88** rearranged to give a mixture (1:2) of **2.89** and compound **2.90** (Scheme 2.23). Through extensive 2D-NMR analysis, it was determined that the structure was strikingly similar to the *spiro*-bicyclononane core of aspernomine and sespenine.

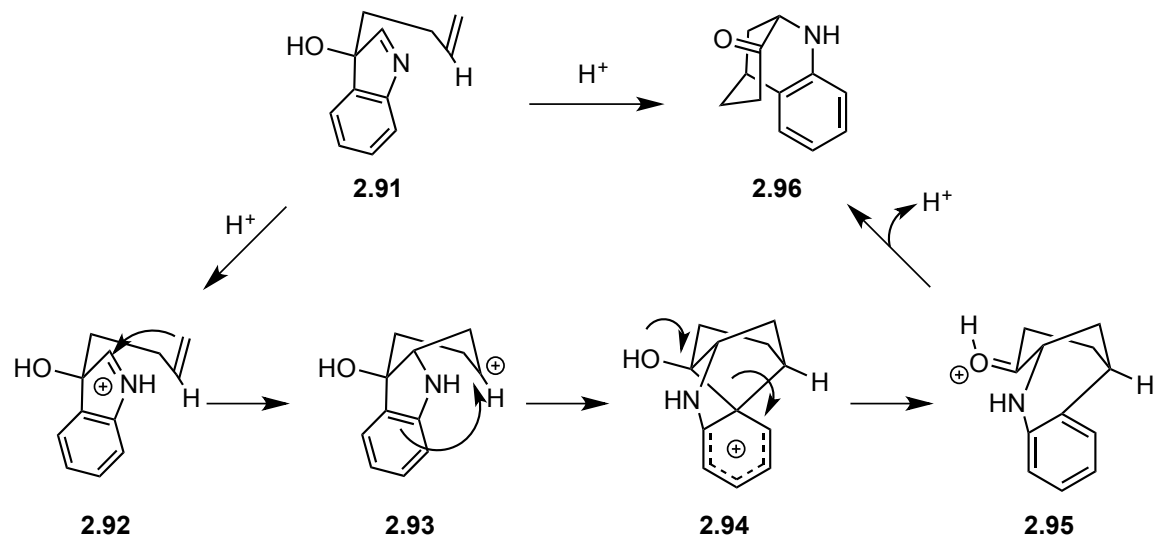
Thus, the authors proposed that a 3-hydroxyindole intermediate is involved in the biosynthesis of the indolosesquiterpenes.

Scheme 2.23. Unexpected Rearrangement Observed of 3-Hydroxyindole Species **2.88**



Mechanistically, it is believed that this transformation proceeds via a boat conformation in which the alkene of **2.92** aligns with the iminium to form a 2° carbocation **2.93** that is stabilized by the proximal aniline moiety, subsequently forming arenium **2.94**. The arenium ion is then quenched via the formation of ketone **2.95** (Scheme 2.24). This mechanism for oxidative rearrangement is supported by quantum chemical calculation in which Tantillo *et al* suggests that the pathway involves a concerted yet asynchronous [4+2] cycloaddition that avoids the formation of a 2° carbocation.⁷⁴

Scheme 2.24. Proposed Mechanism of Oxidative Rearrangement

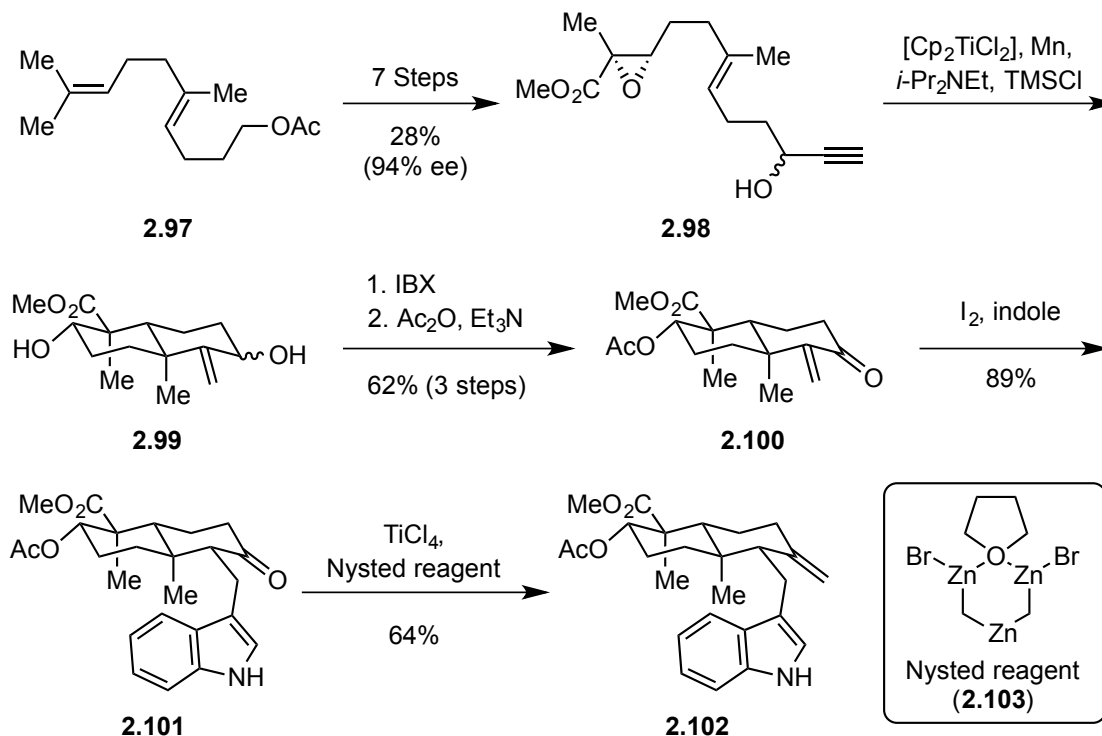


2.3.2.2 Bioinspired Total Synthesis of Sespentine

When our investigations of these natural products began in 2012, there were no published syntheses of either aspernomine or sespentine. However, in 2014, Sun *et al* published the first total synthesis of sespentine in which they performed a bioinspired oxidative carbocation rearrangement to form the *spiro*-bicyclononane core of **2.83** in a manner analogous to the proposed biosynthetic rearrangement (Scheme 2.24, **2.91** to **2.96**).⁷⁵ As of this writing, the related natural product aspernomine has not been synthesized.

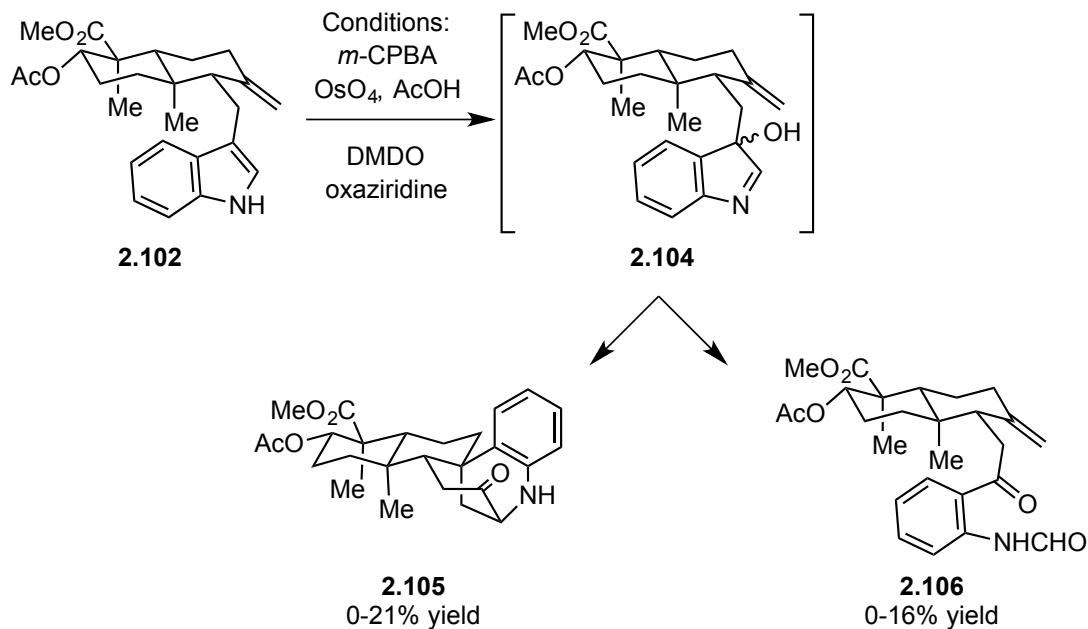
Sun's total synthesis of sespentine started with the known alkene **2.97**, which was converted to propargyl alcohol **2.98** in seven steps (Scheme 2.25). Compound **2.98** underwent a radical cyclization using $[Cp_2TiCl_2]$ and Mn^0 to afford decalin system **2.99**. Subsequent oxidation and alcohol protection afforded enone **2.100** in 62% yield over three steps. A conjugate addition of indole to **2.100** under mild conditions provided **2.101** in 89% yield. Olefination of **2.101** using $TiCl_4$ /Nysted reagent (Scheme 2.25, **2.103**) provided the desired olefin **2.102** in 64% yield.

Scheme 2.25. Synthesis of Precursor to Oxidative Rearrangement



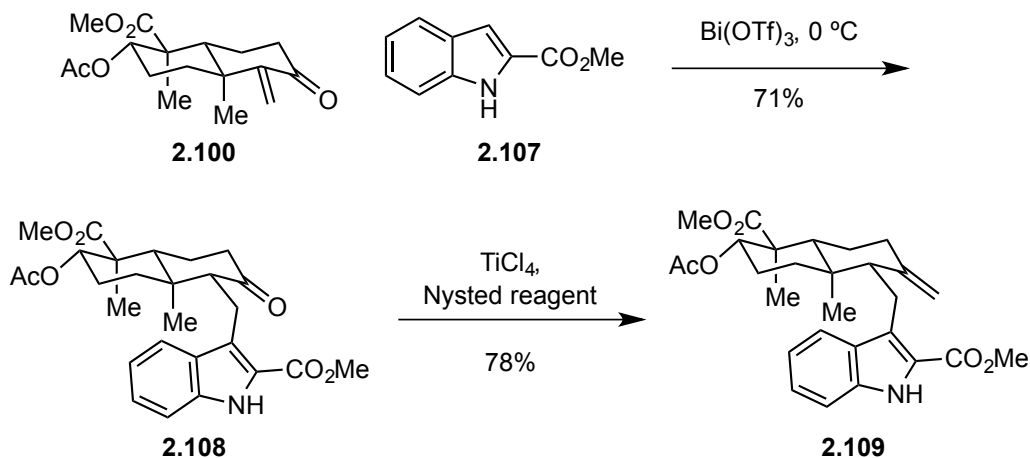
With **2.102** in hand, a large number of oxidants were screened with the intention of optimizing the formation of **2.105**. However, **2.105** was isolated only in 0-21% yield, and in several instances the over oxidized product **2.106** (0-16% yield) was isolated (Scheme 2.26). The authors speculated that the 3-hydroxyindole intermediate **2.104** that forms upon initial oxidation of the indole moiety was highly unstable and readily underwent undesired reaction pathways such as over oxidation and rearrangement to compounds other than the desired product **2.105**. Thus, they proposed that the conversion of **2.102** to **2.105** would proceed more efficiently if the 3-hydroxyindole intermediate **2.104** were stabilized with an electron withdrawing group at the 2-position.

Scheme 2.26. Attempted Oxidative Rearrangement



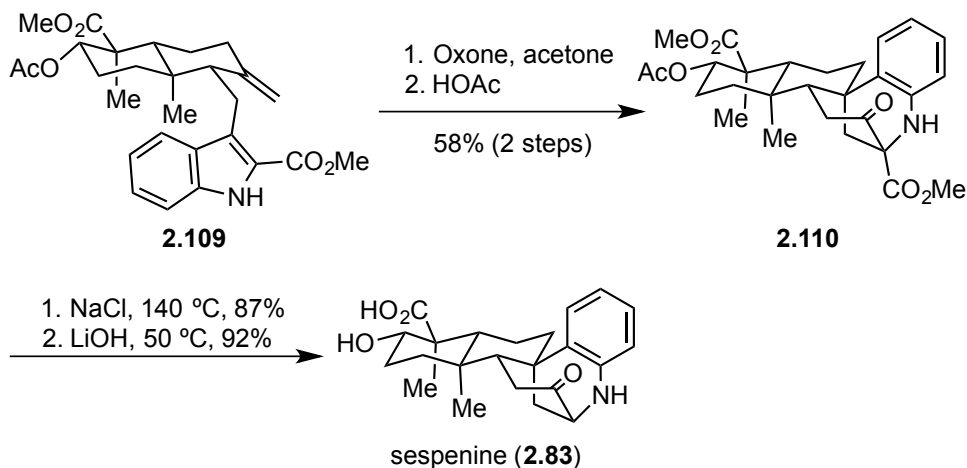
To stabilize the 3-hydroxyindole intermediate **2.104**, Sun and coworkers utilized indole 2-methyl ester **2.107** in lieu of indole. Using slightly modified conditions, Bi(OTf)₃ catalyzed the 1,4-addition of **2.107** to afford **2.108** in 71% yield. Subsequent olefination of **2.108** with Nysted reagent provided olefin **2.109** in 78% yield (Scheme 2.27).

Scheme 2.27. Revised Approach Utilizing Indole Methyl Ester **2.107**



Subjecting the modified system to oxidation with oxone/acetone provided the 3-hydroxyindole species as a stable mixture of diastereomers that readily converged to the desired *spiro*-bicyclonone system **2.110** present in the natural product in 58% yield over two steps (Scheme 2.28). A Krapcho-demethoxycarbonylation of **2.110** followed by saponification of the ester and acetyl moieties afforded that natural product sespenine (**2.83**) in high yields.

Scheme 2.28. Successful Oxidative Rearrangement and Completion of the Natural Product



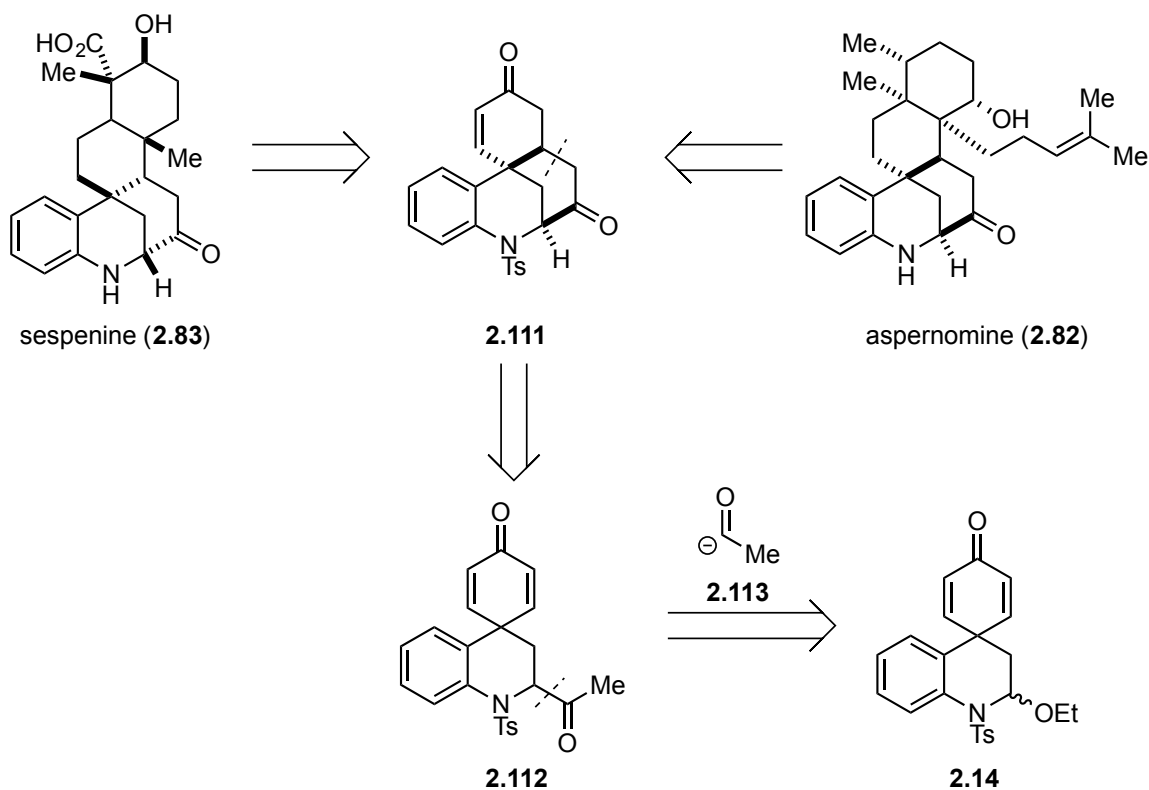
In summary, sespenine (**2.83**) was formed in 21 steps from commercially available material. Employing a radical cyclization, the authors formed the decalin system, and a bioinspired oxidative carbocation rearrangement synthesized the *spiro*-bicyclononane core. Due to the *spiro*-bicyclononane core being formed last, this synthesis could not be used to access the related natural product aspernomine. Thus, we propose that a synthetic strategy in which the *spiro*-bicyclonone core is formed first would allow for a divergent synthesis of both natural products.

2.3.3 Synthetic Efforts Towards the Synthesis of Aspernomine and Sespenine

2.3.3.1 Retrosynthetic Analysis of the spiro-Bicyclononane Core

In our analysis of the synthetic challenges posed by sespenine (**2.83**) and aspernomine (**2.82**), we hypothesized that the tetracyclic compound **2.111** could serve as a divergent intermediate (Scheme 2.29). We envisioned that **2.111** could arise from an intramolecular conjugate addition of ketone **2.112**, which could be synthesized from dienone **2.14** via addition of an acyl anion (**2.113**) equivalent to an *N*-tosyliminium ion that would be formed *in situ*.

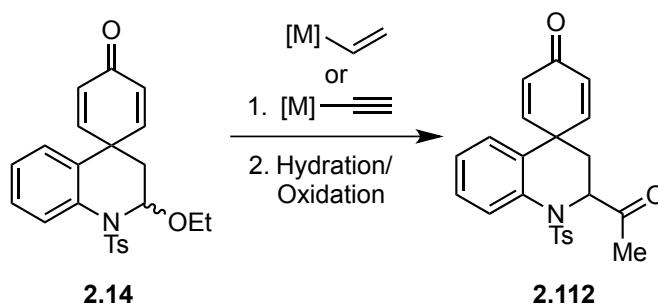
Scheme 2.29. Retrosynthetic Analysis of Sespenine and Aspernomine



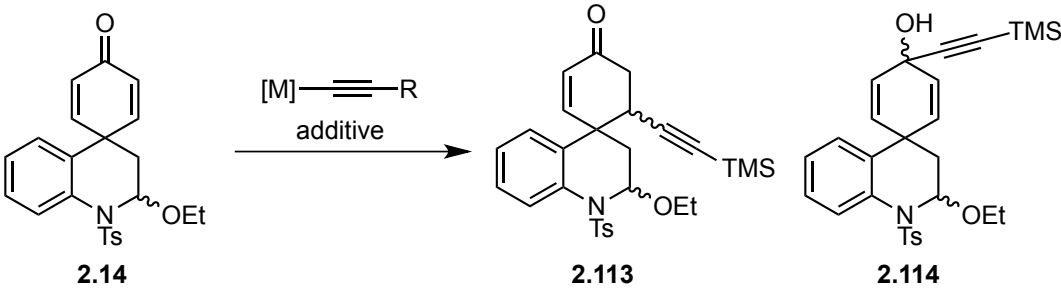
2.3.3.2 Initial Strategy for Addition of Acyl Anion Equivalent

Our strategy to form ketone **2.112** involved nucleophilic addition of a two-carbon unit to the iminium ion generated from dienone **2.14**, which could be either oxidized (in the case of an alkene) or hydrated (in the case of an alkyne) to afford the desired ketone (Scheme 2.30).

Scheme 2.30. Initial Strategy for Installation of Acyl Anion Equivalent



Initial attempts to form the desired alkyne adduct with lithium and sodium acetylides resulted in exclusively 1,2-addition to the enone (Table 2.5, entries 1 and 2). In order for a chemoselective addition to the acetal to occur, we envisioned that the carbon nucleophile must be mild enough to not react with the dienone, yet reactive enough to add into the *N*-tosyl iminium ion. It was then determined that less reactive metal species were needed because we wanted the nucleophile to react exclusively with the transiently formed iminium ion. Subsequent attempts using a zinc acetylide, formed either stoichiometrically with *n*-BuLi and ZnCl₂, or catalytically with ZnOTf₂ and (*i*-Pr)₂NEt, afforded primarily 1,4-addition products (Table 2.5, entries 3).

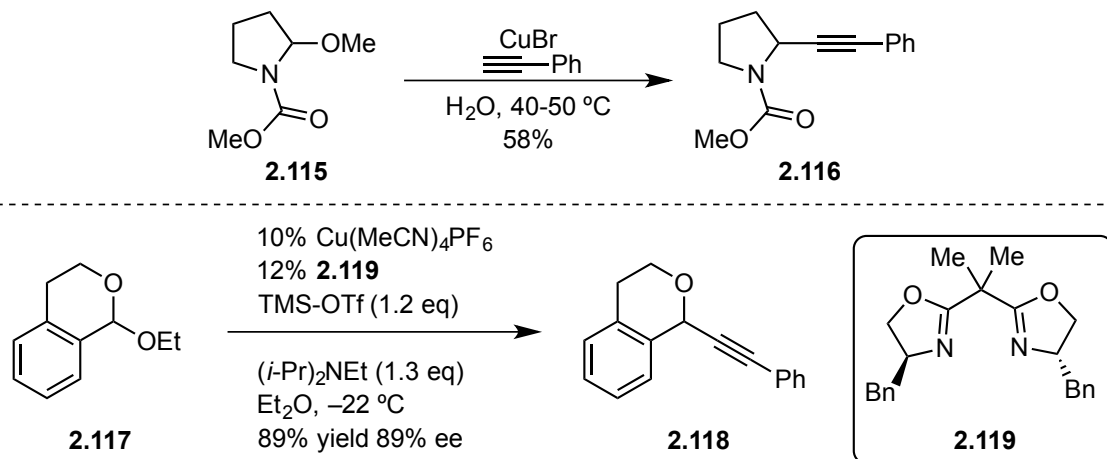
Table 2.5. Li, Na, and Zn Acetylide Addition to Dienone **2.14**

Entry	[M]	Additive	R	Temp	Solvent	Product
1	Li	None	TMS	-78 °C → 0 °C	THF	2.114
2	Na	None	H	-78 °C	THF	2.114
3	Zn	None	TMS	0 °C	CH ₂ Cl ₂	2.113

Thinking that an even milder metal acetylide species might be needed, copper acetylides were explored. It was found that the copper acetylide species formed with CuBr and *i*-Pr₂NEt did not react with dienone **2.14** at room temperature; however, upon heating the reaction 1,4-addition (**2.114**) was observed (Table 2.6, entries 1 and 2). This result was particularly disheartening given a report by Zhang *et al* in which a copper acetylide added to hemiaminal ether **2.115** (Figure 2.9).⁷⁶ In a different report, Watson *et al* found that copper acetylides can add enantioselectively to isochroman acetals (**2.117**) when Lewis acid co-catalysts were employed (Figure 2.9).⁷⁷ Unfortunately, only 1,4-addition was observed when the Lewis acids BF₃•OEt₂ and TMS-OTf were used as co-catalysts (Table 2.6, entries 3 and 4).

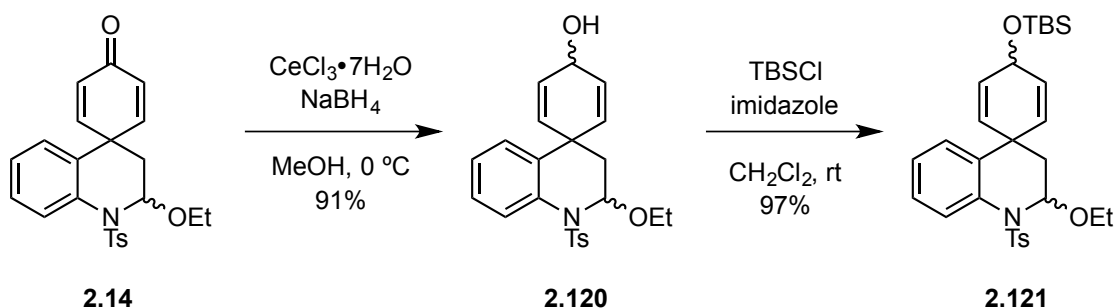
Table 2.6. Cu Acetylide Addition to Dienone **2.14**

Entry	[M]	Additive	R	Temp	Solvent	Product
1	Cu	None	TMS	rt	CH ₂ Cl ₂	no RXN
2	Cu	None	TMS	reflux	DCE	2.113
3	Cu	BF ₃ •OEt ₂	TMS	0 °C → rt	CH ₂ Cl ₂	2.113
4	Cu	TMS-OTf/ (<i>i</i> -Pr) ₂ NEt	TMS	0 °C → rt	CH ₂ Cl ₂	2.113

Figure 2.9. Copper Acetylide Addition to Hemiaminal Ethers and Acetals

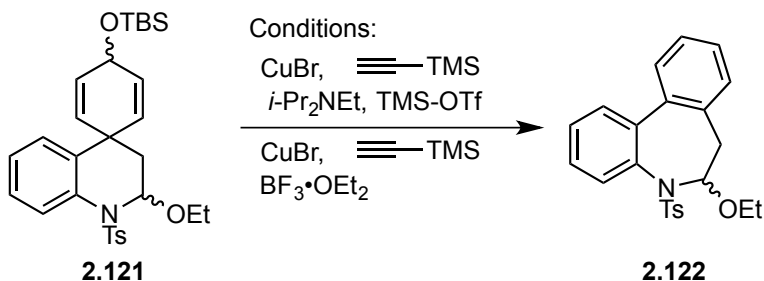
At this juncture, we reasoned that blocking the reactivity of the dienone via a Luche reduction might allow for nucleophilic addition to the hemiaminal ether. Using CeCl₃•7H₂O/NaBH₄/MeOH, dienone **2.14** was reduced to alcohol **2.120** in 91% yield.⁷⁸ The double allylic alcohol **2.120** was subsequently protected as the silyl ether to afford **2.121** in 97% yield (Scheme 2.31).

Scheme 2.31. Synthesis of Protected Allylic Alcohol **2.121**



Unfortunately, it was found that **2.121** was much less stable than dienone **2.14** and rapidly ionized under Lewis acidic conditions. When **2.121** was subjected to identical conditions used previously $\text{CuBr}/i\text{-Pr}_2\text{NEt}/\text{TMS-OTf}$ or $\text{CuBr}/i\text{-Pr}_2\text{NEt}/\text{BF}_3 \cdot \text{OEt}_2$, **2.121** rapidly degraded to **2.122**. Because **2.121** showed poor stability, it was determined that this approach should not be pursued further.

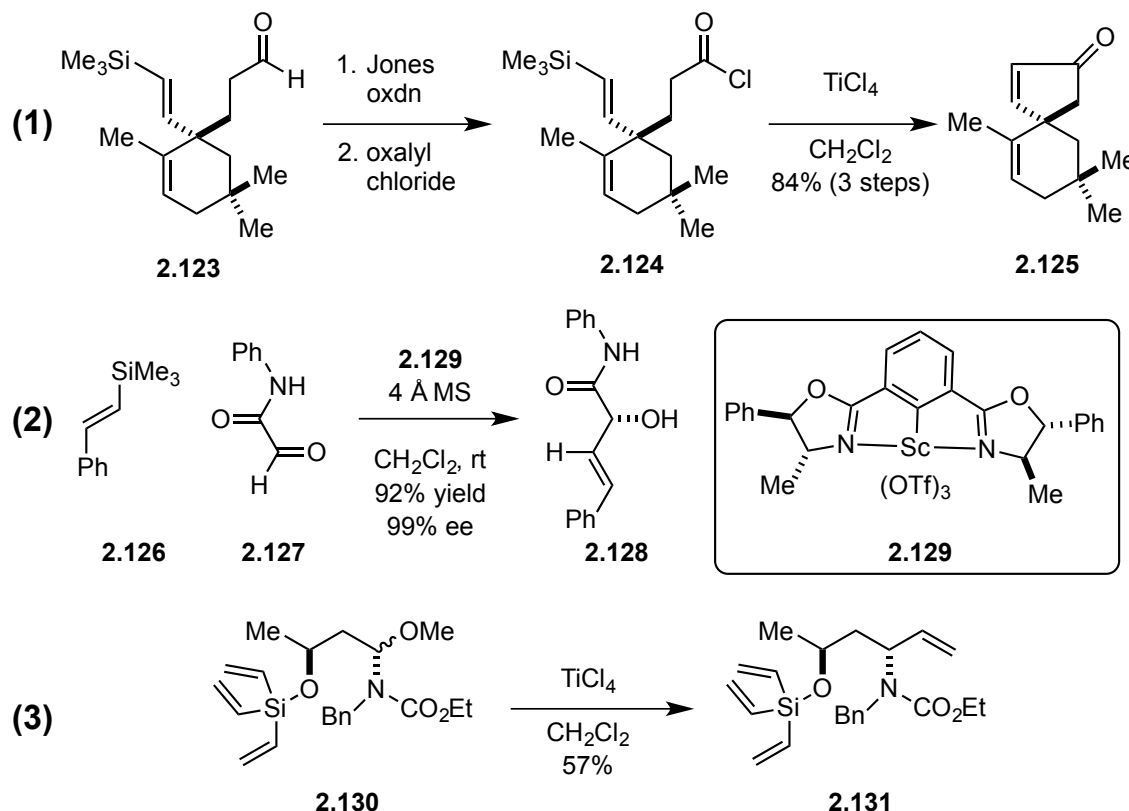
Scheme 2.32. Protected Allylic Alcohol Undergoes Rapid Degradation



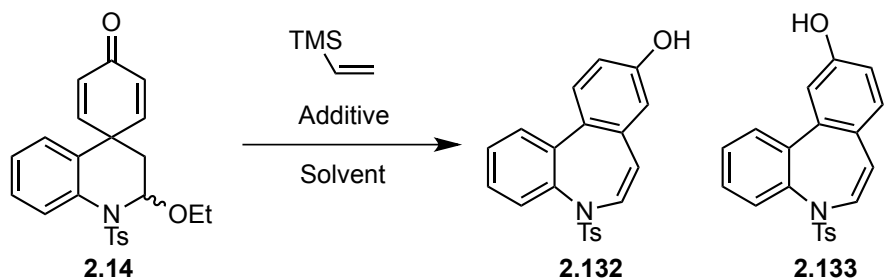
While efforts were being undertaken to add metal acetylides into hemiaminal ether **2.14**, we were concurrently investigating vinyl nucleophiles as an alternative. The addition of vinylsilanes to iminiums and other highly reactive electrophiles is well preceded (Figure 2.10).⁷⁹⁻⁸¹ For example, as an intermediate in the synthesis of (\pm)-quadron, Burke *et al* formed cyclopentenone **2.125** via an intramolecular vinylsilane addition (Figure 2.10, entry 1).⁸² Evans *et al* have also reported an enantioselective intermolecular vinyl silane addition using the chiral scandium catalyst **2.129** (Figure 2.10,

entry 2),³¹ and in a report by Hioki *et al*, they perform an intramolecular vinylsilane addition to a hemiaminal ether using TiCl_4 as a Lewis acid catalyst (Scheme 2.10, entry 3).

Figure 2.10. Examples of Inter- and Intramolecular Vinylsilane Additions

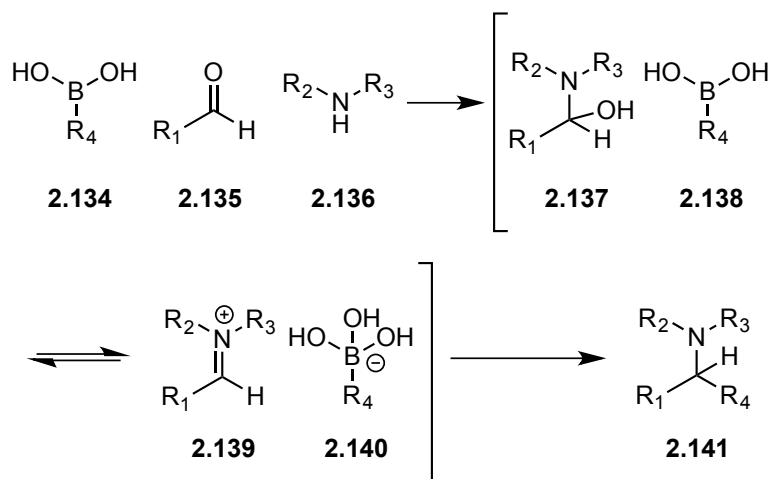


Several attempts to convert **2.14** to the vinyl adduct were unsuccessful (Table 2.7). For example, when vinyltrimethylsilane was combined with dienone **2.14** in the presence of $\text{BF}_3 \cdot \text{OEt}_2$, degradation of starting material to **2.132** and **2.133** was observed (Table 2.7, entry 1). The same results were obtained when the vinylsilane reagent was used as the solvent for the reaction (Table 2.7, entry 2). When trifluoroacetic acid was used in lieu of $\text{BF}_3 \cdot \text{OEt}_2$, starting material was recovered due to the Brønsted acid induced degradation of the vinyltrimethylsilane (Table 2.7, entry 3).

Table 2.7. Attempted Addition of Vinyltrimethylsilane


Entry	Additive	Temperature	Solvent	Product
1	BF ₃ •OEt ₂	rt	CH ₂ Cl ₂	2.132 and 2.133
2	BF ₃ •OEt ₂	rt	None	2.132 and 2.133
3	CF ₃ CO ₂ H	rt	CH ₂ Cl ₂	No RXN

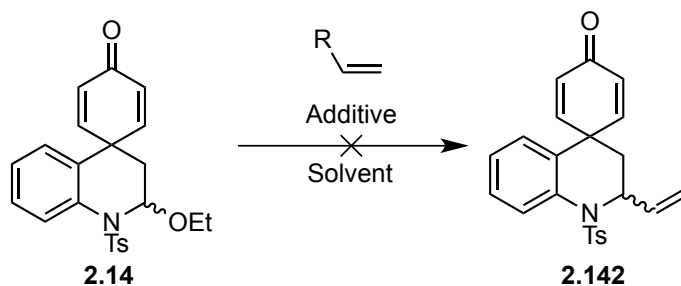
The Petasis borono-Mannich reaction is a well-studied multicomponent reaction in which an aldehyde, amine, and boronic acid combine to form highly substituted amine (Scheme 2.33).⁸³

Scheme 2.33. General Mechanism for Petasis Borono-Mannich Reaction

We envisioned that a boronic acid or ester might ionize the hemiaminal ether **2.14** to form the *N*-tosyliminium ion, which would in turn react with the boronate to form the desired adduct. Unfortunately, vinyl boroxine and vinyl potassium trifluoroborate did not react with the system, returning mostly starting material at elevated temperature (Table

2.8). After these results, it was hypothesized that the boronic esters used (vinyl boroxine/pyridine complex and vinyl potassium trifluoroborate) were not Lewis acidic enough to ionize the hemiaminal ether.

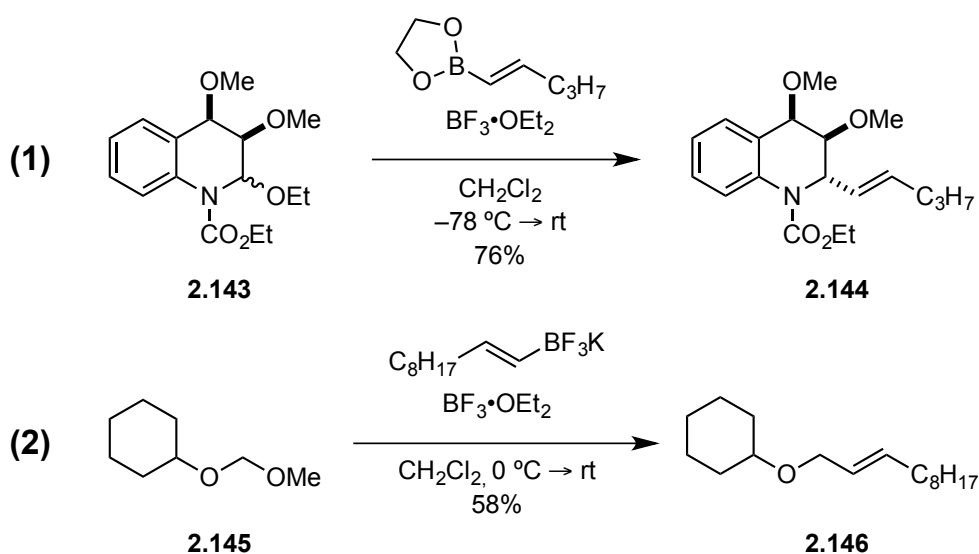
Table 2.8. Failed Attempts to Form Alkene Adduct **2.142**



Entry	Additive	R	Temperature	Solvent	Product
1	none	Boroxine•pyridine	rt → reflux	DCE	No RXN
2	none	Boroxine•pyridine	rt → reflux	MeCN	No RXN
3	none	BF ₃ K	rt → reflux	DCE	No RXN
4	none	BF ₃ K	rt → reflux	MeCN	No RXN

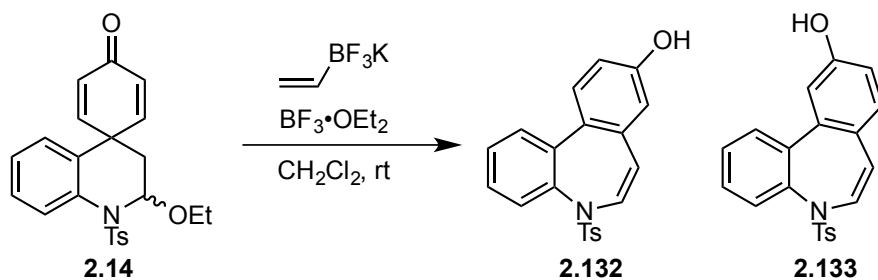
There have been numerous reports of reactions of boronic acids with acetals.⁸³ Although in some cases, additional Lewis acids are required to activate the system to nucleophilic attack (Figure 2.11). In both cases, BF₃•OEt₂ was added to make the reaction proceed.^{84,85}

Figure 2.11. Vinyl Borate Addition to Acetals



When **2.14** was combined with vinyl potassium trifluoroborate and $\text{BF}_3 \cdot \text{OEt}_2$, none of the desired alkene adduct was obtained (Scheme 2.34). Instead, products resulting from dienone-phenol rearrangement were observed. These experiments suggest vinyl boronic acid addition is slower than dienone-phenol rearrangement. Given that none of the desired product was observed for any of these transformations, we began to pursue other strategies for forming C-C bonds.

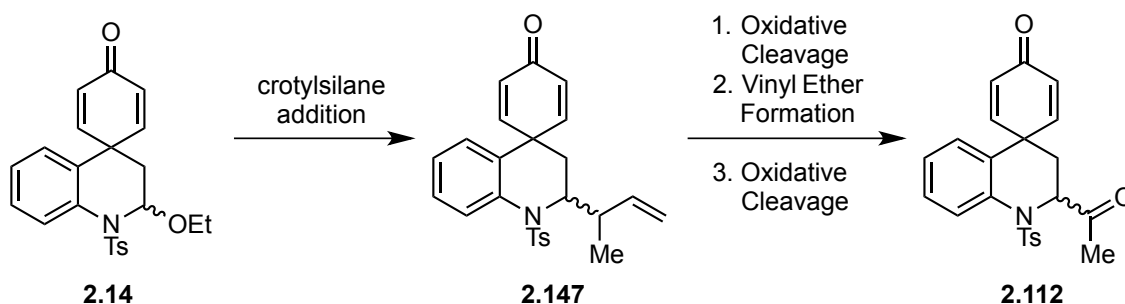
Scheme 2.34. Attempted Lewis Acid Catalyzed Petasis Reaction



2.3.3.3 Revised Strategy for Addition of Acyl Anion Equivalent

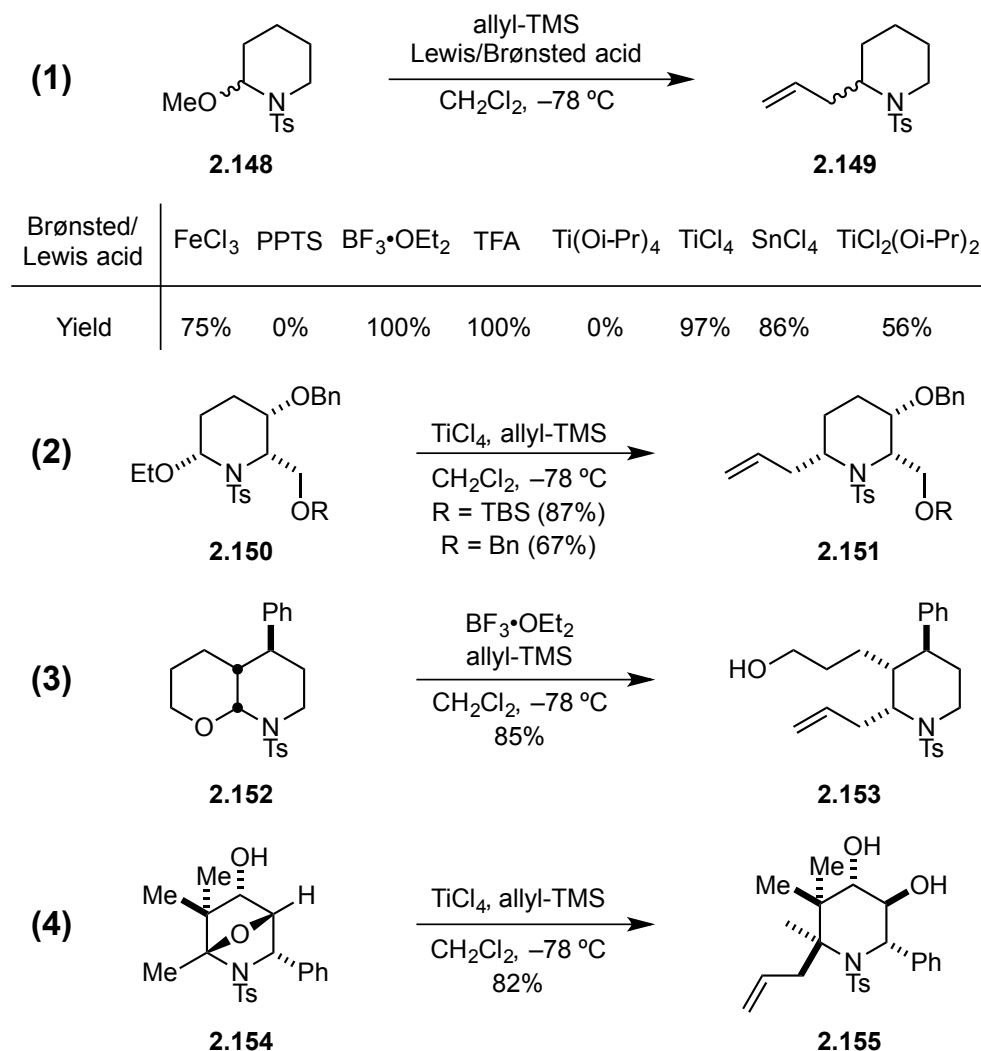
At this juncture, we then envisioned that the addition of a three carbon crotyl group to hemiaminal ether **2.14** could give terminal alkene (**2.147**), which could be converted to ketone **2.112** via successive oxidative cleavages (Scheme 2.35).

Scheme 2.35. Revised Strategy for Installation of Acyl Anion Equivalent



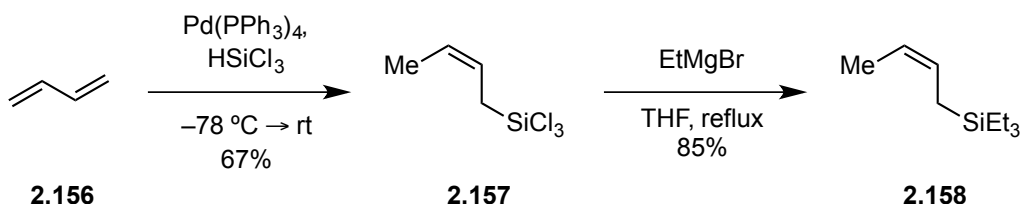
There are numerous examples in the literature for the addition of an allylsilane to an imine or an *N*-tosyl hemiaminal ether (Figure 2.12).⁸⁶⁻⁹¹ In a report by Somfai *et al*, it was found that TMS allylsilane added readily and efficiently to hemiaminal ether **2.148** in the presence of several different Lewis acid catalysts (Figure 2.12, entry 1).⁸⁶ This transformation was later employed by Zhou *et al* in the synthesis of (+)-desoxoprosophylline⁸⁸ and by Haroutounian *et al* in their approach to the synthesis of alkaloid lipids (Figure 2.12, entry 2).⁸⁷ The bicyclic hemiaminal ether **2.152** was also shown to react stereospecifically with TMS allylsilane under strong Lewis acidic conditions (Figure 2.12, entry 3). More recently, the oxa-bridged piperidine system **2.154** was combined with TMS allylsilane in a stereospecific manner to afford highly substituted piperidine systems (Figure 2.12, entry 4).

Figure 2.12. Precedent for Addition of Allyltrimethylsilane to Cyclic *N*-Tosyl Hemiaminal Ether



The synthesis of the crotylsilane began via palladium catalyzed hydrosilation of butadiene (**2.156**) with trichlorosilane to afford (*Z*)-trichlorocrotyl silane (**2.157**) in 67% yield. Trichlorosilane **2.157** was subsequently converted to (*Z*)-triethylcrotylsilane **2.158** in 85% yield on multigram scale by reacting with ethylmagnesium bromide (Scheme 2.36).⁹² The (*Z*)-isomer was chosen because the materials used to make it were readily available at the time; we envision that the (*E*)-isomer could be used as well.

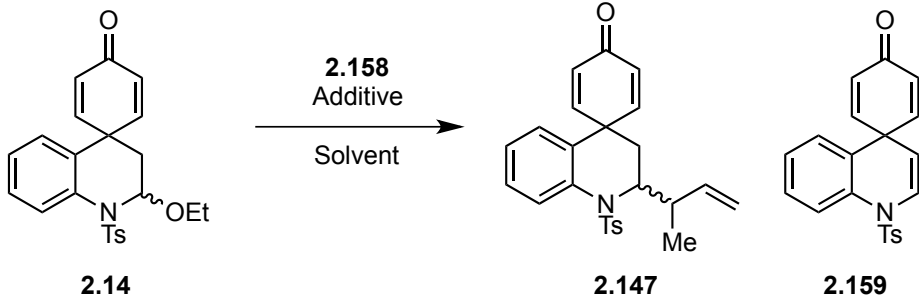
Scheme 2.36. Synthesis of (Z)-Crotylsilane **2.158**



With crotylsilane **2.158** in hand, reaction conditions for addition to hemiaminal ether **2.14** were screened. In analogy with the prior art (Figure 2.12), titanium tetrachloride, trifluoroacetic acid, and boron trifluoride etherate were evaluated for their ability to induce addition of crotylsilane to **2.14** (Table 2.9). Even at reduced temperatures ($-78\text{ }^\circ\text{C}$), rapid and complete degradation of the starting material was observed when TiCl_4 was used as a Lewis acid. The Brønsted acid TFA did afford the desired crotyl adduct **2.147**, but only as the minor product. The major product **2.159** arose from elimination to the *N*-tosylenamine (Table 2.9, entry 2). The Lewis acid $\text{BF}_3 \cdot \text{OEt}_2$ gave the best results, and although no elimination product was observed, starting material was not completely consumed (Table 2.9, entry 3). In fact, the reaction gave rather inconsistent results, with yields ranging from 30-89%. We hypothesized that the presumptive *N*-tosyliminium ion was highly destabilized; thus a more polar solvent would stabilize the transiently formed *N*-tosyl iminium ion and accelerate the rate of the reaction. In the event, switching the solvent from dichloromethane to acetonitrile improved the transformation dramatically. The product distribution for the transformation employing TFA switched from 1:4 to 1:1 in favor of crotyl adduct **2.147** (Table 2.9, entry 4). When $\text{BF}_3 \cdot \text{OEt}_2$ was used at room temperature, complete conversion of starting material was observed, and **2.147** was isolated in 83% yield (Table 2.9, entry 5). Upon further experimentation, we found that reducing the reaction temperature to $0\text{ }^\circ\text{C}$ afforded **2.147** in slightly higher yields (92%) (Table 2.9, entry 6). Due to poor solubility of **2.14**

in acetonitrile, temperatures colder than 0 °C were not explored. Finally, the optimized conditions were determined to be two equivalents $\text{BF}_3 \cdot \text{OEt}_2$ and two equivalents of triethylcrotylsilane **2.158**. The reaction proceeded quantitatively on a 100 mg scale and gave comparable yields on a gram scale (97%) (Table 2.9, entries 7 and 8).

Table 2.9. Optimization of Crotylsilane Addition

						
<div style="display: flex; justify-content: space-around; align-items: center;"> <div style="text-align: center;"> 2.14 </div> <div style="text-align: center;"> 2.147 </div> <div style="text-align: center;"> 2.159 </div> </div>						
Entry	Additive	eq 2.158	Temp	Solvent	Yield	Product
1	1.1 eq TiCl_4	5.0	−78 °C	CH_2Cl_2	100%	decomposition
2	5 eq TFA	3.0	rt	CH_2Cl_2	100%	2.147 : 2.159 (1:4)
3	3-5 eq $\text{BF}_3 \cdot \text{OEt}_2$	3-5	rt	CH_2Cl_2	30-89%	2.147
4	5 eq TFA	3	rt	MeCN	~70%	2.147 : 2.159 (1:1)
5	1.1 eq $\text{BF}_3 \cdot \text{OEt}_2$	1.5	rt	MeCN	83%	2.147
6	1.1 eq $\text{BF}_3 \cdot \text{OEt}_2$	1.5	0 °C	MeCN	92%	2.147
7	2.0 eq $\text{BF}_3 \cdot \text{OEt}_2$	2.0	0 °C	MeCN	quant ¹	2.147
8	2.0 eq $\text{BF}_3 \cdot \text{OEt}_2$	2.0	0 °C	MeCN	97% ²	2.147

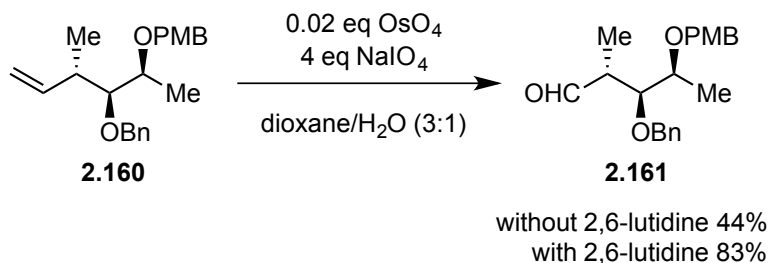
¹ Reaction run on 100 mg scale
² Reaction run on 1 gram scale

2.3.3.4 Bis Oxidative Cleavage of Terminal Olefin

Having developed a methodology that produces large amounts of terminal alkene **2.147**, we examined the oxidative cleavage of the terminal olefin to give **2.162** under Johnson-Lemieux oxidative cleavage conditions. Alkene **2.147** was thus converted to aldehyde **2.162** in 62% yield (Table 2.10, entry 1). Reducing the number of equivalents of NaIO_4 (10 eq to 5 eq) made no significant change to the reaction profile (Table 2.10, entry 2). Examination of the literature revealed that 2,6-lutidine improved the yields

dramatically for the conversion of **2.160** to **2.161** by suppressing over-oxidation and buffering the pH of the reaction media (Scheme 2.37).⁹³

Scheme 2.37. 2,6-Lutidine as an Additive for a Johnson-Lemieux Oxidation



Subjecting alkene **2.147** to the modified conditions of Jin *et al* resulted in a significant improvement in yield of **2.162** (Table 2.10, entry 3 and 4).

Table 2.10. Optimization of Johnson-Lemieux Oxidation

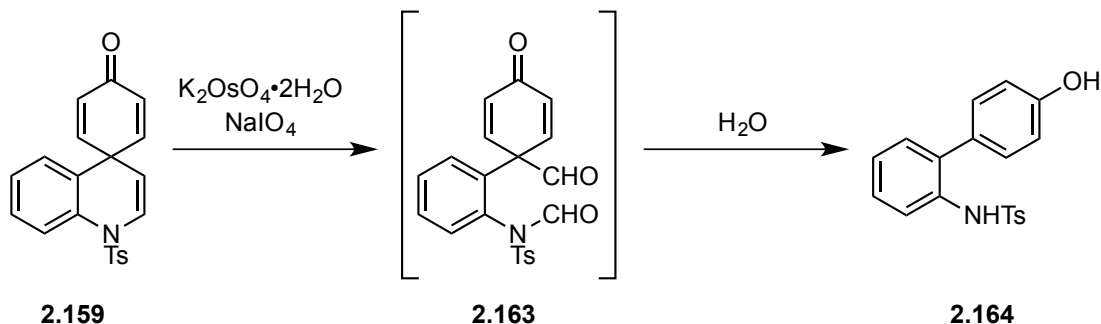
Reaction scheme showing the conversion of **2.147** to **2.162**. The starting material **2.147** is a complex molecule with a quinone-like structure and a vinyl group. The reaction conditions are 5% $\text{K}_2\text{OsO}_4 \cdot 2\text{H}_2\text{O}$ oxidant, solvent, and room temperature (rt). The product **2.162** is the corresponding aldehyde.

Entry	Additive	Oxidant	Solvent	Yield
1	None	10 eq NaIO_4	<i>tert</i> -BuOH:THF: H_2O (4:4:1)	62%
2	None	5 eq NaIO_4	<i>tert</i> -BuOH:THF: H_2O (4:4:1)	57%
3	None	5 eq NaIO_4	Dioxane: H_2O (4:1)	65%
4	2 eq 2,6-lutidine	4 eq NaIO_4	Dioxane: H_2O (4:1)	81%

Curiously, during the course of synthesizing appreciable amounts of **2.162**, varying quantities of phenol **2.164** were isolated from the reaction mixture. We hypothesized that this by-product was observed as a result of Johnson-Lemieux oxidation of enamine **2.159** to dialdehyde **2.163**, which under the aqueous reaction conditions could generate two equivalents of formic acid to afford phenol **2.164** (Scheme 2.38). Although

it is possible that enamine **2.159** could arise via gamma deprotonation and retro-aldol of aldehyde **2.162**, resubjecting **2.162** to the reaction conditions resulted in no degradation.

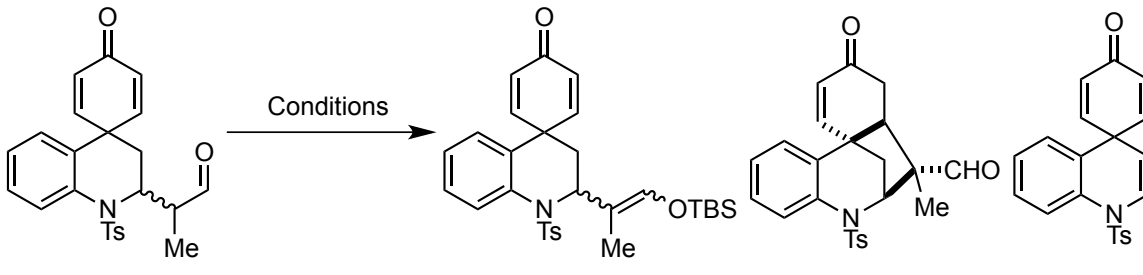
Scheme 2.38. Rationalization for the Observation of Phenol **2.164**



The formation of silyl enol ether **2.165** proved to be a troublesome transformation. Initial attempts using TBS-Cl with imidazole as the base provided the desired enol ether in 30-50% yields (Table 2.11, entry 1). However, the reaction was quite sluggish and required heating to 50 °C to consume all of the starting material. In addition to silyl enol ether **2.165**, the crude reaction mixture contained compounds that were bearing a phenol group, likely arising from acid catalyzed dienone-phenol rearrangement. When the more reactive TBS-OTf was used, the reaction went to completion at room temperature and afforded **2.165** in 63% yield (Table 2.11, entry 2). Unfortunately, attempts to optimize the reaction further were not successful. The stronger base DBU gave no product and caused rapid dimerization of the aldehyde. (Table 2.11, entry 3). We hypothesized that the imidazolium triflate formed when imidazole combines with TBS-OTf was causing starting material degradation, yet switching to *N*-methylimidazole resulted in no improvement in yield (Table 2.11, entry 4). Switching the base to 2,6-lutidine resulted in worse yields (30-40%) (Table 2.11, entry 5). Curiously, **2.166**, which arises from the intramolecular Michael addition, was isolated in 10-20% yield when 2,6-lutidine was employed. We attributed this observation to the increased

acidity of the conjugate acid of 2,6-lutidine, which would in turn activate the dienone moiety to nucleophilic attack. Attempts were also made to form the silyl enol ether under strong base condition; however, none of the desired product was observed. Instead, the gamma elimination/retroaldol product **2.159** was observed. Although further optimization is needed, we decided to investigate the feasibility of subsequent oxidative cleavage steps before continuing with these synthetic efforts.

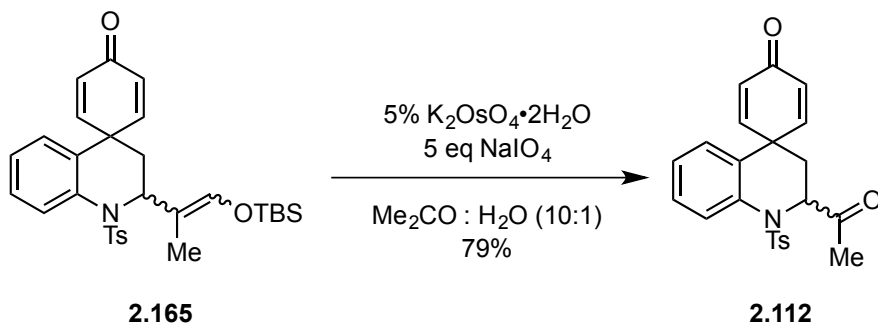
Table 2.11. Attempts to Optimize the Formation of Silyl Enol Ether **2.165**

					
2.162		2.165	2.166	2.159	
Entry	Reagent	Base	Temp	Solvent	Yield of 2.165
1	TBS-Cl	imidazole	50 °C	DCE	30-50%
2	TBS-OTf	imidazole	rt	CH ₂ Cl ₂	63%
3	TBS-OTf	DBU	rt	CH ₂ Cl ₂	0%
4	TBS-OTf	<i>N</i> -methylimidazole	rt	MeCN	50%
5	TBS-OTf	2,6-lutidine	rt	CH ₂ Cl ₂	30-40%
6	TBS-Cl	LDA	-78 °C	THF	0%

LDA = lithium diisopropylamide; DBU = 1,8-Diazabicyclo[5.4.0]undec-7-ene
DCE = dichloroethane

Johnson-Lemieux oxidation of silyl enol ether **2.165** proceeded readily to ketone **2.112**. Using conditions similar to those used for terminal alkene **2.147**, **2.112** was formed in 79% yield, thereby affording the desired alpha amino ketone moiety (Scheme 2.39).

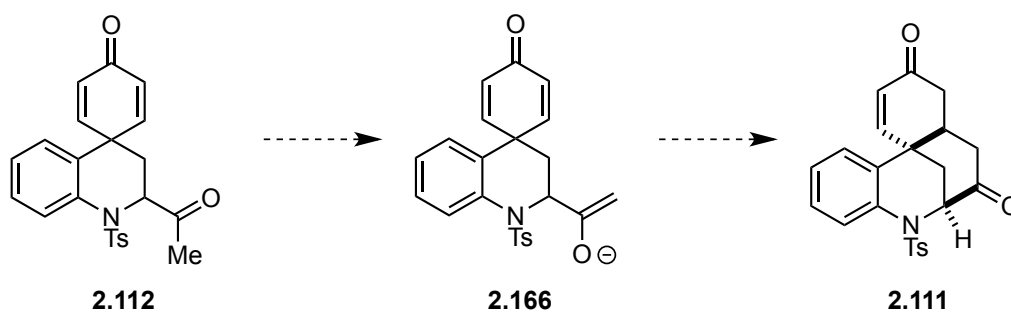
Scheme 2.39. Johnson-Lemieux Oxidation of Silyl Enol Ether **2.165**



2.3.3.5 Attempted Intramolecular Michael Addition to Synthesize spiro-Bicyclononane Core

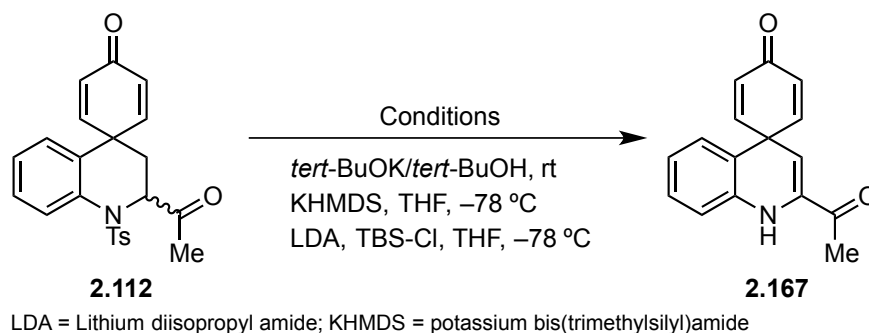
We had initially hypothesized that the intramolecular conjugate addition would proceed readily if the kinetic enolate **2.166** could be formed (Scheme 2.40). To test that hypothesis, we screened several bulky strong bases to see if the less substituted enolate could be formed quantitatively.

Scheme 2.40. Proposed Route to Tetracycle **2.111**



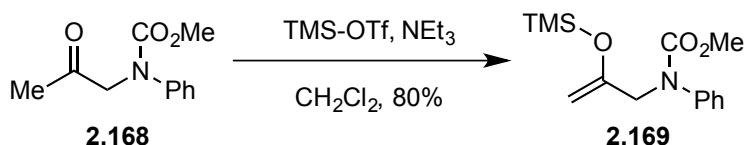
Unfortunately, all attempts to stoichiometrically form the kinetic enolate failed (Scheme 2.41). Instead, elimination of the sulfonamide and isomerization to enamine **2.167** was observed. Attempts to trap the kinetic enolate via addition of TBS-Cl failed as well, once again affording only the elimination product.

Scheme 2.41. Attempts to Stoichiometrically Form the Kinetic Enol Ether



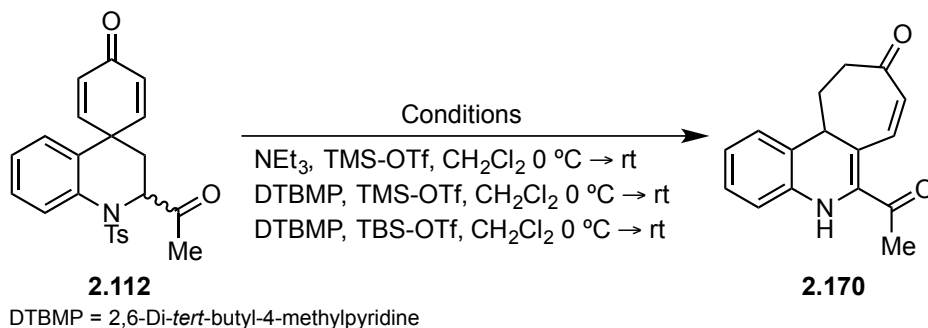
It has also been shown that kinetic enolates can form in high yields under general base conditions (Scheme 2.42).⁹⁴ For example, Pecunioso *et al* demonstrated that ketone **2.168** could be converted to silyl enol ether **2.169** in high yields using TMS-OTf and triethylamine.⁹⁴

Scheme 2.42. Alternative Method to Form Kinetic Enolates



Unfortunately, all attempts to form **2.111** under general base conditions were unsuccessful. Using the conditions published by Pecunioso *et al* did not afford any of the desired enol ether. Instead, a complex mixture of products was formed that, upon quenching with tetrabutylammonium fluoride, funneled to compound **2.170**. Quenching the reaction at -78 °C did not effect the product distribution. We then speculated that a bulkier base might lead to deprotonation at the less hindered position to form the desired enol ether, yet 2,6-di-*tert*-butyl-4-methylpyridine provided virtually identical reaction profiles.

Scheme 2.43. Failed Attempts to Form Kinetic Enolate Under General Base Conditions

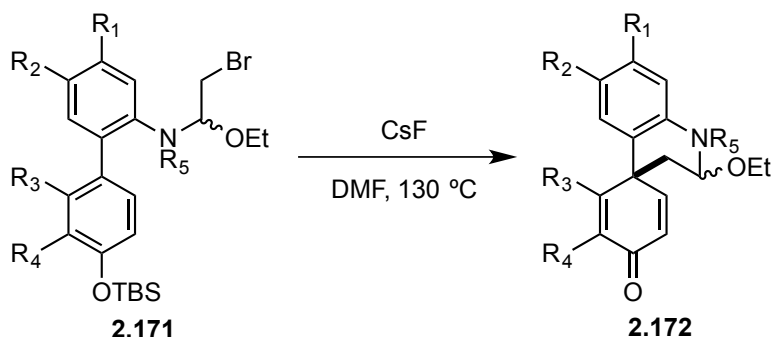


Given that all attempts to induce intramolecular conjugate addition were unsuccessful coupled with the untimely retirement of Phil Magnus (advisor while this work was undertaken), these synthetic efforts were abandoned.

2.4 SUMMARY

In this investigation into the phenolic *C*-alkylation of aniline based systems, it was found that the readily synthesized scaffold **2.171** forms dienones of the form **2.172** in high yields (84-99%) and was tolerant of substitution on both arene rings (Table 2.12). Due to the high yields and broad substrate scope, this approach compares very favorably to the other methods enumerated in Chapter 1. As of this moment, this strategy is also the only published methodology that can synthesize derivatives with a methyl substituent *meta*- to the aniline nitrogen (Table 2.12, compound **2.32e**).

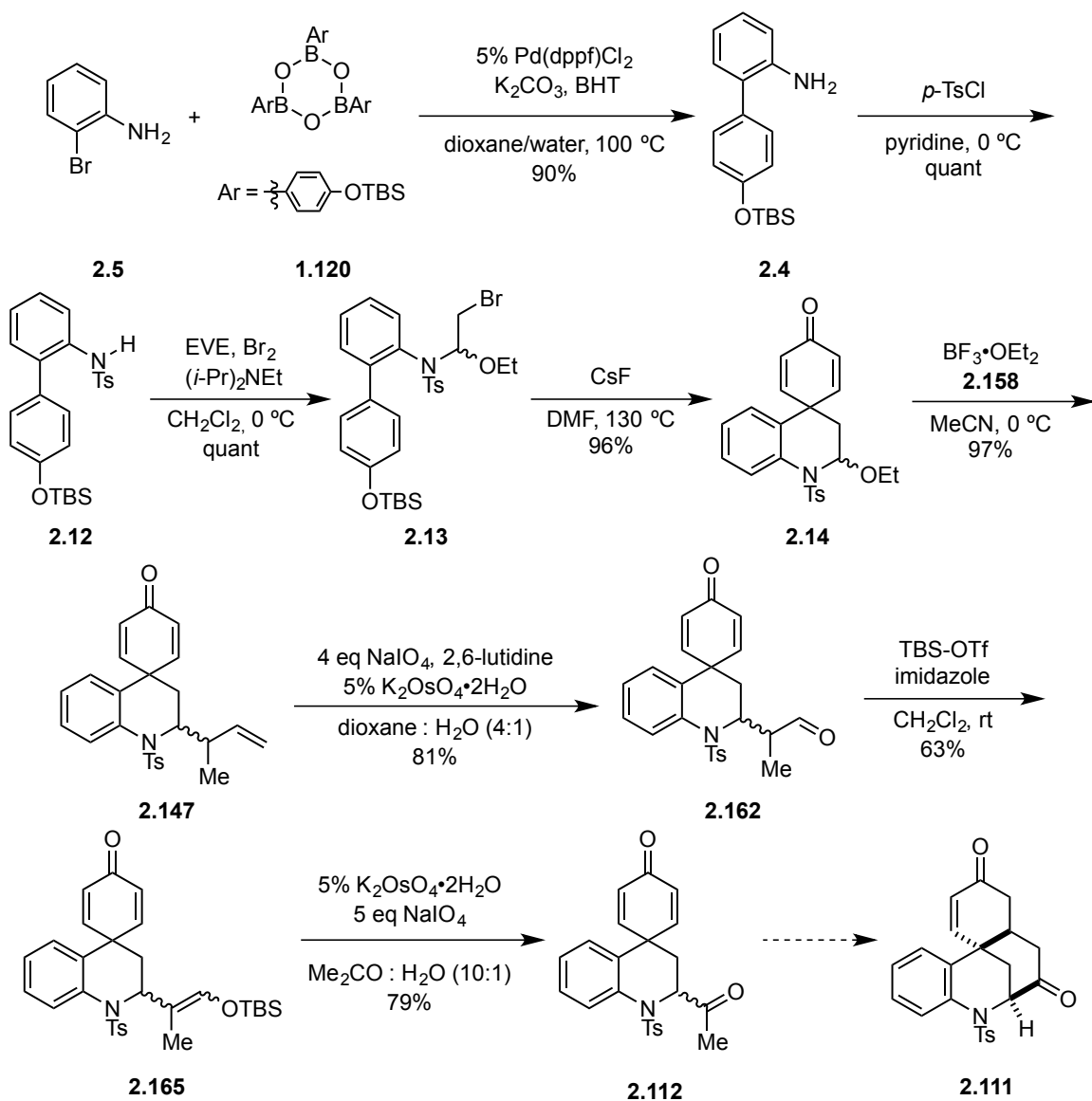
Table 2.12. Summary of Results for *para*-Phenolic C-Alkylation of Aniline Derived *spiro*-Cyclohexyldienones



R ₁	R ₂	R ₃	R ₄	R ₅	Product	Yield
H	H	H	H	Ts	2.14	96%
H	H	H	H	Ms	2.20	83%
H	H	H	H	Ns	2.21	34%
H	Me	H	H	Ts	2.32a	89%
H	OMe	H	H	Ts	2.32b	99%
H	Cl	H	H	Ts	2.32c	98%
OMe	H	H	H	Ts	2.32d	95%
Me	H	H	H	Ts	2.32e	98%
H	H	H	OMe	Ts	2.32g	91%
H	H	-C ₄ H ₄ -	-C ₄ H ₄ -	Ts	2.40	84%

Studies were also undertaken to synthesize the *spiro*-bicyclic nonane core of aspernomine (**2.82**) and sespenine (**2.83**). A sequence was developed in which ketone **2.112** was synthesized in 8 steps and 34% yield from known materials (Scheme 2.44). The key transformation in this sequence is a chemoselective addition of crotylsilane to **2.14**. Efforts to elaborate **2.112** into **2.111** have been unsuccessful, primarily due to the inability to form the less substituted enolate or enol ether. Moving forward, future studies should be focused towards forming the less substituted enol ether. One may be able to preferentially form the desired enolate via pre-installing a halogen alpha to the ketone that could be reduced in a Reformansky reaction. Additionally, one may consider removing the sulfonamide protecting group and attempting the intramolecular conjugate addition on the free aniline.

Scheme 2.44. Summary of Synthetic Efforts Towards the *spiro*-Bicyclic Nonane Core of Aspernomine and Sespentine



Chapter 3: Previous Synthesis of Actinophyllic Acid and Previous Evaluation of Diverted Intermediates for Anticancer Activity

Portions of this chapter are reproduced with permission from Knezevic, C. E. “Development of Poly(ADP-Ribose) Glycohydrolase Inhibitors and Tetracyclic Indoles as Anticancer Compounds.” Ph. D. dissertation, University of Illinois at Urbana-Champaign, 2013.⁹⁵ Parkinson, E. I. “Deoxynyboquinones as NQO1-Targeted Anticancer Compounds and Deoxynybomycins as Potent and Selective Antibiotics.” Ph.D. dissertation, University of Illinois at Urbana-Champaign, 2015.⁹⁶

3.1 NATURAL PRODUCTS AND THEIR DERIVATIVES AS SOURCES OF NEW CHEMOTHERAPEUTICS

3.1.1 Introduction

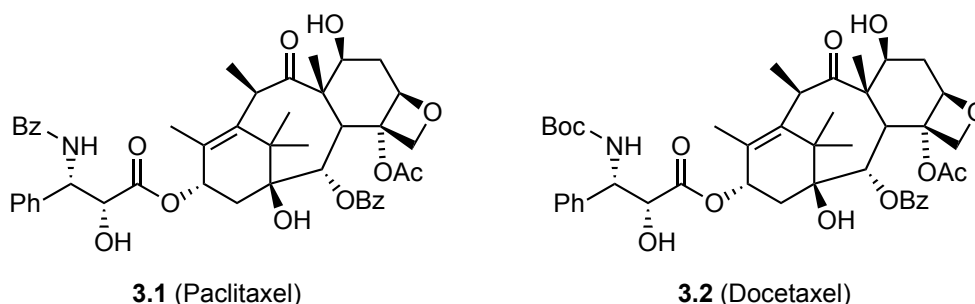
In 2015, the American Cancer Society estimated over 1,650,000 individuals were diagnosed with cancer in the United States and nearly 590,000 deaths were attributed to the disease. There are an estimated 14.5 million Americans living with a history of cancer (either currently or previously diagnosed), and the direct medical costs for treatment and care are estimated to be roughly 88.7 billion dollars.⁹⁷ Although the five year survival rate for cancer has risen dramatically from 49% (for years 1975-1977) to 68% (for years 2004-2010), the disease is far from eradicated, and newer, better treatments are needed.⁹⁷

3.1.2 Natural Products as a Source for New Therapeutics

Over the last 76 years, natural products have been a source of new and potent anti-cancer therapeutics. From 1940 to 2010, 140 anti-cancer agents have been approved by the FDA. Of these 140 approved agents, 126 are small molecules, and 67% of the small molecules are natural in origin, meaning they are either natural products or are a

semi-synthetic analog.⁹⁸ Indeed, over one third of the anti-cancer agents named to the World Health Organization's list of essential medications required for basic healthcare are natural product derived.⁹⁹ For example, one of the most studied classes of anticancer natural products are the taxanes (Figure 3.1, representative examples **3.1** and **3.2**). The natural product paclitaxel (**3.1**) and the semi-synthetic taxane docetaxel (**3.2**) are frontline chemotherapeutics and are listed on the WHO List of Essential Medicines.⁹⁹

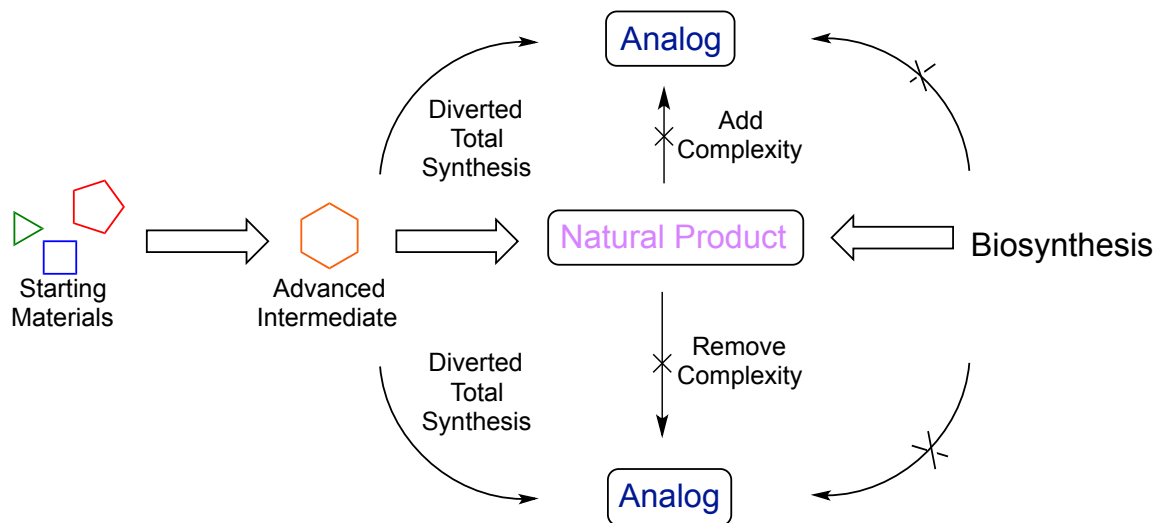
Figure 3.1. The Natural Product Paclitaxel and Derivative Docetaxel



3.1.3 Diverted Total Synthesis as a Strategy for Drug Discovery

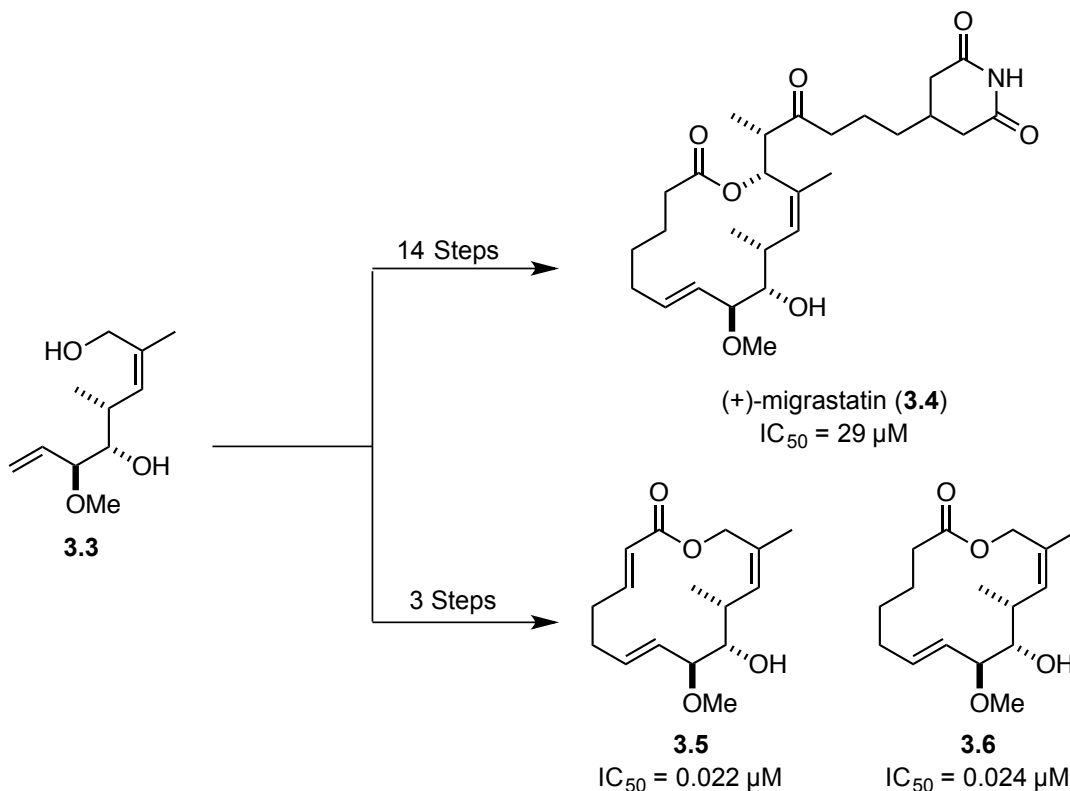
In recent years, the strategy of evaluating analogs of intermediates and their analogs encountered during the course of total synthesis has become an effective approach to access unique natural product derivatives. Researchers are often more interested in natural product analogs than the natural products themselves because the analogs may have unique activity,¹⁰⁰ higher potency,¹⁰¹ or better pharmacokinetic properties.¹⁰² The strategy of diverted total synthesis (DTS) was first coined by Danishefsky *et al* during his work on the natural product migrastatin.¹⁰¹ In DTS, advanced intermediates are diverted to create unique analogs that would not be otherwise accessible through biosynthetic or semi-synthetic means (Figure 3.2). Additionally, the analogs synthesized via DTS may provide valuable insight into which structural elements compose the active pharmacophore and contribute to the desired phenotypic outcome.

Figure 3.2. Graphic Depiction of Diverted Total Synthesis¹⁰¹



In the synthesis of (+)-migrastatin (**3.4**), Danishefsky *et al* found that the structurally simpler analogs **3.5** and **3.6** were 10^3 times more potent against 4T1 cell in a cellular migration assay (Scheme 3.1).¹⁰¹ Using a DTS approach, advanced intermediate **3.3** was converted to the more potent derivatives **3.5** and **3.6** in three steps, whereas the natural product (+)-migrastatin (**3.4**) required 14 additional transformations. Since the initial publication of the (+)-migrastatin analogs, the pharmacophore was minimized further, and these simplified derivatives are under pre-clinical investigation for their ability to suppress lung and breast cancer metastases.¹⁰³ This example demonstrates the powerful results a DTS approach can provide. The more potent intermediates **3.5** and **3.6** would not have been accessible by any other means than laboratory synthesis, be they biosynthetic or semi-synthetic.

Scheme 3.1. Synthesis of (+)-Migrastatin and Analogs by Danishefsky *et al*¹⁰¹



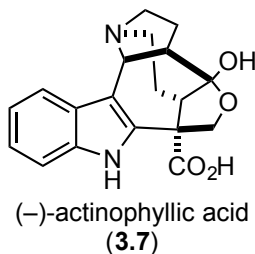
Indeed, the concept of DTS has found application outside of the Danishefsky research group. The amphidinolide,¹⁰⁴ latrunculin,¹⁰⁵ gambierol,¹⁰⁶ mycolactone,¹⁰⁷ ainsliatrimmer,¹⁰⁸ hyperlactone,¹⁰⁹ and many other classes¹¹⁰ of natural products have been subjects of DTS studies that have shed insight into what structural motifs lead to biological activity. Hence, total synthesis of biologically relevant natural products has been, and will continue to be, a valuable method to identify and evaluate new pharmacological leads.

3.2 ISOLATION AND PRIOR SYNTHESIS OF ACTINOPHYLLIC ACID

3.2.1 Isolation and Initial Biological Evaluation of Actinophyllic Acid

The indole alkaloid actinophyllic acid (**3.7**) was first isolated by Carroll *et al* in 2005 from the aqueous leaf extracts of *Alstonia actinophylla*, a plant native to Queensland, Australia via bioassay-guided fractionation (Figure 3.3).¹¹¹ The authors claimed that the natural product exhibited potent inhibitory activity against carboxypeptidase U (CPU) (IC_{50} = 0.84 μ M), which is an endogenous inhibitor of fibrinolysis.¹¹¹ The compound was also of interest to the synthetic community because it contained a unique hexacyclic indole core.

Figure 3.3. The Indole Alkaloid Actinophyllic Acid

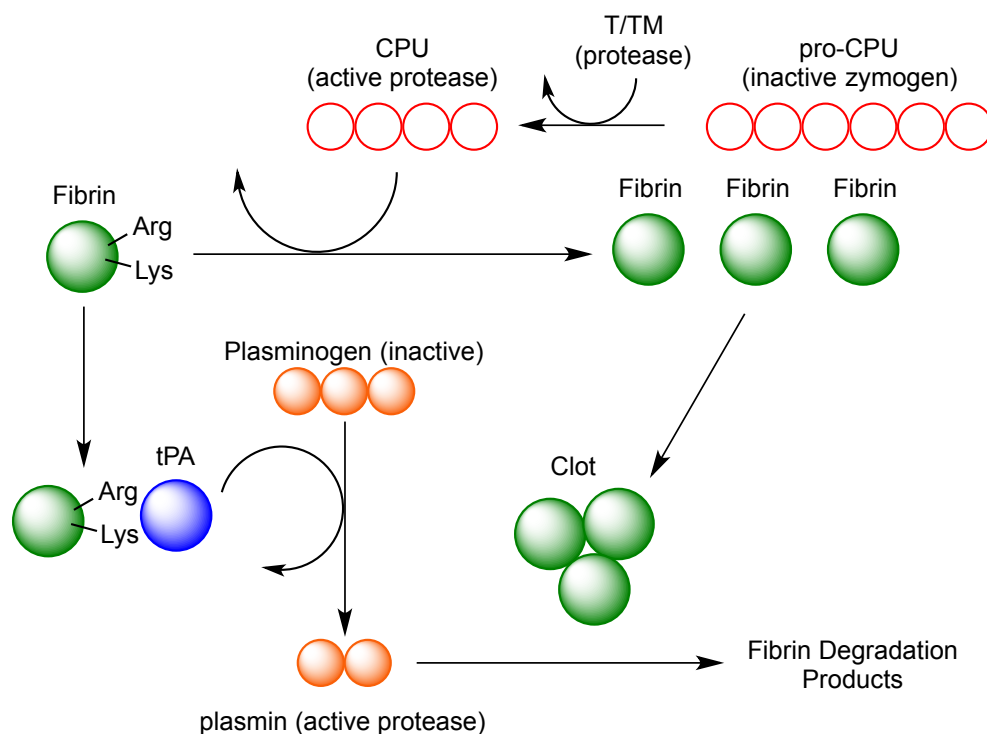


3.2.1.1 Carboxypeptidase U and Its Role Fibrinolysis

Fibrinolysis is a biological process in which fibrin is degraded to prevent the clogging of blood vessels. Fibrin is a globular protein in the clotting response that polymerizes and combines with platelets to repair damaged blood vessels.¹¹² Biochemically, fibrinolysis occurs when fibrin forms a ternary complex with the proteins plasminogen and tissue-type plasminogen activator (tPA).¹¹³ Once the complex is formed, inactive plasminogen is cleaved to the active serine protease plasmin, which in turn degrades fibrin. Carboxypeptidase U does not exist in its active form. Instead, it exists as the inactive zymogen pro-CPU that is cleaved to its active form (CPU) by the enzymes thrombin, trypsin, or the thrombin/thrombomodulin complex (T/TM).^{114,115} CPU in turn

cleaves the C-terminal arginine and lysine residues of fibrin. The C-terminal arginine and lysine residues are necessary for fibrin to form the ternary complex with plasminogen and tPA.¹¹³ Thus, CPU inhibits fibrinolysis by preventing the formation of the ternary complex, resulting in no plasmin formation (Figure 3.4).

Figure 3.4. Graphical Depiction of Fibrinolysis Signalling Pathways



3.2.1.2 Implications of CPU in Cancer

In addition to the role CPU plays in fibrinolysis, the protein has been shown to be upregulated in the plasma samples of lung cancer patients.¹¹⁶ Specifically, individuals with small cell carcinoma of the lung (SCCL) possess plasma levels of CPU greater than ten times that of a healthy control.¹¹⁶ The reason for the upregulation of CPU is unknown; however, some lung cancer cell lines have been shown to express mRNA for CPU. Thus,

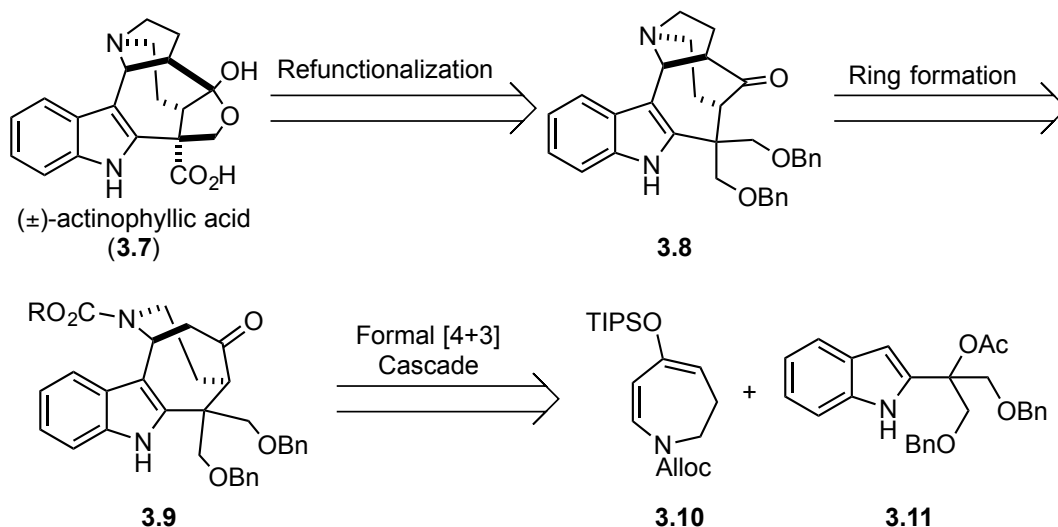
it is not known whether the upregulation of CPU is a direct result of translation from the cancerous cells or a phenotypic response of the body to the cancer.¹¹⁶

The plasminogen/plasmin system, which is regulated by CPU, is involved in processes that mediate tumor growth, including cell proliferation and angiogenesis.¹¹⁷ Angiogenesis, the process by which new blood vessels are formed, relies heavily on coagulation and fibrinolysis to facilitate the rapid and continuous rearrangement of the extracellular matrix (ECM) that is required during cancer proliferation.^{118,119} Therefore, we speculated that CPU would promote the constant remodeling of the ECM that is required for angiogenesis and sustained tumor formation. We further speculated that an inhibitor of CPU, such as actinophyllic acid (**3.7**), would inhibit tumor growth and prevent tumor metastases. To evaluate this hypothesis, the Martin lab and Hergenrother lab at the University of Illinois at Urbana-Champaign collaborated to synthesize and evaluate the anticancer properties of actinophyllic acid (**3.7**).

3.2.2 Martin Synthesis of Actinophyllic Acid

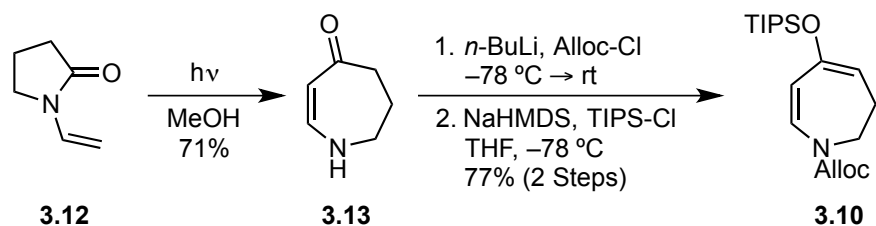
Through the efforts of Dr. Brett Granger and Dr. Ivan Jewitt, the Martin lab completed the synthesis of (±)-actinophyllic acid (**3.7**) in 2013.¹⁰⁰ Retrosynthetically, the Martin lab envisioned that actinophyllic acid (**3.7**) could arise from deprotection and oxidation of pentacycle **3.3**, which in turn could be synthesized from tetracycle **3.9** via an intramolecular alkylation (Figure 3.2). The key step in this synthesis was a proposed formal [4+3] cascade between vinylogous amide enol ether **3.10** and indolo-acetate **3.11** that would form the tetracyclic core **3.9** in one operation.

Scheme 3.2. Retrosynthetic Analysis of (±)-Actinophyllic Acid (**3.7**)



Before the proposed cascade could be evaluated, the individual components **3.10** and **3.11** were synthesized (Schemes 3.3, 3.4, and 3.5). The vinylogous amide **3.13** was formed in 71% yield from *N*-vinylpyridone (**3.12**) via a Norrish type 1 rearrangement. Subsequent protection of the amide nitrogen atom as the allyl carbamate followed by silyl enol ether formation afforded the π -nucleophile **3.10** in 77% over two steps (Scheme 3.3).¹⁰⁰

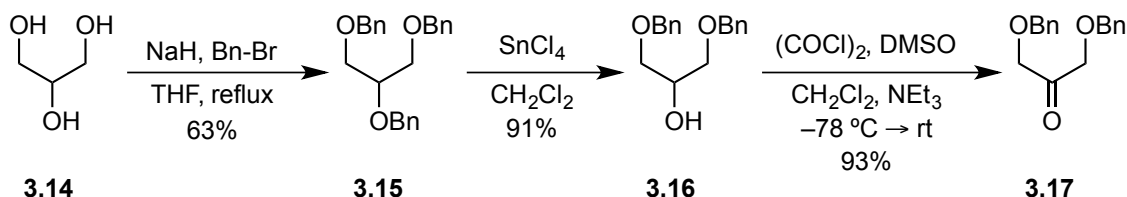
Scheme 3.3. Synthesis of π -Nucleophile **3.10**



Ketone **3.17** was synthesized in three steps from glycerol (**3.14**) by per-benzylation with benzyl bromide to give compound **3.15** in 63% yield. The protected glycerol species **3.15** was selectively deprotected using SnCl_4 to afford secondary alcohol

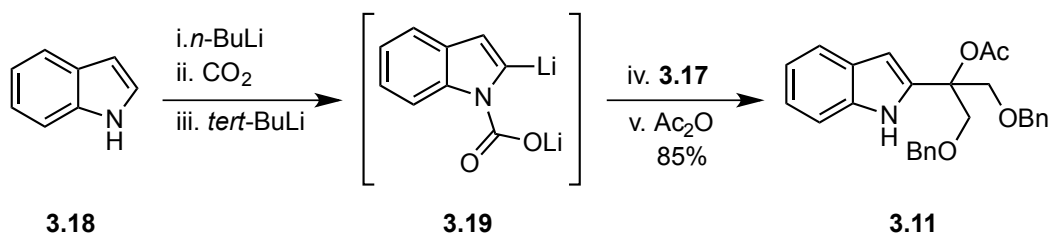
3.16 in 91% yield. Subsequent Swern oxidation of alcohol **3.16** gave ketone **3.17** in 93% yield (Scheme 3.4).¹⁰⁰

Scheme 3.4. Synthesis of Ketone **3.17**



The indolo-acetate **3.11** was synthesized from indole (**3.18**) via a one-pot multistep protocol (Scheme 3.5). First, indole (**3.18**) was deprotonated with *n*-BuLi to give the lithium anion that was then combined with dry CO₂ gas to give the lithium carboxylate salt. The carboxylate salt then underwent a directed deprotonation at the 2-position with *tert*-BuLi to give dianion **3.19**. Dianion **3.19** was then added via cannula to a solution of ketone **3.17** to give the corresponding alcohol. Acetic anhydride was then added, and the reaction mixture was allowed to warm to room temperature. This one-pot, five-step protocol afforded indolo-acetate **3.11** in 85% yield.¹⁰⁰

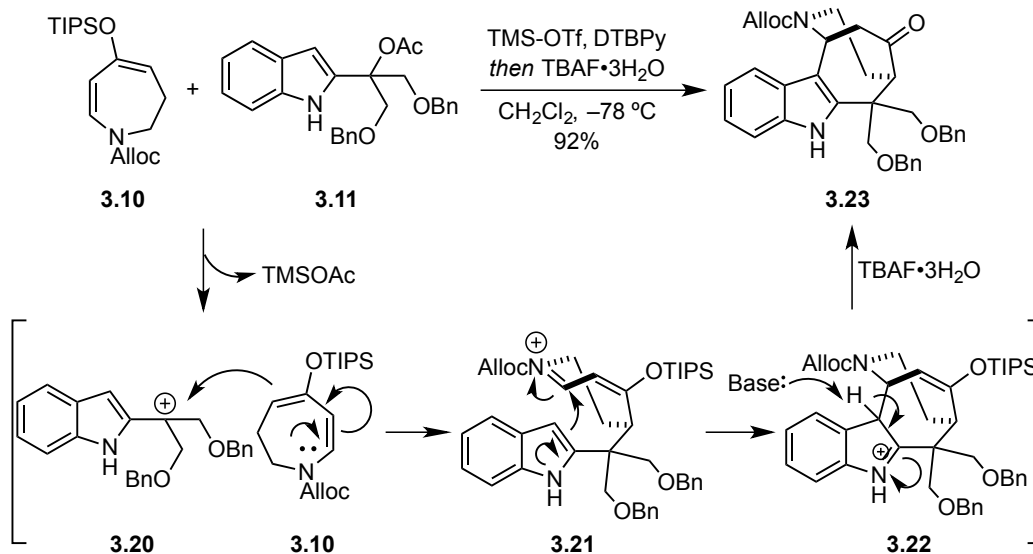
Scheme 3.5. One Pot Synthesis of Indolo-Acetate **3.11**



Having completed the synthesis of compounds **3.10** and **3.11**, it was found that, after much optimization, the cascade progressed as intended to form tetracycle **3.23** in high yield (Scheme 3.6).¹⁰⁰ It is believed that the reaction proceeded via ionization of **3.11** by TMS-OTf to give tertiary carbocation **3.20**, which could then reacted with the π -

nucleophile **3.10** in an S_N1 manner to afford *N*-acyl iminium **3.21**. Iminium **3.21** then would react in an intramolecular fashion to give compound **3.22**, which would rapidly deprotonate and rearomatize the indole moiety. The reaction was quenched with tetrabutylammonium fluoride at $-78\text{ }^{\circ}\text{C}$ to give ketone **3.23** in 92% yield. It was observed that the choice of base was vital to the success of this transformation. If 2,6-lutidine was used instead of 2,6-di-*tert*-butylpyridine, the reaction did not initiate and starting material was recovered.^{120,121} The lack of reactivity was attributed to TMS-OTf forming a Lewis acid/Lewis base pair with 2,6-lutidine, thus attenuating its reactivity. Although a step-wise reaction is shown in Scheme 3.6, there is a distinct possibility the that reaction proceeds through a concerted [4+3] reaction pathway, further mechanistic studies would be needed to determine which pathway is preferred.

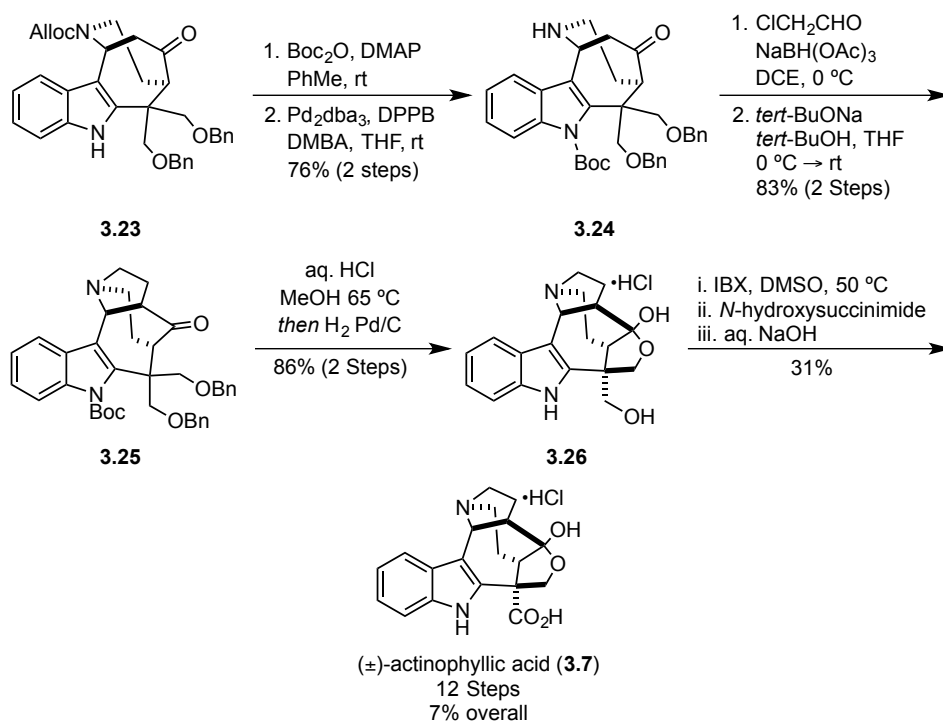
Scheme 3.6. Successful Formation of the Tetracyclic Core of Actinophyllic Acid



Dr. Brett Granger completed the synthesis of actinophyllic acid in six additional steps (Scheme 3.7). Beginning with the tetracycle **3.23**, the nitrogen atom was protected using Boc anhydride/DMAP, followed by removal of the allyl carbamate using

$\text{Pd}_2\text{dba}_3/\text{DPPB}$ and the allyl cation scavenger *N,N*-dimethylbarbituric acid to afford the 2° amine **3.24** in 76% overall yield. Reductive amination of compound **3.24** with chloroacetaldehyde and $\text{NaBH}(\text{OAc})_3$, followed immediately by intramolecular alkylation afforded pentacycle **3.25** in 83% yield. The Boc group of **3.25** was removed using hydrochloric acid in methanol then the *O*-Bn groups were removed in the same pot via hydrogenolysis to give primary alcohol **3.26** in 86% yield. Oxidation of **3.26** to the natural product **3.7** proved unexpectedly troublesome. A three-step protocol was used in which the alcohol was first oxidized to the aldehyde with excess IBX, *N*-hydroxysuccinimide was added to form the hydroxysuccinimide ester, and then saponification of the ester afforded (\pm)-actinophyllic acid (**3.7**) in 31% yield. In summary, the natural product (\pm)-actinophyllic acid (**3.7**) was prepared in 12 steps and 7% overall yield from readily available, known compounds.^{100,122}

Scheme 3.7. Completion of the Natural Product



3.3 DISCOVERY OF A LEAD COMPOUND

Having completed the synthesis of (±)-actinophyllic acid (**3.7**), we next sought to test our hypothesis that actinophyllic acid (**3.7**) might inhibit cancer cell growth through its CPU activity by evaluating the anticancer properties in a cell death assay. Recalling the work pioneered by Danishefsky *et al* on diverted total synthesis (Figure 3.2 and Scheme 3.1), we became curious as to whether the less structurally complex intermediates, specifically **3.23**, displayed any anticancer activity. We were particularly interested in compound **3.23**, or a derivative thereof, because its unique carbon framework was not readily accessible by other means. Additionally, **3.23** could be synthesized on multi-gram scale in 40% yield from commercially available materials, making the material readily accessible for biological evaluation.

3.3.1 Discovery of Cytotoxic Properties

Upon completion of the total synthesis, (±)-actinophyllic acid (**3.7**) and select derivatives prepared by Dr. Brett Granger and Bruce Hua (Figures 3.6 and 3.7) were tested by the Hergenrother lab against several cancer cell lines. Initially, each compound was screened against the triple-negative breast cancer cell line Hs578t at 100 μ M, and the viability of the cells was determined using the dye alamar blue. In the presence of healthy cells with properly functioning mitochondria, the active ingredient of alamar blue, resazurin (**3.27**), is reduced to the highly florescent blue chromophore resorufin (**3.28**) (Figure 3.5).¹²³ Since florescence is a function of cell viability, the percent cell viability can be determined by the relative UV absorption of cells dosed with a compound to a negative control (DMSO) and a positive control (doxorubicin).

Figure 3.5. The Cell Viability Probe Alamar Blue

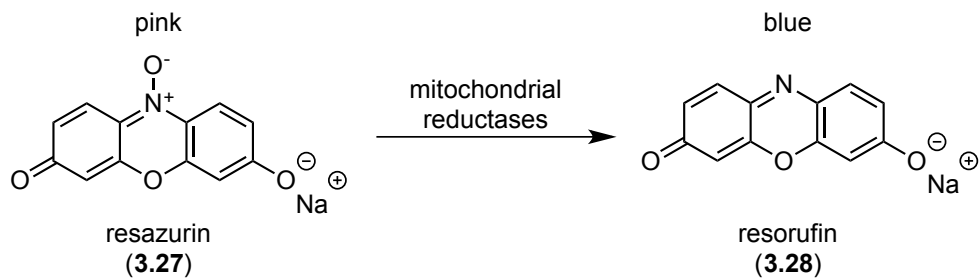


Figure 3.6. Compounds That Showed No or Minimal Cytotoxicity

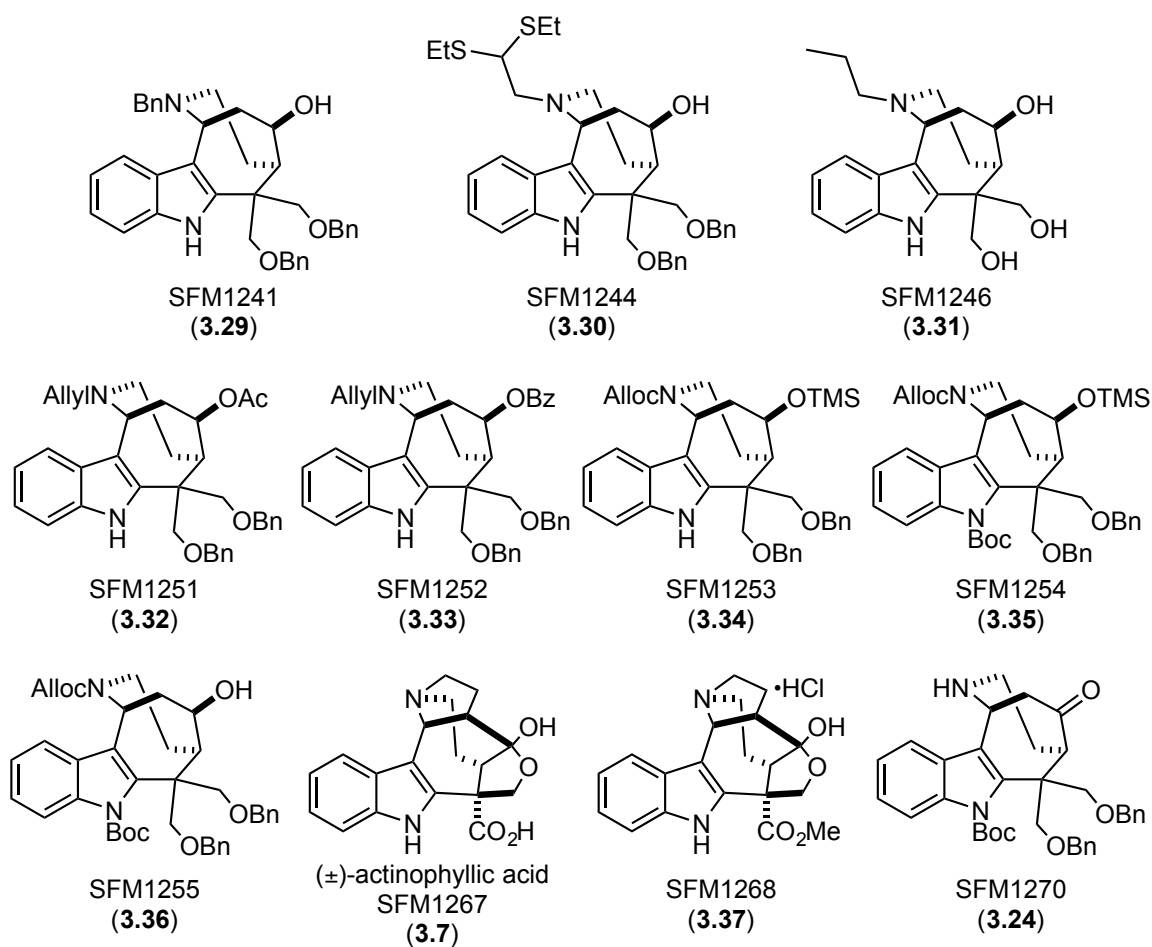
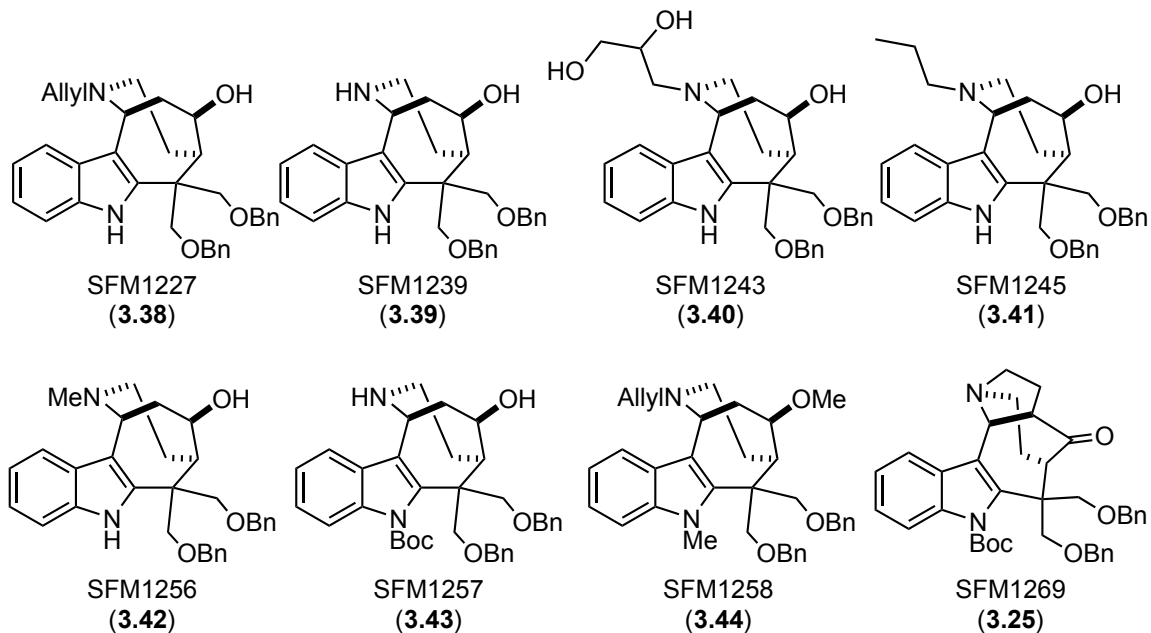


Figure 3.7. Compounds That Showed Cytotoxicity



The initial experiments, performed by Dr. Claire Knezevic and Dr. Betsy Parkinson, indicated that actinophyllic acid (SFM1267, **3.7**), actinophyllic acid methyl ester (SFM1268, **3.37**), and a number of other intermediates were not active against cancer cells (Figure 3.6, Figure 3.8); however, multiple compounds derived from the tetracyclic cascade product **3.23** were efficacious and demonstrated anticancer activity at high concentrations (Figure 3.7, Figure 3.8). The compounds that showed positive results in the initial cytotoxicity screen were further evaluated, and their IC_{50} values were determined (Table 3.1). Of the active compounds, it was found that the IC_{50} values ranged from 63.0 to 6.6 μ M. The most potent compound, SFM1257 (**3.43**), was further evaluated against a diverse panel of cancer cell lines, and SFM1257 (**3.43**) was found to exhibit relatively uniform anticancer activity across a number of cell lines (Table 3.1).^{95,96}

Figure 3.8. Initial Screen For Cytotoxicity⁹⁵

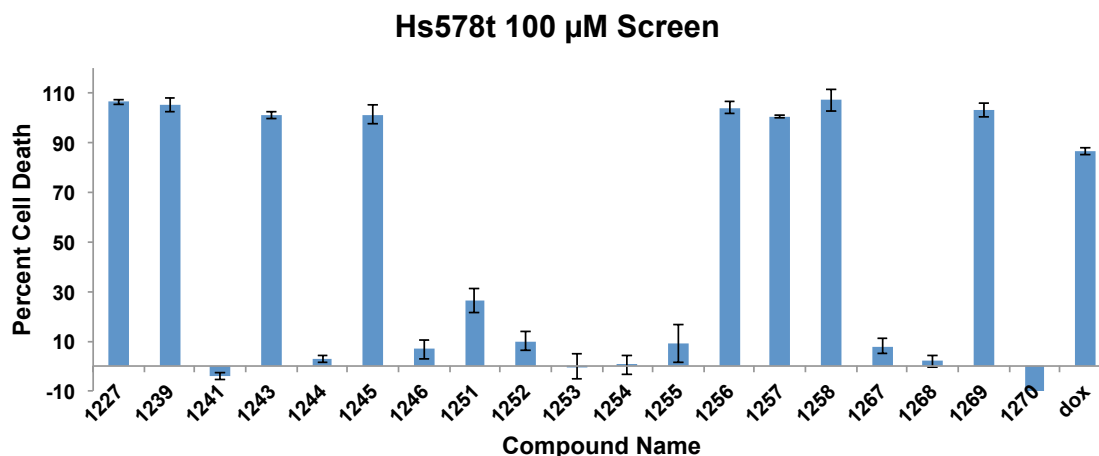


Table 3.1. Further Evaluation of Cytotoxic Compounds^{95,96}

A)	Compound	Hs578t IC ₅₀ (μM)*
	SFM1227	63 ± 16.0
	SFM1239	14.9 ± 4.8
	SFM1243	20.4 ± 3.6
	SFM1245	13.2 ± 1.3
	SFM1256	12.6 ± 2.5
	SFM1257	6.6 ± 0.7
	SFM1258	15.5 ± 2.8
	SFM1269	11.2 ± 1.9

B)	Cell Line	Cancer Cell Type	IC ₅₀ (μM)*
	Hs578t	triple-negative breast	6.6 ± 0.7
	BT549	triple-negative breast	8.0 ± 0.6
	MDA-MB-231	triple-negative breast	3.4 ± 0.02
	4T1	murine breast	6.1 ± 1.5
	T47D	ER+ breast	10 ± 2.3
	MCF-7	ER+ breast	4.3 ± 0.4
	U937	lymphoma	3.3 ± 0.2
	HeLa	cervical	9.7
	U87	brain	4.8 ± 0.5
	A549	lung	6.8 ± 1.3
	MIA-PaCa-2	pancreatic	4.3 ± 0.2

A) IC₅₀ values for active compounds B) Evaluation of SFM1257 (3.43) against a panel of cell lines. *N= 3, s.e.m. where error is indicated. No error implies N= 1.

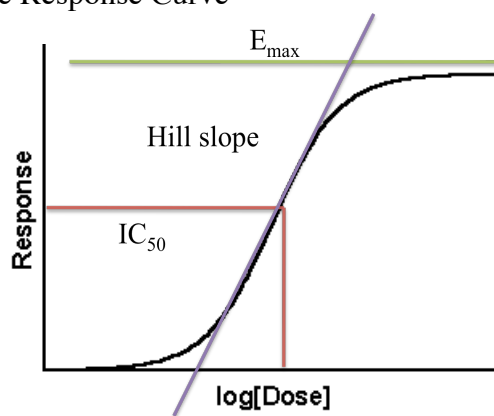
3.3.2 Analysis of Dose-Response-Curves

3.3.2.1 The Importance of IC₅₀, E_{max}, and Hill Slope

The ultimate goal during the preclinical assessment of a drug candidate is to find a small molecule that will have the highest probability of providing positive clinical outcomes. In order for a drug to work, sufficient levels of a drug must reach a target site,

remain at the site for a sufficient duration, and not be overly toxic. A major assumption in much of academia and pharmaceutical drug development is that a compound possessing high potency in cells (low IC_{50}) has a higher likelihood to be efficacious in human patients.¹²⁴ The logic is that high potency implies lower therapeutic doses will be required, and lower therapeutic doses will, in turn, lead to less off-target toxicity or accumulated deleterious metabolites. Unfortunately, these common assumptions about cancer therapeutics are not supported by preclinical and clinical data.¹²⁴⁻¹²⁷ In a retro-analysis of FDA approved chemotherapy drugs against the NCI-60 panel of cancer cell lines, it was determined that high potency (nanomolar IC_{50} values) bore little relevance to clinical efficacy, and most major classes of cytotoxic chemotherapeutics lacked nanomolar potency in cells.¹²⁶ However, there are other metrics determined from a dose-response curve that may help predict the effectiveness of a compound for the treatment of cancer. Specifically, those metrics are the Hill slope (HS) (Figure 3.9, purple line) and E_{max} (Figure 3.9, green line).

Figure 3.9. Example Dose Response Curve



The HS is defined as the slope of the dose response curve at the point of inflection.¹²⁸ Qualitatively, the HS is a quantification of how quickly a compound approaches the maximum response (E_{max}). In the context of a cell death assay, the

theoretical E_{\max} is 100, meaning 100% percent cell death. The percent cell death at a given concentration can be determined mathematically from the equation shown in Figure 3.10.¹²⁹ For example, a compound with $E_{\max}= 100$, $IC_{50}= 1 \mu\text{M}$, and $HS= 1$ would require a concentration of $19 \mu\text{M}$ to achieve 95% cell death. If $E_{\max}= 100$, $IC_{50}= 1 \mu\text{M}$, but $HS= 2$, a concentration of only $\sim 3.5 \mu\text{M}$ is needed to achieve 95% cell death. In the case of a potential anticancer compound, the desired therapeutic outcome is 100% cancer cell death. Therefore, one is lead to conclude that compounds that display larger HS values may have a higher probability to show positive therapeutic outcomes.

Figure 3.10. Equation Used to Calculate Percent Cell Death¹²⁹

$$\text{Percent Cell Death} = E_{\max} + \left(\frac{E_0 - E_{\max}}{1 + \left(\frac{\text{Dose}}{IC_{50}} \right)^{HS}} \right)$$

Indeed, studies have shown a positive correlation between clinical efficacy of drugs and HS. For BCR-ABL inhibitors used in the treatment of myeloid leukemia, Druker *et al* found that there was a strong correlation between clinical response and HS for various cell lines containing point mutations in the BCR-ABL kinase domain.¹³⁰ Inhibitors that displayed lower HS values were associated with poorer clinic responses, and inhibitors with higher HS values were associated with better clinical outcomes.¹³⁰ The authors noted that a mutation that led to a worse IC_{50} but maintained a high HS could be treated clinically by simply increasing the dose. A similar observation was reported by Siliciano *et al* for HIV-targeted retrovirals. The authors noted that genetic mutations in the drug target modulated the IC_{50} and HS of an inhibitor, and if a mutation causes a slight change in IC_{50} but a dramatic change in HS, the efficacy of a drug at concentrations

above the IC_{50} is dramatically reduced.¹³¹ Thus, chemotherapeutic kinase inhibitors and HIV retroviral inhibitors both benefit clinically from steeper Hill slopes.

In a recent report by Sorger *et al*, the authors analyzed 64 cancer drugs over 53 breast cancer cell lines and found that HS values varied by drug class and did not correlate to IC_{50} .¹²⁹ For example, mTOR inhibitors were found to have an average HS of 0.41, and it was determined that the major driver of the shallow dose-response curve was the high degree of cell-to-cell variability within a cellular population that contributes to a non-uniform response to the cytotoxins.¹²⁹ Even at high doses well above the IC_{50} value, wide variations in response to the mTOR inhibitors were observed. This fact is particularly troublesome because partial or fractional killing leads to selection bias and the development of resistance.¹²⁹ On the other hand, proteasome and HSP90 (heat shock protein 90) inhibitors showed the highest average HS values (~2). Through meta-analysis, the authors showed that compounds with a similar mode-of-action displayed comparable HS values.¹²⁹

Since HS strongly correlates with mode-of-action, a HS greater than one could imply that a compound impacts a single biological target that in turn modulates multiple biological processes or that a compound impacts multiple biological targets (polypharmacology). Although polypharmacology is typically associated with non-specific toxicity, a recent report found that approved drugs have on average six biological targets,¹³² and other reports have found that complex, multigenic diseases like cancer may benefit from polypharmacology as an alternative to complex therapeutic approaches.¹³³⁻¹³⁵ Thus, the HS exhibited by a compound in a cell death assay is more accurately viewed as an innate characteristic rather than a parameter that is capable of being optimized.

The E_{max} is another often overlooked metric that quantifies the percentage of cells remaining after the dose-response-curve reaches a plateau. This parameter is key for

determining how effective a compound is at killing cells at high concentrations. Sorger *et al* demonstrated that compounds that display a high E_{\max} across several cancer cell lines did not develop resistant upon regrowth and retained the same overall levels of sensitivity to the cytotoxins.¹²⁹ As a result, compounds that display a high E_{\max} across multiple cell lines have a lower risk of developing resistance.

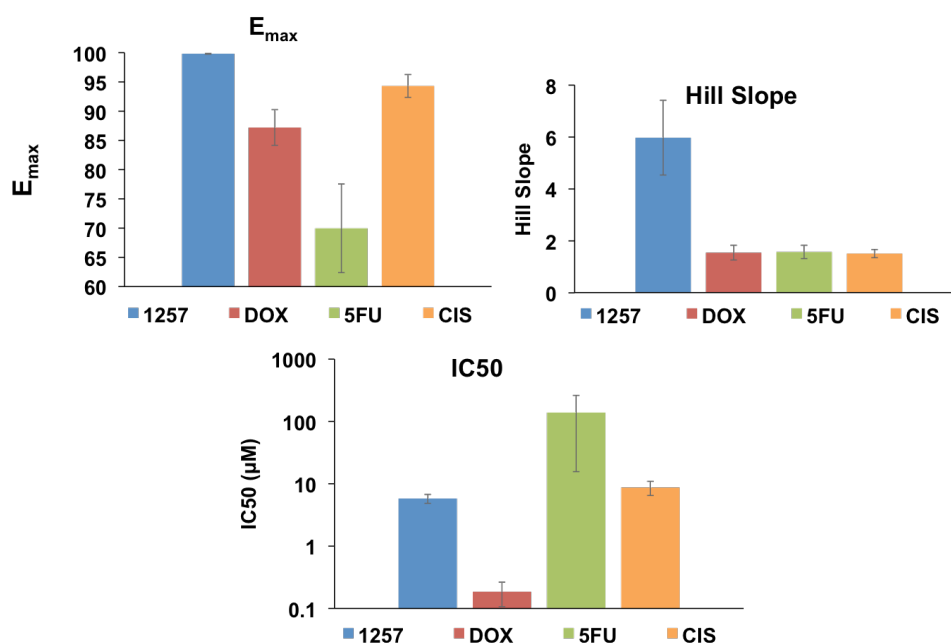
3.3.2.2 Actinophyllic Acid Intermediates Show Consistently Steep Hill Slopes and High E_{\max}

Upon screening SFM1257 (**3.43**), it became evident to Dr. Claire Knezevic and Dr. Betsy Parkinson that this novel compound killed cancer cells with uniformly steep Hill slopes and E_{\max} either at or approaching the theoretical maximum (100% cell death) (Table 3.2). As compared to the FDA approved frontline anticancer drugs doxorubicin, 5-fluorouracil, and cisplatin, SFM1257 (**3.43**) showed significantly higher average HS values over the cancer cell lines tested (Figure 3.11).⁹⁶ Additionally, SFM1257 (**3.43**) showed consistently higher average E_{\max} values than all three of the other compounds tested (Figure 3.11).⁹⁶ The IC_{50} values for the compounds varied rather dramatically; doxorubicin was the most potent with low nanomolar values, but the values for SFM1257 (**3.43**), 5-fluorouracil, and cisplatin were comparable over the cell lines examined. Given that a steep Hill slope and high value for E_{\max} is shown to correlates well with positive clinical outcomes and IC_{50} does not, they decided to continue pursuing investigations into these novel cytotoxins.

Table 3.2. IC_{50} , Hill slope, and E_{max} Values For SFM1257 Versus FDA Approved Anticancer Drugs⁹⁶

Cell Line (tumor type)	SFM1257			Doxorubicin			5-Fluorouracil			Cisplatin		
	IC_{50} (μ M)	Hill Slope	E_{max}	IC_{50} (μ M)	Hill Slope	E_{max}	IC_{50} (μ M)	Hill Slope	E_{max}	IC_{50} (μ M)	Hill Slope	E_{max}
A549 (lung)	6.8 ± 1.3	7.9 ± 3.2	100 ± 0.1	0.19 ± 0.05	0.91 ± 0.06	89.9 ± 0.5	11 ± 5.4	2.1 ± 0.8	73.6 ± 4.4	8.6 ± 4.5	2.6 ± 0.4	91.1 ± 3.6
Hs578t (breast)	6.6 ± 0.7	7.6 ± 2.3	100 ± 0.1	0.16 ± 0.1	1.3 ± 0.2	93.0 ± 3.0	17 ± 11	9.5 ± 4.0	69.4 ± 5.8	9.6 ± 2.4	3.0 ± 0.7	95.9 ± 1.6
MCF-7 (breast)	4.3 ± 0.4	3.3 ± 0.3	98.9 ± 0.2	1.1 ± 0.21	6.3 ± 2.5	65 ± 4.4	>1000	1.8 ± 0.3	22.3 ± 3.3	18 ± 5.0	0.94 ± 0.1	99.5 ± 6.5
MDA-MB- 231 (breast)	3.4 ± 0.02	15.7 ± 0.5	100 ± 0.1	0.29 ± 0.06	0.96 ± 0.1	80.7 ± 0.5	45 ± 11	1.3 ± 0.08	59.3 ± 1.7	11 ± 3.4	1.4 ± 0.2	90.2 ± 3.9
Mia PaCa-2 (pancreatic)	4.3 ± 0.2	3.2 ± 0.3	100 ± 0.3	0.021 ± 0.004	1.9 ± 0.3	90.8 ± 1.0	7.5 ± 2.5	5.8 ± 3.8	80.8 ± 2.0	6.3 ± 0.7	1.6 ± 0.1	94.4 ± 0.4
T47D (breast)	10 ± 2.3	10 ± 2.9	99.9 ± 0.04	0.092 ± 0.007	1.8 ± 0.5	82 ± 2.0	25 ± 3.2	2.1 ± 0.1	65.3 ± 1.8	8.0 ± 2.3	10.9 ± 3.8	75.6 ± 1.9
U937 (lymphoma)	3.3 ± 0.2	11 ± 3.7	100 ± 0.2	0.021 ± 0.001	1.8 ± 0.1	98.3 ± 0.7	10 ± 2.2	1.8 ± 0.3	92 ± 5.5	2.5 ± 1.0	2.1 ± 0.3	100 ± 0.7
4T1 (murine breast)	6.1 ± 1.5	9.8 ± 4.1	100 ± 0.1	0.11 ± 0.005	1.5 ± 0.2	91.2 ± 1.3	2.7 ± 0.3	0.95 ± 0.06	88.5 ± 0.5	3.5 ± 1.2	2.8 ± 0.6	95.9 ± 0.6

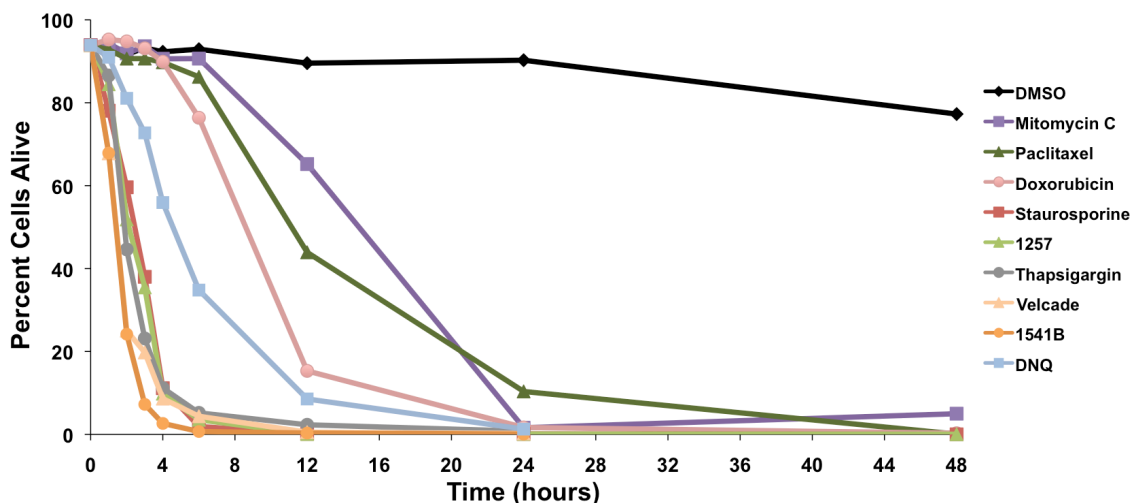
Figure 3.11. Average E_{max} and Hill Slope Values of SFM1257, Doxorubicin, 5-Fluorouracil, and Cisplatin Over All Cell Lines⁹⁶



3.3.3 Actinophyllic Acid Intermediates Induce Rapid Cell Death

During the course of evaluating SFM1257 (**3.43**) and other derivatives, Dr. Claire Knezevic and Dr. Betsy Parkinson observed that the rate of cell death was very rapid, and incubation times past 12 h did not increase the amount of observed cell death.⁹⁵ Thus, they sought to compare the rate of SFM1257 (**3.43**) induced cell death to that of known cytotoxins. The rate of cell death was determined via incubation of U937 lymphoma cell with 10 μ M cytotoxin (20 μ M for thapsigargin) and evaluation of their viability by flow cytometry at set time points. They found that SFM1257 (**3.43**) elicited >95% cell death in only six hours. (Figure 3.12).⁹⁵ The FDA approved anti-cancer agents mitomycin C (**3.46**) (purple line), paclitaxel (**3.1**) (dark green line), and doxorubicin (**3.48**) (pink line) as well as the catalytic ROS generator DNQ (**3.50**) (blue line) all killed cancer cells slower than SFM1257 (**3.43**) (light green line).^{95,136} Interestingly, mitomycin C (**3.46**), doxorubicin (**3.48**), and DNQ (**3.50**) elicit cell death via damage to the cellular DNA, indicating that rate of cell death may correlate to mode-of-action, as expected.

Figure 3.12. Relative Rate of SFM1257 (**3.43**) Induced Cell Death Versus Other Known Cytotoxins⁹⁵

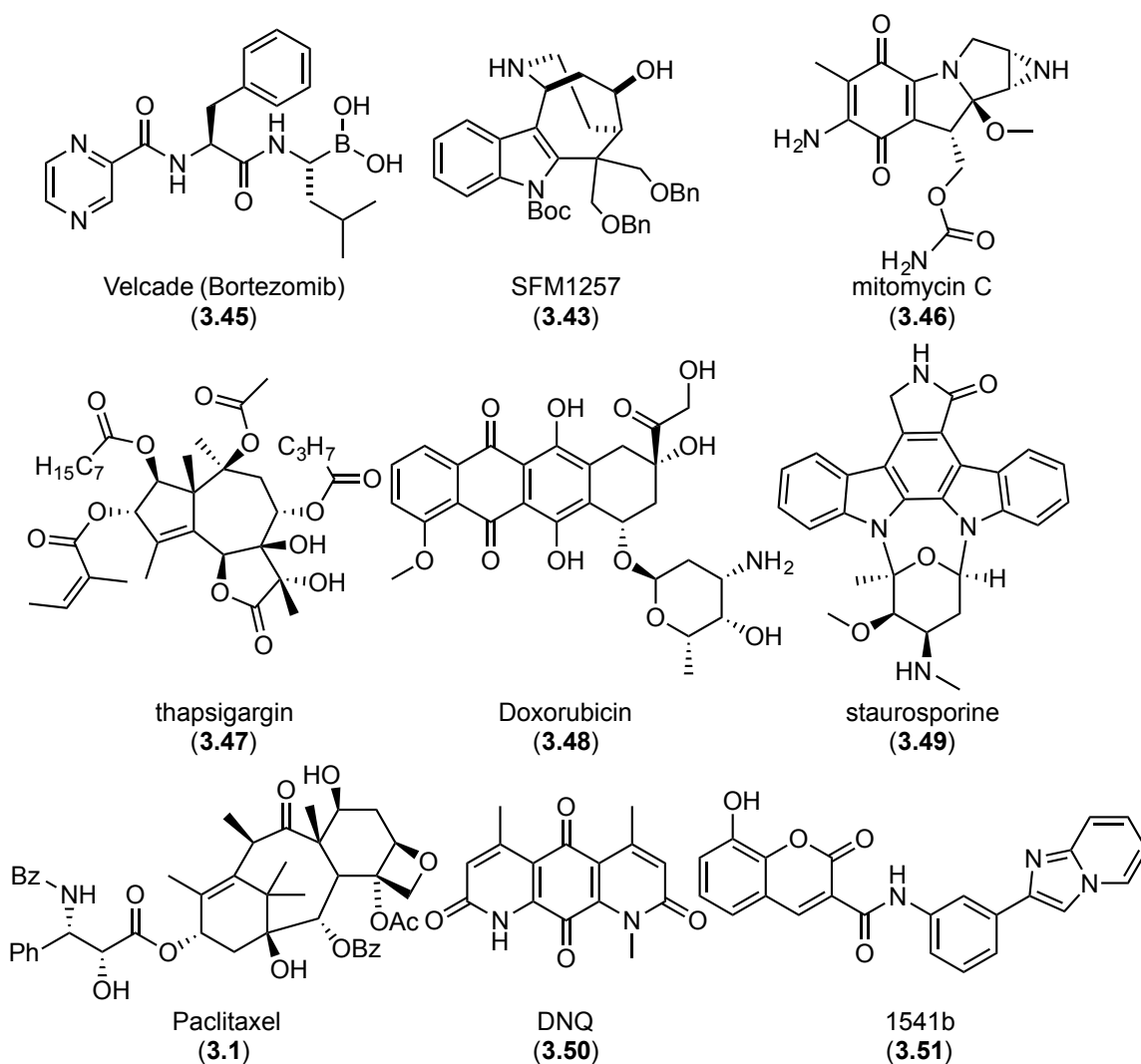


In other experiments, SFM1257 (**3.43**) was found to work with speeds comparable to thapsigargin (**3.47**), velcade (**3.45**), staurosporine (**3.49**), and 1541b (**3.51**). The tool compound thapsigargin (**3.46**) is a SERCA (sarco/endoplasmic reticulum Ca^{2+} -ATPase) that induces a build up of cytosolic calcium, which in turn triggers apoptosis and other cell death pathways.¹³⁷ Velcade (bortezomib) (**3.45**) is a potent proteasome inhibitor FDA approved for the treatment of relapsed multiple myeloma and mantle cell lymphoma.¹³⁸ The indole alkaloid staurosporine (**3.49**) is a nonspecific pan-kinase inhibitor known as the gold-standard for rapid induction of cell death.¹³⁹ The cytotoxin 1541b (**3.51**) is a procaspase-3 activator, which is the final ‘executioner’ caspase in the apoptotic signaling pathway.¹⁴⁰ These four compounds have little in common with regards to mode-of-action or structure, so no real mechanistic insights could be garnered from comparing SFM1257 (**3.43**) to the compounds.

As shown in Figure 3.12, the rate of cell death induction can vary dramatically from one therapeutic agent to another. Although there has not been a report published correlating the speed of cell death induction with clinical outcome, there are several

reasons to infer that rapid cell death may be a desirable characteristic. The rapid induction of cell death may compensate for poor pharmacokinetic characteristics of a cytotoxin because a shorter exposure time will be needed to elicit death. Additionally, rapid induction of cell death may reduce the probability of a cell developing resistance by limiting the amount of time each cell has to adapt to the toxic insult. Thus, eliciting rapid cell death may be a beneficial trait of SFM1257 (**3.43**) induced cell death.

Figure 3.13. Cytotoxins Evaluated For Speed of Cell Death



3.3.4 Hemolysis Assays

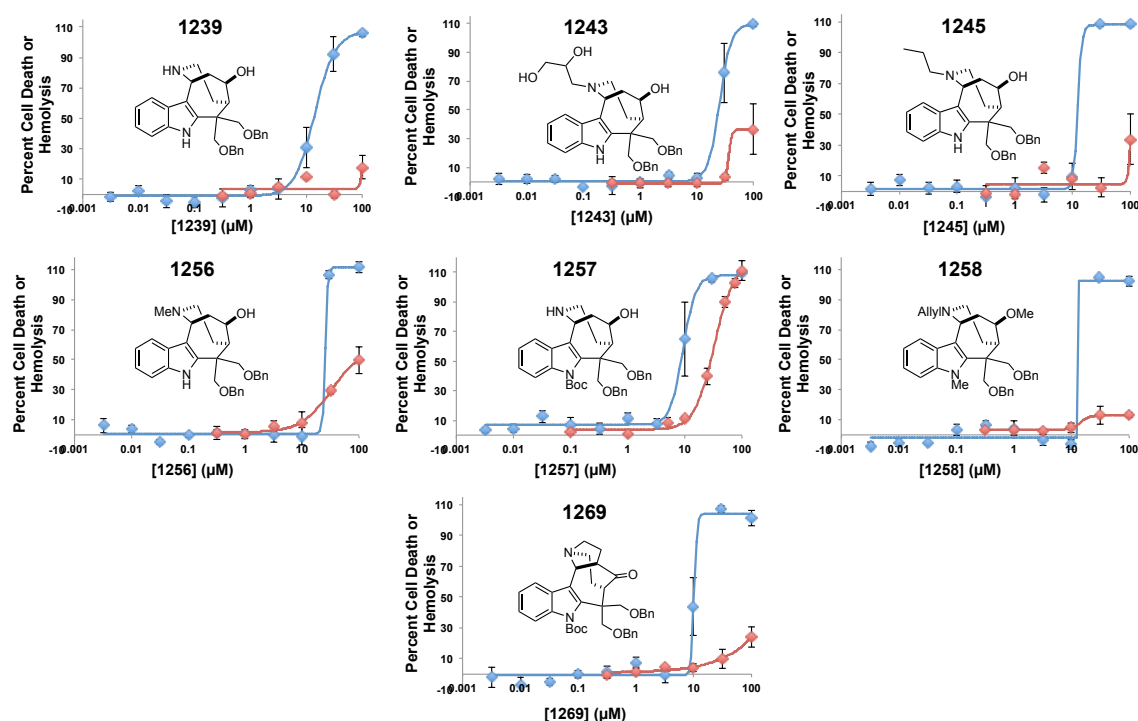
To further assess the translational value of these compounds, the derivatives were evaluated for their ability to elicit hemolysis. Drug induced immune-independent hemolytic anemia is a form of acute toxicity that will prevent a compound from progressing to the clinic. Most often, drug-induced hemolytic anemia occurs when a compound interferes with hemoglobin function, typically via oxidation of Fe^{2+} to Fe^{3+} . For example, the antibiotic dapsone, which is used for the treatment of leprosy and other skin conditions, causes hemolysis when the compound is oxidized to the *N*-hydroxy moiety that in turn forms methemoglobin and leads to eventual lysis.¹⁴¹ Similarly, the antimalarial drug primaquine induces hemolysis via an accumulation of intracellular hydrogen peroxide. Indeed, individuals harboring mutations to glucose-6-phosphate dehydrogenase (G6PD) are more prone to hemolysis, which is likely due to a significant reduction in synthesis of the antioxidant NADPH. Thus, compounds that are easily oxidized or create an oxidative cellular environment run the risk of being hemolytic.

Simple *in vitro* hemolysis assays were used to assess the potential for these compounds to induce immune system independent hemolysis, and *in vitro* analysis has been shown to be a good indicator of *in vivo* toxicity.^{142,143} Dr. Claire Knezevic and Dr. Besty Parkinson evaluated the hemolytic potential of SFM1257 (**3.43**) and other active derivatives by incubating washed and purified red blood cells with the test compound for 2 h at 37 °C. The supernatant was then removed, and the absorbance at 540 nm, which corresponded to the amount of hemoglobin released, was determined.

The dose-response curves for hemolysis (red) versus Hs578t toxicity (blue) are shown in the graphs in Figure 3.12. Most of the active anticancer compounds did not induce significant hemolysis (>10%) until a dose of 100 μM achieved. Unfortunately, the most potent compound SFM1257 (**3.43**) showed significant hemolytic activity at 30

μM .⁹⁵ Fortunately, other derivatives with similar potency showed no hemolytic activity, leading one to reach several conclusions: 1) the mechanism of cell death in cancer cells is different from the mechanism that causes hemolysis; and 2) the hemolytic activity can be attenuated via structure-activity studies.

Figure 3.14. Dose Response Curve for Hemolysis and Cell Death⁹⁵



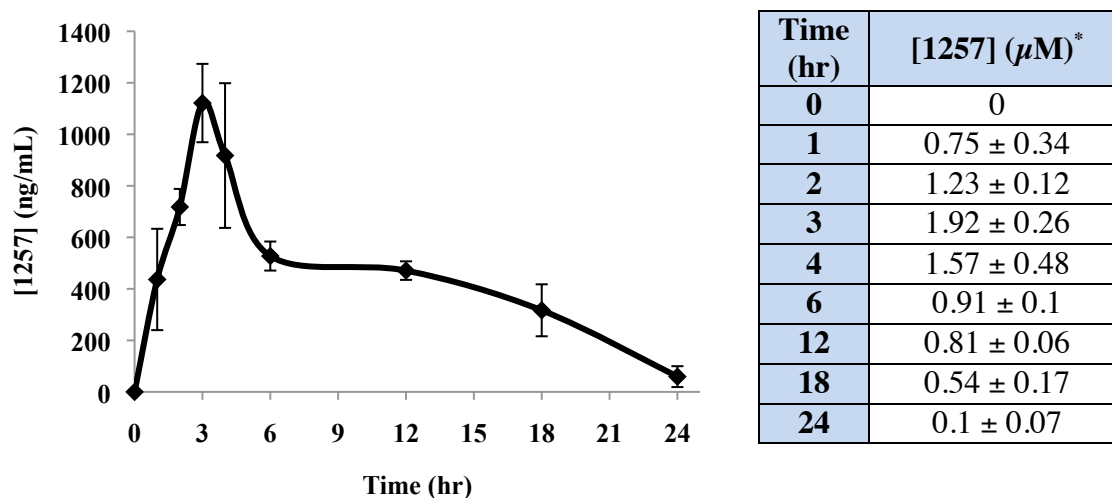
3.3.5 Preliminary *in vivo* Analysis

3.3.5.1 Determination of Maximum Tolerated Dose and Pharmacokinetic Analysis

Before the discovery that SFM1257 (**3.43**) induced hemolysis, preliminary *in vivo* mouse studies were performed by Dr. Hyang Yeon Lee, and it was found that SFM1257 had a maximum tolerated dose (MTD) of 20 mg/kg for a single intraperitoneal (IP) injection with no lasting effects.¹⁴⁴ Lethargy and minor weight loss was observed at 20 mg/kg, but the mice recovered completely after 24 hours.¹⁴⁴ Upon determining the MTD,

preliminary pharmacokinetic (PK) studies were undertaken. For the PK analysis, three C57/BL6 mice were injected (IP) with SFM1257 (**3.43**) at 20 mg/kg as a PEG 400 formula, and the plasma concentrations were determined via HPLC. It was found that SFM1257 achieved a peak plasma concentration of 1.9 μ M with a half-life of 5.8 hours.¹⁴⁴ The preliminary MTD analysis was promising because it demonstrated that SFM1257 (**3.43**) was not overtly toxic. Additionally, the preliminary PK study showed that the compound is stable in a living system.

Figure 3.15. Pharmacokinetic Analysis of SFM1257 (**3.43**)¹⁴⁴



*N= 3, error bars represent standard error of mean (S.E.M.)

Despite these promising results, *in vivo* work with SFM1257 (**3.43**) was halted due to concerns about its hemolytic properties. As a result, the focus of further animal studies was shifted to SFM1258 (**3.44**) because it did not elicit hemolysis at high concentrations and was comparable in activity to SFM1257 (**3.43**). The MTD analysis performed for SFM1257 (**3.43**) was repeated for SFM1258 (**3.44**), and Dr. Hyang Yeon Lee determined that SFM1258 (**3.44**) was better tolerated than SFM1257 (**3.43**), with a MTD of 60 mg/kg.¹⁴⁴ Once again, Dr. Lee observed minor weight loss and general

lethargy, but the mice had recovered completely within 48 hours post treatment.^{96,144} No PK analysis was performed for SFM1258 (**3.44**).

3.3.5.2 Evaluation in Mouse Model for Breast Cancer

After determining that SFM1258 (**3.44**) was decently tolerated in mice and not overtly toxic, we sought to evaluate whether the compound had *in vivo* efficacy in a mouse model for breast cancer. The 4T1 syngeneic mouse model was used to evaluate the *in vivo* efficacy of the compound, and SFM1258 (**3.44**) was determined to be active against this particularly cell line ($IC_{50} = 10 \pm 3.1 \mu M$; $E_{max} = 99.7 \pm 0.5$; $HS = 4.0 \pm 0.9$).

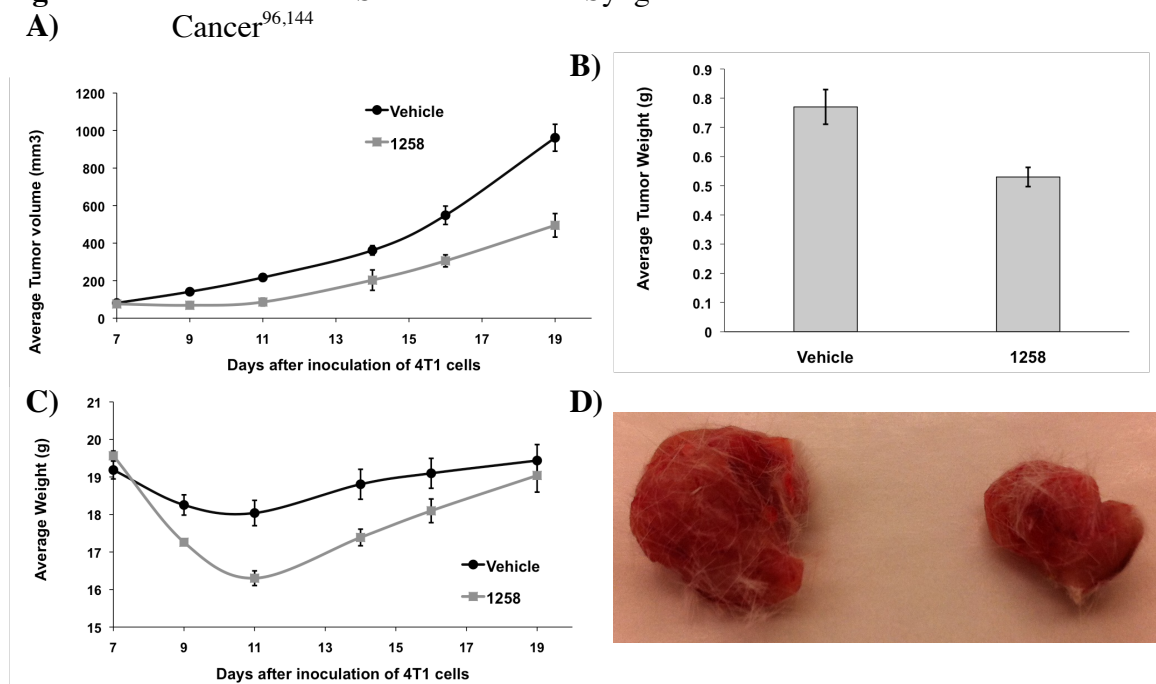
The 4T1 breast cancer model mimics very aggressive, highly metastatic breast cancer and correlates well to naturally occurring cancers. For starters, the tumor model is orthotopic and not a xenograph. Namely, the tumor is grown in the anatomically correct place, and the mouse has an intact immune system.¹⁴⁵ Additionally, the 4T1 model develops metastases spontaneously from the primary tumor and spreads to the draining lymph nodes and other organs in a manner similar to that of human breast cancer.¹⁴⁵

The experiment was set up as follows: Ten eight-week-old female Balb/c mice were injected with 10^6 4T1 murine breast cancer cells, and the mice were injected on days 7, 9, and 11 post inoculation (Figure 3.16) with SFM1258 (**3.44**) at 60 mg/kg IP in PEG-400 or an equal volume of PEG-400 (vehicle). The tumor volume and mouse weight was recorded every 2-3 days, and on day 19, the mice were sacrificed and the tumors excised (Figure 3.16).^{96,144}

Upon completion of the study, average tumor volumes and masses of mice treated with SFM1258 (**3.44**) were significantly reduced over those of the control group (Figure 3.16A and B), and an image of an excised tumor relative to the control is pictured in Figure 3.16D.^{96,144} Additionally, no overt toxicity was observed during the course of the

experiment, and although the mice did lose weight upon initial treatment of SFM1258 (3.44), they were fully recovered by the end of the experiment (Figure 3.16C). This exciting data showed that the SFM1258 (3.44) was efficacious in a very challenging mouse model for breast cancer, further validating the translational potential for these compounds.

Figure 3.16. Evaluation of SFM1258 in 4T1 Syngeneic Mouse Model for Breast Cancer^{96,144}



A) Tumor volume of SFM1258 treated mice vs vehicle **B)** Average tumor weight of SFM1258 and vehicle treated mice after excision **C)** Average weight of SFM1258 and vehicle treated mice during course of experiment **D)** Image of excised tumors treated with vehicle (left) and SFM1258 (right)

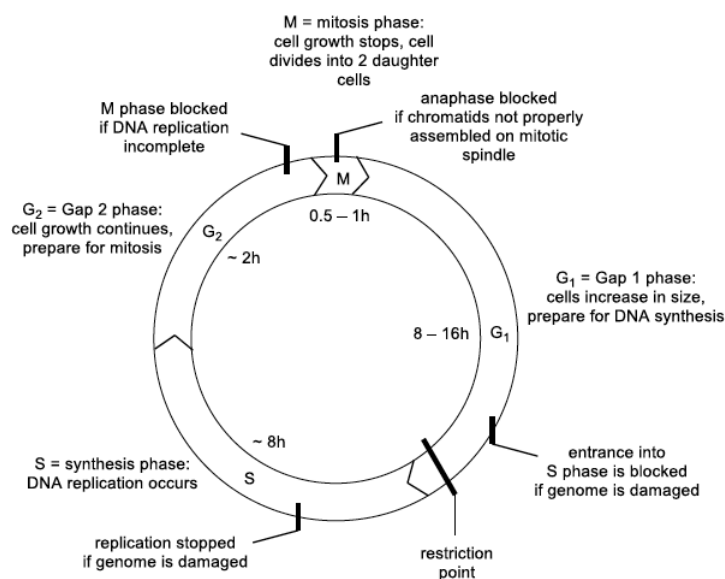
3.4 INVESTIGATION INTO MODE-OF-ACTION

While efforts were underway to evaluate the translational potential of SFM1257 (3.43) and SFM1258 (3.44), concurrent studies were being performed by Dr. Claire Knezevic to determine the mode-of-action for these compounds and identify their biological targets. Identifying the biological target will help guide structure-activity studies so that potency can be increased and non-specific interactions can be minimized.

3.4.1 Cell Cycle Arrest Assays

A cell cycle arrest analysis is a common experiment that can help elucidate the mode-of-action of a cytotoxin. For example, the FDA-approved chemotherapeutic paclitaxel (**3.1**) stabilizes microtubules and prevents chromosomes from achieving metaphase spindle configuration, subsequently blocking the progression of mitosis.^{146,147} As a result, cells dosed with paclitaxel or a different microtubule stabilizing reagent will overwhelmingly display G2/M cell cycle arrest.¹⁴⁷ Similarly, the topoisomerase inhibitor topotecan arrests progression through the cell cycle and demonstrates G2/M cell arrest by causing replication fork collisions in dividing cells.¹⁴⁸ Other toxins, such as the proteasome inhibitor bortezomib (velcade) or the nucleoside analog gemcitabine, induce cell death independent of the cell cycle phase.¹⁴⁹ Due to the extended times required to induce cell death (days) and their relatively short half-lives *in vivo* (hours), drugs that rely heavily on the phase of the cell cycle often induce fractional killing.¹⁵⁰ As a result, it has been shown that topotecan is more effective in treating ovarian cancer when delivered in smaller, more frequent doses than short exposure to high doses.¹⁵¹ Hence, knowledge pertaining to the cell cycle dependence of a drug is clinically relevant. Compounds that are associated with DNA damage, such as *cis*-platin, often show a preference for G1 phase cell death.¹⁵² The tumor suppressor protein p53 is activated upon detection of DNA damage and regulates the G1/S cell cycle checkpoint.¹⁵³ Thus, if a compound shows a strong preference for G1 cell cycle arrest, the mode-of-action may be p53 dependent.

Figure 3.17. The Cell Cycle and its Checkpoints¹⁵⁴



The cell cycle arrest analysis of SFM1257 (**3.43**) induced cell death proceeded as follows: Dr. Claire Knezevic synchronized U937 cells in the M phase using the non-toxic microtubule polymerization inhibitor nocodazole (**3.52**) (Figure 3.18).¹⁵⁵ Once the cells were synchronized, they were pelleted and washed to remove the nocodazole. The cells were then dosed with 4 μ M SFM1257 (**3.43**), and aliquots were removed and analyzed by flow cytometry. The phase of the cell cycle was determined by staining with propidium iodide (PI). PI is a DNA dye that fluoresces brightly when bound to DNA,¹⁵⁶ and the phase of the cell cycle is determined by the relative amount of PI fluorescence for each cell. If the relative fluorescence is equal to one, then the cell is in the G₁ phase, a fluorescence of two implies the G₂/M phase, and an intermediate amount of fluorescence implies the S phase. It was found that SFM1257 (**3.43**) overwhelmingly elicited arrest of the cell cycle in the G₁ phase (Figure 3.19).⁹⁵ This indicates that SFM1257 (**3.43**) likely does not act through the stabilization or destabilization of microtubules or inhibition of

topoisomerase, as this would trigger G2/M arrest. It indicates that the mode-of-action may be p53 dependent, but further investigation is required to validate that assertion.

Figure 3.18. The Structure of Nocodazole (**3.52**)

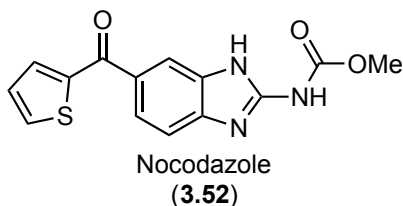
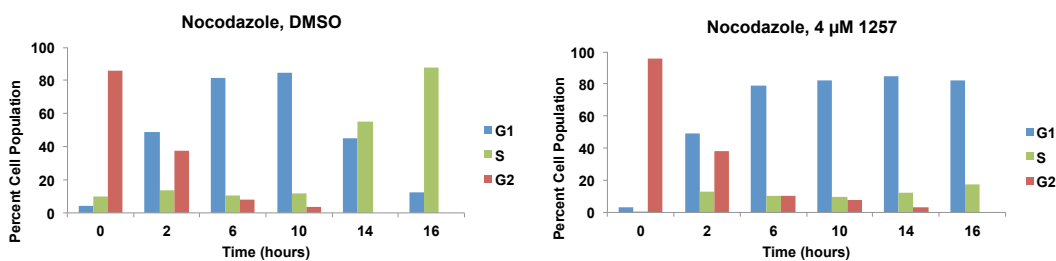


Figure 3.19. Cell Cycle Analysis of SFM1257 (**3.43**) Induced Cytotoxicity^{95,120}



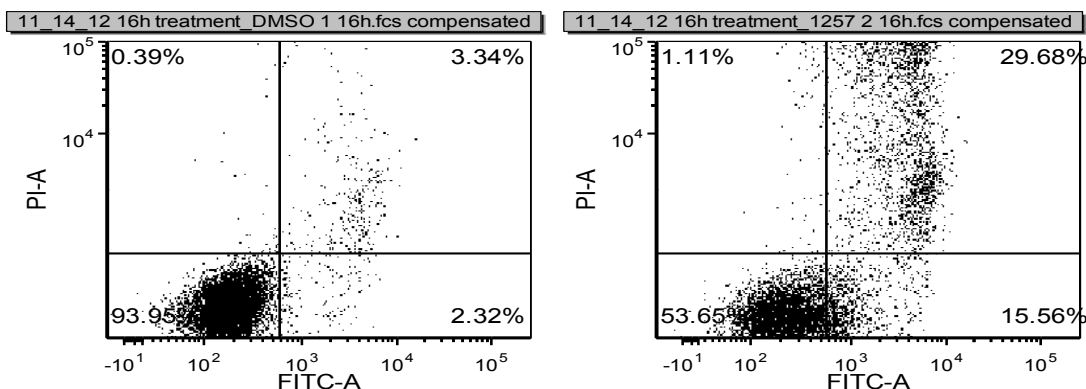
3.4.2 Annexin V and Propidium Iodide Staining

Apoptosis is an extensively studied form of programmed cell death that has well defined and well characterized biochemical pathways.¹⁵⁷⁻¹⁵⁹ Although apoptosis occurs naturally as a way of discarding and recycling old or damaged cells, external insults like radiation, heat, or a small molecule can trigger apoptosis.¹⁵⁸ An early indicator of apoptosis is the presence of phosphatidylserine (PTS) on the outer cell membrane. PTS is normally located on the inward-facing side of the cell membrane and inverts once the apoptotic mechanisms are triggered.¹⁵⁸ Once activated, PTS serves as a marker for phagocytic recognition so that apoptotic cells can be recognized and recycled by the immune system.¹⁵⁸ The fluorophore conjugated PTS antibody Annexin V-FITC is used to identify the presence of PTS on the outside of a cell. Annexin V is usually used in

conjunction with the DNA dye propidium iodide (PI).¹⁵⁶ In the context of flow cytometry, PI determines whether a cell is viable because PI cannot penetrate the cell membrane; thus if the wavelength for PI fluorescence is observed, the outer membrane of a cell has been compromised, and the cell is no longer viable.¹⁵⁶ When Annexin-V and PI are used in unison, a cell that is positive for Annexin-V but negative for PI is in the early stages of apoptosis. If a cell is positive for PI and Annexin-V, the cell is no longer viable and may or may not have undergone apoptosis.

To evaluate whether SFM1257 (**3.43**) elicits apoptotic cell death, U937 lymphoma cells were incubated with 4 μ M SFM1257 (**3.43**) for 16 hours, and the cells were evaluated by PI/Annexin V staining using flow cytometry.⁹⁵ It was found that a small percentage of the cells (~15%) were in the classical apoptotic quadrant (PI negative/Annexin V positive; lower right corner Figure 3.20).⁹⁵ This result indicates that at least some of the cells underwent classical apoptosis. However, this result alone is not enough to unambiguously determine that apoptosis is the major driver of cell death; other experiments must be run to further validate this finding.

Figure 3.20. Dot Plots for PI/Annexin V-FITC Staining



3.4.3 Small Molecule Inhibitors

One way to probe the mechanism of action of a cytotoxic agent is to determine which proteins are necessary for its function. There is a litany of small molecule probes with well-defined and well-characterized biological targets that can be used to block specific cell signaling pathways. Thus, if a small molecule inhibitor reduces or prevents the toxicity attributed to a cytotoxin, it can be inferred that the pathway blocked by the inhibitor is involved in the mode-of-action of the cytotoxin.

3.4.3.1 Small Molecule Inhibitors of Apoptosis

Given that the preliminary flow cytometry experiments indicated that SFM1257 (**3.43**) was causing apoptosis, Dr. Claire Knezevic screened numerous small molecule inhibitors of apoptosis (Figure 3.21, **3.53-63**) to further evaluate that observation. A graphical depiction of the various apoptotic signal transduction pathways and known small molecule inhibitors of those pathways are shown in Figure 3.22. The general procedure for evaluating effect of tool compounds on SFM1257 (**3.43**) toxicity was to preincubate U937 cells with the tool compound for two hours, then add SFM1257 (**3.43**) as a DMSO solution so that the final concentration was 9 μM . After three hours of incubation with SFM1257 (**3.43**), the cellular viability was assessed via flow cytometry.⁹⁵

Figure 3.21. Structures of Apoptosis Inhibitors

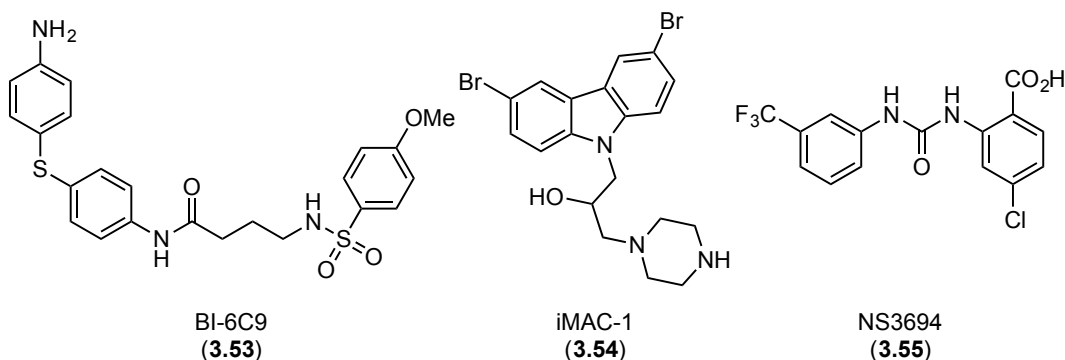


Figure 3.21., cont.

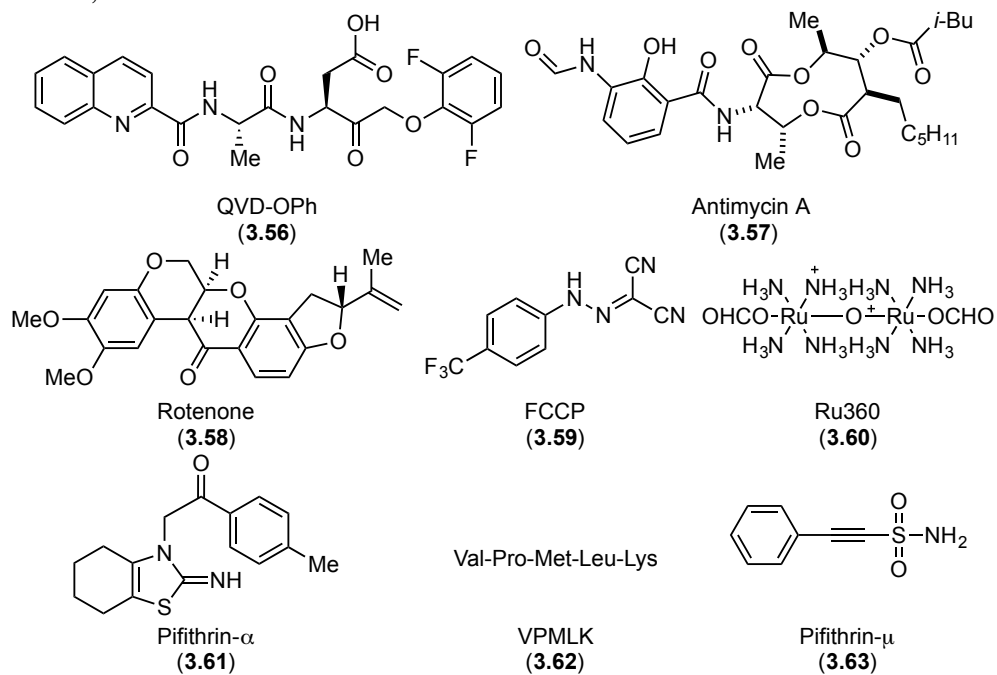
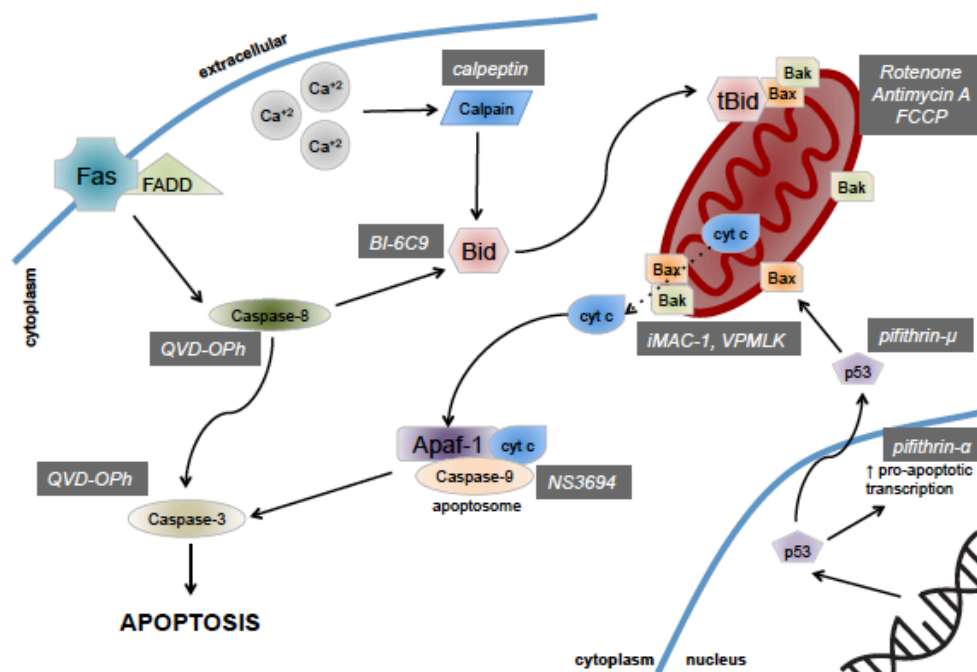


Figure 3.22. Apoptotic Signaling Pathways and Their Small Molecule Inhibitors⁹⁵



Initially, the pan-caspase inhibitor Q-VD-OPh (**3.55**) was used, and no cytoprotection was observed (Figure 3.23).⁹⁵ Q-VD-OPh inhibits caspase 9/3, caspase 8/10, and caspase 12;¹⁶⁰ thus, Dr. Knezevic concluded that SFM1257 (**3.43**) does not rely exclusively on caspase activation to elicit cell death. Given that apoptosis can occur in both caspase-dependent and caspase-independent pathways, other apoptotic pathways were examined.

The compounds antimycin A (**3.57**), rotenone (**3.58**), and FCCP (**3.59**) are chemical probes that disrupt ATP synthesis by interfering with oxidative phosphorylation; since ATP is required for apoptosis, blocking ATP production should prevent apoptosis.^{161,162} No protection was observed for rotenone (**3.58**) and FCCP (**3.59**), yet modest cytoprotection was seen with antimycin A (**3.57**) (Figure 3.23).⁹⁵ Since antimycin A (**3.57**) was in disagreement with the rotenone (**3.58**) and FCCP (**3.59**), Dr. Knezevic concluded that the observed cytoprotection by antimycin A was likely attributed to something other than the decoupling of oxidative phosphorylation.

Variations in cytosolic calcium levels effect mitochondrial function, and the regulation of mitochondrial calcium levels is key to preserving proper cellular function. When there is a build up of cytosolic calcium, the mitochondrial permeability transition pore (MPTP) is activated, and pro-apoptotic proteins, such as cytochrome C, are released.¹⁶³ The ruthenium complex Ru360 (**3.60**) blocks the MPTP, affording cytoprotection.¹⁶³ Since Dr. Knezevic observed no cytoprotection, it is likely that cytosolic calcium build up is not causing cell death (Figure 3.23).⁹⁵

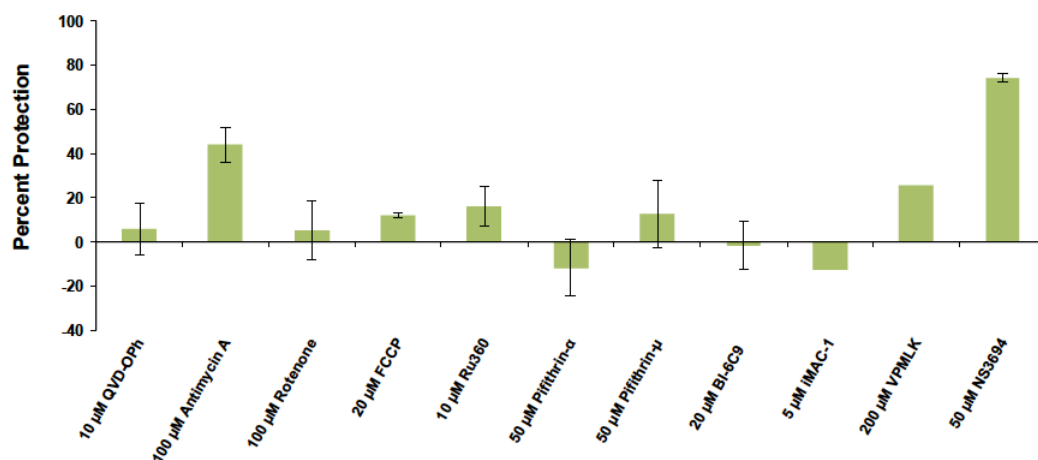
The pifithrins are used to evaluate the role of p53 signalling in cell death. The transcription factor p53 is often referred to as the ‘tumor suppressor protein’ because it is capable of identifying DNA damage and triggering apoptosis.^{164,165} The compound pifithrin- α (**3.61**) blocks p53 from transcribing pro-apoptotic genes, and pifithrin- μ (**3.63**)

blocks pro-apoptotic signaling caused when p53 binds to the mitochondria and the mitochondrial proteins Bcl-xL and Bcl-2.^{164,166} Since no protection was observed with either compound, Dr. Knezevic concluded that p53 did not play a role in SFM1257 (**3.43**) induced cell death (Figure 3.23).⁹⁵

The compound BI-6C9 (**3.53**) inhibits the cleavage of the pro-apoptotic enzyme Bid by caspase 8 (Figure 3.22).¹⁶⁷ The cleaved fragment of Bid, tBid, localizes to the mitochondria and causes the oligomerization of Bax and Bak, which in turn permeabilizes the mitochondrial membrane to allow for release of the proapoptotic protein cytochrome C.¹⁶⁷ The compounds iMAC-1 (**3.54**) and VPMLK (**3.62**) work to prevent Bax and Bak mediated release of cytochrome C.^{168,169} Since Dr. Knezevic observed no protection with any of the three compounds, it was concluded that Bid, Bax, or Bak do not play a key role in SFM1257 (**3.43**) mediated cell death (Figure 3.23).⁹⁵

In caspase-dependent apoptosis, cytochrome C is released from the mitochondria and combines with apaf-1 (apoptotic protease activating factor 1) to form a 700 kDa heptamer complex called the apoptosome, which in turn activates procaspase-9 and procaspase-3.¹⁷⁰ The tool compound NS3694 (**3.55**) inhibits the formation of the apoptosome and prevents the activation of procaspase-9.¹⁷¹ Oddly, Dr. Knezevic found that NS3694 (**3.55**) afforded robust cytoprotection, implying that apoptosome formation is necessary for SFM1257 (**3.43**) induced cytotoxicity, but caspase activation and cytochrome C release is not.⁹⁵ Given the inconsistent nature of these results, Dr. Knezevic hypothesized that NS3694 is preventing SFM1257 (**3.43**) toxicity through a manner other than inhibiting the apoptosome.

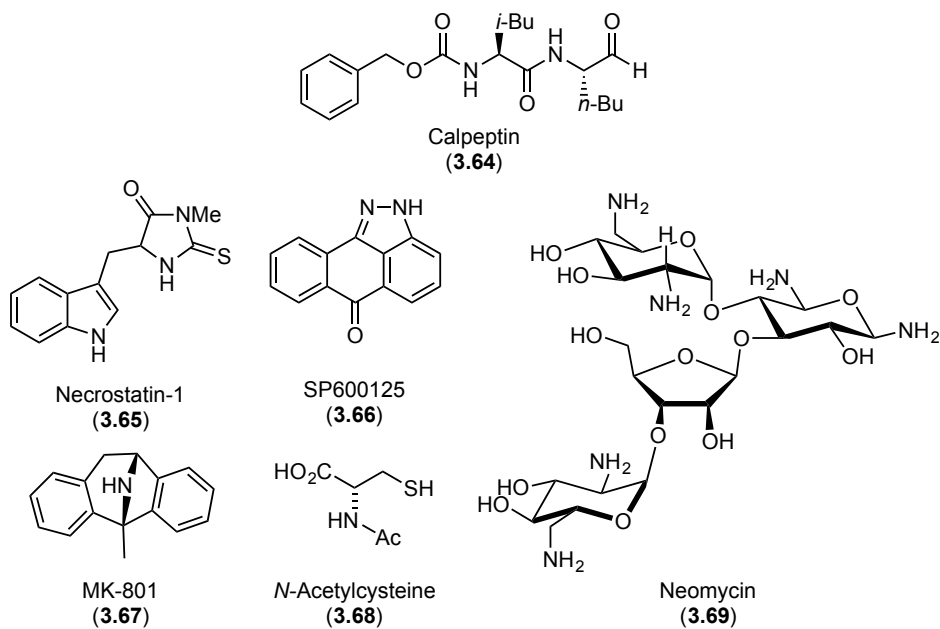
Figure 3.23. Tool Compounds Used to Block Apoptosis⁹⁵



3.4.3.2 Necrosis and Other inhibitors

The lack of robust and consistent cytoprotection by apoptosis inhibitors led Dr. Knezevic to conclude that cell death caused by SFM1257 (**3.43**) is not exclusively apoptotic. To elucidate what other pathways may be involved, small molecule inhibitors of necrosis and other forms of cell death were investigated (Figure 3.24, **3.64-69**).

Figure 3.24. Structures of Tool Compounds Used to Block Non-Apoptotic Cell Death



Necrosis is a form of non-programmed inflammatory cell death that is characterized by the rupturing of the cell membrane and the spilling of the cytosolic components into the extracellular space; it is typically a result of external factors such as infection, toxins, or trauma.¹⁵⁷ Similarly, necroptosis is a form of cell death that is characterized by necrotic morphologies, yet it is activated through a well-defined nonapoptotic pathway.¹⁷² The kinase inhibitors necrostatin-1 (**3.65**) and SP600125 (**3.66**) target key signaling pathways involved in necroptosis; Necrostatin-1 (**3.65**) inhibits RIP Kinase (RIPK)¹⁷² and SP600125 (**3.66**) inhibits c-Jun N-terminal kinases (JNK).¹⁷³ Unfortunately, Dr. Knezevic observed that neither compound afforded significant protection from SFM1257 (**3.43**) induced cell death (Figure 3.25).⁹⁵

The calpains are a class of calcium-activated proteases that have roles in both apoptosis and necrosis; overactivity of the calpains is tied to neurological disorders and Alzheimer's disease.¹⁷⁴ The calpain inhibitor calpeptin (**3.64**)¹⁷⁵ afforded no cytoprotection, meaning SFM1257 (**3.43**) toxicity is not coupled to calpain activity (Figure 3.25).⁹⁵

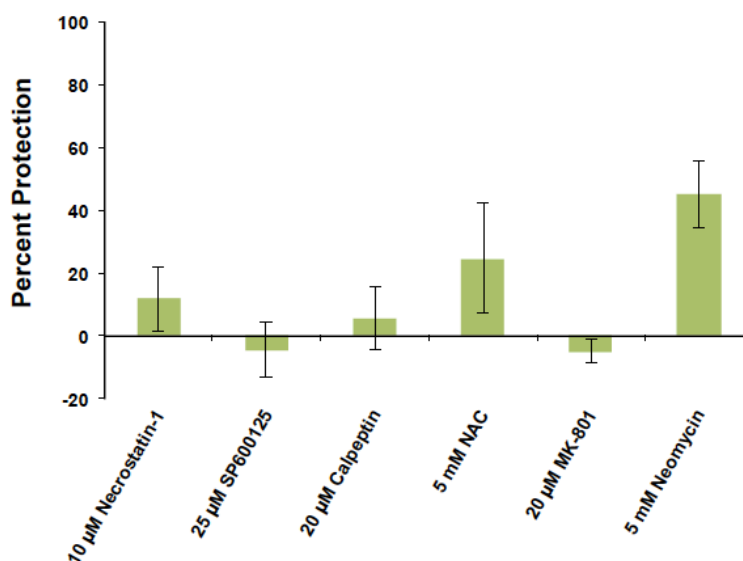
Excitotoxicity is a form of cell death caused by hyperactivity of the NMDA receptor, which leads to a massive influx of extracellular Ca^{2+} .¹⁷⁶ The NMDA antagonist MK-801,¹⁷⁷ which blocks the extracellular Ca^{2+} influx associated with excitotoxicity and other neurological disorders, provided no cytoprotection from SFM1257 (**3.43**) induced cell death (Figure 3.25),⁹⁵ indicating that extracellular calcium influx through the NMDA receptor is not a cause of cell death.

Disruption of normal mitochondrial function can lead to an accumulation of reactive oxygen species (ROS), which in turn can cause DNA damage and PARP-1 induced cell death, parthanatos.¹⁷⁸ Dr. Knezevic evaluated the ROS scavenger *N*-acetyl cysteine (NAC)¹⁷⁹ for its ability to mitigate SFM1257 (**3.43**) induced cytotoxicity, and

modest protection was observed (Figure 3.25).⁹⁵ This implies that ROS generation may play a role in SFM1257 (**3.43**) toxicity, but ROS generation is only a minor driver of SFM1257 (**3.43**) induced cell death.

The inositol triphosphate receptor (IP₃R) is an endoplasmic reticulum membrane-bound protein that regulates intracellular Ca²⁺ homeostasis, and consequences of IP₃R dysregulation are tied to necrotic and apoptotic cell death.^{180,181} The antibiotic neomycin (**3.69**) binds to and sequesters inositol triphosphate (IP₃), which is a native ligand for IP₃R. If agonism of IP₃R is causing SFM1257 (**3.43**) induced cell death, neomycin (**3.69**) should mitigate that effect.¹⁸² Dr. Knezevic found that neomycin (**3.69**) decreased sensitivity of U937 cells to SFM1257 (**3.43**), affording roughly 50% cytoprotection (Figure 3.25).⁹⁵ Since dysregulation of IP₃R is associated with endoplasmic reticulum (ER) stress, Dr. Knezevic determined that small molecule inhibitors of ER stress related pathways should be investigated next.

Figure 3.25. Tool Compounds Used to Block Non-Apoptotic Cell Death⁹⁵



3.4.3.3 Endoplasmic Reticulum Stress Inhibitors

The unfolded protein response is a biochemical process used to mitigate cellular stress resulting from the accumulation of misfolded proteins in the endoplasmic reticulum (ER). ER stress can be caused by a number of diseases and pathologies, including cancer,^{183,184} viral infection,¹⁸⁵ Alzheimer's disease,^{186,187} and other neurological disorders.¹⁸⁸ As a result, the biochemical constituents that control the UPR have become targets of interest for numerous drug discovery campaigns.¹⁸⁹

The UPR initiates when misfolded proteins accumulate in the ER and cause binding immunoglobulin protein (BiP) to dissociate from the luminal side of the transmembrane proteins inositol-requiring enzyme 1 alpha (IRE1 α), protein kinase RNA-like endoplasmic reticulum kinase (PERK), and activating transcription factor 6 (ATF6) (Figure 3.26).¹⁹⁰ Upon dissociation of BiP, PERK and IRE1 α homodimerize and autophosphorylate, leading to downstream signaling of pro-survival processes, and ATF6 translocates and serves as a transcription factor for pro-cell survival proteins.¹⁹⁰ There is a delicate balance between the initial pro-survival signaling and eventual pro-death signaling of PERK, IRE1 α , and ATF6; sustained activation of the UPR eventually leads to the transcription of pro-apoptotic proteins.¹⁹⁰ To investigate the role of ER stress in SFM1257 (**3.43**) induced toxicity, Dr. Knezevic screened several small molecule inhibitors (Figure 3.27, **3.70-76**) of ER stress related pathways. A diagram summarizing the signaling pathways involved in the UPR and their small molecule inhibitors is shown in Figure 3.26.

Figure 3.26. The Unfolded Protein Response Signaling Pathway and Its Small Molecule Inhibitors⁹⁵

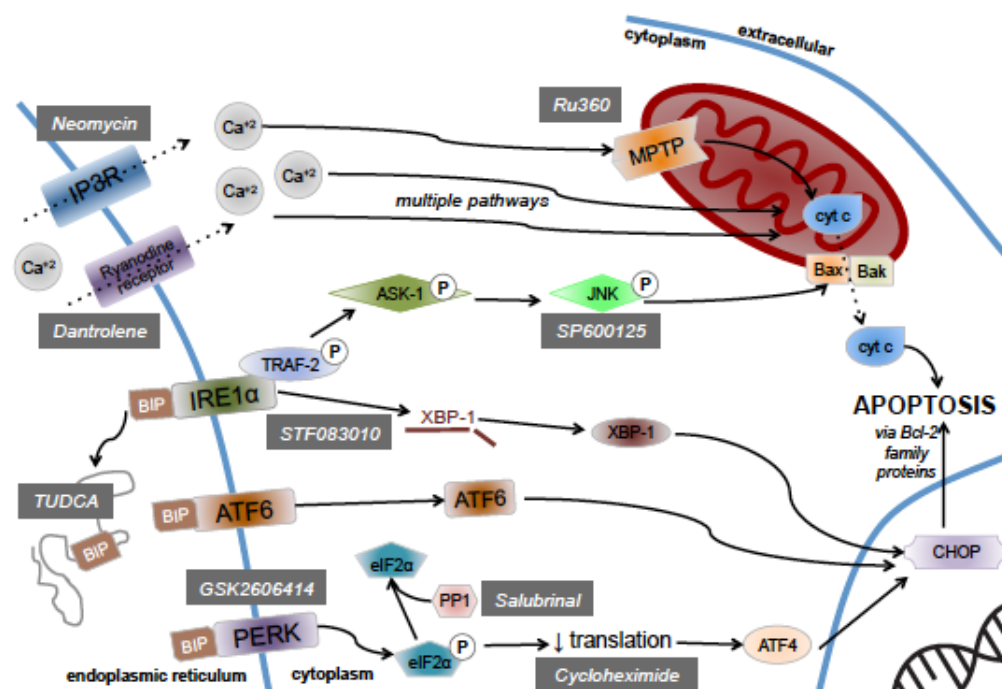
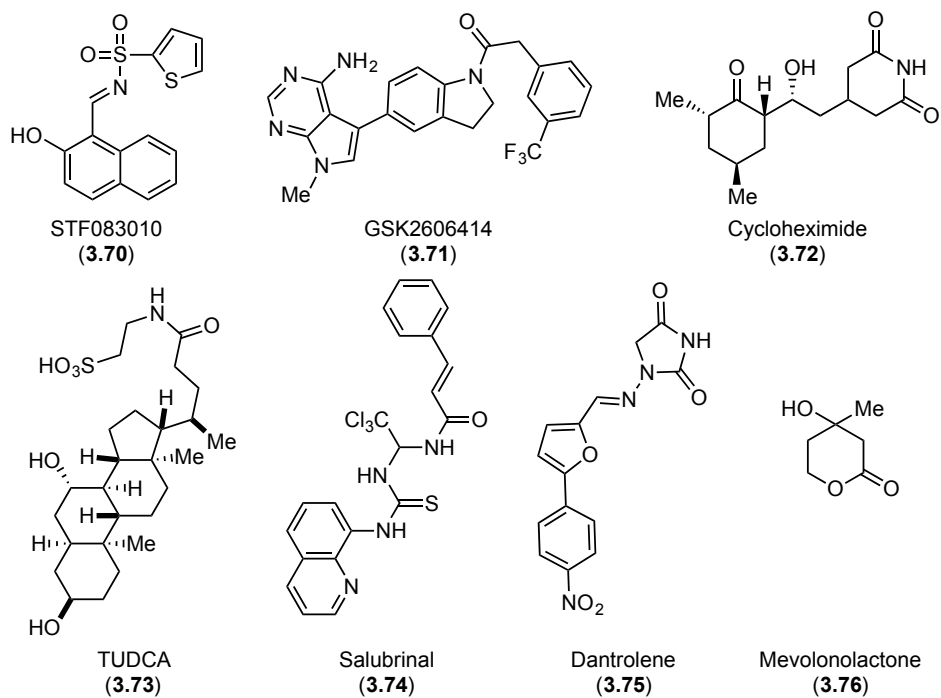


Figure 3.27. Structures of Endoplasmic Reticulum Stress Inhibitors



One of the pro-survival mechanisms of IRE1 α is its endonuclease activity, which works in parallel to its kinase activity.¹⁹⁰ The chemical probe SF083010 (**3.70**) blocks the activation of X-box binding protein 1 (XBP1) mRNA by IRE1 α , which in turn prevents the transcription of pro-survival proteins.¹⁹¹ It was found that SF083010 (**3.70**) enhanced SFM1257 (**3.43**) toxicity, indicating ER stress may play a role in the mode-of-action of SFM1257 (**3.43**) (Figure 3.28).⁹⁵

The small molecule GSK2606414 (**3.71**) is an inhibitor of PERK, and since prolonged activation of PERK leads to pro-apoptotic signaling, inhibition of PERK may impart cytoprotection in cell experiencing ER stress.¹⁹² the PERK inhibitor GSK2606414 (**3.71**) afforded no cytoprotection against (Figure 3.28), implying PERK signaling is not necessary for SFM1257 (**3.43**) induced cell death.⁹⁵

ER stress can be a result of the accumulation of misfolded proteins; the small molecules TUDCA (**3.73**) and cycloheximide (**3.72**) are known to mitigate that insult. TUDCA (**3.73**) upregulates chaperone proteins that assist with folding and cycloheximide (**3.72**) inhibits protein translation.^{193,194} Dr. Knezevic observed that neither compound afforded cytoprotection (Figure 3.28), implying SFM1257 (**3.43**) does not cause a build up of misfolded proteins.⁹⁵

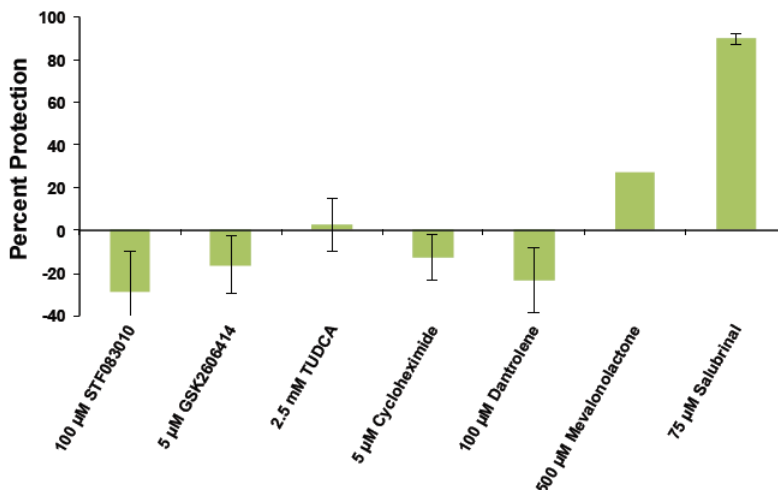
Since neomycin afforded cytoprotection, the role of calcium efflux was investigated further. The ryanodine receptor works in conjunction with the IP₃R receptor to regulate cytosolic Ca²⁺ levels.¹⁹⁵ The ryanodine receptor inhibitor dantrolene (**3.75**)¹⁹⁶ afforded no cytoprotection, implying calcium efflux through the ryanodine reception does not play a role in SFM1257 (**3.43**) toxicity (Figure 3.28).⁹⁵

The ER is also responsible for the synthesis of cholesterol, and interference with cholesterol synthesis can lead to ER stress.¹⁹⁷ However, supplementing cholesterol

synthesis with mevalonolactone (**3.76**)¹⁹⁷ afforded only slight cytoprotection (Figure 3.28), indicating SFM1257 (**3.43**) is likely not due to inhibition of cholesterol synthesis.⁹⁵

The compound salubrinal (**3.74**) is an inhibitor of both the ER stress-induced holoenzyme protein phosphatase 1/growth arrest and DNA damage-inducible protein 34 (PP1/GADD34) as well as the constitutively active holoenzyme phosphatase protein phosphatase 1/constitutive repressor of eIF2 α phosphorylation (PP1/CreP).^{189,198} Dr. Knezevic found that salubrinal (**3.74**) provided robust protection against SFM1257 (**3.43**) toxicity (Figure 3.28), providing strong evidence that ER stress is one key driver of SFM1257 (**3.43**) cytotoxicity.⁹⁵

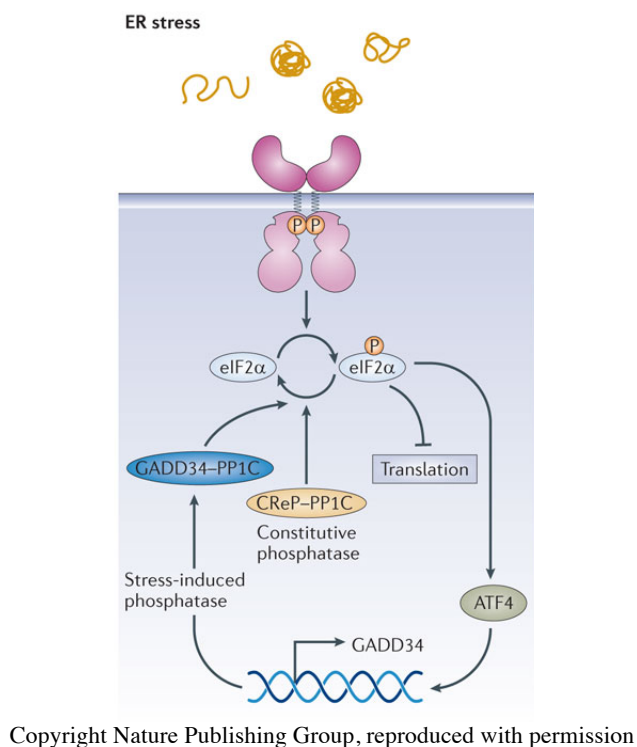
Figure 3.28. Tool Compounds Used to Mitigate Endoplasmic Reticulum Stress⁹⁵



The cytoprotective properties of salubrinal (**3.74**) are well documented; it has been demonstrated to mitigate the effects of ER stress caused by tunicamycin,¹⁹⁸ rotenone,¹⁹⁹ and kainic acid²⁰⁰ but not thapsigargin.²⁰¹ When the UPR is activated, PERK phosphorylates eukaryotic translation initiation factor 2 α (eIF2 α), which in turn works to reduce the stress applied to the ER by halting met-tRNA initiated protein translation and upregulating translation of activating transcription factor 4 (ATF4)

(Figure 3.29).¹⁸⁹ ATF4 is a transcription factor for GADD34, and the phosphatases PP1/CreP and PP1/GADD34 dephosphorylate p-eIF2 α to return translation to normal levels; thus, GADD34 serves in a negative feedback loop.¹⁸⁹ Salubrinal (**3.74**) inhibits both phosphatases and thus reduces ER stress by maintaining low levels of protein translation. Additionally, the decrease in global translation is accompanied by an increase in chaperone proteins that aid in protein folding.¹⁸⁹ Thus, salubrinal (**3.74**) decreases the protein load applied to the ER and increases the folding capacity of the ER to counteract ER stress. Therefore, it is likely that SFM1257 (**3.43**) is causing toxic levels of ER stress that are capable of being mitigated through innate cellular processes.

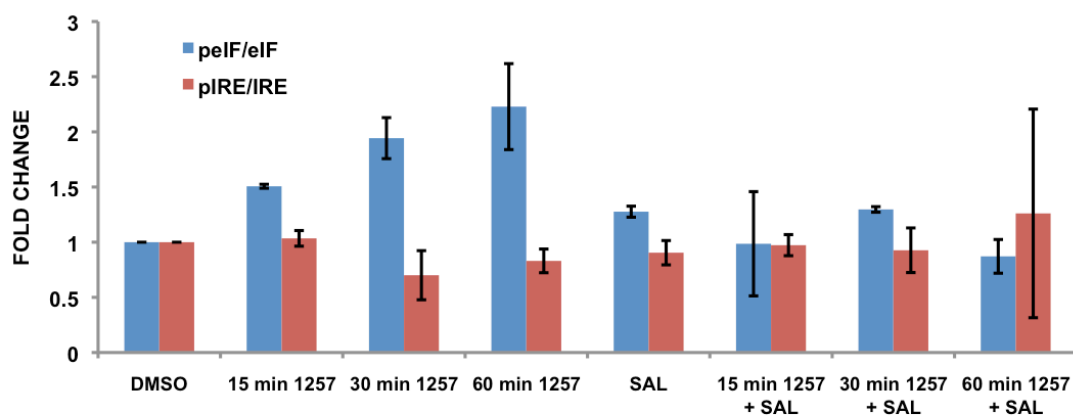
Figure 3.29. Schematic Representation of PERK Signalling¹⁸⁹



3.4.4 Western Blot Analysis for ER Stress Markers

After discovering that salubrinal (**3.74**) provided robust cytoprotection from SFM1257 (**3.43**) induced cytotoxicity, ER stress was assigned as the mode-of-action for SFM1257 (**3.43**). To further validate this hypothesis, specific biochemical markers were analyzed and quantified. Since the unfolded protein response activates PERK and IRE1 simultaneously, one would expect to see increased levels of p-eIF2 α and p-IRE1 (Figure 3.30). As expected, SFM1257 (**3.43**) caused an immediate and dramatic increase in the levels of p-eIF2 α , yet little to no change was observed in p-IRE1 levels (Figure 3.30).^{95,96} This would imply that PERK was activated in the absence of IRE1, which would be unlikely unless SFM1257 (**3.43**) was activating PERK directly. Given that the PERK inhibitor GSK2606414 (**3.71**) provided no cytoprotection (Figure 3.28), that hypothesis is unlikely. Additionally, one would expect the levels of p-eIF2 α to be roughly equivalent with or without the addition of salubrinal (**3.74**). In fact, cells treated with salubrinal (**3.74**) typically see a slight increase in p-eIF2 α levels because salubrinal (**3.74**) inhibits the phosphatases that reduce p-eIF2 α levels.¹⁹⁸ Instead, it was observed that salubrinal (**3.74**) prevented the phosphorylation of eIF2 α . This observation has several potential implications: 1) though highly unlikely, salubrinal (**3.74**) may be reacting irreversibly with SFM1257 (**3.43**); 2) salubrinal (**3.74**) may prevent cellular uptake of SFM1257 (**3.43**); and/or 3) salubrinal (**3.74**) may out compete SFM1257 (**3.43**) for the same target, implying SFM1257 (**3.43**) triggers ER stress by directly inhibiting eIF2 α phosphatases PP1/GADD34 and PP1/CreP. Thus, additional small molecule inhibitors of eIF2 α phosphatases need to be evaluated in order to verify that the observed protection with salubrinal (**3.74**) is due to inhibition of PP1/GADD34 and not an off-target effect.

Figure 3.30. Western Blot Analysis of eIF2 α and IRE1 Levels⁹⁶



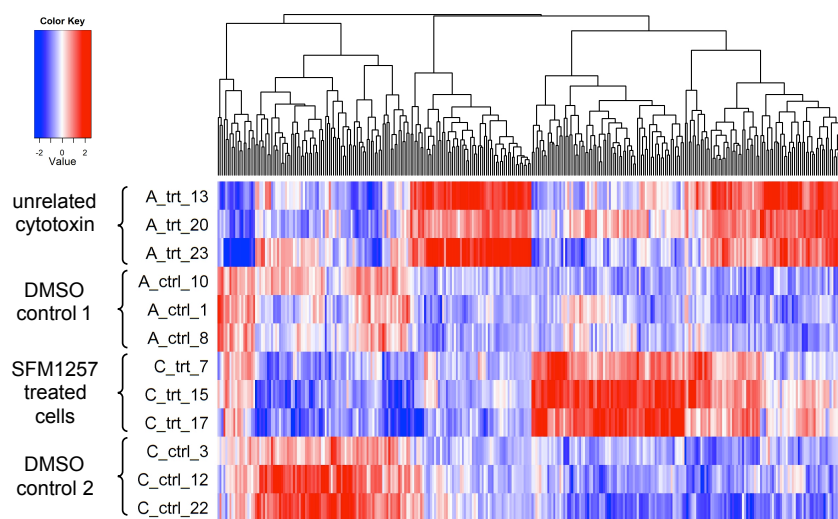
3.4.5 Transcript Profiling and Connectivity Map Analysis

To help shed further insight into the mode-of-action of SFM1257 (**3.43**), transcript profiling was performed to analyze how the transcriptome responds to SMF1257 (**3.43**). To describe simplistically, transcript profiling involves isolating the mRNA from a cell, using high-throughput microarray technology to determine the level of each transcript, and analyzing the levels of each transcript relative to a control.²⁰²

3.4.5.1 Initial Results and Preliminary Analysis

The transcript profiles of U937 cells incubated with SFM1257 (**3.43**), DMSO, and an unrelated cytotoxin were obtained. The collected data were converted to the heat map shown in Figure 3.31, and it was found that the transcript profile of SFM1257 (**3.43**) treated cells differed from the DMSO controls.⁹⁵ Additionally, the SFM1257 (**3.43**) transcript profile also differed from an unrelated cytotoxin, which is to be expected due to the toxins having unrelated mode-of-action.⁹⁵

Figure 3.31. Heat Map Analysis of Transcript Levels⁹⁵



The list of up- and down-regulated genes are listed in Table 3.3. The most up-regulated gene was IFIT-2 (interferon-induced protein with tetraco peptide repeats 2), and IFIT-2 has been shown to promote apoptosis when it forms complexes with IFIT-1 and IFIT-3.²⁰³ Since IFIT-1 and IFIT-3 were upregulated as well, it is possible that the cytotoxicity of SFM1257 (**3.43**) is tied to these genes. The IFIT genes are involved in a number of cellular processes designed to fight viral infections, and coincidentally, ER stress plays a key role in stopping viral infections by preventing the synthesis of viral proteins.^{185,204} Therefore, SFM1257 (**3.43**) may induce ER stress in a manner that mimics a viral infection. The gene CCNG2 was enriched as well, which is interesting because CCNG2 codes for cyclin G2, and cyclin G2 is known to cause G1 arrest, which is in agreement with cell cycle arrest studies (Figure 3.19).²⁰⁵ Additionally, there are automated analysis methods that are capable of comparing the transcript profile of a given compound a database of literature compounds that have known modes-of-action.²⁰⁶ Thus, if the transcript profile of SFM1257 (**3.43**) has high similarity with a known

cytotoxin, it is likely they share a similar mode-of-action. One such analysis method is the Connectivity Map database developed by the Broad Institute.

Table 3.3. Genes Significantly Up- and Down-regulated by SFM1257 (**3.43**)⁹⁵

Gene Name	Fold Change	Gene Name	Fold Change
IFIT2	11.17	TPGS1	-2.68
CYP51A1	5.84	RRP9	-2.69
RNA28S5	5.30	ZMAT5	-2.70
CCNG2	4.75	LTBP3	-2.71
PLEKHF2	4.54	LPHN1	-2.73
RANGRF	4.54	MCAT	-2.74
SLC26A11	4.21	GAMT	-2.75
MSMO1	4.21	TMEM161A	-2.77
SLC38A2	3.91	ECE2	-2.79
KRBA1	3.87	DESI1	-2.81
LY96	3.87	PRAM1	-2.92
CTH	3.81	ATP5D	-3.02
STAT2	3.65	LOC150223	-3.03
TMUB2	3.61	HYAL2	-3.10
TSC22D3	3.60	ZMAT5	-3.15
INSIG1	3.55	BIK	-3.23
TXNIP	3.55	UNC93B1	-3.30
ALB	3.53	CERCAM	-3.30
HMGCS1	3.49	TPSAB1	-3.50
FAM214A	3.45	NFKBIB	-3.50
CLIC4	3.36	ADRM1	-3.51
FAM27E3	3.35	TPSAB1	-3.57
IFIT3	3.27	FAM108A1	-3.67
IFIT1	3.25	FAM101B	-3.71
ASNS	3.14	AZU1	-3.76
C4orf34	3.11	LRRC33	-3.83
FAM214A	3.02	CCDC86	-4.08
RGS12	3.02	SPI1	-4.35
BCL2A1	3.00	NCF1	-4.36
HAVCR2	2.98	PRTN3	-4.53

3.4.5.2 Connectivity Map Analysis

The Broad Institute developed the Connectivity Map database (CMAP) to allow for the easy comparison of the transcript profiles for over 10,000 known compounds.²⁰⁶ The use of the Connectivity Map to uncover the mode-of-action for a compound has been well documented and reviewed.²⁰² Inputting the data obtained from the transcript profiling experiment to CMAP uncovered a number of compounds (Figure 3.32, **3.77-93**) with high similarity; however, none of compounds identified would be described as anticancer agents. Instead, the majority of the matches are in use as antihistamines, antipsychotics, or antibiotics (Table 3.4).⁹⁵

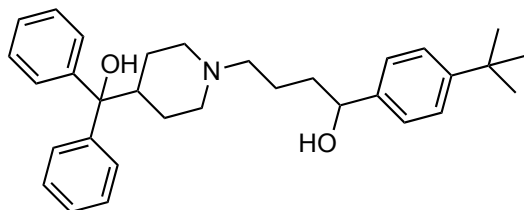
The majority of the compounds identified can cause an imbalance in cytosolic Ca^{2+} level, thus indicating SFM1257 (**3.43**) may trigger an imbalance in Ca^{2+} levels. Since ER stress is often associated with changes in cytosolic Ca^{2+} levels, it is not surprising the Ca^{2+} channel blockers tetrandine (**3.84**)²⁰⁷ and prenylamine (**3.87**)²⁰⁸ showed high similarity to SFM1257 (**3.43**). Tetrandine (**3.84**) has also been shown to block autophagic flux and trigger apoptosis in cancer cells through lysosomal deacidification.²⁰⁹ The anti-diarrhea drug loperamide (**3.86**) is a μ -receptor agonist that has also been shown to act as a Ca^{2+} channel blocker.²¹⁰ Dopamine receptors have also been shown to regulate intercellular calcium levels in neurons,²¹¹ so the similarity to the dopamine antagonists thioridazine (**3.83**), trifluoperazine (**3.88**), fluspirilene (**3.89**), prochlorperazine (**3.90**), and desipramine (**3.92**) is understandable.²¹² ER stress is also associated with the arrest of protein translation, so the high similarity to translation inhibiting aminonucleotide puromycin (**3.81**) is not unexpected.²¹³ The heat shock protein 90 (Hsp90) inhibitor geldanamycin (**3.93**) has been also shown to induce ER stress as well as hemolysis,²¹⁴ which are both characteristics of the cellular response to SFM1257 (**3.43**).

The highest similarity match was the antihistamine terfinadine (**3.77**), which is not longer used clinically due to concerns over cardiotoxicity.²¹⁵ Like SFM1257 (**3.43**), terfinadine elicits G1 phase cell cycle arrest and apoptotic cell death.²¹⁶ Additionally, it has also been shown that the anticancer effects of terfinadine (**3.77**) are not due to its antihistamine properties, but rather a result of large increases in cytosolic calcium levels.²¹⁷ As a result, the CMAP analysis appears to indicate that Ca²⁺ regulation is key characteristic of the cellular response to SFM1257 (**3.43**).

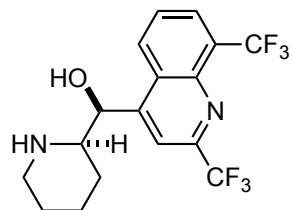
Table 3.4. Compound Identified by Connectivity Map Analysis⁹⁵

Perturbagen	Mean Score	Clinical Use(s)	Target (molecule/pathway)
Terfenadine (3.77)	0.808	antihistamine, cardiotoxic	histamine H1 receptor and HERG antagonist
Mefloquine (3.78)	0.77	antimalarial	heme polymerase inhibitor, analogous to chloroquine
Benzethonium Chloride (3.79)	0.77	food additive, surfactant, antiinfective, topical antimicrobial	unknown
Puromycin (3.81)	0.749	antibiotic	translation inhibitor, aminonucleoside
MG-262 (3.80)	0.702	Lon protease inhibitor	selective and reversible inhibitor of proteasome
Astemizole (3.81)	0.697	antihistamine	histamine H1 receptor antagonist, similar to terfenadine
Thioridazine (3.83)	0.685	antipsychotic	inhibits dopamine D1 and D2 receptors, block alpha-andrenergic effect
Tetrandrine (3.84)	0.663	Ca ²⁺ channel blocker	Ca ²⁺ channel inhibitor, causes G1 arrest and apoptosis
Metixene (3.85)	0.646	anticholinergic	muscarinic acetylcholine receptor M1-5
Loperamide (3.86)	0.645	antidiarrheal (imodium)	μ -opioid receptor agonist, similar to morphine
Prenylamine (3.87)	0.642	Ca ²⁺ channel blocker	depletes myocardial catecholamine stores, monoamine transporter inhibitor
Trifluoperazine (3.88)	0.629	antipsychotic	inhibits dopamine D1 and D2 receptors
Fluspirilene (3.89)	0.628	antipsychotic	inhibits dopamine D2 receptor and voltage-dependent Ca ²⁺ channel gamma-1 subunit
Prochlorperazine (3.90)	0.617	antipsychotic	inhibits dopamine receptor
Rescinnamine (3.91)	0.609	antihypertensive	angiotensin-converting enzyme inhibitor
Desipramine (3.92)	0.608	antidepressant	inhibits reuptake of norepinephrine and serotonin
Geldanamycin (3.93)	0.602	antibiotic	inhibits HSP90 and GRP94

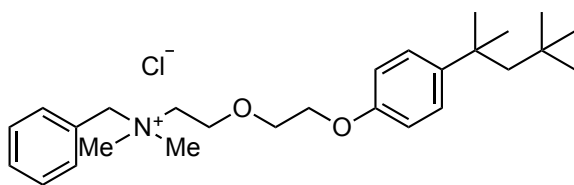
Figure 3.32. Structures of High Similarity Matches



terfenadine
(3.77)



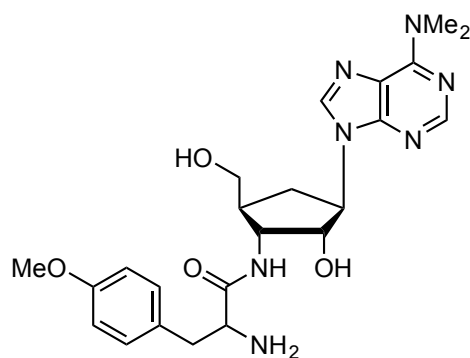
mefloquine
(3.78)



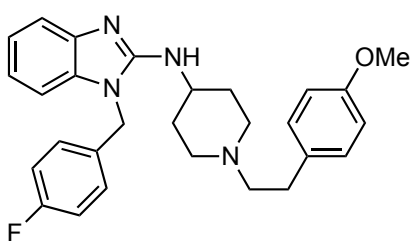
benzethonium chloride
(3.79)

Cbz-Leu-Leu-Leu-B(OH)₂

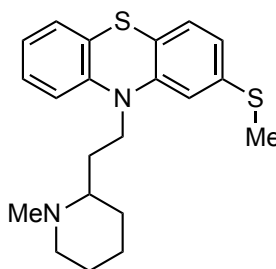
MG-262
(3.80)



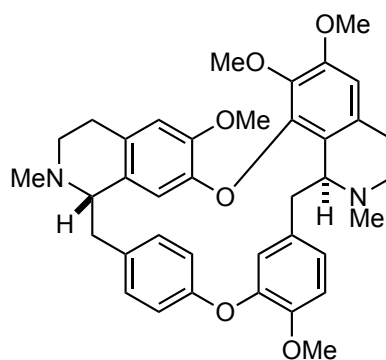
puromycin
(3.81)



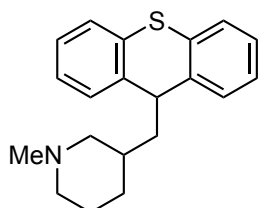
astemizole
(3.82)



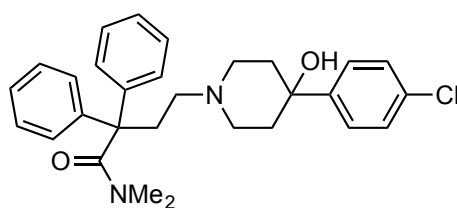
thioridazine
(3.83)



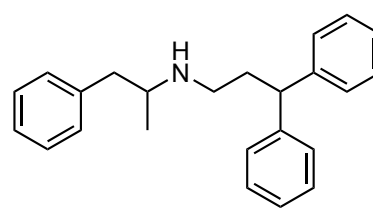
tetrandrine
(3.84)



metixene
(3.85)

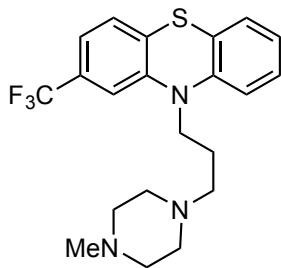


loperamide
(3.86)

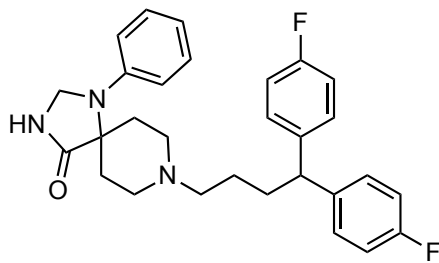


prenylamine
(3.87)

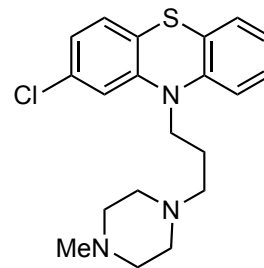
Figure 3.32., cont.



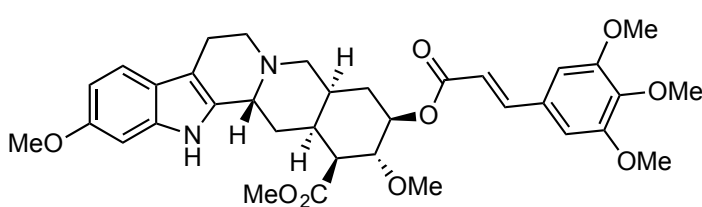
trifluoroperazine
(3.88)



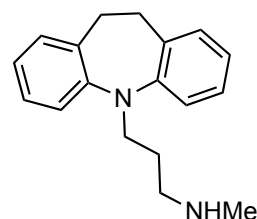
fluspirilene
(3.89)



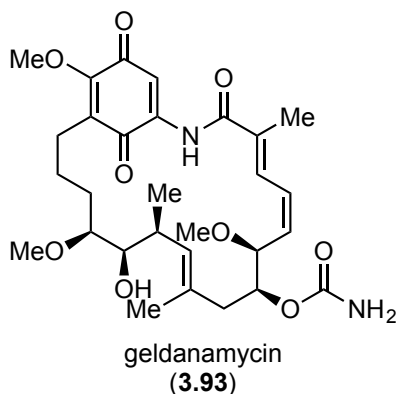
prochlorperazine
(3.90)



rescinnamine
(3.91)



desipramine
(3.92)



geldanamycin
(3.93)

3.4.6 Whole Genome shRNA Screening and siRNA Validation

To further aid in the elucidation of the biological target of SFM1257 (3.43), Dr. Claire Knezevic performed a positive selection whole genome shRNA screen. In this experiment, MiaPaca-2 cells were virally transduced with over 200,000 shRNA constructs targeting 47,500 human genes (3-5 constructs per gene), so that the cells incorporate the shRNA into their genome and express less of the target protein. The cells

were then incubated with 6.5 μ M SFM1257 (**3.43**) for six hours, which is a high enough concentration to elicit >90% cell death. The surviving cells were grown to confluency, and their DNA was isolated, amplified with PCR, and analyzed using next-gen sequencing.⁹⁵ Of the roughly 200,000 constructs in the library, over 62,000 were present in the final samples, and those constructs represented approximately 44% of the human genome.⁹⁵

In theory, the remaining cells survived because the specific shRNA constructs mitigated the effects of SFM1257 (**3.43**) toxicity. The relative amounts of shRNA constructs identified in the surviving cells were compared to the shRNA constructs found in the DMSO control, and the fold changes varied from 383 to 33 (Table 3.5).⁹⁵ The most enriched constructs in the SFM1257 (**3.43**) treated samples were ones coding for the ITPR3 gene, which codes for the inositol 1,4,5-triphosphate 3 receptors (IP₃R).⁹⁵ IP₃R is a ligand-gated calcium channel on the ER that participates in ER stress signaling.²¹⁸ The construct for gene ESR1, which codes for estrogen receptor alpha (ER α), was enriched as well, and ESR1 has also been implicated in ER stress pathways.²¹⁹ Additionally, a number of the other enriched constructs code for proteins involved in glycosyl transfer or ubiquitination, which play key roles in ER function. To confirm these results, the observed cytoprotection was subsequently verified via siRNA knockdown studies.

Table 3.5. shRNA Constructs and Their Enrichment⁹⁵

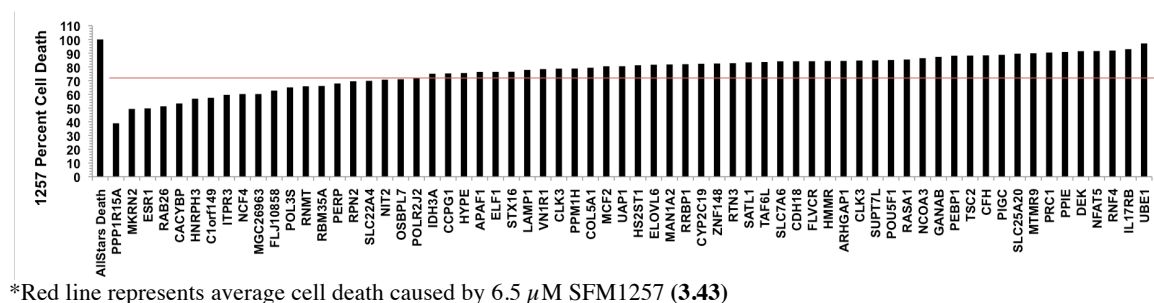
Symbol	Gene Name	Fold Change 1257 vs DMSO	Symbol	Gene Name	Fold Change 1257 vs DMSO
ITPR3	inositol 1,4,5-triphosphate receptor 3	383	CDH18	cadherin 18	70
NCF4	neutrophil cytosolic factor 4	333	POLR2J2	polymerase (RNA) II (DNA directed) polypeptide J2	70
PRSS53	protease, serine, 53	315	ZNF148	zinc finger protein 148	66
NCOA3	nuclear receptor coactivator 3	209	SKIV2L2	superkiller viralicidic activity 2-like 2 (S. cerevisiae)	65
ELF1	E74-like factor 1 (ets domain transcription factor)	184	ZNF85	zinc finger protein 85	65
GNAT2	guanine nucleotide binding protein (G protein)	165	FICD	FIC domain containing	64
RNMT	RNA (guanine-7-) methyltransferase	150	MTMR9	myotubularin related protein 9	64
HNRNPH3	heterogeneous nuclear ribonucleoprotein H3 (2H9)	147	UAP1	UDP-N-acetylglucosamine pyrophosphorylase 1	63
RASA1	RAS p21 protein activator (GTPase activating protein) 1	141	DPPA4	developmental pluripotency associated 4	63
CACYBP	calcyclin binding protein	135	NIT2	nitrilase family	62
IL17RB	interleukin 17 receptor B	134	PEBP1	phosphatidylethanolamine binding protein 1	62
RRBP1	ribosome binding protein 1	133	IDH3A	isocitrate dehydrogenase 3 (NAD+) alpha	62
CLK3	CDC-like kinase 3	124	CCPG1	cell cycle progression 1	61
RNF4	ring finger protein 4	123	MCAT	malonyl CoA:ACP acyltransferase (mitochondrial)	61
RNASE2	ribonuclease, Rnase A family, 2	116	SCNM1	sodium channel modifier 1	61
GANAB	alpha glucosidase 2	111	VN1R1	vomeroneasal 1 receptor 1	60
TSC2	tuberous sclerosis 2	104	CYP2C19	cytochrome P450	60
TTY1	testis-specific transcript	102	CMTR1	cap methyltransferase 1	59
UTP11L	UTP11-like	100	SUGP1	SURP and G patch domain containing 1	59
NEIL3	nei endonuclease VIII-like 3	99	PERP	PERP, TP53 apoptosis effector	59
PPM1H	protein phosphatase	94	TAF6L	TAF6-like RNA polymerase II	56
SLC7A6	solute carrier family 7 (amino acid transporter light chain)	94	MRT04	mRNA turnover 4 homolog (S. cerevisiae)	54

Table 3.5., cont.

KIAA0430	KIAA0430	93	HS2ST1	heparan sulfate 2-O-sulfotransferase 1	54
HIST1H2BG	histone cluster 1	92	LAMP1	lysosomal-associated membrane protein 1	53
RTN3	reticulon 3	87	CFH	complement factor H	52
ARHGAP1	Rho GTPase activating protein 1	85	DPYSL3	dihydropyrimidinase-like 3	52
KBTBD7	kelch repeat and BTB (POZ) domain containing 7	84	SUPT7L	suppressor of Ty 7 (S. cerevisiae)-like	51
SLC22A4	solute carrier family 22 (organic cation/zwitterion transporter)	83	SLC25A20	solute carrier family 25 (carnitine/acylcarnitine translocase)	50
FEZ2	fasciculation and elongation protein zeta 2 (zygin II)	82	UBA1	ubiquitin-like modifier activating enzyme 1	47
MEAF6	MYST/Esa1-associated factor 6	78	SYN1	synapsin I	46
RAB26	RAB26, member RAS-oncogene family	77	CYP2A7P1	cytochrome P450	45
ESRP1	epithelial splicing regulatory protein 1	77	PRC1	protein regulator of cytokinesis 1	44
NTN3	netrin 3	76	PIGC	phosphatidylinositol glycan anchor biosynthesis	44
COBL1	cordon-bleu WH2 repeat protein-like 1	75	HMMR	hyaluronan-mediated motility receptor (RHAMM)	44
MKRN2	makorin ring finger protein 2	75	DEK	DEK oncogene	44
MAN1A2	mannosidase	74	RPN2	ribophorin II	43
REEP5	receptor accessory protein 5	74	COL5A1	collagen	40
SATL1	spermidine/spermine N1-acetyl transferase-like 1	74	MCF2	MCF.2 cell line derived transforming sequence	39
OSBPL7	oxysterol binding protein-like 7	74	STX16	syntaxin 16	39
FLVCR1	feline leukemia virus subgroup C cellular receptor 1	73	TJAP1	tight junction associated protein 1 (peripheral)	39
SGMS2	sphingomyelin synthase 2	73	ELOVL6	ELOVL fatty acid elongase 6	38
ESR1	estrogen receptor 1	72	PRRG4	proline rich Gla (G-carboxyglutamic acid) 4 (transmembrane)	37
PPIE	peptidylprolyl isomerase E (cyclophilin E)	71	NFAT5	nuclear factor of activated T-cells 5	34
POU5F1	POU class 5 homeobox 1	71	GSDMB	gasdermin B	33

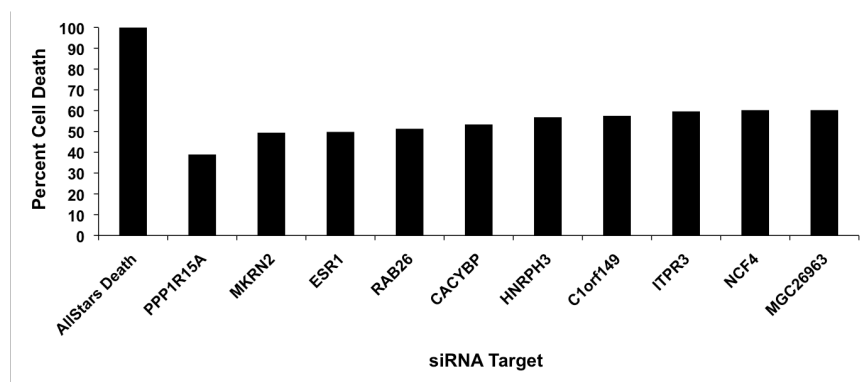
Dr. Betsy Parkinson validated the results of the whole genome shRNA study by selecting one or two siRNAs for 66 of the enriched genes and performing an siRNA knockdown study, and the toxicity of SFM1257 (3.43) at 6.5 μ M in MiaPaca-2 cells transfected with each of these siRNA constructs was determined (Figure 3.33).⁹⁶ In line with the observed cytoprotection seen by PP1/GADD34 inhibitor salubrinal (3.74), robust protection was afforded by siRNA for the gene PPP1R15A, which codes for the protein GADD34 (Figure 3.34).⁹⁶ Additionally, the ER stress related genes ITPR3 and ESR1, which both showed enrichment in the shRNA screen, were also identified as cytoprotective in the siRNA validation screen (Figure 3.34), further supporting the ER stress hypothesis.

Figure 3.33. Validation of shRNA Results with siRNA⁹⁵



*Red line represents average cell death caused by 6.5 μ M SFM1257 (3.43)

Figure 3.34. siRNA Constructs that Mitigated SFM1257 (3.43) Caused Cell Death⁹⁶

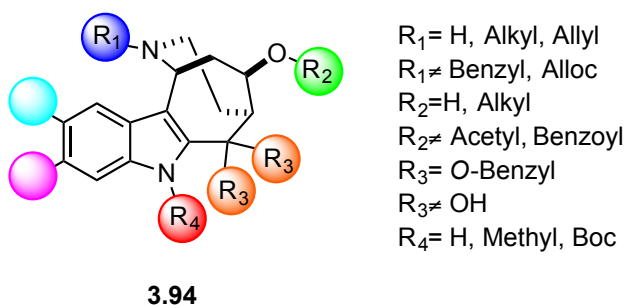


3.5 SUMMARY OF RESULTS AND FUTURE DIRECTIONS

3.5.1 Optimization of Lead Compound

Due to promising preliminary *in vitro* and *in vivo* results, a derivative of compound SFM1257 (**3.43**) is being developed for the ultimate purpose of clinical translation. Moving forward, additional derivatives must be synthesized with the goal of increasing potency while minimizing toxicity. From the initial data collected (Table 3.1, Figure 3.8), a preliminary structure-activity-relationship can be assembled (Figure 3.35). It is clear that large non-polar groups and carbamate groups on the basic nitrogen moiety (Figure 3.35, R₁) are not tolerated (benzyl, dithioacetal, alloc), but smaller groups are tolerated (-H, alkyl, allyl). The oxygen moiety (Figure 3.35, R₂) can be a free hydroxyl or a *O*-Me group, but acylation of the hydroxyl group to afford the corresponding ester is not tolerated. The 1,3-diol moiety (Figure 3.35, R₃) is active when protected with an *O*-benzyl group, but no cytotoxicity was observed when the benzyl groups were removed to give the free alcohols. In addition, substitution on the indole nitrogen atom (Figure 3.35, R₄) is well tolerated (-H, Boc, methyl).

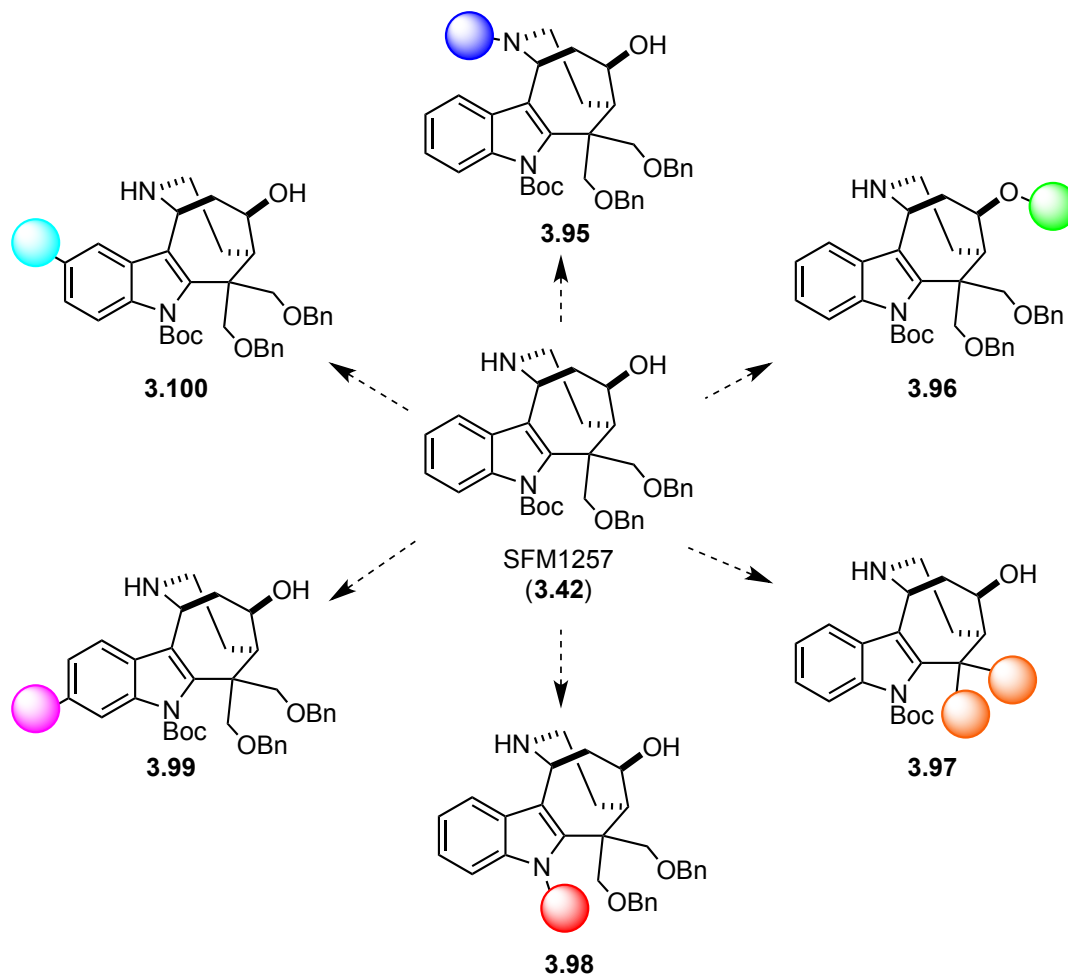
Figure 3.35. Preliminary SAR Analysis



Though the data presented in Figure 3.35 provides preliminary insight, additional analogs must be synthesized to more fully establish the SAR. Using SFM1257 (**3.43**) as the lead compound, there are six sites that must still be investigated to establish a

thorough SAR profile (Figure 3.36). The substituents at those positions need to be varied iteratively in order to elucidate the effects of each position on the efficacy and potency of the compound (Figure 3.36). Reducing the complexity of the molecule is also of interest. It must be determined whether substituents smaller than benzyl are tolerated on the 1,3-diol moiety. If the *O*-benzyl moieties could be replaced with *O*-Me or *-H*, the molar mass and complexity would be reduced dramatically. Once single site modifications are completed, the effects of modifying multiple sites simultaneously must be investigated. Additionally, all of derivatives synthesized to date are racemic. As these compounds continue down the pipeline for pre-clinical development, there will be a need to evaluate and determine the efficacy of each enantiomer independently because each enantiomer may be responsible for unique aspects of the phenotypic response to these compounds. Hence, approaches for enantioselective synthesis of SFM1257 (**3.43**) must be developed.

Figure 3.36. Examples of Iterative Change to be Made to SFM1257 (**3.43**)



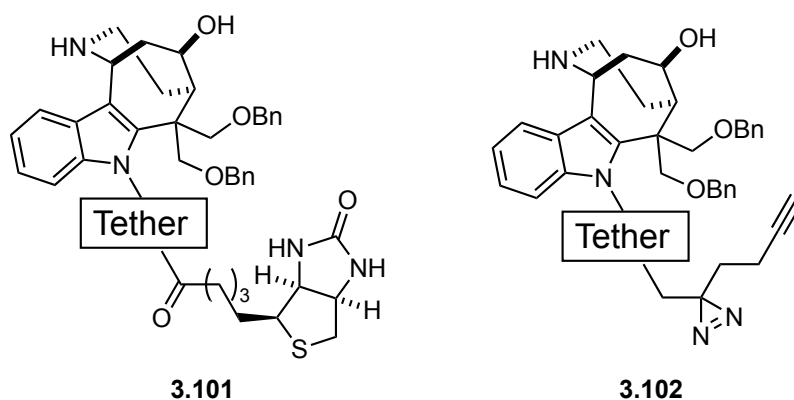
3.5.2 Mode-of-Action Studies

The mode-of-action for these compounds has tentatively been assigned as early induction of endoplasmic reticulum (ER) stress, followed by caspase-independent cell death. Through exhaustive analysis with small molecule chemical probes, it was determined that SFM1257 (**3.43**) can cause apoptotic cell death but can utilize non-apoptotic pathways when apoptosis is inhibited. Additionally, the cytotoxicity of SFM1257 (**3.43**) has been correlated to the phosphorylation level of eIF2 α , which is a biochemical marker for ER stress, by showing that inhibition and knockdown of the p-

eIF2 α phosphatase PP1/GADD34 reduces sensitivity to SFM1257 (**3.43**). Through transcriptomic analysis and RNA interference studies, it was determined that Ca²⁺ dysregulation, likely through the IP₃R receptor, plays a role in the mode-of-action for SFM1257 (**3.43**), but it is not known whether the Ca²⁺ dysregulation causes ER stress or is a result of the ER stress.

At the moment, the molecular targets of SFM1257 (**3.43**) remain unknown, and several additional experiments should be run to aid in elucidating the targets. Additional small molecule inhibitors need to be evaluated to validate the observation that inhibiting PP1/GADD34 is cytoprotective; this would further verify the observed response to salubrinal (**3.74**). To identify the biological targets, chemical probes with a tethered biotin (**3.101**) or tethered alkyne (**3.102**) can be used for biotin pull-down experiment and other photoaffinity studies (Figure 3.37). A biotin or alkyne handle would also allow for one to visualize the sub-cellular localization of the compounds via addition of a streptavidin bound fluorophore or a ‘click’ reaction with a fluorophore tethered to an azide.

Figure 3.37. Chemical Probes Derived From SFM1257 (**3.43**)

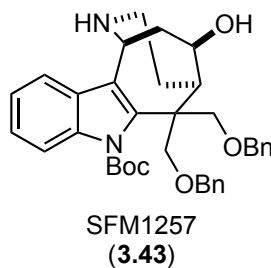


Chapter 4: Synthesis and Biological Evaluation of Novel Tetracyclic Indole Derivatives and Tool Compounds

4.1 INTRODUCTION

It is clear from previous work that further investigations are required before more *in vivo* studies are performed on SFM1257 (**3.43**) and derivatives thereof. Additional biological analyses of toxicity induced by SFM1257 (**3.43**) with known chemical probes and novel SFM1257 (**3.43**)-derived tool compounds are needed to advance mode-of-action studies. Specifically, derivatives of SFM1257 (**3.43**) that contain a tethered biotin moiety, and photoaffinity cross-linker are needed for target identification studies. Derivatives of SFM1257 (**3.43**) must also be synthesized and a more thorough structure-activity-relationship established in order to maximize potency and minimize toxicity. Furthermore, pharmacophore minimization studies are needed to determine what structural characteristics contribute most to the biological activity.

Figure 4.1. Structure of SFM1257 (**3.43**)



4.2. TOOL COMPOUNDS FOR MODE-OF-ACTION STUDIES

4.2.1. Introduction

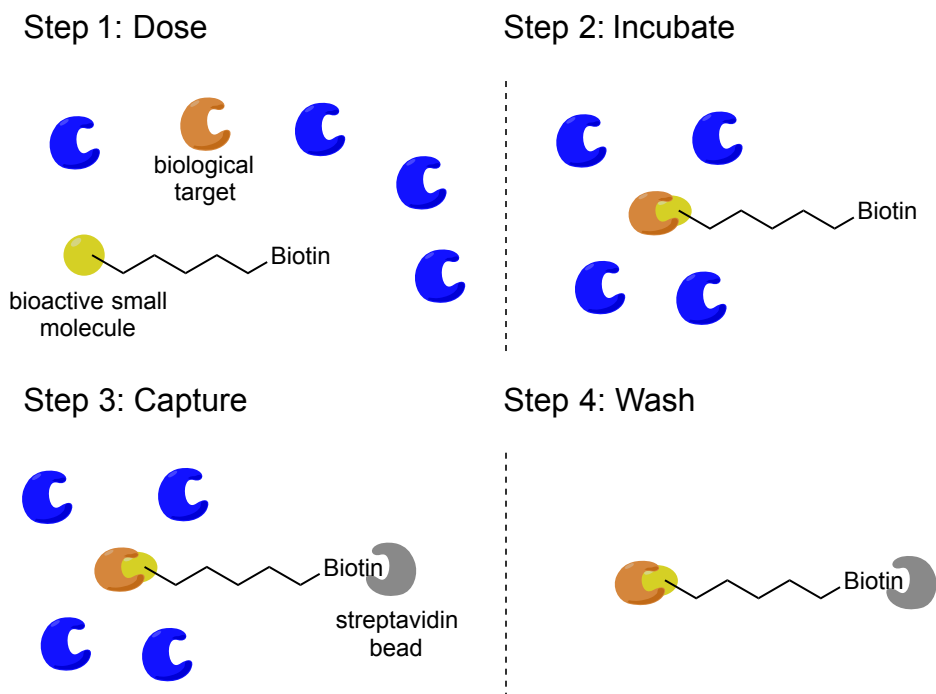
Determining the protein targets of bioactive small molecules is an important exercise that is used to expand the druggable genome and provide valuable insight into the mode-of-action of a biologically active compounds. A compound discovered via

phenotypic screening will sometimes have an unknown or previously uncharacterized biological target, and there are several common methods and techniques used to aid in the identification of the target. There are several thorough reviews of the use of tool compounds for target identification studies and examples thereof.²²⁰⁻²²³

4.2.1.1 Biotinylated Chemical Probes for Target Identification

A common technique for target identification involves the use of a biotinylated probe.²²⁴⁻²⁴¹ Biotin, vitamin B₇, forms one of the strongest known non-covalent bonds ($K_d \sim 10^{-15}$ M) with the protein streptavidin,²⁴² and as a result, small molecules with a biotin-terminated or containing tether are used to create non-covalent affinity matrices for protein isolation and purification.²²⁰ A standard biotin pull-down experiment can be performed in either whole cells or cellular lysate, and a simplified pictorial description is shown in Figure 4.2.

Figure 4.2. Pictorial Description of Biotin Pull-Down Experiment



The first step in a biotin pull-down experiment is to incubate cells or cellular lysate with the biotin-conjugated bioactive small molecule (Step 1, Figure 4.2.). The small molecule will bind to the biological target (Step 2, Figure 4.2.). The cells are then lysed, and a solid-supported streptavidin bead is added to the lysate. The streptavidin bead immediately binds to the biotin, forming a conjugate with the biological target (Step 3, Figure 4.2.). The bead is then washed, removing all the miscellaneous proteins and biomolecules that are not bound to the bioactive small molecule. The streptavidin bead is then removed by boiling with a standard denaturant (i.e. SDS), leaving behind the isolated biological target (Step 4, Figure 4.2.). The biological target is then typically analyzed via tandem mass spectrometry to determine its sequence and identity.²²⁰

The biotin tether does not necessarily have to be pre-installed on the molecular probe to perform the pull-down assay. A strategy that has proven to be very effective in recent years is to attach the biotin tether to the chemical probe after incubating the probe in the cells or cellular lysate via an azide-alkyne ‘click’ reaction.²⁴³⁻²⁴⁶ This strategy has several distinct advantages over pre-tethering the biotin, most notably because the biotin tag can make synthesis and purification of the probe difficult, adversely affect binding to the target, and negatively impact the solubility of the compound.²²⁰

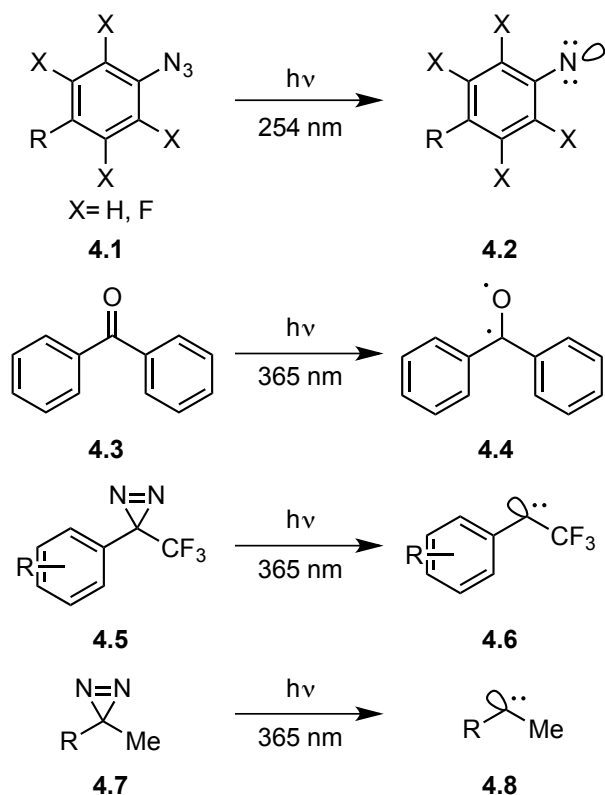
Biotinylated probes have spectacular utility in a vast number of target identification experiments. Imaging agents attached to streptavidin and biotin antibodies have been used for immunoblots and microscopy experiments,²³⁵ and the microscopy experiments would allow one to visualize where a compound may be localizing within a cell. Biotinylated probes have also been used to synthesize solid phase supports for protein purification via affinity chromatography. This approach has been used to isolate and identify novel insulin receptors,²⁴⁷ new phosphatase holoenzyme complexes,²⁴⁸ previously unknown transcription factors,²⁴⁹ and many other proteins.²⁵⁰ In the context of

this work, the primary focus will be upon the design and synthesis of chemical probes for target identification via a standard pull-down experiment.

4.2.1.2 Photoaffinity Probes and Their Use in Target Identification

The strategy of tethering a biotin directly to a small molecule and performing a pull-down study works well if either the biological target is in high concentration or if the probe is a very strong binder; thus, pull down studies typically work best if the compound covalently binds to its biological target.²³⁸ If the small molecule is a weak binder or the biological target has a low abundance, a pull-down assay may yield inconclusive results.²²⁰ An advantage of this method is that one can potentially identify all of the biological targets that contribute to the phenotypic response of a drug. If one only identifies the highest affinity biological target of a compound, one may miss weaker binding targets that are associated with deleterious toxicity or off-target drug effects, which was illustrated by Peters *et al* in their method to assay the binding partners of kinase inhibitors.²⁵¹ To address these issues, reactive cross-linking moieties were developed so that the small molecule probe covalently binds to the target protein.²²⁰ The most commonly employed photoaffinity cross-linking moieties are shown in Figure 4.3, and these four structural motifs have been effectively utilized in a number of photoaffinity studies.²⁵²⁻²⁵⁵ The reactive functional groups, upon exposure to UV light, create high energy nitrene, radical, or carbene species that insert very effectively into peptides, covalently tethering the molecular probe to the biological target.

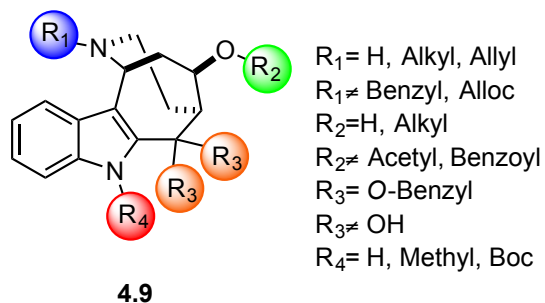
Figure 4.3. Commonly Used Photoaffinity Cross-Linking Moieties



4.2.2. Synthesis and Evaluation of Tool Compounds

Before commencing with the synthesis of a tool compound derived from SFM1257 (**3.43**), care had to be taken to ensure that the compound would not lose bioactivity. The preliminary structure-activity analysis indicated that large non-polar substituents were not tolerated on the basic nitrogen moiety, yet large non-polar substituents were tolerated on the indole nitrogen atom (Figure 4.4). Thus, it was decided that the indole nitrogen atom was the optimal location to append a tethered biotin or photoaffinity cross-linker.

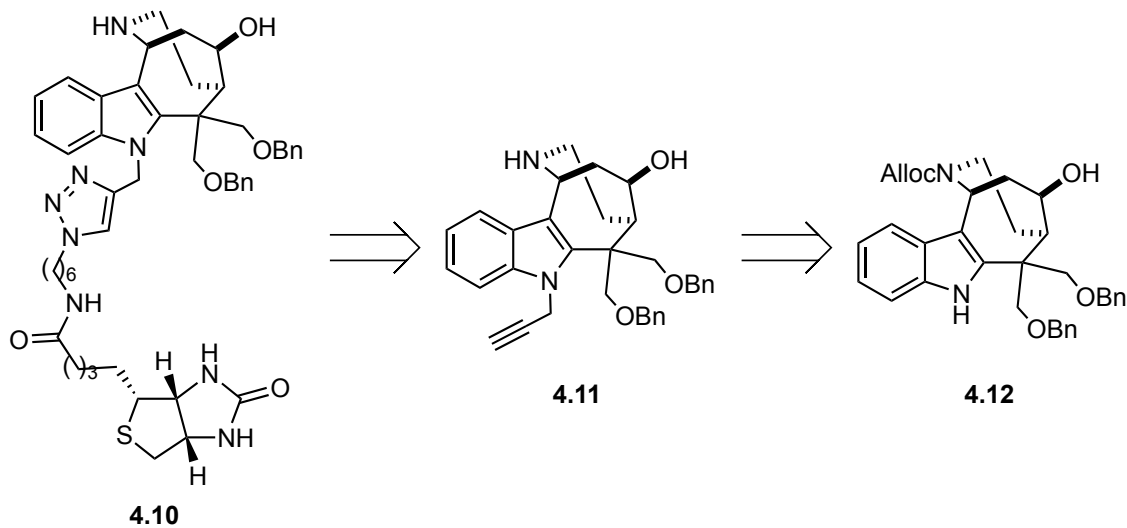
Figure 4.4. Preliminary Structure-Activity Analysis



4.2.2.1 Synthesis of Biotinylated Tool Compound

Initially, we sought to synthesize a tool compound tethered directly to biotin. We thus envisioned that the biotinylated compound **4.10** could be synthesized from alkyne **4.11** via an azide-alkyne ‘click’ reaction, and alkyne **4.11** could be accessed from compound **4.12**.

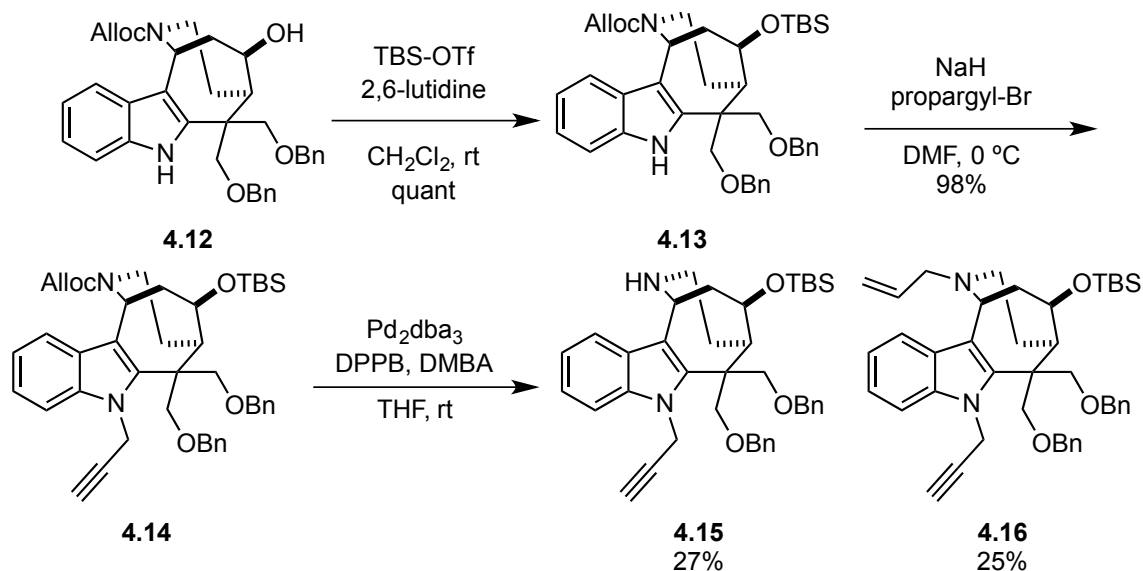
Figure 4.5. Retrosynthetic Analysis for Biotinylated Tool Compound



The synthesis of a biotinylated tool compound began via protection of alcohol **4.12** as the silyl ether. It was found that **4.12** could be converted to **4.13** quantitatively using *tert*-butyldimethylsilyltriflate and 2,6-lutidine. The indole nitrogen atom of **4.13**

was then alkylated with sodium hydride and propargyl bromide to give alkyne **4.14** in 98% yield. The allyl carbamate of **4.14** was removed using Pd_2dba_3 and 1,3-dimethylbarbituric acid (DMBA) as an allyl scavenger to give **4.15** and **4.16** in 27% and 25% yields, respectively. Although the yield of the final deprotection was poor, a sufficient amount of material was synthesized, so optimization of the reaction was not undertaken.

Scheme 4.1. Synthesis of Protected Alkyne **4.15**

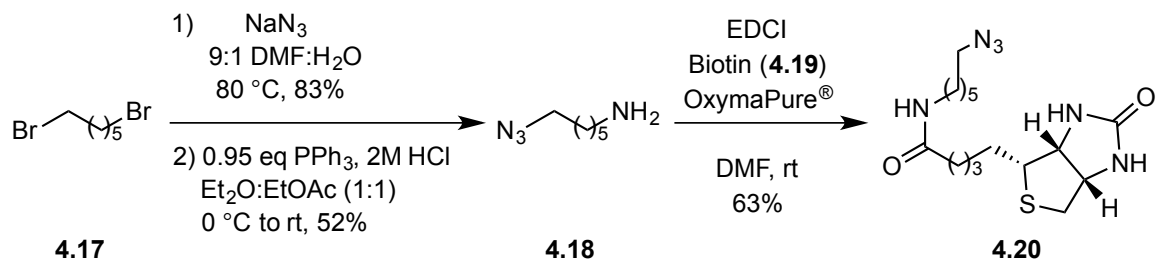


DPPB= 1,4-bis(diphenylphosphino)butane; dba= dibenzylideneacetone

With the synthesis of first half of the biotinylated derivative nearly completed, our focus was shifted to the preparation of the azide coupling partner for the impending ‘click’ reaction (Scheme 4.2). The synthesis of **4.20** was carried out according to a literature procedure.²⁵⁶ Reaction of 1,6-dibromohexane (**4.17**), with sodium azide afforded the diazido compound that was subsequently selectively reduced to monoamine **4.18** via a Staudinger reaction with a substoichiometric amount of triphenylphosphine. Monoamine **4.18** was appended to biotin (**4.19**) using standard peptide coupling

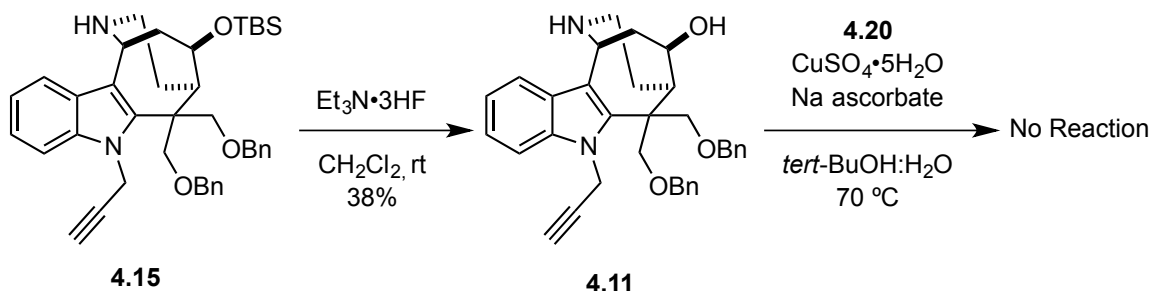
conditions (EDCI/OxymaPure®/DMF), and the desired biotin tethered azide **4.20** was synthesized in 63% yield.

Scheme 4.2. Synthesis of Biotin Tether²⁵⁶



Initially, we planned to complete the synthesis of **4.10** by performing the azide-alkyne ‘click’ reaction last, so alkyne **4.15** was deprotected with Et₃N•3HF to give **4.11** in 38% yield. With alkyne **4.11** in hand, the click reaction with azide **4.20** was attempted. Unfortunately, the reaction afforded none of the desired product, and only returned starting material was isolated. Increasing the number of equivalents of CuSO₄ or sodium ascorbate did not affect the reaction. Extended reaction times and elevated temperatures did not afford any of the desired cycloaddition product.

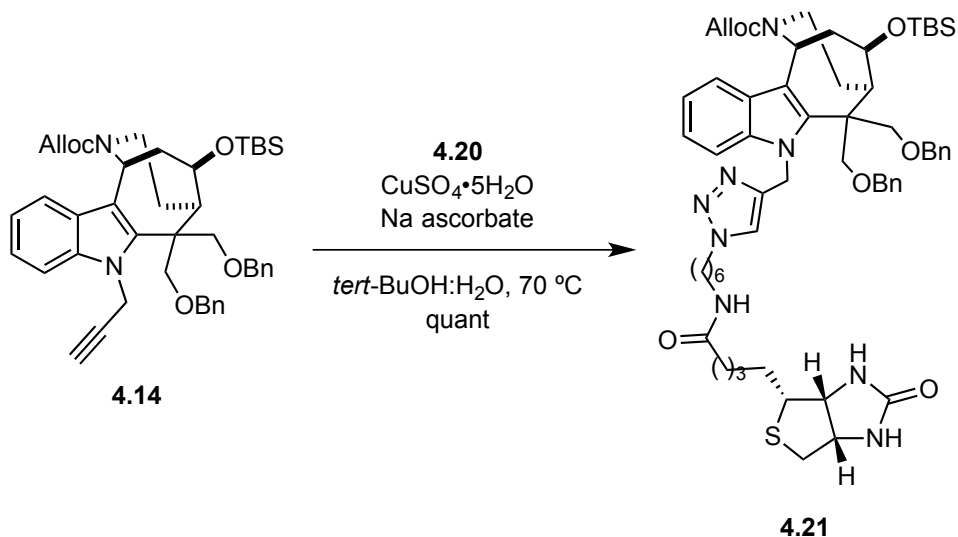
Scheme 4.3. Initial Attempt at Formation of Biotinylate Derivative



We hypothesized that the Lewis basic atoms on **4.11** may be chelating or binding to copper species preventing the reaction from proceeding as desired. To test this hypothesis, compound **4.14** was subjected to the same conditions for the ‘click’ reaction,

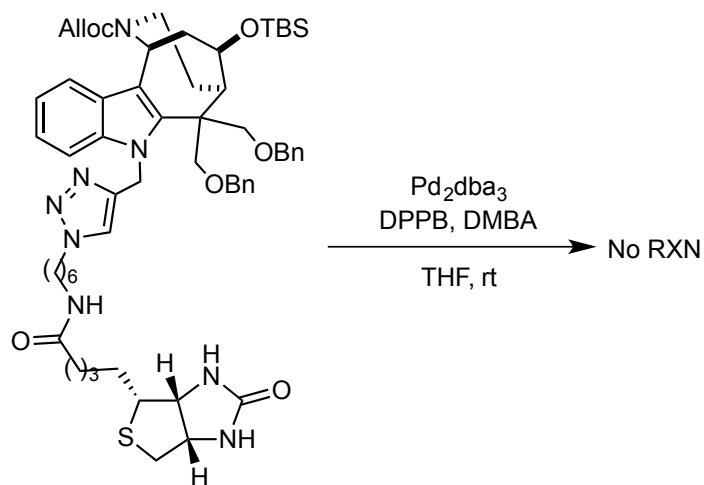
and the reaction proceeded cleanly to afford the biotin-tethered compound **4.21** in quantitative yield (Scheme 4.4).

Scheme 4.4. Successful ‘Click’ Reaction



Encouraged by this result, efforts were undertaken to deprotect compound **4.21**. Unfortunately, attempts to remove the allyl carbamate group under the previous conditions were unsuccessful, and only starting material was observed (Scheme 4.5). Extended reaction times and increased Pd_2dba_3 loading did not afford any of the desired compound. When elevated temperatures were employed ($100\text{ }^\circ\text{C}$, DMF), decomposition of the starting material was observed.

Scheme 4.5. Attempted Removal of Allyl Carbamate Group of **4.21**

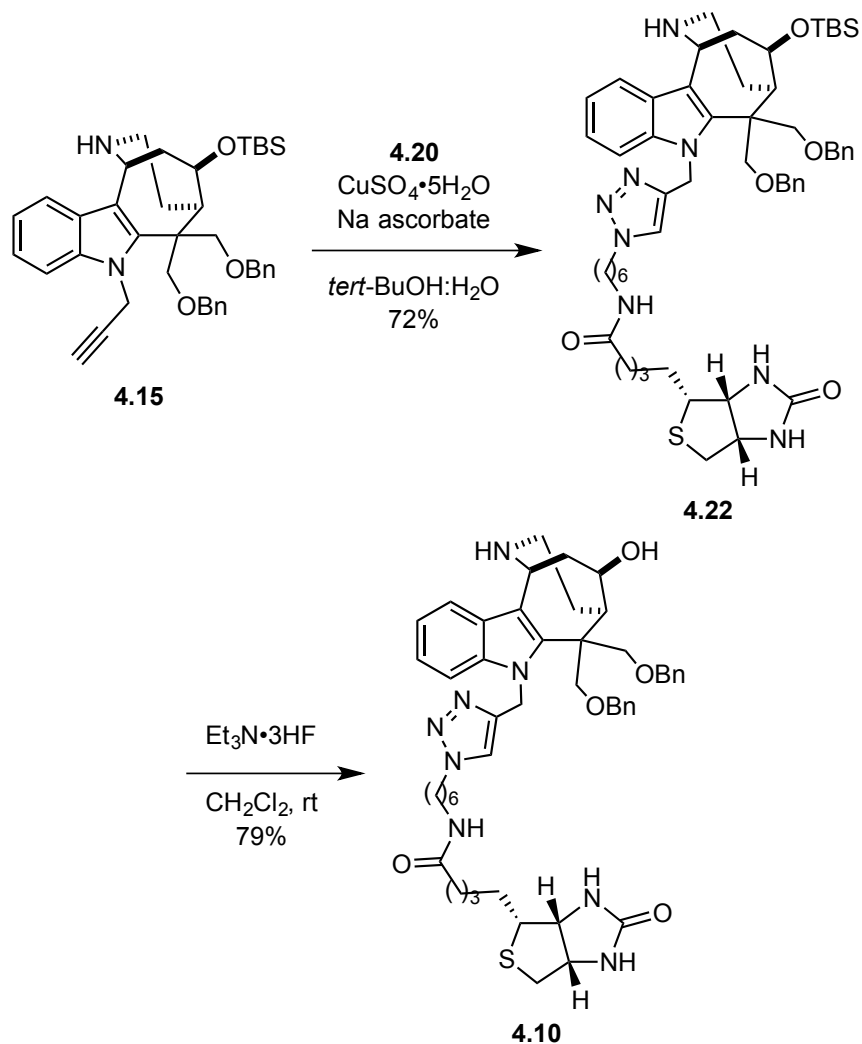


4.21

DPPB= 1,4-bis(diphenylphosphino)butane; dba= dibenzylideneacetone

Since we now had evidence to support the hypothesis that the Lewis basic moieties were likely inhibiting the ‘click’ reaction, the next logical step was to evaluate which Lewis basic site was preventing the progression of the reaction. Since compound **4.15** had previously been synthesized, it was subjected to the ‘click’ reaction conditions, and the reaction furnished the biotin tether compound **4.22** in 72% yield (Scheme 4.6). The TBS group of **4.22** was then removed using $\text{Et}_3\text{N} \cdot 3\text{HF}$ to afford the desired biotinylated compound **4.10** in 79% yield.

Scheme 4.6. Synthesis of Biotinylated Probe **4.10**

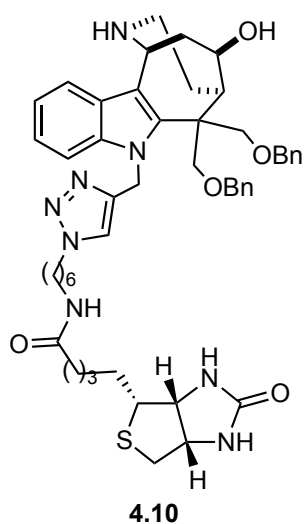


4.2.2.2 Evaluation of Biotinylated Tool Compound

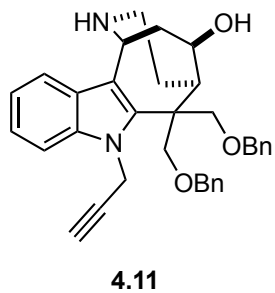
After completing the synthesis of **4.10**, its biological activity was evaluated by Dr. Betsy Parkinson. It was found that **4.10** was active against U937 lymphoma cells ($\text{IC}_{50} = 34.9 \pm 6.1 \mu\text{M}$) (Figure 4.6), but the activity was diminished by a factor of 10 when compared to the parent compound, SFM1257 (**3.43**) ($\text{IC}_{50} = 3.3 \pm 0.2 \mu\text{M}$). Additionally, it was found that compound **4.11** containing the alkyne handle was cytotoxic against U937 cells ($\text{IC}_{50} = 22.5 \pm 4.7 \mu\text{M}$). Compound **4.11** could also be used in a pull-down

assay if the ‘click’ reaction were done in the cellular lysate. At this time, we became concerned that these compounds may not be binding to their biological target with particularly high affinity because of the high micromolar IC₅₀ values. Thus, it was determined that the best course of action would be to synthesize a different derivative containing a photoaffinity cross-linker.

Figure 4.6. Biological Evaluation of Biotinylated Tool Compound⁹⁶



4.10	
Hill slope	1.9 ± 0.2
E _{max}	101 ± 1.5
U937 IC ₅₀ (μM)	34.9 ± 6.1
Hemolysis IC ₅₀ (μM)	310 ± 30

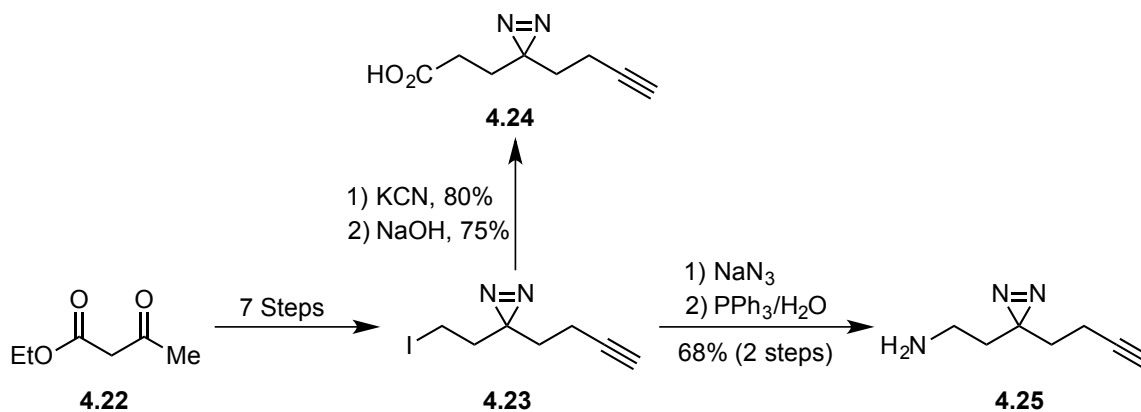


4.11	
Hill slope	9.3 ± 3.9
E _{max}	99.9 ± 0.1
U937 IC ₅₀ (μM)	22.5 ± 4.7
Hemolysis IC ₅₀ (μM)	>333

4.2.3.1 Synthesis of Photoaffinity Probe

Given that there are several common cross-linking moieties found in the literature (Figure 4.3), we sought to use a cross linker that could be easily attached to the indole nitrogen atom of **4.13**. While determining which approach to take to design a photoaffinity tether, we became aware of a report by Li *et al* in which they designed and evaluated the diazirine tether shown in Scheme 4.7.²⁵⁷ We were drawn to this approach for several reasons: 1) the tether could be synthesized on large scale from cheap materials; 2) the tether could be appended to our scaffold via alkylation (**4.23**), nucleophilic addition (**4.25**), or peptide coupling (**4.24**); and 3) the authors applied the tether to proteomic analysis of several known kinase inhibitors. Following literature procedures, **4.23**, **4.24**, and **4.25** were synthesized (Scheme 4.7).²⁵⁷

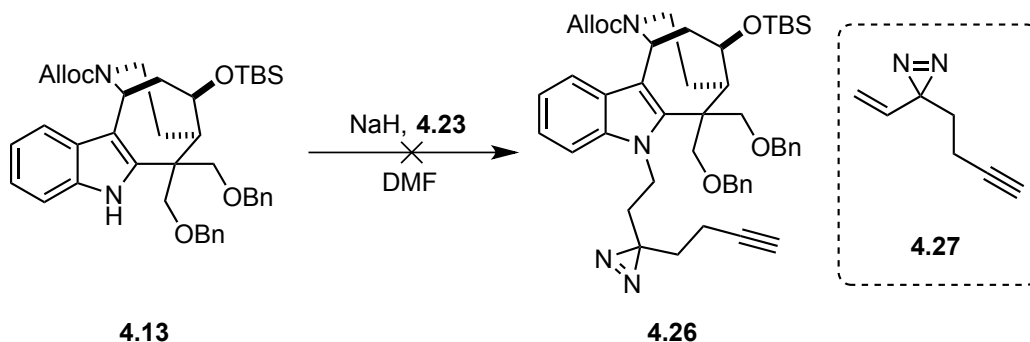
Scheme 4.7. Photoaffinity Tether Published by Li *et al*²⁵⁷



Initial attempts to append the photoaffinity probe to the indole nitrogen atom of **4.13** by alkylation with iodide **4.23** were unsuccessful (Scheme 4.8). The ¹H-NMR spectra of the crude reaction mixture showed alkene **4.27** and unreacted starting material. Increasing the number of equivalents of **4.23** or inverting the order of addition (adding **4.13**/NaH to **4.23**) did not change the product distribution. We speculated that the substitution on the proximal quaternary carbon to the indole nitrogen atom was sterically

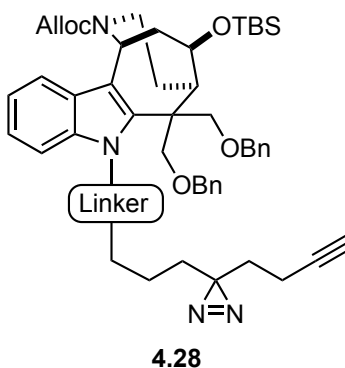
preventing nucleophilic attack. To overcome this preference for elimination, we proposed that a more reactive electrophile that cannot eliminate would be better suited to alkylate the indole nitrogen atom.

Scheme 4.8. Initial Attempt to Alkylate Indole Nitrogen



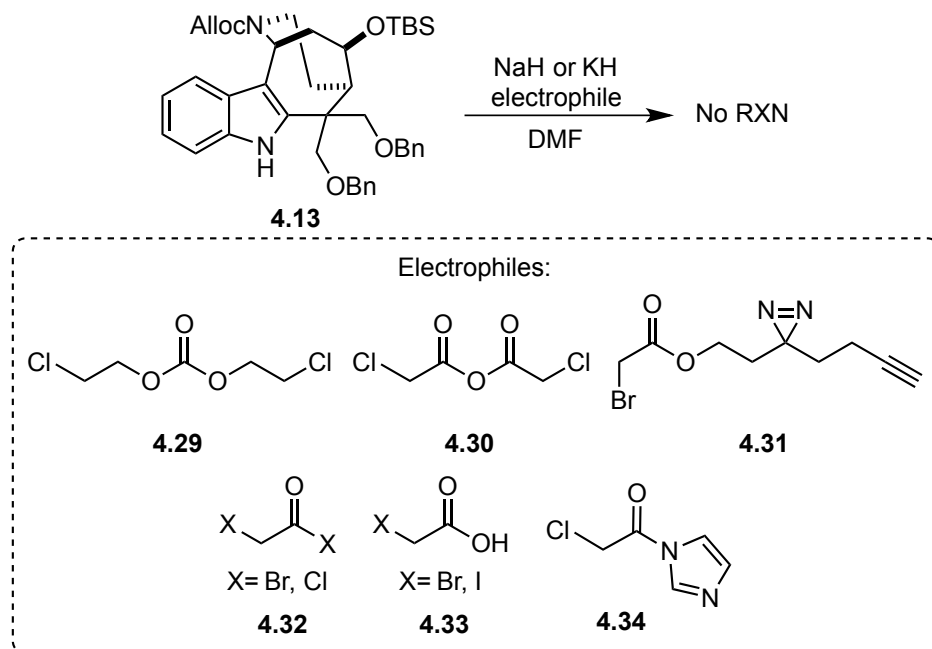
Although the synthesis of **4.23** was straightforward, it was a time-consuming, seven-step reaction sequence. As such, we felt that it would be a more prudent use of material if a short carbon linker was attached to the indole nitrogen atom, so the photoaffinity tether could be subsequently appended to the linker. By so doing, more reactive electrophiles could be used to alkylate or acylate the indole nitrogen atom, and then the photoaffinity tether can be readily attached to the linker.

Figure 4.7. Revised Strategy



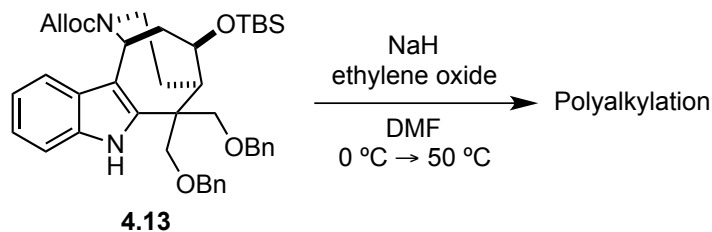
Various electrophiles (Scheme 4.9, **4.29-34**) were screened for their ability to alkylate or acylate the indole nitrogen atom of **4.13**. All of these electrophiles had two electrophilic sites so that the indole nitrogen atom could occupy one site, and amine **4.25** would be attached to the second site. Unfortunately, all attempts to alkylate **4.13** with these electrophiles were unsuccessful, and only starting material was returned in every attempt.

Scheme 4.9. Attempted Alkylation With Various Electrophiles



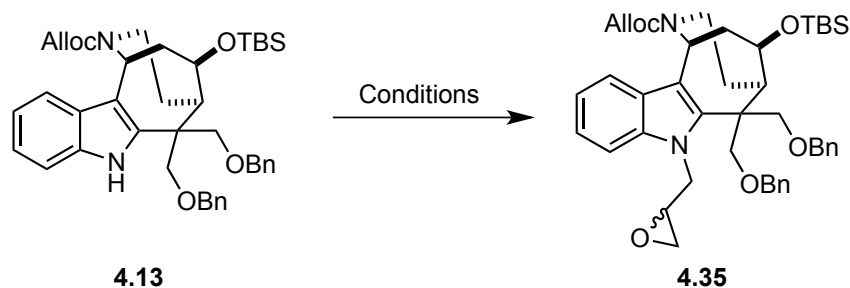
Due to our inability to acylate or alkylate the indole nitrogen atom, we determined that an electrophile that cannot eliminate or enolize would be better suited for this transformation. We found that ethylene oxide did alkylate the indole nitrogen atom at 50 °C, but the resulting alcohol reacted with additional equivalents of ethylene oxide to create a mixture of polymeric products (Scheme 4.10).

Scheme 4.10. Attempted Alkylation with Ethylene Oxide



After determining that ethylene oxide was not a good choice for a linker, *epi*-chlorohydrin was examined. We discovered that quantitative deprotonation of **4.13** with sodium hydride in dimethylformamide (DMF) followed by addition of *epi*-chlorohydrin afforded the desired product **4.35** in 30-50% yield (Table 4.1, entry 1); the majority of the mass balance was unreacted starting material. Adding sodium iodide to the reaction to form the more reactive alkyl iodide *in situ* did not improve the yield (Table 4.1, entry 2). Switching to potassium hydride provided no benefit over sodium hydride (Table 4.1, entry 3). *N*-Methylpyrrolidone (NMP) was evaluated as a solvent, and it was found that the reaction profile was cleaner with NMP than DMF, but the yields still varied greatly (Table 4.1, entry 4). Attempts to deprotonate **4.13** with dimsyl anion (deprotonated DMSO) and alkylate in THF (Table 4.1, entry 5) also afforded none of the desired product. Additionally, use of acetonitrile as the solvent resulted in no formation of the desired product (Table 4.1, entry 6). The most consistent yields were obtained with the polar aprotic solvent hexamethylphosphoramide (HMPA), and the alkylated indole **4.35** was thus obtained in 64% yield (99% BRSM) (Table 4.1, entry 7).

Table 4.1. Successful Alkylation with *epi*-Chlorohydrin

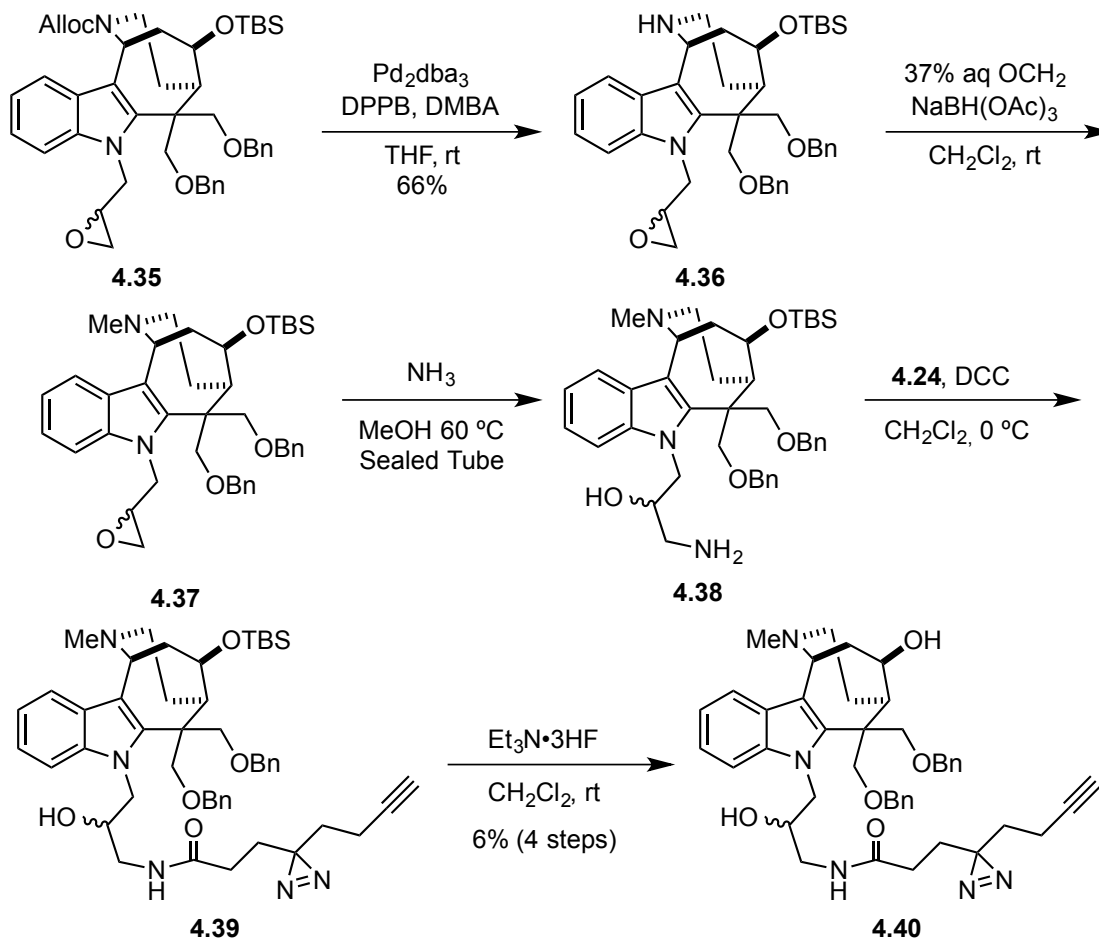


Entry	Conditions	Yield
1	NaH, <i>epi</i> -chlorohydrin, DMF	30-50%
2	NaH, <i>epi</i> -chlorohydrin, NaI, DMF	30-50%
3	KH, <i>epi</i> -chlorohydrin, DMF	30-50%
4	NaH, <i>epi</i> -chlorohydrin, NMP	30-90%
5	NaH, DMSO, <i>epi</i> -chlorohydrin, THF	0%
6	NaH, <i>epi</i> -chlorohydrin, MeCN	0%
7	NaH, <i>epi</i> -chlorohydrin, HMPA	64% (99%)*

*BRSM

With an appreciable amount of epoxide **4.35** in hand, the allyl carbamate group was removed using Pd₂dba₃/DPPB and 1,3-dimethylbarbituric acid (DMBA) as an allyl scavenger to afford compound **4.36** in 66% yield. Secondary amine **4.36** was converted to the tertiary amine **4.37** via a reductive amination with 37% aqueous formaldehyde and NaBH(OAc)₃. After work up, the crude reaction mixture containing **4.37** was dissolved in methanolic ammonia and heated at 60 °C for 36 hours in a sealed tube to provide amino alcohol **4.38**; the crude reaction mixture was carried on without performing an aqueous workup or further purification. The amino alcohol **4.38** was then coupled to carboxylic acid **4.24** using the peptide coupling reagent *N,N*-dicyclohexylcarbodiimide (DCC) to afford compound **4.39**. After a quick aqueous work up, the crude reaction mixture was stirred at room temperature in a mixture (1:3 v/v) of Et₃N•3HF and CH₂Cl₂ to afford photoaffinity probe **4.40** in 6% yield over four steps after purification by reverse-phase HPLC.

Scheme 4.11. Completion of the Photoaffinity Probe



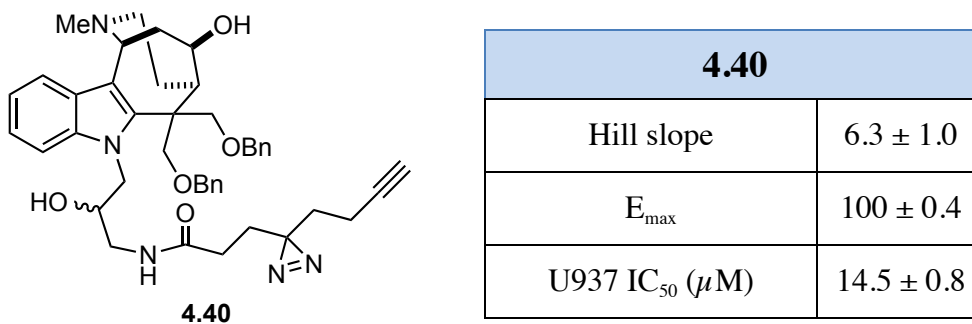
DPPB= 1,4-bis(diphenylphosphino)butane; dba= dibenzylideneacetone

4.2.3.2 Evaluation of Photoaffinity Probe

Having completed the synthesis of photoaffinity probe **4.40**, it was evaluated for its ability to induce cell death in U937 lymphoma cells (Figure 4.8) and was found to be active *in vitro* ($\text{IC}_{50} = 14.5 \pm 0.8$), although it was approximately four-fold less active than SFM1257 (**3.43**). Notably, **4.40** was approximately two-fold more active than the biotinylated derivative **4.10** ($\text{IC}_{50} = 34.9 \pm 6.1 \mu\text{M}$) and slightly more active than the *N*-propargyl compound **4.11** ($\text{IC}_{50} = 22.5 \pm 4.7 \mu\text{M}$). Thus, it was decided that photoaffinity

probe **4.40** would likely be the better choice going forward for subsequent pull-down studies.

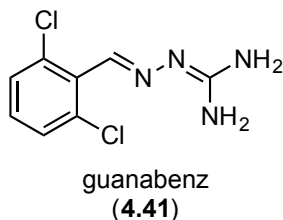
Figure 4.8. Biological Evaluation of Photoaffinity Probe



4.2.4. Evaluation SFM1257 Mode-of-Action With Small Molecule Tool Compounds

While work was being done to synthesize the new chemical probes in the previous section, the mode-of-action of SFM1257 (**3.43**) was being further evaluated using known tool compounds. Initial work performed by Dr. Claire Knezevic found the tool compound salubrinal (**3.74**), which is known to reduce endoplasmic reticulum (ER) stress, was cytoprotective against SFM1257 (**3.43**)-induced toxicity.⁹⁵ To investigate whether the protection afforded by salubrinal (**3.74**) was due to PP1/GADD34 inhibition, the selective PP1/GADD34 inhibitor guanabenz²⁵⁸ (**4.41**) was used.

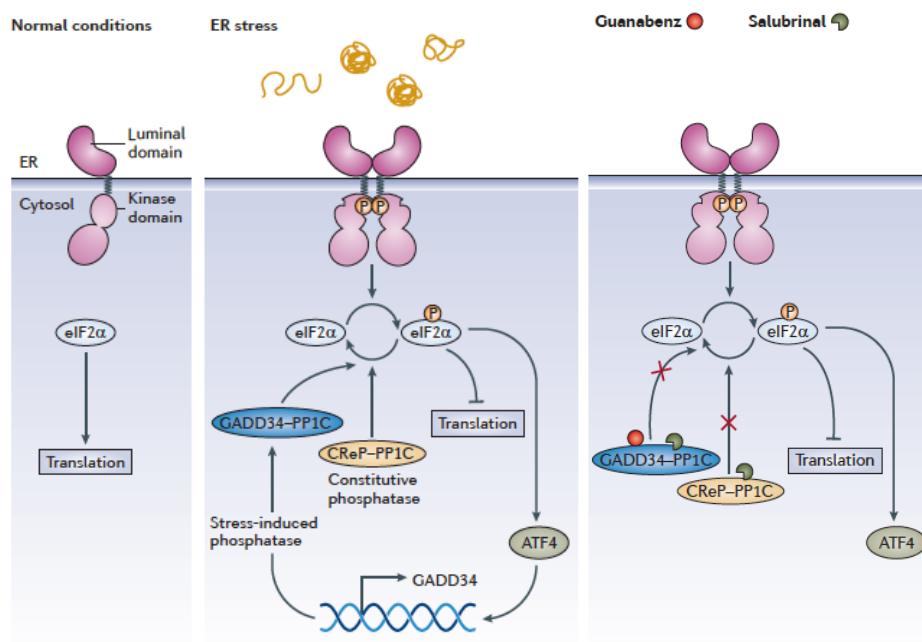
Figure 4.9. The Selective PP1/GADD34 Inhibitor Guanabenz (**4.41**)²⁵⁸



4.2.4.1 Guanabenz as a Cytoprotectant

Guanabenz (**4.41**) is an alpha agonist of the α_2 -adrenergic receptor, and it was approved by the FDA in 1982 for the treatment of hypertension.²⁵⁹ However, Bertolotti *et al* discovered in 2011 that guanabenz (**4.41**) also selectively inhibited growth arrest and DNA damage inducible protein (GADD34), which is the regulatory subunit of protein phosphatase 1 (PP1).²⁵⁸ When a cell experiences ER stress, it activates the unfolded protein response (UPR), and the ER signaling protein PERK phosphorylates eIF2 α (Figure 4.10).¹⁸⁹ The phosphorylation of eIF2 α causes a reduction in protein translation and upregulates other proteins designed to mitigate ER stress. The two phosphatases that act on p-eIF2 α are PP1/GADD34 and PP1/CReP; these holoproteins work to resume normal levels of protein translation.^{198,258} By inhibiting these phosphatases, salubrinal (**3.74**) and guanabenz (**4.41**) reduce the protein production rate to a level manageable by the ER, thereby mitigating the ER stress.

Figure 4.10. ER Stress and the Inhibitors Salubrinal (**3.74**) and Guanabenz (**4.41**)¹⁸⁹



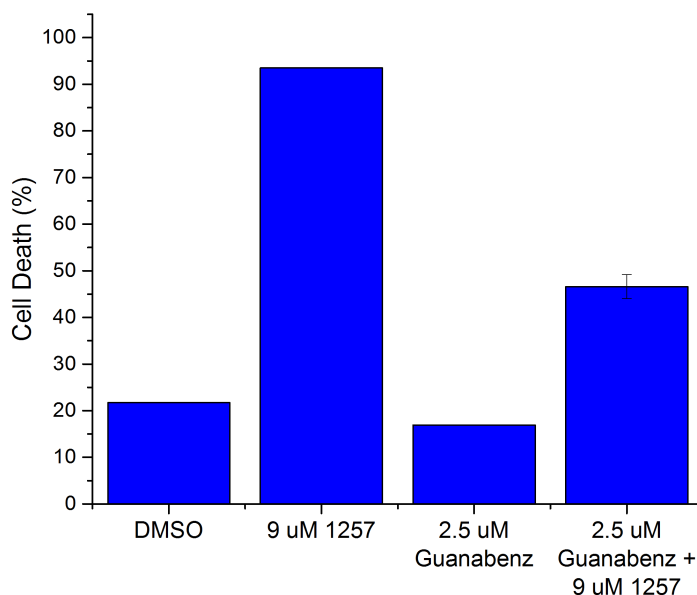
Copyright Nature Publishing Group; Reproduced with permission¹⁸⁹

Guanabenz (**4.41**) is considered a better tool to for studying the effects of ER stress because it is selective for the stress induced phosphatase PP1/GADD34 and does not affect the constitutively active phosphatase PP1/CReP, whereas salubrinal inhibits both phosphatases. Because salubrinal (**3.74**) inhibits the constitutively active phosphatase PP1/CReP, cells incubated with salubrinal (**3.74**) will show an increase in the level of p-eIF2 α regardless of whether the cell is undergoing ER stress. On the other hand, cells incubated with guanabenz (**4.41**) will only show an increase in p-eIF2 α levels if the cell has activated the UPR because PP1/GADD34 is only transcribed when the UPR is initiated.²⁶⁰

4.2.4.2 Evaluation of Guanabenz

To evaluate the cytoprotective ability of guanabenz (**4.41**), U937 cells were incubated with 2.5 μ M guanabenz (**4.41**) for two hours, and SFM1257 (**3.43**) was then added so that the final concentration of SFM1257 (**3.43**) was 9 μ M. After three hours, the viability of the cells was determined via flow cytometry by staining with PI/Annexin V-FITC (Figure 4.11). It was observed that guanabenz (**4.41**) provided robust cytoprotection (~67%) against SFM1257 (**3.43**)-induced cell death. This result provided one more piece of evidence that SFM1257 (**3.43**)-induced cell death results from ER stress and further validated that the results obtained with salubrinal (**3.74**). Additionally, it demonstrated that inhibiting the constitutively active phosphatase PP1/CReP was not necessary to afford cytoprotection.

Figure 4.11. Guanabenz (**4.41**) Protects against SFM1257 (**3.43**) Induced Cytotoxicity



4.2.5 Future Studies

Moving forward, additional studies must be performed to identify the biological target and correlate the cytotoxicity to a biochemical marker. Before the photoaffinity probe (**4.41**) can be used to perform target identification studies via biotin pull-down experiments, it would be prudent to verify that **4.41** has the same mode-of-action as SFM1257 (**3.43**). At the moment, it has only been shown that **4.41** is cytotoxic. To validate that **4.41** has the same mode-of-action as SFM1257 (**3.43**), cytoprotection should be observed with salubrinal (**3.74**) and guanabenz (**4.41**). Additionally, further studies must be performed to evaluate the connection between p-eIF2 α levels and cell death. Previous work by Dr. Claire Knezevic⁹⁵ and Dr. Betsy Parkinson⁹⁶ has shown high levels of p-eIF2 α were seen in cell incubated with cytotoxic amounts of SFM1257 (**3.43**), and normal levels were seen when the cytoprotectant small molecule salubrinal (**3.74**) was used. It would be of interest to see if similar results are obtained when guanabenz (**4.41**) is used as a cytoprotectant. Another experiment that would provide further insight into

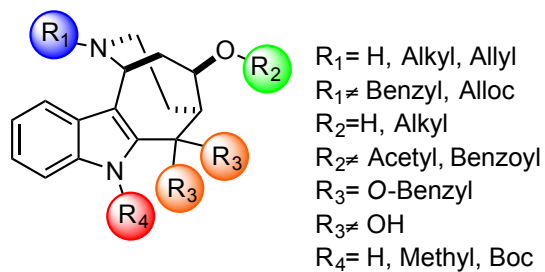
the mode-of-action would be to evaluate SFM1257 (**3.43**) against cells that are eIF2 α phosphorylation incompetent. By preventing the formation of p-eIF2 α , one would be able to determine whether phosphorylation is a direct cause of the cell death or is secondary effect of SFM1257 (**3.43**) toxicity.

4.3 STRUCTURE ACTIVITY ANALYSIS OF NOVEL TETRACYCLIC INDOLE DERIVATIVES

4.3.1 Introduction

Prior to the commencement of this work, a number of novel tetracyclic indole containing derivatives had been synthesized and their anticancer properties had been evaluated (Table 4.2).^{95,96,120} From these data, a preliminary structure-activity-relationship (SAR) was formed (Table 4.2). It was clear that large non-polar groups and carbamates on the basic nitrogen moiety (benzyl, dithioacetal, alloc) (Table 4.2, R₁) were not tolerated, but smaller groups (-H, alkyl, allyl) were. The oxygen moiety (Table 4.2, R₂) could be left as the free hydroxyl group or methylated to the *O*-Me, but acylation with acetyl and benzoyl chloride to afford the corresponding ester was not tolerated. Derivatives with an *O*-benzyl group on the 1,3-diol moiety (Table 4.2, R₃) were biologically active, but no cytotoxicity was observed when the benzyl groups were removed to give the free alcohols. In addition, substitution at the indole nitrogen atom (Table 4.2, R₄) was well tolerated (-H, Boc, methyl). Although these data provided some initial insights of the SAR, it was not clear what constituted the minimum active pharmacophore, nor was it obvious if the Lewis basic positions (Table 4.2, R₁, R₂, R₄) were necessary for the compound to interact with its biological target.

Table 4.2. Preliminary SAR and Evaluation of Cytotoxicity^{95,96,120}



4.9

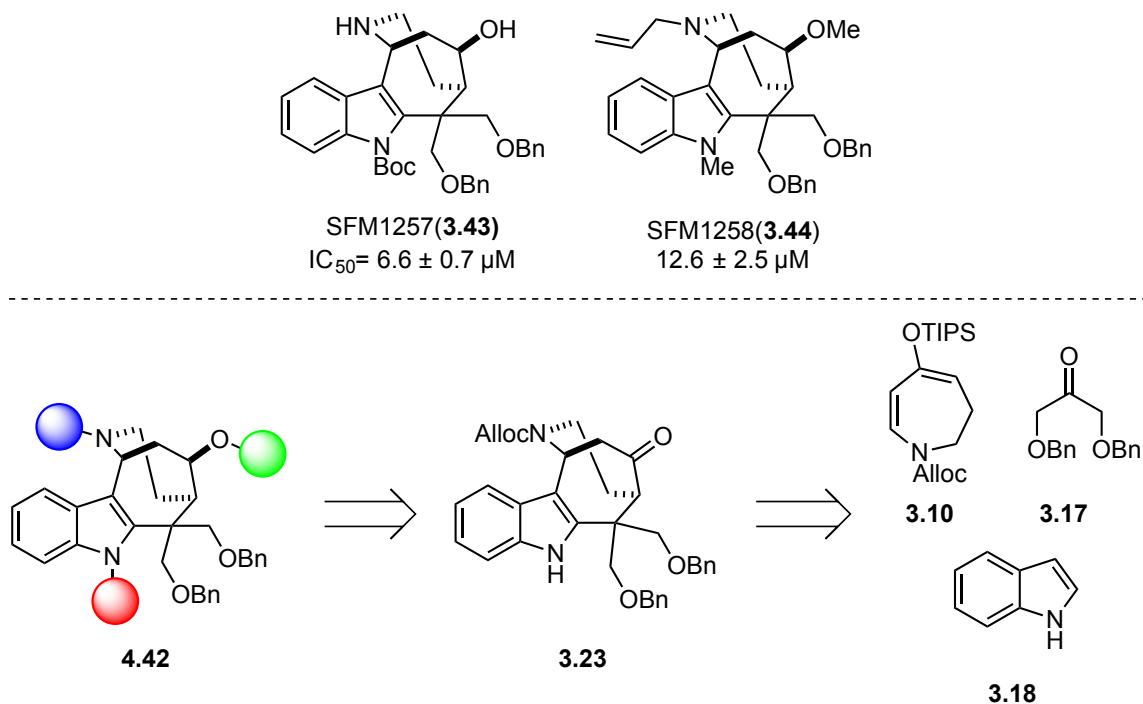
Compound	R ₁	R ₂	R ₃	R ₄	Hs578t IC ₅₀ (μM)	U937 IC ₅₀ (μM)	Hemolysis IC ₅₀ (μM)
3.38	Allyl	OH	OBn	H	63 ± 16.0	14.1	>100 μM
3.39	H	OH	OBn	H	14.9 ± 4.8	ND	>100 μM
3.40	-CH ₂ CH(OH) CH ₂ OH	OH	OBn	H	20.4 ± 3.6	ND	>100 μM
3.41	<i>n</i> -Propyl	OH	OBn	H	13.2 ± 1.3	9.8	>100 μM
3.42	Me	OH	OBn	H	12.6 ± 2.5	9.6	~100 μM
3.43	H	OH	OBn	Boc	6.6 ± 0.7	3.3 ± 0.2	28 μM
3.44	Allyl	OMe	OBn	Me	15.5 ± 2.8	ND	>100 μM
3.25	-CH ₂ CH ₂ -	=O	OBn	H	11.2 ± 1.9	ND	>100 μM
3.32	Allyl	OAc	OBn	H	>100 μM	ND	ND
3.33	Allyl	OBz	OBn	H	>100 μM	ND	ND
3.34	Alloc	OTMS	OBn	H	>100 μM	ND	ND
3.35	Alloc	OTMS	OBn	Boc	>100 μM	ND	ND
3.36	Alloc	OH	OBn	Boc	>100 μM	ND	ND
3.29	Bn	OH	OBn	H	>100 μM	ND	ND
3.31	<i>n</i> -Propyl	OH	OH	H	>100 μM	ND	ND
3.24	H	=O	OBn	Boc	>100 μM	ND	ND
3.30	-CH ₂ CH(SEt) ₂	OH	OBn	H	>100 μM	ND	ND

ND= Not Determined

4.3.2 Structure Activity Relationship of Lewis Basic Atoms

We commenced our studies by focusing, on determining how substitution at the Lewis basic sites modulated the biological activity of the two lead compounds, SFM1257 and SFM1258. The initial derivatives screened (Table 4.2) had sporadic substitution patterns that made it difficult to draw conclusions. For example, we observed a drop in potency between SFM1257 (**3.43**) and SFM1258 (**3.44**), but we were not sure whether modification of the basic amine, indole nitrogen atom, or alcohol group was responsible for the loss in potency. Thus, we sought to make iterative changes to the scaffold so that direct comparisons between analogs could be made, and the effect of substitution at each Lewis basic position could be deduced. Additionally, the Lewis basic positions were chosen first because they could be accessed from known intermediates in the synthesis of (±)-actinophyllic acid (**3.7**) by Martin *et al* (Figure 4.12).¹⁰⁰

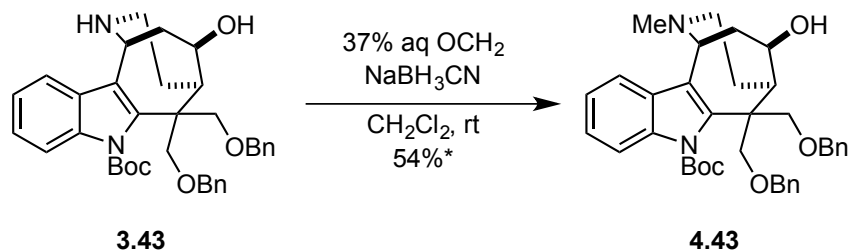
Figure 4.12. SAR Studies of Lewis Basic Atoms



4.3.2.1 Synthesis of Tetracyclic Derivatives

We began by synthesizing analogs of SFM1257 (**3.43**) and SFM1258 (**3.44**) that possessed different substituents at single Lewis basic sites. Thus, the *N*-methyl SFM1257 (**3.43**) analog was synthesized in 54% yield via a reductive amination of **3.43** with formaldehyde (Scheme 4.12).

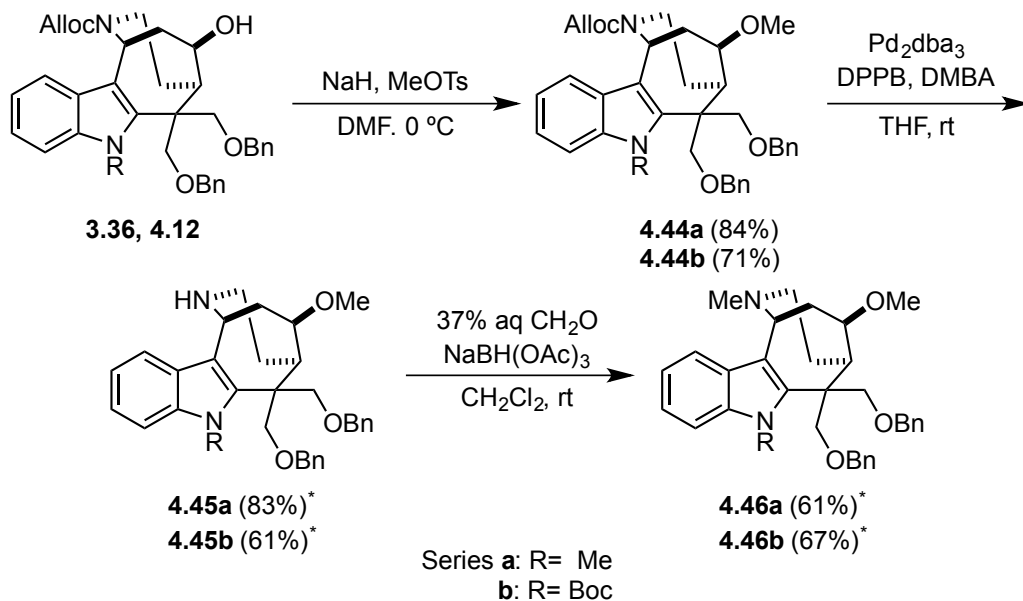
Scheme 4.12. Synthesis of Derivative **4.43**



*Reaction was only run once

Additional derivatives of SFM1257 (**3.43**) and SFM1258 (**3.44**) were synthesized from compounds **4.12** and **3.36**, which were readily accessible intermediates from the Martin synthesis of (±)-actinophyllic acid (**3.7**) (Scheme 4.13).¹²² Alkylation of **4.12** and **3.36** with sodium hydride and methyl *p*-toluenesulfonate afforded compounds **4.44a** and **4.44b** in 84% and 71% yields, respectively. The allyl carbamate protecting group was removed with Pd₂dba₃/DPPB and 1,3-dimethylbarbituric acid (DMBA) to give compounds **4.45a** and **4.45b** in 83% and 61% yields. Lastly, a reductive amination of **4.45a** and **4.45a** with formaldehyde afforded tertiary amines **4.46a** and **4.46b** in 61% and 67% yields.

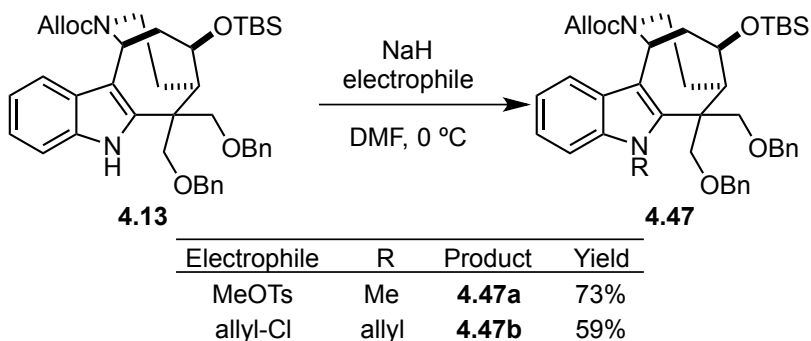
Scheme 4.13. Synthesis of Derivatives **4.45a**, **4.45b**, **4.46a**, and **4.46b**



*Reaction was only run once

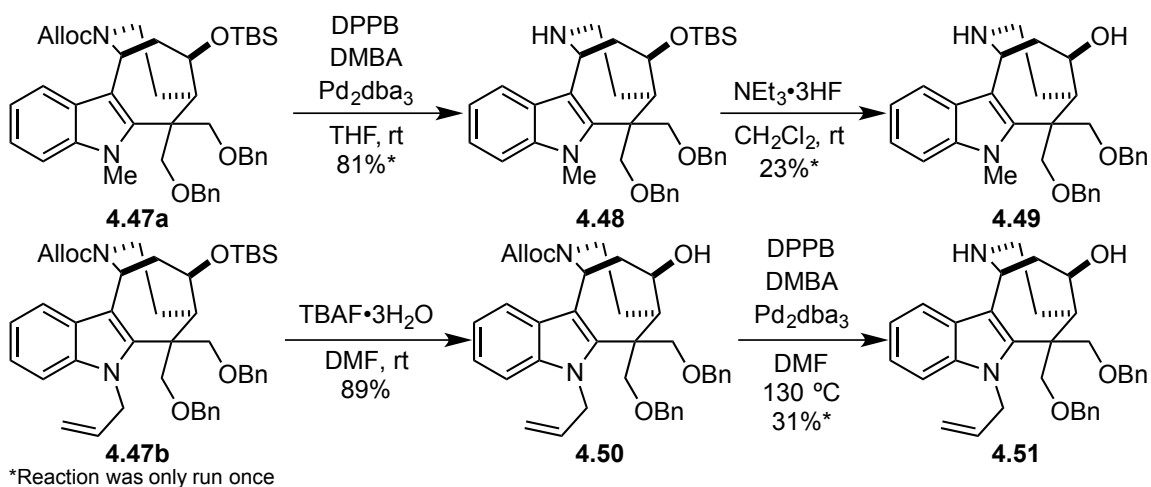
To gauge the importance of the Boc group on SFM1257 (**3.43**) bioactivity, various substitution patterns on the indole nitrogen atom were investigated (Scheme 4.14). From the work done to synthesize the photoaffinity tethered compound **4.40**, we knew that only highly reactive electrophiles without acidic protons would readily alkylate the indole nitrogen atom. Thus, compound **4.13** was alkylated with methyl *p*-toluenesulfonate and allyl chloride to give compound **4.47a** and **4.47b** in 73% and 59% yields, respectively.

Scheme 4.14. Alkylation of Indole Nitrogen Atom



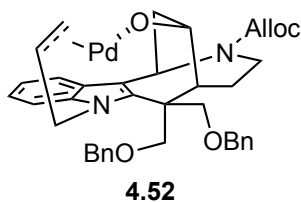
With compounds **4.47a** and **4.47b** in hand, the TBS group and allyl carbamate moiety were removed to afford new derivatives with differing substitution on the indole nitrogen atom. The allyl carbamate of **4.47a** was removed with Pd₂dba₃/DPPB using 1,3-dimethylbarbituric acid (DMBA) as the allyl scavenger to afford **4.48** in 81% yield. A small amount of **4.48** was reserved for biological evaluation, and the remaining material was deprotected with NEt₃•3HF to give **4.49** in 23% yield after HPLC purification. Additionally, allyl derivative **4.51** was formed in two steps from **4.47b** by TBS removal with TBAF•3H₂O to afford **4.50**, then allyl carbamate removal with Pd₂dba₃/DPPB/DMBA to give **4.51** in 28% yield over two steps (Figure 4.13).

Figure 4.13. Synthesis of Derivatives **4.48**, **4.49** and **4.51**



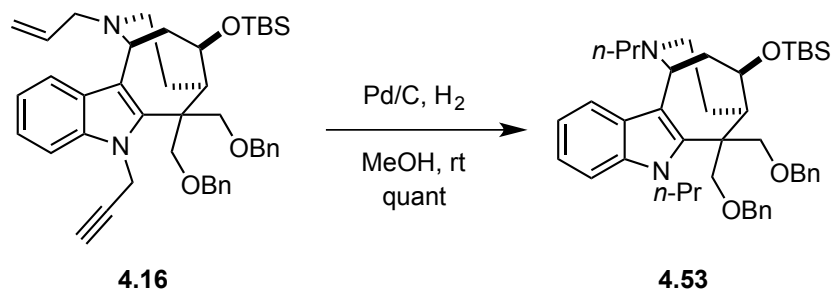
Unexpectedly, removing the allyl carbamate group from **4.50** with Pd₂dba₃/DPPB did not proceed in THF or refluxing dioxane. Instead, heating the reaction to 130 °C in DMF was required. Given that the allyl carbamate group was removed from similar compounds without employing such harsh conditions,^{100,122} it was postulated that the Pd⁰ species in the reaction might be coordinating with the indole *N*-allyl group first, then forming a chelate with the Lewis basic oxygen, thereby preventing the metal from performing the desired transformation. (Figure 4.14).

Figure 4.14. Proposed Intramolecular Palladium Chelate

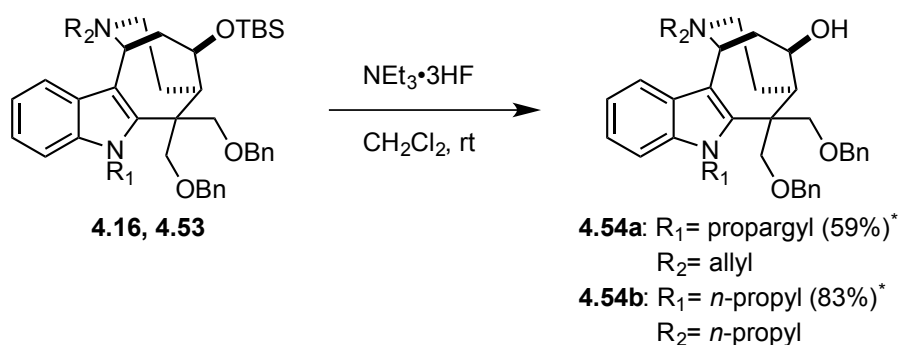


In the course of synthesizing the biotin tethered derivative **4.10**, an appreciable amount of compound **4.16** was isolated as an unintended byproduct. Thus, we decided to use **4.16** to synthesize additional derivatives (Scheme 4.15). Accordingly, a portion of **4.16** was quantitatively reduced to compound **4.53** using Pd/C and hydrogen gas. Compounds **4.16** and **4.53** were deprotected to give **4.54a** and **4.54b** in 59% and 83% yields, respectively (Scheme 4.16), thus providing derivatives **4.54a** and **4.54b** for biological evaluation.

Scheme 4.15. Reduction of Compound **4.16**



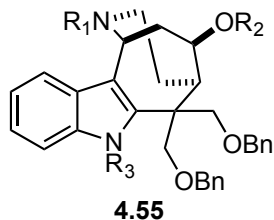
Scheme 4.16. Synthesis of Derivatives **4.54a** and **4.54b**



*Reaction was only run once

4.3.2.2 Evaluation of Tetracyclic Derivatives

Upon completing the synthesis of these novel derivatives, the compounds were evaluated for their ability to induce cell death in Hs578t cells (triple negative breast cancer) U937 cells (human lymphoma), and red blood cells (Table 4.3).

Table 4.3. Evaluation of Varying Substitution at Lewis Basic Sites

Entry	Cmpd	R ₁	R ₂	R ₃	Hs578t IC ₅₀ (μM)	U937 IC ₅₀ (μM)	Hem* IC ₅₀ (μM)
1	1257 (3.43)	H	H	Boc	6.6 ± 0.7*	3.3 ± 0.2*	28
2	4.43	Me	H	Boc	ND	5.3 ± 0.1*	140 ± 60
3	4.45b	H	Me	Boc	ND	4.0 ± 0.1*	50 ± 12
4	4.46b	Me	Me	Boc	ND	57.0 ± 1.5*	>333
5	1258 (3.44)	Allyl	Me	Me	20 ± 2.9*	5.6 ± 2.3*	>100
6	4.45a	H	Me	Me	ND	12.0 ± 0.2*	170 ± 60
7	4.46a	Me	Me	Me	ND	8.5 ± 0.7*	120 ± 40
8	4.49	H	H	Me	6.5 ± 0.6	6.8 ± 0.2	ND
9	4.48	H	TBS	Me	5.2 ± 0.3	6.8 ± 2.4	ND
10	4.51	H	H	Allyl	ND	10.7 ± 0.4*	110 ± 10
11	4.11	H	H	Propargyl	ND	22.5 ± 4.7*	>333
12	4.54a	Allyl	H	Propargyl	ND	9.4 ± 0.1*	>333
13	4.54b	<i>n</i> -Pr	H	<i>n</i> -Pr	ND	4.0 ± 0.1*	54 ± 9.8

ND= Not Determined; *Data collected by Dr. Betsy Parkinson⁹⁶

After analyzing the data, several conclusions were drawn about the structure-activity-relationship of these compounds. The first observation is that the oxygen moiety

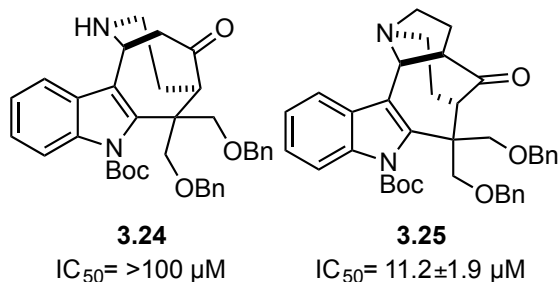
(R₂) is likely neither a hydrogen bond donor nor a major contributor to the phenotypic response. That observation is supported by comparing entry 1 to entry 3 and entry 8 to entry 9. When the oxygen atom was alkylated to the methyl ether (Table 4.3, entry 1 to entry 3), there was no significant change in activity. Additionally, blocking the oxygen atom with a large, greasy silyl group (Table 4.3, entry 8 and entry 9) did not impact the cytotoxicity of the compound. It is also clear that a Boc group on the indole nitrogen atom enhances cytotoxicity but it is not necessary. When the Boc group was substituted for a methyl group (Table 4.3, entry 1 and entry 8), no significant difference in activity was seen. However, the *N*-allyl and *N*-propargyl derivatives (Table 4.3, entry 10 and entry 11) showed a decrease in activity. One rather unexpected observation was that methylating both the basic nitrogen atom (R₁) and oxygen atom (R₂) of SFM1257 (**3.43**) caused a 10-fold reduction in potency (Table 4.3, entry 4), but methylating each position individually (Table 4.3, entry 2 and entry 3) had only a nominal impact on activity. A positive trend was observed in regards to hemolytic activity; methylation of the secondary amine of SFM1257 (**3.43**) (Table 4.3, entry 2) resulted in a dramatic decrease in hemolytic activity (28 μ M vs 140 μ M) but little to no loss in cytotoxicity. Overall, the SAR provided little insight, as various modifications across the scaffold provided little to no change in potency. Thus, we determined that substitution at the Lewis basic positions were not major contributors to the cytotoxicity of SFM1257 (**3.43**) and SFM1258 (**3.44**).

4.3.2.3 Synthesis of Pentacyclic Derivatives

An appreciable amount of the advanced intermediate **3.25** remained from the synthesis of (\pm)-actinophyllic acid (**3.7**) by Dr. Brett Granger. Since the pentacyclic derivative **3.25** was shown to be biologically active in the initial cytotoxicity screens (Table 4.2, **3.25**), we decided to prepare several pentacyclic derivatives to examine how

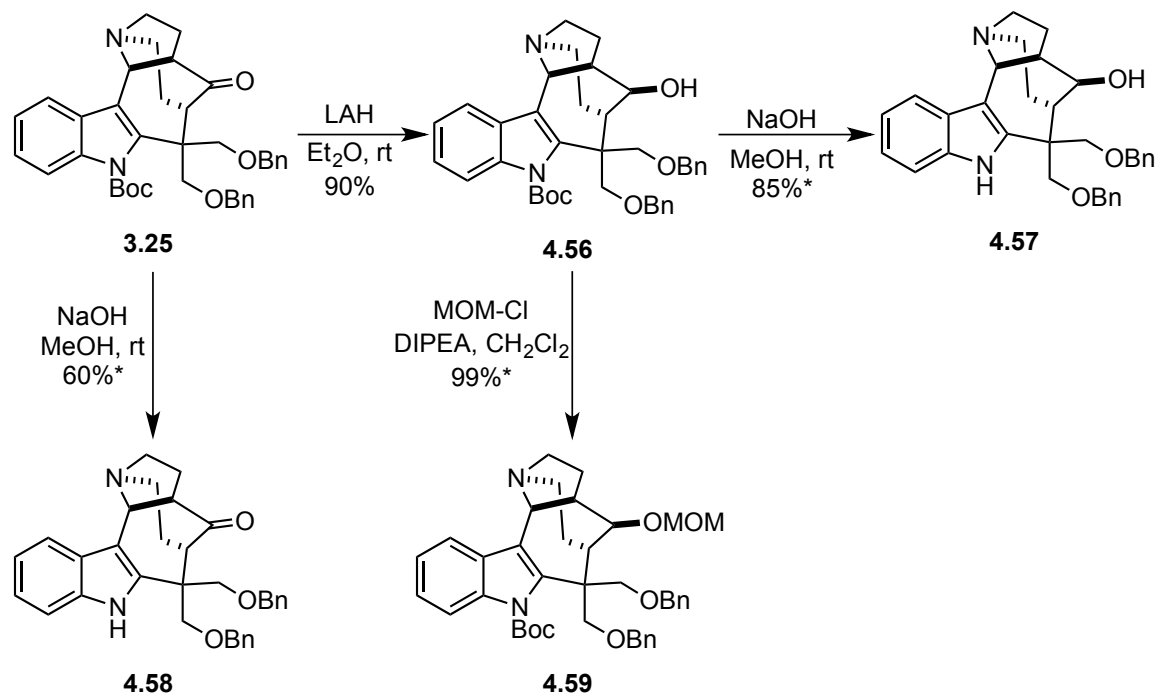
forming the additional ring affected the SAR. In addition, we found it curious that compound **3.25** was biologically active, but **3.24** was not (Figure 4.15). Given that tetracyclic compound **3.24** is known to degrade under acidic conditions,¹²⁰ we hypothesized that the lack of observed cytotoxicity may be due to degradation *in vitro*. Thus, pentacyclic compounds derived from **3.25** may be useful to help mitigate potential issues that may arise if our lead compound shows poor oral bioavailability due to rapid *in vivo* degradation.

Figure 4.15. Comparison of Pentacyclic **3.25** to Tetracyclic **3.24**



The syntheses of the novel pentacyclic derivatives **4.56-59** are shown in Scheme 4.17. Beginning from the pentacycle **3.25**, the ketone moiety was reduced to the alcohol **4.56** in 90% yield. The Boc groups of **3.25** and **4.56** were removed with NaOH/MeOH to give **4.58** and **4.57** in 65% and 85% yields, respectively. Lastly, a methoxymethyl ether was appended to compound **4.59** in 99% yield using diisopropylethylamine and MOM-Cl.

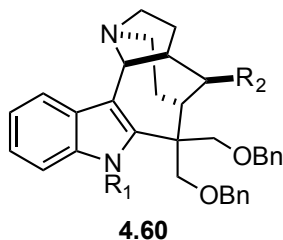
Scheme 4.17. Synthesis of Pentacyclic Derivatives **4.56**, **4.57**, **4.58**, and **4.59**.



*Reaction was only run once

4.3.2.4 Evaluation of Pentacyclic Derivatives

Upon completing the synthesis of these novel derivatives, the compounds were evaluated for their ability to induce cell death in U937 cells (human lymphoma) and red blood cells (Table 4.4).

Table 4.4. Evaluation of Pentacyclic Derivatives

Entry	Compound	R ₁	R ₂	Hs578t [*] IC ₅₀ (μM)	U937 [*] IC ₅₀ (μM)	Hem [*] IC ₅₀ (μM)
1	3.25	Boc	=O	11.2 ± 1.9	ND	ND
2	4.56	Boc	OH	ND	6.9 ± 0.5	80 ± 10
3	4.57	H	OH	ND	10.8 ± 0.3	210 ± 40
4	4.58	H	=O	ND	12.1 ± 0.1	>333
5	4.59	Boc	OMOM	ND	12.6 ± 0.1	140 ± 30

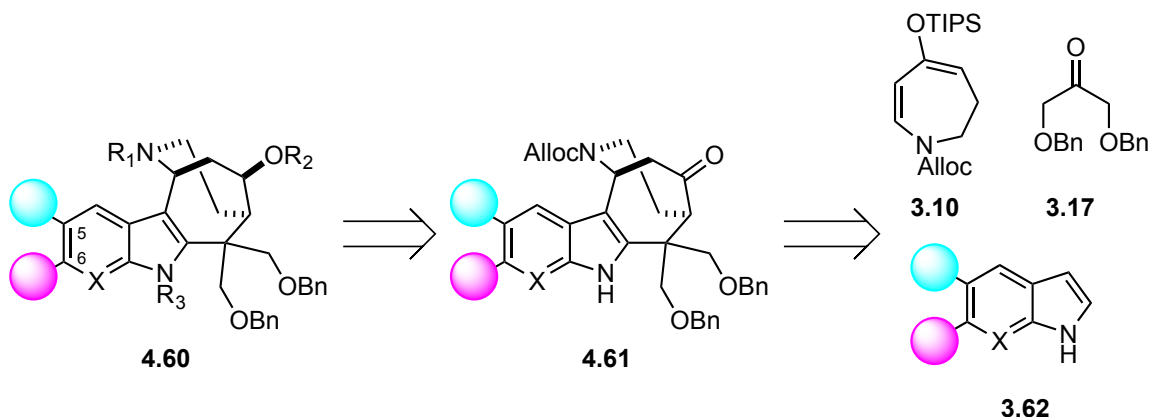
^{*}Data collected by Dr. Betsy Parkinson⁹⁶

The pentacyclic derivatives were found to be either comparable to or slightly less potent than the analogous tetracyclic compounds. However, the IC₅₀ data collected for these derivatives does provide additional insight into the role of the oxygen moiety (R₂) in the active pharmacophore. For example, comparing **4.57** to **4.58** (Table 4.4, entry 3 and entry 4) shows that the oxidation state of the alcohol does not affect the potency of the compound. Additionally, it was found that a Boc group on the indole nitrogen atom slightly improved potency, but activity was not dependent on the Boc group (Table 4.4, entry 2 and entry 3). Given that pentacyclic compounds **4.56-59** showed no clear superiority over the tetracyclic derivatives, no additional derivatives of **3.25** were prepared.

4.3.3 Structure Activity Relationship Associated with Indole Ring

After evaluating the SAR of the Lewis basic moieties on the tetra- and pentacyclic systems, we expanded into new a chemical space by synthesizing derivatives with substitution at the 5- and 6-positions of the indole ring. In addition, we sought to explore how derivatives based on 7-azaindole would affect the biological activity because the additional Lewis basic position would improve the water solubility and decrease the ClogD. Unfortunately, the substitution that we desired would not be accessible via late stage functionalization of SFM1257 (**3.43**) or SFM1258 (**3.44**), so it was necessary to use a prefunctionalized indole species from the beginning. To form the desired 5- and 6-substituted indole derivatives, we envisioned that the analogs could be formed from the common tetracyclic intermediate **4.61**, which in turn could be synthesized from substituted indole (**4.62**), π -nucleophile **3.10**, and ketone **3.17** (Figure 4.16).

Figure 4.16. Indole Ring SAR Studies



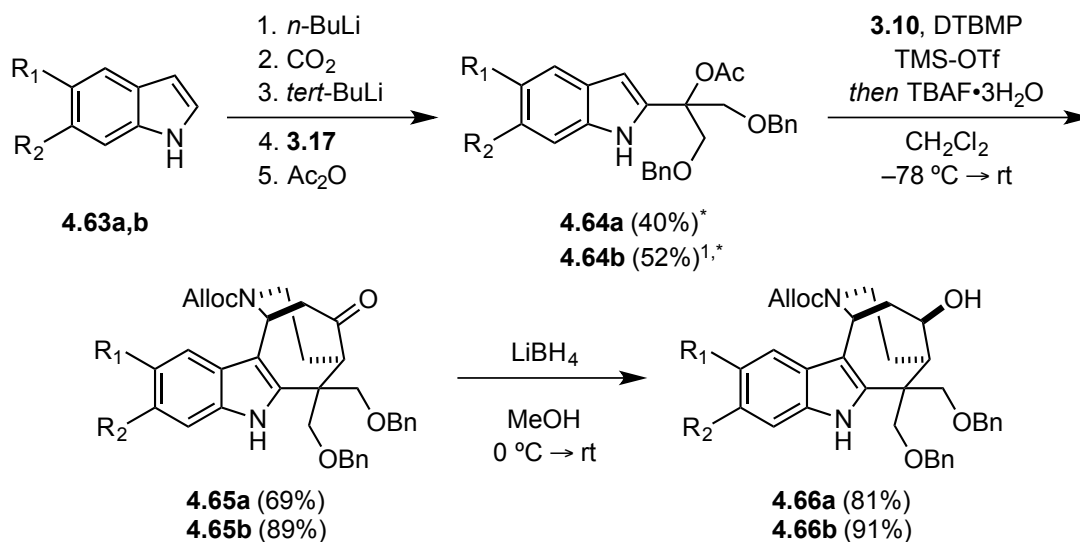
4.3.3.1 Synthesis of 5- and 6-Substituted Indole Derivatives

To install substituents at the 5- and 6-position of the indole ring, we reasoned that the best course of action was to make derivatives starting from commercially available 5-

and 6-chloroindole (**4.63a,b**). This approach would allow us to synthesize a diverse library of compounds via palladium catalyzed cross couplings.

The chemistry developed by Dr. Ivan Jewitt and Dr. Brett Granger for the synthesis of (±)-actinophyllic acid (**3.7**) worked well on the corresponding substituted indoles. Using the five step one-pot protocol, 5- and 6-chloroindole (**4.63a,b**) were converted to the corresponding 2-substituted indole acetates **4.64a,b** in 40% and 52% yields, respectively. Compounds **4.64a,b** were then combined with **3.10** and TMS-OTf to form the corresponding tetracyclic compounds **4.65a,b** in 69% and 89% yields. Reduction of **4.65a,b** with lithium borohydride gave the corresponding alcohols **4.66a,b** in 81% and 91% yields (Scheme 4.18).

Scheme 4.18. Synthesis of 5- and 6-Chloro Indole Scaffolds



Series **a**: $\text{R}_1 = \text{Cl}, \text{R}_2 = \text{H}$

b: $\text{R}_1 = \text{H}, \text{R}_2 = \text{Cl}$

TBAF= tetrabutylammonium fluoride; DTBMP= 2,6-di-*tert*-butyl-4-methylpyridine

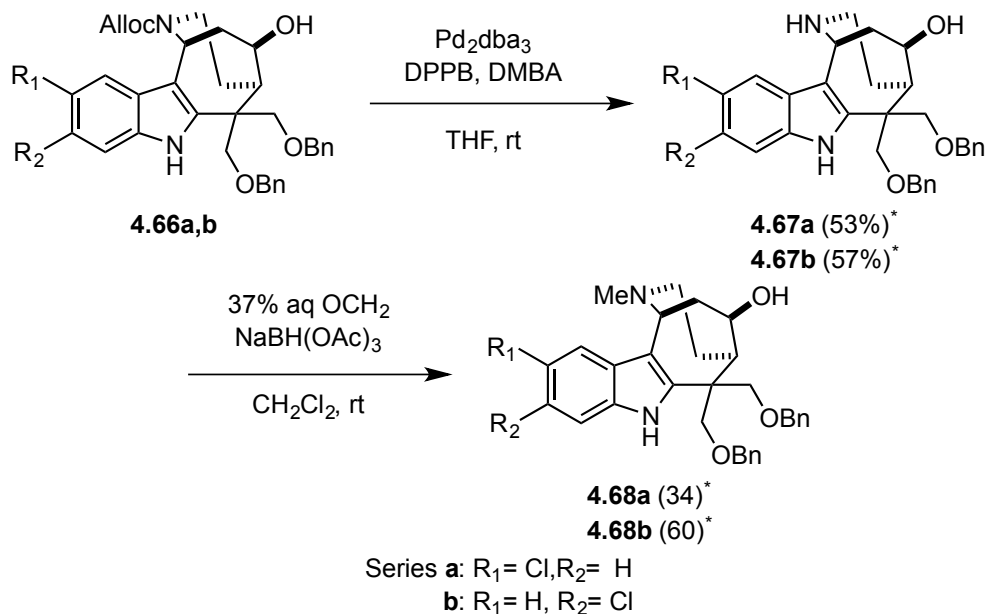
¹The alcohol (**4.64c**) was isolated in 31% yield

*Reaction was only run once

With compounds **4.66a,b** in hand, the allyl carbamate was removed with $\text{Pd}_2\text{dba}_3/\text{DPPB}/\text{DMBA}$ to provide the amines **4.67a,b** in 53% and 57% yields,

respectively (Scheme 4.19). Compounds **4.67a,b** were converted to the corresponding tertiary amines **4.68a,b** in 34% and 60% yields.

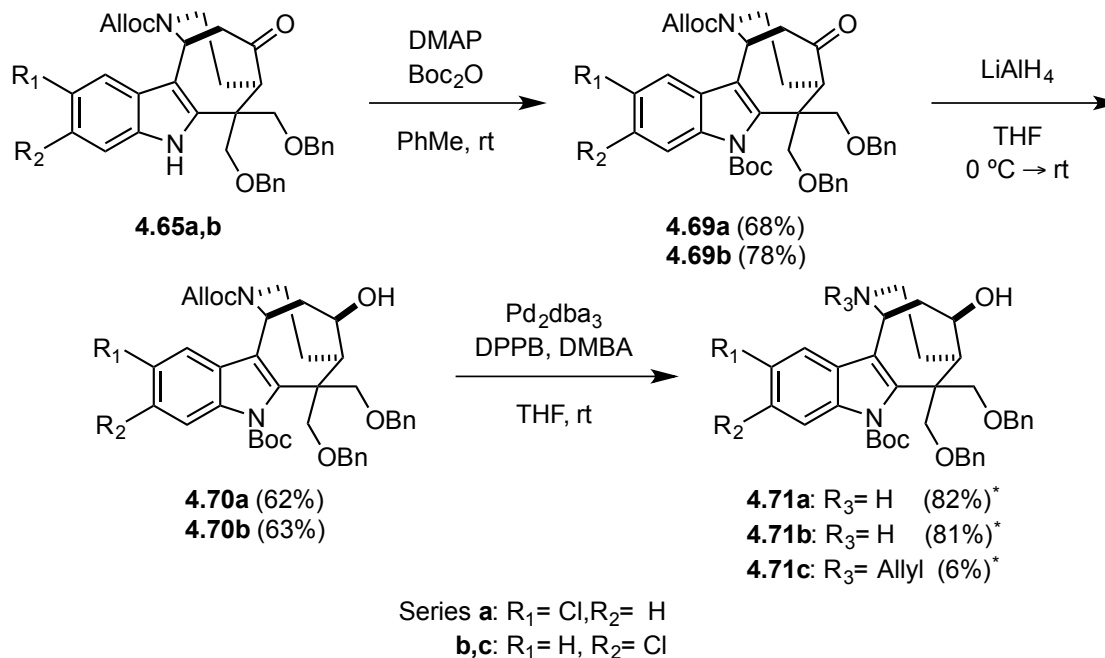
Scheme 4.19. Synthesis of 5- and 6-Chloro Derivative **4.67a-b** and **4.68a-b**



DPPB= 1,4-bis(diphenylphosphino)butane
 DMBA= 1,3-dimethylbarbituric acid; dba= dibenzylideneacetone
 *Reaction was only run once

The 5- and 6-chloroindole derivatives of SFM1257 (**3.43**) were then prepared in three steps from ketones **4.65a,b** (Scheme 4.20). The indole nitrogen atom of compounds **4.65a,b** were protected with di-*tert*-butyldicarbonate and 4-dimethylaminopyridine to afford **4.69a,b** in 68% and 78% yields, respectively. Compounds **4.69a,b** were reduced with lithium aluminum hydride to provide alcohols **4.70a,b** in 62% and 63% yields. The allyl carbamate of **4.70a,b** was removed with $\text{Pd}_2\text{dba}_3/\text{DPPB}/\text{DMBA}$ to give **4.71a,b** in 82% and 81% yield. Additionally, the *N*-allyl derivative **4.71c** was isolated as a minor product in 6% yield.

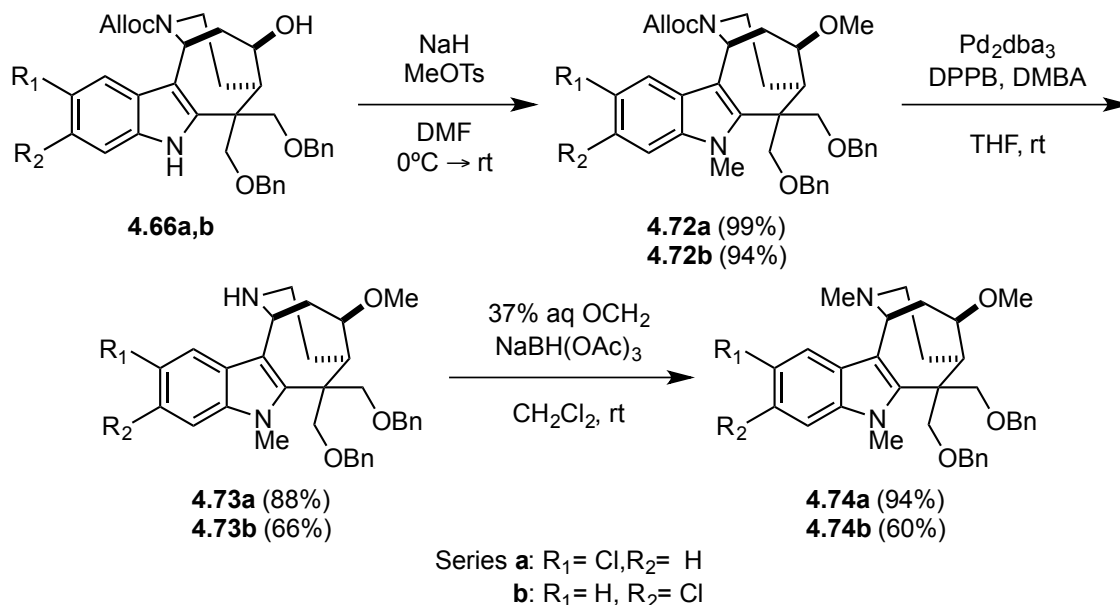
Scheme 4.20. Synthesis of 5- and 6-Chloro Derivatives of SFM1257 (**3.43**)



DPPB= 1,4-bis(diphenylphosphino)butane; DMAP= Dimethylaminopyridine
 DMBA= 1,3-dimethylbarbituric acid; dba= dibenzylideneacetone; Boc₂O= di-*tert*-butyldicarbonate
 *Reaction was only run once

The synthesis of 5- and 6-substituted derivatives continued with methylation of **4.66a,b** using sodium hydride and methyl *p*-toluenesulfonate to give **4.72a,b** in 99% and 94% yield (Scheme 4.21). The allyl carbamates of **4.72a,b** were removed with Pd₂dba₃/DPPB/DMBA to give the corresponding amines **4.73a-b** in 88% and 66% yield. Subsequent reductive amination with 37% aqueous formaldehyde and sodium triacetoxyborohydride afforded tertiary amines **4.74a,b** in 94% and 60% yield.

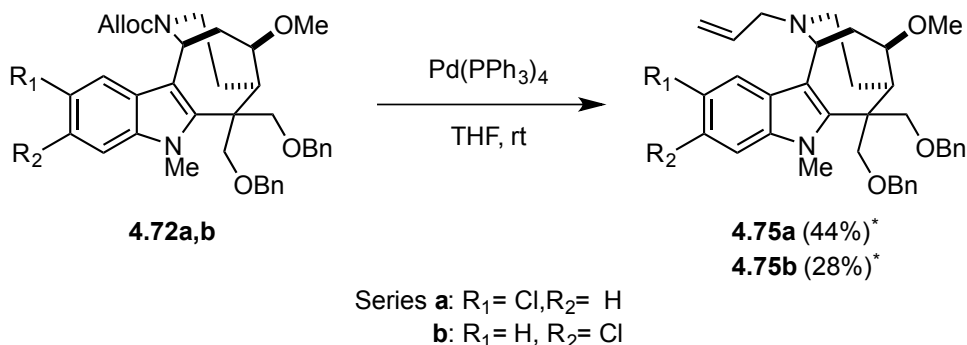
Scheme 4.21. Synthesis of 5- and 6-Substituted Derivatives **4.73a,b** and **4.74a,b**



DPPB= 1,4-bis(diphenylphosphino)butane
 DMBA= 1,3-dimethylbarbituric acid; dba= dibenzylideneacetone

The 5- and 6-chloro derivative of SFM1258 (**3.44**) were prepared in one step from compounds **4.72a,b**. A palladium catalyzed decarboxylative allylation using $\text{Pd}(\text{Ph}_3)_4$ afforded the 5- and 6-chloro-*N*-allyl derivatives (**4.75a,b**) in 44% and 28% yields, respectively (Scheme 4.22).

Scheme 4.22. Synthesis of 5- and 6-Chloro Analogs of SFM1258 (**3.44**)

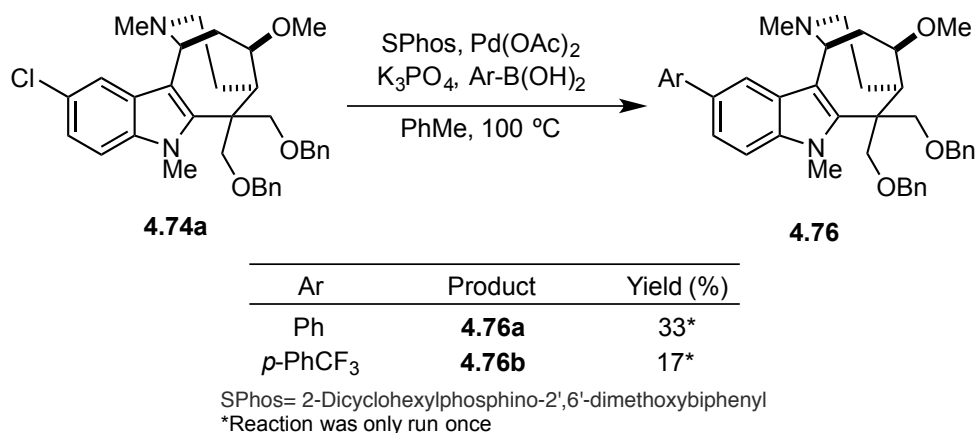


*Reaction was only run once

To expand further into new chemical space, preliminary work was undertaken to form novel derivatives with varying substitution at the 5-position of the indole subunit.

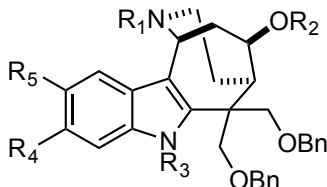
Using conditions developed by Buchwald *et al*,²⁶¹ a Suzuki coupling on **4.74a** with phenylboronic acid and 4-(trifluoromethyl)phenylboronic acid using Pd(OAc)₂/SPhos/K₃PO₄ in toluene at 100 °C afforded the desired products **4.75a,b** in 33% and 17% yield (Scheme 4.23).

Scheme 4.23. Synthesis of Suzuki Adducts **4.76a-b**



4.3.3.2 Evaluation

Upon completing the synthesis of these novel 5- and 6-substituted indole derivatives, the compounds were evaluated for their ability to induced cell death in Hs578t cells (triple negative breast cancer) U937 cells (human lymphoma), and red blood cells (Table 4.5).

Table 4.5. Evaluation of 5- and 6-Substituted Derivatives

Entry	Cmpd	R ₁	R ₂	R ₃	R ₄	R ₅	Hs578t IC ₅₀ (μM)	U937 IC ₅₀ (μM)	Hem IC ₅₀ (μM)
1	1257 (3.43)	H	H	Boc	H	H	6.6 ± 0.7*	3.3 ± 0.2*	28*
2	1258 (3.44)	Allyl	Me	Me	H	H	20 ± 2.9*	5.6 ± 2.3*	>100
3	4.68a	Me	H	H	H	Cl	ND	4.9 ± 0.1*	190 ± 60*
4	4.67a	H	H	H	H	Cl	ND	6.0 ± 0.2*	120 ± 20*
5	4.68b	Me	H	H	Cl	H	5.9 ± 0.4	6.7 ± 0.9	ND
6	4.67b	H	H	H	Cl	H	3.1 ± 0.4	4.5 ± 1.0	ND
7	4.71a	H	H	Boc	H	Cl	5.1 ± 1.0	3.8 ± 0.4	ND
8	4.71b	H	H	Boc	Cl	H	4.8 ± 1.0	3.9 ± 0.5	ND
9	4.71c	Allyl	H	Boc	Cl	H	15.1 ± 2.9	12.2 ± 2.0	ND
10	4.75a	Allyl	Me	Me	H	Cl	36.4 ± 2.3	11.9 ± 0.5	ND
11	4.73a	H	Me	Me	H	Cl	7.2 ± 1.1	9.0 ± 1.6	ND
12	4.74a	Me	Me	Me	H	Cl	6.9 ± 0.6	6.0 ± 0.2	ND
13	4.75b	Allyl	Me	Me	Cl	H	32.5 ± 3.8	12.8 ± 0.2	ND
14	4.73b	H	Me	Me	Cl	H	5.6 ± 0.3	4.5 ± 0.5	ND
15	4.74b	Me	Me	Me	Cl	H	4.5 ± 0.8	5.1 ± 1.4	ND
16	4.76a	Me	Me	Me	H	Ph	10.2 ± 1.6	6.9 ± 0.7	ND
17	4.76b	Me	Me	Me	H	<i>p</i> -PhCF ₃	6.3 ± 0.1	6.2 ± 0.1	ND

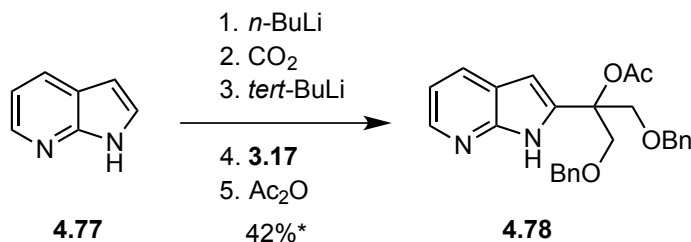
*Data collected by Betsy Parkinson⁹⁶; ND= Not Determined

Analysis of the data presented in Table 4.5 shed light on several trends with the 5- and 6-chloroindole derivatives. First and foremost, all of the 5- and 6-chloroindoles as well as the 5-phenyl derivatives were active *in vitro* ($IC_{50} < 20 \mu M$). However, there were no significant differences in potency between the 5- and 6-chloro derivatives and no enhancement in activity over the unsubstituted derivatives. For example, the most potent compound SFM1257 (**3.43**) showed almost identical activity to its 5- and 6-chloro analogs (Table 4.5, entry 1 vs. entry 7 and entry 8), and the 5- and 6-chloro analogs of SFM1258 (**3.44**) showed a slight drop in potency (entry 2 vs. entry 10 and entry 13). However, the data did clearly showed that an allyl group on the basic nitrogen atom (R_1) causes a significant reduction in cytotoxicity (Table 4.5, entry 7 vs. entry 9, entry 10 vs. entry 11, entry 13 vs. entry 14). On a positive note, the two derivatives that were evaluated for hemolytic activity (Table 4.5, entry 3 and entry 4) had an $IC_{50} > 100 \mu M$.

4.3.3.3 Synthesis of 7-Azaindole Derivatives

After evaluating the effects of substitution at the 5- and 6-positions, we investigated whether 7-azaindole derivatives would be tolerated in our system. The synthesis of 7-azaindole derived compounds commenced with the synthesis of indolo-acetate **4.78**. Using the five step one-pot protocol, 7-azaindole (**4.77**) was converted to indolo-acetate **4.78** in 42% overall yield.

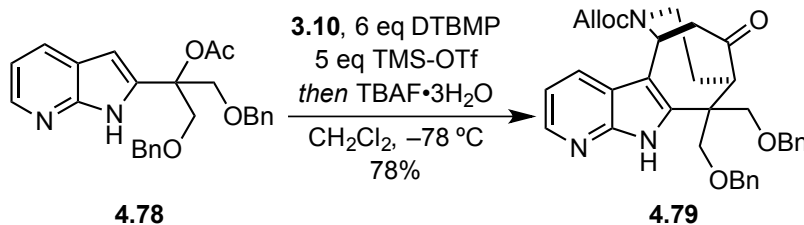
Scheme 4.24. Synthesis of Indolo-acetate **4.78**



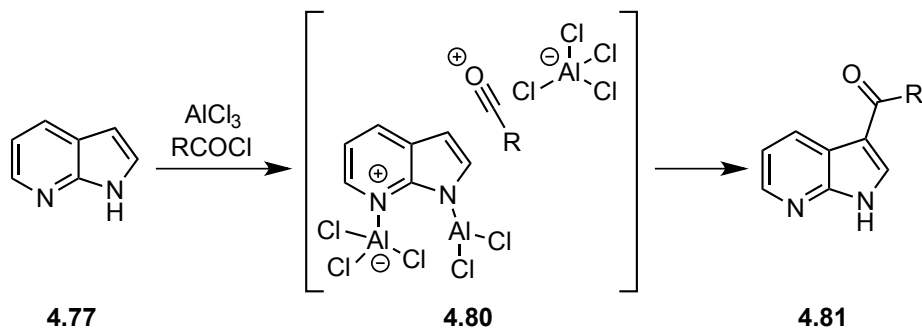
*Reaction was only run once

With indolo-acetate **4.78** in hand, the cascade sequence was performed to deliver **4.79** in 78% yield (Scheme 4.25). Notably, this reaction required an excess of TMS-OTf (5 eq) to go to completion. We hypothesized that the excess Lewis acid was required because the additional Lewis basic position of the 7-azaindole moiety sequestered the TMS-OTf, which inhibits carbocation formation. Indeed, Zhang *et al* made a similar hypothesis in Friedel-Crafts acylations of 7-azaindole (**4.77**), when they observed that an excess of aluminum trichloride was needed to obtain optimum yields.²⁶² They hypothesized that the AlCl₃ reacted with azaindole (**4.77**) to give complex **4.80** before activating the acylating agents (Scheme 4.26).

Scheme 4.25. Synthesis of 7-Azaindole Derived Tetracycle **4.79**



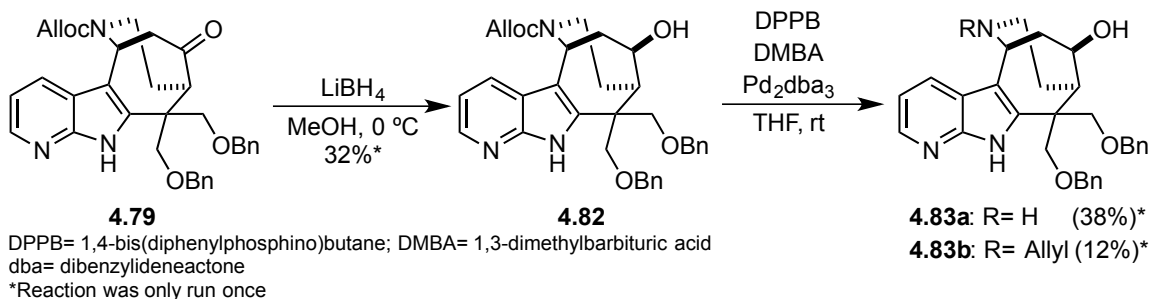
Scheme 4.26. Friedel Craft Acylation of 7-Azaindole²⁶²



After successfully synthesizing tetracyclic **4.79**, the ketone moiety was reduced to an alcohol group **4.82** in 32% yield using lithium borohydride, and the allyl carbamate of

4.82 was removed with Pd₂dba₃/DPPB/DMBA to provide **4.83a** and **4.83b** in 38% and 12% yield, respectively.

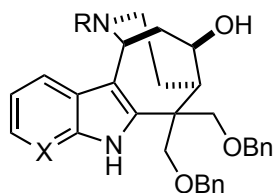
Scheme 4.27. Synthesis of 7-Azaindole Derivatives **4.83a** and **4.83b**



4.3.3.4 Evaluation of 7-Azaindole Derived Compounds

Upon completing the synthesis of the 7-azaindole derivatives, the compounds were evaluated for their ability to induce cell death in Hs578t cells (triple negative breast cancer) and U937 cell (human lymphoma) (Table 4.6). Unfortunately, the derivatives derived from 7-azaindole did not see an enhancement in potency. As a result, this series of derivatives was not pursued further.

Table 4.6. Evaluation of 7-Azaindole Derivatives



4.83

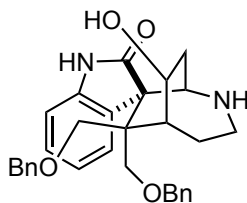
Compound	X	R	Hs578t IC ₅₀ (μM)	U937 IC ₅₀ (μM)
3.39	C	H	14.9 ± 4.8	ND
3.38	C	Allyl	63 ± 16.0	14.1
4.83a	N	H	23.7 ± 4.3	11.9 ± 1.7
4.83b	N	Allyl	44.6 ± 0.6	28.4 ± 0.5

ND= Not Determined

4.3.3.4 Attempted Synthesis of Oxindole Derivatives

During the course of these studies, we became curious as to whether major structural changes in the conformation of the indole moiety would affect biological activity. We hypothesized that an oxidative rearrangement of the indole moiety to 2-oxindole **4.84** (Figure 4.17) would dramatically alter the orientation of the molecule. If no changes in cytotoxicity were observed upon rearrangement, we would conclude that the indole moiety has a nominal role in binding to the biological target.

Figure 4.17 Proposed Oxindole Derivative



4.84

We found that compounds **4.12** and **4.13** underwent facile rearrangement upon reaction with *meta*-chloroperoxybenzoic acid to give the 3-oxindole **4.86a**, not the 2-oxindole **4.85** that was initially expected (Scheme 4.28). Indeed, free alcohol **4.12** and the TBS-protected alcohol **4.13** afforded the highly fluorescent 3-oxindole species as a single diastereomer in 80% and 77% yields, respectively. The structure and the relative stereochemistry of **4.86b** was unambiguously determined via X-ray crystallography (Figure 4.18).

Scheme 4.28. Synthesis of 3-Oxindole Derivative **4.86a** and **4.86b**

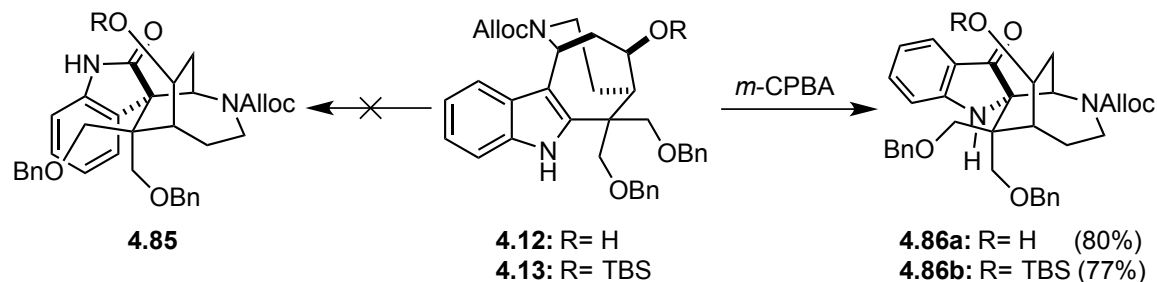
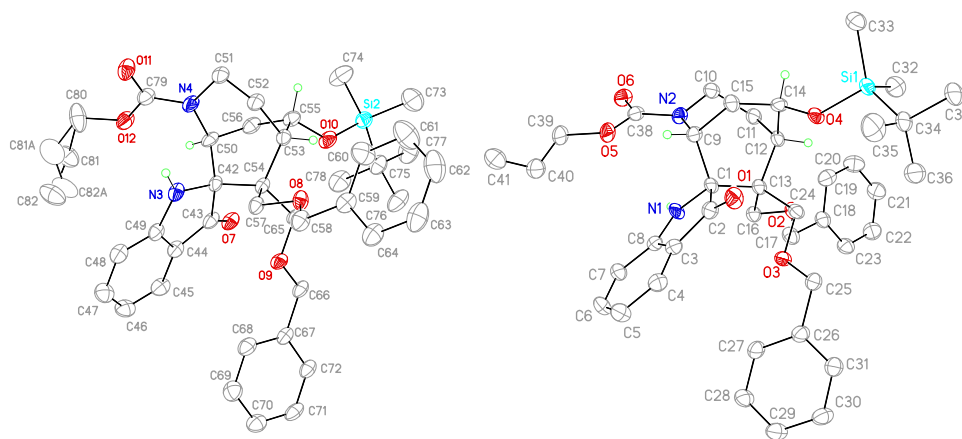


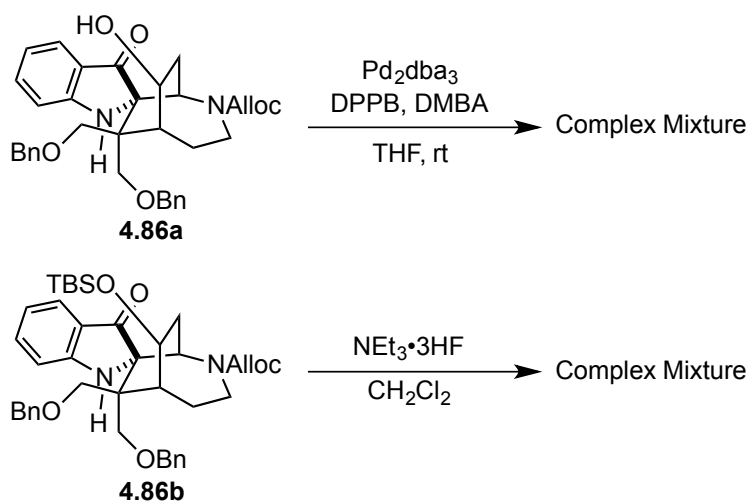
Figure 4.18. X-Ray Structures of Both **4.86b** Enantiomers



Unfortunately, attempts to remove the allyl carbamate from **4.86a** or the TBS ether from **4.86b** provided complex mixtures of products (Figure 4.19). LCMS analysis

of the crude reaction mixtures showed a variety of compounds with mass hits corresponding to either addition of DMBA or HF. We hypothesized that the acidic conditions of these transformations may be causing a retro-mannich reaction that would cleave the bridgehead C-C bond and react with whatever nucleophile is in the reaction. Because of concerns that these compounds may not be stable in a biological system, we did not pursue them any further.

Figure 4.19: Attempted Deprotection of 3-Oxindole Derivative

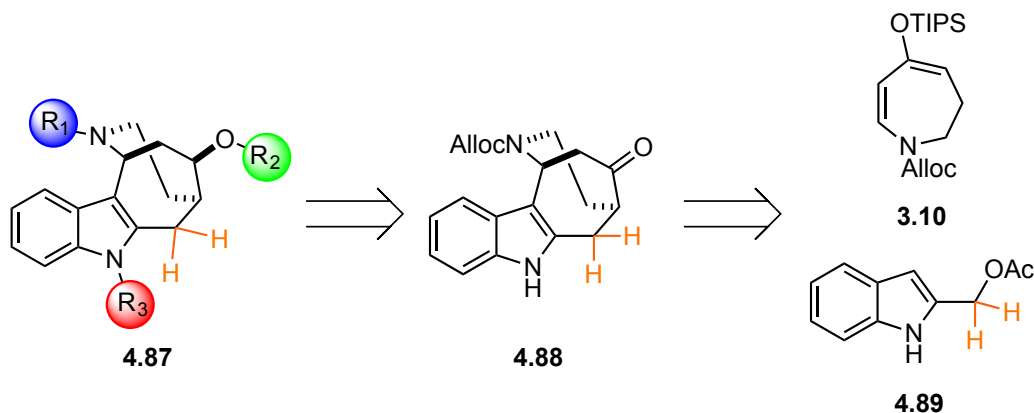


4.3.4 Minimization of 1,3-Diol Moiety

After exploring the SAR of substitution on the indole ring, we next sought to explore the chemical space around the 1,3-diol moiety. Specifically, we wanted to determine whether the 1,3-diol structural moiety was necessary for SFM1257 (**3.43**) bioactivity. If the 1,3-diol structural motif was deemed unnecessary, derivatives the form **4.87** would dramatically reduce the molecular weight and ClogD (Figure 4.20). The synthesis of these derivatives would require modification of the 1,3-diol functionality at the beginning of the synthesis. In particular, we envisioned that analogs of SFM1257 (**3.43**) and SFM1258 (**3.44**) could be formed from common tetracyclic intermediate **4.88**,

which in turn could be synthesized from the primary acetate **4.89** and π -nucleophile **3.10** (Figure 4.20).

Figure 4.20. Proposed Synthesis of Derivatives Lacking 1,3-Diol Moiety

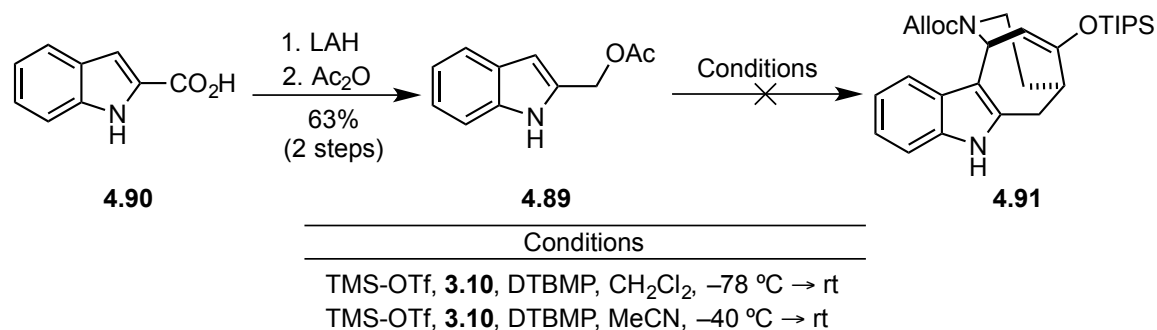


4.3.4.1 Attempted Synthesis of Derivatives Lacking the 1,3-Diol Moiety

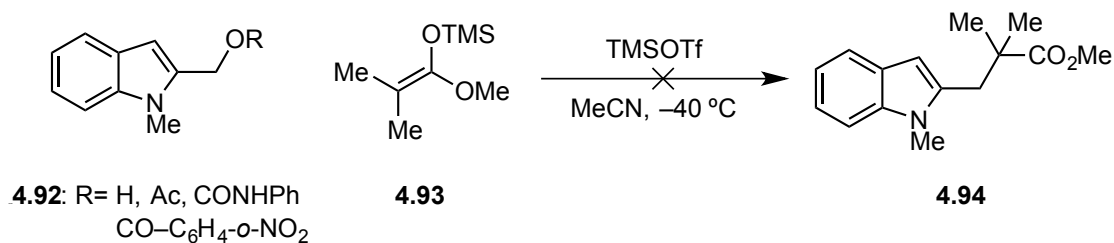
The attempted synthesis of **4.88** began with commercially available indole-2-carboxylic acid (**4.90**) (Table 4.7). Following literature procedures, compound **4.90** was reduced with lithium aluminum hydride to the corresponding primary alcohol, which was acylated with acetic anhydride to give **4.89** in 63% yield over two steps.²⁶³ When attempts were made to react **4.89** with **3.10** using the previously optimized conditions (TMS-OTf, DTBMP, CH_2Cl_2 , -78°C), no reaction was observed, and starting material was recovered. When the reaction was warmed to room temperature or higher, none of the desired product **4.91** was detected by $^1\text{H-NMR}$ or LCMS analysis, and degradation of **4.89** was observed. Identical results were obtained when acetonitrile was used as solvent. Hypothesizing that the reaction occurs through an $\text{S}_{\text{N}}1$ pathway, it is not surprising that **4.89** is less prone to ionization than the original substrate **3.11** because **4.89** would require the formation of a primary carbocation. This observation is in agreement with

previous work in the Martin lab in which compound **4.92** did not react with ketene acetals in the presence of Lewis acid (Scheme 4.29).²⁶⁴

Table 4.7. Attempted Cascade Reaction on Primary Acetate



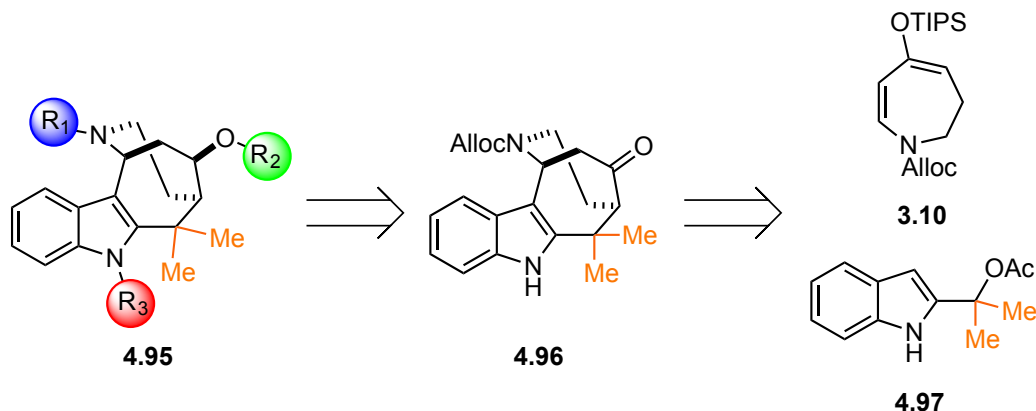
Scheme 4.29. Previous Work in Martin Group²⁶⁴



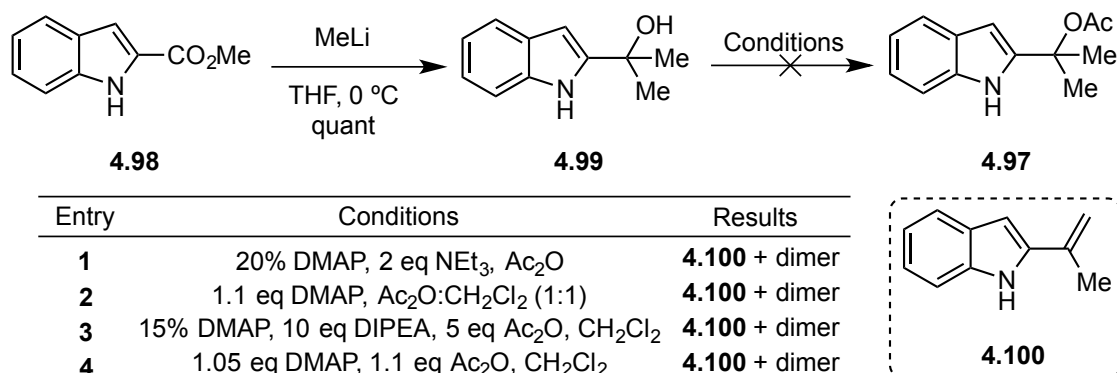
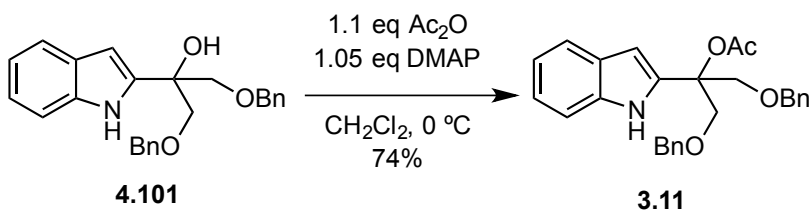
4.3.4.2 Synthesis of *gem*-Dimethyl Derivative

Given the unreactive nature of **4.89**, we turned our attention to *gem*-dimethyl derivatives with the general form of **4.95** (Figure 4.21). Analogous to the previous compounds, we envisioned that these would arise via a Lewis acid mediated addition of **3.10** to **4.97**.

Figure 4.21. Revised Approach to Derivatives Lacking 1,3-Diol Moiety



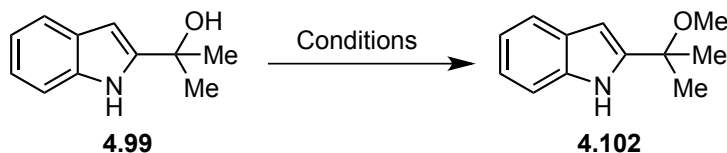
Synthetic efforts towards *gem*-dimethyl derivatives **4.95** commenced from commercially available indole-2-methyl ester **4.98**. Following literature procedure, methyl ester **4.98** was converted to tertiary alcohol **4.99** by reaction with methyllithium.²⁶⁵ Unfortunately, attempts at acylation of alcohol **4.99** did not afford any isolable quantities of acetate **4.97** (Table 4.8). Instead, elimination product **4.100** and other unidentified dimeric compounds were observed by ¹H-NMR spectroscopy and LCMS analysis of crude reaction mixtures. These results were somewhat unexpected, because Dr. Ivan Jewett successfully converted **4.101** to **3.11** in 74% yield (Scheme 4.30).¹²¹ We hypothesized that the inductively withdrawing *O*-benzyl substituents make **3.11** less prone to ionization than **4.97**, thereby stabilizing **3.11**. Thus, we hypothesized that a methyl ether derivative of **4.99** might be sufficiently stable to isolate yet labile enough to ionize under Lewis acidic conditions.

Table 4.8. Attempted Synthesis of Acetate **4.97****Scheme 4.30.** Previously Reported Conversion of **4.101** to **3.11**¹²¹

Numerous conditions were examined to optimize the solvolysis of **4.99** to give the methyl ether **4.102** (Table 4.9). For example, it was found that heating **4.99** in anhydrous methanol under reflux for extended reaction times returned only starting material (Table 4.9, entry 1). Several Brønsted acids were then screened, and it was found that 1 M HCl provided methyl ether **4.102** in 46% yield (Table 4.9, entry 2), whereas 10 mol% *p*-toluenesulfonic acid lead to an intractable mixture (Table 4.9, entry 3). The less acidic Brønsted acid pyridinium *p*-toluenesulfonate afforded methyl ether **4.102** in 85% yield but some elimination was also observed (Table 4.9, entry 4). We then found that silica gel slowly catalyzed the conversion of **4.99** to **4.102** (Table 4.9, entry 5). As a result, several Brønsted acid-doped silica gels were prepared and evaluated, and it was found that 10% oxalic acid/SiO₂ quantitatively formed methyl ether **4.102** within two hours on a 25 mg

scale (Table 4.9, entry 8). However, the reaction did not go to completion once scaled up to 250 mg, affording **4.102** in 75% yield (98% BRSM) (Table 4.9, entry 9).

Table 4.9. Optimization of Solvolysis Reaction with MeOH

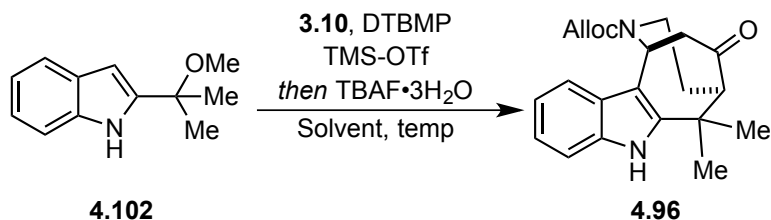


Entry	Conditions	Results
1	MeOH, reflux	No Reaction
2	1 M HCl, MeOH, 100 °C (sealed tube)	46% 4.102 (100% conversion)
3	10% <i>p</i> -TsOH, MeOH	intractable mixture (100% conversion)
4	10% PPTS, MeOH, rt	~85% 4.102 (100% conversion)
5	SiO ₂ , MeOH, 100 °C (sealed tube)	~20% 4.102 (~20% conversion)
6	10% H ₃ PO ₄ /SiO ₂ , MeOH, rt	~50% 4.102 (~50% conversion)
7	10% fumaric acid/SiO ₂ , MeOH, rt	~50% 4.102 (~50% conversion)
8	10% oxalic acid/SiO ₂ , MeOH, rt	quant (25 mg scale)
9	10% oxalic acid/SiO ₂ , MeOH, rt	75% (98 BRSM) (250 mg scale)

PPTS= pyridinium *p*-toluenesulfonate

With an appreciable amount of **4.102** in hand, it was treated with **3.10** in the presence of TMS-OTf and DTBMP to give **4.96** in 22% yield (Table 4.10, entry 1). Significant amount of starting material remained, so we hypothesized that increasing the solvent polarity by changing the solvent from CH₂Cl₂ to MeCN might facilitate the ionization of **4.102** and lead to higher conversion. Indeed, higher conversion was observed, but a significant amount of gramine fragmentation was also observed (Table 4.10, entry 2), which we attributed to the higher reaction temperature (−40 °C vs. −78 °C). Because MeCN freezes below −40 °C, a mixture (2:3) of MeCN/CH₂Cl₂ was used to increase the solvent polarity but still allow the reaction to be performed at −78 °C. The mixed solvent system reaction afforded **4.96** in 43% yield (Table 4.10, entry 3). Although additional optimization was needed, sufficient material was synthesized for our purposes.

Table 4.10. Synthesis of Tetracycle **4.96**

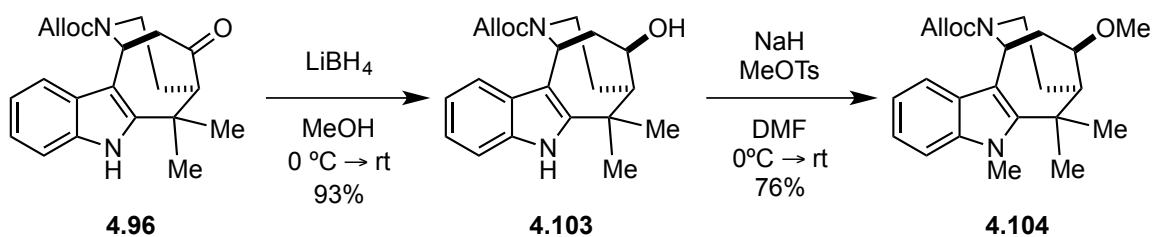


Entry	Conditions	Yield (%)
1	CH ₂ Cl ₂ , -78 °C	22
2	MeCN, -40 °C	31
3	MeCN/CH ₂ Cl ₂ (2:3), -78 °C	43

TBAF= tetrabutylammonium fluoride
DTBMP= 2,6-di-*tert*-butyl-4-methylpyridine

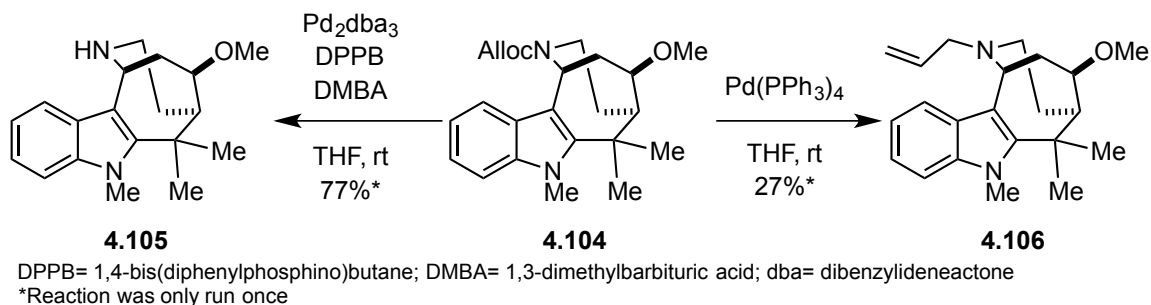
The synthesis of *gem*-dimethyl derivatives commenced via the reduction of **4.96** with lithium borohydride to give alcohol **4.103** in 93% yield, and dimethylation with NaH/MeOTs then furnished compound **4.104** in 76% yield (Scheme 4.31).

Scheme 4.31. Reduction and Alkylation of *gem*-Dimethyl Tetracycle **4.104**



Removal of the allyl carbamate from **4.104** using Pd₂dba₃/DPPB/DMBA afforded amine **4.105** in 77% yield. Alternatively, removal of the allyl carbamate with Pd(PPh₃)₄ in the absence of DMBA afforded *N*-allyl compound **4.106** in 27% yield (Scheme 4.32).

Scheme 4.32. Synthesis of Derivative **4.105** and **4.106**



4.3.4.4 Evaluation of Derivatives

The *gem*-dimethyl derivatives were then evaluated by Dr. Betsy Parkinson for their ability to induce cell death in U937 cells (human lymphoma) and human red blood cells (Table 4.11).⁹⁶ Because the *gem*-dimethyl compounds showed no biological activity, this series was not pursued further. However, these results provide valuable insight to what constitutes the active pharmacophore. It is clearly evident that the oxygen atoms and/or the benzyl groups are necessary for biological activity.

Table 4.11. Evaluation of *gem*-Dimethyl Derivatives

Entry	Cmpd	R ₁	R ₂	R ₃	U937*	Hem*
					IC ₅₀ (μM)	IC ₅₀ (μM)
1	4.106	Allyl	Me	Me	>100	>333
2	4.105	H	Me	Me	>100	>333

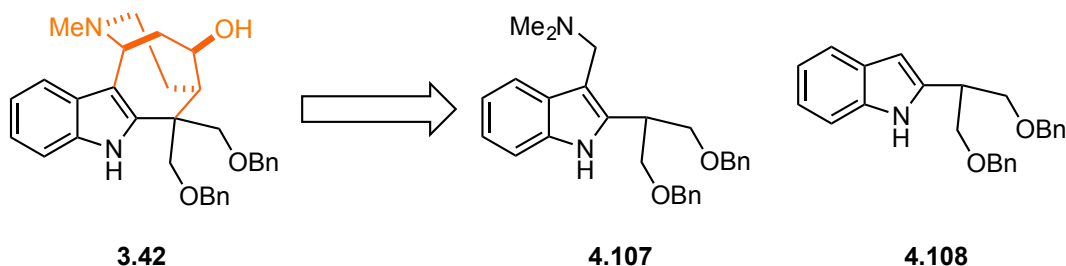
*Data collected Dr. Betsy Parkinson⁹⁶

4.3.5 Further Pharmacophore Elucidation

We sought to further to determine which structural features were necessary for biological activity. From the previous set of studies, it was clear that the *O*-benzyl

moieties were necessary for biological activity. As a result, we sought to simplify the carbon structure to determine how dependent the biological activity was on the tetracyclic framework. Accordingly, we decided to evaluate compounds **4.107** and **4.108** (Figure 4.22). Compound **4.107** would elucidate whether the basic nitrogen atom was needed for biological activity, and compound **4.108** would inform us as to what extent the observed biological activity was dependent on the *O*-benzyl groups.

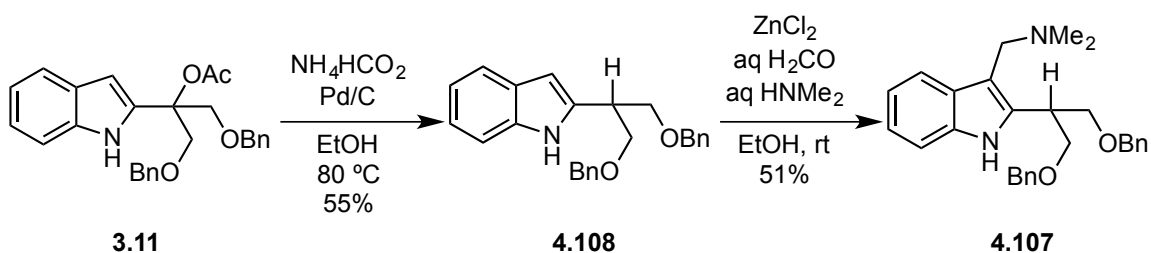
Figure 4.22. Derivatives to Further Minimize Pharmacophore



4.3.5.1 Synthesis of Dissected Carbon Framework

Compounds **4.107** and **4.108** were readily synthesized from indolo-acetate **3.11**. For example, heterogeneous transfer hydrogenation of **3.11** with ammonium formate and Pd/C afforded compound **4.108** in 55% yield. Utilizing the conditions reported by Li *et al*, compound **4.107** was synthesized in 51% yield using 37% aqueous formaldehyde, dimethylamine, and zinc chloride.²⁶⁶

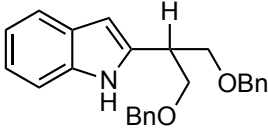
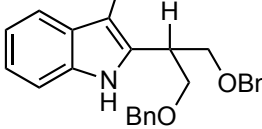
Scheme 4.33. Synthesis of Derivatives **4.107** and **4.108**



4.3.5.2 Evaluation of Compounds 4.107 and 4.108

Compounds **4.107** and **4.108** were evaluated for their ability to induce cell death in Hs578t cells (triple negative breast cancer) and U937 cells (human lymphoma) (Table 4.12). Compound **4.108** was slightly active *in vitro* (Hs578t $IC_{50} >100 \mu M$ and U937 $IC_{50} = 48.0 \pm 11.4 \mu M$); whereas, compound **4.107** was significantly more active (Hs578t $IC_{50} = 24.4 \pm 1.9 \mu M$ and U937 $IC_{50} = 17.8 \pm 3.9 \mu M$). These data suggest that the basic nitrogen atom is necessary for biological activity.

Table 4.12. Evaluation of Compounds **4.107** and **4.108**

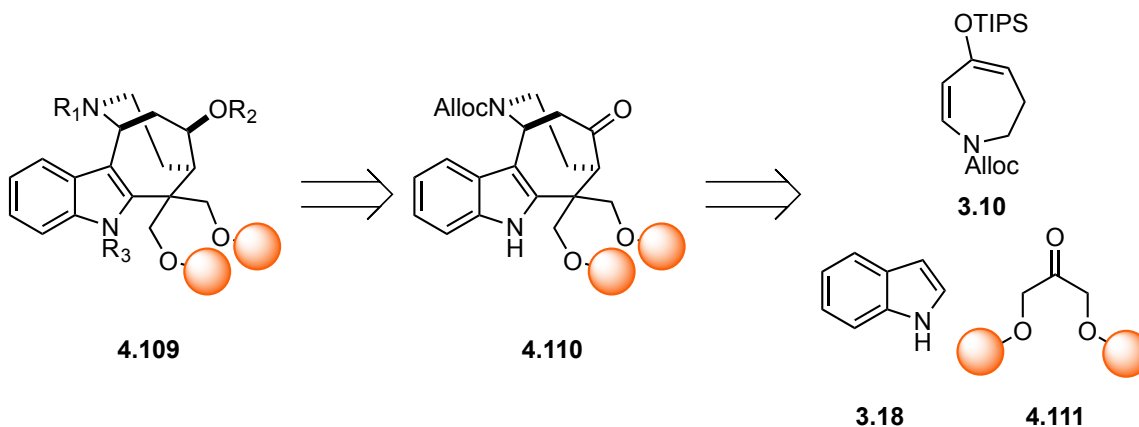
 4.108	 4.107	
Compound	Hs578t IC ₅₀ (μM)	U937 IC ₅₀ (μM)
4.108	>100	48.0 ± 11.4
4.107	24.4 ± 1.9	17.8 ± 3.9

4.3.6 Structure Activity Relationship of 1,3-Diol Moiety

As a result of the studies thus far, it seemed clear that the 1,3-diol moiety played an integral role in the biological activity of SFM1257 (**3.43**). Thus, we next sought to

synthesize several *O*-substituted derivatives in order to probe the SAR in that section of the molecule (Figure 4.23, **4.109**). Specifically, we wanted to explore the effects that exchanging the *O*-benzyl moieties for *O*-methyl, *O*-phenyl, and substituted *O*-phenyl groups would have on the biological activity of these compounds. Because these structural variations could not be introduced via late stage functionalization of SFM1257 (**3.43**) or SFM1258 (**3.44**), we embarked on their *de novo* synthesis. We envisioned that the analogs could be formed from common tetracyclic intermediate **4.110**, which in turn could be synthesized from indole (**3.18**), π -nucleophile **3.10**, and the desired substituted ketone (**4.111**) (Figure 4.23).

Figure 4.23. Retrosynthetic Analysis for 1,3-Diol Substituted Derivatives

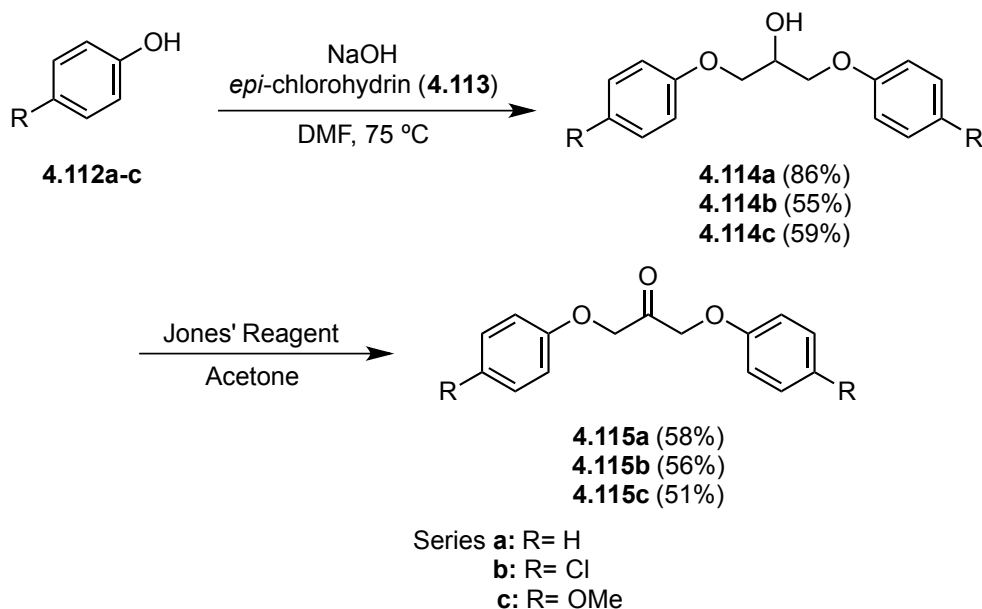


4.3.6.1 Synthesis of *O*-Substituted Derivatives

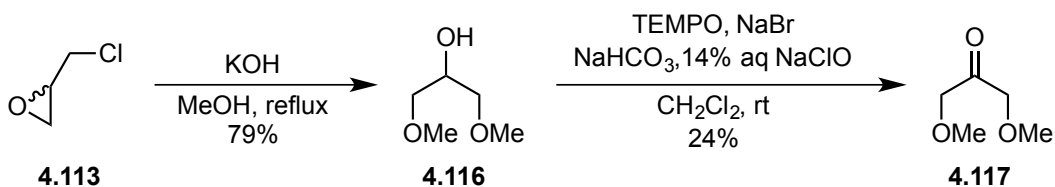
The synthesis of the 1,3-diol derivatives commenced with the formation of the desired substituted ketone. These compounds were synthesized in two steps according to literature procedures (Scheme 4.34).²⁶⁷ Starting with the substituted phenols **4.112a-c**, a double nucleophilic substitution with *epi*-chlorohydrin (**4.113**) afforded alcohols **4.114a-c** in 55-86% yield. The alcohols **4.114a-c** were oxidized to the corresponding ketones (**4.115a-c**) in 51-58% yield. Similarly, the methoxy-substituted ketone **4.117** was

synthesized in two steps via double substitution of MeOH with *epi*-chlorohydrin (**4.113**) to give alcohol **4.116** in 79% yield, and subsequent TEMPO oxidation to give ketone **4.117** in 24% yield (Scheme 4.34).²⁶⁸

Scheme 4.34. Synthesis of Ketone **4.114a-c**

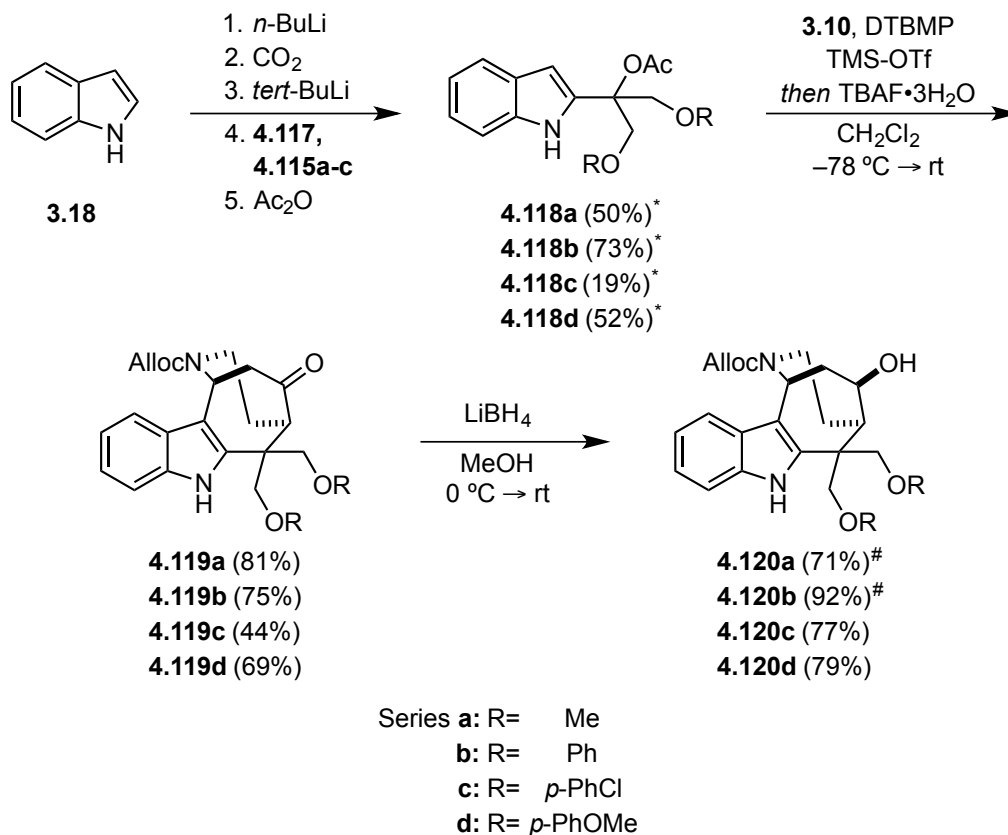


Scheme 4.35. Synthesis of Ketone **4.117**



The synthesis of the differentially substituted 1,3-diol derivatives continued with the formation of indolo-acetates **4.118a-d** in 19-73% yield via the five step one-pot procedure utilizing ketones **4.117** and **4.115a-c** (Scheme 4.36). The indolo-acetate compounds **4.118a-d** were next subjected to the cascade reaction conditions to provide the desired tetracycles **4.119a-d** in 44-81% yield. The tetracyclic compounds (**4.119a-d**) were reduced with lithium borohydride to the desired alcohols **4.120a-d** in 38-79% yield.

Scheme 4.36. Synthesis of Differentially Substituted 1,3-Diol Scaffold

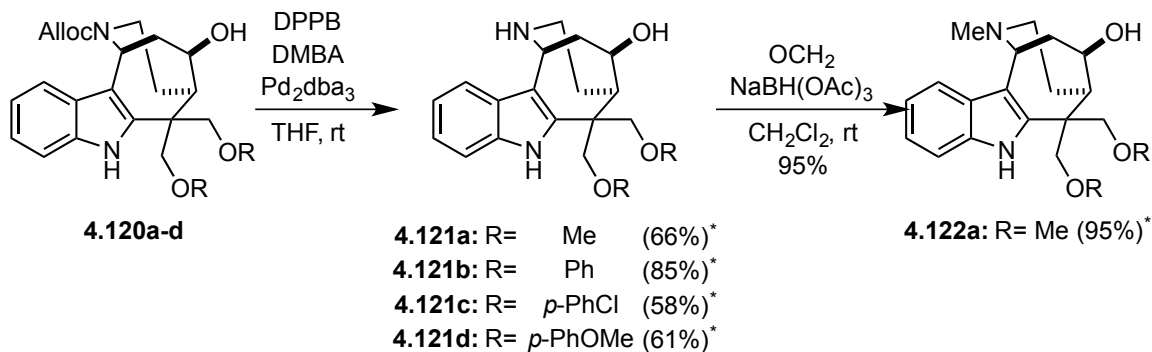


TBAF= tetrabutylammonium fluoride; DTBMP= 2,6-di-*tert*-butyl-4-methylpyridine

#BRSM; *Reaction only run once

The allyl carbamate groups in **4.120a-d** were then removed with $\text{Pd}_2\text{dba}_3/\text{DPPB}/\text{DMBA}$ to afford **4.121a-d** in 58-85% yield. Compound **4.122a** was prepared via reductive amination of **4.121a** with 37% aqueous formaldehyde to provide the tertiary amine **4.122a** in 95% yield.

Scheme 4.37. Synthesis of Derivative **4.121a-d** and **4.122a**



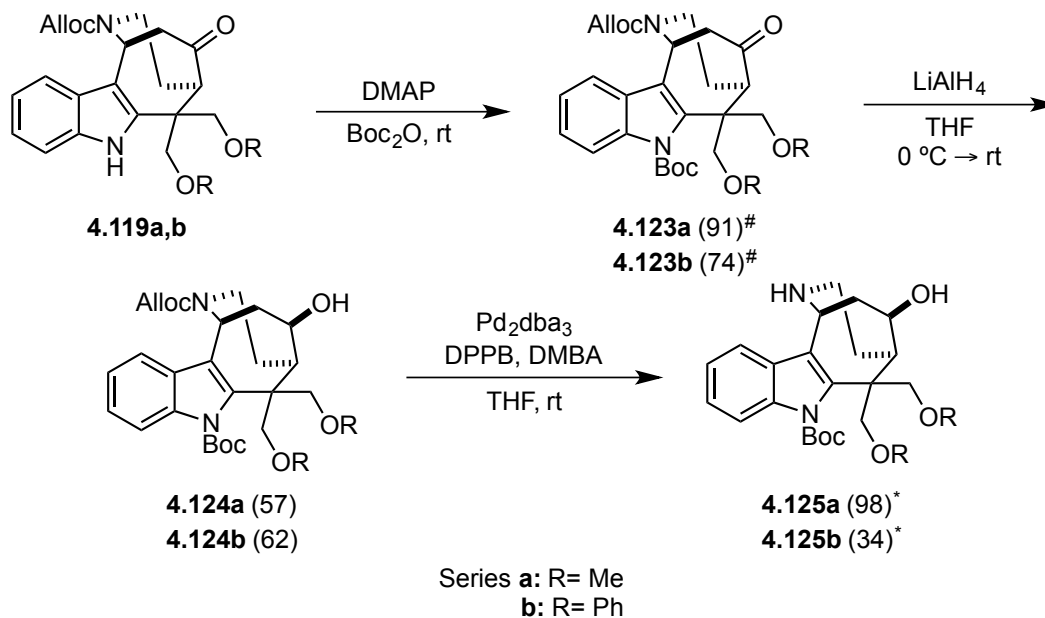
DMBA= 1,3-dimethylbarbituric acid; dba= dibenzylideneacetone

DPPB= 1,4-bis(diphenylphosphino)butane

*Reaction was only run once

To prepare analogs structurally similar to SFM1257 (**4.43**), the indole nitrogen atom of **4.119a,b** was protected with DMAP/Boc₂O to afford compounds **4.123a,b** in 63% and 40% yield, respectively. Ketones **4.123a,b** were reduced with lithium aluminum hydride to afford alcohols **4.124a,b** in 57% and 62% yield. The allyl carbamate of **4.124a,b** was removed with Pd₂dba₃/DPPB/DMBA to provide derivatives **4.125a,b** in 98% and 34% yield (Scheme 4.38).

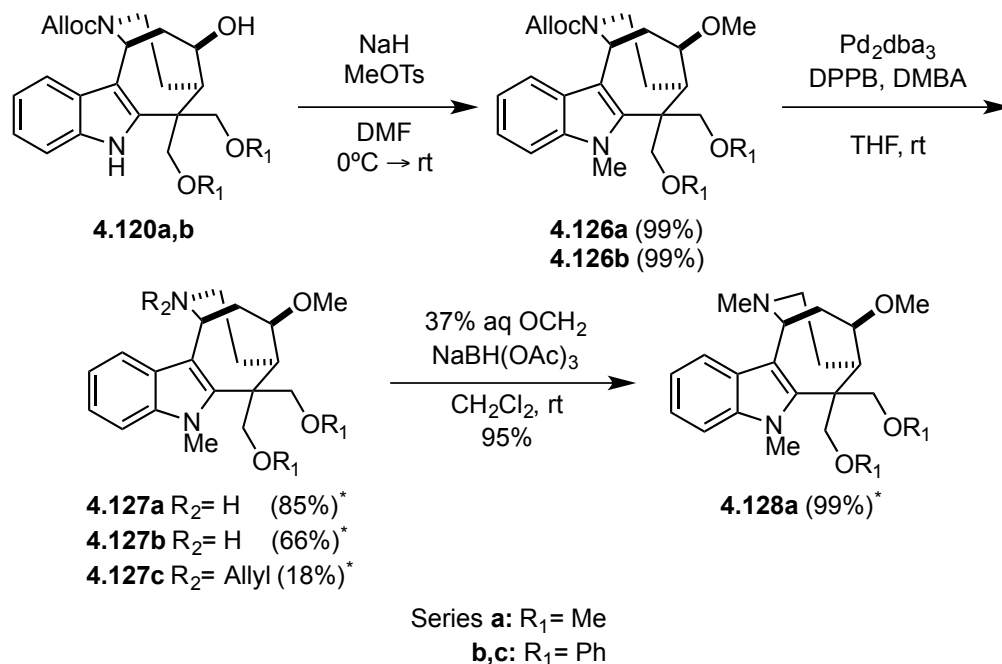
Scheme 4.38. Synthesis of Derivative 4.125a,b



DPPB= 1,4-bis(diphenylphosphino)butane; DMBA= 1,3-dimethylbarbituric acid; dba= dibenzylideneacetone
[#]BRSM; ^{*}Reaction only run once

In other experiments, alkylation of **4.120a,b** with NaH/MeOTs gave compounds **4.126a,b** in 99% yield each. Removal of the allyl carbamate group from compound **4.126a** with Pd₂dba₃/DPPB/DMBA provided amine **4.127a** in 85% yield, and removal of the allyl carbamate group from **4.126b** furnished compound **4.127b** and the *N*-allyl derivative **4.127c** in 66% and 18% yields, respectively. A reductive amination of **4.127a** with 37% aqueous formaldehyde provided tertiary amine **4.128a** in 99% yield (Scheme 4.39).

Scheme 4.39. Synthesis of Derivatives **4.127a-c** and **4.128a**

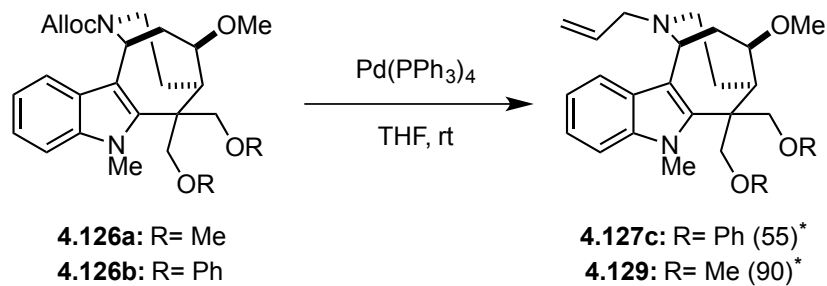


DPPB= 1,4-bis(diphenylphosphino)butane; DMBA= 1,3-dimethylbarbituric acid; dba= dibenzylideneacetone

*Reaction only run once

Several additional analogs of SFM1258 (**3.44**) were synthesized from **4.127a-b** by a decarboxylative allylation to afford *N*-allyl compounds **4.129** and **4.127c** in 90% and 55% yield (Scheme 4.40).

Scheme 4.40. Synthesis of Derivative **4.127c** and **4.129**

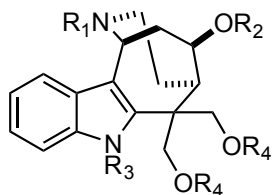


*Reaction was only run once

4.3.6.2 Evaluation of *O*-Substituted Derivatives

These novel 1,3-diol analogs were evaluated for their ability to induce cell death in Hs578t cells (triple negative breast cancer) U937 cells (human lymphoma), and human red blood cells (Table 4.13). The data collected for these derivatives provided further insight into the structure-activity-relationship of the compounds. In particular, exchanging the *O*-benzyl groups for *O*-methyl groups rendered the compounds inactive (Table 4.13, entries 3-8). On the other hand, exchanging the *O*-benzyl groups for *O*-phenyl or *p*-substituted *O*-phenyl groups did not dramatically affect potency (Table 4.13, entries 9-14). However, the *O*-phenyl derivative of SFM1257 (**3.43**) and SFM1258 (**3.44**) did show a slight reduction in potency (Table 4.13, entry 1 vs. entry 11 and entry 2 vs. 10). These data indicate that larger, non-polar moieties on the 1,3-diol are necessary for biological activity. Additionally, the *p*-substituted phenyl groups on the 1,3-diol were biologically active, and the *p*-chloro derivative **4.121c** showed comparable activity to SFM1257 (**3.43**) (Table 4.13, entry 1 and entry 13). Interestingly, the *p*-methoxy phenyl substituted derivative **4.121d** showed comparable activity to *p*-chloro derivative **4.121c** (Table 4.13, entry 13 vs 14), thereby indicating that the electronics of the arene may not be very relevant for binding to the biological target. This series of compound also reinforced the previous observation that appending an allyl group to the basic nitrogen adversely affects potency (Table 4.13, entry 9 vs. entry 10).

Table 4.13. Evaluation of Differentially Substituted 1,3-Diol Derivatives



4.130

Entry	Compound	R ₁	R ₂	R ₃	R ₄	Hs578t IC ₅₀ (μM)	U937 IC ₅₀ (μM)	Hem* IC ₅₀ (μM)
1	SFM1257 (3.43)	H	H	Boc	Bn	6.6 ± 0.7	3.3 ± 0.2	28
2	SFM1258 (3.44)	Allyl	Me	Me	Bn	20 ± 2.9	5.6 ± 2.3	>100
3	4.121a	H	H	H	Me	ND	>100*	>333
4	4.122a	Me	H	H	Me	ND	>100*	>333
5	4.127a	H	Me	Me	Me	ND	>100*	>333
6	4.128a	Me	Me	Me	Me	ND	>100*	>333
7	4.129	Allyl	Me	Me	Me	ND	>100*	>333
8	4.125a	H	H	Boc	Me	ND	>100*	>333
9	4.127b	H	Me	Me	Ph	5.3 ± 0.9	6.4 ± 0.1	ND
10	4.127c	Allyl	Me	Me	Ph	35.4 ± 6.2	20.9 ± 1.5	ND
11	4.125b	H	H	Boc	Ph	9.2 ± 1.2	7.2 ± 0.9	ND
12	4.121b	H	H	H	Ph	6.1 ± 0.1	6.4 ± 0.1	ND
13	4.121c	H	H	H	<i>p</i> -PhCl	4.7 ± 0.3	4.2 ± 0.6	ND
14	4.121d	H	H	H	<i>p</i> -PhOMe	10.2 ± 1.6	4.4 ± 1.0	ND

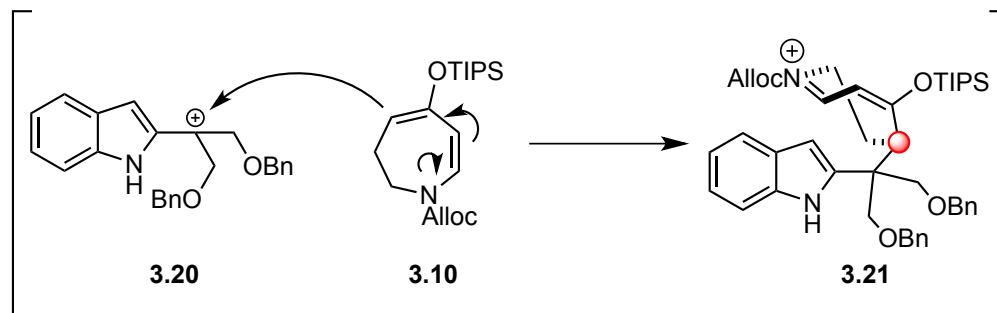
*Data collected by Dr. Betsy Parkinson⁹⁶

4.4 PRELIMINARY EFFORTS TOWARDS THE SYNTHESIS OF ENANTIOENRICHED DERIVATIVES

4.4.1 Introduction

All of the derivatives prepared to date have been racemic, but it is necessary to evaluate the biological properties for each enantiomer independently because each enantiomer may be responsible for a unique aspect of the phenotypic response. Enantiopure material may be obtained by chiral HPLC separation or chiral resolution with a chiral auxiliary, but given the impracticality of large-scale chiral HPLC separation and the step-inefficiency of a resolution with a chiral auxiliary, enantioselective synthesis is the method of choice. In the synthesis of SFM1257 (**3.43**), the addition of π -nucleophile **3.10** to tertiary carbocation **3.20** is the chirality-determining step, so the focus of these efforts will be to impart stereoselectivity onto this transformation (Figure 4.24).

Figure 4.24. The Chirality Forming Step in the Synthesis of SFM1257 (**3.43**)

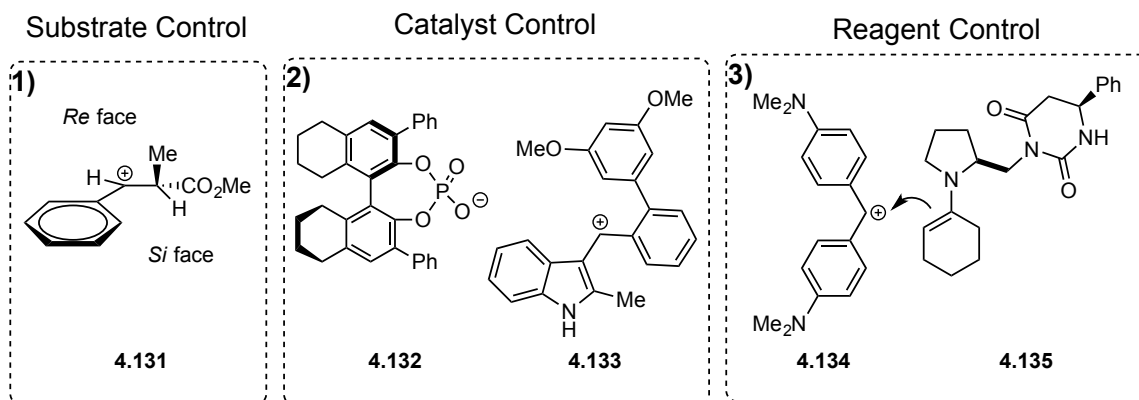


4.4.2 Strategies For Stereoselective Additions to Carbocations

There are three general strategies employed to perform these types of transformations asymmetrically: substrate control, catalyst control, and reagent control (Figure 4.25).²⁶⁹

Substrate control (Figure 4.25, 1): stereochemistry is controlled by a chiral group covalently attached to the carbocation. This approach has been successfully employed in natural product synthesis and on kilogram scale of an active pharmaceutical ingredient (API).²⁷⁰⁻²⁷⁶ Catalyst control (Figure 4.25, 2): a prochiral carbocation forms an ion pair with a chiral counterion by blocking one face of the carbocation that subsequently controls stereochemistry. This strategy has been used for enantioselective polyene cyclization,²⁷⁷ Friedel-Crafts alkylation and acylation,^{278,279} allylic substitution,²⁸⁰ and enamide addition.²⁸¹ Reagent control (Figure 4.25, 3): stereochemistry at an achiral carbocation is controlled through stereochemical interaction with a chiral nucleophile. This approach has been used effectively with a chiral ketene acetal,²⁶⁴ enamine,²⁸²⁻²⁸⁵ and thiourea catalysis.^{286,287} In the context of our system, substrate control is not an option because both of the reactants (**3.10** and **3.11**) are achiral. Catalyst control cannot be applied given that carbocation **3.20** is not prochiral. Thus, the better option for our system is reagent control with a chiral nucleophile.

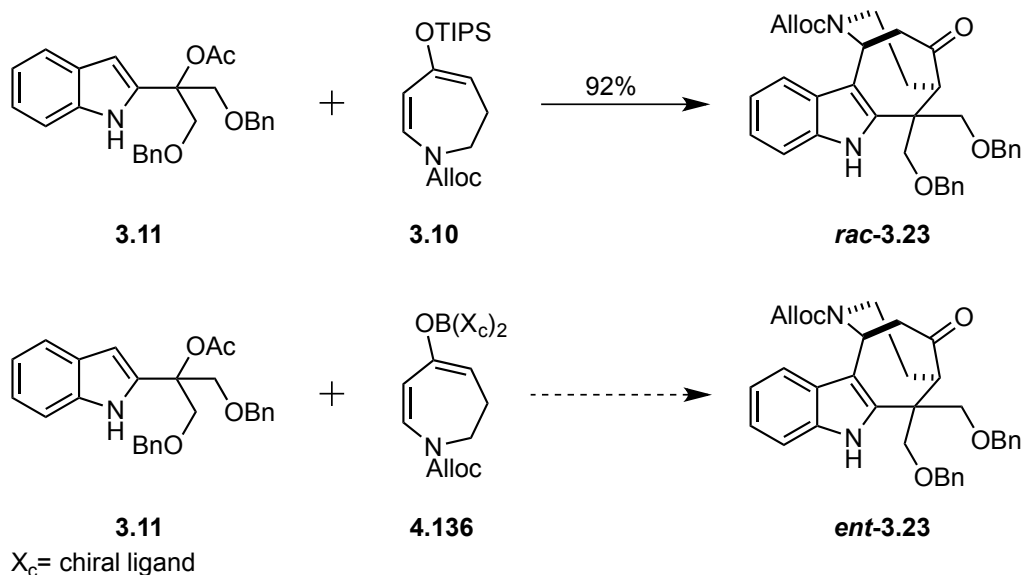
Figure 4.25 Carbocations in Asymmetric Synthesis



4.4.3 Chiral Boron Enolate Strategy

Towards the goal of stereoselective addition to carbocation **3.20**, we envision that the π -nucleophile **3.10** can be modified to include an easily removed chiral auxiliary in place of the TIPS groups (Figure 4.26). This would impart chirality onto π -nucleophile **3.10** and hopefully afford a product with high levels of enantioenrichment after removal of the auxiliary.

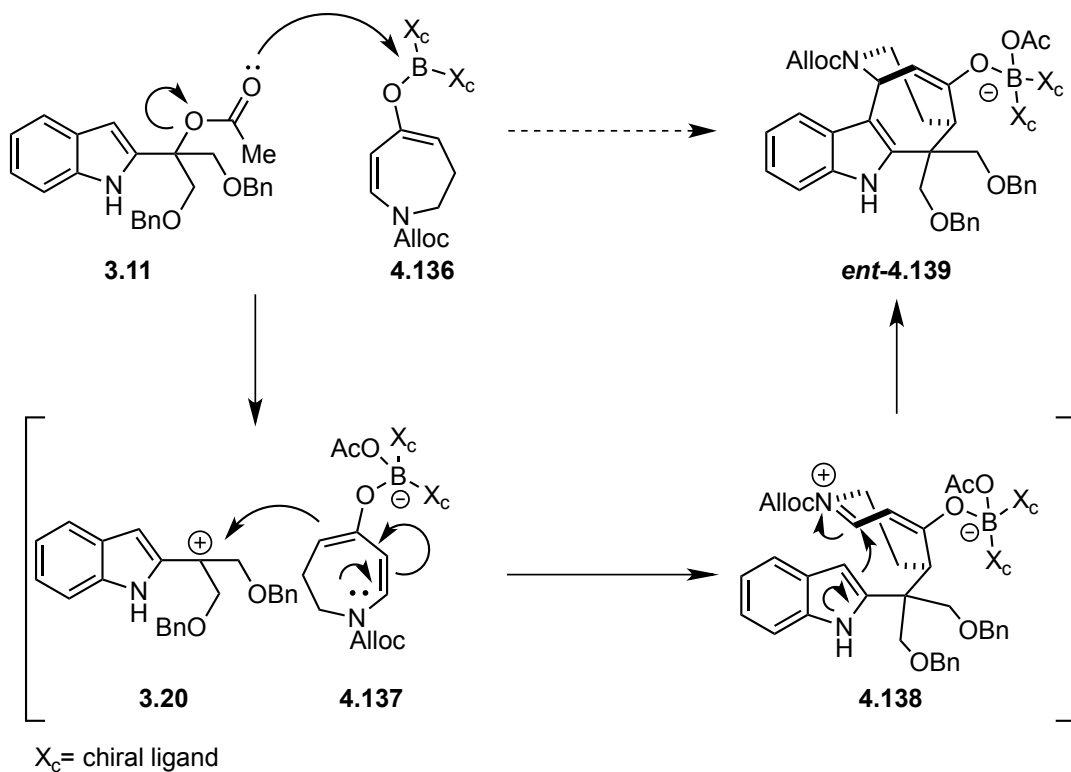
Figure 4.26. Proposed Strategy for Obtaining Enantioenriched Material



We reasoned that use of a chiral boron enolate would be the optimal strategy to make the transformation of **3.11** to **4.139** stereoselective because the reactivity of such enolates is analogous to a silyl enol ether (Scheme 4.41). One could envision a reaction pathway in which chiral borate **4.136** would coordinate with the acetoxyl group of **3.10** to facilitate ionization and give carbocation **3.20** and boronate **4.137**. Chiral boronate **4.137** would then react with carbocation **3.20** to afford the *N*-acyliminium species **4.138**, which would in turn react with the 3-position of indole to afford enantioenriched **4.139**. We

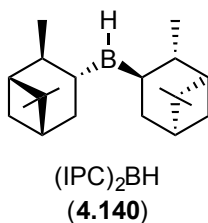
envision the key stereodetermining step would be the alkylation of **3.20** with **4.137**, and the stereochemistry of the alkylation would be controlled by the chirality of the boronate.

Scheme 4.41. Proposed Enantioselective Cascade Reaction



There are a number of chiral groups that could be attached to the boron for potential use in this transformation,²⁸⁸⁻²⁹² The boron enolate derived from diisopinocampheylborane (**4.140**) was chosen for initial investigation in this system because the reagent can be readily prepared on decagram scale from cheap materials,²⁹³ and its use in enantioselective aldol reactions for reagent control of absolute stereochemistry is well documented.²⁹⁴⁻²⁹⁷

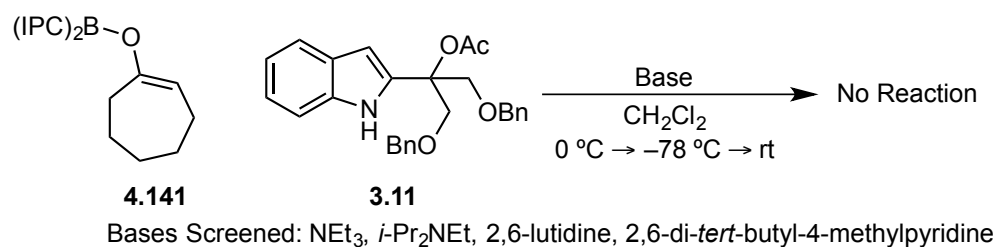
Figure 4.27. Structure of (IPC)₂BH



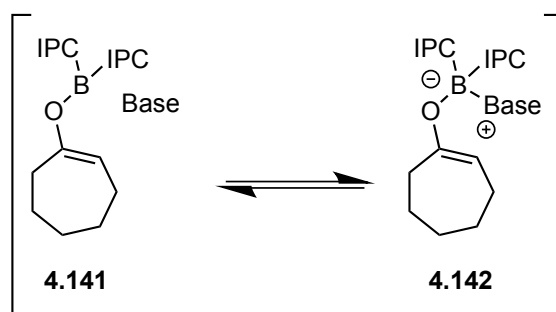
4.4.4 Cycloheptanone Model Study

Given the complexity of this transformation, cycloheptanone was chosen as a model system to evaluate the Lewis acidity of the boron enolate. In this model study, the IPC boron enolate **4.141** was first formed *in situ* using general base catalysis with a titrated²⁹⁸ solution of (IPC)₂BOTf in CH₂Cl₂, followed by dropwise addition of a solution of **3.10** in CH₂Cl₂. The initial attempts with triethylamine as the base failed to facilitate the addition of **4.141** to **3.11** (Scheme 4.42). Since no reaction was observed and only starting material was recovered, the boron enolate did not appear to be sufficiently Lewis acidic to initiate the reaction. To verify that boron enolate **4.141** was being formed, a control reaction was run with **4.141** and benzaldehyde. The base used to form the boron enolate can also coordinate to the boron, thereby attenuating Lewis acidity (Scheme 4.43). For that reason, several additional bases were screened (*i*-Pr₂NEt, 2,6-lutidine, and 2,6-di-*tert*-butyl-4-methylpyridine), each subsequent base bulkier than the previous (Scheme 4.42). It was found that switching to a bulkier base did not sufficiently enhance the Lewis acidity to promote ionization.

Scheme 4.42. Initial Attempts with Cycloheptanone Model System

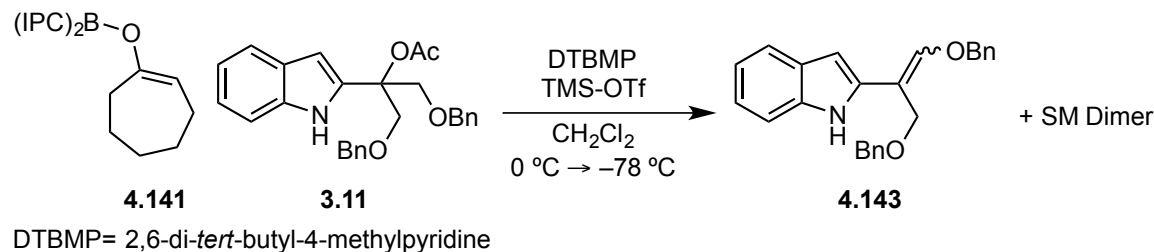


Scheme 4.43. Base Can Coordinate to Boron Enolate



We reasoned that a Lewis acid co-catalyst might be necessary to initiate the reaction. When TMS-OTf was added to the reaction, ionization of the indolo-acetate (**3.11**) occurred, but no addition of the boron enolate to the indolo-acetate was observed. Instead, elimination of the acetate (**4.143**) as well as dimerization of the starting material was observed upon quenching the reaction (Scheme 4.44). Thus, we concluded that boron enolate **4.141** was not sufficiently nucleophilic to facilitate the addition of **4.141** to **3.11**.

Scheme 4.44. Cycloheptanone Model System With Lewis Acid Co-catalyst



4.4.5 Vinylogous Amide Boron Enolate Formation Using Weak Base

After the failure with the cycloheptanone model system, we turned our attention to forming the boron enolate of the vinylogous amide **4.144** because we predicted the resulting boron enolate would be significantly more nucleophilic (Figure 4.28). To evaluate whether the boron enolate could be formed under general base conditions, the spectroscopy reaction was performed in CD₂Cl₂, and aliquots were analyzed via ¹H-NMR and ¹³C-NMR by monitoring the carbonyl resonance in the ¹³C-NMR spectra and the alpha proton resonance in the ¹H-NMR spectra of **4.144**. It was found that the base chosen had a dramatic effect on the outcome of the reaction. The very bulky base 2,6-di-*tert*-butyl-4-methylpyridine (DTBMP) afforded none of the desired boron enolate. A complete loss of the carbonyl resonance was observed in the ¹³C-NMR spectra, but no discernable resonances were observed in the ¹H-NMR. On the other hand, approximately ~70% conversion was observed when *i*-Pr₂NEt was used as the base. This conclusion was supported by the loss of resonance at 4 ppm in the ¹H-NMR spectra, and a new doublet ¹H-NMR resonance at 5.2 ppm. We believe the doublet at 5.2 ppm is the boron enolate proton (**4.145**, H₁) because the analogous proton on **3.10** comes at roughly the same ppm (Figure 4.29). Additionally, the carbonyl peak was still seen in the ¹³C-NMR, but its intensity had significantly diminished.

Figure 4.28. Observations From ^1H -NMR Studies of Boron Enolate Formation

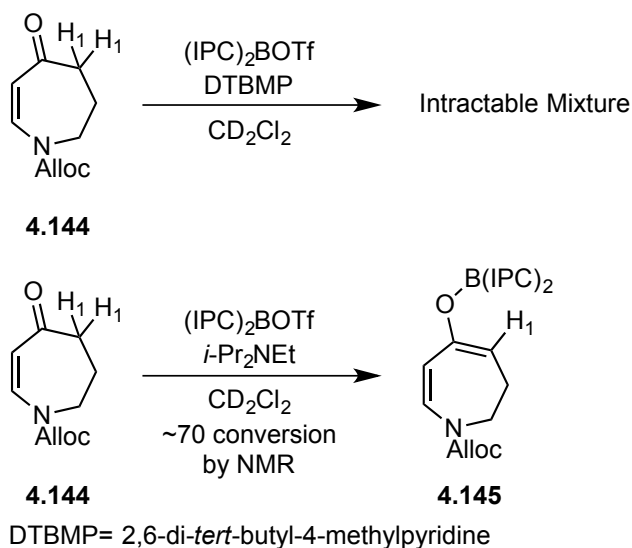
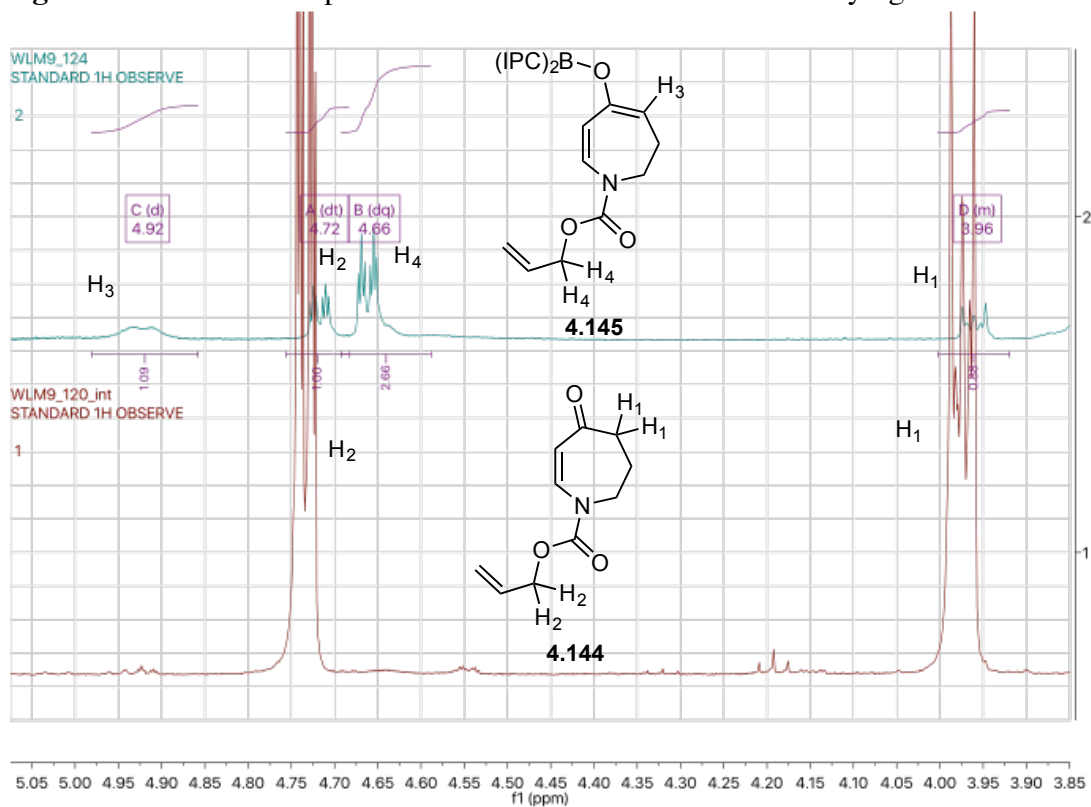
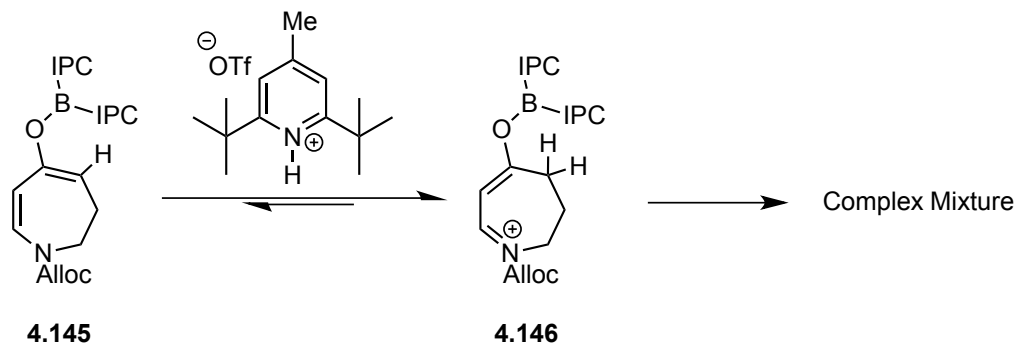


Figure 4.29. ^1H -NMR Spectrum of Boron Enolate **4.145** and Vinylogous Amide **4.144**



We hypothesized that the inability of DTBMP to convert **4.144** to **4.145** was due to protonation of boron enolate **4.144** by the resulting conjugate acid of DTBMP which has a pKa of 4.95 (Scheme 4.45).²⁹⁹ Given that TIPS enol ether **3.10** is very acid labile and rapidly decomposes on silica, it is not surprising that decomposition of the material was observed. Despite successfully forming **4.145** with *i*-Pr₂NEt, previous reports by Dr. Brett Granger¹²⁰ and Dr. Ivan Jewett¹²¹ found that the TMS-OTf mediated reaction between **3.11** and **3.10** does not proceed cleanly if bases other than DTBMP are used. Thus, we concluded that forming the boron enolate under general base condition is not a viable approach to this transformation.

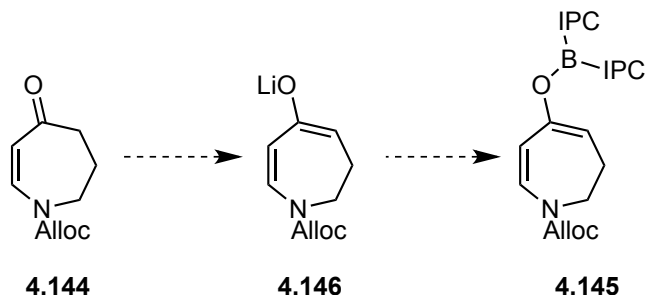
Scheme 4.45. Rationalization for Lack of Boron Enolate Formation with DTBMP



4.4.6 Future Studies

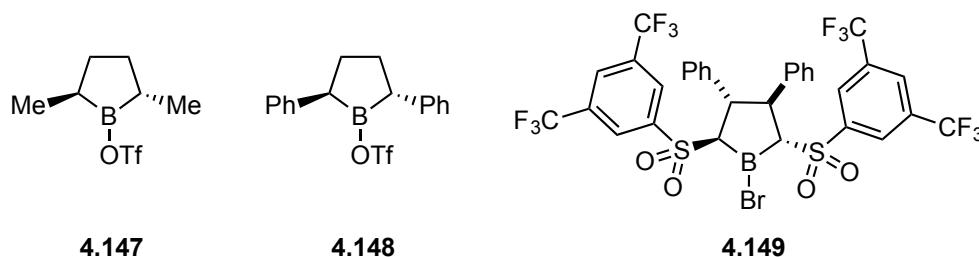
The development of a stereoselective variant of the Lewis acid catalyzed reaction between **3.10** and **3.11** is an ongoing effort. Moving forward, we believe the best course of action will be to synthesize the boron enolate by first quantitatively forming the lithium enolate with a bulky base, then reacting the lithium enolate with (IPC)₂BOTf (Scheme 4.46). The use of a strong base to quantitatively deprotonate **4.144** will mitigate the issues pertaining to the acidity of the conjugate acid.

Scheme 4.46. Proposed Future Attempt at Boron Enolate Formation



After the boron enolate has been successfully synthesized, the addition of **4.145** to **3.11** will be attempted with and without the addition of TMS-OTf. If it is found that the reaction proceeds, but does not impart significant enantioenrichment, additional boron enolates can be evaluated (Figure 4.30).²⁸⁸⁻²⁹²

Figure 4.30. Additional Boron Reagent Capable of Controlling Absolute Stereochemistry

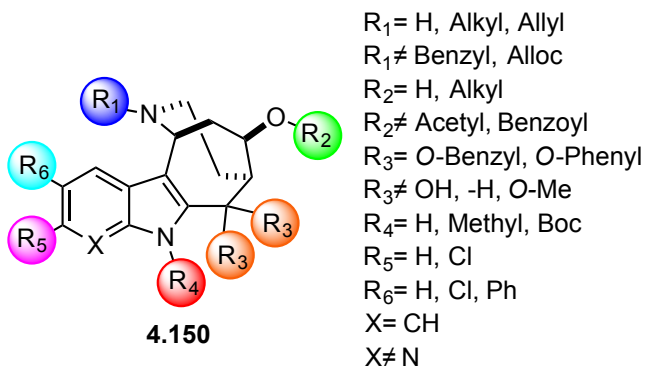


4.5 CONCLUSION

A number of significant advances have been made towards understanding how SFM1257 (**3.43**) interacts with biological systems. For example, the hypothesis that SFM1257 (**3.43**) induces cell death via induction of ER stress was supported by demonstrating that guanabenz (**4.41**), a small molecule inhibitor of PP1/GADD34, afforded robust cytoprotection against SFM1257 (**3.43**) induced toxicity. This also demonstrated that inhibition of PP1/CReP was not necessary to mitigate the effects of SFM1257 (**3.43**). Additionally, two novel tool compounds containing a tethered biotin and photoaffinity cross-linker were created for future target identification studies.

Through the synthesis and biological evaluation of over 40 novel derivatives of SFM1257 and SFM1258, an extensive structure-activity-relationship has been established for these compounds, and key insights have been developed as summarized in Figure 4.31. Through the synthesis of truncated derivatives, we have determined that the key structural features that contribute significantly to the biological activity are large, non-polar groups on the 1,3-diol moiety (Figure 4.31, R₃). If the *O*-benzyl groups (Figure 4.31, R₃) are exchanged for *O*-Me or *-H*, the compounds show no *in vitro* potency. Further studies demonstrated that the alcohol moiety (Figure 4.31, R₂) is likely not critical for binding to the biological target. It was found that substitution is tolerated at the 5- and 6-position on the indole ring (Figure 4.31, R₅ and R₆), but decreasing the electron density of the indole ring leads to less potent compounds (Figure 4.31, X= N). These studies have also indicated that the availability of the basic nitrogen atom to act as a hydrogen bond donor or acceptor is crucial to maintaining activity. If a carbamate or large, non-polar group is appended to the basic amine (Figure 4.31: R₁= benzyl, alloc), potency is decreased. However, smaller alkyl substituents are tolerated on the basic amine and also lead to lower levels of hemolysis. Overall, the SAR of these compounds has not been very pronounced, and many fairly large changes have resulted in only small differences in potency (i.e. Figure 4.31: IC₅₀ ≈ R₅= H, Cl, Ph, and *p*-CF₃Ph). These data, combined with the previous biological evaluation by the Hergenrother lab, has led us to conclude that these compounds are likely not binding to an individual target with high affinity (IC₅₀ < 1 μM). Thus, it is not clear that future SAR studies would lead to a significant improvement over our current lead compounds, SFM1257 (**3.43**) and SFM1258 (**3.44**).

Figure 4.31. Summary of SAR to Date



Preliminary work has also been undertaken to access enantioenriched material. It has been found that formation of a chiral boron enolate using DTBMP is not a viable approach to this transformation, likely due a deleterious reaction between the conjugate acid and the boron enolate. Thus, future studies will focus on the formation of the boron enolate under strong base conditions.

Chapter 5: Experimental Procedures

5.1 GENERAL EXPERIMENTAL SECTION

Methanol (MeOH), acetonitrile (MeCN), and *N,N*-dimethylformamide (DMF) were dried by filtration through two column of activated molecular sieves. Tetrahydrofuran (THF) and toluene were passed through two columns of activated neutral alumina prior to use. Triethylamine (Et₃N), diisopropylethylamine (DIPEA), *N,N*-diisopropylamine (*i*-Pr₂NH), pyridine, trimethylsilyl chloride (TMS-Cl), benzene, dichloromethane (CH₂Cl₂), trimethylsilyl trifluoromethanesulfonate (TMS-OTf), acetic anhydride (Ac₂O), 2,6-lutidine, and *tert*-butyldimethylsilyl trifluoromethanesulfonate (TBS-OTf) were distilled fresh from CaH₂. *N*-vinylpyrrolidone was distilled under reduced pressure prior to use. All other reagents and solvents were reagent grade and were purchased and used as received unless otherwise noted. Water sensitive reactions were performed with oven- or flame-dried glassware, stir-bars, and steel needles. Reaction temperatures are reported as the temperature of the bath surrounding the vessel. Sensitive reagents and solvents were transferred using plastic syringes and steel needles using standard techniques. Thin layer chromatography (TLC) was performed on EMD 60 F₂₅₄ glass-backed pre-coated silica gel plates and were visualized using one or more of the following techniques: UV light (254 nm) and staining with basic potassium permanganate (KMnO₄) or *p*-anisaldehyde (PAA). Flash chromatography was performed using glass columns and Silicycle SiliaFlash F60 (40-63 μm) silica gel eluting with the solvents indicated according to Still.³⁰⁰ Purity was determined using an LCMS system comprised of an Agilent 1200 Series HPLC and an Agilent 6130 Series single quadrupole mass spectrometer. Samples were injected onto a Phenomenex Gemini C18 column (5 micron, 2.1 x 50 mm) and eluted at 0.7 mL/min using a gradient of 10-90% acetonitrile, 0.1% formic acid (11 minute linear ramp). Positive mode electrospray ionization was

used to verify the identity of the major component, and a UV chromatogram recorded as 214 nm was integrated to determine compound purity. Reverse phase high performance liquid chromatography (RP HPLC) was conducted using a binary solvent system, where solvent A was 0.1% aqueous TFA and solvent B was 0.1% TFA in MeCN, with a Phenomenex Gemini C18 column (10 μ m particle size, 300Å pore size), 250 mm x 21.2 mm diameter (flow rate of 15 mL/min) being used for preparative work. Proton nuclear magnetic resonance (^1H -NMR) and carbon nuclear magnetic resonance (^{13}C -NMR) chemical shifts are reported in parts per million (ppm, δ), downfield from tetramethylsilane (TMS, δ = 0.00 ppm) and referenced to residual solvent. Coupling constants (J) are reported in hertz (Hz) and the resonance abbreviations used are: s, singlet; d, doublet; t, triplet; dt, doublet of triplets; td, triplet of doublets; dd, doublet of doublets; ddd, doublet of doublet of doublets; m, multiplet; comp, overlapping multiplets of magnetically non-equivalent protons. The abbreviations br and app stand for broad and apparent, respectively. Melting points were measured on a Thomas-Hoover capillary tube apparatus and are uncorrected. Infrared spectra were recorded with a Nicolet FT-IR spectrophotometer as thin films on a NaCl disc unless otherwise noted.

Hs578t (human breast cancer) cells were cultured in Dulbecco's modified Eagle medium (DMEM) containing 4.5 g/L glucose and supplemented with 10% (v/v) fetal bovine serum (Gemini Bio-Products, West Sacramento, CA), 1 mM sodium pyruvate, 100 U/ml penicillin (Cellgro, Manassas, VA), and 100 μ g/mL streptomycin (Cellgro, Manassas, VA). U937 (human lymphoma) cells were grown in RPMI 1640 supplemented with 10% (v/v) fetal bovine serum, 100 U/ml penicillin, and 100 μ g/mL streptomycin. All cells were maintained in a humidified atmosphere with 95% air and 5% CO₂. All adherent cell lines were detached using 0.05% trypsin/EDTA.

5.2 EXPERIMENTAL PROCEDURES AND COMPOUND CHARACTERIZATION

Dose Response (IC₅₀) curves

To a 96-well plate, 100 μ L of 2% compound dilution or 2% DMSO-containing media were added (final volume of 1% DMSO in all wells). On each plate at least 3 wells per compound concentration were prepared. Next, 100 μ L of a 150,000-300,000 cells/mL suspension was added to each well, yielding a final concentration of 3,000 (Hs578t) or 5,000 cells/well (U937). To multiple wells in column 2 was added 20 μ L of 10 mM doxorubicin (final concentration of 100 μ M) as a positive control. Plates were sealed with gas-permeable seals and incubated at 37 °C for 48 h. At that time, 50 μ L of 3-(4,5-dimethylthiazol-2-yl)-2,5-diphenyltetrazolium bromide (MTT) in sterile PBS (3 mg/mL) was added, and the plates were re-sealed and incubated for 4-8 hours. The plates were subsequently aspirated and the precipitate formazan was dissolved in 50 μ L DMSO. Absorbance values at 560-650 nm were measured using a microplate reader (Molecular Devices, Sunnyvale, CA) and normalized to the average of non-edge untreated wells (0% cell death) and the average of 100 μ M doxorubicin wells (100% cell death). The data were plotted as compound concentration versus percent dead cells, and fitted to a logistic-dose response curve using OriginPro. Hill Slope values were obtained from curve fitted by OriginPro. The data were generated in triplicate, and IC₅₀ values are reported as the average of three separate experiments along with standard error of the mean.

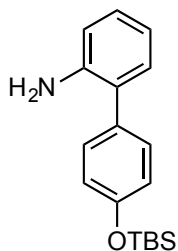
Cell viability via flow cytometry

U937 cells were plated at 300,000 cells/well in 500 μ L in 24-plates 2 h prior to addition of cytotoxic compound. A 500X dilution of compound in DMSO was added to media, followed by agitation to mix. The cells were incubated for the indicated time, and then transferred to polystyrene flow tubes. The tubes were centrifuged (3 min, 500xg)

and the supernatant was aspirated. The pellet was resuspended in binding buffer (10 mM HEPES, 140 mM NaCl, 2.5 mM CaCl₂, pH = 7.4) containing 2 µg/mL propidium iodide and 1X Annexin V-FITC Conjugate antibody. Cell suspensions were placed on ice and analyzed by flow cytometry, where cells were considered viable if they were both PI- and AnnV-negative.

With use of protectant compounds

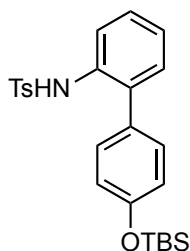
Protectant compounds were added as DMSO stocks to wells prior to addition of cell suspension, such that cells were pre-incubated with protectant compound for 2 h prior to cytotoxin addition. DMSO or 500X compound was then added and incubated for the indicated time period before analysis as described above.



4'-((*tert*-Butyldimethylsilyl)oxy)-[1,1'-biphenyl]-2-amine. (2.4). (WLM5_120).

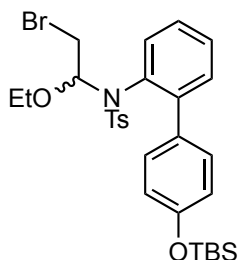
To a degassed (30 min Ar) mixture of 1,4-dioxane (75 mL) and water (25 mL) was added powdered K₂CO₃ (4.1 g, 29.64 mmol), 2-bromoaniline (1.70 g, 9.88 mmol), boroxine **1.120** (3.00 g, 4.28 mmol), Pd(dppf)Cl₂ dichloromethane adduct (403 mg, 0.494 mmol), and 2,6-di-*tert*-butyl-4 methylphenol (BHT) (spatula tip). The mixture was then heated to 100 °C under an argon atmosphere for 6 hours until all starting material was consumed, as judged by TLC. The resulting dark colored solution was diluted with EtOAc (1 L), washed with H₂O (500 mL), brine (500 mL), dried with Na₂SO₄, and concentrated under reduced pressure. The resulting black oil was purified by flash chromatography eluting

with Hexanes : EtOAc (10:1) to give 2.96 g (90%) of **2.4** as a brown oil: $^1\text{H-NMR}$ (400 MHz, CDCl_3) δ 7.35 (d, $J = 8.8$ Hz, 2 H) 7.19-7.14 (comp, 2 H) 6.95 (d, $J = 8.4$ Hz, 2 H) 6.85 (td, $J = 8.0$ Hz, 1 H) 6.78 (d, $J = 7.6$ Hz, 1 H) 3.77 (br, 2 H) 1.06 (s, 9 H) 0.29 (s, 6 H); $^{13}\text{C-NMR}$ (100 MHz, CDCl_3) δ 154.9, 143.7, 132.4, 130.6, 130.2, 128.2, 127.6, 120.4, 118.7, 115.6, 25.8, 18.3, -4.2; IR (thin film) 3470, 3377, 2956, 2929, 2885, 2858 cm^{-1} ; HRMS (ESI) m/z observed 300.17750 [$\text{C}_{18}\text{H}_{25}\text{NOSi}$ ($\text{M}+\text{H}$) $^+$ requires 300.17782].



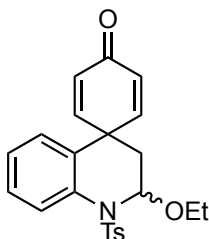
***N*-(4'-((*tert*-butyldimethylsilyl)oxy)-[1,1'-biphenyl]-2-yl)-4-methylbenzenesulfonamide. (2.12). (WLM3_6).** To a solution of **2.4** (973 mg, 3.25 mmol) in pyridine (6.5 mL) at 0 °C was added p-toluenesulfonyl chloride (1.25 g, 6.5 mmol). The reaction was allowed stir overnight until all starting material was consumed, as judged by TLC. The resulting brown solution was diluted with EtOAc (50 mL), washed with H_2O (25 mL), brine (25 mL), dried with Na_2SO_4 , and concentrated *in vacuo* to give a brown oil, which was subsequently azeotroped with cyclohexane (3 x 25 mL). Subsequent purification by flash chromatography eluting with Hexanes : EtOAc (10:1) gave 1.47 g (quant) of **2.12** as a sappy clear oil that solidified upon standing: $^1\text{H-NMR}$ (400 MHz, CDCl_3) δ 7.70 (d, $J = 8.0$ Hz, 1 H) 7.47 (d, $J = 8.8$ Hz, 2 H) 7.29 (td, $J = 8.2$ Hz, 1 H) 7.18 (d, $J = 8.4$ Hz, 2 H) 7.13-7.06 (comp, 2 H), 6.80 (d, $J = 8.8$, 2 H) 6.72 (d, $J = 8.8$ Hz, 2 H) 6.67 (br, 1 H) 2.38 (s, 3 H) 1.03 (s, 9 H) 0.26 (s, 6 H); $^{13}\text{C-NMR}$ (100 MHz, CDCl_3) δ 155.9, 144.1, 136.4, 134.1, 134.0, 130.7, 130.3, 130.2, 129.8, 128.6, 127.4, 125.1, 121.6, 120.8, 25.9, 21.8, 18.5, -4.1; IR (thin film) 3344, 3064, 3034, 2955,

2929, 2886, 2858 cm^{-1} ; HRMS (ESI) m/z observed 454.18624 [$\text{C}_{25}\text{H}_{31}\text{NO}_3\text{SSi}$ ($\text{M}+\text{H}$) $^+$ requires 454.18667].



***N*-(2-bromo-1-ethoxyethyl)-*N*-(4'-((*tert*-butyldimethylsilyl)oxy)-[1,1'-biphenyl]-2-yl)-4-methylbenzenesulfonamide. (2.13). (WLM6_66).** To a solution of Br_2 (2.63 g, 0.85 mL, 16.44 mmol) in CH_2Cl_2 (41 mL) at 0 °C under argon was added ethyl vinyl ether (1.48 g, 1.98 mL, 20.55 mmol) drop-wise until the solution turned colorless. The mixture was stirred for 30 min and diisopropylethylamine (4.25 g, 5.73 mL, 32.88 mmol) was added. After 30 min, a solution of **2.12** (3.73 g, 8.22 mmol) in CH_2Cl_2 (41 mL) was added drop-wise, and the mixture was allowed to slowly warm to room temperature overnight under an argon atmosphere. After complete consumption of starting material, as judged by TLC, the reaction mixture was poured onto saturated aqueous NH_4Cl (75 mL) and extracted with EtOAc (3 x 75 mL). The combined extracts were washed with H_2O (100 mL), brine (100 mL), dried with Na_2SO_4 , and concentrated *in vacuo*. The resulting brown oil was purified by flash chromatography eluting with Hexanes : EtOAc (20:1) gave 5.0 g (quant) of **2.13** as a clear oil that crystallized upon standing: M.p. 118-122 °C; ^1H -NMR (400 MHz, CDCl_3 , as a mixture of rotamers) δ 7.83-7.78 (comp, 2 H) 7.54-7.49 (comp, 2 H) 7.42-7.34 (comp, 4 H) 7.29-7.17 (m, 1 H) 7.00-6.84 (comp, 3 H) 5.10-4.93 (m, 1 H) 3.27-3.18 (m, 1 H) 3.09-3.03 (m, 1 H) 2.87-2.83 (m, 1 H) 2.70-2.66 (m, 1 H) 2.48 (s, 3 H) 1.02 (s, 9 H) 0.94-0.86 (comp, 3 H) 0.24 (s, 6 H); ^{13}C -NMR (100 MHz, CDCl_3 , as a mixture of rotamers) δ 155.5, 155.2, 144.4,

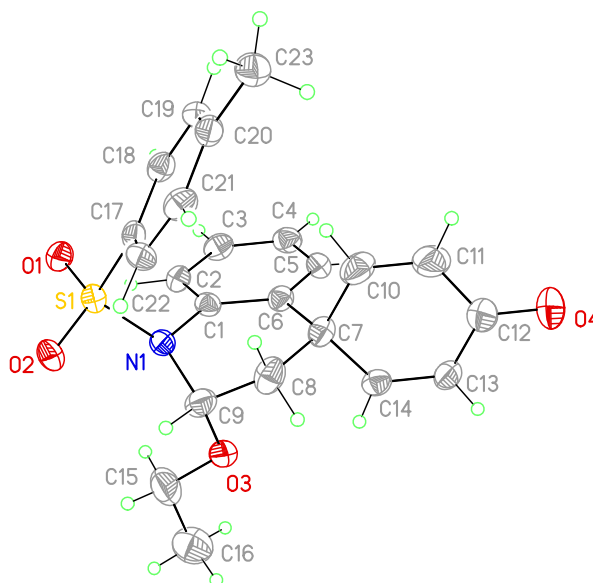
144.1, 143.9, 138.3, 137.6, 135.0, 132.8, 132.6, 132.4, 132.1, 131.8, 131.2, 130.9, 129.7, 129.6, 129.3, 129.1, 129.0, 128.4, 128.1, 127.2, 127.2, 119.9, 119.7, 91.5, 89.8, 66.9, 65.3, 33.6, 33.5, 25.7, 21.6, 18.3, 18.2, 14.5, 14.2, -4.4; IR (thin film) 3065, 3031, 2956, 2929, 2897, 2858 cm^{-1} ; HRMS (ESI) m/z observed 626.13680 [$\text{C}_{29}\text{H}_{38}\text{BrNO}_4\text{SSi}$ ($\text{M}+\text{Na}$) $^+$ requires 626.13664].



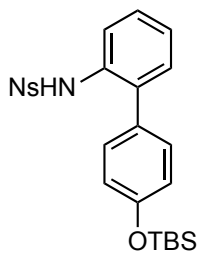
2'-Ethoxy-1'-tosyl-2',3'-dihydro-1'H-spiro[cyclohexa[2,5]diene-1,4'-quinolin]-4-one. (2.14). (WLM6_72). To a solution of **2.13** (4.43 g, 7.33 mmol) in anhydrous DMF (73 mL, stored over 4Å molecular sieves) at 50 °C was added flame-dried CsF (3.34 g, 21.98 mmol). The reaction mixture was immediately heated to 130 °C for 1 h under an argon atmosphere. After complete consumption of the starting material, as judged by TLC, the reaction mixture was diluted with EtOAc (200 mL), washed with H_2O (100 mL), brine (100 mL), dried with Na_2SO_4 , and concentrated *in vacuo* to afford a brown oil. Purification by flash chromatography eluting with Hexanes : EtOAc (3:1) to afford 2.88 g (96%) of **2.14** as a white crystalline solid: M.p. 158-160 °C; ^1H -NMR (400 MHz, CDCl_3) δ 7.92 (d, J = 9.2 Hz, 1 H) 7.43 (d, J = 8.4 Hz, 2 H) 7.30 (td, J = 4.4 Hz, 1 H) 7.27-7.24 (comp, 3 H) 7.12 (td, J = 8.0 Hz, 1 H) 6.86 (dd, J = 9.2 Hz, 1 H) 6.12 (dd, J = 12.0 Hz, 1 H) 6.07 (dd, J = 12.0 Hz, 1 H) 5.71 (dd, J = 19.6 Hz, 1 H) 5.67 (t, J = 2.8 Hz, 1 H) 3.84-3.76 (m, 1 H) 3.64-3.56 (m, 1 H) 2.41 (s, 3 H) 1.92 (dd, J = 16.8 Hz, 1 H) 1.58 (dd, J = 18.0 Hz, 1 H) 1.13 (t, J = 7.2 Hz, 3 H); ^{13}C -NMR (100 MHz, CDCl_3) δ 185.9, 155.3, 154.3, 144.6, 135.9, 133.1, 130.0, 129.4, 128.8, 128.3, 127.4, 127.3, 126.6, 126.4,

125.1, 83.0, 63.8, 41.6, 35.0, 21.8, 15.0; IR (thin film) 3058, 2976, 2929, 1668 cm^{-1} .

HRMS (CI) m/z observed 409.1346 [$\text{C}_{23}\text{H}_{23}\text{NO}_4\text{S}$ (M) $^+$ requires 409.1348].

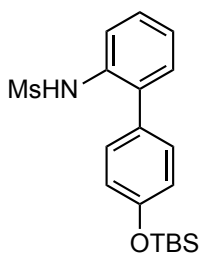


ORTEP View of **2.14**. Displacement ellipsoids are scaled to the 50% probability level.



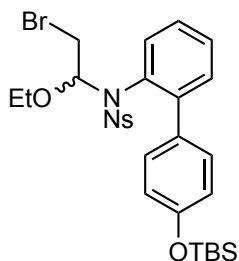
***N*-(4'-((*tert*-butyldimethylsilyl)oxy)-[1,1'-biphenyl]-2-yl)-4-nitrobenzenesulfonamide. (2.16). (WLM4_132).** To a solution of **2.4** (284 mg, 0.95 mmol) in CH_2Cl_2 : pyridine (1 : 1) (10 mL) under argon at 0 $^\circ\text{C}$ was added *p*-

nitrosulfonyl chloride (420 mg, 1.90 mmol). The reaction was allowed stir overnight until all starting material was consumed, as judged by TLC. The resulting brown solution was diluted with EtOAc (50 mL), washed with H₂O (25 mL), brine (25 mL), dried with Na₂SO₄, and concentrated *in vacuo* to give a brown oil, which was subsequently azeotroped with cyclohexane (3 x 15 mL). Purification by flash chromatography eluting with Hexanes : EtOAc (8:1) gave 313 mg (68%) of **2.16** as a yellow solid: M.p. 127-129°C; ¹H-NMR (400 MHz, CDCl₃) δ 8.16 (d, *J* = 8.8 Hz, 2 H) 7.65 (d, *J* = 8.8 Hz, 2 H) 7.68-7.66 (m, 1 H) 7.34 (td, *J* = 7.8, 1.6 Hz, 1 H) 7.19 (td, *J* = 7.6, 1.2 Hz, 1 H) 7.10 (dd, *J* = 7.6, 1.6 Hz, 1 H) 6.78 (d, *J* = 8.4 Hz, 2 H) 6.70 (d, *J* = 8.8 Hz, 2 H) 1.02 (s, 9 H) 0.26 (s, 6 H); ¹³C-NMR (100 MHz, CDCl₃) δ 155.9, 150.2, 144.7, 135.0, 132.6, 130.7, 129.8, 129.7, 128.6, 128.4, 126.3, 124.1, 123.1, 120.7, 25.7, 18.3, -4.3; IR (thin film) 3338, 2930, 2858, 1532, 1348 cm⁻¹; HRMS (ESI) *m/z* observed 507.13911 [C₂₄H₂₈N₂O₅SSi (M+Na)⁺ requires 507.13804].



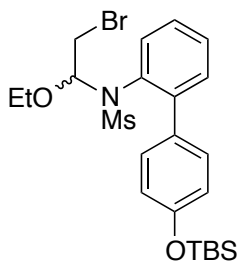
***N*-(4'-((*tert*-butyldimethylsilyl)oxy)-[1,1'-biphenyl]-2-yl)methanesulfonamide. (2.17). (WLM4_50).** To a solution of **2.4** (213 mg, 0.71 mmol) in CH₂Cl₂ (6 mL) under argon at 0 °C was added triethylamine (108 mg, 1.07 mmol, 0.15 mL) and methanesulfonyl chloride (1 M in CH₂Cl₂, 0.71 mL). After 3 hr, the reaction was poured onto saturated aqueous NH₄Cl (20 mL) and extracted with EtOAc (3 x 15 mL). The combined organic extracts were washed with H₂O (20 mL), brine (20 mL), dried with

Na₂SO₄ and concentrated under reduced pressure. The resulting a brown oil was purified by flash chromatography eluting with Hexanes : EtOAc (4:1) to afford 187 mg (69%) of **2.17** as a yellow oil: ¹H-NMR (400 MHz, CDCl₃) δ 7.63 (dd, *J* = 8.8 Hz, 1 H) 7.35 (td, *J* = 8.0 Hz, 1 H) 7.25 (dd, *J* = 7.6 Hz, 1 H) 7.22-7.18 (comp, 3 H) 6.95 (d, *J* = 8.8 Hz, 2 H) 6.56 (br, 1 H) 2.85 (s, 3 H) 1.02 (s, 9 H) 0.26 (s, 6 H); ¹³C-NMR (100 MHz, CDCl₃) δ 156.1, 134.3, 133.4, 131.2, 130.4, 130.3, 128.9, 125.1, 121.2, 120.3, 39.9, 25.9, 18.4, -4.1. IR (thin film) 3355, 3064, 3034, 2956, 2886, 2858 cm⁻¹; HRMS (ESI) *m/z* observed 400.13681 [C₁₉H₂₇NO₃SSi (M+Na)⁺ requires 400.13731].



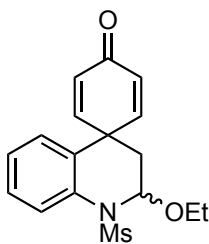
***N*-(2-bromo-1-ethoxyethyl)-*N*-(4'-((*tert*-butyldimethylsilyl)oxy)-[1,1'-biphenyl]-2-yl)-4-nitrobenzenesulfonamide. (2.18). (WLM4_133).** To a solution of Br₂ (133 mg, 0.043 mL, 0.834 mmol) in CH₂Cl₂ (2.1 mL) at 0°C under argon was added ethyl vinyl ether (75 mg, 0.10 mL, 1.05 mmol) drop-wise until the solution turned colorless. The mixture was stirred for 30 min and diisopropylethylamine (217 mg, 0.29 mL, 1.68 mmol) was added. After 30 min, a solution of **2.16** (202 mg, 0.42 mmol) in CH₂Cl₂ (2.1 mL) was added drop-wise, and the mixture was allowed to slowly warm to room temperature overnight under an argon atmosphere. After complete consumption of starting material, as judged by TLC, the reaction mixture was poured onto saturated aqueous NH₄Cl (25 mL) and extracted with EtOAc (3 x 20 mL). The combined extracts were washed with H₂O (30 mL), brine (30 mL), dried with Na₂SO₄, and concentrated under reduced pressure. The resulting brown oil was purified by flash chromatography

eluting with Hexanes : EtOAc (10:1) to afford 230 mg (87%) of **2.18** as a yellow solid: M.p. 140-143°C; ¹H-NMR (400 MHz, CDCl₃, as a mixture of rotamers) δ 8.42-8.38 (comp, 2 H) 8.16-8.05 (comp, 2 H) 7.48-7.41 (comp, 4 H) 7.28-7.24 (m, 1 H) 6.96-6.83 (comp, 3 H) 5.15-4.83 (m, 1 H) 3.47-2.56 (comp, 4 H) 1.03 (s, 9 H) 1.92-1.87 (comp, 3 H) 0.26 (s, 6 H); ¹³C-NMR (100 MHz, CDCl₃, as a mixture of rotamers) δ 155.9, 155.7, 150.3, 147.3, 146.3, 144.3, 144.0, 136.0, 133.3, 132.7, 132.4, 131.6, 131.2, 131.0, 130.0, 129.9, 129.6, 128.5, 127.9, 127.7, 124.2, 120.2, 120.1, 93.7, 90.6, 67.3, 66.4, 33.7, 33.9, 25.9, 18.4, 14.7, 14.6, -4.2; IR (thin film) 2956, 2929, 2858, 1533, 1349 cm⁻¹; HRMS calcd. C₂₈H₃₅BrN₂NaO₆SSi (MNa)⁺ 657.10607, found 657.10696.



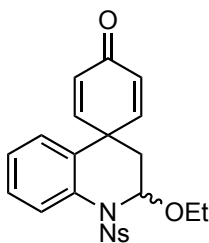
***N*-(2-bromo-1-ethoxyethyl)-*N*-(4'-((*tert*-butyldimethylsilyl)oxy)-[1,1'-biphenyl]-2-yl)methanesulfonamide. (2.19). (WLM4_51).** To a solution of Br₂ (157 mg, 0.051 mL, 0.985 mmol) in CH₂Cl₂ (3 mL) at 0°C under argon was added ethyl vinyl ether (89 mg, 0.12 mL, 1.23 mmol) drop-wise until the solution turned colorless. The mixture was stirred for 30 min and diisopropylethylamine (255 mg, 0.34 mL, 1.97 mmol) was added. After 30 min, a solution of **2.17** (187 mg, 0.493 mmol) in CH₂Cl₂ (3 mL) was added drop-wise, and the mixture was allowed to slowly warm to room temperature overnight under an argon atmosphere. After complete consumption of starting material, as judged by TLC, the reaction mixture was poured onto saturated aqueous NH₄Cl (25 mL) and extracted with EtOAc (3 x 15 mL). The combined extracts were washed with

H₂O (25 mL), brine (25 mL), dried with Na₂SO₄, and concentrated under reduced pressure. The resulting brown oil was purified by flash chromatography eluting with Hexanes : EtOAc (10:1) to afford 192 mg (74%) of **2.19** as a yellow oil: ¹H-NMR (400 MHz, CDCl₃, as a mixture of rotamers) δ 7.48-7.35 (comp, 6 H) 6.95-6.89 (comp, 2 H) 5.05-4.80 (m, 1 H) 3.80-2.75 (comp, 7 H) 1.26-1.19 (comp, 3 H) 1.03-1.0 (comp, 9 H) 0.23-0.21 (comp, 6 H); ¹³C-NMR (100 MHz, CDCl₃, as a mixture of rotamers) δ 155.5, 155.3, 143.8, 143.2, 136.0, 133.1, 132.7, 132.5, 132.3, 132.2, 131.7, 130.9, 130.8, 129.3, 129.1, 129.0, 127.9, 120.1, 119.8, 119.7, 92.3, 89.9, 67.3, 66.1, 43.2, 42.9, 41.1, 33.5, 32.5, 25.6, 18.2, 14.9, 14.6, -4.4; IR (thin film) 2957, 2930, 2896, 2858 cm⁻¹; HRMS (ESI) *m/z* observed 550.10506 [C₂₃H₃₄BrNO₄SSi (M+Na)⁺ requires 550.10534].



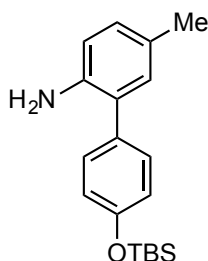
2'-Ethoxy-1'-(methylsulfonyl)-2',3'-dihydro-1'*H*-spiro[cyclohexa[2,5]diene-1,4'-quinolin]-4-one. (2.20). (WLM4_54). To a solution of **2.19** (159 mg, 0.301 mmol) in anhydrous DMF (3 mL, stored over 4Å molecular sieves) at 50 °C was added flame-dried CsF (228 mg, 1.504 mmol). The reaction mixture was immediately heated to 130 °C for 1 h under an argon atmosphere. After complete consumption of the starting material, as judged by TLC, the reaction mixture was diluted with EtOAc (30 mL), washed with H₂O (20 mL), brine (20 mL), dried with Na₂SO₄, and concentrated under reduced pressure. The resulting brown oil was purified by flash chromatography eluting with Hexanes : EtOAc (3:2) to afford 83 mg (83%) of **2.20** as a white crystalline solid: M.p. 118-121 °C (decomp); ¹H-NMR (400 MHz, CDCl₃) δ 7.79 (dd, *J* = 8.4, 0.8 Hz, 1 H)

7.42 (dd, $J = 10.0, 3.2$ Hz, 1 H) 7.29 (td, $J = 8.0, 1.6$ Hz, 1 H) 7.09 (td, $J = 8.0$ Hz, 1 H) 7.01 (dd, $J = 8.0, 1.6$ Hz, 1 H) 6.76 (dd, $J = 10.0, 3.2$ Hz, 1 H) 6.36 (dd, $J = 10.0, 2.0$ Hz, 1 H) 6.19 (dd, $J = 10.0, 2.0$ Hz, 1 H) 5.76 (t, $J = 3.2$ Hz, 1 H) 3.75-3.67 (m, 1 H) 3.61-3.54 (m, 1 H) 3.07 (s, 3 H) 2.29 (d, $J = 3.2$ Hz, 2 H) 1.16 (t, $J = 7.6$ Hz, 3 H); ^{13}C -NMR (100 MHz, CDCl_3) δ 185.7, 154.6, 154.1, 133.6, 129.7, 129.0, 128.4, 125.4, 125.1, 125.0, 122.8, 82.4, 63.7, 41.9, 40.0, 36.7, 14.8; IR (thin film) 2976, 2931, 1663 cm^{-1} ; HRMS (ESI) m/z observed 356.09309 [$\text{C}_{17}\text{H}_{19}\text{NO}_4\text{S}$ ($\text{M}+\text{Na}$) $^+$ requires 356.09270].



2'-Ethoxy-1'-((4-nitrophenyl)sulfonyl)-2',3'-dihydro-1'H-spiro[cyclohexa[2,5]diene-1,4'-quinolin]-4-one. (2.21). (WLM5_7). To a solution of **2.18** (135 mg, 0.212 mmol) in anhydrous DMF (2.2 mL, stored over 4Å molecular sieves) at 50 °C was added flame-dried CsF (161 mg, 1.06 mmol). The reaction mixture was immediately heated to 130 °C for 1 h under an argon atmosphere. After complete consumption of the starting material, as judged by TLC, the reaction mixture was diluted with EtOAc (25 mL), washed with H_2O (10 mL), brine (10 mL), dried with Na_2SO_4 , and concentrated under reduced pressure. The resulting brown oil was purified by flash chromatography eluting with Hexanes : EtOAc (1:1) to afford a semi-crude white solid that was subsequently recrystallized from MeOH to give 50 mg (34%) of pure **2.21**: ^1H NMR (500 MHz, CDCl_3) δ 8.32 (d, $J = 9.0$ Hz, 2 H) 7.90 (dd, $J = 8.75, 1.75$ Hz, 1 H) 7.80 (d, $J = 9.0$ Hz, 2 H) 7.33 (td, $J = 7.5$ Hz, 1 H) 7.25 (dd, $J = 8.4, 3.0$ Hz, 1 H) 7.17 (td, $J = 7.5, 1.0$ Hz, 1 H) 6.92 (dd, $J = 8.0, 1.5$ Hz, 1 H) 6.19 (dd, $J = 10.5$ Hz, 1.75 Hz, 1 H)

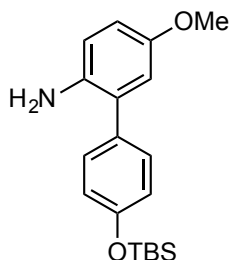
6.10 (dd, $J = 10.0$ Hz, 2.0 Hz, 1 H) 5.79 (dd, $J = 10.0$, 3.0 Hz, 1 H) 5.77-5.76 (m, 1 H) 3.84-3.78 (m, 1 H) 3.67-3.61 (m, 1 H) 2.06 (dd, $J = 14.5$, 2.5 Hz, 1 H) 1.63 (dd, $J = 14.5$, 3.5 Hz, 1 H) 1.17 (t, $J = 7.0$ Hz, 1 H); ^{13}C -NMR (125 MHz, CDCl_3) δ 185.3, 154.3, 153.1, 150.3, 144.4, 132.2, 129.7, 128.9, 128.6, 128.4, 126.7, 126.6, 126.1, 125.2, 124.4, 83.2, 64.0, 41.4, 35.7, 14.7; IR (thin film) 3104, 2973, 1668, 1539, 1351 cm^{-1} ; HRMS (ESI) m/z observed 463.09349 [$\text{C}_{22}\text{H}_{20}\text{N}_2\text{O}_6\text{S}$ ($\text{M}+\text{Na}$) $^+$ requires 463.09343].



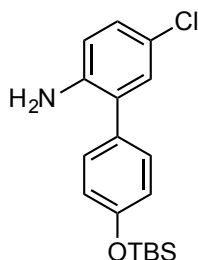
4'-((*tert*-Butyldimethylsilyl)oxy)-5-methyl-[1,1'-biphenyl]-2-amine. (2.27a).

(WLM4_148). To a degassed (30 min) mixture of 1,4-dioxane (4.0 mL) and water (1.3 mL) was added powdered K_2CO_3 (224 mg, 1.62 mmol), **2.26a** (100 mg, 0.54 mmol), **1.120** (165 mg, 0.234 mmol), $\text{Pd}(\text{dppf})\text{Cl}_2$ dichloromethane adduct (13 mg, 0.0159 mmol), and 2,6-di-*tert*-butyl-4-methylphenol (BHT) (spatula tip). The mixture was then heated to 100 $^\circ\text{C}$ under an argon atmosphere for 4 hours until all starting material was consumed, as judged by TLC. The resulting dark colored solution was diluted with EtOAc (20 mL), washed with H_2O (10 mL), brine (10 mL), dried with Na_2SO_4 , and concentrated under reduced pressure. The resulting black oil was purified by flash chromatography eluting with Hexanes: EtOAc (10:1) to afford 99 mg (59% yield) of **2.27a** as a brown oil: ^1H NMR (400 MHz, CDCl_3) δ 7.33 (d, $J = 8.4$ Hz, 2 H) 6.97-6.96 (comp, 2 H) 6.92 (d, $J = 8.4$ Hz, 2 H) 6.69 (d, $J = 8.8$ Hz, 1 H) 3.64 (br, 2 H) 2.29 (s, 3 H) 1.04 (s, 9 H) 0.26 (s, 6 H); ^{13}C -NMR (100 MHz, CDCl_3) δ 154.9, 141.2, 132.6, 131.2, 130.3, 128.8, 127.9, 127.7, 120.4, 115.9, 25.9, 20.6, 18.4, -4.2; IR (thin film) 3461, 3371,

2956, 2929, 2858 cm^{-1} ; HRMS (ESI) m/z observed 314.1930 [$\text{C}_{19}\text{H}_{27}\text{NOSi}$ ($\text{M}+\text{H}$) $^{+}$ requires 314.1940].

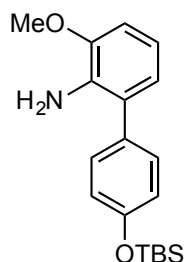


4'-((*tert*-Butyldimethylsilyl)oxy)-5-methoxy-[1,1'-biphenyl]-2-amine. (2.27b). (**WLM3_84**). To a degassed (30 min) mixture of 1,4-dioxane (40 mL) and water (13 mL) was added powdered K_2CO_3 (2.5g, 17.8 mmol), **2.26b** (1.23 g, 5.94 mmol), **1.120** (1.81 g, 2.57 mmol), $\text{Pd}(\text{dppf})\text{Cl}_2$ dichloromethane adduct (240 mg, 0.297 mmol), and 2,6-di-*tert*-butyl-4 methylphenol (BHT) (spatula tip). The mixture was then heated to 100 $^{\circ}\text{C}$ under an argon atmosphere for 6 hours until all starting material was consumed, as judged by TLC. The resulting dark colored solution was diluted with EtOAc (250 mL), washed with H_2O (125 mL), brine (125 mL), dried with Na_2SO_4 , and concentrated under reduced pressure. The resulting black oil was purified by flash chromatography eluting with Hexanes: EtOAc (10:1) to afford 1.830 g (93%) of **2.27b** as a brown oil: ^1H NMR (400 MHz, CDCl_3) δ 7.34 (d, $J = 8.8$ Hz, 2 H) 6.93 (d, $J = 8.4$ Hz, 2 H) 6.78-6.71 (comp, 3 H) 3.78 (s, 3 H) 3.71 (br, 2 H) 1.04 (s, 9 H) 0.27 (s, 6 H); ^{13}C NMR (100 MHz, CDCl_3) δ 155.2, 153.0, 137.5, 132.6, 130.4, 128.9, 120.6, 117.1, 116.0, 114.3, 56.0, 26.0, 18.5, -4.1; IR (thin film) 3444, 3362, 3031, 2930, 2857, 2831 cm^{-1} ; HRMS (ESI) m/z observed 330.18839 [$\text{C}_{19}\text{H}_{27}\text{NO}_2\text{Si}$ ($\text{M}+\text{H}$) $^{+}$ requires 330.18838].

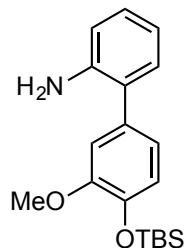


4'-((*tert*-Butyldimethylsilyl)oxy)-5-chloro-[1,1'-biphenyl]-2-amine. (2.27c).

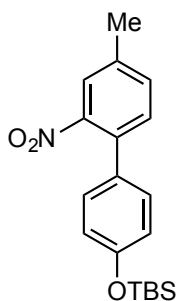
(WLM4_154). To a degassed (30 min) mixture of 1,4-dioxane (9.0 mL) and water (3.0 mL) was added powdered K_2CO_3 (560 mg, 4.05 mmol), 2-bromo-4-chloroaniline (278 mg, 1.35 mmol), **2** (441 mg, 1.75 mmol), $Pd(dppf)Cl_2$ dichloromethane adduct (55 mg, 0.0675 mmol), and 2,6-di-*tert*-butyl-4-methylphenol (BHT) (spatula tip). The mixture was then heated to 100 °C under an argon atmosphere for 4 hours until all starting material was consumed, as judged by TLC. The resulting dark colored solution was diluted with EtOAc (50 mL), washed with H_2O (25 mL), brine (25 mL), dried with Na_2SO_4 , and concentrated under reduced pressure. The resulting black oil was purified by flash chromatography eluting with Hexanes: EtOAc (10:1) to afford 342 mg (76% yield) of **2.27c** as a clear oil: 1H -NMR (400 MHz, $CDCl_3$) δ 7.33 (d, J = 8.8 Hz, 2 H) 7.15 (d, J = 2.4 Hz, 1 H) 7.11 (dd, J = 8.6 Hz, 2.6 Hz, 1 H) 6.99 (d, J = 8.4 Hz, 2 H) 6.66 (d, J = 8.4 Hz, 1 H) 3.77 (br, 2 H) 1.12 (s, 9 H) 0.34 (s, 6 H); ^{13}C -NMR (100 MHz, $CDCl_3$) δ 155.3, 142.4, 131.2, 130.1, 130.0, 128.7, 127.8, 122.9, 120.5, 116.6, 25.8, 18.3, -4.3; IR (thin film) 3474, 3385, 2931, 2886, 2861 cm^{-1} ; HRMS (ESI) m/z observed 334.13890 [$C_{18}H_{23}ClNOSi$ ($M+H$) $^+$ requires 334.13880].



4'-((*tert*-Butyldimethylsilyl)oxy)-3-methoxy-[1,1'-biphenyl]-2-amine. (2.27d). (**WLM3_82**). To a degassed (30 min) mixture of 1,4-dioxane (40 mL) and water (13 mL) was added powdered K_2CO_3 (2.36 g, 17.1 mmol), **2.26d** (1.18 g, 5.69 mmol), **1.120** (1.73 g, 2.46 mmol), $\text{Pd}(\text{dppf})\text{Cl}_2$ dichloromethane adduct (230 mg, 0.284 mmol), and 2,6-di-*tert*-butyl-4-methylphenol (BHT) (spatula tip). The mixture was then heated to 50 °C under an argon atmosphere for 12 hours until all starting material was consumed, as judged by TLC. The resulting dark colored solution was diluted with EtOAc (100 mL), washed with H_2O (50 mL), brine (50 mL), dried with Na_2SO_4 , and concentrated under reduced pressure. The resulting black oil was purified by flash chromatography eluting with Hexanes : EtOAc (10:1) to give 1.69 g (90% yield) **2.27d** as a brown oil; ^1H NMR (400 MHz, CDCl_3) δ (2H, d, $J = 8.8$ Hz) 7.056-7.040 (comp, 2 H) 6.87 (d, $J = 8.4$ Hz, 2 H) 6.80 (d, $J = 8.4$ Hz, 1 H) 4.07 (br, 2 H) 3.94 (s, 3 H) 1.07 (s, 9 H) 0.29 (s, 6 H); ^{13}C NMR (100 MHz, CDCl_3) δ 154.8, 147.9, 135.2, 135.1, 132.2, 127.8, 120.6, 119.7, 115.7, 109.4, 55.8, 26.0, 18.6, -4.1; IR (thin film) 3380, 2956, 2930, 2857 cm^{-1} ; HRMS (CI) m/z observed 329.1812 [$\text{C}_{19}\text{H}_{27}\text{NO}_2\text{Si}$ (M) $^+$ requires 329.181].

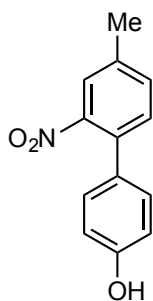


4'-((*tert*-Butyldimethylsilyl)oxy)-3'-methoxy-[1,1'-biphenyl]-2-amine. (2.27e). (**WLM3_76**). To a degassed (30 min) mixture of 1,4-dioxane (6.0 mL) and water (2.0 mL) was added powdered K₂CO₃ (315 mg, 2.29 mmol), 2-bromoaniline (135 mg, 0.762 mmol), (4'-((*tert*-butyldimethylsilyl)oxy)-3-methoxyphenyl)boronic acid (235 mg, 0.897 mmol), Pd(dppf)Cl₂ dichloromethane adduct (30 mg, 0.038 mmol), and 2,6-di-*tert*-butyl-4-methylphenol (BHT) (spatula tip). The mixture was then heated to 100 °C under an argon atmosphere for 6 hours until all starting material was consumed, as judged by TLC. The resulting dark colored solution was diluted with EtOAc (20 mL), washed with H₂O (10 mL), brine (10 mL), dried with Na₂SO₄, and concentrated under reduced pressure. The resulting black oil was purified by flash chromatography eluting with Hexanes: EtOAc (10:1) to afford 200 mg (80%) of **2.27e** as a brown oil: ¹H-NMR (400 MHz, CDCl₃) δ 7.20-7.16 (comp, 2 H) 7.01-6.94 (comp, 3 H) 6.86 (dt, *J* = 7.6 Hz, 1 H) 6.78 (d, *J* = 8.0 Hz, 1 H) 3.86 (s, 3 H) 3.85 (br, 2 H) 1.11 (s, 9 H) 0.28 (s, 6 H); ¹³C NMR (100 MHz, CDCl₃) δ 151.3, 144.5, 143.9, 133.3, 130.7, 128.5, 128.0, 121.7, 121.4, 118.8, 115.8, 113.3, 55.8, 26.1, 18.8, -4.2; IR (thin film) 3470, 3376, 2929, 2895, 2857 cm⁻¹; HRMS (ESI) *m/z* observed 330.18821 [C₁₉H₂₇NO₂Si (M+H)⁺ requires 330.18838].

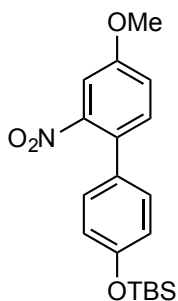


***tert*-Butyldimethyl((4'-methyl-2'-nitro-[1,1'-biphenyl]-4-yl)oxy)silane. (2.29a).** (**WLM4_135**). To a degassed (30 min) mixture of 1,4-dioxane (13.5 mL) and water (4.5 mL) was added powdered K₂CO₃ (730 mg, 5.28 mmol), 2-bromo-5-methylnitrobenzene

(380 mg, 1.76 mmol), **1.120** (536 mg, 0.763 mmol), Pd(dppf)Cl₂ dichloromethane adduct (72 mg, 0.088 mmol), and 2,6-di-*tert*-butyl-4-methylphenol (BHT) (spatula tip). The mixture was then heated to 100 °C under an argon atmosphere for 4 hours until all starting material was consumed, as judged by TLC. The resulting dark colored solution was diluted with EtOAc (100 mL), washed with H₂O (50 mL), brine (50 mL), dried with Na₂SO₄, and concentrated under reduced pressure. The resulting black oil was purified by flash chromatography eluting with Hexanes : EtOAc (10:1) to afford 399 mg (66%) of **2.29a** as a yellow oil and 60 mg (15%) of **2.29c** as a brown oil: ¹H-NMR (400 MHz, CDCl₃) δ 7.07 (d, *J* = 0.8 Hz, 1 H) 7.38 (dd, *J* = 8.0, 1.2 Hz, 1 H) 7.30 (d, *J* = 8.0 Hz, 1 H) 7.17 (d, *J* = 8.8 Hz, 2 H) 6.87 (d, *J* = 8.4 Hz, 2 H) 2.45 (s, 3 H) 1.00 (s, 9 H) 0.24 (s, 6 H); ¹³C-NMR (100 MHz, CDCl₃) δ 155.9, 149.4, 138.3, 133.3, 133.0, 131.8, 130.3, 129.3, 124.4, 120.4, 25.8, 21.0, 18.4, -4.2; IR (thin film) 2956, 2930, 2858, 1532, 1352 cm⁻¹; HRMS (ESI) *m/z* observed 366.15041 [C₁₉H₂₅NO₃Si (M+Na)⁺ required 366.14959].

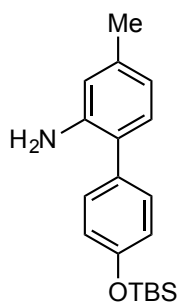


4'-Methyl-2'-nitro-[1,1'-biphenyl]-4-ol. (2.29c). Isolated as a by-product: ¹H-NMR (400 MHz, CDCl₃) δ 7.61 (d, *J* = 0.8 Hz, 1 H) 7.39 (dd, *J* = 8.0, 1.6 Hz, 1 H) 7.29 (d, *J* = 7.6 Hz, 1 H) 7.16 (d, *J* = 8.8 Hz, 2 H) 6.85 (d, *J* = 8.8 Hz, 2 H) 5.90 (br, 1 H) 2.44 (s, 3 H); ¹³C-NMR (100 MHz, CDCl₃) δ 155.9, 149.2, 138.4, 133.2, 131.9, 129.6, 129.4, 124.5, 115.9, 20.9; IR (thin film) 3421, 1517, 1354 cm⁻¹; HRMS (ESI) *m/z* observed 252.06329 [C₁₃H₁₁NO₃ (M+Na)⁺ required 252.06311].

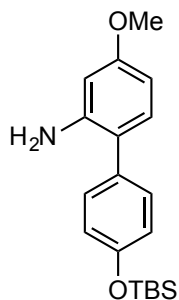


***tert*-Butyl((4'-methoxy-2'-nitro-[1,1'-biphenyl]-4-yl)oxy)dimethylsilane.**

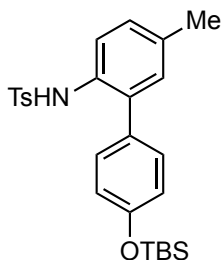
(2.29b). (WLM3_64). To a degassed (30 min) mixture of 1,4-dioxane (15 mL) and water (5 mL) was added powdered K_2CO_3 (1.07 g, 7.76 mmol) 1-bromo-4-methoxy-2-nitrobenzene (600 mg, 2.59 mmol), **1.120** (787 mg, 1.12 mmol), $Pd(dppf)Cl_2$ dichloromethane adduct (106 mg, 0.130 mmol), and 2,6-di-*tert*-butyl-4 methylphenol (BHT) (spatula tip). The mixture was then heated to 100 °C under an argon atmosphere for 6 hours until all starting material was consumed, as judged by TLC. The resulting dark colored solution was diluted with EtOAc (100 mL), washed with H_2O (50 mL), brine (50 mL), dried with Na_2SO_4 , and concentrated under reduced pressure. The resulting black oil was purified by flash chromatography eluting with Hexanes : EtOAc (10:1) to afford 761 mg (82%) of **2.29b** as a yellow oil: 1H -NMR (400 MHz, $CDCl_3$) δ 7.33-7.32 (d, J = 2.8 Hz, 1 H) 7.31 (d, J = 3.2 Hz, 1 H) 7.15 (d, J = 8.8 Hz, 2 H) 7.11 (dd, J = 11.2 Hz, 1 H) 6.88 (d, J = 8.8 Hz, 2 H) 3.87 (s, 3 H) 1.02 (s, 9 H) 0.25 (s, 6 H); ^{13}C -NMR (100 MHz, $CDCl_3$) δ 159.0, 155.8, 149.9, 133.0, 130.3, 129.4, 128.5, 120.4, 118.7, 109.1, 56.1, 25.9, 18.4, -4.1; IR (thin film) 2956, 2930, 2858, 1534, 1265 cm^{-1} ; HRMS (ESI) m/z observed 360.16258 [$C_{19}H_{25}NO_4Si$ (M+H) $^+$ requires 360.16256].



4'-((*tert*-Butyldimethylsilyl)oxy)-4-methyl-[1,1'-biphenyl]-2-amine. (2.30a).
(WLM4_136). A suspension of **2.29a** (347 mg, 1.01 mmol) and palladium 10% wt on activated carbon (54 mg) in EtOAc (5 mL) was allowed to stir overnight at room temperature under a hydrogen atmosphere. After complete consumption of starting material, as judged by TLC, the suspension was diluted with EtOAc (25 mL) and filtered through a pad of Celite® that was subsequently washed with EtOAc (3 x 25 mL). The resulting filtrate was concentrated *in vacuo* to give 240 mg (76%) of **2.30a** as a brown oil that required no further purification: ¹H-NMR (400 MHz, CDCl₃) δ 7.31 (d, *J* = 8.8 Hz, 2 H) 7.02 (d, *J* = 8.0 Hz, 1 H) 6.91 (d, *J* = 8.8 Hz, 2 H) 6.65 (dd, *J* = 8.0, 0.8 Hz, 1 H) 6.61 (s, 1 H) 3.65 (br, 2 H) 2.31 (3H, s) 1.03 (s, 9 H) 0.25 (s, 6 H); ¹³C-NMR (100 MHz, CDCl₃) δ 154.8, 143.5, 138.2, 132.5, 130.5, 130.3, 125.0, 120.4, 119.7, 116.4, 25.9, 21.4, 18.4, -4.1; IR (thin film) 3465, 3373, 2956, 2929, 2858 cm⁻¹; HRMS (ESI) *m/z* observed 314.19458 [C₁₉H₂₇NOSi (M+Na)⁺ requires 314.19347].

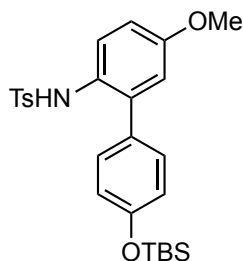


4'-((*tert*-Butyldimethylsilyl)oxy)-4-methoxy-[1,1'-biphenyl]-2-amine. (2.30b). (WLM3_65). A suspension of **2.29b** (355 mg, 0.988 mmol) and palladium 10% wt on activated carbon (100 mg) in EtOAc (3 mL) was allowed to stir overnight at room temperature under a hydrogen atmosphere. After complete consumption of starting material, as judged by TLC, the suspension was diluted with EtOAc (25 mL) and filtered through a pad of Celite® that was subsequently washed with EtOAc (3 x 25 mL). The resulting filtrate was concentrated *in vacuo* to give 321 mg (99%) of **2.30b** as a yellow oil that required no further purification: ¹H-NMR (400 MHz, CDCl₃) δ 7.32 (d, *J* = 8.4 Hz, 2 H) 7.06 (d, *J* = 8.0 Hz, 1 H) 6.94 (d, *J* = 8.4 Hz, 2 H) 6.42 (dd, *J* = 10.4 Hz, 1 H) 6.34 (d, *J* = 2.4 Hz, 1 H) 3.81 (s, 3 H) 1.06 (s, 9 H) 0.29 (s, 6 H); ¹³C-NMR (100 MHz, CDCl₃) δ 160.1, 154.9, 145.0, 132.4, 131.5, 130.5, 120.9, 120.6, 104.4, 101.3, 55.4, 26.0, 18.5, -4.1; IR (thin film) 34712, 3377, 2956, 2858 cm⁻¹; HRMS (ESI) *m/z* observed 330.18820 [C₁₉H₂₇NO₂Si (M+H)⁺ requires 330.18838].



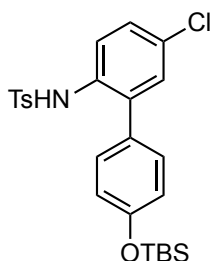
N-(4'-((*tert*-butyldimethylsilyl)oxy)-5-methyl-[1,1'-biphenyl]-2-yl)-4-methylbenzenesulfonamide. (2.31a). (WLM4_152). To a solution of **2.27a** (100 mg, 0.32 mmol) in pyridine (3 mL) at 0 °C was added p-toluenesulfonyl chloride (122 mg, 0.638 mmol). The reaction was allowed stir overnight until all starting material was consumed, as judged by TLC. The resulting brown solution was diluted with EtOAc (20 mL), washed with H₂O (10 mL), brine (10 mL), dried with Na₂SO₄, and concentrated *in vacuo* to give a brown oil, which was subsequently azeotroped with cyclohexane (3 x 10

mL). Purification by flash chromatography eluting with Hexanes : EtOAc (SiO₂ 10:1) gave 110 mg (74%) of **2.31a** as a brown oil: ¹H-NMR (400 MHz, CDCl₃) δ 7.56 (d, *J* = 8.4 Hz, 1 H) 7.44 (d, *J* = 8.4 Hz, 2 H) 7.17 (d, *J* = 8.0 Hz, 2 H) 7.11 (dd, *J* = 8.4, 2.0 Hz, 1 H) 6.88 (d, *J* = 2.0 Hz, 1 H) 6.77 (d, *J* = 8.4 Hz, 2 H) 6.67 (d, *J* = 8.4 Hz, 2 H) 6.53 (s, 1 H) 2.39 (s, 3 H) 2.29 (s, 3 H) 1.03 (s, 9 H) 0.26 (s, 6 H); ¹³C-NMR (100 MHz, CDCl₃) δ 155.6, 143.8, 136.4, 134.8, 134.1, 131.3, 131.1, 130.3, 130.1, 129.6, 129.1, 127.3, 122.0, 120.6, 25.8, 21.7, 20.9, 18.4, -4.2; IR (thin film) 3346, 2955, 2929, 2858 cm⁻¹; HRMS (ESI) *m/z* observed 490.18409 [C₂₆H₃₃NO₃SSi (M+Na)⁺ 490.18426].

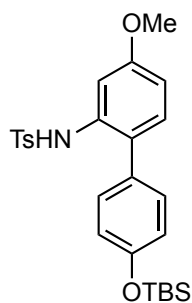


***N*-(4'-((*tert*-butyldimethylsilyl)oxy)-5-methoxy-[1,1'-biphenyl]-2-yl)-4-methylbenzenesulfonamide. (2.31b). (WLM3_53).** To a solution of **2.27b** (165 mg, 0.501 mmol) in pyridine (2 mL) at 0 °C was added *p*-toluenesulfonyl chloride (191 mg, 1.001 mmol). The reaction was allowed stir overnight until all starting material was consumed, as judged by TLC. The resulting brown solution was diluted with EtOAc (20 mL), washed with H₂O (10 mL), brine (10 mL), dried with Na₂SO₄, and concentrated *in vacuo* to give a brown oil, which was subsequently azeotroped with cyclohexane (3 x 15 mL). Purification by flash chromatography eluting with Hexanes: EtOAc (10:1) to afford 207 (86%) of **2.31b** as a white solid: M.p. 91-93 °C; ¹H-NMR (400 MHz, CDCl₃) δ 7.62 (d, *J* = 8.8 Hz, 1 H) 7.34 (d, *J* = 8.4 Hz, 2 H) 7.14 (d, *J* = 8.0 Hz, 2 H) 6.86 (dd, *J* = 12.0 Hz, 1 H) 6.73 (d, *J* = 8.0 Hz, 2 H) 6.61-6.59 (comp, 3 H) 6.45 (s, 1 H) 3.76 (s, 3 H) 2.39 (s, 3 H) 1.02 (s, 9 H) 0.25 (s, 6 H); ¹³C-NMR (100 MHz, CDCl₃) δ 157.3, 155.8, 143.8,

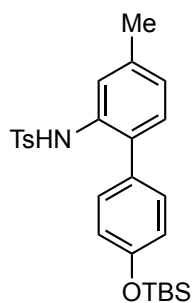
136.7, 136.3, 130.4, 130.0, 129.7, 127.4, 126.8, 125.2, 120.6, 115.8, 113.8, 55.7, 25.9, 21.8, 18.5, -4.1; IR (thin film) 3346, 2955, 2930, 2858 cm^{-1} ; HRMS (ESI) m/z observed 484.19715 [$\text{C}_{26}\text{H}_{33}\text{NO}_4\text{SSi}$ ($\text{M}+\text{H}$) $^+$ requires 484.19723].



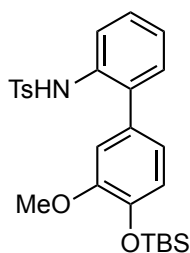
***N*-(4'-((*tert*-butyldimethylsilyl)oxy)-5-chloro-[1,1'-biphenyl]-2-yl)-4-methylbenzenesulfonamide. (2.31c). (WLM5_4).** To a solution of **2.27c** (352 mg, 1.05 mmol) in pyridine (5 mL) at 0 °C was added *p*-toluenesulfonyl chloride (402 mg, 2.11 mmol). The reaction was allowed stir overnight until all starting material was consumed, as judged by TLC. The resulting brown solution was diluted with EtOAc (50 mL), washed with H_2O (25 mL), brine (25 mL), dried with Na_2SO_4 , and concentrated *in vacuo* to give a brown oil, which was subsequently azeotroped with cyclohexane (3 x 15 mL). Purification by flash chromatography eluting with Hexanes : EtOAc (10:1) afforded 411 mg (84%) of **2.31c** as a white solid: M.p. 101-102°C; ^1H -NMR (400 MHz, CDCl_3) δ 7.64 (d, J = 8.8 Hz, 1 H) 7.45 (d, J = 8.4 Hz, 2 H) 7.26 (dd, J = 8.6 Hz, 2.6 Hz, 1 H) 7.20 (d, J = 8.0 Hz, 2 H) 7.07 (d, J = 2.8 Hz, 1 H) 6.79 (d, J = 8.8 Hz, 2 H) 6.68 (d, J = 8.8 Hz, 2 H) 6.57 (s, 1 H) 2.41 (s, 3 H) 1.02 (s, 9 H) 0.25 (s, 6 H); ^{13}C -NMR (100 MHz, CDCl_3) δ 156.2, 144.2, 136.1, 135.5, 132.7, 130.4, 130.3, 130.0, 129.8, 128.8, 128.5, 127.3, 122.8, 120.9, 25.8, 21.7, 18.4, -4.2; IR (thin film) 3344, 2955, 2929, 2857 cm^{-1} ; HRMS (ESI) m/z observed 510.12811 [$\text{C}_{25}\text{H}_{30}\text{ClNO}_3\text{SSi}$ ($\text{M}+\text{Na}$) $^+$ requires 510.12964].



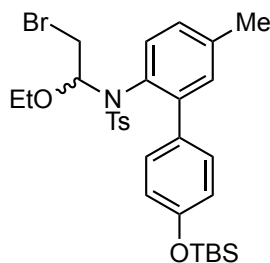
***N*-(4'-((*tert*-butyldimethylsilyl)oxy)-4-methoxy-[1,1'-biphenyl]-2-yl)-4-methylbenzenesulfonamide. (2.31d). (WLM3_69).** To a solution of **2.30a** (145 mg, 0.44 mmol) in pyridine (2 mL) at 0 °C was added *p*-toluenesulfonyl chloride (168 mg, 0.88 mmol). The reaction was allowed stir overnight until all starting material was consumed, as judged by TLC. The resulting brown solution was diluted with EtOAc (20 mL), washed with H₂O (10 mL), brine (10 mL), dried with Na₂SO₄, and concentrated *in vacuo* to give a brown oil, which was subsequently azeotroped with cyclohexane (3 x 15 mL). Purification by flash chromatography eluting with Hexanes: EtOAc (10:1) to give 194 mg (91%) of **2.31d** as a white solid: M.p. 90-92 °C; ¹H-NMR (400 MHz, CDCl₃) δ 7.51 (d, *J* = 8.4 Hz, 2 H) 7.28 (d, *J* = 2.4 Hz, 1 H) 7.18 (d, *J* = 7.6 Hz, 2 H) 6.97 (d, *J* = 8.4 Hz, 1 H) 6.80 (d, *J* = 8.4 Hz, 2 H) 6.71 (d, *J* = 8.4 Hz, 2 H) 6.67 (s, 1 H) 6.64 (dd, *J* = 10.4 Hz, 1 H) 3.79 (s, 3 H) 2.37 (s, 3 H) 1.03 (s, 9 H) 0.26 (s, 6 H); ¹³C-NMR (100 MHz, CDCl₃) δ 159.7, 155.7, 144.1, 136.4, 135.0, 131.4, 130.6, 130.1, 129.8, 127.4, 126.2, 120.8, 111.0, 106.7, 55.6, 25.9, 21.779, 18.5, -4.1; IR (thin film) 3346, 2930, 2858 cm⁻¹; HRMS (ESI) *m/z* observed 484.19724 [C₂₆H₃₃NO₄SSi (M+H)⁺ requires 484.19723].



***N*-(4'-((*tert*-butyldimethylsilyl)oxy)-4-methyl-[1,1'-biphenyl]-2-yl)-4-methylbenzenesulfonamide. (2.31e). (WLM4_137).** To a solution of **2.30b** (240 mg, 0.766 mmol) in pyridine (4 mL) at 0 °C was added p-toluenesulfonyl chloride (292 mg, 1.531 mmol). The reaction was allowed stir overnight until all starting material was consumed, as judged by TLC. The resulting brown solution was diluted with EtOAc (20 mL), washed with H₂O (10 mL), brine (10 mL), dried with Na₂SO₄, and concentrated *in vacuo* to give a brown oil, which was subsequently azeotroped with cyclohexane (3 x 10 mL). Purification by flash chromatography eluting with Hexanes : EtOAc (10:1) gave 342 mg (96%) of **2.31e** as a brown oil: ¹H-NMR (400 MHz, CDCl₃) δ 7.54 (s, 1 H) 7.47 (d, *J* = 8.4 Hz, 2 H) 7.17 (d, *J* = 8.4 Hz, 2 H) 6.97-6.91 (comp, 2H) 6.79 (d, *J* = 8.4 Hz, 2 H) 6.69 (d, *J* = 8.4 Hz, 2 H) 6.62 (s, 1 H) 2.38 (s, 3 H) 2.37 (s, 3 H) 1.03 (s, 9 H) 0.26 (s, 6 H); ¹³C-NMR (100 MHz, CDCl₃) δ 155.5, 143.7, 138.3, 136.3, 133.6, 131.1, 130.2, 130.1, 130.1, 129.5, 127.2, 125.8, 122.1, 120.5, 25.7, 21.6, 21.4, 18.3, -4.3; IR (thin film) 3347, 2955, 2929, 2858 cm⁻¹; HRMS (ESI) *m/z* observed 490.18537 [C₂₆H₃₃NO₃SSi (M+Na)⁺ requires 490.18426].

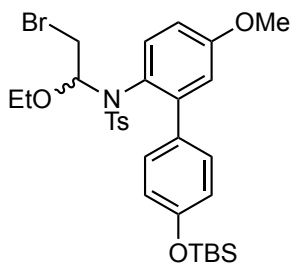


***N*-(4'-(((*tert*-butyldimethylsilyl)oxy)-3'-methoxy-[1,1'-biphenyl]-2-yl)-4-methylbenzenesulfonamide. (2.31f). (WLM3_54).** To a solution of **2.27d** (272 mg, 0.825 mmol) in pyridine (2 mL) at 0 °C was added p-toluenesulfonyl chloride (315 mg, 1.65 mmol). The reaction was allowed stir overnight until all starting material was consumed, as judged by TLC. The resulting brown solution was diluted with EtOAc (30 mL), washed with H₂O (15 mL), brine (15 mL), dried with Na₂SO₄, and concentrated *in vacuo* to give a brown oil, which was subsequently azeotroped with cyclohexane (3 x 15 mL). Purification by flash chromatography eluting with Hexanes : EtOAc (10:1) to afford 355 mg (89%) of **2.31f** as a white solid: M.p. 78-80 °C; ¹H-NMR (400 MHz, CDCl₃) δ 7.68 (d, *J* = 8.4 Hz, 1 H) 7.46 (d, *J* = 8.4 Hz, 2 H) 7.31-7.26 (m, 1 H) 7.16 (d, *J* = 8.0 Hz, 2 H) 7.11 (d, *J* = 4.0 Hz, 2 H) 6.82 (d, *J* = 7.6 Hz, 1 H) 6.78 (s, 1 H) 6.44 (d, *J* = 2.0 Hz, 1 H) 6.33 (dd, *J* = 10.0 Hz, 1 H) 3.72 (s, 3 H) 2.37 (s, 3 H) 1.04 (s, 9 H) 0.22 (s, 6 H); ¹³C-NMR (100 MHz, CDCl₃) δ 151.5, 145.2, 143.9, 136.6, 134.2, 134.1, 130.8, 130.6, 129.8, 128.6, 127.4, 125.1, 121.5, 121.5, 121.3, 113.0, 55.7, 26.0, 21.8, 18.7, -4.2; IR (thin film) 3340, 2955, 2929, 2857 cm⁻¹; HRMS (ESI) *m/z* observed 484.19695 [C₂₆H₃₃NO₄SSi (M+H)⁺ requires 484.19723].

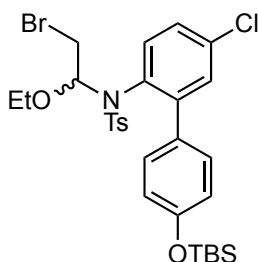


***N*-(2-bromo-1-ethoxyethyl)-*N*-(4'-(((*tert*-butyldimethylsilyl)oxy)-5-methyl-[1,1'-biphenyl]-2-yl)-4-methylbenzenesulfonamide. (2.32a). (WLM5_6).** To a solution of Br₂ (85 mg, 0.03 mL, 0.531 mmol) in CH₂Cl₂ (1.5 mL) at 0 °C under argon was added ethyl vinyl ether (48 mg, 0.6 mL, 0.663 mmol) drop-wise until the solution turned

colorless. The mixture was stirred for 30 min and diisopropylethylamine (136 mg, 0.18 mL, 1.06 mmol) was added. After 30 min, a solution of **2.31a** (124 mg, 0.265 mmol) in CH₂Cl₂ (1.5 mL) was added drop-wise, and the mixture was allowed to slowly warm to room temperature overnight under an argon atmosphere. After complete consumption of starting material, as judged by TLC, the reaction mixture was poured onto saturated aqueous NH₄Cl (20 mL) and extracted with EtOAc (3 x 20 mL). The combined extracts were washed with H₂O (30 mL), brine (30 mL), dried with Na₂SO₄, and concentrated under reduced pressure. The resulting brown oil was purified by flash chromatography eluting with Hexanes: EtOAc (20:1) to give 159 mg (97%) of **2.32a** as a white solid: M.p. 125-128°C; ¹H-NMR (400 MHz, CDCl₃, as a mixture of rotamers) δ 7.82-7.78 (comp, 2 H) 7.53-7.48 (comp, 2 H) 7.37-7.73 (comp, 2 H) 7.23-7.19 (m, 1 H) 7.09-6.98 (m, 1 H) 6.93-6.70 (comp, 3 H) 5.09-4.94 (m, 1 H) 3.23-3.16 (m, 1 H) 3.08-3.04 (m, 1 H) 2.86-2.81 (m, 1 H) 2.71-2.64 (m, 1 H) 2.48 (s, 3 H) 2.38-2.35 (comp, 3 H) 1.03-1.01 (comp, 9 H) 0.94-0.86 (comp, 3 H) 0.24 (s, 6 H); ¹³C-NMR (100 MHz, CDCl₃, as a mixture of rotamers) δ 155.6, 155.3, 144.3, 144.2, 144.0, 143.7, 139.5, 139.2, 138.6, 137.9, 133.6, 133.1, 133.0, 132.8, 132.4, 131.8, 131.3, 131.1, 130.0, 129.8, 129.7, 129.0, 128.6, 128.3, 128.2, 128.1, 120.1, 119.8, 91.6, 89.9, 67.1, 65.3, 33.8, 33.7, 25.9, 21.8, 21.3, 21.2, 18.5, 18.4, 14.7, 14.4, -4.2; IR (thin film) 2956, 2929, 2896, 2858 cm⁻¹; HRMS (ESI) *m/z* observed 640.15470 [C₃₀H₄₀BrNO₄SSi (M+Na)⁺ 640.15230].

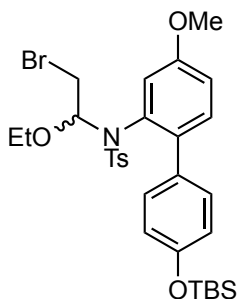


***N*-(2-bromo-1-ethoxyethyl)-*N*-(4'-((*tert*-butyldimethylsilyl)oxy)-5-methoxy-[1,1'-biphenyl]-2-yl)-4-methylbenzenesulfonamide. (2.32b). (WLM3_90).** To a solution of Br₂ (240 mg, 0.077 mL, 1.49 mmol) in CH₂Cl₂ (4 mL) at 0°C under argon was added ethyl vinyl ether (135 mg, 0.18 mL, 1.87 mmol) drop-wise until the solution turned colorless. The mixture was stirred for 30 min and diisopropylethylamine (387 mg, 0.52 mL, 2.99 mmol) was added. After 30 min, a solution of **2.31b** (361 mg, 0.75 mmol) in CH₂Cl₂ (4 mL) was added drop-wise, and the mixture was allowed to slowly warm to room temperature overnight under an argon atmosphere. After complete consumption of starting material, as judged by TLC, the reaction mixture was poured onto saturated aqueous NH₄Cl (20 mL) and extracted with EtOAc (3 x 10 mL). The combined extracts were washed with H₂O (20 mL), brine (20 mL), dried with Na₂SO₄, and concentrated under reduced pressure. The resulting brown oil was purified by flash chromatography eluting with Hexanes: EtOAc (10:1) to afford 464 mg (98%) of **2.32b** as a clear oil that crystallized upon standing: M.p. 126-127°C; ¹H-NMR (400 MHz, CDCl₃, as a mixture of rotamers) δ 7.81-7.77 (comp, 2 H) 7.57-7.52 (comp, 2 H) 7.37-7.34 (comp, 2 H) 6.94-6.88 (comp, 3 H) 6.81-6.69 (comp, 2 H) 5.11-4.97 (m, 1 H) 3.82-3.79 (comp, 3 H) 3.27-3.11 (m, 1 H) 3.11-3.04 (m, 1 H) 2.86-2.78 (m, 1 H) 2.72-2.61 (m, 1 H) 2.47 (s, 3 H) 1.03-1.03 (comp, 9 H) 0.95-0.87 (comp, 3 H) 0.25 (s, 6 H); ¹³C-NMR (100 MHz, CDCl₃, as a mixture of rotamers) δ 159.9, 159.5, 155.8, 155.5, 146.1, 145.5, 144.3, 144.1, 138.6, 137.9, 133.2, 132.8, 131.4, 131.2, 130.5, 130.0, 129.8, 128.6, 128.3, 127.5, 125.2, 120.2, 119.9, 117.7, 117.0, 113.2, 113.1, 91.5, 89.9, 67.2, 65.3, 55.7, 33.9, 33.7, 26.0, 21.9, 18.5, 18.5, 14.8, 14.5, -4.1; IR (thin film) 2956, 2930, 2897, 2858 cm⁻¹; HRMS (ESI) *m/z* observed 656.14652 [C₃₀H₄₀BrNO₅SSi (M+Na)⁺ requires 656.14720].



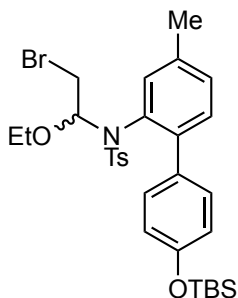
***N*-(2-bromo-1-ethoxyethyl)-*N*-(4'-((*tert*-butyldimethylsilyl)oxy)-5-chloro-[1,1'-biphenyl]-2-yl)-4-methylbenzenesulfonamide. (2.32c). (WLM5_8).** To a solution of Br₂ (211 mg, 0.07 mL, 1.322 mmol) in CH₂Cl₂ (3.5 mL) at 0°C under argon was added ethyl vinyl ether (119 mg, 0.16 mL, 1.65 mmol) drop-wise until the solution turned colorless. The mixture was stirred for 30 min and diisopropylethylamine (342 mg, 0.46 mL, 2.644 mmol) was added. After 30 min, a solution of **2.31c** (322 mg, 0.661 mmol) in CH₂Cl₂ (3.5 mL) was added drop-wise, and the mixture was allowed to slowly warm to room temperature overnight under an argon atmosphere. After complete consumption of starting material, as judged by TLC, the reaction mixture was poured onto saturated aqueous NH₄Cl (30 mL) and extracted with EtOAc (3 x 30 mL). The combined extracts were washed with H₂O (45 mL), brine (45 mL), dried with Na₂SO₄, and concentrated under reduced pressure. The resulting brown oil was purified by flash chromatography eluting with Hexanes : EtOAc (20:1) to afford 413 mg (98%) of **2.32c** as a white solid: M.p. 144-145°C; ¹H-NMR (400 MHz, CDCl₃, as a mixture of rotamers) δ 7.80-7.76 (comp, 2 H) 7.52-7.47 (comp, 2 H) 7.42-7.35 (comp, 3 H) 7.25-7.15 (m, 1 H) 6.94-6.77 (comp, 3 H) 5.10-4.93 (m, 1 H) 3.26-3.14 (m, 1 H) 3.08-3.03 (m, 1 H) 2.83-2.78 (m, 1 H) 2.68-2.62 (m, 1H) 2.48 (s, 3 H) 1.01 (s, 9 H) 0.95-0.85 (comp, 3 H) 0.23 (s, 6 H); ¹³C-NMR (100 MHz, CDCl₃, as a mixture of rotamers) δ 156.1, 155.8, 146.5, 145.9, 144.6, 144.4, 138.2, 137.5, 135.2, 134.9, 133.6, 133.3, 132.9, 132.1, 131.8, 131.4, 131.3, 131.1, 130.6, 130.0, 129.9, 128.6, 128.3, 127.4, 120.3, 120.0, 91.5, 89.9, 67.3, 65.5, 33.5, 33.3,

21.8, 18.5, 18.4, 14.7, 14.4, -4.2; IR (thin film) 2956, 2929, 2858 cm^{-1} ; HRMS (ESI) m/z observed 660.09870 [$\text{C}_{29}\text{H}_{37}\text{BrClINO}_4\text{SSi}$ ($\text{M}+\text{Na}$) $^+$ requires 660.09770].



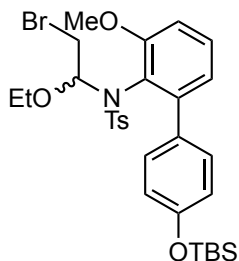
***N*-(2-bromo-1-ethoxyethyl)-*N*-(4'-((*tert*-butyldimethylsilyl)oxy)-4-methoxy-[1,1'-biphenyl]-2-yl)-4-methylbenzenesulfonamide. (2.32d). (WLM3_25).** To a solution of Br_2 (330 mg, 0.11 mL, 2.067 mmol) in CH_2Cl_2 (5 mL) at 0 °C under argon was added ethyl vinyl ether (186 mg, 0.25 mL, 2.585 mmol) drop-wise until the solution turned colorless. The mixture was stirred for 30 min and diisopropylethylamine (535 mg, 0.72 mL, 4.136 mmol) was added. After 30 min, a solution of **2.31d** (500 mg, 1.034 mmol) in CH_2Cl_2 (5 mL) was added drop-wise, and the mixture was allowed to slowly warm to room temperature overnight under an argon atmosphere. After complete consumption of starting material, as judged by TLC, the reaction mixture was poured onto saturated aqueous NH_4Cl (50 mL) and extracted with EtOAc (3 x 25 mL). The combined extracts were washed with H_2O (50 mL), brine (50 mL), dried with Na_2SO_4 , and concentrated under reduced pressure. The resulting brown oil was purified by flash chromatography eluting with Hexanes: EtOAc (10:1) to afford 647 mg (99%) of **2.32d** as a clear oil that crystallized upon standing: M.p. 99-101 °C; ^1H -NMR (400 MHz, CDCl_3 , as a mixture of rotamers) δ 7.86-7.81 (comp, 2 H) 7.50-7.46 (comp, 2 H) 7.38-7.34 (comp, 2 H) 7.32-7.26 (m, 1 H) 7.00-6.88 (comp, 3 H) 6.56-6.42 (m, 1 H) 5.11-4.92 (m, 1 H) 3.72-3.68 (comp, 3 H) 3.29-3.23 (m, 1 H) 3.14-3.06 (m, 1 H) 2.92-2.84 (m, 1 H)

2.73-2.65 (m, 1 H) 2.47 (s, 3 H) 1.02 (s, 9 H) 0.95-0.87 (comp, 3 H) 0.24 (s, 6 H); ^{13}C -NMR (100 MHz, CDCl_3 , as a mixture of rotamers) δ 158.5, 155.4, 155.2, 144.5, 144.2, 138.6, 137.8, 136.8, 136.5, 136.2, 133.5, 133.4, 132.8, 132.7, 132.6, 131.5, 131.3, 129.9, 129.8, 128.7, 128.5, 127.3, 122.6, 120.1, 119.9, 117.6, 115.3, 115.1, 114.6, 92.1, 90.0, 67.2, 65.6, 55.5, 33.7, 25.927, 21.8, 21.2, 18.5, 18.4, 14.8, 14.5, -4.2; IR (thin film) 2930.09, 2858.21 cm^{-1} ; HRMS (ESI) m/z observed 656.14749 [$\text{C}_{30}\text{H}_{40}\text{BrNNaO}_5\text{SSi}$ ($\text{M}+\text{Na}$) $^+$ requires 656.14720].



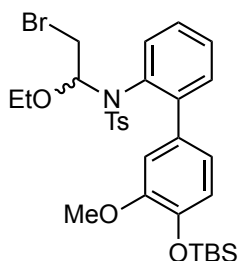
***N*-(2-bromo-1-ethoxyethyl)-*N*-(4'-((*tert*-butyldimethylsilyl)oxy)-4-methyl-[1,1'-biphenyl]-2-yl)-4-methylbenzenesulfonamide. (2.32e). (WLM4_138).** To a solution of Br_2 (205 mg, 0.066 mL, 1.28 mmol) in CH_2Cl_2 (3 mL) at 0°C under argon was added ethyl vinyl ether (115 mg, 0.15 mL, 1.6 mmol) drop-wise until the solution turned colorless. The mixture was stirred for 30 min and diisopropylethylamine (331 mg, 0.45 mL, 2.56 mmol) was added. After 30 min, a solution of **2.31e** (299 mg, 0.64 mmol) in CH_2Cl_2 (3 mL) was added drop-wise, and the mixture was allowed to slowly warm to room temperature overnight under an argon atmosphere. After complete consumption of starting material, as judged by TLC, the reaction mixture was poured onto saturated aqueous NH_4Cl (20 mL) and extracted with EtOAc (3 x 20 mL). The combined extracts were washed with H_2O (30 mL), brine (30 mL), dried with Na_2SO_4 , and concentrated under reduced pressure. The resulting brown oil was purified by flash chromatography

eluting with Hexanes: EtOAc (20:1) to afford 391 mg (99%) of **2.32e** as a white solid: M.p. 144-146°C; ¹H-NMR (400 MHz, CDCl₃, as a mixture of rotamers) δ 7.82-7.78 (comp, 2 H) 7.52-7.44 (comp, 2 H) 7.39-7.35 (comp, 2 H) 7.31-7.16 (comp, 2 H) 6.94-6.6.86 (comp, 2 H) 6.81-6.63 (m, 1 H) 5.08-5.05 (m, 1 H) 3.27-3.18 (m, 1 H) 3.10-3.02 (m, 1 H) 2.88-2.81 (m, 1 H) 2.74-2.64 (m, 1 H) 2.49-2.48 (comp, 3 H) 2.32-2.26 (comp, 3 H) 1.03-1.01 (comp, 9 H) 0.96-0.86 (comp, 3 H) 0.24 (s, 6 H); ¹³C-NMR (100 MHz, CDCl₃, as a mixture of rotamers) δ 155.5, 155.2, 144.3, 144.1, 141.6, 141.0, 138.6, 137.8, 137.2, 134.8, 133.0, 132.8, 132.7, 132.4, 132.0, 131.3, 131.1, 130.2, 129.9, 129.8, 129.7, 129.6, 128.6, 128.4, 120.1, 119.8, 91.5, 90.0, 67.1, 65.4, 33.8, 33.7, 21.8, 21.0, 21.0, 18.4, 18.4, 14.6, 14.4, -4.2; IR (thin film) 2928, 2896, 2858 cm⁻¹; HRMS (ESI) *m/z* observed 640.15380 [C₃₀H₄₀BrNO₄SSi (M+Na)⁺ requires 640.15230].



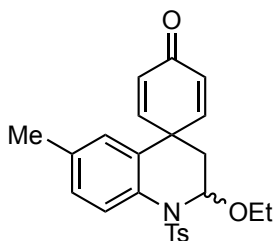
***N*-(2-bromo-1-ethoxyethyl)-*N*-(4'-((*tert*-butyldimethylsilyl)oxy)-3-methoxy-[1,1'-biphenyl]-2-yl)-4-methylbenzenesulfonamide. (2.32f). (WLM3_86).** To a solution of Br₂ (196 mg, 0.063 mL, 1.23 mmol) in CH₂Cl₂ (3mL) at 0 °C under argon was added ethyl vinyl ether (111 mg, 0.15 mL, 1.54 mmol) drop-wise until the solution turned colorless. The mixture was stirred for 30 min and diisopropylethylamine (320 mg, 0.43 mL, 2.46 mmol) was added. After 30 min, a solution of **2.31f** (298 mg, 0.616 mmol) in CH₂Cl₂ (3 mL) was added drop-wise, and the mixture was allowed to slowly warm to room temperature overnight under an argon atmosphere. After complete consumption of starting material, as judged by TLC, the reaction mixture was poured onto saturated

aqueous NH_4Cl (20 mL) and extracted with EtOAc (3 x 20 mL). The combined extracts were washed with H_2O (30 mL), brine (30 mL), dried with Na_2SO_4 , and concentrated under reduced pressure. The resulting brown oil was purified by flash chromatography eluting with Hexanes: EtOAc (20:1) to afford 335 mg (86%) of **2.32f** as a brown oil: ^1H -NMR (400 MHz, CDCl_3 , as a mixture of rotamers) δ 7.65 (d, J = 8.0 Hz, 2 H), 7.44 (d, J = 8.4 Hz, 2 H) 7.25 (d, J = 8.0 Hz, 2 H) 7.13-7.11 (m, 1 H) 7.05-7.03 (m, 1 H) 6.94-6.90 (m, 1 H) 6.91 (d, J = 8.4 Hz, 2 H) 5.65-5.49 (m, 1 H) 4.09-3.08 (comp, 7 H) 2.41 (s, 3 H) 1.30-1.16 (comp, 3 H) 1.01 (s, 9 H) 0.24 (s, 6 H); ^{13}C -NMR (100 MHz, CDCl_3 , as a mixture of rotamers) δ 159.2, 158.5, 157.9, 156.0, 144.1, 144.0, 143.8, 143.6, 143.5, 138.2, 137.8, 136.3, 135.2, 133.7, 133.1, 129.4, 129.3, 128.5, 128.1, 124.2, 121.5, 120.7, 120.6, 119.4, 118.8, 115.6, 111.1, 110.2, 89.2, 88.5, 88.4, 65.7, 65.2, 55.6, 55.2, 33.0, 32.8, 32.7, 30.0, 26.0, 21.8, 18.5, 15.5, 14.9, 14.8, -4.1; IR (thin film) 2956, 2928, 2857 cm^{-1} ; HRMS (ESI) m/z observed 656.14709 [$\text{C}_{30}\text{H}_{40}\text{BrNO}_5\text{SSi}$ ($\text{M}+\text{Na}$) $^+$ requires 656.14720].



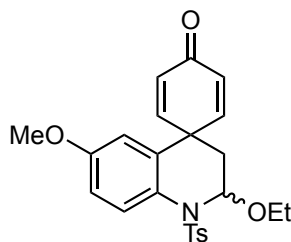
***N*-(2-bromo-1-ethoxyethyl)-*N*-(4'-((*tert*-butyldimethylsilyl)oxy)-3'-methoxy-[1,1'-biphenyl]-2-yl)-4-methylbenzenesulfonamide. (2.32g). (WLM3_83).** To a solution of Br_2 (218 mg, 0.046 mL, 0.90 mmol) in CH_2Cl_2 (2 mL) at 0°C under argon was added ethyl vinyl ether (81 mg, 0.11 mL, 1.13 mmol) drop-wise until the solution turned colorless. The mixture was stirred for 30 min and diisopropylethylamine (234 mg, 0.31 mL, 1.80 mmol) was added. After 30 min, a solution of **2.31g** (218 mg, 0.45 mmol) in

CH₂Cl₂ (2 mL) was added drop-wise, and the mixture was allowed to slowly warm to room temperature overnight under an argon atmosphere. After complete consumption of starting material, as judged by TLC, the reaction mixture was poured onto saturated aqueous NH₄Cl (10 mL) and extracted with EtOAc (3 x 10 mL). The combined extracts were washed with H₂O (20 mL), brine (20 mL), dried with Na₂SO₄, and concentrated *in vacuo* to give a brown oil. Purification by flash chromatography eluting with Hexanes : EtOAc (20:1) to afford 250 mg (87%) **2.32g** as a clear oil that crystallized upon standing: M.p. 123-124 °C; ¹H-NMR (400 MHz, CDCl₃, as a mixture of rotamers) δ 7.84-7.80 (comp, 2 H) 7.62-7.52 (m, 1 H) 7.49-7.36 (comp, 4 H) 7.28-7.18 (m, 1 H) 6.94-6.82 (comp, 3 H) 5.12-4.89 (m, 1 H) 3.91 (s, 3 H) 3.25-3.14 (m, 1 H) 3.14-3.06 (m, 1 H) 2.88-2.84 (m, 1 H) 2.67-2.56 (m, 1 H) 2.49 (s, 3 H) 1.03 (s, 9 H) 0.90 (t, *J* = 7.2 Hz, 3 H) 0.21-0.19 (m, 6 H); ¹³C-NMR (100 MHz, CDCl₃, as a mixture of rotamers) δ 150.8, 150.6, 145.0, 144.8, 144.7, 144.5, 144.4, 144.2, 138.9, 138.1, 135.7, 133.5, 133.3, 133.0, 132.8, 132.4, 131.8, 130.0, 129.9, 129.6, 129.3, 129.1, 128.5, 128.3, 127.5, 122.7, 122.2, 121.1, 121.0, 114.4, 92.2, 90.0, 67.2, 65.7, 55.9, 33.9, 33.8, 30.4, 26.0, 21.9, 18.8, 18.8, 14.7, 14.6, -4.3, -4.4; IR (thin film) 2956, 2928, 2857 cm⁻¹; HRMS (ESI) *m/z* observed 656.14709 [C₃₀H₄₀BrNO₅SSi (M+Na)⁺ requires 656.14720].



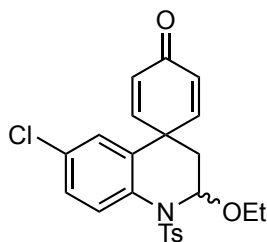
2'-Ethoxy-6'-methyl-1'-tosyl-2',3'-dihydro-1'H-spiro[cyclohexa[2,5]diene-1,4'-quinolin]-4-one. (2.33a). (WLM5_12). To a solution of **2.32a** (93 mg, 0.15 mmol) in anhydrous DMF (1.5 mL, stored over 4Å molecular sieves) at 50 °C was added flame-

dried CsF (114 mg, 0.75 mmol). The reaction mixture was immediately heated to 130 °C for 1 h under an argon atmosphere. After complete consumption of the starting material, as judged by TLC, the reaction mixture was diluted with EtOAc (15 mL), washed with H₂O (10 mL), brine (10 mL), dried with Na₂SO₄, and concentrated under reduced pressure. The resulting brown oil was purified by flash chromatography eluting with Hexanes : EtOAc (3:1) to provide 57 mg (89%) of **2.33a** as a white crystalline solid: M.p. 186-187°C; ¹H-NMR (400 MHz, CDCl₃) δ 7.79 (d, *J* = 8.4 Hz, 1 H) 7.42 (d, *J* = 8.0 Hz, 2 H) 7.26-7.23 (comp, 3 H) 7.10 (dd, *J* = 8.4 Hz, 1.6 Hz, 1 H) 6.63 (d, *J* = 1.6 Hz, 1 H) 6.12 (dd, *J* = 9.8 Hz, 1.8 Hz, 1 H) 6.07 (dd, *J* = 10.2 Hz, 1.8 Hz, 1 H) 5.69 (dd, *J* = 10.0, 2.8 Hz, 1 H) 5.61-5.63 (m, 1 H) 3.83-3.75 (m, 1 H) 3.63-3.55 (m, 1 H) 2.41 (s, 3 H) 2.23 (s, 3 H) 1.88 (dd, *J* = 14.4, 2.4 Hz, 1 H) 1.53 (dd, *J* = 14.4, 3.6 Hz, 1 H) 1.12 (t, *J* = 7.0 Hz, 3 H); ¹³C-NMR (100 MHz, CDCl₃) δ 185.9, 155.4, 154.4, 144.4, 136.2, 135.9, 130.4, 129.9, 129.6, 129.6, 128.1, 127.3, 127.1, 126.1, 124.9, 82.9, 63.7, 41.5, 34.8, 21.7, 21.0, 14.9; IR (thin film) 2972, 2927, 1668 cm⁻¹; HRMS (ESI) *m/z* observed 446.14047 [C₂₄H₂₅NO₄S (M+Na)⁺ required 446.13965].



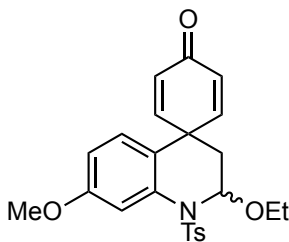
2'-Ethoxy-6'-methoxy-1'-tosyl-2',3'-dihydro-1'*H*-spiro[cyclohexa[2,5]diene-1,4'-quinolin]-4-one. (2.33b). (WLM3_81). To a solution of **2.32b** (209 mg, 0.33 mmol) in anhydrous DMF (3.5 mL, stored over 4Å molecular sieves) at 50 °C was added flame-dried CsF (250 mg, 1.65 mmol). The reaction mixture was immediately heated to 130 °C for 1 h under an argon atmosphere. After complete consumption of the starting material,

as judged by TLC, the reaction mixture was diluted with EtOAc (30 mL), washed with H₂O (15 mL), brine (15 mL), dried with Na₂SO₄, and concentrated under reduced pressure. The resulting brown oil was purified by flash chromatography eluting with Hexanes : EtOAc (3:1) to afford 143 mg (99%) of **2.32a** as a white crystalline solid: M.p. 125-126 °C; ¹H-NMR (400 MHz, CDCl₃) δ 7.81 (d, *J* = 8.8 Hz, 1 H) 7.37 (d, *J* = 8.0 Hz, 2 H) 7.23-7.19 (comp, 3 H) 6.83 (dd, *J* = 11.6 Hz, 1 H) 6.33 (d, *J* = 2.8 Hz, 1 H) 6.07 (dd, *J* = 11.6 Hz, 1 H) 6.02 (dd, *J* = 11.6 Hz, 1 H) 5.62-5.58 (comp, 2 H) 3.79-3.72 (m, 1 H) 3.68 (s, 3 H) 3.60-3.52 (m, 1 H) 2.38 (s, 3 H) 1.82 (dd, *J* = 16.8 Hz, 1 H) 1.48 (dd, *J* = 18.0 Hz, 1 H) 1.09 (t, *J* = 7.2 Hz, 3 H); ¹³C-NMR (100 MHz, CDCl₃) δ 185.8, 157.8, 155.4, 154.2, 144.5, 135.7, 130.0, 128.9, 128.2, 128.1, 127.4, 125.7, 124.9, 114.4, 114.0, 82.9, 63.6, 55.6, 41.7, 34.6, 21.8, 15.0; IR (thin film) 2974, 1668 cm⁻¹; HRMS (ESI) *m/z* observed 462.13445 [C₂₄H₂₅NO₅S (M+Na)⁺ required 462.13456].



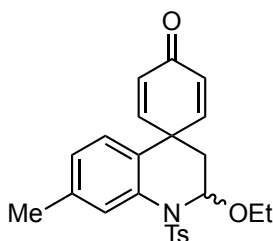
6'-Chloro-2'-ethoxy-1'-tosyl-2',3'-dihydro-1'H-spiro[cyclohexa[2,5]diene-1,4'-quinolin]-4-one. (2.33c). (WLM5_9). To a solution of **2.32c** (227 mg, 0.355 mmol) in anhydrous DMF (3.6 mL, stored over 4Å molecular sieves) at 50 °C was added flame-dried CsF (270 mg, 1.78 mmol). The reaction mixture was immediately heated to 130 °C for 1 h under an argon atmosphere. After complete consumption of the starting material, as judged by TLC, the reaction mixture was diluted with EtOAc (50 mL), washed with H₂O (25 mL), brine (25 mL), dried with Na₂SO₄, and concentrated under reduced pressure. The resulting brown oil was purified by flash chromatography eluting with

Hexanes : EtOAc (3:1) to afford 155 mg (98%) of **2.33c** as a white crystalline solid: M.p. 169-170 °C; ¹H-NMR (400 MHz, CDCl₃) δ 7.90 (d, *J* = 9.2 Hz, 1 H) 7.46 (d, *J* = 8.4 Hz, 2 H) 7.31-7.23 (comp, 4 H) 6.84 (d, *J* = 2.8 Hz, 1 H) 6.16 (dd, *J* = 10.0 Hz, 2.5 Hz, 1 H) 6.12 (dd, *J* = 10.0 Hz, 1.6 Hz, 1 H) 5.71 (dd, *J* = 10.0 Hz, 2.8 Hz, 1 H) 5.67-5.66 (m, 1 H) 3.83-3.75 (m, 1 H) 3.65-3.57 (m, 1 H) 2.44 (s, 3 H) 1.94 (dd, *J* = 14.8 Hz, 2.4 Hz, 1 H) 1.55 (dd, *J* = 14.8 Hz, 3.2 Hz, 1 H) 1.15 (t, *J* = 7.0 Hz, 3 H); ¹³C-NMR (100 MHz, CDCl₃) δ 185.3, 154.3, 153.2, 144.8, 135.5, 131.8, 131.6, 130.0, 129.1, 128.9, 128.6, 128.5, 128.4, 127.2, 125.4, 82.8, 63.8, 41.3, 34.7, 21.7, 14.8; IR (thin film) 2972, 2928, 2884, 1668 cm⁻¹; HRMS (ESI) *m/z* observed 466.08470 [C₂₃H₂₂ClNO₄S (M+Na)⁺ requires 466.08500].



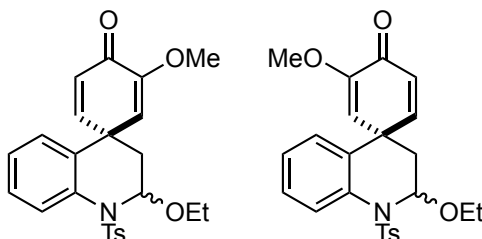
2'-Ethoxy-7'-methoxy-1'-tosyl-2',3'-dihydro-1'*H*-spiro[cyclohexa[2,5]diene-1,4'-quinolin]-4-one. (2.33d). (WLM3_27). To a solution of **2.32d** (150 mg, 0.24 mmol) in anhydrous DMF (2.5 mL, stored over 4 Å molecular sieves) at 50 °C was added flame-dried CsF (180 mg, 1.18 mmol). The reaction mixture was immediately heated to 130 °C for 1 h under an argon atmosphere. After complete consumption of the starting material, as judged by TLC, the reaction mixture was diluted with EtOAc (20 mL), washed with H₂O (10 mL), brine (10 mL), dried with Na₂SO₄, and concentrated under reduced pressure. The resulting brown oil was purified by flash chromatography eluting with Hexanes: EtOAc (3:1) to afford 99 mg (95%) of **2.33d** as a white crystalline solid: M.p. 158-161 °C; ¹H NMR (400 MHz, CDCl₃) δ 7.48-7.44 (comp, 3 H) 7.26-7.21 (comp, 3 H)

6.74 (d, $J = 8.8$ Hz, 1 H) 6.68 (dd, $J = 11.2$ Hz, 1 H) 6.09 (dd, $J = 12.0$ Hz, 1 H) 6.03 (dd, $J = 12$ Hz, 1 H) 5.69 (dd, $J = 12.8$ Hz, 1 H) 5.66 (t, $J = 2.4$ Hz, 1 H) 3.83 (s, 3 H) 3.84-3.76 (m, 1 H) 3.64-3.58 (m, 1 H) 2.40 (s, 3 H) 1.89 (dd, $J = 17.2$ Hz, 1 H) 1.51 (dd, $J = 17.6$ Hz, 1 H) 1.13 (t, $J = 6.8$ Hz, 3 H); ^{13}C -NMR (100 MHz, CDCl_3) δ 186.0, 159.5, 155.6, 154.7, 144.7, 135.9, 134.1, 130.2, 130.0, 128.0, 127.4, 124.8, 118.0, 113.3, 111.6, 83.1, 63.9, 55.7, 41.2, 34.9, 21.8, 15.0; IR (thin film) 2974, 2932, 1668 cm^{-1} ; HRMS (ESI) m/z observed 462.13455 [$\text{C}_{24}\text{H}_{25}\text{NO}_5\text{S}$ ($\text{M}+\text{Na}$) $^+$ required 462.13456].



2'-Ethoxy-7'-methyl-1'-tosyl-2',3'-dihydro-1'H-spiro[cyclohexa[2,5]diene-1,4'-quinolin]-4-one. (2.33e). (WLM4_139). To a solution of **2.32e** (186 mg, 0.3 mmol) in anhydrous DMF (3.0 mL, stored over 4Å molecular sieves) at 50 °C was added flame-dried CsF (228 mg, 1.5 mmol). The reaction mixture was immediately heated to 130 °C for 1 h under an argon atmosphere. After complete consumption of the starting material, as judged by TLC, the reaction mixture was diluted with EtOAc (40 mL), washed with H_2O (20 mL), brine (20 mL), dried with Na_2SO_4 , and concentrated under reduced pressure. The resulting brown oil was purified by flash chromatography eluting with Hexanes : EtOAc (4:1) to afford 124 mg (98%) of **2.33e** as a white crystalline solid: M.p. 163-164°C; ^1H -NMR (500 MHz, CDCl_3) δ 7.71 (s, 1 H) 7.42 (dd, $J = 6.5$ Hz, 1.5 Hz, 2 H) 7.24 (d, $J = 8.0$ Hz, 2 H) 7.21 (dd, $J = 10.0$ Hz, 3.0 Hz, 1 H) 6.92 (dd, $J = 8.5$, 1.5 Hz, 1 H) 6.73 (d, $J = 8.0$ Hz, 1 H) 6.09 (dd, $J = 10.0$, 2.0 Hz, 1 H) 6.03 (dd, $J = 10.0$, 2.0 Hz, 1 H) 5.69 (dd, $J = 10.0$ Hz, 3.0 Hz, 1 H) 5.64-5.63 (m, 1 H) 3.81-3.75 (m, 1 H) 3.61-3.55

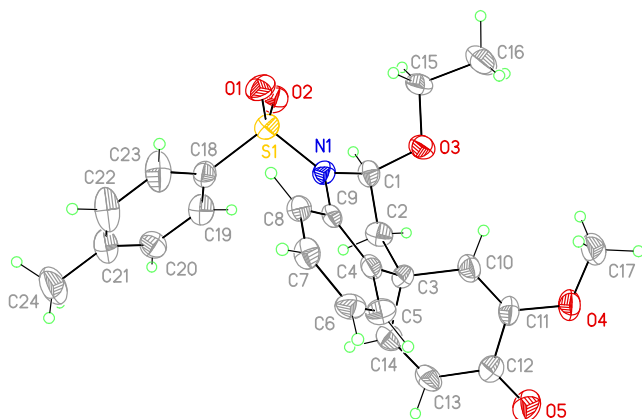
(m, 1 H) 2.39 (s, 3 H) 2.35 (s, 3 H) 1.88 (dd, $J = 14.5$ Hz, 2.0 Hz, 1 H) 1.53 (dd, $J = 14.5$ Hz, 3.5 Hz, 1 H) 1.11 (t, $J = 7.25$ Hz, 3 H); ^{13}C -NMR (125 MHz, CDCl_3) δ 185.5, 155.1, 154.1, 144.2, 138.5, 135.7, 132.6, 129.6, 128.8, 127.8, 127.3, 127.1, 127.0, 124.6, 123.1, 82.7, 63.4, 41.1, 34.7, 21.7, 21.4, 14.8; IR (thin film) 3032, 2975, 2928 cm^{-1} ; HRMS (ESI) m/z observed 446.13925 [$\text{C}_{24}\text{H}_{25}\text{NO}_4\text{S}$ ($\text{M}+\text{Na}$) $^+$ requires 446.13965].



2'-Ethoxy-3-methoxy-1'-tosyl-2',3'-dihydro-1'*H*-spiro[cyclohexa[2,5]diene-1,4'-quinolin]-4-one. (2.33g). (WLM3_87). To a solution of **2.32g** (105 mg, 0.165 mmol) in anhydrous DMF (2 mL, stored over 4Å molecular sieves) at 50 °C was added flame-dried CsF (125 mg, 0.827 mmol). The reaction mixture was immediately heated to 130 °C for 1 h under an argon atmosphere. After complete consumption of the starting material, as judged by TLC, the reaction mixture was diluted with EtOAc (20 mL), washed with H_2O (10 mL), brine (10 mL), dried with Na_2SO_4 , and concentrated under reduced pressure. The resulting brown oil was purified by flash chromatography eluting with Hexanes : EtOAc (3:1) to afford 66 mg (91%) of a 5 : 4 diastomeric mixture of *cis*-**2.33g** : *trans*-**2.33g** as a white crystalline solids.

cis-**2.33g**: ^1H -NMR (400 MHz, CDCl_3) δ 7.94 (dd, $J = 9.2$ Hz, 1 H) 7.43 (dd, $J = 8.4$ Hz, 2 H) 7.32-7.24 (comp, 3 H) 7.11 (dt, $J = 8.0$ Hz, 1 H) 6.77 (dd, $J = 9.2$ Hz, 1 H) 6.35 (dd, $J = 2.4$ Hz, 1 H) 6.16 (d, $J = 9.6$ Hz, 1 H) 5.75 (dd, $J = 12.4$ Hz, 1 H) 5.71 (t, $J = 2.8$ Hz, 1 H) 3.86-3.82 (m, 1 H) 3.64-3.60 (m, 1 H) 3.53 (s, 3 H) 2.41 (s, 3 H) 1.95 (dd, $J = 16.8$ Hz, 1 H) 1.64 (dd, $J = 17.6$ Hz, 1 H) 1.15 (t, $J = 7.2$ Hz, 3 H); ^{13}C -NMR (100

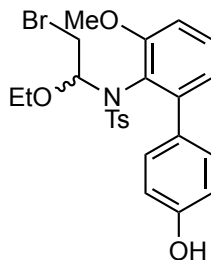
MHz, CDCl₃) δ 180.8, 154.4, 148.2, 144.4, 135.7, 132.7, 129.8, 129.1, 128.3, 127.6, 127.4, 127.1, 126.7, 126.1, 124.0, 82.9, 63.6, 54.6, 42.0, 35.9, 21.6, 14.7; IR (thin film) 2974, 1674 cm⁻¹; HRMS (ESI) m/z observed 462.13438 [C₂₄H₂₅NO₅S (M+Na)⁺ requires 462.13456].



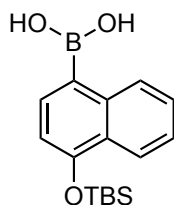
ORTEP view of *cis*-**2.33g**. Displacement ellipsoids are scaled to the 50% probability level.

trans-**2.33g**: ¹H NMR (400 MHz, CDCl₃) δ 7.87 (dd, J = 9.6 Hz, 1 H) 7.43 (dd, J = 8.4 Hz, 2 H) 7.31-7.21 (comp, 3 H) 7.14 (dd, J = 8.8 Hz, 1 H) 7.12 (dt, J = 7.6 Hz, 1 H) 6.87 (dd, J = 9.2 Hz, 1 H) 6.08 (d, J = 10.0 Hz, 1 H) 5.64 (t, J = 2.8 Hz, 1 H) 4.54 (d, J = 2.4 Hz, 1 H) 3.81-3.77 (m, 1 H) 3.62-3.57 (m, 1 H) 3.39 (s, 3 H) 2.37 (s, 3 H) 1.93 (1H, dd, J = 16.8 Hz) 1.67 (dd, J = 18.0 Hz, 1 H) 1.12 (t, J = 7.2 Hz, 3 H); ¹³C-NMR (100 MHz, CDCl₃) δ 180.8, 155.2, 150.3, 144.0, 136.0, 132.7, 129.6, 129.0, 128.3, 128.1, 127.6, 127.5, 126.4, 124.2, 122.4, 83.3, 63.6, 54.5, 41.8, 35.7, 21.5, 14.7; IR (thin film)

2976, 1670 cm^{-1} ; HRMS (ESI) m/z observed 462.13434 [$\text{C}_{24}\text{H}_{25}\text{NO}_5\text{S}$ ($\text{M}+\text{Na}$) $^+$ requires 462.13456].

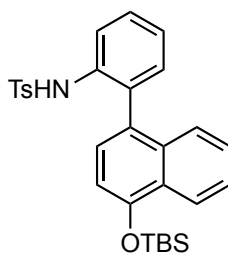


***N*-(2-bromo-1-ethoxyethyl)-*N*-(4'-hydroxy-3-methoxy-[1,1'-biphenyl]-2-yl)-4-methylbenzenesulfonamide. (2.34). (WLM3_91).** To a solution of **2.32f** (298 mg, 0.47 mmol) in anhydrous DMF (5 mL, stored over 4Å molecular sieves) at 50 °C was added flame-dried CsF (360 mg, 2.35 mmol). The reaction mixture was immediately heated to 130 °C for 1 h under an argon atmosphere. After complete consumption of the starting material, as judged by TLC, the reaction mixture was diluted with EtOAc (60 mL), washed with H_2O (30 mL), brine (30 mL), dried with Na_2SO_4 , and concentrated under reduced pressure. The resulting brown oil was purified by flash chromatography eluting with Hexanes: EtOAc (3:1) to afford 39 mg (16%) of **2.32f** as a yellow oil: ^1H NMR (400 MHz, CDCl_3) δ 7.57 (d, J = 8.4 Hz, 2 H) 7.25 (d, J = 8.8 Hz, 2 H) 7.04 (d, J = 8.0 Hz, 1 H) 6.97-6.80 (comp, 3 H) 6.71 (d, J = 8.4 Hz, 2 H) 5.51-5.39 (m, 1 H) 3.83-3.00 (comp, 4 H) 3.58 (s, 3 H) 3.36 (s, 3 H) 2.31 (s, 3 H) 1.17-1.07 (comp, 3 H); ^{13}C -NMR (100 MHz, CDCl_3) δ 158.8, 157.5, 156.3, 143.9, 143.7, 143.5, 143.4, 137.5, 137.4, 134.6, 132.5, 131.9, 129.1, 129.0, 128.2, 127.6, 120.6, 119.8, 118.9, 118.3, 115.6, 110.5, 109.7, 88.8, 88.2, 65.4, 65.0, 60.5, 55.1, 54.8, 32.5, 32.3, 25.5, 25.5, 21.4, 20.9, 15.4, 14.4, 14.3, 14.0; IR (thin film) 3441, 3033, 2975 cm^{-1} ; HRMS (ESI) m/z observed 542.0206000 [$\text{C}_{24}\text{H}_{26}\text{BrNO}_5\text{S}$ ($\text{M}+\text{Na}$) $^+$ requires 542.06000].



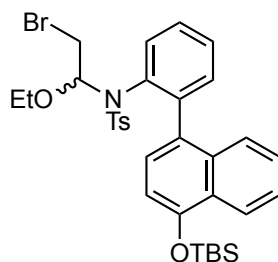
(4-((*tert*-Butyldimethylsilyl)oxy)naphthalen-1-yl)boronic acid. (2.37).

(WLM4_5). To a solution of **2.36** (6.09 g, 18.05 mmol) in THF (20 mL) at $-78\text{ }^{\circ}\text{C}$ was added drop-wise *n*-butyllithium (2.5 M in hexanes, 45 mL, 45.13 mmol). After letting stir for 1 h, triisopropylborate (20.8 mL, 90.27 mmol) was added drop-wise to above solution, and the mixture was allowed to slowly warm to room temperature overnight. The mixture was poured onto 10% aqueous KHSO_4 (30 mL) and extracted with EtOAc (3 x 100 mL). The combined organic extracts were washed with H_2O (100 mL), brine (100 mL), dried with Na_2SO_4 , and concentrated under reduced pressure. The crude white solid was purified by flash chromatography eluting with Hexanes: EtOAc (5:1 \rightarrow 100% EtOAc) to afford 3.60 g (66%) of **2.37** as a white solid; $^1\text{H-NMR}$ (400 MHz, CDCl_3) δ 9.01 (d, $J = 8.0$ Hz, 1 H) 8.28 (d, $J = 7.6$ Hz, 1 H) 7.65-7.45 (comp, 3 H) 6.92 (d, $J = 7.6$ Hz, 1 H) 1.11 (s, 9 H) 0.33 (s, 6 H); $^{13}\text{C-NMR}$ (100 MHz, CDCl_3) δ 156.1, 139.4, 138.8, 127.9, 127.7, 127.0, 124.8, 122.9, 111.9, 13.9, -4.2; IR (thin film) 3217, 2958, 2928, 2859 cm^{-1} ; HRMS (ESI) m/z observed 300.14680 [$\text{C}_{16}\text{H}_{23}\text{BO}_3\text{Si}$ (M-H) $^-$] requires 300.14730].



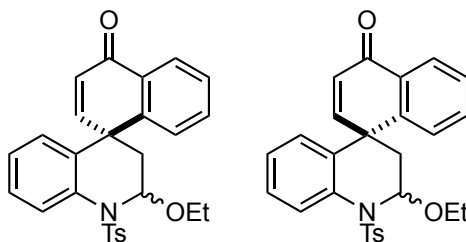
***N*-(2-(4-((*tert*-butyldimethylsilyl)oxy)naphthalen-1-yl)phenyl)-4-methylbenzenesulfonamide. (2.38). (WLM4_17).** To a degassed (30 min) mixture of

1,4-dioxane (9 mL) and water (3 mL) was added powdered Na_2CO_3 (324 mg, 3.054 mmol), **2.36** (400 mg, 1.32 mmol), 2-bromoaniline (179 mg, 1.018 mmol), $\text{Pd}(\text{dppf})\text{Cl}_2$ dichloromethane adduct (42 mg, 0.0509 mmol), and 2,6-di-*tert*-butyl-4 methylphenol (BHT) (spatula tip). The mixture was then heated to 50 °C under an argon atmosphere for 12 hours until all starting material was consumed, as judged by TLC. The resulting dark colored solution was diluted with EtOAc (30 mL), washed with H_2O (10 mL), brine (10 mL), dried with Na_2SO_4 , and concentrated *in vacuo* to yield a black oil. The crude mixture was then dissolved in pyridine (6 mL) and cooled to 0 °C. p-Toluenesulfonyl chloride (388 mg, 2.036 mmol) was then added and the reaction was allowed to stir overnight under argon. The reaction mixture was then diluted with EtOAc (30 mL), washed with H_2O (15 mL), brine (15 mL), dried with Na_2SO_4 and concentrated under reduced pressure. The resulting brown oil was purified by flash chromatography eluting with Hexanes : EtOAc (10:1) to afford 123 mg (24%) of **2.38** as a yellow oil: ^1H -NMR (400 MHz, CDCl_3) δ 8.25 (dd, J = 8.8 Hz, 1 H) 7.82 (dd, J = 9.2 Hz, 1 H) 7.48 (dt, J = 8.0 Hz, 1 H) 7.40 (dt, J = 8.0 Hz, 1 H) 7.32 (d, J = 8.0 Hz, 1 H) 7.25 (dt, J = 7.6 Hz, 1 H) 7.17 (dt, J = 7.6 Hz, 1 H) 7.12 (dd, J = 7.6 Hz, 1 H) 7.07 (d, J = 9.2 Hz, 2 H) 7.01 (d, J = 8.4 Hz, 1 H) 6.76 (d, J = 7.6 Hz, 1 H) 6.69 (d, J = 7.6 Hz, 1 H) 6.31 (s, 1 H) 2.38 (s, 3 H) 1.15 (s, 9 H) 0.39 (s, 3 H) 0.35 (s, 3 H); ^{13}C -NMR (100 MHz, CDCl_3) δ 152.2, 143.6, 135.9, 135.0, 133.0, 131.5, 131.5, 129.4, 128.7, 128.0, 127.5, 127.2, 127.1, 126.6, 125.5, 124.9, 124.6, 123.1, 120.7, 111.8, 25.9, 21.6, 18.5, -4.1, -4.2; IR (thin film) 3337, 3064, 2956, 2929, 2885, 2858 cm^{-1} ; HRMS (CI) m/z observed 503.1952 [$\text{C}_{29}\text{H}_{33}\text{NO}_3\text{SSi}$ (M) $^+$ requires 503.1950].



***N*-(2-bromo-1-ethoxyethyl)-*N*-(2-(4-((*tert*-butyldimethylsilyl)oxy)naphthalen-1-yl)phenyl)-4-methylbenzenesulfonamide. (2.39). (WLM4_34).** To a solution of Br₂ (51 mg, 0.016 mL, 0.318 mmol) in CH₂Cl₂ (0.75 mL) at 0°C under argon was added ethyl vinyl ether (29 mg, 0.4 mL, 0.397 mmol) drop-wise until the solution turned colorless. The mixture was stirred for 30 min and diisopropylethylamine (82 mg, 0.11 mL, 0.635 mmol) was added. After 30 min, a solution of **2.38** (80 mg, 0.159 mmol) in CH₂Cl₂ (0.75 mL) was added drop-wise, and the mixture was allowed to slowly warm to room temperature overnight under an argon atmosphere. After complete consumption of starting material, as judged by TLC, the reaction mixture was poured onto saturated aqueous NH₄Cl (10 mL) and extracted with EtOAc (3 x 5 mL). The combined extracts were washed with H₂O (10 mL), brine (10 mL), dried with Na₂SO₄, and concentrated under reduced pressure. The resulting brown oil was purified by flash chromatography eluting with Hexanes : EtOAc (10:1) to afford 84 mg (81%) of **2.39** as a yellow oil. ¹H NMR (400 MHz, CDCl₃, as a mixture of rotamers) δ 8.27-8.23 (m, 1H) 7.92-7.70 (comp, 3 H) 7.53-6.97 (comp, 10 H) 4.89-4.01 (m, 1 H) 3.51-2.57 (comp, 2 H) 2.48-2.38 (comp, 3 H) 1.66-1.59 (m, 1 H) 1.37-1.30 (m, 1 H) 1.15-1.13 (comp, 9 H) 0.95-0.38 (comp, 3 H) 0.35-0.32 (comp, 6 H); ¹³C-NMR (100 MHz, CDCl₃, as a mixture of rotamers) δ 151.5, 145.7, 145.4, 144.6, 143.9, 143.8, 142.5, 138.5, 136.8, 134.7, 134.2, 134.1, 133.9, 132.8, 130.2, 129.8, 129.6, 129.5, 129.4, 129.2, 128.8, 128.5, 128.5, 128.3, 128.2, 128.1, 128.0, 127.9, 127.7, 127.6, 127.3, 127.2, 127.1, 126.7, 126.3, 125.8, 125.2, 125.1, 124.9, 124.8, 123.1, 122.8, 121.8, 118.4, 111.9, 111.8, 111.7, 91.5, 90.6, 70.4, 66.2, 65.0, 33.3, 33.2,

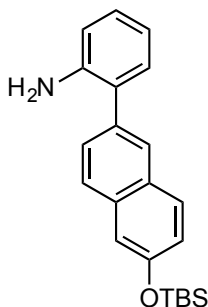
30.8, 25.9, 25.9, 25.9, 21.7, 21.6, 18.6, 18.5, 14.2, 13.6, 13.4, -4.1, -4.2, -4.3; IR (thin film) 3065, 2957, 2929, 2896, 2858 cm^{-1} ; HRMS (ESI) m/z observed 676.15299 [$\text{C}_{33}\text{H}_{40}\text{BrNO}_4\text{SSi}$ ($\text{M}+\text{Na}$) $^+$ requires 676.15229].



2'-Ethoxy-1'-tosyl-2',3'-dihydro-1'*H*,4*H*-spiro[naphthalene-1,4'-quinolin]-4-one **55. (2.40). (WLM4_35).** To a solution of **2.39** (75 mg, 0.115 mmol) in anhydrous DMF (1. mL, stored over 4Å molecular sieves) at 50 °C was added flame-dried CsF (87 mg, 0.573 mmol). The reaction mixture was immediately heated to 130 °C for 1 h under an argon atmosphere. After complete consumption of the starting material, as judged by TLC, the reaction mixture was diluted with EtOAc (20 mL), washed with H₂O (10 mL), brine (10 mL), dried with Na₂SO₄, and concentrated under reduced pressure. The resulting brown oil was purified by PTLC eluting with Hexanes : EtOAc (8:1) to afford 44 mg (84%) of a 4:1 inseparable diastereomeric mixture of **2.40**

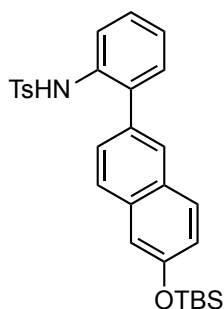
major product **2.40**: ^1H -NMR (400 MHz, CDCl_3) δ 8.10 (dd, J = 8.0, 1.2 Hz, 1 H) 7.84 (dd, J = 8.2 Hz, 1 H) 7.59 (d, J = 8.4 Hz, 2 H) 7.55 (dd, J = 8.2 Hz, 1 H) 7.43 (td, J = 8.0 Hz, 1 H) 7.37-7.24 (comp, 4 H) 6.99 (td, J = 7.6 Hz, 1 H) 6.47 (dd, J = 7.8 Hz, 1 H) 5.95 (d, J = 10.0 Hz, 1 H) 5.73 (dd, J = 4.8, 2.0 Hz, 1 H) 5.32 (d, J = 10.0 Hz, 1 H) 3.85-3.79 (m, 1 H) 3.65-3.59 (m, 1 H) 2.44 (s, 3 H) 2.36 (dd, J = 15.2, 1.6 Hz, 1 H) 2.25 (dd, J = 15.2, 4.8 Hz, 1 H) 1.17 (t, J = 7.6 Hz, 3 H); ^{13}C -NMR (100 MHz, CDCl_3) δ 184.6, 154.6, 149.8, 144.4, 136.6, 133.9, 133.2, 133.0, 131.2, 130.6, 129.9, 129.8, 128.0, 127.3, 127.2, 126.6, 126.4, 125.8, 124.1, 82.4, 63.3, 41.9, 41.6, 21.5, 14.6; IR (thin film)

3066, 2973, 2927, 1665 cm^{-1} ; HRMS (ESI) m/z observed 482.13948 [$\text{C}_{27}\text{H}_{25}\text{NO}_4\text{S}$ ($\text{M}+\text{Na})^+$ requires 482.13965].

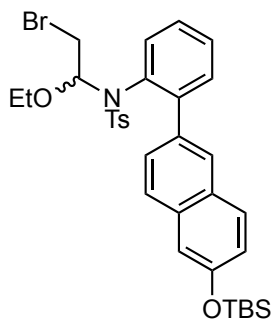


2-(6-((*tert*-Butyldimethylsilyl)oxy)naphthalen-2-yl)aniline. (2.41b).

(WLM3_148). To a degassed (30 min) mixture of 1,4-dioxane (3 mL) and water (1 mL) was added powdered K_2CO_3 (170 mg, 1.22 mmol), 2-bromoaniline (72 mg, 0.408 mmol), **2.41** (160 mg, 0.529 mmol), $\text{Pd}(\text{dppf})\text{Cl}_2$ dichloromethane adduct (17 mg, 0.0204 mmol), and 2,6-di-*tert*-butyl-4 methylphenol (BHT) (spatula tip). The mixture was then heated to 100 $^\circ\text{C}$ under an argon atmosphere for 6 hours until all starting material was consumed, as judged by TLC. The resulting dark colored solution was diluted with EtOAc (20 mL), washed with H_2O (10 mL), brine (10 mL), dried with Na_2SO_4 , and concentrated under reduced pressure. The resulting black oil was purified by flash chromatography eluting with Hexanes : EtOAc (10:1) to afford 90 mg (63%) of **2.41b** as a brown oil: ^1H -NMR (400 MHz, CDCl_3) δ 7.87 (s, 1 H) 7.78 (t, $J = 9.6$ Hz, 1 H) 7.56 (dd, $J = 12.4$ Hz, 1 H) 7.27-7.18 (comp, 3H) 7.14 (dd, $J = 11.2$ Hz, 1 H) 6.89 (dt, $J = 7.2$ Hz, 1 H) 6.82 (dd, $J = 8.8$ Hz, 1 H) 3.82 (br, 2 H) 1.07 (s, 9 H) 0.30 (s, 6 H); ^{13}C -NMR (100 MHz, CDCl_3) δ 153.7, 143.7, 134.8, 133.6, 130.6, 129.4, 128.4, 127.6, 127.5, 127.1, 122.5, 118.7, 115.6, 114.8, 25.7, 18.3, -4.3; IR (thin film) 3470, 3377, 3053, 3024, 2929, 2885, 2857 cm^{-1} ; HRMS (ESI) m/z observed 350.19351 [$\text{C}_{22}\text{H}_{27}\text{NOSi}$ ($\text{M}+\text{H})^+$ requires 350.19347].

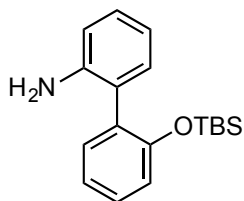


***N*-(2-(6-((*tert*-butyldimethylsilyl)oxy)naphthalen-2-yl)phenyl)-4-methylbenzenesulfonamide. (2.42). (WLM3_145).** To a solution of **2.41b** (84 mg, 0.24 mmol) in pyridine (2.5 mL) at 0 °C was added p-toluenesulfonyl chloride (92 mg, 0.48 mmol). The reaction was allowed stir overnight until all starting material was consumed, as judged by TLC. The resulting brown solution was diluted with EtOAc (20 mL), washed with H₂O (10 mL), brine (10 mL), dried with Na₂SO₄, and concentrated *in vacuo* to give a brown oil, which was subsequently azeotroped with cyclohexane (3 x 5 mL). Purification by flash chromatography eluting with Hexanes : EtOAc (10:1) gave 117 mg (97%) of **2.42** as a brown solid: M.p. 109-111 °C; ¹H-NMR (400 MHz, CDCl₃) δ 7.78 (d, *J* = 8.0 Hz, 1 H) 7.68 (d, *J* = 8.4 Hz, 1 H) 7.60 (d, *J* = 8.8 Hz, 1 H) 7.44 (d, *J* = 8.4 Hz, 2 H) 7.38-7.35 (m, 1 H) 7.24 (d, *J* = 2.0 Hz, 1 H) 7.19-7.14 (comp, 6 H) 6.93 (dd, *J* = 8.4 Hz, 1 H) 6.67 (s, 1 H) 2.41 (s, 3 H) 1.07 (s, 9 H) 0.31 (s, 6 H); ¹³C-NMR (100 MHz, CDCl₃) δ 154.1, 143.7, 136.1, 134.2, 133.8, 132.3, 130.4, 129.5, 129.3, 129.0, 128.5, 127.7, 127.5, 127.1, 126.7, 125.0, 123.0, 121.7, 114.8, 25.7, 21.5, 18.3, -4.3; IR (thin film) 3340, 3054, 2955, 2929, 2885, 2858 cm⁻¹; HRMS (ESI) *m/z* observed 504.20180 [C₂₉H₃₃NO₃SSi (M+H)⁺ 504.20230].



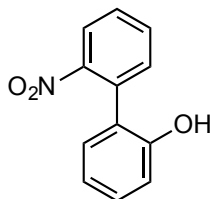
***N*-(2-bromo-1-ethoxyethyl)-*N*-(2-(6-((*tert*-butyldimethylsilyl)oxy)naphthalen-2-yl)phenyl)-4-methylbenzenesulfonamide. (2.43). (WLM4_6).** To a solution of Br₂ (126 mg, 0.04 mL, 0.786 mmol) in CH₂Cl₂ (2 mL) at 0°C under argon was added ethyl vinyl ether (71 mg, 0.1 mL, 0.983 mmol) drop-wise until the solution turned colorless. The mixture was stirred for 30 min and diisopropylethylamine (204 mg, 0.27 mL, 1.57 mmol) was added. After 30 min, a solution of **2.42** (198 mg, 0.393 mmol) in CH₂Cl₂ (2 mL) was added drop-wise, and the mixture was allowed to slowly warm to room temperature overnight under an argon atmosphere. After complete consumption of starting material, as judged by TLC, the reaction mixture was poured onto saturated aqueous NH₄Cl (10 mL) and extracted with EtOAc (3 x 15 mL). The combined extracts were washed with H₂O (20 mL), brine (20 mL), dried with Na₂SO₄, and concentrated under reduced pressure. The resulting brown oil was purified by flash chromatography eluting with Hexanes : EtOAc (10:1) to afford 206 mg (80%) of **2.43** as a yellow foam: ¹H-NMR (400 MHz, CDCl₃, as a mixture of rotamers) δ 8.05-8.04 (m, 1 H) 7.83-7.12 (comp, 12 H) 6.94-6.92 (d, 1 H) 5.64-5.03 (m, 1 H) 3.30-2.55 (comp, 4 H) 2.48-2.46 (comp, 3 H) 1.06-1.05 (comp, 9 H) 0.95-0.55 (comp, 3 H) 0.31-0.28 (comp, 6 H); ¹³C-NMR (100 MHz, CDCl₃, as a mixture of rotamers) δ 153.9, 153.6, 144.9, 144.2, 144.1, 144.0, 138.2, 137.4, 135.2, 135.2, 134.6, 134.5, 133.9, 133.7, 133.6, 132.9, 132.8, 132.4, 132.1, 130.6, 129.8, 129.7, 129.5, 129.5, 129.4, 129.3, 129.1, 128.9, 128.8, 128.7, 128.4, 128.2, 128.0, 127.9, 127.8, 127.5, 127.4, 126.5, 126.2, 122.5, 122.3, 114.6, 114.5, 91.0,

89.7, 88.6, 67.0, 66.8, 65.4, 33.6, 33.1, 32.9, 21.6, 18.2, 18.2, 14.7, 14.5, 13.9, -4.3;
 HRMS (ESI) m/z observed 676.15164 [$C_{33}H_{40}BrNO_4SSi$ ($M+Na$)⁺ requires 676.15229].

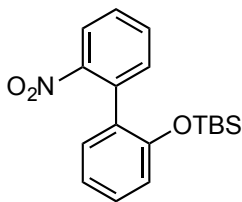


2'-((*tert*-Butyldimethylsilyl)oxy)-[1,1'-biphenyl]-2-amine (2.47). (WLM3_128).

A suspension of **2.51** (252 mg, 0.765 mmol) and palladium 10% wt on activated carbon (50 mg) in EtOAc (1.5 mL) was allowed to stir overnight at room temperature under a hydrogen atmosphere. After complete consumption of starting material, as judged by TLC, the suspension was diluted with EtOAc (25 mL) and filtered through a pad of Celite® that was subsequently washed with EtOAc (3 x 15 mL). The resulting filtrate was concentrated under reduced pressure to give 222 mg (97%) of **2.47** as a yellow oil that required no further purification; ¹H-NMR (400 MHz, CDCl₃) δ 7.32-7.26 (comp, 2 H) 7.19-7.07 (comp, 3 H) 6.97 (d, J = 8.0 Hz, 1 H) 6.83 (dt, J = 8.2 Hz, 1 H) 6.75 (d, J = 7.6 Hz, 1 H) 3.81 (br, 2 H) 0.84 (s, 9 H) 0.09 (s, 3 H) -0.11 (s, 3 H); ¹³C-NMR (100 MHz, CDCl₃) δ 153.0, 144.9, 132.1, 131.8, 131.6, 128.9, 128.6, 125.9, 122.4, 120.6, 118.5, 116.0, 25.7, 18.2; IR (thin film) 3466, 3382, 3062, 3024, 2955, 2929, 2884, 2857 cm⁻¹; HRMS (ESI) m/z observed 300.00000 [$C_{18}H_{25}NOSi$ ($M+H$)⁺ requires 300.00000].

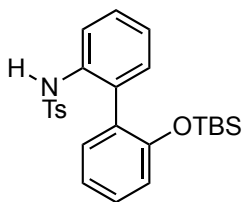


2'-Nitro-[1,1'-biphenyl]-2-ol. (2.50). (WLM3_123). To a degassed (30 min) mixture of 1,4-dioxane (3 mL) and water (1 mL) was added powdered Cs_2CO_3 (503 mg, 1.54 mmol), 2-nitrobromobenzene (104 mg, 0.515 mmol), **2.48** (92 mg, 0.669 mmol), Pd(dppf)Cl_2 dichloromethane adduct (21mg, 0.0257 mmol), and 2,6-di-*tert*-butyl-4 methylphenol (BHT) (spatula tip). The mixture was then heated to 100 °C under an argon atmosphere for 6 hours until all starting material was consumed, as judged by TLC. The resulting dark colored solution was diluted with EtOAc (50 mL), washed with H_2O (25 mL), brine (25 mL), dried with Na_2SO_4 , and concentrated under reduced pressure. The resulting black oil was purified by flash chromatography eluting with Hexanes : EtOAc (5:1) to afford 110 mg (99% yield) of **2.50** as a yellow solid: M.p. 134-136 °C; $^1\text{H-NMR}$ (400 MHz, CDCl_3) δ 7.97 (dd, J = 9.2 Hz, 1 H) 7.66 (dt, J = 8.0 Hz, 1 H) 7.51 (dt, J = 8.4 Hz, 1 H) 7.44 (dd, J = 8.8 Hz, 1 H) 7.29-7.23 (comp, 2 H) 7.04 (t, J = 7.6 Hz, 1 H) 6.83 (d, J = 8.4 Hz, 1 H) 5.15 (br, 1 H); $^{13}\text{C-NMR}$ (100 MHz, CDCl_3) δ 152.3, 149.6, 132.9, 132.7, 132.6, 129.9, 128.5, 125.0, 124.2, 121.4, 115.7; IR (thin film) 3447, 3067, 2925, 2854, 1525, 1356 cm^{-1} ; HRMS (ESI) m/z observed 238.04738 [$\text{C}_{12}\text{H}_9\text{NO}_3$ ($\text{M}+\text{Na}$) $^+$ requires 238.04746].



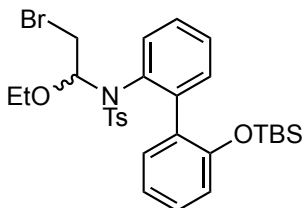
***tert*-Butyldimethyl((2'-nitro-[1,1'-biphenyl]-2-yl)oxy)silane. (2.51). (WLM3_127).** To a stirred solution of **2.50** (302 mg, 1.40 mmol) in 1,2 dichloroethane (2 mL) at room temperature was added imidazole (285 mg, 4.2 mmol). After 15 min, *tert*-butyldimethylsilylchloride (235 mg, 1.54 mmol) was added, and the resulting solution

was stirred at room temperature until all starting material was consumed, as judged by TLC. The mixture was cooled to rt, poured onto saturated NH_4Cl (25 mL) and extracted with EtOAc (4 x 20 mL). The combined organic extracts were washed with H_2O (25 mL), brine (25 mL), dried with Na_2SO_4 , and concentrated under reduced pressure. The resulting yellow oil was purified by flash chromatography eluting with Hexanes : EtOAc (10:1) to give 445 mg (96%) of **2.51** as a yellow oil that crystalized upon standing: M.p. 74-76 °C; ^1H -NMR (400 MHz, CDCl_3) δ 7.98 (dd, J = 9.6 Hz, 1 H) 7.63 (dt, J = 7.8 Hz, 1 H) 7.47 (dt, J = 8.8 Hz, 1 H) 7.42 (dd, J = 9.2 Hz, 1 H) 7.31-7.26 (comp, 2 H) 7.08 (dt, J = 8.2 Hz, 1 H) 6.89 (d, J = 8.0 Hz, 1 H) 0.73 (s, 9 H) 0.00 (br, 6 H); ^{13}C -NMR (100 MHz, CDCl_3) δ 152.6, 149.9, 134.4, 133.0, 132.8, 130.2, 129.9, 129.7, 128.3, 124.4, 122.0, 119.7, 25.6, 18.2, -4.3; IR (thin film) 3066, 3026, 2956, 2930, 2885, 2858, 1532, 1354 cm^{-1} ; HRMS (ESI) m/z observed 330.15237 [$\text{C}_{18}\text{H}_{23}\text{NO}_3\text{Si}$ ($\text{M}+\text{H}$) $^+$ 330.15200].



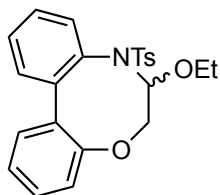
***N*-(2'-((*tert*-butyldimethylsilyl)oxy)-[1,1'-biphenyl]-2-yl)-4-methylbenzenesulfonamide. (2.52). (WLM3_129).** To a solution of **2.47** (220 mg, 0.735 mmol) in pyridine (1 mL) at 0 °C was added *p*-toluenesulfonyl chloride (280 mg, 1.47 mmol). The reaction was allowed stir overnight until all starting material was consumed, as judged by TLC. The resulting brown solution was diluted with EtOAc (30 mL), washed with H_2O (15 mL), brine (15 mL), dried with Na_2SO_4 , and concentrated *in vacuo* to give a brown oil, which was subsequently azeotroped with cyclohexane (3 x 10 mL). Purification by flash chromatography eluting with Hexanes : EtOAc (10:1) gave

316 mg (95%) of **2.52** as a white solid: $^1\text{H-NMR}$ (400 MHz, CDCl_3) δ 7.67 (dd, $J = 9.2$ Hz, 1 H) 7.37 (dt, $J = 8.8$ Hz, 1 H) 7.34 (s, 1 H) 7.23 (dt, $J = 8.4$ Hz, 1 H) 7.21-7.16 (m, 1 H) 7.07-7.03 (comp, 3 H) 6.89 (d, $J = 8.0$ Hz, 2 H) 6.86 (dd, $J = 9.2$ Hz, 1 H) 6.74 (dt, $J = 8.2$ Hz, 1 H) 6.34 (dd, $J = 9.6$ Hz, 1 H) 2.32 (s, 3 H) 0.77 (s, 9 H) 0.08 (s, 3 H) -0.33 (s, 3 H); $^{13}\text{C-NMR}$ (100 MHz, CDCl_3) δ 151.1, 142.6, 136.1, 134.5, 134.0, 131.5, 130.8, 130.1, 129.1, 128.9, 128.5, 126.9, 126.6, 126.5, 122.1, 120.3, 25.3, 21.4, 17.9, -4.3, -5.3; IR (thin film) 3304, 2930, 2859 cm^{-1} ; HRMS (ESI) m/z observed 454.18690 [$\text{C}_{25}\text{H}_{31}\text{NO}_3\text{SSi}$ ($\text{M}+\text{H}$) $^+$ requires 454.18667].



***N*-(2-bromo-1-ethoxyethyl)-*N*-(2'-((*tert*-butyldimethylsilyl)oxy)-[1,1'-biphenyl]-2-yl)-4-methylbenzenesulfonamide. (2.53). (WLM3_130).** To a solution of Br_2 (140 mg, 0.045 mL, 0.86 mmol) in CH_2Cl_2 (2 mL) at 0°C under argon was added ethyl vinyl ether (140 mg, 0.104 mL, 1.075 mmol) drop-wise until the solution turned colorless. The mixture was stirred for 30 min and diisopropylethylamine (223 mg, 0.3 mL, 1.72 mmol) was added. After 30 min, a solution of **2.52** (195 mg, 0.43 mmol) in CH_2Cl_2 (2 mL) was added drop-wise, and the mixture was allowed to slowly warm to room temperature overnight under an argon atmosphere. After complete consumption of starting material, as judged by TLC, the reaction mixture was poured onto saturated aqueous NH_4Cl (20 mL) and extracted with EtOAc (3 x 20 mL). The combined extracts were washed with H_2O (30 mL), brine (30 mL), dried with Na_2SO_4 , and concentrated under reduced pressure. The resulting brown oil was purified by flash chromatography

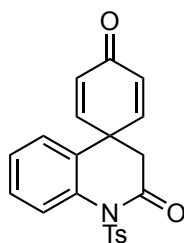
eluting with Hexanes : EtOAc (10:1) to afford 142 mg (55%) of **2.53** as a clear oil that solidified upon standing: $^1\text{H-NMR}$ (400 MHz, CDCl_3 , as a mixture of rotamers) δ 7.80-7.74 (comp, 2 H) 7.47-7.16 (comp, 7 H) 7.05-6.84 (m, 3 H) 4.91-4.80 (m, 1 H) 3.63-3.58 (m, 1 H) 3.22-3.05 (comp, 2 H) 2.47-2.41 (comp, 4 H) 1.00-0.82 (comp, 3 H) 0.71-0.68 (comp, 9 H) 0.21-0.15 (comp, 6 H); $^{13}\text{C-NMR}$ (100 MHz, CDCl_3 as a mixture of rotamers) δ 152.9, 152.7, 143.5, 140.2, 138.8, 138.3, 133.6, 133.4, 132.4, 132.0, 131.7, 130.2, 129.3, 129.1, 129.0, 128.4, 128.1, 128.0, 127.5, 127.4, 120.7, 120.4, 118.4, 118.0, 93.3, 66.5, 65.6, 34.4, 33.2, 25.4, 21.6, 17.8, 14.5, 1.00, -3.7, -4.2, -4.4, -4.5; IR (thin film) 3064, 2958, 2929, 2896, 2857 cm^{-1} ; HRMS (ESI) m/z observed 626.13697 [$\text{C}_{29}\text{H}_{38}\text{BrNO}_4\text{SSi}$ ($\text{M}+\text{Na}$) $^+$ requires 626.13664].



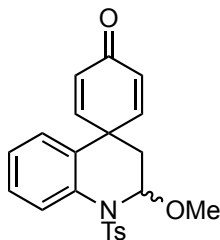
7-Ethoxy-8-tosyl-7,8-dihydro-6H-dibenzo[*e,g*][1,4]oxazocine. (2.56).

(WLM3_96). To a solution of **2.55** (102 mg, 0.169 mmol) in anhydrous DMF (2 mL, stored over 4Å molecular sieves) at 50 °C was added flame-dried CsF (130 mg, 0.843 mmol). The reaction mixture was immediately heated to 130 °C for 1 h under an argon atmosphere. After complete consumption of the starting material, as judged by TLC, the reaction mixture was diluted with EtOAc (30 mL), washed with H_2O (20 mL), brine (20 mL), dried with Na_2SO_4 , and concentrated under reduced pressure. The resulting brown oil was purified by flash chromatography eluting with Hexanes: EtOAc (5:1) gave 69 mg (quant) of **2.56** as a white crystalline solid: M.p. 137-140 °C; $^1\text{H-NMR}$ (400 MHz, CDCl_3) δ 7.48-7.41 (comp, 3 H) 7.32-7.30 (m, 1 H) 7.12 (1H, d, J = 8.4 Hz) 7.06 (dt, J =

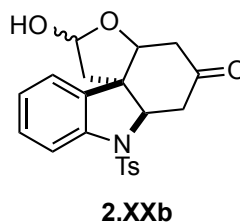
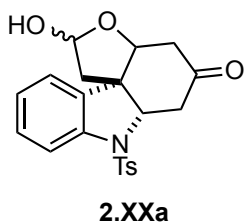
8.4 Hz, 1 H) 6.75 (d, $J = 8.0$ Hz, 2 H) 6.70-6.64 (comp, 2 H) 6.47 (1H, dd, $J = 9.2, 2.0$ Hz) 5.65 (dd, $J = 8.4, 4.0$ Hz, 1 H) 4.21-4.13 (m, 1 H) 4.03 (dd, $J = 13.0, 4.0$ Hz, 1 H) 3.95 (dd, $J = 13.0, 8.4$ Hz, 1 H) 3.86-3.78 (m, 1 H) 2.24 (s, 3 H) 1.28 (t, $J = 7.2$ Hz, 3 H); ^{13}C -NMR (100 MHz, CDCl_3) δ 155.3, 142.7, 141.8, 136.5, 134.3, 134.1, 130.8, 130.2, 129.7, 128.8, 128.1, 126.8, 123.6, 120.9, 119.7, 82.8, 66.7, 64.1, 21.4, 14.9; IR (thin film) 3063, 2978, 2929, 2881 cm^{-1} ; HRMS (ESI) m/z observed 410.14171 [$\text{C}_{23}\text{H}_{23}\text{NO}_4\text{S}$ ($\text{M}+\text{H}$) $^+$ requires 410.14206].



1'-Tosyl-1'*H*-spiro[cyclohexa[2,5]diene-1,4'-quinoline]-2',4'(3'*H*)-dione. (2.73).
(WLM3_45). To a stirred solution of **2.14** (29 mg, 0.071 mmol) and *m*-chloroperoxybenzoic acid (61 mg, 0.354 mmol) in CH_2Cl_2 (0.7 mL) was added $\text{BF}_3 \cdot \text{OEt}_2$ (cat) under argon. The reaction was stirred at room temperature for 2 h. After complete consumption of the starting material, as judged by TLC, the reaction mixture was purified via PTLC eluting with Hexanes : EtOAc (3:1) to afford 15 mg (55%) of **2.73** as a white solid: M.p. 177 $^\circ\text{C}$ (decomp); ^1H -NMR (400 MHz, CDCl_3) δ 8.05 (d, $J = 8.4$ Hz, 2 H) 7.80 (d, $J = 8.0$ Hz, 1 H) 7.43 (dt, $J = 7.6$ Hz, 1 H) 7.41 (d, $J = 8.0$ Hz, 2 H) 7.26 (dt, $J = 7.6$ Hz, 1 H) 7.13 (dd, $J = 9.2$ Hz, 1 H) 6.78 (d, $J = 10.0$ Hz, 2 H) 6.37 (d, $J = 9.6$ Hz, 2 H) 2.72 (s, 2 H) 2.48 (s, 3 H); ^{13}C -NMR (100 MHz, CDCl_3) δ 184.5, 167.6, 147.8, 145.9, 135.7, 135.1, 130.3, 129.6, 129.2, 129.1, 128.7, 127.1, 126.1, 124.4, 44.2, 43.0, 21.8; IR (thin film) 3070, 2921, 1719, 1670 cm^{-1} ; HRMS (ESI) m/z observed 380.0952 [$\text{C}_{21}\text{H}_{17}\text{NO}_4\text{S}$ ($\text{M}+\text{H}$) $^+$ requires 380.0957].

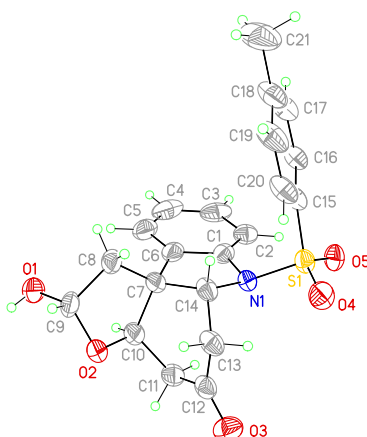


2'-Methoxy-1'-tosyl-2',3'-dihydro-1'H-spiro[cyclohexa[2,5]diene-1,4'-quinolin]-4-one. (2.74). (WLM4_65). To a stirred solution of **2.14** (50 mg, 0.122 mmol) in dry CH₂Cl₂ (0.4 mL) and dry MeOH (0.8 mL) was added trifluoroacetic acid (0.1 mL). The reaction was stirred at 50 °C under argon for 48 hr. After complete consumption of starting material, as judged by TLC, the reaction mixture was purified via PTLC eluting with Hexanes : EtOAc (4:1) to afford 34 mg (71%) of **2.74** as a white solid: M.p. 150-151°C; ¹H-NMR (400 MHz, CDCl₃) δ 7.94 (dd, *J* = 8.4 Hz, 1 H) 7.44 (d, *J* = 8.4 Hz, 2 H) 7.31 (td, *J* = 7.2 Hz, 1 H) 7.26 (d, *J* = 8.4 Hz, 2 H) 7.21 (dd, *J* = 10.0, 3.0 Hz, 1 H) 7.12 (td, *J* = 8.0 Hz, 1 H) 6.87 (dd, *J* = 8.0, 1.6 Hz, 1 H) 6.12 (dd, *J* = 10.0, 2.0 Hz, 1 H) 6.06 (dd, *J* = 10.4, 2.0 Hz, 1 H) 5.71 (dd, *J* = 10.0, 2.8 Hz, 1 H) 5.56 (m, 1 H) 3.42 (s, 3 H) 2.41 (s, 3 H) 1.94 (dd, *J* = 14.4, 2.4 Hz, 1 H) 1.60 (dd, *J* = 14.4, 3.2 Hz, 1 H); ¹³C-NMR (100 MHz, CDCl₃) δ 185.5, 154.8, 153.9, 144.4, 135.6, 132.7, 129.8, 129.2, 128.6, 128.0, 127.2, 127.0, 126.4, 126.2, 124.8, 84.4, 55.7, 41.3, 34.7, 21.6; IR (thin film) 3065, 3001, 2950, 1665 cm⁻¹; HRMS (ESI) *m/z* observed 418.10934 [C₂₂H₂₁NO₄S (M+Na)⁺ requires 418.10835].

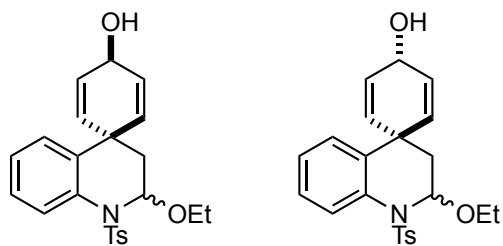


2-Hydroxy-7-tosyl-1,2,3a,4,6a,7-hexahydrofuro[2,3-*d*]carbazol-5(6*H*)-one.

(2.81). (WLM3_66). A stirred solution of **2.14** (134 mg, 0.33 mmol) in 1M HCl (1 mL) and dioxane (3 mL) was heated at 100 °C for 6 hr under argon. After complete consumption of the starting material, as judged by TLC, the reaction was diluted with EtOAc (15 mL), washed with H₂O (10 mL), brine (10 mL), dried with Na₂SO₄ and concentrated under reduced pressure. The resulting white solid was purified by flash chromatography eluting with Hexanes : EtOAc (1:1) to afford 109 mg (84%) of **2.81** as a 2:1 mixture of diastereomers: ¹H NMR (400 MHz, (CD₃)₂SO) δ 7.70 (d, *J* = 8.4 Hz, 2 H) 7.64 (d, *J* = 8.4 Hz, 2 H) 7.58 (d, *J* = 8.0 Hz, 1 H) 7.57 (d, *J* = 8.0 Hz, 1 H) 7.35-7.26 (comp, 6 H) 7.13-7.07 (comp, 2 H) 6.78 (d, *J* = 4.8 Hz, 1 H) 6.52 (d, *J* = 4.8 Hz, 1 H) 5.57-5.54 (m, 1 H) 5.47-5.44 (m, 1 H) 4.45 (t, *J* = 4.8 Hz, 1 H) 4.23-4.20 (comp, 2 H) 4.12 (t, *J* = 4.0 Hz, 1 H) 3.34 (dd, *J* = 4.4 Hz, 1 H) 3.16 (dd, *J* = 17.6, 4.0 Hz, 1 H) 3.03 (dd, *J* = 16.8, 4.8 Hz, 1 H) 2.86 (dd, *J* = 17.6, 4.0 Hz, 1 H) 2.53-2.44 (comp, 2 H) 2.38 (dd, *J* = 13.6, 4.5 Hz, 1 H) 2.34-2.28 (m, 1 H) 2.31 (s, 6 H) 2.25 (dd, *J* = 14.4 Hz, 5.6 Hz, 1 H) 2.18-2.08 (comp, 2 H) 1.63 (dd, *J* = 14.0, 2.4 Hz, 1 H); ¹³C-NMR (100 MHz, (CD₃)₂SO) δ 206.7, 206.3, 144.8, 144.8, 141.3, 140.9, 133.4, 133.0, 132.2, 131.7, 129.9, 129.0, 128.9, 127.8, 127.5, 125.0, 124.0, 115.4, 115.1, 97.4, 96.9, 82.0, 80.8, 67.8, 67.3, 52.4, 51.4, 48.2, 48.0, 42.1, 40.5, 39.2, 21.0; IR (thin film) 3503, 2925, 1718 cm⁻¹; HRMS (ESI) *m/z* observed 400.12109 [C₂₁H₂₂NO₅S (M+H)⁺ requires 400.12132].



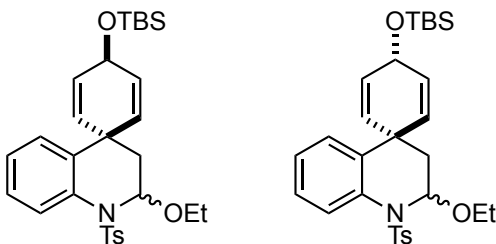
View of **2.81a** showing the atom labeling scheme. Displacement ellipsoids are scaled to the 50% probability level. The diastereomer shown has an R, R, R configuration at C7, C9a and C14, respectively. The hydrogen atom on O9a was not included in the refinement model.



2'-Ethoxy-1'-tosyl-2',3'-dihydro-1'H-spiro[cyclohexa[2,5]diene-1,4'-quinolin]-4-ol. (2.120). (WLM3_136). To a stirred solution of **2.14** (394 mg, 0.962 mmol) in MeOH (2 mL) and CH₂Cl₂ (2 mL) at 0 °C was added CeCl₃•7H₂O (717 mg, 1.92 mmol). After stirring for 30 min, NaBH₄ (75 mg, 1.92 mmol) was added in one portion. After 30 min, the reaction was quenched with saturated NH₄Cl (2 mL) and extracted with EtOAc (3 x 10 mL). The combined organic extracts were washed with H₂O (15 mL), brine (15 mL), dried with Na₂SO₄, and concentrated under reduced pressure. The resulting white solid was purified by flash chromatography eluting with Hexanes : EtOAc (2:1) to afford 359 mg (91%) of **2.120a** and **2.120b** as a 1:1 diastereomeric mixture.

2.120a: $^1\text{H-NMR}$ (400 MHz, CDCl_3) δ 7.83 (dd, $J = 8.0$ Hz, 1 H) 7.40 (d, $J = 8.4$ Hz, 2 H) 7.24-7.19 (comp, 3 H) 7.12 (td, $J = 7.2$ Hz, 1 H) 7.04 (dd, $J = 8.0$ Hz, 1 H) 6.10 (dm, 1 H) 5.77 (dm, 1 H) 5.68 (dm, 1 H) 5.59 (m, 1 H) 4.70 (dm, 1 H) 4.46 (m, 1 H) 3.81-3.73 (m, 1 H) 3.61-3.53 (m, 1 H) 2.38 (s, 3 H) 1.81 (dd, $J = 14.4$ Hz, 1 H) 1.72 (br, 1 H) 1.41 (dd, $J = 14.4$ Hz, 1 H) 1.11 (t, $J = 7.2$ Hz, 3 H); $^{13}\text{C-NMR}$ (100 MHz, CDCl_3) δ 143.9, 137.5, 136.0, 135.5, 132.8, 132.6, 130.3, 129.6, 127.3, 127.2, 126.7, 126.1, 125.8, 123.2, 83.6, 63.3, 61.4, 38.6, 37.8, 21.5, 14.8; IR (thin film) 3420, 3026, 2975, 2928 cm^{-1} ; HRMS (ESI) m/z observed 434.10000 [$\text{C}_{23}\text{H}_{25}\text{NO}_4\text{S}$ ($\text{M}+\text{Na}$) $^+$ requires 434.10000].

2.120b: $^1\text{H-NMR}$ (400 MHz, CDCl_3) δ 7.83 (dd, $J = 8.0$ Hz, 1 H) 7.50 (d, $J = 8.4$ Hz, 2 H) 7.24-7.19 (comp, 3 H) 7.10 (td, $J = 7.2, 1.2$ Hz, 1 H) 6.87 (dd, $J = 7.6, 1.2$ Hz, 1 H) 6.19 (dm, 1 H) 5.79 (dm, 1 H) 5.72 (dm, 1 H) 5.58 (m, 1 H) 4.68 (dm, 1 H) 4.54 (m, 1 H) 3.80-3.73 (m, 1 H) 3.61-3.53 (m, 1 H) 2.38 (s, 3 H) 1.86 (dd, $J = 14.4, 2.4$ Hz, 1 H) 1.70 (br, 1 H) 1.46 (dd, $J = 14.4, 3.2$ Hz, 1 H) 1.10 (t, $J = 7.2$ Hz, 3 H); $^{13}\text{C-NMR}$ (100 MHz, CDCl_3) δ 144.0, 137.4, 136.5, 135.9, 133.0, 132.4, 130.1, 129.6, 127.4, 127.2, 126.5, 126.3, 125.8, 123.2, 83.5, 63.3, 61.4, 38.1, 37.8, 21.5, 14.8; IR (thin film) 3392, 3027, 2975, 2928 cm^{-1} ; HRMS (ESI) m/z observed 412.20000 [$\text{C}_{23}\text{H}_{25}\text{NO}_4\text{S}$ ($\text{M}+\text{H}$) $^+$ requires 412.20000].

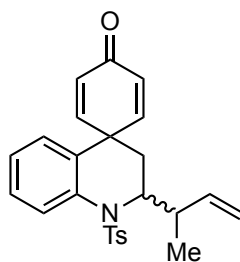


4-((*tert*-Butyldimethylsilyl)oxy)-2'-ethoxy-1'-tosyl-2',3'-dihydro-1'*H*-spiro[cyclohexa[2,5]diene-1,4'-quinoline]. (2.121). (WLM3_147_2). To a stirred solution of **2.120** (127 mg, 0.309 mmol) in DCE (3.0 mL) under argon was added imidazole (65 mg, 0.925 mmol). The reaction mixture was stirred for 15 min, then *tert*-butyldimethylsilylchloride (70 mg, 0.463 mmol) was added and the reaction was allowed to stir overnight. After complete consumption of the starting material, as judged by TLC, the reaction was poured onto saturated NH₄Cl (5.0 mL) and extracted with EtOAc (3 x 5 mL). The combined organic extracts were washed with H₂O (10.0 mL), brine (10.0 mL), dried with Na₂SO₄, and concentrated under reduced pressure. The resulting yellow oil was purified by flash chromatography eluting with Hexanes: EtOAc (10:1) to afford 157 mg (97%) of **2.121a** and **2.121b** as a waxy white solid.

2.121a: ¹H-NMR (400 MHz, CDCl₃) δ 7.82 (dd, *J* = 8.4, 1.2 Hz, 1 H) 7.39 (dd, *J* = 8.4, 1.2 Hz, 2 H) 7.23-7.19 (comp, 4 H) 7.12 (td, *J* = 6.4 Hz, 1 H) 6.04 (dt, *J* = 10.4, 2.0 Hz, 1 H) 5.67-5.63 (dm, 1 H) 5.59-5.54 (comp, 3 H) 4.63 (dt, *J* = 10.0, 2.0 Hz, 1 H) 4.51-4.48 (m, 1 H) 3.81-3.74 (m, 1 H) 3.61-3.53 (m, 1 H) 2.38 (s, 3 H) 1.80 (dd, *J* = 14.4, 2.4 Hz, 1 H) 1.39 (dd, *J* = 14.4, 3.6 Hz, 1 H) 1.10 (t, *J* = 7.2 Hz, 3 H) 0.92 (s, 9 H) 0.10 (s, 6 H); ¹³C-NMR (100 MHz, CDCl₃) δ 143.8, 136.5, 136.0, 134.7, 133.3, 132.4, 131.3, 130.8, 129.5, 127.6, 127.2, 125.9, 124.1, 83.7, 63.2, 61.8, 38.6, 37.6, 25.9, 21.5, 18.3, 14.8, -4.5; IR (thin film) 3027, 2928, 2856 cm⁻¹; HRMS (ESI) *m/z* observed 548.22710 [C₂₉H₃₉NO₄S (M+Na)⁺ requires 548.22613].

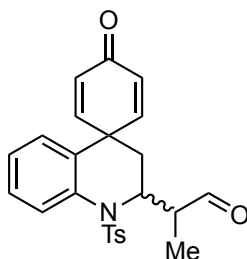
2.121b: ¹H NMR (400 MHz, CDCl₃) δ 7.82 (dd, *J* = 8.4, 1.2 Hz, 1 H) 7.39 (d, *J* = 8.4 Hz, 2 H) 7.23-7.19 (comp, 3 H) 7.11 (td, *J* = 7.8, 1.2 Hz, 1 H) 6.88 (dd, *J* = 7.8 Hz, 1 H) 6.12 (dt, *J* = 10.0, 2.0 Hz, 1 H) 5.68-5.64 (dm, 2 H) 5.62-5.56 (comp, 2 H) 4.67-4.65

(m, 1 H) 4.61 (dt, $J = 10.0, 2.0$ Hz, 1 H) 3.78-3.72 (m, 1 H) 3.61-3.55 (m, 1 H) 2.39 (s, 3 H) 1.93 (dd, $J = 14.8, 2.4$ Hz, 1 H) 1.43 (dd, $J = 14.4$ Hz, 3.6 Hz, 1 H) 1.10 (t, $J = 7.8$ Hz, 3 H) 0.90 (s, 9 H) 0.10 (s, 6 H); ^{13}C -NMR (100 MHz, CDCl_3) δ 143.9, 136.0, 135.9, 135.3, 133.7, 132.6, 130.0, 129.5, 127.2, 127.2, 126.3, 125.7, 124.0, 83.6, 63.3, 62.3, 37.8, 37.7, 26.0, 21.5, 18.4, 14.7, -4.3; IR (thin film) 3026, 2955, 2928, 2885, 2856 cm^{-1} ; HRMS (ESI) m/z 548.22686 [$\text{C}_{29}\text{H}_{39}\text{NNaO}_4\text{S}$ ($\text{M}+\text{Na}$) $^+$ 548.22613].



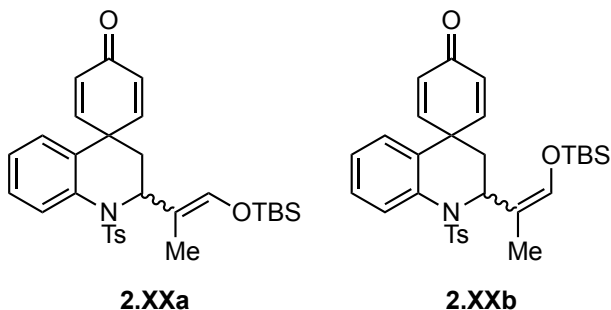
2'-(but-3-en-2-yl)-1'-tosyl-2',3'-dihydro-1'H-spiro[cyclohexane-1,4'-quinoline]-2,5-dien-4-one. (2.147). (WLM6_79). Freshly distilled boron trifluoride etherate (651 mg, 4.59 mmol, 0.56 mL) was added dropwise to a solution of **2.14** (940 mg, 2.30 mmol) and **2.158** (782 mg, 4.59 mmol) in dry MeCN (11.5 mL) at 0 °C, and the reaction was stirred for 6 h at 0 °C. The reaction mixture was quenched with saturated aq NaHCO_3 (5.0 mL) and stirred at room temperature for 10 min. The reaction mixture was diluted with H_2O (20 mL) and extracted with CH_2Cl_2 (3 x 20 mL). The combined organic extracts were washed with brine (40 mL), dried (Na_2SO_4), filtered, and concentrated *in vacuo* to afford a yellow oil. Subsequent purification by flash chromatography eluting with Hexanes : EtOAc (3 : 1) provided 934 mg (97%) of **2.147** as a white solid: ^1H -NMR (400 MHz, CDCl_3) δ 7.84 (d, $J = 8.0$ Hz, 0.4 H) 7.78 (d, $J = 8.0$ Hz, 0.6 H) 7.41-7.40 (comp, 1 H) 7.29-7.20 (comp, 3 H) 7.10-7.09 (comp, 1 H) 6.85 (d, $J = 7.2$ Hz, 1.2 H)

6.80 (d, $J = 10.4$ Hz, 0.8 H) 6.21 (d, $J = 10.0$ Hz, 0.6 H) 6.15 (d, $J = 10.0$ Hz, 0.4 H) 5.86-5.64 (comp, 2 H) 5.43 (d, $J = 9.2$ Hz, 0.6 H) 5.33 (d, $J = 9.6$ Hz, 0.4 H) 5.06-4.82 (comp, 2 H) 4.19 (comp, 1 H) 2.58 (m, 0.6 H) 2.49 (m, 0.4 H) 1.90-1.80 (comp, 2 H) 1.09 (d, $J = 6.4$ Hz, 1.2 H) 1.00 (d, $J = 6.0$ Hz, 1.8 H); ^{13}C -NMR (100 MHz, CDCl_3) δ 185.2, 185.1, 153.5, 152.9, 152.9, 152.8, 144.3, 144.3, 140.1, 139.2, 136.4, 136.3, 134.6, 134.2, 129.9, 129.8, 129.5, 129.3, 128.7, 128.6, 128.2, 128.1, 127.5, 127.4, 127.0, 126.9, 126.6, 126.5, 126.3, 117.2, 115.4, 57.8, 41.9, 41.6, 40.8, 40.6, 32.7, 32.5, 21.6, 18.1, 15.3; HRMS (ESI) m/z observed 442.14470 [$\text{C}_{25}\text{H}_{25}\text{NO}_3\text{S}$ ($\text{M}+\text{Na}$) $^+$ requires 442.14470].



2-(4-oxo-1'-tosyl-2',3'-dihydro-1'H-spiro[cyclohexane-1,4'-quinoline]-2,5-dien-2'-yl)propanal. (2.162). (WLM6_88). Sodium periodate (224 mg, 1.048 mmol) was added to a solution of **2.147** (110 mg, 0.262 mmol), 2,6-lutidine (55 mg, 0.524 mmol, 59 μL), and $\text{K}_2\text{OsO}_4 \cdot 2\text{H}_2\text{O}$ (5 mg, 0.0131 mmol) in dioxane/ H_2O (4:1) (5.2 mL) at room temperature. After 12 h, the reaction mixture was diluted with H_2O (10 mL) and extracted with CH_2Cl_2 (3 x 15 mL). The combined organic extracts were washed with brine (20 mL), dried (Na_2SO_4), filtered, and concentrated *in vacuo* to afford a brown oil. Subsequent purification by flash chromatography eluting with Hexanes : EtOAc (3 : 2) provided 89 mg (81%) of **2.162** as a white solid: ^1H -NMR (400 MHz, CDCl_3) δ 9.72 (d, $J = 2.0$ Hz, 0.5 H) 9.70 (d, $J = 2.0$ Hz, 0.5 H) 7.90 (d, $J = 8.8$ Hz, 0.5 H) 7.84 (d, $J = 8.8$ Hz, 0.5 H) 7.46 (d, $J = 8.4$ Hz, 1 H) 7.42 (d, $J = 8.4$ Hz, 1 H) 7.35 (dt, $J = 8.0, 2.0$ Hz, 1

H) 7.26 (d, $J = 8.8$ Hz, 2 H) 7.16 (t, $J = 8.0$ Hz, 1 H) 6.89 (dd, $J = 8.0, 2.0$ Hz, 1 H) 6.78 (dd, $J = 10.8, 3.2$ Hz, 0.5 H) 6.71 (dd, $J = 10.8, 3.2$ Hz, 0.5 H) 6.26 (dd, $J = 10.8, 1.6$ Hz, 0.5 H) 6.24 (dd, $J = 10.8, 1.6$ Hz, 0.5 H) 5.85 (dd, $J = 10.4, 1.6$ Hz, 0.5 H) 5.83 (dd, $J = 10.4, 1.6$ Hz, 0.5 H) 5.35 (dd, $J = 10.4, 2.8$ Hz, 0.5 H) 5.30 (dd, $J = 10.4, 2.8$ Hz, 0.5 H) 4.70 (q, $J = 6.0$ Hz, 0.5 H) 4.59 (q, $J = 6.0$ Hz, 0.5 H) 2.97 (m, 0.5 H) 2.82 (m, 0.5 H) 2.41 (s, 3 H) 1.95-1.80 (comp, 2 H) 1.23 (d, $J = 7.2$ Hz, 1.5 Hz) 1.14 (d, $J = 7.2$ Hz, 1.5 Hz); ^{13}C -NMR (100 MHz, CDCl_3) δ 202.4, 201.9, 185.1, 185.0, 152.2, 152.2, 151.9, 145.0, 144.9, 135.8, 135.5, 134.2, 130.2, 129.7, 129.6, 129.2, 129.1, 128.5, 128.3, 128.2, 128.0, 127.6, 127.6, 127.5, 127.3, 127.1, 127.0, 54.2, 53.9, 49.8, 49.5, 41.7, 41.7, 35.0, 32.7, 21.8, 21.7, 11.8, 10.0; HRMS (ESI) m/z observed 444.12470 [$\text{C}_{24}\text{H}_{23}\text{NO}_4\text{S}$ ($\text{M}+\text{Na}$) $^+$ requires 444.12400].

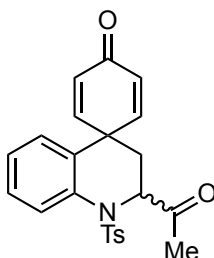


2'-(1-((*tert*-butyldimethylsilyl)oxy)prop-1-en-2-yl)-1'-tosyl-2',3'-dihydro-1'*H*-spiro[cyclohexane-1,4'-quinoline]-2,5-dien-4-one. (2.165). (WLM6_83). Freshly distilled *tert*-butyldimethylsilyl triflate (226 mg, 0.854 mmol) was added to a solution of **2.162** (36 mg, 0.85 mmol) and imidazole (87 mg, 1.281 mmol) in dry CH_2Cl_2 (0.85 mL), and the reaction was stirred at room temperature overnight. The reaction was quenched with saturated aq NaHCO_3 (1.0 mL) and stirred at room temperature for 10 min. The reaction mixture was diluted with H_2O (5 mL) and extracted with CH_2Cl_2 (3 x 5 mL). The combined organic extracts were washed with brine (10 mL), dried (Na_2SO_4), filtered, and

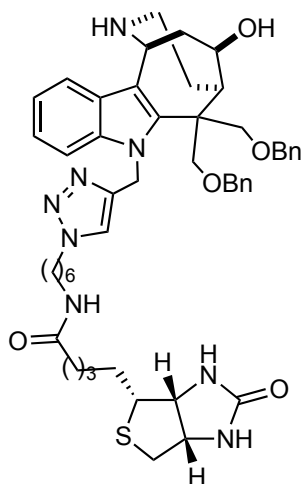
concentrated *in vacuo* to afford a brown oil. Subsequent purification by flash chromatography eluting with Hexanes : EtOAc (6 : 1) provided 29 mg (63%) of **2.165** as a clear oil:

2.165a: $^1\text{H-NMR}$ (400 MHz, CDCl_3) δ 7.70 (dd, $J = 8.0, 1.0$ Hz, 1 H) 7.59 (d, $J = 8.4$ Hz, 2 H) 7.30-7.26 (comp, 3 H) 7.07 (td, $J = 7.6, 1.2$ Hz, 1 H) 6.90 (dd, $J = 8.0, 1.6$, 1 H) 6.82 (dd, $J = 10.0, 3.0$ Hz, 1 H) 6.33-6.27 (comp, 3 H) 6.11 (dd, $J = 10.0, 2.0$ Hz, 1 H) 4.90 (t, $J = 7.2$ Hz, 1 H) 2.42 (s, 3 H) 2.01 (dd, $J = 13.6, 7.6$ Hz, 1 H) 1.82 (dd, $J = 14.0, 6.4$ Hz, 1 H) 1.47 (d, $J = 1.2$ Hz, 3 H) 0.85 (s, 9 H) 0.06 (s, 3 H) 0.04 (s, 3 H); $^{13}\text{C-NMR}$ (100 MHz, CDCl_3) δ 185.7, 152.4, 151.3, 144.2, 139.1, 137.3, 136.3, 129.9, 129.7, 128.9, 128.5, 128.4, 127.8, 127.5, 125.9, 125.7, 114.3, 56.3, 43.1, 37.7, 25.7, 21.8, 18.3, 9.8, -5.1, -5.2; HRMS (ESI) m/z observed 558.21060 [$\text{C}_{30}\text{H}_{37}\text{NO}_4\text{SSi}$ ($\text{M}+\text{Na}$) $^+$ requires 558.21050].

2.165b: $^1\text{H-NMR}$ (400 MHz, CDCl_3) δ 7.97 (d, $J = 7.2$ Hz, 1 H) 7.50 (d, $J = 8.0$ Hz, 2 H) 7.34 (td, $J = 8.0, 3.2$ Hz, 1 H) 7.23 (d, $J = 8.0$ Hz, 2 H) 7.09 (td, $J = 7.2, 1.2$ Hz, 1 H) 6.89 (dd $J = 7.6, 1.2$ Hz, 1 H) 6.76 (dd, $J = 10.0, 3.2$ Hz, 1 H) 6.35 (dd, $J = 10.0, 1.6$ Hz, 1 H) 6.06 (s, 1 H) (dd) (dd) 5.21 (dd, $J = 10.4, 6.8$ Hz, 1 H) 2.41 (s, 3 H) 1.91 (dd, $J = 13.2, 6.8$ Hz, 1 H) 1.84 (dd, $J = 13.6, 6.8$ Hz, 1 H) 1.52 (d, $J = 1.2$ Hz, 3 H) 0.92 (9 H) 0.20 (s, 3 H) 0.10 (s, 3 H); $^{13}\text{C-NMR}$ (100 MHz, CDCl_3) δ 185.6, 152.7, 150.1, 144.4, 136.4, 135.4, 135.0, 131.8, 129.9, 129.5, 128.8, 127.9, 127.7, 127.0, 125.6, 117.2, 52.5, 43.6, 39.3, 29.9, 25.7, 21.7, 18.2, 12.7, -5.0, -5.1; IR (thin film) 2953, 2928, 2856, 1670 cm^{-1} ; HRMS (ESI) m/z observed 558.21040 [$\text{C}_{30}\text{H}_{37}\text{NO}_4\text{SSi}$ ($\text{M}+\text{Na}$) $^+$ requires 558.21050].

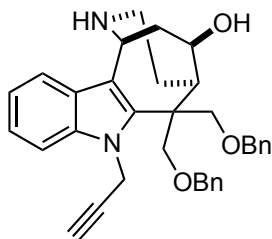


2'-acetyl-1'-tosyl-2',3'-dihydro-1'H-spiro[cyclohexane-1,4'-quinoline]-2,5-dien-4-one. (2.112). (WLM6_49). Sodium periodate (40 mg, 0.185 mmol) was added to a solution of **2.165** (20 mg, 0.037 mmol) and $\text{K}_2\text{OsO}_4 \cdot 2\text{H}_2\text{O}$ (0.7 mg, 0.00187 mmol) in acetone/ H_2O (10:1) (0.4 mL) at room temperature. After 5 h, the reaction mixture was diluted with H_2O (5 mL) and extracted with CH_2Cl_2 (3 x 5 mL). The combined organic extracts were washed with brine (5 mL), dried (Na_2SO_4), filtered, and concentrated *in vacuo* to afford a brown oil. Subsequent purification by flash chromatography eluting with Hexanes : EtOAc (1 : 1) provided 12 mg (79%) of **2.112** as a white solid: ^1H -NMR (400 MHz, CDCl_3) δ 8.06 (d, J = 8.8 Hz, 1 H) 7.48 (d, J = 8.0 Hz, 2 H) 7.38 (td, J = 7.2, 1.6 Hz, 1 H) 7.28 (d, J = 8.0 Hz, 2 H) 7.15 (t, 7.2, 1 H) 6.89 (dd, J = 8.0, 1.6 Hz, 1 H) 6.73 (dd, J = 10.0, 3.2 Hz, 1 H) 6.25 (dd, J = 10.0, 1.6 Hz, 1 H) 5.83 (dd, J = 10.0, 1.6 Hz, 1 H) 5.21 (dd, J = 10.4, 3.2 Hz, 1 H) 4.72 (t, J = 6.4 Hz, 1 H) 2.42 (s, 3 H) 2.33 (s, 3 H) 2.25 (dd, J = 14.0, 6.4 Hz, 1 H) 1.90 (dd, J = 14.0, 6.4 Hz, 1 H); ^{13}C -NMR (125 MHz, CDCl_3) δ 206.5, 184.9, 152.4, 151.1, 145.1, 134.8, 134.2, 130.1, 129.1, 129.1, 128.4, 127.7, 127.5, 127.4, 126.8, 126.7, 62.3, 41.5, 32.9, 26.3, 21.6; HRMS (ESI) m/z observed 430.10780 [$\text{C}_{23}\text{H}_{21}\text{NO}_4\text{S}$ ($\text{M}+\text{Na}$) $^+$ requires 430.10830].



***N*-(6-(4-(((1*S*/*R*, 5*R*/*S*, 12*R*/*S*)-6,6-bis((benzyloxy)methyl)-12-hydroxy-3,4,5,6-tetrahydro-1*H*-5,1-ethanoazocino[4,3-*b*]indol-7(2*H*)-yl)methyl)-1*H*-1,2,3-triazol-1-yl)hexyl)-5-((3*aR*,4*R*,6*aS*)-2-oxohexahydro-1*H*-thieno[3,4-*d*]imidazol-4-yl)pentanamide. (4.10). (WLM7_270_2).** NEt₃•3HF (0.1 mL) was added to a solution of **4.21** (11.5 mg, 0.012 mmol) in CH₂Cl₂ (0.1 mL) in a plastic vial. The reaction was stirred at room temperature for 36 h, whereupon excess NEt₃•3HF was quenched with SiO₂ (spatula tip). The reaction mixture was diluted with MeOH (1.0 mL) and filtered through a sub-micron syringe filter. Subsequent purification by RP HPLC H₂O : MeCN (10% MeCN → 95% MeCN over 30 min) provided 8.1 mg (79%) of **4.10** as a white solid: ¹H-NMR (500 MHz, CD₃OD) δ 7.60 (m, 1 H) 7.25-7.21 (comp, 7 H) 7.17-7.13 (comp, 5H) 7.13-7.08 (comp, 2H) 5.82 (d, *J* = 12.5 Hz, 1 H) 5.47 (d, 12.0 Hz, 1 H) 5.31 (d, *J* = 5.0 Hz, 1 H) 4.49-4.44 (m, 1 H) 4.41 (d, *J* = 11.0 Hz, 1 H) 4.35 (d, *J* = 12.0 Hz, 2 H) 4.30-4.24 (m, 1 H) 4.21 (d, *J* = 10.5 Hz, 1 H) 4.14-4.05 (comp, 3 H) 3.99 (d, *J* = 11.0 Hz, 1 H) 3.95 (d, *J* = 9.5 Hz, 1 H) 3.20-3.15 (comp, 2 H) 3.06 (t, *J* = 7.0 Hz, 2 H) 3.02-2.94 (comp, 3 H) 2.93-2.87 (m, 1 H) 2.68 (t, *J* = 13.0 Hz, 1 H) 2.28 (dm, *J* = 15.5 Hz, 1 H), 2.20-2.15 (comp, 3 H) 1.93 (m, 1 H) 1.74-1.55 (comp, 6 H) 1.45-1.34 (comp, 4 H) 1.23 (m, 2 H) 1.14 (m, 2 H); ¹³C-NMR (125 MHz, CD₃OD) δ 175.9, 166.1, 146.3, 141.7,

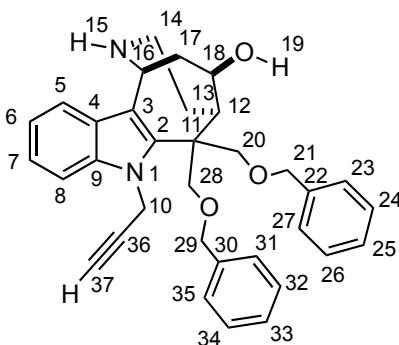
139.2, 139.0, 138.9, 129.5, 129.4, 128.9, 128.8, 128.8, 128.7, 127.6, 124.0, 123.7, 121.6, 118.5, 114.9, 111.4, 110.3, 76.6, 75.4, 74.6, 74.2, 74.1, 63.4, 61.6, 57.2, 51.4, 51.2, 50.8, 49.9, 43.7, 42.0, 41.0, 40.2, 40.1, 36.8, 31.0, 30.2, 29.8, 29.5, 28.9, 27.5, 27.2, 27.0; HRMS (ESI) m/z observed 911.45980 [$C_{50}H_{64}N_8O_5S$ ($M+Na$)⁺ requires 911.46130].



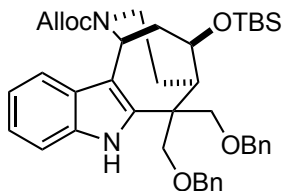
(1*S*/R, 5*R*/S, 12*R*/S)-6,6-bis((benzyloxy)methyl)-7-(prop-2-yn-1-yl)-2,3,4,5,6,7-hexahydro-1*H*-5,1-ethanoazocino[4,3-*b*]indol-12-ol. (4.11). (WLM7_279_2).

NEt₃•3HF (0.05 mL) was added to a solution of **4.15** (12 mg) in CH₂Cl₂ (0.1 mL) in a plastic vial. The reaction was stirred at room temperature for 36 h, whereupon excess NEt₃•3HF was quenched with SiO₂ (spatula tip). The reaction mixture was diluted with MeOH (1.0 mL) and filtered through a sub-micron syringe filter. Subsequent purification by RP HPLC H₂O : MeCN (10% MeCN → 95% MeCN over 30 min) provided 4 mg (38%) of **4.15** as a white solid: ¹H-NMR (500 MHz, CD₃OD) δ 7.57 (d, J = 8.0 Hz, 1 H) 7.47 (d, J = 8.5 Hz, 1 H) 7.29-7.16 (comp, 12 H) 5.36 (dd, J = 9.0, 2.0 Hz, 1 H) 5.26 (d, J = 5.5 Hz, 1 H) 4.87 (dd, J = 9.0, 2.0 Hz, 1 H) 4.59 (d, J = 12.0 Hz, 1 H) 4.53 (d, J = 12.0 Hz, 1 H) 4.50 (d, J = 12.0 Hz, 1 H) 4.45 (d, J = 12.0 Hz, 1 H) 4.38 (td, J = 9.0, 2.0 Hz, 1 H) 4.18 (d, J = 10.5 Hz, 1 H) 4.09 (d, J = 10.5 Hz, 3 H) 2.95-2.87 (comp, 4 H) 2.68 (t, J = 2.5 Hz, 1 H) 2.25 (m, 1 H) 2.11 (dd, J = 14.0, 9.0 Hz, 1 H) 1.91 (m, 1 H); ¹³C-NMR (150 MHz, CD₃OD) δ 141.2, 139.2, 139.0, 138.6, 129.4, 129.4, 129.2, 128.9, 128.8, 127.3, 124.0, 121.7, 118.3, 111.3, 110.1, 80.1, 77.0, 76.0, 75.3, 74.5, 74.4, 74.3, 51.0, 50.7, 49.8,

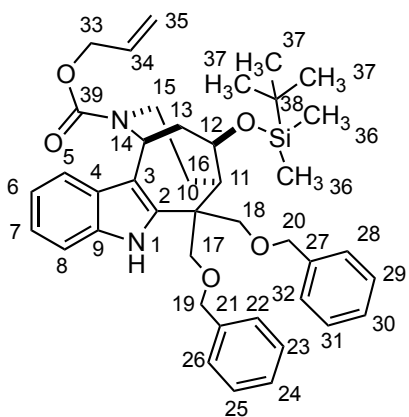
41.9, 39.5, 36.9, 28.8; HRMS (ESI) m/z observed 543.26130 [$C_{34}H_{36}N_2O_3$ (M+Na) $^+$ requires 543.26180].



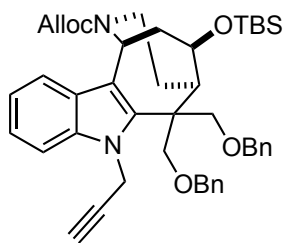
Assignments: 1H -NMR (500 MHz, CD_3OD) δ 7.57 (d, J = 8.0 Hz, 1 H, C5-H) 7.47 (d, J = 8.5 Hz, 1 H, C8-H) 7.29-7.16 (comp, 12 H) 5.36 (dd, J = 9.0, 2.0 Hz, 1 H, C10-H) 5.26 (d, J = 5.5 Hz, 1 H, C16-H) 4.87 (dd, J = 9.0, 2.0 Hz, 1 H, C10-H) 4.59 (d, J = 12.0 Hz, 1 H, C21-H or C29-H) 4.53 (d, J = 12.0 Hz, 1 H, C21-H or C29-H) 4.50 (d, J = 12.0 Hz, 1 H, C21-H or C29-H) 4.45 (d, J = 12.0 Hz, 1 H, C21-H or C29-H) 4.38 (td, J = 9.0, 2.0 Hz, 1 H, C18-H) 4.18 (d, J = 10.5 Hz, 1 H, C20-H or C28-H) 4.09 (d, J = 10.5 Hz, 3 H, C20-H₂ or C28-H₂) 2.95-2.87 (comp, 4 H, C12-H, C15-H₂, and C17-H) 2.68 (t, J = 2.5 Hz, 1 H, C37-H) 2.25 (m, 1 H, C13-H) 2.11 (dd, J = 14.0, 9.0 Hz, 1 H, C17-H) 1.91 (m, 1 H, C13-H); ^{13}C -NMR (150 MHz, CD_3OD) δ 141.2, 139.2, 139.0, 138.6, 129.4, 129.4, 129.2, 128.9, 128.8, 127.3, 124.0 (C7), 121.7 (C6), 118.3 (C5), 111.3 (C8), 110.1 (C3), 80.1 (C37), 77.0 (C36), 76.0 (C20 or C28), 75.3 (C20 or C28), 74.5 (C18), 74.4 (C21 or C29), 74.3 (C21 or C29), 51.0 (C11), 50.7 (C16), 49.8 (C12), 41.9 (C14), 39.5 (C17), 36.9 (C10), 28.8 (C13).



(1R/S, 5R/S, 12R/S)-Allyl-6,6-bis((benzyloxy)methyl)-12-((tert-butyltrimethylsilyl)oxy)-3,4,5,6-tetrahydro-1H-5,1-ethanoazocino[4,3-b]indole-2(7H)-carboxylate. (**4.13**). (WLM7_123_2_frac1). A mixture of **4.12** (33 mg, 0.058 mmol) and freshly distilled 2,6-lutidine (31 mg, 0.291 mmol, 33 μ L) in CH₂Cl₂ (0.6 mL) at room temperature under N₂ was added freshly distilled *tert*-butyltrimethylsilyl trifluoromethanesulfonate (39 mg, 0.146 mmol, 33 μ L) and the reaction was stirred for 2 h at room temperature. The reaction was quenched with saturated aq NaHCO₃ (1.0 mL), diluted with H₂O (1.0 mL), and extracted with CH₂Cl₂ (3 x 1.5 mL). The combined organic extracts were washed with brine (3.0 mL), dried (Na₂SO₄), filtered, and concentrated *in vacuo* to afford a clear oil. Subsequent purification by flash chromatography Hexanes : EtOAc (5 : 1) afforded 36 mg (91%) of **4.13** as a clear oil: ¹H-NMR (500 MHz, CD₃CN, 70 °C) δ 9.29 (br, 1 H) 7.39 (d, *J* = 8.0 Hz, 1 H) 7.37-7.20 (comp, 11 H) 7.10 (app t, *J* = 8.0 Hz, 1 H) 7.03 (app t, *J* = 7.0 Hz, 1 H) 6.03 (br, 1 H) 5.56 (d, *J* = 6.5 Hz, 1 H) 5.35 (br, 1 H) 5.23 (br, 1 H) 4.65 (m, 2 H) 4.62 (d, *J* = 12.0 Hz, 1 H) 4.59 (d, *J* = 12.0 Hz, 1 H) 4.50 (d, *J* = 12.5 Hz, 1 H) 4.47 (d, *J* = 12.5 Hz, 1 H) 4.36 (t, *J* = 9.0 Hz, 1 H) 4.28 (d, *J* = 9.5 Hz, 1 H) 4.06 (d, *J* = 9.5 Hz, 1 H) 3.93 (d, *J* = 9.5 Hz, 1 H) 3.80 (m, 1 H) 3.68 (d, *J* = 9.5 Hz, 1 H) 2.96 (m, 1 H) 2.69 (m, 1 H) 2.62 (m, 1 H) 1.98-1.96 (m, 1 H) 1.89-1.85 (m, 1 H) 1.80-1.73 (m, 1 H) 0.85 (s, 9 H) 0.03 (s, 3 H) 0.03 (s, 3 H); ¹³C-NMR (125 MHz, CD₃CN, 70 °C) δ 156.4, 141.2, 140.2, 140.1, 136.9, 135.2, 129.7, 129.5, 129.4, 129.1, 129.0, 128.9, 128.8, 128.8, 128.7, 128.5, 127.6, 122.7, 120.5, 118.3, 117.4, 113.1, 112.1, 77.3, 74.5, 74.5, 74.3, 72.5, 66.6, 48.7, 48.3, 47.7, 41.9, 31.1, 26.6, 18.9, -4.3, -4.4; HRMS (CI) *m/z* observed 680.3644 [C₄₁H₅₂N₂O₅Si (M)⁺ requires 680.3646].

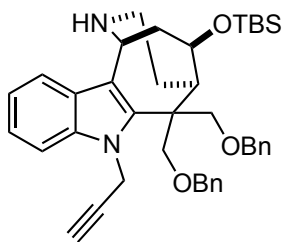


Assignments: ^1H -NMR: δ 9.29 (br, 1 H, N1-H) 7.39 (d, $J = 8.0$ Hz, 1 H, C5-H) 7.37-7.20 (comp, 11 H, C8-H, C22-H, C23-H, C24-H, C25-H, C26-H, C28-H, C29-H, C30-H, C31-H, C32-H) 7.10 (app t, $J = 8.0$ Hz, 1 H, C7-H) 7.03 (app t, $J = 7.0$ Hz, 1 H, C6-H) 6.03 (br, 1 H, C34-H) 5.56 (d, $J = 6.5$ Hz, 1 H, C14-H) 5.35 (br, 1 H, C35-H) 5.23 (br, 1 H, C35-H) 4.65 (m, 2 H, C33-H₂) 4.62 (d, $J = 12.0$ Hz, 1 H, C19-H or C20-H) 4.59 (d, $J = 12.0$ Hz, 1 H, C19-H or C20-H) 4.50 (d, $J = 12.5$ Hz, 1 H, C19-H or C20-H) 4.47 (d, $J = 12.5$ Hz, 1 H, C19-H or C20-H) 4.36 (t, $J = 9.0$ Hz, 1 H, C12-H) 4.28 (d, $J = 9.5$ Hz, 1 H, C18-H) 4.06 (d, $J = 9.5$ Hz, 1 H, C17-H) 3.93 (d, $J = 9.5$ Hz, 1 H, C17-H) 3.80 (m, 1 H, C15-H) 3.68 (d, $J = 9.5$ Hz, 1 H, C18-H) 2.96 (m, 1 H, C13-H) 2.69 (m, 1 H, C15-H) 2.62 (m, 1 H, C11-H) 1.98-1.96 (m, 1 H, C16-H) 1.89-1.85 (m, 1 H, C13-H) 1.80-1.73 (m, 1 H, C16-H) 0.85 (s, 9 H, C37-CH₃) 0.03 (s, 3 H, C36-CH₃) 0.03 (s, 3 H, C36-CH₃); ^{13}C -NMR: δ 156.4 (C39), 141.2, 140.2, 140.1, 136.9, 135.2, 129.7, 129.5, 129.4, 129.1, 129.0, 128.9, 128.8, 128.8, 128.7, 128.5, 127.6, 122.7 (C7), 120.5 (C6), 118.3 (C5), 117.4, 113.1, 112.1 (C8), 77.3 (C12), 74.5 (C17 or C19 or C20), 74.5 (C17 or C19 or C20), 74.3 (C17 or C19 or C20), 72.5 (C18), 66.6 (C33), 48.7 (C10), 48.3 (C14), 47.7 (C11), 41.9 (C15), 31.1 (C16), 26.6 (C37), 18.9 (C38), -4.3 (C36), -4.4 (C36).



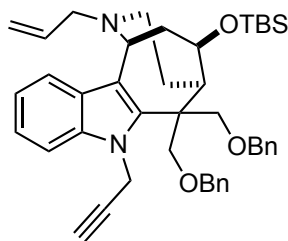
(1*S*/*R*, 5*R*/*S*, 12*R*/*S*)-allyl 6,6-bis((benzyloxy)methyl)-12-((*tert*-butyldimethylsilyl)oxy)-7-(prop-2-yn-1-yl)-3,4,5,6-tetrahydro-1*H*-5,1-ethanoazocino[4,3-*b*]indole-2(7*H*)-carboxylate. (**4.14**). (WLM7_257_2). A mixture of **4.13** (150 mg, 0.22 mmol) and 60% NaH dispersion in mineral oil (18 mg, 0.44 mmol) in DMF (1.1 mL) at 0 °C under N₂ was stirred for five min and propargyl bromide (131 mg of 80% solution in toluene, 0.88 mmol, 95 μ L) was added in one portion. After 1 h, the reaction was quenched with saturated aq NaHCO₃ (1.5 mL), diluted with H₂O (1.5 mL), and extracted with EtOAc (3 x 20 mL). The combined organic extracts were washed with brine (25 mL), dried (Na₂SO₄), filtered, and concentrated *in vacuo* to afford a clear oil. Purification by flash chromatography eluting with Hexanes : EtOAc (10 : 1) to provide 155 mg (98%) of **4.14** as a clear oil: ¹H-NMR (500 MHz, CD₃CN, rotamers) δ 7.41-7.07 (comp, 14 H) 6.09-6.03 (m, 0.5 H) 5.98-5.92 (m, 0.5 H) 5.74 (d, *J* = 2.5 Hz, 0.5 H) 5.70 (d, *J* = 2.5 Hz, 0.5 H) 5.57 (d, *J* = 7.0 Hz, 0.5 H) 5.54 (d, *J* = 7.0 Hz, 0.5 H) 5.39 (d, *J* = 17.5 Hz, 0.5 H) 5.48 (d, *J* = 12.0 Hz, 1 H) 5.16 (d, *J* = 11.0 Hz, 0.5 H) 4.89 (d, *J* = 2.5 Hz, 0.5 H) 4.86 (d, *J* = 2.5 Hz, 0.5 H) 4.74-4.70 (m, 0.5 H) 4.63 (m, 1 H) 4.59-4.50 (comp, 2.5 H) 4.49-4.44 (comp, 2 H) 4.32 (d, *J* = 10.0 Hz, 1 H) 4.29 (m, 1 H) 4.13 (d, *J* = 10.0 Hz, 1 H) 3.97 (d, *J* = 10.0 Hz, 1 H) 3.92 (dd, *J* = 10.0, 3.0 Hz, 1 H) 3.77 (dd, *J* = 14.0, 6.0 Hz, 1 H) 3.71 (dd, *J* = 14.0, 6.0 Hz, 1 H) 2.85 (m, 1 H) 2.72 (m, 1 H) 2.57 (td, *J* = 13.5, 4.0 Hz, 0.5 H) 2.52 (m, 1 H) 2.49 (td, *J* = 13.5, 4.0 Hz, 0.5 H) 1.89-1.70 (comp, 3 H) 0.834 (s, 9 H) 0.01 (s, 6 H); ¹³C-NMR (125 MHz, CD₃CN, rotamers) δ 155.8, 141.0, 140.8, 139.4, 138.2, 134.9, 129.3, 129.2, 128.8, 128.8, 128.5, 128.5, 127.3, 123.2, 121.0,

117.4, 116.9, 115.5, 110.9, 81.0, 76.5, 75.2, 74.0, 73.9, 73.7, 73.3, 66.4, 66.1, 50.7, 50.7, 48.3, 48.1, 41.6, 41.2, 40.1, 37.3, 32.6, 31.33, 30.7, 30.4, 26.3, 18.6, -4.7, -4.7; HRMS (ESI) m/z observed 741.36900 [$C_{44}H_{54}N_2O_5Si$ ($M+Na$) $^+$ requires 741.36940].



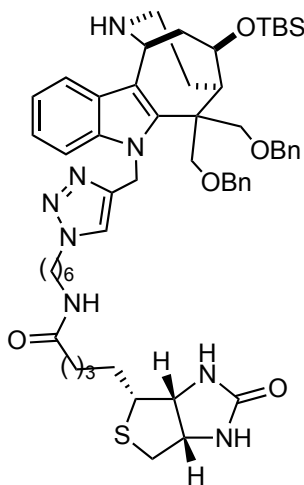
(1*S*/*R*, 5*R*/*S*, 12*R*/*S*)-6,6-bis((benzyloxy)methyl)-12-((*tert*-butyldimethylsilyl)oxy)-7-(prop-2-yn-1-yl)-2,3,4,5,6,7-hexahydro-1*H*-5,1-ethanoazocino[4,3-*b*]indole. (**4.15**). (WLM7_258_2). A round bottom flask charged with $Pd_2(dba)_3$ (2.0 mg, 0.0022 mmol) and 1,4-bis(diphenylphosphino)butane (1.8 mg, 0.0043 mmol) was placed under vacuum and backfilled with N_2 three times. A second round bottom flask was charged with **4.14** (155 mg, 0.22 mmol) and 1,3-dimethylbarbituric acid (337 mg, 2.16 mmol) and placed under vacuum and backfilled with N_2 three times. THF (1.0 mL) was then added to both flasks, and the mixtures were stirred at room temperature under N_2 for 5 min. The Pd/ligand mixture was added via syringe to the flask containing **4.15**, and stirring was continued at room temperature until **4.15** was gone by TLC. The reaction was quenched with saturated aq $NaHCO_3$ (2.0 mL) and stirred at room temperature for 15 min. The reaction mixture was diluted with H_2O (10 mL) extracted with CH_2Cl_2 (3 x 20 mL). The combined organic extracts were washed with brine (25 mL), dried (Na_2SO_4), filtered, and concentrated *in vacuo* to afford a brown oil. Subsequent purification by flash chromatography eluting with Hexanes : EtOAc (1 : 1 to 100% EtOAc) provided 31 mg (27%) of **4.15** and 37 mg (25%) of **4.16** as a white solids: 1H -NMR (500 MHz, $CDCl_3$) δ 7.65 (d, J = 8.0 Hz, 1 H) 7.41 (d, J = 8.5 Hz, 1 H)

7.33-7.14 (comp, 12 H) 5.77 (dd, $J = 9.0, 2.5$ Hz, 1 H) 5.29 (br, 1 H) 4.73 (dd, $J = 9.0, 2.5$ Hz, 1 H) 4.69 (app t, $J = 9.0$ Hz, 1 H) 4.60 (d, $J = 12.0$ Hz, 1 H) 4.57 (d, $J = 12.0$ Hz, 1 H) 4.46 (d, $J = 12.5$ Hz, 1 H) 4.41 (d, $J = 11.5$ Hz, 1 H) 4.26 (d, $J = 9.5$ Hz, 1 H) 4.11 (d, $J = 10.5$ Hz, 1 H) 3.97 (d, $J = 10.0$ Hz, 1 H) 3.96 (d, $J = 10.5$ Hz, 1 H) 3.03 (comp, 3 H) 2.81 (comp, 2 H) 2.21 (app t, $J = 2.5$ Hz, 1 H) 2.17-2.10 (comp, 2 H) 0.84 (s, 9 H) 0.06 (s, 3 H) 0.03 (s, 3 H); ^{13}C -NMR (125 MHz, CDCl_3) δ 140.89, 137.90, 137.73, 137.45, 128.56, 128.54, 128.18, 127.98, 127.89, 127.84, 123.28, 121.05, 118.04, 109.97, 109.18, 79.59, 77.73, 74.70, 73.98, 73.64, 73.57, 72.85, 72.36, 50.00, 49.32, 48.37, 40.36, 39.40, 36.74, 27.16, 25.94, -4.89, -5.08. HRMS (ESI) m/z observed 657.34680 [$\text{C}_{43}\text{H}_{50}\text{N}_2\text{O}_3\text{Si}$ ($\text{M}+\text{Na}$) $^+$ requires 657.34830].



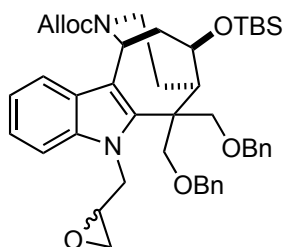
(1*S*/*R*, 5*R*/*S*, 12*R*/*S*)-2-allyl-6,6-bis((benzyloxy)methyl)-12-((*tert*-butyldimethylsilyl)oxy)-7-(prop-2-yn-1-yl)-2,3,4,5,6,7-hexahydro-1*H*-5,1-ethanoazocino[4,3-*b*]indole. (4.16). (WLM7_258_2). ^1H -NMR (500 MHz, CD_3CN) δ 7.46 (d, $J = 8.0$ Hz, 1 H) 7.34 (d, $J = 8.5$ Hz, 1 H) 7.31-7.16 (comp, 11 H) 7.07 (td, $J = 7.0, 2.0$ Hz, 1 H) 5.96 (m, 1 H) 5.79 (dd, $J = 9.0, 2.5$ Hz, 1 H) 5.28 (dm, $J = 17.0$ Hz, 1 H) 5.15 (dd, $J = 10.5, 1.5$ Hz, 1 H) 4.84 (dd, $J = 9.0, 2.5$ Hz, 1 H) 4.58 (d, $J = 12.0$ Hz, 1 H) 4.55 (d, $J = 12.0$ Hz, 1 H) 4.50 (td, $J = 9.0, 2.0$ Hz, 1 H) 4.44 (d, $J = 12.0$ Hz, 1 H) 4.41 (d, $J = 12.0$ Hz, 1 H) 4.38 (d, $J = 9.5$ Hz, 1 H) 4.05 (d, $J = 10.0$ Hz, 1 H) 3.95 (d, $J = 9.5$ Hz, 1 H) 3.93 (d, $J = 10.0$ Hz, 1 H) 3.28-3.23 (m, 1 H) 2.99-2.95 (m, 1 H) 2.68 (m, 1 H) 2.56 (ddd, $J = 13.5, 8.5, 7.0$ Hz, 1 H) 2.50 (t, $J = 2.5$ Hz, 1 H) 2.39 (dd, $J = 12.5, 10.5$

Hz, 1 H) 2.07 (td, $J = 12.5, 3.5$ Hz, 1 H) 1.96 (m, 1 H) 1.78-1.68 (comp, 2 H) 0.84 (s, 9 H) 0.03 (s, 6 H); ^{13}C -NMR (125 MHz, CD_3CN) δ 140.3, 139.5, 139.5, 139.0, 138.1, 129.2, 129.2, 129.1, 128.8, 128.7, 128.5, 128.4, 122.7, 120.5, 119.4, 116.8, 110.4, 105.7, 81.2, 76.8, 76.0, 74.0, 73.9, 73.5, 73.1, 62.6, 53.7, 50.8, 50.2, 49.9, 43.9, 37.2, 31.3, 28.7, 26.3, -4.5, -4.6. HRMS (ESI) m/z observed 675.39670 [$\text{C}_{43}\text{H}_{54}\text{N}_2\text{O}_3\text{Si}$ ($\text{M}+\text{H}$) $^+$ requires 675.39760].



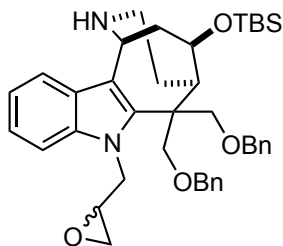
***N*-(6-(4-(((1*S*/*R*, 5*R*/*S*, 12*R*/*S*)-6,6-bis((benzyloxy)methyl)-12-((*tert*-butyldimethylsilyl)oxy)-3,4,5,6-tetrahydro-1*H*-5,1-ethanoazocino[4,3-*b*]indol-7(2*H*)-yl)methyl)-1*H*-1,2,3-triazol-1-yl)hexyl)-5-(((3*aR*,4*R*,6*aS*)-2-oxohexahydro-1*H*-thieno[3,4-*d*]imidazol-4-yl)pentanamide. (4.21). (WLM7_260_2).** A mixture of *tert*-BuOH : H₂O (1 : 1) (0.4 mL) was added to a flask charged with CuSO₄•5H₂O (1.2 mg, 0.0049 mmol), **4.14** (31 mg, 0.049 mmol), azide **4.20** (27 mg, 0.073 mmol) and sodium ascorbate (1.9 mg, 0.0098 mmol). The reaction mixture was heated to 70 °C. After 1.5 h, the reaction was cooled to room temperature, and aq ammonia (0.3 mL) was added. The reaction was then diluted with MeOH (2 mL) and extracted with CH₂Cl₂ (3 x 5 mL). The combined organic extracts were washed with brine (5 mL), dried (Na₂SO₄), and

concentrated under reduced pressure to afford a brown solid. Purification by flash chromatography eluting with CH₂Cl₂ : MeOH (100% CH₂Cl₂ → 95:5 → 80:20) containing 1% NEt₃ provided 35.5 mg (72%) of **4.21** as a white solid: ¹H-NMR (500 MHz, CD₃OD) δ 7.59 (d, *J* = 8.4 Hz, 1 H) 7.31 (s, 1 H) 7.26-7.22 (comp, 3 H) 7.21-7.13 (comp, 6 H) 7.12-7.09 (comp, 4 H) 6.15 (d, *J* = 18.0 Hz, 1 H) 5.51 (d, *J* = 18.0 Hz, 1 H) 5.29 (d, *J* = 5.4 Hz, 1 H) 4.50-4.44 (comp, 2 H) 4.47 (d, *J* = 12.6 Hz, 1 H) 4.43 (d, *J* = 12.0 Hz, 1 H) 4.37 (d, *J* = 12.0 Hz, 1 H) 4.34 (d, *J* = 11.4 Hz, 1 H) 4.26 (m, 1 H) 4.19-4.15 (comp, 2 H) 4.12-4.01 (comp, 2 H) 4.06 (d, 10.2 Hz, 1 H) 4.02 (d, *J* = 10.2 Hz, 1 H) 3.18-3.16 (m, 1 H) 3.07 (t, *J* = 7.2 Hz, 2 H) 2.99 (dd, *J* = 13.2, 6.0 Hz, 1 H) 2.92-2.86 (comp, 4 H) 2.67 (d, *J* = 13.2 Hz, 1 H) 2.26 (dm, *J* = 16.8 Hz, 1 H) 2.20-2.17 (m, 1 H) 2.17 (t, *J* = 7.2 Hz, 2 H) 1.88 (m, 1 H) 1.73-1.54 (comp, 6 H) 1.44-1.36 (comp, 4 H) 1.24 (m, 2 H) 1.16 (m, 2 H) 0.87 (s, 9 H) 0.09 (s, 6 H); ¹³C-NMR (125 MHz, CD₃OD) δ 175.9, 166.1, 142.7, 139.3, 139.2, 139.1, 129.4, 129.4, 128.9, 128.8, 128.7, 128.7, 128.6, 127.5, 124.1, 123.6, 121.6, 118.4, 111.5, 109.7, 75.7, 75.3, 74.5, 74.2, 74.1, 63.4, 61.6, 57.0, 51.4, 51.2, 49.8, 49.6, 44.3, 41.7, 41.0, 40.4, 40.1, 36.8, 31.0, 30.2, 29.8, 29.8, 29.5, 28.5, 27.2, 27.0, 26.4, 18.8, -4.7, -4.7; HRMS (ESI) *m/z* observed 1025.54580 [C₅₆H₇₈N₈O₅SSi (M+Na)⁺ requires 1025.54770].



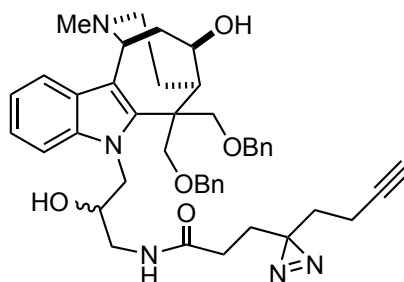
Allyl (1*S*/*R*, 5*R*/*S*, 12*R*/*S*)-6,6-Bis((benzyloxy)methyl)-12-((*tert*-butyldimethylsilyl)oxy)-7-(oxiran-2-ylmethyl)-1,3,4,5,6,7-hexahydro-2*H*-5,1-ethanoazocino[4,3-*b*]indole-2-carboxylate. (4.35). (WLM9_75). 60% NaH dispersion

in mineral oil (21 mg, 0.521 mmol) was added to a solution of **4.13** (71 mg, 0.104 mmol) in HMPA (0.52 mL) at 0 °C. After 15 min, *epi*-chlorohydrin (96 mg, 1.04 mmol, 82 μ L) was added in one portion. The cooling bath was removed, and the reaction was stirred at rt for 36 h. The reaction mixture was quenched via the addition of saturated aq NaHCO₃ (1.0 mL) and extracted with CH₂Cl₂ (3 x 15 mL). The combined organic extracts were washed with 1 M HCl (15 mL), brine (15 mL), dried (Na₂SO₄), filtered, and concentrated *in vacuo* to afford a yellow oil. Subsequent purification by flash chromatography eluting with Hexanes : EtOAc (10 : 1) to afford 49 mg (64%) **4.35** and 26 mg (36%) of **4.13**: ¹H-NMR (500 MHz, CD₃CN, 70 °C) δ 7.51 (dd, *J* = 19.0, 8.0 Hz, 1H), 7.33 (comp, 13H), 7.19 – 7.06 (m, 1H), 6.21 – 5.98 (m, 1H), 5.66 (d, *J* = 6.7 Hz, 1H), 5.40 (comp, 3H), 4.74 (comp, 2H), 4.63 (comp, 3H), 4.58 – 4.46 (m, 3H), 4.41 (t, *J* = 9.2 Hz, 1H), 4.33 (d, *J* = 9.8 Hz, 1H), 4.21 (comp, 1H), 4.08 (comp, 2H), 3.91 (comp, 2H), 3.20 – 3.04 (m, 1H), 3.04 – 2.92 (m, 1H), 2.87 (comp, 1H), 2.70 (comp, 1H), 2.48 (comp, 1H), 0.94 (s, 10H), 0.11 (s, 6H); ¹³C-NMR (125 MHz, CD₃CN, 70 °C) δ 156.3, 139.8, 139.8, 139.7, 139.7, 139.5, 135.2, 129.5, 129.5, 129.5, 129.0, 129.0, 128.9, 128.8, 128.8, 128.7, 128.7, 127.9, 123.3, 123.2, 121.0, 121.0, 115.9, 112.1, 112.1, 111.3, 77.1, 76.1, 75.8, 74.4, 74.3, 74.3, 74.2, 66.6, 53.3, 53.0, 51.7, 51.4, 51.3, 50.1, 49.5, 48.8, 46.2, 46.1, 42.0, 30.6, 26.6, 18.9, 6.3, -4.3, -4.3; HRMS (ESI) *m/z* observed 759.37970 [C₄₄H₅₆N₂O₆Si (M+Na)⁺ requires 759.38000].



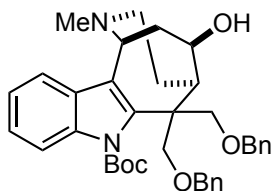
(1*S*/*R*, 5*R*/*S*, 12*R*/*S*)-6,6-Bis((benzyloxy)methyl)-12-((*tert*-butyldimethylsilyl)oxy)-7-(oxiran-2-ylmethyl)-2,3,4,5,6,7-hexahydro-1*H*-5,1-ethanoazocino[4,3-*b*]indole. (**4.36**). (WLM9_76). A round bottom flask charged with Pd₂(dba)₃ (15 mg, 0.0166 mmol) and 1,4-bis(diphenylphosphino)butane (14 mg, 0.0332 mmol) was placed under vacuum and backfilled with N₂ three times. A second round bottom flask was charged with **4.35** (49 mg, 0.0665 mmol) and 1,3-dimethylbarbituric acid (104 mg, 0.665 mmol) and placed under vacuum and backfilled with N₂ three times. THF (0.5 mL) was then added to both flasks, and the mixtures were stirred at room temperature under N₂ for 5 min. An aliquot of the Pd/ligand mixture (50 μL) was added via syringe to the flask containing **4.35**, and stirring was continued at room temperature until **4.35** was gone by TLC. The reaction was quenched with saturated aq NaHCO₃ (1.0 mL) and stirred at room temperature for 15 min. The reaction mixture was diluted with H₂O (5 mL) extracted with CH₂Cl₂ (3 x 10 mL). The combined organic extracts were washed with brine (15 mL), dried (Na₂SO₄), filtered, and concentrated *in vacuo* to afford a brown oil. Subsequent purification by flash chromatography eluting with EtOAc : Hexanes (10 : 1 → 100% EtOAc) containing 1% NEt₃ provided 28.5 mg (66%) of **4.36** as a white solid: ¹H-NMR (500 MHz, CD₃CN) δ 7.51 – 7.44 (m, 1H), 7.40 (comp, 1H), 7.25 (comp, 10H), 7.11 (comp, 1H), 7.03 (comp, 1H), 5.43 (comp, 1H), 4.79 (comp, 1H), 4.57 (comp, 4H), 4.43 (comp, 2H), 4.28 (comp, *J* = 9.5, 6.7 Hz, 1H), 4.01 (comp, 3H), 3.78 (comp, 1H), 3.10 – 2.96 (m, 1H), 2.71 (comp, 2H), 2.54 (comp, 2H), 2.36 (comp, 3H), 2.05 – 1.96 (m, 1H), 1.89 – 1.79 (m, 1H), 1.77 – 1.57 (m, 1H), 0.87 (comp, 9H), 0.06 (comp, 6H); ¹³C NMR (125 MHz, CD₃CN) δ 140.8, 140.8, 139.6, 139.6, 139.6, 139.4, 139.3, 129.3, 129.3, 129.2, 129.2, 129.2, 128.8, 128.7, 128.7, 128.7, 128.6, 128.6, 128.6, 128.6, 128.6, 128.5, 128.5, 128.5, 128.4, 128.4, 128.4, 128.4, 128.4, 127.7, 122.5, 122.3, 120.1, 120.0, 118.5, 118.5, 116.5, 116.4, 111.6, 111.5, 77.1, 77.1, 76.2, 76.0, 73.9, 73.9,

73.9, 73.8, 73.8, 73.7, 53.2, 52.9, 51.2, 51.0, 51.0, 51.0, 49.8, 48.7, 48.2, 48.2, 45.9, 45.6, 44.5, 44.5, 42.5, 42.5, 32.2, 26.4, 26.4, 18.7, 18.7, 18.6, -4.5, -4.6, -4.6; HRMS (ESI) m/z observed 675.35710 [$C_{40}H_{52}N_2O_4Si$ ($M+Na$) $^+$ requires 675.35890].



***N*-(3-((1*S*/*R*, 5*R*/*S*, 12*R*/*S*)-6,6-Bis((benzyloxy)methyl)-12-hydroxy-2-methyl-1,2,3,4,5,6-hexahydro-7*H*-5,1-ethanoazocino[4,3-*b*]indol-7-yl)-2-hydroxypropyl)-3-(3-(but-3-yn-1-yl)-3*H*-diazirin-3-yl)propanamide. (4.40). (WLM9_87).** 37% aq formaldehyde (1.2 mg, 0.0398 mmol, 3.3 μ L) was added to a stirred solution of **4.36** (13 mg, 0.0199 mmol) in CH_2Cl_2 (0.2 mL). After 5 min, sodium triacetoxymethylborohydride (12.7 mg, 0.0597 mmol) was added in one portion. After 1 h, the reaction was quenched with saturated aq $NaHCO_3$ (0.3 mL) and extracted with CH_2Cl_2 (3 x 5 mL). The combined organic extracts were washed with brine (10 mL), dried (Na_2SO_4), filtered, and concentrated *in vacuo* to afford a yellow oil. The crude reaction mixture was dissolved in saturated methanolic ammonia (0.5 mL) and heated to 80 $^{\circ}C$ in a sealed vial for 48 h. Upon cooling the reaction to rt, the solvent was removed *in vacuo* to afford a yellow oil. The crude reaction mixture was subsequently dissolved in CH_2Cl_2 (0.2 mL) and cooled to 0 $^{\circ}C$. After stirring for 5 min, **4.24** (3.6 mg, 0.0219) and *N,N'*-dicyclohexylcarbodiimide (4.5 mg, 0.0219 mmol) were added to the reaction. After 10 min, the reaction was quenched with saturated aq $NaHCO_3$ (0.5 mL) and extracted with CH_2Cl_2 (3 x 10 mL). The combined organic extracts were washed with brine (10 mL), dried (Na_2SO_4), filtered,

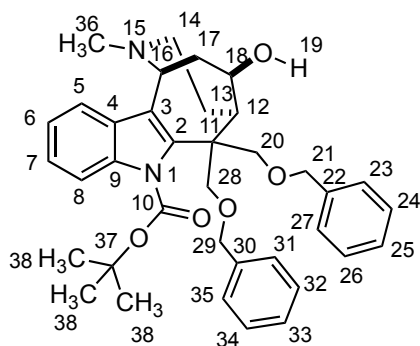
and concentrated *in vacuo* to afford a yellow oil. The crude reaction mixture was dissolved in CH₂Cl₂ (0.3 mL) and NEt₃•3HF (0.1 mL) and stirred at rt. After 36 h, SiO₂ (10 mg) was added to quench excess HF. The solvent was removed *in vacuo* and MeOH (1.0 mL) was added to the crude reaction mixture. The reaction mixture was filtered with a submicron syringe filter and purified via RPHPLC eluting with H₂O : MeCN (75 : 25 → 90 : 10 over 120 min) containing 0.1% TFA to afford 0.85 mg (6%) of **4.40** as a white solid: ¹H-NMR (600 MHz, CD₃OD) δ 7.59 (comp, *J* = 8.0, 4.8 Hz, 1H), 7.57 – 7.50 (m, 1H), 7.25 (comp, 11H), 7.13 – 7.08 (m, 1H), 5.18 (d, *J* = 5.7 Hz, 1H), 4.43 (comp, 9H), 4.11 (dd, *J* = 29.9, 10.2 Hz, 1H), 3.94 (dd, *J* = 40.9, 10.1 Hz, 1H), 3.47 – 3.35 (m, 1H), 3.20 (comp, 3H), 3.05 (comp, 3H), 2.85 (s, 4H), 2.35 – 2.20 (m, 1H), 2.04 (comp, 4H), 1.97 (comp, 2H), 1.76 (comp, 2H), 1.57 (td, *J* = 7.4, 2.6 Hz, 2H); HRMS (ESI) *m/z* observed 718.39600 [C₄₃H₅₁N₅O₅ (M+H)⁺ requires 718.39630].



(1S/R, 5R/S, 12R/S)-tert-Butyl 6,6-bis((benzyloxy)methyl)-12-hydroxy-2-methyl-3,4,5,6-tetrahydro-1H-5,1-ethanoazocino[4,3-b]indole-7(2H)-carboxylate.

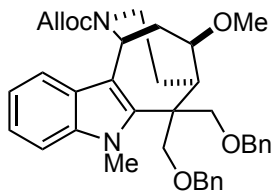
(4.43). (WLM7_176_2). A mixture of **3.34** (5.5 mg, 0.00944 mmol) and 37% aq formaldehyde solution (7.7 mg, 0.0944 mmol, 7.7 μL) in CH₂Cl₂ (0.3 mL) was stirred for 5 min at room temperature and sodium cyanoborohydride (9 mg, 0.142 mmol) was added in one portion. Stirring was continued for 3 h at room temperature. The reaction was quenched with saturated aq Rochelle's salt (0.1 mL), diluted with MeOH (0.5 mL), and extracted with CH₂Cl₂ (3 x 2 mL). The combined organic extracts were washed with brine (4 mL), dried (Na₂SO₄), filtered, and concentrated *in vacuo* to afford a brown oil.

Subsequent purification by RPHPLC H₂O : MeCN (90 : 10 → 5 : 95 over 20 min) afforded 3.0 mg (54%) of **4.43** as a white solid. ¹H-NMR (500 MHz, CD₃OD) δ 7.76 (d, *J* = 8.5 Hz, 1 H) 7.65 (d, *J* = 7.5 Hz, 1 H) 7.38 (t, *J* = 8.0 Hz, 1 H) 7.31 (t, *J* = 7.5 Hz, 1 H) 7.22-7.17 (comp, 7 H) 7.14 (comp, 3 H) 5.24 (d, *J* = 5.0 Hz, 1 H) 4.54-4.38 (comp, 7 H) 4.32 (td, *J* = 8.5 Hz, 1 H) 3.67 (d, *J* = 10.0 Hz, 1 H) 3.06-2.96 (comp, 3H) 2.91-2.88 (m, 1 H) 2.86 (s, 3 H) 2.27-2.18 (comp, 2 H) 1.93 (m, 1 H) 1.60 (s, 9 H); ¹³C-NMR (125 MHz, CD₃OD) δ 152.4, 142.1, 139.4, 139.0, 137.8, 129.3, 129.3, 129.0, 128.8, 128.7, 128.6, 128.1, 125.9, 123.9, 118.8, 115.3, 113.8, 86.8, 77.7, 74.7, 74.3, 74.2, 73.9, 59.9, 53.2, 53.1, 46.4, 38.7, 30.7, 29.6, 28.2; HRMS (ESI) *m/z* observed 597.33250 [C₃₇H₄₄N₂O₅ (M+H)⁺ requires 597.33230].



Assignments: ¹H-NMR (500 MHz, CD₃OD) δ 7.76 (d, *J* = 8.5 Hz, 1 H, C8-H) 7.65 (d, *J* = 7.5 Hz, 1 H, C5-H) 7.38 (t, *J* = 8.0 Hz, 1 H, C7-H) 7.31 (t, *J* = 7.5 Hz, 1 H, C6-H) 7.22-7.17 (comp, 7 H) 7.14 (comp, 3 H) 5.24 (d, *J* = 5.0 Hz, 1 H, C16-H) 4.54-4.38 (comp, 7 H, C20-H and C21-H and C28-H and C29-H) 4.32 (td, *J* = 8.5 Hz, 1 H, C18-H) 3.67 (d, *J* = 10.0 Hz, 1 H, C20-H or C21-H or C28-H or C29-H) 3.06-2.96 (comp, 3H, C14-H₂ and C17-H) 2.91-2.88 (m, 1 H, C12-H) 2.86 (s, 3 H, C36-H₃) 2.27-2.18 (comp, 2 H, C13-H and C17-H) 1.93 (m, 1 H, C13-H) 1.60 (s, 9 H, C38-H₃); ¹³C-NMR (125 MHz, CD₃OD) δ 152.4, 142.1, 139.4, 139.0, 137.8, 129.3, 129.3, 129.0,

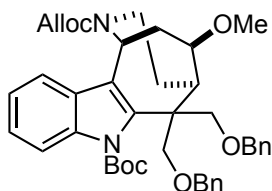
128.8, 128.7, 128.6, 128.1, 125.9, 123.9, 118.8 (C5), 115.3 (C8), 113.8 (C3), 86.8 (C10), 77.7 (C20 or C21 or C28 or C29), 74.7 (C20 or C21 or C28 or C29), 74.3 (C18), 74.2 (C20 or C21 or C28 or C29), 73.9 (C20 or C21 or C28 or C29), 59.9 (C16), 53.2 (C12), 53.1 (C14), 51.2 (C11) 46.4 (C36), 38.7 (C14), 29.6 (C13), 28.2 (C38).



(1R/S, 5R/S, 12R/S)-Allyl-6,6-bis((benzyloxy)methyl)-12-methoxy-7-methyl-3,4,5,6-tetrahydro-1H-5,1-ethanoazocino[4,3-b]indole-2(7H)-carboxylate (4.44a).

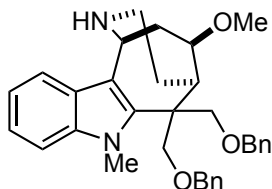
(WLM7_114_2). A mixture of **4.12** (43 mg, 0.076 mmol) and 60% NaH dispersion in mineral oil (30 mg, 0.76 mmol) in DMF (0.75 mL) at 0 °C under N₂ was stirred for five min and methyl *p*-toluenesulfonate (71 mg, 0.38 mmol) was added in one portion. The reaction was allowed to warm slowly to room temperature overnight. The reaction was quenched with saturated aq NaHCO₃ (0.75 mL), diluted with H₂O (5 mL), and extracted with EtOAc (3 x 10 mL). The combined organic extracts were washed with brine (20 mL), dried (Na₂SO₄), filtered, and concentrated *in vacuo* to afford a clear oil. Purification by flash chromatography eluting with Hexanes : EtOAc (4:1 → 2:1) to provide 38 mg (84%) of **4.44a** as a clear oil: ¹H-NMR (500 MHz, CD₃CN, 70 °C) δ 7.38 (d, *J* = 8.0 Hz, 1 H) 7.33-7.22 (comp, 9 H) 7.19-7.18 (comp, 2 H) 7.15 (td, *J* = 7.0, 1.0 Hz, 1 H) 7.04 (td, *J* = 7.5, 1.0 Hz, 1 H) 6.03 (br, 1 H) 5.66 (d, *J* = 6.5 Hz, 1 H) 5.34 (br, 1 H) 5.22 (br, 1 H) 4.66 (br, 1 H) 4.53-4.47 (comp, 3 H) 4.42 (d, *J* = 12.0 Hz, 1 H) 4.38 (d, *J* = 10.5 Hz, 1 H) 3.99 (d, *J* = 9.5 Hz, 1 H) 3.96 (d, *J* = 9.5 Hz, 1 H) 3.95 (d, *J* = 10.5 Hz, 1 H) 3.83 (s, 3 H) 3.78 (app t, *J* = 8.8 Hz, 1 H) 3.31 (s, 3 H) 3.05-3.00 (comp, 2 H) 2.82 (br, 1 H) 2.16 (dt, *J* = 18.0, 5.0 Hz, 1 H) 1.83-1.70 (comp, 2 H); ¹³C-NMR (125 MHz, CD₃CN, 70°C) δ 156.3,

140.8, 140.1, 139.5, 139.0, 135.3, 129.5, 129.5, 129.0, 128.9, 128.8, 128.6, 127.5, 122.9, 120.5, 117.4, 115.5, 110.3, 86.4, 78.1, 75.3, 74.3, 74.0, 66.6, 57.5, 50.6, 48.5, 47.0, 42.1, 33.7; HRMS (ESI) m/z observed 617.29900 [$C_{37}H_{42}N_2O_5$ ($M+Na$)⁺ requires 617.29860].



(1R/S, 5R/S, 12R/S)-2-Allyl-7-tert-butyl-6,6-bis((benzyloxy)methyl)-12-methoxy-3,4,5,6-tetrahydro-1H-5,1-ethanoazocino[4,3-b]indole-2,7-dicarboxylate (4.44b). (WLM7_122_2_frac1). A mixture of **3.36** (44 mg, 0.0659 mmol) and 60% NaH dispersion in mineral oil (10.5 mg, 0.2636 mmol) in DMF (0.6 mL) under N₂ at 0 °C was stirred for five min and methyl *p*-toluenesulfonate (24.5 mg, 0.1318 mmol) was added in one portion. The reaction was allowed to warm slowly to room temperature overnight. The reaction was quenched with saturated aq NaHCO₃ (0.75 mL), diluted with H₂O (5 mL), and extracted with EtOAc (3 x 10 mL). The combined organic extracts were washed with brine (20 mL), dried (Na₂SO₄), filtered, and concentrated *in vacuo* to afford a clear oil. Subsequent purification by flash chromatography eluting with Hexanes : EtOAc (4 : 1 → 2 : 1) afforded 32 mg (71%) of **4.44b** as a white solid: ¹H-NMR (500 MHz, C₆D₆, mixture of rotamers) δ 7.92-7.88 (m, 0.5 H) 7.68-7.57 (m, 0.5 H) 7.41-7.38 (m, 1 H) 7.28-7.02 (comp, 10 H) 6.98-6.89 (comp, 2 H) 6.16 (d, *J* = 6.5 Hz, 0.5 H) 5.95-5.73 (dm, 1 H) 5.29-5.25 (m, 0.5 H) 5.11-5.00 (comp, 1 H) 4.95-4.92 (m, 0.5 H) 4.83-4.81 (m, 0.5 H) 4.77-4.73 (m, 1 H) 4.71-4.65 (comp, 1 H) 4.62-4.58 (m, 1 H) 4.56-4.53 (m, 1 H) 4.48-4.45 (m, 1 H) 4.34-4.19 (comp, 3 H) 4.14-4.02 (comp, 1 H) 3.86-3.71 (m, 1 H) 3.65-3.60 (m, 1 H) 3.43-3.37 (m, 1 H) 3.17-3.02 (comp, 4 H) 2.97-2.89 (comp, 1 H) 2.18-2.06 (comp, 1 H) 1.92-1.85 (m, 1 H) 1.73-1.54 (comp, 2 H) 1.40-1.30 (comp, 9 H); ¹³C-NMR

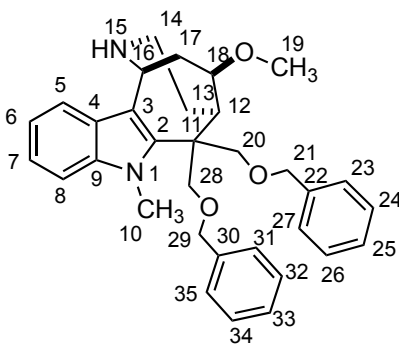
(125 MHz, C₆D₆, mixture of rotamers) δ 204.6, 155.4, 155.3, 151.5, 139.9, 139.8, 139.3, 139.1, 139.1, 138.7, 138.5, 138.0, 136.9, 134.0, 133.8, 128.8, 128.6, 128.5, 127.6, 127.4, 127.1, 127.1, 126.5, 126.4, 124.6, 122.6, 122.5, 122.4, 122.3, 122.1, 121.9, 118.7, 118.2, 117.2, 116.9, 114.6, 114.5, 85.3, 83.3, 83.2, 78.8, 78.6, 73.8, 73.6, 73.3, 73.1, 72.6, 72.5, 72.4, 66.1, 57.0, 56.9, 50.1, 47.5, 47.2, 46.7, 46.1, 41.5, 41.2, 37.9, 36.6, 33.9, 32.3, 32.2, 31.4, 30.1, 30.1, 30.0, 29.8, 29.8, 29.6, 29.4, 27.8, 25.1, 23.1, 14.3, 1.4; HRMS (ESI) m/z observed 703.33500 [C₄₁H₄₈N₂O₇ (M+Na)⁺ requires 703.33500].



(1R/S, 5R/S, 12R/S)-6,6-Bis((benzyloxy)methyl)-12-methoxy-7-methyl-2,3,4,5,6,7-hexahydro-1H-5,1-ethanoazocino[4,3-b]indole (4.45a).

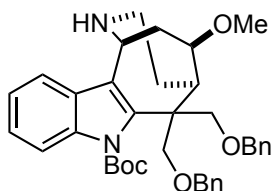
(WLM7_116_2_frac2). A round bottom flask charged with Pd₂(dba)₃ (0.7 mg, 0.00079 mmol) and 1,4-bis(diphenylphosphino)butane (0.34 mg, 0.00079 mmol) was placed under vacuum and backfilled with N₂ three times. A second round bottom flask was charged with **4.44a** (47 mg, 0.079 mmol) and 1,3-dimethylbarbituric acid (123 mg, 0.79 mmol) and placed under vacuum and backfilled with N₂ three times. THF (0.4 mL) was then added to both flasks, and the mixtures were stirred at room temperature under N₂ for 5 min. The Pd/ligand mixture was added via syringe to the flask containing **4.44a**, and stirring was continued at room temperature until **4.44a** was gone by TLC. The reaction was quenched with saturated aq NaHCO₃ (0.8 mL) and stirred at room temperature for 15 min. The reaction mixture was diluted with H₂O (2 mL) extracted with Et₂O (3 x 10 mL). The combined organic extracts were washed with brine (10 mL), dried (Na₂SO₄), filtered, and concentrated *in vacuo* to afford a brown oil. Subsequent purification by flash

chromatography eluting with EtOAc : MeOH (9 : 1 → 5 : 1) to provide 33 mg (83%) of **4.45a** as a white solid: $^1\text{H-NMR}$ (500 MHz, CD_3CN) δ 7.44 (d, J = 8.0 Hz, 1 H) 7.33-7.17 (comp, 11 H) 7.10 (td, J = 7.5, 1.0 Hz, 1 H) 6.99 (td, J = 7.5, 1.0 Hz, 1 H) 4.60 (d, J = 6.5 Hz, 1 H) 4.50-4.44 (comp, 3 H) 4.37 (app t, 2 H) 3.97 (td, J = 9.3, 2.0 Hz, 1 H) 3.94 (d, J = 9.5 Hz, 1 H) 3.88 (d, J = 10.0 Hz, 1 H) 3.86 (d, J = 9.0 Hz, 1 H) 3.79 (s, 3 H) 3.30 (s, 3 H) 2.93 (m, 1 H) 2.72-2.67 (m, 1 H) 2.54-2.47 (comp, 2 H) 2.20 (br, 1 H) 2.11 (dm, J = 14.0 Hz, 1 H) 1.75 (ddd, J = 14.0, 9.5, 1.0 Hz, 1 H) 1.64-1.57 (m, 1 H); $^{13}\text{C-NMR}$ (125 MHz, CD_3CN) δ 139.9, 139.5, 139.4, 138.7, 129.2, 129.2, 128.7, 128.6, 128.5, 128.4, 127.3, 122.0, 119.5, 116.5, 109.7, 86.7, 78.3, 75.3, 73.8, 73.5, 57.2, 50.0, 48.0, 46.4, 42.7, 42.4, 33.5, 33.2; HRMS (ESI) m/z observed 511.29540 [$\text{C}_{33}\text{H}_{38}\text{N}_2\text{O}_3$ ($\text{M}+\text{H}$) $^+$ requires 511.29550].



Assignments: $^1\text{H-NMR}$: δ 7.44 (d, J = 8.0 Hz, 1 H, C5-H) 7.33-7.17 (comp, 11 H, C8-H, C23-H, C24-H, C25-H, C26-H, C27-H, C31-H, C32-H, C33-H, C34-H, C35-H) 7.10 (td, J = 7.5, 1.0 Hz, 1 H, C7-H) 6.99 (td, J = 7.5, 1.0 Hz, 1 H, C6-H) 4.60 (d, J = 6.5 Hz, 1 H, C16-H) 4.50-4.44 (comp, 3 H, C21-H₂, C29-H or C21-H, C29-H₂) 4.37 (app t, 2 H, C20-H, C21-H or C29-H) 3.97 (td, J = 9.3, 2.0 Hz, 1 H, C18-H) 3.94 (d, J = 9.5 Hz, 1 H, C20-H or C28-H) 3.88 (d, J = 10.0 Hz, 1 H, C20-H or C28-H) 3.86 (d, J = 9.0 Hz, 1 H, C20-H or C28-H) 3.79 (s, 3 H, C10-CH₃) 3.30 (s, 3 H, C19-CH₃) 2.93 (m, 1

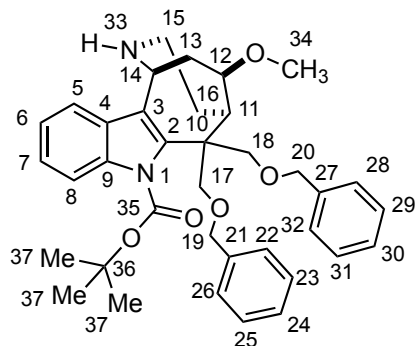
H, C12-H) 2.72-2.67 (m, 1 H, C17-H) 2.54-2.47 (comp, 2 H, C14-H2) 2.20 (br, 1 H, N15-H) 2.11 (dm, $J = 14.0$ Hz, 1 H, C13-H) 1.75 (ddd, $J = 14.0, 9.5, 1.0$ Hz, 1 H, C17-H) 1.64-1.57 (m, 1 H, C13-H). ^{13}C -NMR: δ 139.9, 139.5, 139.3, 138.7, 129.2, 129.2, 128.7, 128.6, 128.5, 128.4, 127.3, 122.0 (C7), 119.5 (C6), 116.5 (C5), 109.7 (C8), 86.7 (C18), 78.3 (C20), 75.3 (C28), 73.8 (C21 or C29), 73.5 (C21 or C29), 57.2 (C19), 50.0 (C11), 48.0 (C16), 46.4 (C12), 42.7 (C14), 42.4 (C17), 33.5 (C13), 33.2 (C10).



(5R/S, 12R/S)-tert-Butyl-6,6-bis((benzyloxy)methyl)-12-methoxy-3,4,5,6-tetrahydro-1H-5,1-ethanoazocino[4,3-b]indole-7(2H)-carboxylate (4.45b).

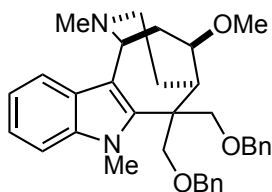
(WLM7_134_2). A round bottom flask charged with $\text{Pd}_2(\text{dba})_3$ (0.43 mg, 0.00047 mmol) and 1,4-bis(diphenylphosphino)butane (0.20 mg, 0.00047 mmol) was placed under vacuum and backfilled with N_2 three times. A second round bottom flask was charged with **4.44b** (32 mg, 0.047 mmol) and 1,3-dimethylbarbituric acid (73 mg, 0.47 mmol) and placed under vacuum and backfilled with N_2 three times. THF (0.25 mL) was then added to both flasks, and the mixtures were stirred at room temperature under N_2 for five min. The Pd/ligand mixture was added via syringe to the flask containing **4.44b**, and stirring was continued at room temperature until **4.44b** was gone by TLC. The reaction was quenched with saturated aq NaHCO_3 (1.0 mL) and stirred at room temperature for 15 min. The reaction mixture was diluted with H_2O (1.0 mL) extracted with Et_2O (3 x 5 mL). The combined organic extracts were washed with brine (10.0 mL), dried (Na_2SO_4), filtered, and concentrated *in vacuo* to afford a brown oil. Subsequent purification by flash chromatography CH_2Cl_2 : MeOH (100% \rightarrow 19 : 1) with 1% NEt_3 afforded 17 mg (61%)

of **4.45b** as a white solid: $^1\text{H-NMR}$ (600 MHz, CD_3OD) δ 7.77 (dm, $J = 8.4$ Hz, 1 H) 7.59 (d, $J = 7.8$ Hz, 1 H) 7.37-7.31 (comp, 5 H) 7.27-7.24 (comp, 2 H) 7.13-7.01 (comp, 3 H) 7.05-7.04 (comp, 2 H) 5.29 (d, $J = 5.4$ Hz, 1 H) 4.81 (d, $J = 7.8$ Hz, 1 H) 4.62 (d, $J = 10.2$ Hz, 1 H) 4.54 (d, $J = 7.8$ Hz, 1 H) 4.52 (d, $J = 8.4$ Hz, 1 H) 4.45 (d, $J = 12.0$ Hz, 1 H) 4.41 (d, $J = 12.0$ Hz, 1 H) 4.09 (d, $J = 8.4$ Hz, 1 H) 3.86 (t, $J = 9.6$ Hz, 1 H) 3.73 (d, $J = 10.8$ Hz, 1 H) 3.40 (s, 3H) 3.28 (m, 1H) 2.98 (m, 1H) 2.87 (dd, $J = 13.8, 4.8$ Hz, 1 H) 2.73 (td, $J = 13.8, 4.8$ Hz, 1 H) 2.29-2.22 (comp, 2 H) 1.82 (tm, 1 H) 1.59 (s, 9H); $^{13}\text{C-NMR}$ (150 MHz, CD_3OD) δ 152.2, 141.5, 139.9, 139.0, 137.7, 129.2, 129.1, 128.4, 128.3, 128.3, 127.7, 127.2, 125.9, 123.3, 118.5, 115.9, 115.0, 86.2, 84.8, 78.6, 73.8, 73.6, 73.5, 58.0, 51.1, 45.8, 42.0, 37.1, 29.2, 28.3; HRMS (ESI) m/z observed 597.33210 [$\text{C}_{37}\text{H}_{44}\text{N}_2\text{O}_5$ (M+H) $^+$ requires 597.33230].



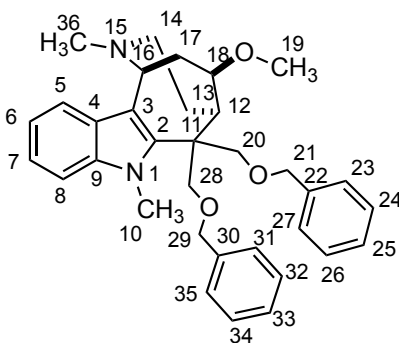
Assignments: $^1\text{H-NMR}$ δ 7.77 (dm, $J = 8.4$ Hz, 1H, C8-H) 7.59 (d, $J = 7.8$ Hz, 1H, C5-H) 7.37-7.31 (comp, 5H) 7.27-7.24 (comp, 2H) 7.13-7.10 (comp, 3H) 7.05-7.04 (comp, 2H) 5.29 (d, $J = 5.4$ Hz, 1H, C14-H) 4.81 (d, $J = 7.8$ Hz, 1H, C17-H or C18-H C19-H or C20-H) 4.62 (d, $J = 10.2$ Hz, 1H, C17-H or C18-H C19-H or C20-H) 4.54 (d, $J = 7.8$ Hz, 1H, C17-H or C18-H C19-H or C20-H) 4.52 (d, $J = 8.4$ Hz, 1H, C17-H or C18-H C19-H or C20-H) 4.45 (d, $J = 12.0$ Hz, 1H, C17-H or C18-H C19-H or C20-H) 4.41 (d, $J = 12.0$ Hz, 1H, C17 or C18 or C19 or C20) 4.09 (d, $J = 8.4$ Hz, 1H, C17 or C18 or

C19 or C20) 3.86 (t, $J = 9.6$ Hz, 1H, C12-H) 3.73 (d, $J = 10.8$ Hz, 1H, C17-H or C18-H C19-H or C20-H) 3.40 (s, 3H, C34-H₃) 3.28 (m, 1H, C11-H) 2.98 (m, 1H, C13-H) 2.87 (dd, $J = 13.8, 4.8$ Hz, 1H, C15-H) 2.73 (td, $J = 13.8, 4.8$ Hz, 1H, C15-H) 2.29-2.22 (comp, 2H, C13-H and C16-H) 1.82 (tm, 1H, C16-H) 1.59 (s, 9H, C37-H₃); ¹³C-NMR δ 152.2 (C35), 141.5, 139.9, 139.0, 137.7, 129.2, 129.1, 128.4, 128.3, 128.3, 127.7, 127.2, 125.9, 123.3, 118.5 (C6), 115.9, 115.0 (C8), 86.2 (C36), 84.8 (C12), 78.6 (C17 or C18 or C19 or C20), 73.8 (C17 or C18 or C19 or C20), 73.6 (C17 or C18 or C19 or C20), 73.5 (C17 or C18 or C19 or C20), 58.0 (C34), 51.1 (C10), 45.8 (C11), 42.0 (C15), 37.1 (C13), 29.2 (C16), 28.3 (C37).



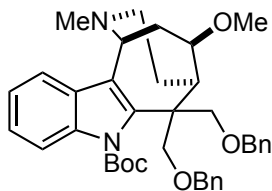
(1R/S, 5R/S, 12R/S)-6,6-Bis((benzyloxy)methyl)-12-methoxy-2,7-dimethyl-2,3,4,5,6,7-hexahydro-1H-5,1-ethanoazocino[4,3-b]indole (4.46a). (WLM7_121_2). A mixture of **4.45a** (10 mg, 0.0196 mmol) and 37% aq formaldehyde solution (16 mg, 0.196 mmol, 16 μ L) in CH₂Cl₂ (0.2 mL) was stirred for 5 min at room temperature and sodium cyanoborohydride (18.5 mg, 0.294 mmol) was added in one portion. Stirring was continued for 3 h at room temperature. The reaction was quenched with saturated aq Rochelle's salt (1.0 mL), diluted with MeOH (1.0 mL), and extracted with CH₂Cl₂ (3 x 2 mL). The combined organic extracts were washed with brine (3 mL), dried (Na₂SO₄), filtered, and concentrated *in vacuo* to afford a brown oil. Subsequent purification by flash chromatography eluting with CH₂Cl₂ : MeOH (9 : 1) afforded 6.3 mg (61%) of **4.46a** as a yellow solid. ¹H-NMR (600 MHz, CD₃CN) δ 7.51 (d, $J = 7.8$ Hz, 1H) 7.36-7.32 (comp, 5H) 7.30-7.23 (m, 1H) 7.26-7.22 (comp, 3 H) 7.19 (td, $J = 7.8, 1.2$ Hz, 1 H) 7.16-7.15

(comp, 2 H) 7.11 (td, $J = 7.2, 0.6$ Hz, 1 H) 4.87 (d, $J = 5.4$ Hz, 1 H) 4.50 (d, $J = 12.0$ Hz, 1 H) 4.47-4.44 (comp, 3 H) 4.39 (d, $J = 12.0$ Hz, 1 H) 4.17 (td, $J = 9.0, 1.8$ Hz, 1 H) 4.01 (d, $J = 9.6$ Hz, 1 H) 3.85 (d, $J = 9.0$ Hz, 1 H) 3.81 (s, 3 H) 3.79 (d, $J = 10.8$ Hz, 1 H) 3.33 (s, 3 H) 3.27-3.21 (m, 1 H) 3.08 (m, 1 H) 2.84-2.81 (comp, 2 H) 2.61 (s, 3 H) 2.26-2.21 (m, 1 H) 2.16 (m, 1 H) 1.92-1.90 (m, 1 H); ^{13}C -NMR (150 MHz, CD_3CN) δ 141.6, 139.6, 138.7, 138.6, 129.4, 129.3, 129.0, 128.8, 128.6, 128.5, 128.0, 123.0, 121.1, 118.3, 110.5, 84.6, 78.6, 74.5, 74.0, 73.4, 58.6, 57.7, 52.2, 50.0, 45.8, 44.8, 37.8, 33.4, 29.1; HRMS (ESI) m/z observed 525.31090 [$\text{C}_{34}\text{H}_{40}\text{N}_2\text{O}_3$ ($\text{M}+\text{H}$) $^+$ requires 525.31120].



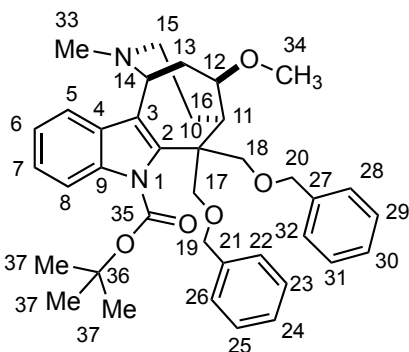
Assignments: ^1H -NMR: 7.51 (d, $J = 7.8$ Hz, 1 H, C5-H) 7.36-7.32 (comp, 5 H, C8-H, C23-H, C27-H, C31-H, C35-H) 7.30-7.28 (m, 1 H, C24-H or C26-H or C32-H or C34-H) 7.26-7.22 (comp, 3 H, C24-H or C26-H or C32-H or C34-H) 7.19 (td, $J = 7.8, 1.2$ Hz, 1 H, C7-H) 7.16-7.15 (comp, 2 H, C25-H, C33-H) 7.11 (td, $J = 7.2, 0.6$ Hz, 1 H, C6-H) 4.87 (d, $J = 5.4$ Hz, 1 H, C16-H) 4.50 (d, $J = 12.0$ Hz, 1 H, C21-H or C29-H) 4.47-4.44 (comp, 3 H, C20-H, C21-H2 or C29-H2) 4.39 (d, $J = 12.0$ Hz, 1 H, C21-H or C29-H) 4.17 (td, $J = 9.0, 1.8$ Hz, 1 H, C18-H) 4.01 (d, $J = 9.6$ Hz, 1 H, C28-H) 3.85 (d, $J = 9.0$ Hz, 1 H, C28-H) 3.81 (s, 3 H, C10-CH3) 3.79 (d, $J = 10.8$ Hz, 1 H, C20-H) 3.33 (s, 3 H, C19-CH3) 3.27-3.21 (m, 1 H, C17-H) 3.08 (m, 1 H, C12-H) 2.84-2.81 (comp, 2 H, C14-H2) 2.61 (s, 3 H, C36-CH3) 2.26-2.21 (m, 1 H, C13-H) 2.16 (m, 1 H, C13-H) 1.92-

1.90 (m, 1 H, C17-H). ^{13}C -NMR: 141.6, 139.6, 138.7, 138.6, 129.4, 129.3, 129.0, 128.8, 128.6, 128.5, 128.0, 123.0 (C7), 121.1 (C6), 118.3 (C5), 110.5 (C8), 84.6 (C18), 78.6 (C20), 74.5 (C28), 74.0 (C29), 73.4 (C21), 58.6 (C16), 57.7 (C19), 52.2 (C14), 50.0 (C11), 45.8 (C36), 44.8 (C12), 37.8 (C17), 33.4 (C10), 29.1 (C13).

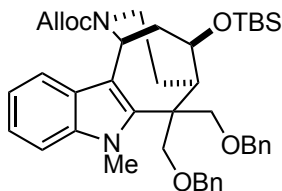


(1S/R, 5R/S, 12R/S)-tert-Butyl-6,6-bis((benzyloxy)methyl)-12-methoxy-2-methyl-3,4,5,6-tetrahydro-1H-5,1-ethanoazocino[4,3-b]indole-7(2H)-carboxylate (4.46b). (WLM7_139_2). A mixture of **4.45b** (4.5 mg, 0.00754 mmol) and 37% aq formaldehyde solution (6 mg, 0.0754 mmol, 6 μL) in CH_2Cl_2 (0.3 mL) was stirred for five min at room temperature and sodium cyanoborohydride (7 mg, 0.1131 mmol) was added in one portion. Stirring was continued for 3 h at room temperature. The reaction was quenched with saturated aq Rochelle's salt (1.0 mL), diluted with MeOH (1.0 mL) and extracted with CH_2Cl_2 (3 x 5 mL). The combined organic extracts were washed with brine (10.0 mL), dried (Na_2SO_4), filtered, and concentrated *in vacuo* to afford a brown oil. Subsequent purification by preparative RP HPLC H_2O : MeCN (90 : 10 \rightarrow 5 : 95 over 30 min) afforded 3 mg (67%) of **4.46b** as a white solid: ^1H -NMR (500 MHz, CD_3OD) δ 7.76 (d, J = 8.5 Hz, 1 H) 7.64 (d, J = 7.5 Hz, 1 H) 7.38-7.26 (comp, 7 H) 7.17-7.09 (comp, 5 H) 5.25 (d, J = 5.5 Hz, 1 H) 4.77 (d, J = 8.5 Hz, 1H) 4.61 (d, J = 10.5 Hz, 1 H) 4.55 (d, J = 8.5 Hz, 1H) 4.53 (d, J = 8.0 Hz, 1 H) 4.44 (d, J = 10.5 Hz, 1 H) 4.42 (d, J = 12.0 Hz, 1 H) 4.08 (d, J = 8.0 Hz, 1 H) 3.84 (t, J = 9.0 Hz, 1 H) 3.73 (d, J = 10.5 Hz, 1 H) 3.40 (s, 3 H) 3.25 (m, 1 H) 3.10-3.06 (m, 1 H) 2.98-2.97 (m, 1 H) 2.93-2.90 (m, 1 H) 2.88 (s, 3 H) 2.26-2.22 (comp, 2 H) 1.92-1.81 (m, 1 H) 1.61 (s, 9H); ^{13}C -NMR (125

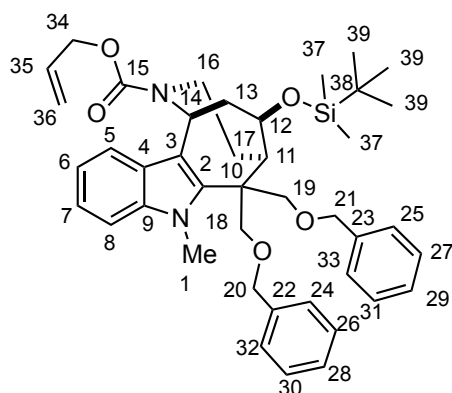
MHz, CD₃OD) δ 152.3, 142.3, 140.0, 139.2, 137.8, 129.3, 128.7, 128.6, 128.5, 128.5, 128.0, 125.9, 123.9, 118.8, 115.2, 113.5, 86.7, 84.7, 78.6, 74.1, 73.8, 73.7, 59.7, 58.1, 53.2, 51.3, 46.5, 45.3, 37.1, 29.6, 28.2. HRMS (CI) m/z observed 609.3318 [C₃₈H₄₅N₂O₅ (M)⁺ requires 609.3328].



Assignments: ¹H-NMR: δ 7.76 (d, J = 8.5 Hz, 1 H, C8-H) 7.64 (d, J = 7.5 Hz, 1 H, C5-H) 7.38-7.26 (comp, 7 H) 7.17-7.09 (comp, 5 H) 5.25 (d, J = 5.5 Hz, 1 H, C14-H) 4.77 (d, J = 8.5 Hz, 1 H, C17-H or C18-H) 4.61 (d, J = 10.5 Hz, 1 H, C17-H or C18-H) 4.55 (d, J = 8.5 Hz, 1 H, C20-H or C21-H) 4.53 (d, J = 8.0 Hz, 1 H, C20-H or C21-H) 4.44 (d, J = 10.5 Hz, 1 H, C20-H or C21-H) 4.42 (d, J = 12.0 Hz, 1 H, C20-H or C21-H) 4.08 (d, J = 8.0 Hz, 1 H, C17-H or C18-H) 3.84 (t, J = 9.0 Hz, 1 H, C12-H) 3.73 (d, J = 10.5 Hz, 1 H, C17-H or C18-H) 3.40 (s, 3 H, C34-H₃) 3.25 (m, 1 H, C11-H) 3.10-3.06 (m, 1 H, C13-H) 2.98-2.97 (m, 1 H, C15-H) 2.93-2.90 (m, 1 H, C15-H) 2.88 (s, 3 H, C33-H₃) 2.26-2.22 (comp, 2 H, C13-H and C16-H) 1.92-1.81 (m, 1 H, C16-H) 1.61 (s, 9 H, C37-H₃).

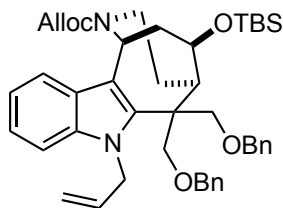


Allyl (1S/R, 5R/S, 12R/S)-6,6-bis((benzyloxy)methyl)-12-((tert-butyltrimethylsilyl)oxy)-7-methyl-1,3,4,5,6,7-hexahydro-2H-5,1-ethanoazocino[4,3-b]indole-2-carboxylate. (4.47a). (WLM8_210). A mixture of **4.13** (28 mg, 0.0411 mmol) and 60% NaH dispersion in mineral oil (5 mg, 0.123 mmol) in DMF (0.4 mL) at 0 °C under N₂ was stirred for five min and methyl *p*-toluenesulfonate (15 mg, 0.0822 mmol) was added in one portion. The reaction was allowed to warm slowly to room temperature overnight. The reaction was quenched with saturated aq NH₄Cl (2 mL), diluted with H₂O (10 mL), and extracted with Et₂O (3 x 15 mL). The combined organic extracts were washed with brine (20 mL), dried (Na₂SO₄), filtered, and concentrated *in vacuo* to afford a clear oil. Purification by flash chromatography eluting with Hexanes : EtOAc (20 : 1 → 10 : 1) to provide 21 mg (73%) of **4.47a** as a clear oil: ¹H-NMR (500 MHz, CD₃OD) δ 7.39 (d, *J* = 7.9 Hz, 1H), 7.33 (d, *J* = 8.4 Hz, 2H), 7.27 (comp, 10H), 7.19 (td, *J* = 7.7, 1.3 Hz, 1H), 7.07 (td, *J* = 7.7, 0.5 Hz, 1H), 6.05 (br, 1H), 5.62 (d, *J* = 6.7 Hz, 1H), 5.42 (br, *J* = 34.7 Hz, 1H), 5.25 (br, 1H), 4.67 (dd, *J* = 13.9, 4.6 Hz, 2H), 4.56 (comp, 2H), 4.52 (d, *J* = 12.1 Hz, 1H), 4.45 (d, *J* = 12.2 Hz, 1H), 4.36 (t, *J* = 8.9 Hz, 1H), 4.31 (d, *J* = 9.9 Hz, 1H), 4.17 (d, *J* = 10.0 Hz, 1H), 4.12 (d, *J* = 9.9 Hz, 1H), 3.99 (d, *J* = 10.1 Hz, 1H), 3.92 (s, 3H), 3.86 – 3.66 (m, 1H), 3.08 – 2.81 (m, 1H), 2.72 (comp, 2H), 2.21 – 2.07 (m, 1H), 1.94 – 1.87 (m, 1H), 1.86 – 1.71 (m, 1H), 0.91 (s, 9H), 0.08 (s, 3H), 0.08 (s, 3H). ¹³C-NMR (125 MHz, CD₃OD) δ 156.3, 141.6, 139.9, 139.7, 139.2, 135.2, 129.4, 129.4, 128.9, 128.8, 128.7, 128.6, 127.4, 122.8, 120.4, 118.1, 115.1, 110.4, 106.0, 77.3, 75.9, 75.9, 74.3, 74.2, 66.5, 53.2, 51.2, 48.7, 42.0, 34.2, 31.9, 26.6, 26.6, 18.9, -4.4, -4.4. HRMS (ESI) *m/z* observed 717.36940 [C₄₂H₅₄N₂O₅Si (M+Na)⁺ requires 717.36940].



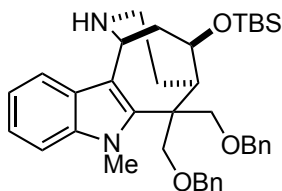
Assignments: ^1H -NMR (500 MHz, CD_3OD) δ 7.39 (d, $J = 7.9$ Hz, 1H, C5-H), 7.33 (d, $J = 8.4$ Hz, 1H, C8-H), 7.27 (comp, 10H, C24-H, C25-H, C26-H, C27-H, C28-H, C29-H, C30-H, C31-H, C32-H, and C33-H), 7.19 (td, $J = 7.7, 1.3$ Hz, 1H, C7-H), 7.07 (td, $J = 7.7, 0.5$ Hz, 1H, C6-H), 6.05 (br, 1H, C35-H), 5.62 (d, $J = 6.7$ Hz, 1H, C14-H), 5.42 (br, $J = 34.7$ Hz, 1H, C36-H), 5.25 (br, 1H, C36-H), 4.67 (dd, $J = 13.9, 4.6$ Hz, 2H, C34-H₂), 4.56 (comp, 2H, C18-H₂ or C19-H₂), 4.52 (d, $J = 12.1$ Hz, 1H, C18-H or C19-H), 4.45 (d, $J = 12.2$ Hz, 1H, C18-H or C19-H), 4.36 (t, $J = 8.9$ Hz, 1H, C12-H), 4.31 (d, $J = 9.9$ Hz, 1H, C20-H or C21-H), 4.17 (d, $J = 10.0$ Hz, 1H, C20-H or C21-H), 4.12 (d, $J = 9.9$ Hz, 1H, C20-H or C21-H), 3.99 (d, $J = 10.1$ Hz, 1H, C20-H or C21-H), 3.92 (s, 3H), 3.86 – 3.66 (m, 1H, C16-H), 3.08 – 2.81 (m, 1H, C13-H), 2.72 (comp, 2H, C11-H and C16-H), 2.21 – 2.07 (m, 1H, C17-H), 1.94 – 1.87 (m, 1H, C13-H), 1.86 – 1.71 (m, 1H, C17-H), 0.91 (s, 9H, C39-H₃), 0.08 (s, 3H, C37-H₃), 0.08 (s, 3H, C37-H₃). ^{13}C -NMR (125 MHz, CD_3OD) δ 156.3 (C15), 141.6 (C2), 139.9 (C22 or C23), 139.7 (C22 or C23), 139.2 (C9), 135.2 (C35), 129.4 (C24 and C32 or C25 and C33), 129.4 (C24 and C32 or C25 and C33), 128.9 (C26 and C30 or C27 and C31), 128.8 (C26 and C30 or C27 and C31), 128.7 (C28 or C29), 128.6 (C28 or C29), 127.4 (C4), 122.8 (C7), 120.4 (C6), 118.1 (C5), 115.1 (C36), 110.4 (C8), 106.0 (C3), 77.3 (C12), 75.9 (C18 or C19), 75.9 (C18 or C19), 74.3 (C20 or C21), 74.2 (C20 or C21), 66.5 (C34), 53.2 (C10), 51.2 (C11), 48.7

(C14), 42.0 (C16), 40.6 (C13), 34.2 (C1), 31.9 (C17), 26.6 (C39), 18.9 (C38), -4.4 (C37), -4.4 (C37).



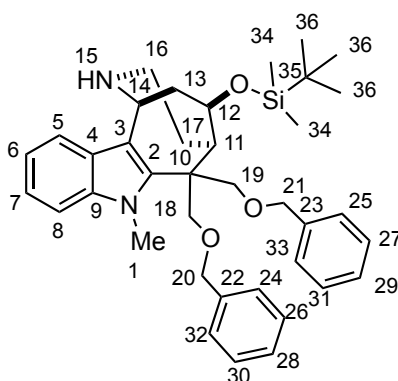
(1R/S, 5R/S, 12R/S)-Allyl-7-allyl-6,6-bis((benzyloxy)methyl)-12-((tert-butyldimethylsilyl)oxy)-3,4,5,6-tetrahydro-1H-5,1-ethanoazocino[4,3-b]indole-2(7H)-carboxylate (**4.47b**). (WLM7_126_2). A mixture of **4.13** (32 mg, 0.047 mmol) and 60% NaH dispersion in mineral oil (19 mg, 0.47 mmol) in DMF (0.5 mL) was stirred for 5 min at 0 °C under N₂ and allyl chloride (18 mg, 0.235 mmol) was added in one portion. The reaction was allowed to warm slowly to room temperature overnight. The reaction was quenched with saturated aq NaHCO₃ (2.0 mL), diluted with H₂O (2.0 mL), and extracted with EtOAc (3 x 10 mL). The combined organic extracts were wash with brine (15.0 mL), dried (Na₂SO₄), filtered, and concentrated *in vacuo* to afford a clear oil. Subsequent purification by flash chromatography eluting with Hexanes : EtOAc (8 : 1) afford 20 mg (59%) of **4.47b** as a clear oil: ¹H-NMR (500 MHz, CDCl₃, mixture of rotamers) δ 7.56 (d, *J* = 7.5 Hz, 0.5 H) 7.45 (d, *J* = 8.0 Hz, 0.5 H) 7.34-7.24 (comp, 8 H) 7.21-7.16 (comp, 4 H) 7.14-7.10 (m, 1 H) 6.12-6.05 (m, 0.5 H) 6.01-5.93 (m, 0.5 H) 5.89-5.82 (m, 1 H) 5.77 (d, *J* = 6.5 Hz, 0.5 H) 5.67-5.62 (comp, 1.5 H) 5.44 (dd, *J* = 17.0, 1.5 Hz, 0.5 H) 5.32-5.28 (comp, 1 H) 5.20 (app d, 0.5 H) 5.06 (app d, 1 H) 4.83-4.68 (comp, 2.5 H) 4.63-4.59 (comp, 1.5 H) 4.58-4.52 (comp, 2 H) 4.47 (d, *J* = 12.0 Hz, 1 H) 4.43 (d, *J* = 12.0 Hz, 1 H) 4.36 (d, *J* = 9.0 Hz, 0.5 H) 4.32 (d, *J* = 9.5 Hz, 0.5 H) 2.29 (d, *J* = 9.5 Hz, 1 H) 4.12-4.04 (comp, 2 H) 3.91 (dd, *J* = 14.5, 6.0 Hz, 0.5 H) 3.78 (dd, *J* = 14.5, 6.0 Hz,

0.5 H) 3.74 (dd, $J = 9.5, 1.5$ Hz, 1 H) 2.30 (m, 0.5 H) 2.89 (m, 0.5 H) 2.86 (m, 1 H) 2.79-2.66 (m, 1 H) 1.99-1.90 (comp, 2 H) 1.86-1.71 (m, 1 H) 0.87 (s, 9 H) 0.06-0.04 (comp, 6 H); ^{13}C -NMR (125 MHz, CDCl_3 , mixture of rotamers) δ 155.4, 155.1, 140.4, 140.3, 138.3, 138.2, 138.2, 137.7, 137.6, 135.1, 135.0, 133.5, 128.2, 127.6, 127.5, 127.5, 127.5, 127.4, 126.5, 126.4, 122.0, 119.5, 117.9, 117.5, 117.3, 116.8, 115.3, 115.2, 114.1, 114.0, 110.3, 110.1, 75.8, 75.6, 75.0, 74.9, 73.3, 73.2, 72.0, 71.8, 65.9, 65.6, 49.9, 49.8, 49.1, 48.7, 47.6, 47.3, 40.9, 40.8, 40.5, 39.5, 30.7, 30.0, 25.8, 18.0, -4.8, -4.9, -5.0; HRMS (ESI) m/z observed 743.38390 [$\text{C}_{44}\text{H}_{56}\text{N}_2\text{O}_5\text{Si}$ ($\text{M}+\text{Na}$) $^+$ requires 743.38510].



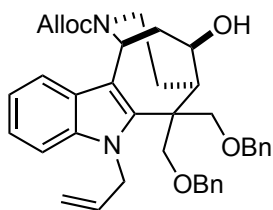
(1*S/R*, 5*R/S*, 12*R/S*)-6,6-Bis((benzyloxy)methyl)-12-((*tert*-butyldimethylsilyl)oxy)-7-methyl-2,3,4,5,6,7-hexahydro-1*H*-5,1-ethanoazocino[4,3-*b*]indole. (**4.48**). (WLM8_214). A round bottom flask charged with $\text{Pd}_2(\text{dba})_3$ (2.8 mg, 0.0030 mmol) and 1,4-bis(diphenylphosphino)butane (2.6 mg, 0.006 mmol) was placed under vacuum and backfilled with N_2 three times. A second round bottom flask was charged with **4.47a** (21 mg, 0.030 mmol) and 1,3-dimethylbarbituric acid (47 mg, 0.302 mmol) and placed under vacuum and backfilled with N_2 three times. THF (0.3 mL) was then added to both flasks, and the mixtures were stirred at room temperature under N_2 for 5 min. A 30 μL aliquot of the Pd/ligand mixture was added via syringe to the flask containing **4.47a**, and stirring was continued at room temperature until **4.47a** was gone by TLC. The reaction was quenched with saturated aq NaHCO_3 (2 mL) and stirred at room temperature for 15 min. The reaction mixture was diluted with H_2O (5 mL) extracted with CH_2Cl_2 (3 x 10 mL). The combined organic extracts were washed with brine (10 mL),

dried (Na₂SO₄), filtered, and concentrated *in vacuo* to afford a brown oil. Subsequent purification by flash chromatography eluting with EtOAc (100%) containing 1% NEt₃ provided 15 mg (81%) of **4.48** as a white solid. ¹H-NMR (500 MHz, CD₃OD) δ 7.51 (dt, *J* = 7.8, 1.0 Hz, 1H), 7.29 (comp, 11H), 7.17 (td, *J* = 7.7, 1.1 Hz, 1H), 7.06 (td, *J* = 7.5, 0.9 Hz, 1H), 4.71 (dd, *J* = 7.0, 1.2 Hz, 1H), 4.62 (td, *J* = 9.0, 1.7 Hz, 1H), 4.57 (d, *J* = 11.6 Hz, 1H), 4.55 (d, *J* = 6.7 Hz, 1H), 4.51 (d, *J* = 12.2 Hz, 1H), 4.45 (d, *J* = 12.2 Hz, 1H), 4.30 (d, *J* = 9.8 Hz, 1H), 4.12 (d, *J* = 9.9 Hz, 1H), 4.10 (d, *J* = 10.1 Hz, 1H), 3.98 (d, *J* = 9.9 Hz, 1H), 3.92 (s, 3H), 2.68 (comp, 2H), 2.58 (ddd, *J* = 12.8, 6.6, 1.5 Hz, 1H), 2.45 (td, *J* = 12.9, 4.1 Hz, 1H), 2.18 – 2.06 (m, 1H), 1.96 – 1.85 (m, 1H), 1.83 – 1.66 (m, 1H), 0.92 (s, 9H), 0.11 (s, 3H), 0.10 (dd, *J* = 7.6, 1.3 Hz, 3H). ¹³C-NMR (125 MHz, CD₃OD) δ 141.2, 140.2, 140.0, 139.3, 129.7, 129.7, 129.1, 129.1, 129.0, 128.8, 127.7, 122.6, 120.0, 118.9, 115.8, 110.4, 77.6, 76.4, 76.3, 74.3, 74.3, 53.5, 51.3, 48.5, 44.7, 42.8, 34.3, 32.8, 26.9, 19.2, -4.0, -4.1. HRMS (ESI) *m/z* observed 633.34810 [C₃₈H₅₀N₂O₃Si (M+Na)⁺ requires 633.34830].



Assignments: ¹H-NMR (500 MHz, CD₃OD) δ 7.51 (dt, *J* = 7.8, 1.0 Hz, 1H, C5-H), 7.29 (comp, 11H, C5-H, C24-H, C25-H, C26-H, C27-H, C28-H, C29-H, C30-H, C31-H, C32-H, and C33-H), 7.17 (td, *J* = 7.7, 1.1 Hz, 1H, C7-H), 7.06 (td, *J* = 7.5, 0.9 Hz, 1H, C6-H), 4.71 (dd, *J* = 7.0, 1.2 Hz, 1H, C14-H), 4.62 (td, *J* = 9.0, 1.7 Hz, 1H, C12-

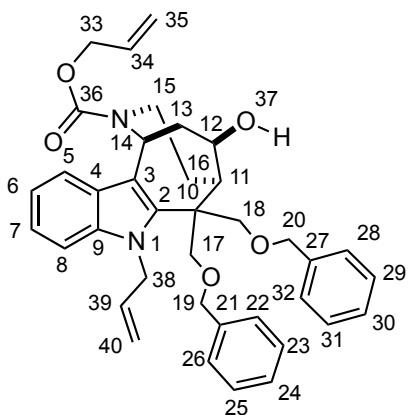
H), 4.57 (d, $J = 11.6$ Hz, 1H, C20-H or C21-H), 4.55 (d, $J = 6.7$ Hz, 1H, C20-H or C21-H), 4.51 (d, $J = 12.2$ Hz, 1H, C20-H or C21-H), 4.45 (d, $J = 12.2$ Hz, 1H, C20-H or C21-H), 4.30 (d, $J = 9.8$ Hz, 1H, C18-H or C19-H), 4.12 (d, $J = 9.9$ Hz, 1H, C18-H or C19-H), 4.10 (d, $J = 10.1$ Hz, 1H, C18-H or C19-H), 3.98 (d, $J = 9.9$ Hz, 1H, C18-H or C19-H), 3.92 (s, 3H, C1-H₃), 2.68 (comp, 2H, C11-H, C13-H), 2.58 (ddd, $J = 12.8, 6.6, 1.5$ Hz, 1H, C16-H), 2.45 (td, $J = 12.9, 4.1$ Hz, 1H, C16-H), 2.18 – 2.06 (m, 1H, C17-H), 1.96 – 1.85 (m, 1H, C13-H), 1.83 – 1.66 (m, 1H, C17-H), 0.92 (s, 9H), 0.11 (s, 3H), 0.10 (s, 3H). ¹³C-NMR (125 MHz, CD₃OD) δ 141.2 (C2), 140.2 (C22 or C23), 140.0 (C22 or C23), 139.3 (C9), 129.7 (C26 and C30 or C27 and C31), 129.7 (C26 and C30 or C27 and C31), 129.1 (C24 and C32 or C25 and C33), 129.1 (C24 and C32 or C25 and C33), 129.0 (C28 or C29), 128.8 (C28 or C29), 127.7 (C4), 122.6 (C7), 120.0 (C6), 118.9 (C5), 115.8 (C3), 110.4 (C8), 77.6 (C12), 76.4 (C20 or C21), 76.3 (C20 or C21), 74.3 (C18 or C19), 74.3 (C18 or C19), 53.5 (C11), 51.3 (C10), 48.5 (C14), 44.7 (C13), 42.8 (C16), 34.3 (C1), 32.8 (C17), 26.9 (C36), 19.2 (C35), -4.0 (C34), -4.1 (C34).



(5R/S, 12R/S)-Allyl-7-allyl-6,6-bis((benzyloxy)methyl)-12-hydroxy-3,4,5,6-tetrahydro-1H-5,1-ethanoazocino[4,3-b]indole-2(7H)-carboxylate (4.50).

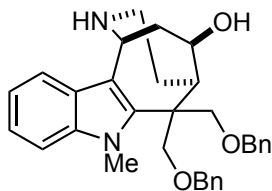
(WLM7_133_2). A mixture of **4.47b** (20 mg, 0.028 mmol) and tetrabutylammonium fluoride trihydrate (18 mg, 0.0555 mmol) in DMF (0.3 mL) was stirred at room temperature under N₂ until starting material was gone by TLC. The reaction was diluted with H₂O (2.0 mL), and extracted with EtOAc (3 x 10 mL). The combined organic

extracts were wash with brine (15 mL), dried (Na₂SO₄), filtered, and concentrated *in vacuo* to afford a clear oil. Subsequent purification by flash chromatography Hexanes : EtOAc (10 : 1 → 4 : 1) afford 15 mg (89%) of **4.50** as a white solid: ¹H-NMR (500 MHz, CD₃CN, 70 °C) δ 7.39 (d, *J* = 9.0 Hz, 1 H) 7.32-7.20 (comp, 11 H) 7.14 (td, *J* = 7.0, 1.0 Hz, 1 H) 7.05 (td, *J* = 7.0 Hz, 0.5 Hz, 1 H) 6.03 (br, 1 H) 5.90-5.83 (m, 1 H) 5.64 (d, *J* = 6.0 Hz, 1 H) 5.33 (br, 1 H) 5.22 (br, 1 H) 5.16 (dm, *J* = 18.5 Hz, 1 H) 5.07 (dd, *J* = 10.5, 1.5 Hz, 1 H) 4.81-4.73 (comp, 2 H) 4.65 (br, 2 H) 4.49-4.43 (comp, 4 H) 4.27 (m, 1 H) 4.10 (d, *J* = 10.0 Hz, 1 H) 4.05 (d, *J* = 10.5 Hz, 2 H) 3.95 (d, *J* = 10.0 Hz, 1 H) 3.82-3.79 (m, 1 H) 3.39-3.36 (m, 1 H) 2.93 (m, 1 H) 2.83 (m, 1 H) 2.76 (m, 1 H) 2.07-1.97 (m, 1 H) 1.86 (m, 1 H) 1.81-1.75 (m, 1 H); ¹³C-NMR (125 MHz, CD₃CN, 70 °C) δ 156.4, 140.4, 139.6, 139.5, 138.9, 136.2, 135.3, 129.6, 129.2, 129.2, 128.9, 128.0, 123.2, 120.8, 117.4, 116.5, 116.1, 111.6, 76.4, 76.1, 76.0, 74.4, 66.7, 51.9, 50.6, 49.8, 42.2; HRMS (ESI) *m/z* observed 629.29880 [C₃₈H₄₂N₂O₅ (M+Na)⁺ requires 629.29860].



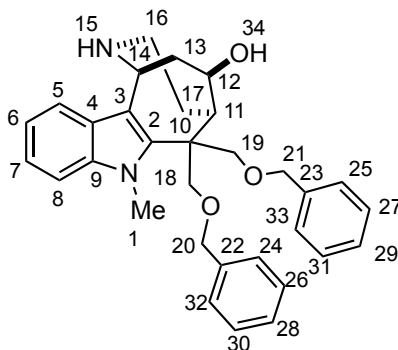
Assignments: ¹H-NMR: δ 7.39 (d, *J* = 9.0 Hz, 1 H, C5-H) 7.32-7.20 (comp, 11 H, C8-H, C22-H, C23-H, C24-H, C25-H, C26-H, C28-H, C29-H, C30-H, C31-H, C32-H) 7.14 (td, *J* = 7.0, 1.0 Hz, 1 H, C7-H) 7.05 (td, *J* = 7.0 Hz, 0.5 Hz, 1 H, C6-H) 6.03 (br, 1 H, C34-H) 5.90-5.83 (m, 1 H, C39-H) 5.64 (d, *J* = 6.0 Hz, 1 H, C14-H) 5.33 (br, 1 H,

C35-H) 5.22 (br, 1 H, C35-H) 5.16 (dm, $J = 18.5$ Hz, 1 H, C38-H) 5.07 (dd, $J = 10.5, 1.5$ Hz, 1 H, C40-H) 4.81-4.73 (comp, 2 H, C40-H and C38-H) 4.65 (br, 2 H, C33-H) 4.49-4.43 (comp, 4 H, C19-H2 and C20-H) 4.27 (m, 1 H, C12-H) 4.10 (d, $J = 10.0$ Hz, 1 H, C17 or C18-H) 4.05 (d, $J = 10.5$ Hz, 2 H, C17-H2 or C18-H2) 3.95 (d, $J = 10.0$ Hz, 1 H, C17-H or C18-H) 3.82-3.79 (m, 1 H, C15-H) 3.39-3.36 (m, 1 H, O37-H) 2.93 (m, 1 H, C13-H) 2.83 (m, 1 H, C11-H) 2.76 (m, 1 H, C15-H) 2.07-1.97 (m, 1 H, C16-H) 1.86 (m, 1 H, C13) 1.81-1.75 (m, 1 H, C16-H); ^{13}C -NMR: δ 156.4 (C-36), 140.4, 139.6, 139.5, 138.9, 136.2 (C39), 135.3, 129.6, 129.2, 129.2, 128.9, 128.0, 123.2 (C7), 120.8 (C6), 117.4, 116.5, 116.1 (C40), 111.6 (C8), 76.4 (C17 or C18), 76.1 (C17 or C18), 76.0 (C12), 74.4 (C19 or C20), 66.7 (C33), 51.9 (C11), 50.6, 49.8 (C38), 42.2 (C15).



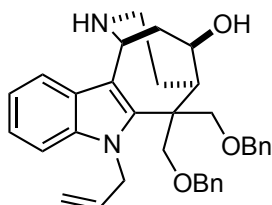
(1S/R, 5R/S, 12R/S)-6,6-Bis((benzyloxy)methyl)-7-methyl-2,3,4,5,6,7-hexahydro-1H-5,1-ethanoazocino[4,3-b]indol-12-ol. (4.49). (WLM8_230). $\text{NEt}_3 \cdot 3\text{HF}$ (50 μL) was added to a solution of **4.48** (15 mg, 0.0246 mmol) in CH_2Cl_2 (0.1 mL) in a plastic vial. The reaction was stirred at room temperature for 36 h, whereupon excess $\text{NEt}_3 \cdot 3\text{HF}$ was quenched with SiO_2 (spatula tip). The reaction mixture was diluted with MeOH (1 mL) and filtered through a sub-micron syringe filter. Subsequent purification by RP HPLC $\text{H}_2\text{O} : \text{MeCN}$ (75 : 25 \rightarrow 95 : 5 over 30 min) provided 2.85 mg (23%) of **4.49** as a white solid: ^1H -NMR (500 MHz, CD_3OD) δ 7.58 (d, $J = 7.9$ Hz, 1H), 7.39 (d, $J = 8.3$ Hz, 1H), 7.27 (comp, 4H), 7.23 (comp, 5H), 7.16 (comp, 3H), 5.28 (dd, $J = 5.3, 1.1$ Hz, 1H), 4.55 (d, $J = 11.9$ Hz, 1H), 4.53 (d, $J = 11.4$ Hz, 1H), 4.51 (d, $J = 11.6$ Hz, 1H), 4.45 (d, $J = 12.0$ Hz, 1H), 4.41 (comp, 2H), 4.13 (d, $J = 9.6$ Hz, 1H), 3.97 (d, $J = 9.5$ Hz,

1H), 3.87 (d, $J = 10.5$ Hz, 1H), 3.79 (s, 3H), 2.96 (comp, 4H), 2.37 (dt, $J = 13.7, 3.9$ Hz, 1H), 2.15 (ddd, $J = 14.8, 9.0, 1.6$ Hz, 1H), 1.95 (tdd, $J = 15.7, 6.2, 2.9$ Hz, 1H). ^{13}C -NMR (125 MHz, CD_3OD) δ 140.1, 137.8, 137.8, 137.5, 128.0, 128.0, 127.7, 127.4, 127.4, 127.4, 125.6, 122.2, 119.7, 116.6, 109.0, 108.2, 76.6, 73.5, 73.3, 72.8, 72.7, 51.2, 49.1, 48.5, 40.5, 38.3, 31.8, 27.9. HRMS (ESI) m/z observed 497.27960 [$\text{C}_{32}\text{H}_{36}\text{N}_2\text{O}_3$ ($\text{M}+\text{H}$) $^+$ requires 497.27990].



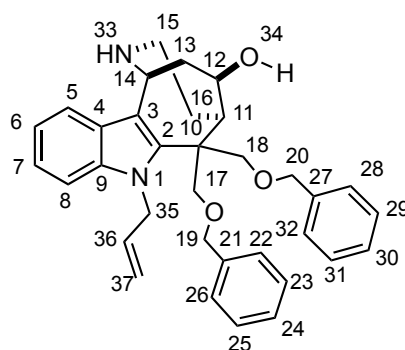
Assignments: ^1H -NMR (500 MHz, CD_3OD) δ 7.58 (d, $J = 7.9$ Hz, 1H, C5-H), 7.39 (d, $J = 8.3$ Hz, 1H, C8-H), 7.27 (comp, 4H, C24-H or C25-H or C26-H or C27-H or C30-H or C31-H or C32-H or C33-H or C28-H or C29-H), 7.23 (comp, 5H, C24-H or C25-H or C26-H or C27-H or C30-H or C31-H or C32-H or C33-H or C28-H or C29-H), 7.16 (comp, 3H, C6-H, C7-H, and C28-H or C29-H), 5.28 (dd, $J = 5.3, 1.1$ Hz, 1H, C14-H), 4.55 (d, $J = 11.9$ Hz, 1H, C20-H or C21-H), 4.53 (d, $J = 11.4$ Hz, 1H, C20-H or C21-H), 4.51 (d, $J = 11.6$ Hz, 1H, C20-H or C21-H), 4.45 (d, $J = 12.0$ Hz, 1H, C20-H or C21-H), 4.41 (comp, 2H, C12-H and C18-H or C19-H), 4.13 (d, $J = 9.6$ Hz, 1H, C18-H or C19-H), 3.97 (d, $J = 9.5$ Hz, 1H, C18-H or C19-H), 3.87 (d, $J = 10.5$ Hz, 1H, C18-H or C19-H), 3.79 (s, 3H, C1-H₃), 2.96 (comp, 4H, C11-H, C13-H, C16-H₂), 2.37 (dt, $J = 13.7, 3.9$ Hz, 1H, C17-H), 2.15 (ddd, $J = 14.8, 9.0, 1.6$ Hz, 1H, C13-H), 1.95 (tdd, $J = 15.7, 6.2, 2.9$ Hz, 1H, C17-H). ^{13}C -NMR (125 MHz, CD_3OD) δ 140.1, 137.8, 137.8, 137.5, 128.0, 128.0, 127.7, 127.4, 127.4, 127.4, 125.6, 122.2, 119.7, 116.6 (C5), 109.0

(C8), 108.2 (C3), 76.6 (C18 or C19), 73.5 (C12), 73.3 (C18 or C19), 72.8 (C20 or C21), 72.7 (C20 or C21), 51.2 (C11), 49.1 (C10), 48.5 (C14), 40.5 (C16), 38.3 (C13), 31.8 (C1), 27.9 (C17).



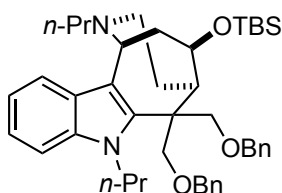
(1S/R, 5R/S, 12R/S)-7-Allyl-6,6-bis((benzyloxy)methyl)-2,3,4,5,6,7-hexahydro-1H-5,1-ethanoazocino[4,3-*b*]indol-12-ol (4.51). (WLM7_138_2). A round bottom flask charged with Pd₂(dba)₃ (0.23 mg, 0.000247 mmol) and 1,4-bis(diphenylphosphino)butane (0.11 mg, 0.000247 mmol) was placed under vacuum and backfilled with N₂ three times. A second round bottom flask was charged with **4.50** (15 mg, 0.0247 mmol) and 1,3-dimethylbarbituric acid (39 mg, 0.247 mmol) and placed under vacuum and backfilled with N₂ three times. DMF (0.2 mL) was then added to both flasks, and the mixtures were stirred at room temperature under N₂ for 5 min. The Pd/ligand mixture was added via syringe to the flask containing **4.50**. The reaction was then heated to 130 °C and stirred for 5 h. The reaction was cooled to room temperature, quenched with saturated aq NaHCO₃ (0.5 mL), and stirred at room temperature for 15 min. The reaction mixture was diluted with MeOH (1.0 mL) and extracted with CH₂Cl₂ (3 x 5.0 mL). The combined organic extracts were washed with H₂O (5.0 mL) brine (5.0 mL), dried (Na₂SO₄), filtered, and concentrated *in vacuo* to afford a yellow oil. Subsequent purification by flash chromatography eluting with CH₂Cl₂ : MeOH (100% to 19 : 1 to 4 : 1) afforded 4 mg (31%) of **4.51** as a white solid: ¹H-NMR (500 MHz, CD₃OD) δ 7.59 (d, *J* = 8.5 Hz, 1 H) 7.30-7.25 (comp, 7 H) 7.24-7.20 (comp, 5 H) 7.16 (td, *J* = 7.0, 1.0 Hz, 1 H) 5.82-5.76 (m,

1 H) 5.27 (dd, $J = 6.5, 1.5$ Hz, 1 H) 5.06 (dm, $J = 18.5$ Hz, 1 H) 5.02 (d, $J = 11.0$ Hz, 1 H) 4.71 (dm, $J = 18.5$ Hz, 1 H) 4.66 (d, $J = 17.5$ Hz, 1 H) 4.53 (d, $J = 12.0$ Hz, 1 H) 4.50 (d, $J = 12.0$ Hz, 1 H) 4.47 (d, $J = 12.0$ Hz, 1 H) 4.41 (td, $J = 9.0, 2.0$ Hz, 1 H) 4.39 (d, $J = 12.0$ Hz, 1 H) 4.09 (d, $J = 10.5$ Hz, 1 H) 4.09 (d, $J = 9.5$ Hz, 1 H) 3.96 (d, $J = 10.5$ Hz, 1 H) 3.95 (d, $J = 9.5$ Hz, 1 H) 2.99-2.92 (comp, 4 H) 2.30-2.27 (m, 1 H) 2.14 (ddd, $J = 14.5, 9.0, 1.5$ Hz, 1 H) 1.95-1.90 (m, 1 H); ^{13}C -NMR (125 MHz, CD_3OD) δ 141.3, 139.2, 138.9, 138.8, 135.4, 129.4, 129.4, 129.2, 129.1, 128.9, 128.9, 127.3, 123.7, 121.3, 118.2, 116.4, 111.7, 109.8, 76.6, 75.1, 74.7, 74.2, 74.1, 50.8, 50.6, 50.0, 49.5, 42.0, 40.0, 29.0; HRMS (CI) m/z observed 521.2789 [$\text{C}_{34}\text{H}_{37}\text{N}_2\text{O}_3$ (M) $^+$ requires 521.2804].

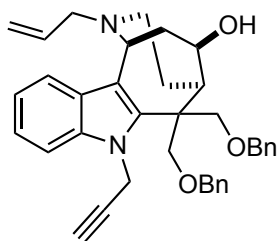


Assignments: ^1H -NMR: δ 7.59 (d, $J = 8.5$ Hz, 1 H, C5-H) 7.30-7.25 (comp, 7 H) 7.24-7.20 (comp, 5 H) 7.16 (td, $J = 7.0, 1.0$ Hz, 1 H, C6-H) 5.82-5.76 (m, 1 H, C36-H) 5.27 (dd, $J = 6.5, 1.5$ Hz, 1 H, C14-H) 5.06 (dm, $J = 18.5$ Hz, 1 H, C35-H) 5.02 (d, $J = 11.0$ Hz, 1 H, C37-H) 4.71 (dm, $J = 18.5$ Hz, 1 H, C37-H) 4.66 (d, $J = 17.5$ Hz, 1 H, C35-H) 4.53 (d, $J = 12.0$ Hz, 1 H, C19-H of C20-H) 4.50 (d, $J = 12.0$ Hz, 1 H, C19-H or C20-H) 4.47 (d, $J = 12.0$ Hz, 1 H, C19-H or C20-H) 4.41 (td, $J = 9.0, 2.0$ Hz, 1 H, C12-H) 4.39 (d, $J = 12.0$ Hz, 1 H, C19-H or C20-H) 4.09 (d, $J = 10.5$ Hz, 1 H, C17-H or C18-H) 4.09 (d, $J = 9.5$ Hz, 1 H, C17-H or C18-H) 3.96 (d, $J = 10.5$ Hz, 1 H, C17-H or C18-H) 3.95 (d, $J = 9.5$ Hz, 1 H, C17-H or C18-H) 2.99-2.92 (comp, 4 H, C11-H and C13-H and

C15-H and C16-H) 2.30-2.27 (m, 1 H, C15-H or C16-H) 2.14 (ddd, $J = 14.5, 9.0, 1.5$ Hz, 1 H, C13-H) 1.95-1.90 (m, 1 H, C15-H or C16-H). ^{13}C -NMR: δ 141.3, 139.2, 138.9, 138.8, 135.4, 129.4, 129.4, 129.2, 129.1, 129.0, 128.9, 127.3, 123.7, 121.3 (C6), 118.2 (C5), 116.4 (C37), 111.7, 109.8, 76.6 (C17 or C18 or C19 or C20), 75.1 (C17 or C18 or C19 or C20), 74.7 (C12), 74.2 (C17 or C18 or C19 or C20), 74.1 (C17 or C18 or C19 or C20), 50.8, 50.6, 50.0 (C14), 49.5 (C35), 42.0, 39.8, 29.0.

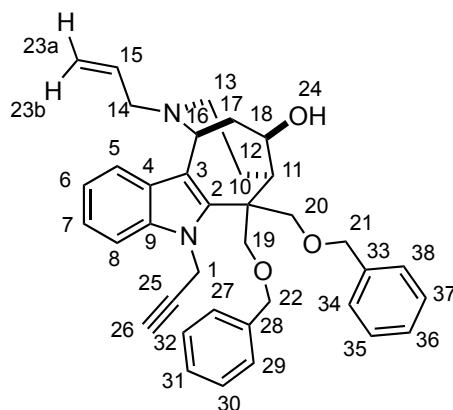


(1*S*/*R*, 5*R*/*S*, 12*R*/*S*)-6,6-Bis((benzyloxy)methyl)-12-((*tert*-butyldimethylsilyl)oxy)-2,7-dipropyl-2,3,4,5,6,7-hexahydro-1*H*-5,1-ethanoazocino[4,3-*b*]indole. (**4.53**). (WLM7_274). Compound **4.16** (16 mg, 0.025 mmol) was stirred with 10% Pd/C (1.6 mg) in MeOH (0.25 mL) under and atmosphere of H₂ (balloon) for 14 h. The reaction mixture was filtered through a pad of celite and concentrated under reduced pressure to afford 16 mg (quant) of **4.53**. The crude material was carried on to the next step without additional purification: ^1H -NMR (500 MHz, CDCl₃) δ 7.46-7.06 (comp, 14 H) 4.76 (m, 1 H) 4.62-4.58 (comp, 2 H) 4.47-4.36 (comp, 3 H) 4.10 (d, $J = 9.5$ Hz, 1 H) 3.97 (m, 1 H) 3.89-3.77 (comp, 2 H) 2.83 (m, 1 H) 2.65-2.61 (comp, 2 H) 2.49-2.28 (comp, 2 H) 1.98-1.94 (comp, 2 H) 1.89 (m, 1 H) 1.75 (comp, 4 H) 1.65 (m, 1 H) 1.54 (m, 1 H) 1.09 (m, 1 H) 0.96 (t, $J = 7.5$ Hz, 3 H) 0.87 (s, 9 H) 0.78 (t, $J = 7.5$ Hz, 3 H) 0.07 (s, 3 H) 0.05 (s, 3 H); HRMS (ESI) m/z observed 681.44390 [C₄₃H₆₀N₂O₃Si (M+H)⁺ requires 681.44460].

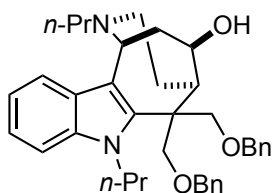


(1*S/R*, 5*R/S*, 12*R/S*)-2-Allyl-6,6-bis((benzyloxy)methyl)-7-(prop-2-yn-1-yl)-2,3,4,5,6,7-hexahydro-1*H*-5,1-ethanoazocino[4,3-*b*]indol-12-ol. (4.54a).

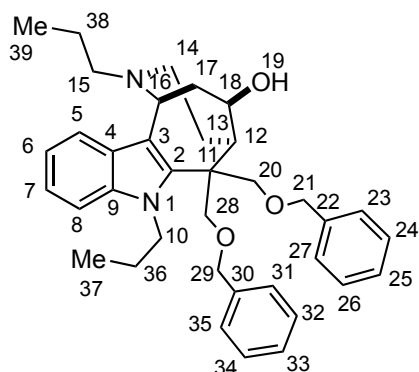
(WLM7_275_2). NEt₃•3HF (0.1 mL) was added to a solution of **4.16** (13.5 mg, 0.020 mmol) in CH₂Cl₂ (0.1 mL) in a plastic vial. The reaction was stirred at room temperature for 36 h, whereupon excess NEt₃•3HF was quenched with SiO₂ (spatula tip). The reaction mixture was diluted with MeOH (1.0 mL) and filtered through a sub-micron syringe filter. Subsequent purification by RP HPLC H₂O : MeCN (10% MeCN → 95% MeCN over 30 min) provided 11.0 mg (98%) of **4.54a** as a white solid: ¹H-NMR (500 MHz, CD₃OD) δ 7.57 (d, *J* = 8.0 Hz, 1 H) 7.50 (d, *J* = 8.0 Hz, 1 H) 7.32-7.17 (comp, 12 H) 6.02 (m, 1 H) 5.56 (d, *J* = 10.0 Hz, 1 H) 5.47 (d, *J* = 17.0 Hz, 1 H) 5.31 (dd, *J* = 14.0, 2.5 Hz, 1 H) 5.22 (d, *J* = 4.5 Hz, 1 H) 4.90 (dd, *J* = 19.0, 2.5 Hz, 1 H) 4.59 (d, *J* = 11.5 Hz, 1 H) 4.52 (d, *J* = 12.0 Hz, 1 H) 4.49 (d, *J* = 11.5 Hz, 1 H) 4.43 (d, *J* = 12.0 Hz, 1 H) 4.39 (td, *J* = 9.0, 2.0 Hz, 1 H) 4.21 (d, *J* = 10.5 Hz, 1 H) 4.11 (d, *J* = 10.0 Hz, 1 H) 4.07 (d, *J* = 9.5 Hz, 1 H) 4.00 (d, *J* = 10.5 Hz, 1 H) 3.97 (dd, *J* = 13.5, 6.5 Hz, 1 H) 3.43 (dd, *J* = 13.5, 7.5 Hz, 1 H) 3.10 (dd, *J* = 13.5, 4.0 Hz, 1 H) 3.02 (m, 1 H) 2.96-2.89 (comp, 2 H) 2.71 (m, 1 H) 2.30 (dm, *J* = 16.5 Hz, 1 H) 2.12 (dd, *J* = 13.5, 8.5 Hz, 1 H) 1.92 (m, 1 H); ¹³C-NMR (125 MHz, CD₃OD) δ 141.9, 139.1, 138.8, 138.4, 129.4, 129.4, 129.3, 129.2, 129.0, 128.9, 128.7, 128.6, 125.9, 124.1, 122.3, 118.1, 111.6, 108.1, 79.8, 76.4, 75.3, 74.8, 74.4, 74.3, 61.6, 59.4, 50.7, 50.6, 50.4, 49.6, 47.9, 39.6, 37.0, 28.9; HRMS (ESI) *m/z* observed 561.31020 [C₃₇H₄₀N₂O₃ (M+H)⁺ requires 561.31120].



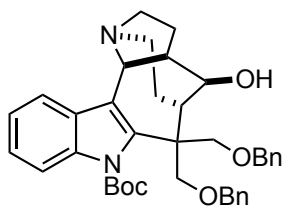
Assignments: $^1\text{H-NMR}$ (500 MHz, CD_3OD) δ 7.57 (d, $J = 8.0$ Hz, 1 H, C5-H) 7.50 (d, $J = 8.0$ Hz, 1 H, C8-H) 7.32-7.17 (comp, 12 H) 6.02 (m, 1 H, C15-H) 5.56 (d, $J = 10.0$ Hz, 1 H, C23_b-H) 5.47 (d, $J = 17.0$ Hz, 1 H, C23_a-H) 5.31 (dd, $J = 14.0, 2.5$ Hz, 1 H, C1-H) 5.22 (d, $J = 4.5$ Hz, 1 H, C16-H) 4.90 (dd, $J = 19.0, 2.5$ Hz, 1 H, C1-H) 4.59 (d, $J = 11.5$ Hz, 1 H, C21-H or C22-H) 4.52 (d, $J = 12.0$ Hz, 1 H, C21-H or C22-H) 4.49 (d, $J = 11.5$ Hz, 1 H, C21-H or C22-H) 4.43 (d, $J = 12.0$ Hz, 1 H, C21-H or C22-H) 4.39 (td, $J = 9.0, 2.0$ Hz, 1 H, C18-H) 4.21 (d, $J = 10.5$ Hz, 1 H, C19-H or C20-H) 4.11 (d, $J = 10.0$ Hz, 1 H, C19-H or C20-H) 4.07 (d, $J = 9.5$ Hz, 1 H, C19-H or C20-H) 4.00 (d, $J = 10.5$ Hz, 1 H, C19-H or C20-H) 3.97 (dd, $J = 13.5, 6.5$ Hz, 1 H, C14-H) 3.43 (dd, $J = 13.5, 7.5$ Hz, 1 H, C14-H) 3.10 (dd, $J = 13.5, 4.0$ Hz, 1 H, C13-H) 3.02 (m, 1 H, C17-H) 2.96-2.89 (comp, 2 H, C11-H and C13-H) 2.71 (m, 1 H, C26-H) 2.30 (dm, $J = 16.5$ Hz, 1 H, C12-H) 2.12 (dd, $J = 13.5, 8.5$ Hz, 1 H, C17-H) 1.92 (m, 1 H, C12-H); $^{13}\text{C-NMR}$ (125 MHz, CD_3OD) δ 141.9, 139.1, 138.8, 138.4, 129.4, 129.4, 129.3, 129.2, 129.0, 128.9, 128.7 (C15), 128.6, 125.9 (C23), 124.1 (C7), 122.3 (C6), 118.1 (C5), 111.6 (C8), 108.1 (C3), 79.8 (C25 or C26), 76.4 (C19 or C20), 75.3 (C19 or C20), 74.8 (C21 or C22), 74.4 (C21 or C22), 74.3 (C18), 61.6 (C14), 59.4 (C16), 50.7 (C11), 50.6 (C13), 50.4 (C10), 39.6 (C17), 37.0 (C1), 28.9 (C12).



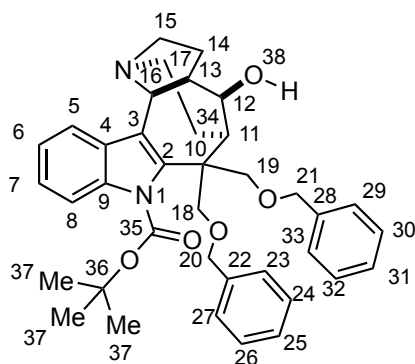
(1S/R, 5R/S, 12R/S)-6,6-Bis((benzyloxy)methyl)-2,7-dipropyl-2,3,4,5,6,7-hexahydro-1H-5,1-ethanoazocino[4,3-b]indol-12-ol. (4.54b). (WLM7_283). NEt₃•3HF (0.1 mL) was added to a solution of **4.53** (14.5 mg, 0.021 mmol) in CH₂Cl₂ (0.1 mL) in a plastic vial. The reaction was stirred at room temperature for 36 h, whereupon excess NEt₃•3HF was quenched with SiO₂ (spatula tip). The reaction mixture was diluted with MeOH (1.0 mL) and filtered through a sub-micron syringe filter. Subsequent purification by RP HPLC H₂O : MeCN (10% MeCN → 95% MeCN over 30 min) provided 10.0 mg (83 %) of **4.54b** as a white solid: ¹H-NMR (500 MHz, CD₃OD) δ 7.50 (d, *J* = 8.0 Hz, 1 H) 7.31-7.19 (comp, 13 H) 5.23 (d, *J* = 4.0 Hz, 1 H) 4.56 (d, *J* = 11.5 Hz, 1 H) 4.51-4.48 (comp, 2 H) 4.40 (m, 1 H) 4.37 (d, *J* = 12.0 Hz, 1 H) 4.19-4.10 (comp, 3 H) 3.97-3.86 (comp, 3 H) 3.18-3.11 (m, 1 H) 3.04-2.93 (comp, 2 H) 2.84-2.76 (m, 1 H) 2.34 (dm, *J* = 16.0 Hz, 1 H) 2.15- 2.09 (m, 1 H) 2.01-1.94 (comp, 2 H) 1.77 (m, 1 H) 1.69 (m, 1 H) 1.55 (m, 1 H) 0.99 (t, *J* = 7.5 Hz, 3 H) 0.80 (t, *J* = 7.5 Hz, 3 H); ¹³C-NMR (125 MHz, CD₃OD) δ 141.6, 139.1, 138.8, 138.4, 129.5, 129.5, 129.3, 129.2, 129.1, 129.0, 128.9, 123.7, 121.8, 117.8, 111.6, 107.3, 77.0, 74.9, 74.5, 74.3, 74.0, 71.5, 60.9, 59.4, 51.1, 50.6, 50.1, 49.5, 39.9, 29.1, 23.6, 19.6, 11.4, 11.3; HRMS (ESI) *m/z* observed 567.35700 [C₃₇H₄₆N₂O₃ (M+H)⁺ requires 567.35810].



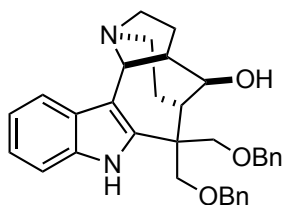
Assignments: $^1\text{H-NMR}$ (500 MHz, CD_3OD) δ 7.50 (d, $J = 8.0$ Hz, 1 H, C5-H) 7.31-7.19 (comp, 13 H) 5.23 (d, $J = 4.0$ Hz, 1 H, C16-H) 4.56 (d, $J = 11.5$ Hz, 1 H, C21-H or C29-H) 4.51-4.48 (comp, 2 H, C21-H₂ or C29-H₂) 4.40 (m, 1 H, C18-H) 4.37 (d, $J = 12.0$ Hz, 1 H, C21-H or C29-H) 4.19-4.10 (comp, 3 H, C10-H, C20-H, and C28-H) 3.97-3.86 (comp, 3 H, C10-H, C20-H, and C28-H) 3.18-3.11 (comp, 2 H, C14-H and C15-H) 3.04-2.93 (comp, 3 H, C12-H, C14-H, and C17-H) 2.84-2.76 (m, 1 H, C15-H) 2.34 (dm, $J = 16.0$ Hz, 1 H, C13-H) 2.15- 2.09 (m, 1 H, C17-H) 2.01-1.94 (comp, 2 H, C13-H and C38-H) 1.77 (m, 1 H, C38-H) 1.69 (m, 1 H, C36-H) 1.55 (m, 1 H, C36-H) 0.99 (t, $J = 7.5$ Hz, 3 H, C39-H₃) 0.80 (t, $J = 7.5$ Hz, 3 H, C37-H₃); $^{13}\text{C-NMR}$ (125 MHz, CD_3OD) δ 141.6, 139.1, 138.8, 138.4, 129.5, 129.5, 129.3, 129.2, 129.1, 129.0, 128.9, 123.7 (C7), 121.8 (C6), 117.8 (C5), 111.6 (C8), 107.3 (C3), 77.0 (C20 or C28), 74.9 (C20 or C28), 74.5 (C18), 74.3 (C21 or C29), 74.0 (C21 or C29), 60.9 (C15), 59.4 (C16), 51.1 (C14), 50.6 (C11), 50.1 (C12), 49.5 (C10), 39.9 (C17), 29.1 (C13), 23.6 (C36), 19.6 (C38), 11.4 (C37), 11.3 (C39).



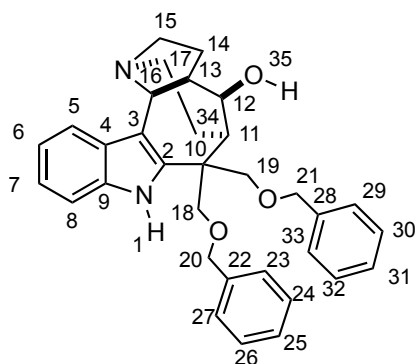
(4S/R, 7R/S, 13cR/S, 14S/R)-*tert*-Butyl-8,8-bis((benzyloxy)methyl)-14-hydroxy-2,3,5,6,7,8-hexahydro-1H-1,7-methanopyrrolo[1',2':1,2]azocino[4,3-b]indole-9(13cH)-carboxylate. (**4.56**). (WLM7_181_2). A mixture of **3.25** (31 mg, 0.051 mmol) in Et₂O (0.5 mL) at room temperature was added lithium aluminum hydride (4 mg, 0.102 mmol) in one portion and the reaction was stirred at room temperature for four h. The reaction mixture was quenched with saturated aq Rochelle's salt (2.0 mL) and allowed to stir at room temperature for 10 min. The reaction mixture was diluted with MeOH (4.0 mL) and extracted with CH₂Cl₂ (3 x 5 mL). The combined organic extracts were washed with H₂O (10.0 mL), brine (10.0 mL), dried (Na₂SO₄), and concentrated *in vacuo* to afford a yellow solid. Subsequent purification by flash chromatography (basic alumina) eluting with CH₂Cl₂ : MeOH (100% → 19 : 1) afforded 28 mg (90%) **4.56** as a white solid: ¹H-NMR (500 MHz, CDCl₃) δ 12.45 (br, 1 H) 7.68 (d, *J* = 7.5 Hz, 1 H) 7.65 (d, *J* = 9.0 Hz, 1 H) 7.34-7.20 (comp, 8 H) 7.16-7.14 (comp, 2 H) 7.07-7.05 (comp, 2 H) 5.20 (app t, *J* = 5.0 Hz, 1 H) 4.65 (d, *J* = 9.5 Hz, 1 H) 4.51 (d, *J* = 12.0 Hz, 2 H) 4.44 (d, *J* = 11.0 Hz, 1 H) 4.36 (d, *J* = 12.0 Hz, 1 H) 4.28 (d, *J* = 9.5 Hz, 1 H) 4.09 (m, 1 H) 4.00 (d, *J* = 9.0 Hz, 1 H) 3.87 (m, 1 H) 3.84 (d, *J* = 9.0 Hz, 1 H) 3.24-3.20 (m, 1 H) 3.09 (app t, *J* = 12.0 Hz, 1 H) 2.88-2.81 (comp, 3 H) 2.52 (m, 1 H) 2.16 (m, 1 H) 2.07-2.03 (m, 1 H) 1.88-1.83 (m, 1 H) 1.63 (s, 9 H); ¹³C-NMR (125 MHz, CDCl₃) δ 151.2, 139.6, 136.9, 136.551, 136.4, 128.5, 128.4, 128.1, 128.0, 128.0, 127.8, 127.5, 125.1, 122.9, 118.4, 113.8, 110.5, 85.1, 80.8, 75.7, 75.1, 73.7, 73.4, 60.8, 49.9, 49.8, 49.2, 48.6, 46.8, 33.3, 28.0, 23.5; HRMS (ESI) *m/z* observed 609.33200 [C₃₈H₄₄N₂O₅ (M+H)⁺ requires 609.33230].



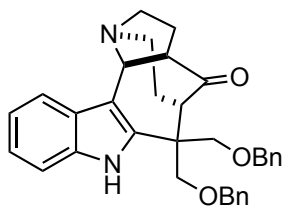
Assignments: $^1\text{H-NMR}$: δ 12.44 (br, 1 H, O38-H) 7.68 (d, $J = 7.5$ Hz, 1 H, C8-H) 7.65 (d, $J = 9.0$ Hz, 1 H, C5-H) 7.34-7.20 (comp, 8 H) 7.16-7.14 (comp, 2 H) 7.07-7.05 (comp, 2 H) 5.20 (app t, $J = 5.0$ Hz, 1 H, C16-H) 4.65 (d, $J = 9.5$ Hz, 1 H, C18-H or C19-H or C20-H or C21-H) 4.51 (d, $J = 12.0$ Hz, 2 H, C18-H or C19-H or C20-H or C21-H) 4.44 (d, $J = 11.0$ Hz, 1 H, C18-H or C19-H or C20-H or C21-H) 4.36 (d, $J = 12.0$ Hz, 1 H, C18-H or C19-H or C20-H or C21-H) 4.28 (d, $J = 9.5$ Hz, 1 H, C18-H or C19-H or C20-H or C21-H) 4.09 (m, 1 H, C15-H) 4.00 (d, $J = 9.0$ Hz, 1 H, C18-H or C19-H or C20-H or C21-H) 3.87 (m, 1 H, C12-H) 3.84 (d, $J = 9.0$ Hz, 1 H, C18-H or C19-H or C20-H or C21-H) 3.24-3.20 (m, 1 H, C15-H) 3.09 (app t, $J = 12.0$ Hz, 1 H, C17-H) 2.88-2.81 (comp, 3 H, C11-H, C13-H, C17-H₂) 2.52 (m, 1 H, C14-H) 2.16 (m, 1 H, C14-H) 2.07-2.03 (m, 1H, C34-H) 1.88-1.83 (m, 1H, C34-H) 1.63 (s, 9H, C37-CH₃). $^{13}\text{C-NMR}$: δ 151.2 (C35), 139.6, 136.892, 136.6, 136.4, 128.6, 128.5, 128.1, 128.0, 128.0, 127.8, 127.5, 125.1, 122.9, 118.4, 113.8, 110.5, 85.1 (C36), 80.8 (C12), 75.7 (C18 or C19 or C20 or C21), 75.1 (C18 or C19 or C20 or C21), 73.7 (C18 or C19 or C20 or C21), 73.4 (C18 or C19 or C20 or C21), 60.8 (C16), 49.9 (C11 or C13), 49.8 (C11 or C13), 49.2 (C10), 48.6 (C15), 46.8 (C17), 33.3 (C14), 28.0 (C37), 23.5 (C34).



(1R/S, 4R/S, 7R/S, 13cS/R, 14S/R)-8,8-Bis((benzyloxy)methyl)-2,3,5,6,7,8,9,13c-octahydro-1H-1,7-methanopyrrolo[1',2':1,2]azocino[4,3-b]indol-14-ol. (**4.57**). (WLM7_149_2). A 1.5 mL screw top vial charged with **4.56** (7 mg, 0.0115 mmol), 40% aq NaOH (0.1 mL), and MeOH (1.0 mL) was stirred at room temperature for one week. The reaction mixture was quenched with saturated aq NH₄Cl (0.5 mL) and extracted with CH₂Cl₂ (3 x 1.0 mL). The combined organic extracts were washed with H₂O (1.0 mL), brine (1.0 mL), dried (Na₂SO₄), and concentrated *in vacuo* to afford a yellow oil. Subsequent purification by RP HPLC H₂O : MeCN (90 : 10 → 5 : 95 over 30 min) afforded 5.0 mg (85%) of **4.57** as a white solid. ¹H-NMR (500 MHz, CD₃OD) δ 10.58 (br, 1 H) 7.58 (d, *J* = 8.0 Hz, 1 H) 7.39 (d, *J* = 8.5 Hz, 1 H) 7.31-7.23 (comp, 10 H) 7.16 (td, *J* = 7.5, 1.0 Hz, 1 H) 7.10 (td, *J* = 7.5, 1.0 Hz, 1 H) 5.22 (d, *J* = 6.5 Hz, 1 H) 4.60-4.53 (comp, 4H) 4.30 (d, *J* = 9.0 Hz, 1 H) 4.21 (d, *J* = 9.5 Hz, 1 H) 4.11 (d, *J* = 5.5 Hz, 1 H) 4.06 (d, *J* = 9.0 Hz, 1 H) 3.76-3.71 (m, 1 H) 3.74 (d, *J* = 9.0 Hz, 1 H) 3.59-3.53 (m, 1 H) 3.25 (td, *J* = 9.0, 3.5 Hz, 1 H) 2.98 (dm, *J* = 14.0 Hz, 1 H) 2.90 (t, *J* = 7.5 Hz, 1 H) 2.80 (app t, *J* = 5.0 Hz, 1 H) 2.64 (m, 1 H) 2.22-2.15 (comp, 2 H) 2.07 (m, 1 H); ¹³C-NMR (125 MHz, CD₃OD) δ 142.9, 139.6, 139.5, 137.1, 129.4, 129.4, 129.0, 128.8, 128.7, 128.6, 123.3, 121.0, 118.0, 112.3, 100.7, 82.3, 76.2, 74.5, 74.4, 73.5, 63.9, 51.6, 50.1, 49.6, 48.2, 43.4, 33.2, 22.6; HRMS (ESI) *m/z* observed 509.28030 [C₃₃H₃₆N₂O₃ (M+H)⁺ requires 509.27990].

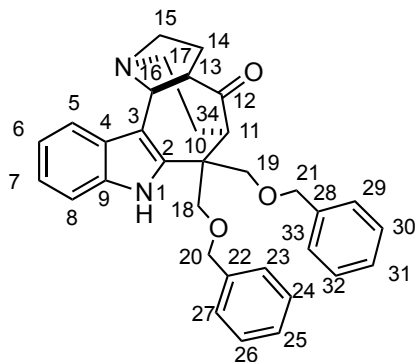


Assignments: ^1H -NMR (500 MHz, CD_3OD) δ 10.58 (br, 1 H, N1-H) 7.58 (d, J = 8.0 Hz, 1 H, C5-H) 7.39 (d, J = 8.5 Hz, 1 H, C8-H) 7.31-7.23 (comp, 10 H, C23-H, C24-H, C25-H, C26-H, C27-H, C29-H, C30-H, C31-H, C32-H, C33-H) 7.16 (td, J = 7.5, 1.0 Hz, 1 H, C7-H) 7.10 (td, J = 7.5, 1.0 Hz, 1 H, C6-H) 5.22 (d, J = 6.5 Hz, 1 H, C16-H) 4.60-4.53 (comp, 4 H, C20-H₂, C21-H₂) 4.30 (d, J = 9.0 Hz, 1 H, C18-H or C19-H) 4.21 (d, J = 9.5 Hz, 1 H, C18-H or C19-H) 4.11 (d, J = 5.5 Hz, 1 H, C12-H) 4.06 (d, J = 9.0 Hz, 1 H, C18-H or C19-H) 3.76-3.71 (m, 1 H, C15-H) 3.74 (d, J = 9.0 Hz, 1 H, C18-H or C19-H) 3.59-3.53 (m, 1 H, C15-H) 3.25 (td, J = 9.0, 3.5 Hz, 1 H, C17-H) 2.98 (dm, J = 14.0 Hz, 1 H, C17-H) 2.90 (t, J = 7.5 Hz, 1 H, C13-H) 2.80 (app t, J = 5.0 Hz, 1 H, C11-H) 2.64 (m, 1 H, C14-H) 2.22-2.15 (comp, 2 H, C14-H, C34-H) 2.07 (m, 1 H, C34-H); ^{13}C -NMR (125 MHz, CD_3OD) δ 142.9, 139.6, 139.5, 137.1, 129.4, 129.4, 129.0, 128.8, 128.7, 128.6, 123.3 (C7), 121.0 (C6), 118.0 (C5), 112.3 (C8), 100.7 (C3), 82.3 (C12), 76.2 (C18 or C19), 74.5 (C20 or C21), 74.4 (C20 or C21), 73.5 (C18 or C19), 63.9 (C16), 51.6 (C13), 50.1 (C15), 49.6 (C10), 48.2 (C17), 43.4 (C11), 33.2 (C14), 22.6 (C34).

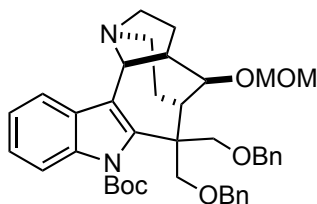


(4S/R, 7R/S, 13cR/S)-8,8-Bis((benzyloxy)methyl)-2,3,5,6,7,8,9,13c-octahydro-1H-1,7-methanopyrrolo[1',2':1,2]azocino[4,3-b]indol-14-one (4.58). (WLM7_130_2).

A 1.5 mL screw top vial charged with **3.25** (4 mg, mmol), 40% aq NaOH (0.1 mL), and MeOH (1.0 mL) was stirred at room temperature for one week. The reaction mixture was diluted with CH₂Cl₂ (2.0 mL), washed with H₂O (1.0 mL), brine (1.0 mL), dried (Na₂SO₄), and concentrated *in vacuo* to afford a yellow oil. Subsequent purification by RP HPLC H₂O : MeCN (90 : 10 → 5 : 95 over 30 min) afforded 2.0 mg (60%) of **4.58** as a yellow solid: ¹H-NMR (500 MHz, CD₃OD) δ 7.60 (d, *J* = 8.0 Hz, 1 H) 7.36 (dm, *J* = 8.0 Hz, 1 H) 7.28-7.16 (comp, 10 H) 7.15 (td, *J* = 7.0, 1.0 Hz, 1 H) 7.08 (td, *J* = 7.0, 1.0 Hz, 1 H) 4.91 (d, *J* = 5.5 Hz, 1 H) 4.59 (d, *J* = 12.0 Hz, 1H) 4.56 (d, *J* = 12.0 Hz, 1 H) 4.44 (d, *J* = 12.0 Hz, 1 H) 4.39 (d, *J* = 12.0 Hz, 1 H) 4.09 (d, *J* = 9.0 Hz, 1 H) 3.82 (d, *J* = 9.0 Hz, 1 H) 3.66 (d, *J* = 9.0 Hz, 1 H) 3.62 (d, *J* = 9.0 Hz, 1 H) 3.52-3.41 (m, 2 H) 3.28-3.25 (m, 2 H) 3.16-3.15 (m, 1 H) 2.82 (m, 1 H) 2.61-2.53 (m, 1 H) 2.24-2.16 (m, 2 H) 2.02-1.98 (m, 1 H) ¹³C-NMR (125 MHz, CD₃OD) δ 215.3, 139.8, 139.4, 139.3, 137.1, 129.4, 130.0, 128.9, 128.8, 128.6, 123.3, 120.7, 118.6, 112.1, 75.5, 74.6, 74.3, 72.5, 60.0, 58.0, 55.6, 51.4, 49.6, 47.0, 31.7, 23.8; HRMS (ESI) *m/z* observed 507.26450 [C₃₃H₃₄N₂O₃ (M+H)⁺ requires 507.26420].

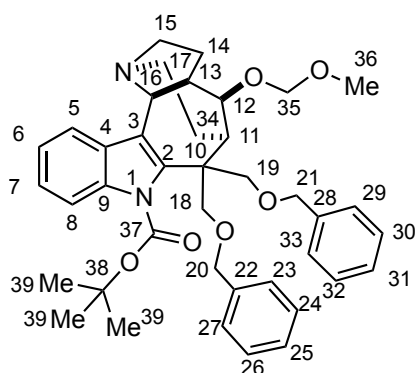


Assignments: $^1\text{H-NMR}$: δ 7.60 (d, $J = 8.0$ Hz, 1 H, C5-H) 7.36 (dm, $J = 8.0$ Hz, 1 H, C8-H) 7.28-7.16 (comp, 10 H, C22-H, C23-H, C24-H, C25-H, C26-H, C27-H, C29-H, C30-H, C31-H, C32-H, C33-H) 7.15 (td, $J = 7.0, 1.0$ Hz, 1 H, C7-H) 7.08 (td, $J = 7.0, 1.0$ Hz, 1 H, C6-H) 4.91 (d, $J = 5.5$ Hz, 1 H, C16-H) 4.59 (d, $J = 12.0$ Hz, 1 H, C20-H or C21-H) 4.56 (d, $J = 12.0$ Hz, 1 H, C20-H or C21-H) 4.44 (d, $J = 12.0$ Hz, 1 H, C20-H or C21-H) 4.39 (d, $J = 12.0$ Hz, 1 H, C20-H or C21-H) 4.09 (d, $J = 9.0$ Hz, 1 H, C19-H) 3.82 (d, $J = 9.0$ Hz, 1 H, C19-H) 3.66 (d, $J = 9.0$ Hz, 1 H, C18-H) 3.62 (d, $J = 9.0$ Hz, 1 H, C18-H) 3.52-3.41 (m, 2 H, C15-H) 3.28-3.25 (m, 2 H, C13-H and C17-H) 3.16-3.15 (m, 1 H, C11-H) 2.82 (m, 1 H, C17-H) 2.61-2.53 (m, 1 H, C14-H) 2.24-2.16 (m, 2 H, C14-H and C34-H) 2.02-1.98 (m, 1 H, C34-H) $^{13}\text{C-NMR}$: δ 215.3 (C12), 139.8, 139.4, 139.3, 137.1, 129.4, 130.0, 128.9, 128.8, 128.6, 123.3 (C7), 120.7 (C6), 118.6 (C5), 112.1 (C8), 75.5 (C18), 74.6 (C20 or C21), 74.3 (C20 or C21), 72.5 (C19), 60.0 (C16), 58.0 (C13), 55.6 (C11), 51.4 (C15), 49.6 (C17), 47.0 (C10), 31.7 (C14), 23.8 (C34).



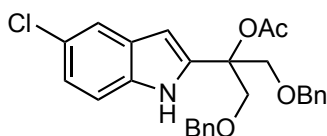
(1R/S, 4R/S, 7R/S, 13cS/R, 14S/R)-8,8-Bis((benzyloxy)methyl)-14-(methoxymethoxy)-2,3,5,6,7,8,9,13c-octahydro-1H-1,7-methanopyrrolo[1',2':1,2]azocino[4,3-b]indole. (4.59). (WLM7_215_2). To a mixture of **4.56** (4.0 mg, 0.00657 mmol) and *N,N*-diisopropylethylamine (4.25 mg, 0.0329 mmol) in dry CH_2Cl_2 (0.3 mL) at 0 °C was added MOM-Cl (0.0197 mmol, 17 μL , 1.18 M in CH_2Cl_2). After 5 h, the reaction was quench by the addition of saturated aq NaHCO_3 (0.5 mL). The reaction was diluted with MeOH (0.5 mL) and extracted with CH_2Cl_2 (3 x 3

mL). The combined organic extracts were washed with brine (1.0 mL), dried (Na_2SO_4), and concentrated *in vacuo* to afford a yellow oil that was purified by flash chromatography (basic Al_2O_3) eluting with CH_2Cl_2 : MeOH (95 : 5) to provide 4.3 mg (quant) of **4.59** as a white solid. ^1H -NMR (500 MHz, CD_3OD) δ 7.70 (d, $J = 8.5$ Hz, 1 H) 7.67 (d, $J = 8.0$ Hz, 1 H) 7.39 (td, $J = 7.0, 1.0$ Hz, 1 H) 7.31 (td, $J = 7.0, 1.0$ Hz, 1 H) 7.25-7.14 (comp, 10 H) 5.46 (d, $J = 6.5$ Hz, 1 H) 4.57-4.46 (comp, 4 H) 4.41 (d, $J = 11.5$ Hz, 1 H) 4.34 (d, $J = 9.0$ Hz, 1 H) 4.27 (d, $J = 9.5$ Hz, 1 H) 4.21 (d, $J = 7.0$ Hz, 1 H) 4.12 (d, $J = 7.0$ Hz, 1 H) 4.08 (dd, $J = 5.5, 1.5$ Hz, 1 H) 3.95-3.90 (m, 1 H) 3.94 (d, $J = 9.5$ Hz, 1 H) 3.81 (dt, $J = 13.0, 9.0$ Hz, 1 H) 3.48 (s, 3 H) 3.34 (td, $J = 14.0, 3.0$ Hz, 1 H) 3.15 (dm, 12.0 Hz, 1 H) 3.02 (m, 1 H) 2.97 (m, 1 H) 2.61 (m, 1 H) 2.23-2.15 (comp, 3 H) 1.60 (s, 9 H); ^{13}C -NMR (125 MHz, CD_3OD) δ 152.3, 143.6, 139.2, 139.1, 137.9, 129.8, 129.4, 129.4, 128.9, 128.8, 128.8, 128.6, 126.0, 124.0, 118.2, 115.1, 108.0, 90.8, 87.1, 81.3, 77.1, 76.1, 74.2, 74.1, 67.7, 59.6, 56.5, 55.8, 51.1, 50.9, 47.8, 32.8, 28.2, 24.6; HRMS (ESI) m/z observed 653.35850 [$\text{C}_{40}\text{H}_{48}\text{N}_2\text{O}_6$ ($\text{M}+\text{H}$) $^+$ requires 653.35850].



Assignments: ^1H -NMR (500 MHz, CD_3OD) δ 7.70 (d, $J = 8.5$ Hz, 1 H, C8-H) 7.67 (d, $J = 8.0$ Hz, 1 H, C5-H) 7.39 (td, $J = 7.0, 1.0$ Hz, 1 H, C7-H) 7.31 (td, $J = 7.0, 1.0$ Hz, 1 H, C6-H) 7.25-7.14 (comp, 10 H, C23-H, C24-H, C25-H, C26-H, C27-H, C29-H, C30-H, C31-H, C32-H, C33-H) 5.46 (d, $J = 6.5$ Hz, 1 H, C16-H) 4.57-4.46 (comp, 4 H,

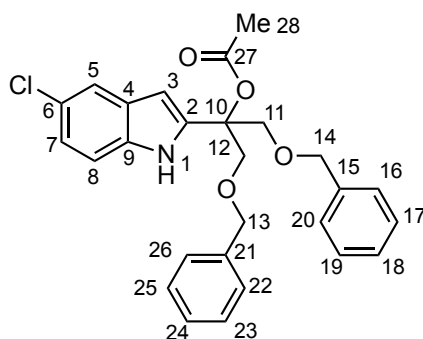
C18-H or C19-H or C20-H or C21-H) 4.41 (d, $J = 11.5$ Hz, 1 H, C18-H or C19-H or C20-H or C21-H) 4.34 (d, $J = 9.0$ Hz, 1 H, C18-H or C19-H or C20-H or C21-H) 4.27 (d, $J = 9.5$ Hz, 1 H, C18-H or C19-H or C20-H or C21-H) 4.21 (d, $J = 7.0$ Hz, 1 H, C35-H) 4.12 (d, $J = 7.0$ Hz, 1 H, C35-H) 4.08 (dd, $J = 5.5, 1.5$ Hz, 1 H, C12-H) 3.95-3.90 (m, 1 H, C15-H) 3.94 (d, $J = 9.5$ Hz, 1 H, C18-H or C19-H or C20-H or C21-H) 3.81 (dt, $J = 13.0, 9.0$ Hz, 1 H, C15-H) 3.48 (s, 3 H, C36-H₃) 3.34 (td, $J = 14.0, 3.0$ Hz, 1 H, C17-H) 3.15 (dm, 12.0 Hz, 1 H, C17-H) 3.02 (m, 1 H, C11-H) 2.97 (m, 1 H, C13-H) 2.61 (m, 1 H, C14-H) 2.23-2.15 (comp, 3 H, C14-H and C34-H₂) 1.60 (s, 9 H, C39-H₃); ¹³C-NMR (125 MHz, CD₃OD) δ 152.3 (C37), 143.6, 139.2, 139.1, 137.9, 129.8, 129.4, 129.4, 128.9, 128.8, 128.8, 128.6, 126.0 (C7), 124.0 (C6), 118.2 (C5), 115.1 (C8), 108.0 (C3), 90.8 (C35), 87.1 (C38), 81.3 (C12), 77.1 (C18 or C19 C20 or C21), 76.1 (C18 or C19 C20 or C21), 74.2 (C18 or C19 C20 or C21), 74.1 (C18 or C19 C20 or C21), 67.7 (C16), 59.6 (C36), 56.5 (C15), 55.8 (C17), 51.1 (C10), 50.9 (C13), 47.8 (C11), 32.8 (C14), 28.2 (C39) 24.6 (C34).



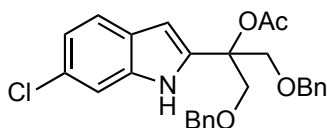
1,3-Bis(benzyloxy)-2-(5-chloro-1H-indol-2-yl)propan-2-yl acetate. (4.64a).

(WLM7_244_2). A solution of *n*-BuLi (3.33 mL of 2.5 M in hexanes, 8.32 mmol) was added dropwise to a solution of 5-chloroindole (**4.63a**) (1.15 g, 7.57 mmol) in dry THF (40 mL) at -78 °C. The reaction was stirred for 30 min, and dried CO₂ gas (passed through a short column of anhydrous CaSO₄) was bubbled through the reaction for 15 min. The reaction was stirred for 15 min, the bath was removed, and the reaction was stirred for 1 h at room temperature. Excess CO₂ was removed via freeze-pump-thaw (3

cycles), and the reaction was evacuated for 30 sec, and then sparged with N₂ for 20 min. The reaction was cooled to -78 °C, whereupon *t*-BuLi (4.62 mL of 1.8 M solution, 8.32 mmol) was added dropwise. The reaction was stirred for 80 min and transferred via cannula to a solution of 1,3-dibenzyloxyacetone (**3.17**) (2.25 g, 8.32 mmol) in dry THF (20 mL) at -78 °C. The reaction was stirred for 2.5 h, freshly distilled acetic anhydride (2.32 g, 22.7 mmol, 2.15 mL) was added dropwise, and the reaction was allowed to warm to room temperature over 7 h. Saturated aq NaHCO₃ (30 mL) was added, and the reaction was stirred for 30 min, whereupon brine (25 mL) and EtOAc (25 mL) were added. The layers were separated, and the aqueous layer was extracted with EtOAc (2 x 25 mL). The combine organic layers were dried (Na₂SO₄), filtered, and concentrated under reduced pressure. The resulting yellow oil was purified by flash chromatography eluting with Hexanes : EtOAc (10 : 1 → 4 : 1) containing 1% NEt₃ to give 1.41 g (40%) of **4.64a** as a white solid: ¹H-NMR (600 MHz, CD₃CN) δ 9.61 (br, 1 H) 7.52 (d, *J* = 1.8 Hz, 1 H) 7.36 (d, *J* = 9.0 Hz, 1 H) 7.33-7.26 (comp, 10 H) 7.10 (dd, *J* = 9.0, 1.8 Hz, 1 H) 6.37 (dd, *J* = 1.8, 0.8 Hz, 1 H) 4.54 (d, *J* = 12.0 Hz, 2 H) 4.51 (d, *J* = 12.0 Hz, 2 H) 4.13 (d, *J* = 11.4 Hz, 2 H) 4.11 (d, *J* = 11.4 Hz, 2 H) 2.03 (s, 3 H); ¹³C-NMR (150 MHz, CD₃CN) δ 170.4, 139.9, 139.2, 135.3, 129.8, 129.3, 128.7, 128.6, 125.3, 122.6, 120.4, 113.5, 100.2, 81.3, 74.1, 71.3, 22.1; HRMS (ESI) *m/z* observed 486.14430 [C₂₇H₂₆ClNO₄ (M+Na)⁺ requires 486.14430].

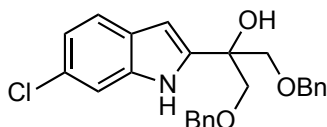


Assignments: $^1\text{H-NMR}$ (600 MHz, CD_3CN) δ 9.61 (br, 1 H, N1-H) 7.52 (d, J = 1.8 Hz, 1 H, C5-H) 7.36 (d, J = 9.0 Hz, 1 H, C8-H) 7.33-7.26 (comp, 10 H, C16-H, C17-H, C18-H, C19-H, C20-H, C22-H, C23-H, C24-H, C25-H, and C26-H) 7.10 (dd, J = 9.0, 1.8 Hz, 1 H, C7-H) 6.37 (dd, J = 1.8, 0.8 Hz, 1 H, C3-H) 4.54 (d, J = 12.0 Hz, 2 H, C13-H and C14-H) 4.51 (d, J = 12.0 Hz, 2 H, C13-H and C14-H) 4.13 (d, J = 11.4 Hz, 2 H, C11-H and C12-H) 4.11 (d, J = 11.4 Hz, 2 H, C11-H and C12-H) 2.03 (s, 3 H, C28- H_3); $^{13}\text{C-NMR}$ (150 MHz, CD_3CN) δ 170.4 (C27), 139.9, 139.2, 135.3, 129.8, 129.3, 128.7, 128.6, 125.3, 122.6 (C7), 120.4 (C5), 113.5 (C8), 100.2 (C3), 81.3 (C10), 74.1 (C13 and C14), 71.3 (C11 and C12), 22.1 (C28).



1,3-Bis(benzyloxy)-2-(6-chloro-1H-indol-2-yl)propan-2-yl acetate. (4.64b). (WLM8_73). A solution of *n*-BuLi (2.9 mL of 2.5 M solution in hexanes, 7.256 mmol) was added dropwise to a solution of **3.63b** (1.00 g, 6.596 mmol) in dry THF (30 mL) at -78°C . The reaction was stirred for 30 min, and dried CO_2 gas (passed through a short column of anhydrous CaSO_4) was bubbled through the reaction for 15 min. The reaction was stirred for 15 min, the bath was removed, and the reaction was stirred for 1 h at room temperature. Excess CO_2 was removed via freeze-pump-thaw (3 cycles), and the reaction

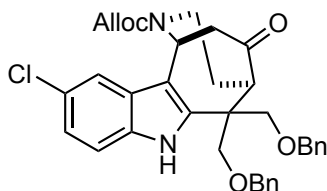
was evacuated for 30 sec, and then sparged with N₂ for 20 min. The reaction was cooled to –78 °C, whereupon *t*-BuLi (4.54 mL of 1.8 M solution in pentane, 7.256 mmol) was added dropwise. The reaction was stirred for 80 min and transferred via cannula to a solution of **3.17** (1.96 g, 7.256 mmol) in dry THF (30 mL) at –78 °C. The reaction was stirred for 2.5 h, freshly distilled acetic anhydride (2.02 g, 19.79 mmol, 1.87 mL) was added dropwise, and the reaction was allowed to warm to room temperature over 7 h. Saturated aq NaHCO₃ (50 mL) was added, and the reaction was stirred for 30 min, whereupon brine (50 mL) and Et₂O (50 mL) were added. The layers were separated, and the aqueous layer was extracted with Et₂O (2 x 50 mL). The combined organic layers were dried (Na₂SO₄), filtered, and concentrated under reduced pressure. The resulting yellow oil was purified by flash chromatography eluting with Hexanes : EtOAc (20:1 → 10:1 → 4:1 → 1:1) containing 1% NEt₃ to give 1.645 g (52%) of **4.64b** as a white solid and 873 mg (31%) of **4.64c** as a brown oil: ¹H-NMR (600 MHz, CD₃CN) δ 9.59 (br, 1 H) 7.48 (d, *J* = 8.4 Hz, 1 H) 7.41 (d, *J* = 2.4 Hz, 1 H) 7.34-7.24 (comp, 10 H) 7.02 (dd, *J* = 8.4, 1.8 Hz, 1 H) 6.41 (d, *J* = 6.41 Hz, 1 H) 4.53 (app d, 4 H) 4.12 (app d, 4 H) 2.03 (s, 3 H); ¹³C-NMR (150 MHz, CD₃CN) δ 170.5, 139.2, 139.2, 137.2, 129.3, 128.7, 128.6, 127.9, 127.4, 122.4, 120.9, 111.8, 100.7, 81.3, 74.1, 71.3, 22.1; HRMS (ESI) *m/z* observed 486.14470 [C₂₇H₂₆ClNO₃ (M+Na)⁺ requires 486.14430].



1,3-Bis(benzyloxy)-2-(6-chloro-1*H*-indol-2-yl)propan-2-ol (4.64c).

(WLM8_73). ¹H-NMR (400 MHz, CD₃CN) δ 9.54 (br, 1H), 7.47 (dt, *J* = 8.4, 0.7 Hz, 1H), 7.45 – 7.39 (m, 1H), 7.30 (comp, 10H), 7.02 (dd, *J* = 8.3, 1.4 Hz, 1H), 6.38 (dd, *J* = 2.2, 0.9 Hz, 1H), 4.54 (s, 4H), 3.77 (d, *J* = 9.5 Hz, 2H), 3.74 (d, *J* = 9.5 Hz, 2H); ¹³C

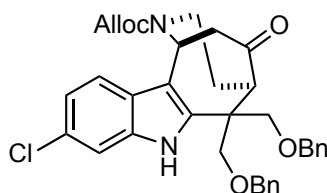
NMR (100 MHz, CD₃CN) δ 143.1, 139.3, 137.0, 129.3, 128.7, 128.5, 127.9, 127.2, 122.1, 120.6, 118.3, 111.8, 99.5, 74.7, 74.1; HRMS (ESI) m/z observed 444.13530 [C₂₅H₂₄ClNO₃ (M+Na)⁺ requires 444.13370].



(1S/R, 5R/S)-Allyl 6,6-bis((benzyloxy)methyl)-10-chloro-12-oxo-3,4,5,6-tetrahydro-1H-1,5-ethanoazocino[4,3-*b*]indole-2(7H)-carboxylate. (4.65a).

(WLM8_97_2). A solution of TMS-OTf (276 mg, 1.242 mmol, 0.225 mL) in dry CH₂Cl₂ (1.0 mL) was added dropwise to a solution of **3.64a** (480 mg, 1.035 mmol), **3.10** (400 mg, 1.14 mmol), and 2,6-di(*tert*-butyl)-4-methylpyridine (425 mg, 2.07 mmol) in dry CH₂Cl₂ (4.0 mL) at –78 °C. The reaction was stirred for 3 h at –78 °C, whereupon a solution of TBAF•3H₂O (980 mg) in CH₂Cl₂ (5.0 mL) was added dropwise. The bath was removed, and the reaction was stirred at room temperature for 1 h. Saturated aq NaHCO₃ (5.0 mL) was added, and the layers were separated. The aqueous layer was extracted with CH₂Cl₂ (3 x 20 mL). The combined organic extracts were washed with brine (25 mL), dried (Na₂SO₄), filtered, and concentrated under reduced pressure. The resultant yellow oil was purified by flash chromatography eluting with Hexanes : EtOAc (10 : 1 → 4 : 1 → 2 : 1) containing 1% NEt₃ to afford 425 mg (69%) of **4.65a** as a yellow foam: ¹H-NMR (500 MHz, CD₃CN, 70 °C) δ 9.68 (br, 1 H) 7.47 (d, J = 2.0 Hz, 1 H) 7.36-7.23 (comp, 9 H) 7.17-7.15 (comp, 2 H) 7.12 (dd, 9.0, 2.0 Hz, 1 H) 6.00 (br, 1 H) 5.78 (app t, J = 3.5 Hz, 1 H) 5.31 (app d, J = 15.0 Hz, 1 H) 5.21 (app d, J = 7.5 Hz, 1 H) 4.63 (d, J = 12.0 Hz, 2 H) 4.59 (d, J = 12.0 Hz, 2 H) 4.39 (d, J = 12.0 Hz, 1 H) 4.33 (d, J = 12.0 Hz, 1 H) 3.98 (d, J = 9.0 Hz, 1 H) 3.92 (d, J = 13.5 Hz, 1 H) 3.76 (d, J = 8.5 Hz, 1 H) 3.73 (d, J

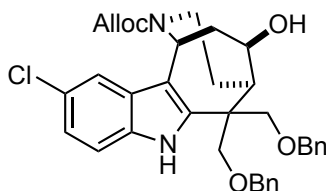
= 8.5 Hz, 1 H) 3.65 (d, J = 8.5 Hz, 1 H) 3.10 (dd, J = 6.0, 3.0 Hz, 1 H) 3.04 (dd, J = 18.5, 9.5 Hz, 1 H) 3.01 (t, J = 13.0 Hz, 1 H) 2.87 (dd, J = 19.0, 3.0 Hz, 1 H) 2.04 (dm, J = 15.0 Hz, 1 H) 1.78 (m, 1 H); ^{13}C -NMR (125 MHz, 70 °C) δ 211.5, 156.0, 141.2, 139.4, 139.3, 135.2, 134.8, 129.6, 129.5, 129.4, 129.1, 129.0, 129.0, 128.9, 128.8, 128.7, 126.2, 123.2, 117.7, 113.7, 110.9, 81.9, 76.0, 74.7, 74.6, 74.4, 71.9, 67.0, 58.3, 46.6, 46.0, 40.9, 28.8; HRMS (ESI) m/z observed 621.21210 [$\text{C}_{35}\text{H}_{35}\text{ClN}_2\text{O}_5$ ($\text{M}+\text{Na}$) $^+$ requires 621.21270].



(1S/R, 5R/S)-Allyl 6,6-bis((benzyloxy)methyl)-9-chloro-12-oxo-3,4,5,6-tetrahydro-1H-1,5-ethanoazocino[4,3-b]indole-2(7H)-carboxylate. (4.65b).

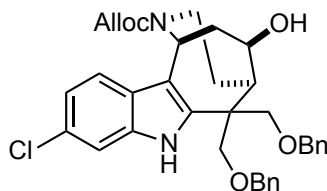
(WLM8_83). A solution of TMS-OTf (370 mg, 1.67 mmol, 0.3 mL) in dry CH_2Cl_2 (2.0 mL) was added dropwise to a solution of **4.64b** (645 mg, 1.39 mmol), **3.10** (540 mg, 1.53 mmol), and 2,6-di(*tert*-butyl)-4-methylpyridine (571 mg, 2.78 mmol) in dry CH_2Cl_2 (5.0 mL) at -78 °C. The reaction was stirred for 3 h at -78 °C, whereupon a solution of TBAF \cdot 3H $_2$ O (1.32 g, 4.17 mmol) in CH_2Cl_2 (5 mL) was added dropwise. The bath was removed, and the reaction was stirred at room temperature for 1 h. Saturated aq NaHCO $_3$ (10 mL) was added, and the layers were separated. The aqueous layer was extracted with CH_2Cl_2 (3 x 20 mL). The combined organic extracts were washed with brine (30 mL), dried (Na $_2$ SO $_4$), filtered, and concentrated under reduced pressure. The resultant yellow oil was purified by flash chromatography eluting with Hexanes : EtOAc (10 : 1 \rightarrow 4 : 1) containing 1% NEt $_3$ to afford 741 mg (89%) of **4.65b** as a yellow foam: ^1H -NMR (500 MHz, CD $_3$ CN, 70 °C) δ 9.69 (br, 1 H) 7.46 (d, J = 8.5 Hz, 1 H) 7.42 (d, J = 2.0 Hz, 1 H) 7.38-7.34 (comp, 4 H) 7.32-7.28 (m, 1 H) 7.27-7.21 (comp, 3 H) 7.18-7.16 (comp, 2 H)

7.06 (dd, $J = 8.5, 1.5$ Hz, 1 H) 6.00 (br, 1 H) 5.84 (app t, 1 H) 5.33 (br, 1 H) 5.21 (br, 1 H) 4.65 (d, $J = 12.0$ Hz, 1 H) 4.63 (m, 2 H) 4.60 (d, $J = 12.0$ Hz, 1 H) 4.40 (d, $J = 12.0$ Hz, 1 H) 4.35 (d, $J = 12.0$ Hz, 1 H) 4.00 (d, $J = 9.5$ Hz, 1 H) 3.95 (d, $J = 14.5$ Hz, 1 H) 3.78 (d, $J = 9.5$ Hz, 1 H) 3.74 (d, $J = 9.0$ Hz, 1 H) 3.68 (d, $J = 9.0$ Hz, 1 H) 3.13 (dd, $J = 6.0, 3.0$ Hz, 1 H) 2.90 (dd, $J = 19.0, 4.0$ Hz, 1 H) 3.02 (d, $J = 13.0$ Hz, 1 H) 2.89 (dd, $J = 19.0, 3.0$ Hz, 1 H) 2.05 (dm, $J = 15.5$ Hz, 1 H) 1.80 (tm, $J = 14.5$ Hz, 1 H); ^{13}C -NMR (125 MHz, CD_3CN , 70 °C) δ 211.5, 156.0, 140.4, 139.3, 139.2, 137.0, 134.7, 129.6, 129.4, 129.0, 128.9, 128.8, 128.7, 128.6, 121.2, 119.9, 117.8, 112.1, 111.2, 75.9, 74.7, 74.4, 73.3, 67.0, 58.2, 50.3, 46.5, 46.0, 40.8, 28.8; HRMS (ESI) m/z observed 599.23080 [$\text{C}_{35}\text{H}_{35}\text{ClN}_2\text{O}_5$ (M+H) $^+$ requires 599.23070].



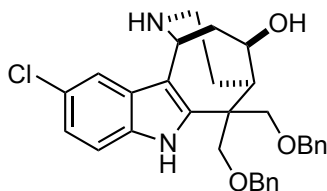
(1*S/R*, 5*R/S*, 12*R/S*)-Allyl 6,6-bis((benzyloxy)methyl)-10-chloro-12-hydroxy-3,4,5,6-tetrahydro-1*H*-5,1-ethanoazocino[4,3-*b*]indole-2(7*H*)-carboxylate. (4.66a). (WLM7_284_2). Lithium borohydride (17 mg, 0.79 mmol) was added to a solution of **4.65a** (95 mg, 0.159 mmol) in dry MeOH (1.6 mL) at 0 °C. After 4 h, saturated aq Rochelle's salt (2.0 mL) was added, and the reaction was stirred for 5 min. the reaction mixture was extracted with CH_2Cl_2 (3 x 10 mL), washed with brine (10 mL), dried (Na_2SO_4), filtered, and concentrated under reduced pressure. Subsequent purification by flash chromatography eluting with Hexanes : EtOAc (3:1 \rightarrow 1:1) afforded 77 mg (81%) of **4.66a** as a white solid: ^1H -NMR (500 MHz, CD_3CN , 70 °C) δ 9.58 (br, 1 H) 7.39-7.23 (comp, 12 H) 7.07 (dd, $J = 8.5, 2.0$ Hz, 1 H) 6.03 (br, 1 H) 5.54 (d, $J = 6.5$ Hz, 1 H) 5.34 (app d, $J = 16.0$ Hz, 1 H) 5.22 (app d, $J = 9.0$ Hz, 1 H) 4.66 (d, $J = 12.0$ Hz, 1 H) 4.60 (d,

$J = 12.0$ Hz, 1 H) 4.50 (d, $J = 12.0$ Hz, 1 H) 4.47 (d, $J = 12.0$ Hz, 1 H) 4.27 (td, $J = 9.0$, 1.5 Hz, 1 H) 4.06 (d, $J = 9.0$ Hz, 1 H) 4.06 (d, $J = 9.0$ Hz, 1 H) 3.99 (d, $J = 9.0$ Hz, 1 H) 3.81 (dd, $J = 10.0$, 5.0 Hz, 1 H) 3.70 (d, $J = 9.0$ Hz, 1 H) 3.19 (br, 1 H) 2.97 (m, 1 H) 2.66 (app t, $J = 12.5$ Hz, 1 H) 2.58 (app t, $J = 5.0$ Hz, 1 H) 2.04 (br, 1 H) 1.90-1.83 (comp, 2 H) 1.80-1.72 (m, 1 H); ^{13}C -NMR (125 MHz, CD_3CN , 70 °C) δ 156.3, 142.9, 139.9, 139.7, 135.2, 135.1, 129.6, 129.5, 129.1, 128.9, 128.9, 128.8, 128.7, 126.0, 122.7, 117.8, 117.4, 113.6, 113.4, 75.9, 74.6, 74.3, 74.3, 74.2, 66.7, 48.2, 47.9, 41.6; HRMS (ESI) m/z observed 623.22820 [$\text{C}_{35}\text{H}_{37}\text{ClN}_2\text{O}_5$ ($\text{M}+\text{Na}$) $^+$ requires 623.22830].



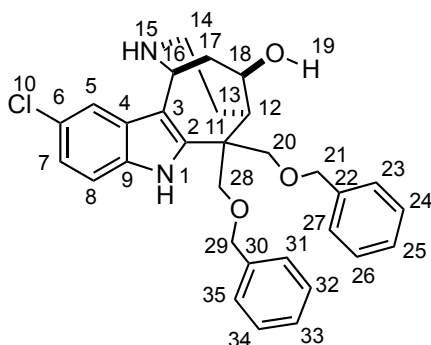
(1*S*/*R*, 5*R*/*S*, 12*R*/*S*)-Allyl 6,6-bis((benzyloxy)methyl)-9-chloro-12-hydroxy-3,4,5,6-tetrahydro-1*H*-5,1-ethanoazocino[4,3-*b*]indole-2(7*H*)-carboxylate. (4.66b). (**WLM8_84**). Lithium borohydride (38 mg, 1.75 mmol) was added to a solution of **4.65b** (525 mg, 0.876 mmol) in dry MeOH (9.0 mL) at 0 °C. After 4 h, saturated aq Rochelle's salt (5.0 mL) was added, and the reaction was stirred for 5 min. the reaction mixture was extracted with CH_2Cl_2 (3 x 25 mL), washed with brine (50 mL), dried (Na_2SO_4), filtered, and concentrated under reduced pressure. The resulting yellow oil was purified by flash chromatography eluting with Hexanes : EtOAc (2 : 1 \rightarrow 1 : 1) to give 481 mg (91%) of **4.66b** as a white solid: ^1H -NMR (500 MHz, CD_3CN , 70 °C) δ 9.56 (br, 1 H) 7.39-7.34 (comp, 6 H) 7.31-7.23 (comp, 6 H) 7.02 (dd, $J = 8.5$, 2.0 Hz, 1 H) 6.01 (br, 1 H) 5.57 (d, $J = 6.5$ Hz, 1 H) 5.33 (br, 1 H) 5.22 (br, 1 H) 4.67-4.64 (comp, 3 H) 4.60 (d, $J = 12.0$ Hz, 1 H) 4.50 (d, $J = 12.0$ Hz, 1 H) 4.47 (d, $J = 12.0$ Hz, 1 H) 4.28 (m, 1 H) 4.06 (d, $J = 8.5$ Hz, 2 H) 4.00 (d, $J = 9.0$ Hz, 1 H) 3.81 (d, $J = 10.0$ Hz, 1 H) 3.69 (d, $J = 9.0$ Hz, 1 H)

3.23 (d, $J = 5.0$ Hz, 1 H) 2.98 (m, 1 H) 2.66 (m, 1 H) 2.59 (m, 1 H) 1.89-1.83 (comp, 2 H) 1.80-1.72 (m, 1 H); ^{13}C -NMR (125 MHz, CD_3CN , 70 $^\circ\text{C}$) δ 156.3, 142.0, 139.8, 139.7, 137.0, 135.1, 129.6, 129.5, 129.0, 128.9, 128.9, 128.7, 128.1, 126.4, 120.9, 119.6, 117.4, 113.6, 112.0, 75.9, 74.6, 74.3, 74.3, 74.2, 66.7, 48.2, 48.2, 47.9, 41.6, 41.5, 31.2; HRMS (ESI) m/z observed 623.22840 [$\text{C}_{35}\text{H}_{37}\text{ClN}_2\text{O}_5$ ($\text{M}+\text{Na}$) $^+$ requires 623.22830].



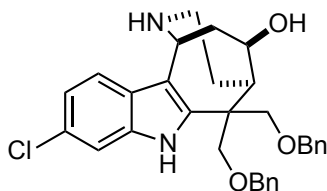
(1*S/R*, 5*R/S*, 12*R/S*)-Allyl 6,6-bis((benzyloxy)methyl)-10-chloro-12-hydroxy-3,4,5,6-tetrahydro-1*H*-5,1-ethanoazocino[4,3-*b*]indole-2(7*H*)-carboxylate. (4.67a). (WLM7_286). A round bottom flask charged with $\text{Pd}_2(\text{dba})_3$ (0.18 mg, 0.0002 mmol) and 1,4-bis(diphenylphosphino)butane (0.17 mg, 0.0004 mmol) was placed under vacuum and backfilled with N_2 three times. A second round bottom flask was charged with **4.66a** (12 mg, 0.02 mmol) and 1,3-dimethylbarbituric acid (31 mg, 0.2 mmol) and placed under vacuum and backfilled with N_2 three times. THF (0.2 mL) was then added to both flasks, and the mixtures were stirred at room temperature under N_2 for 5 min. The Pd/ligand mixture was added via syringe to the flask containing **4.66a**, and stirring was continued at room temperature until **4.66a** was gone by TLC. The reaction was quenched with saturated aq NaHCO_3 (0.5 mL) and stirred at room temperature for 15 min. The reaction mixture was diluted with H_2O (0.5 mL) extracted with CH_2Cl_2 (3 x 5 mL). The combined organic extracts were washed with brine (5 mL), dried (Na_2SO_4), filtered, and concentrated *in vacuo* to afford a brown oil. Subsequent purification by flash chromatography eluting with CH_2Cl_2 : MeOH (100% $\text{CH}_2\text{Cl}_2 \rightarrow 9:1 \rightarrow 4:1$) containing 1% NEt_3 to provide 5.5 mg (53%) of **4.67a** as a white solid: ^1H -NMR (500 MHz,

CD₃OD) δ 7.55 (dd, $J = 2.0, 0.5$ Hz, 1H) 7.36 (dd, $J = 8.5, 0.5$ Hz, 1 H) 7.29-7.20 (comp, 5 H) 7.20-7.16 (comp, 5 H) 7.12 (dd, $J = 9.0, 2.0$ Hz, 1 H) 5.15 (dd, $J = 5.5, 1.5$ Hz, 1 H) 4.60 (d, $J = 11.5$ Hz, 1 H) 4.57 (d, $J = 12.0$ Hz, 1 H) 4.50 (d, $J = 12.5$ Hz, 1 H) 4.47 (d, $J = 12.5$ Hz, 1 H) 4.38 (td, $J = 9.0, 2.0$ Hz, 1 H) 4.19 (d, $J = 9.5$ Hz, 1 H) 3.99 (d, $J = 9.5$ Hz, 1 H) 3.96 (d, $J = 9.5$ Hz, 1 H) 3.79 (d, $J = 9.0$ Hz, 1 H) 2.98-2.91 (comp, 2 H) 2.79-2.73 (comp 2 H) 2.26 (dm, $J = 15.5$ Hz, 1 H) 2.09 (ddd, $J = 15.0, 3.5, 1.5$ Hz, 1 H) 1.89 (m, 1 H); ¹³C-NMR (125 MHz, CD₃OD) δ 143.8, 139.5, 139.5, 135.5, 129.4, 129.3, 128.9, 128.9, 128.8, 128.6, 128.2, 126.7, 123.3, 117.7, 113.5, 106.8, 74.7, 74.6, 74.6, 74.3, 73.6, 49.6, 47.0, 41.5, 40.1, 28.2; HRMS (ESI) m/z observed 539.20730 [C₃₁H₃₃ClN₂O₃ (M+Na)⁺ requires 539.20720].



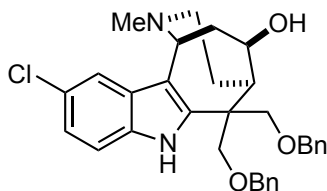
Assignments: ¹H-NMR (500 MHz, CD₃OD) δ 7.55 (dd, $J = 2.0, 0.5$ Hz, 1H, C5-H) 7.36 (dd, $J = 8.5, 0.5$ Hz, 1 H, C8-H) 7.29-7.20 (comp, 5 H) 7.20-7.16 (comp, 5 H) 7.12 (dd, $J = 9.0, 2.0$ Hz, 1 H, C7-H) 5.15 (dd, $J = 5.5, 1.5$ Hz, 1 H, C16-H) 4.60 (d, $J = 11.5$ Hz, 1 H, C21-H or C29-H) 4.57 (d, $J = 12.0$ Hz, 1 H, C21-H or C29-H) 4.50 (d, $J = 12.5$ Hz, 1 H, C21-H or C29-H) 4.47 (d, $J = 12.5$ Hz, 1 H, C21-H or C29-H) 4.38 (td, $J = 9.0, 2.0$ Hz, 1 H, C18-H) 4.19 (d, $J = 9.5$ Hz, 1 H, C20-H or C28-H) 3.99 (d, $J = 9.5$ Hz, 1 H, C20-H or C28-H) 3.96 (d, $J = 9.5$ Hz, 1 H, C20-H or C28-H) 3.79 (d, $J = 9.0$ Hz, 1 H, C20-H or C28-H) 2.98-2.91 (comp, 2 H, C14-H and C17-H) 2.79-2.73 (comp 2 H,

C12-H and C14-H) 2.26 (dm, $J = 15.5$ Hz, 1 H, C13-H) 2.09 (ddd, $J = 15.0, 3.5, 1.5$ Hz, 1 H, C14-H) 1.89 (m, 1 H, C13-H); ^{13}C -NMR (125 MHz, CD_3OD) δ 143.8, 139.5, 139.5, 135.5, 129.4, 129.3, 128.9, 128.9, 128.8, 128.6, 128.2, 126.7, 123.3 (C7), 117.7 (C5), 113.5 (C8), 106.8 (C3), 74.7 (C20 or C28), 74.6 (C18), 74.6 (C21 or C29), 74.3 (C21 or C29), 73.6 (C20 or C28), 49.6 (C16), 47.0 (C12), 41.5 (C14), 40.1 (C17), 28.2 (C13).



(1S/R, 5R/S, 12R/S)-6,6-Bis((benzyloxy)methyl)-9-chloro-2,3,4,5,6,7-hexahydro-1H-5,1-ethanoazocino[4,3-b]indol-12-ol. (**4.67b**). (WLM8_182). A round bottom flask charged with $\text{Pd}_2(\text{dba})_3$ (1.1 mg, 0.00125 mmol) and 1,4-bis(diphenylphosphino)butane (1.1 mg, 0.0025 mmol) was placed under vacuum and backfilled with N_2 three times. A second round bottom flask was charged with **4.66b** (75 mg, 0.125 mmol) and 1,3-dimethylbarbituric acid (195 mg, 1.25 mmol) and placed under vacuum and backfilled with N_2 three times. THF (0.6 mL) was then added to both flasks, and the mixtures were stirred at room temperature under N_2 for 5 min. The Pd/ligand mixture was added via syringe to the flask containing **4.66b**, and stirring was continued at room temperature until **4.66b** was gone by TLC. The reaction was quenched with saturated aq NaHCO_3 (2.0 mL) and stirred at room temperature for 15 min. The reaction mixture was diluted with H_2O (2.0 mL) extracted with CH_2Cl_2 (3 x 10 mL). The combined organic extracts were washed with brine (15 mL), dried (Na_2SO_4), filtered, and concentrated *in vacuo* to afford a brown oil. Subsequent purification by flash chromatography eluting with CH_2Cl_2 : MeOH (98 : 2 \rightarrow 95 : 5) containing 1% NEt_3 provided 37 mg (57%) of **4.67b** as a white solid: ^1H -NMR (500 MHz, CD_3OD) δ 7.44 (d,

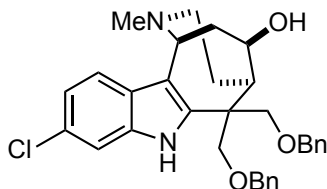
$J = 8.5$ Hz, 1 H) 7.33-7.25 (comp, 6 H) 7.20-7.16 (comp, 5 H) 6.98 (dd, $J = 8.0, 2.0$ Hz, 1 H) 4.72 (d, $J = 5.5$ Hz, 1 H) 4.61 (d, $J = 11.5$ Hz, 1 H) 4.57 (d, $J = 12.0$ Hz, 1 H) 4.46 (comp, 3 H) 4.17 (d, $J = 9.0$ Hz, 1 H) 4.00 (d, $J = 9.5$ Hz, 1 H) 3.97 (d, $J = 9.5$ Hz, 1 H) 3.67 (d, $J = 9.0$ Hz, 1 H) 2.82 (ddd, $J = 14.0, 9.0, 6.5$ Hz, 1 H) 2.70-2.66 (comp, 2 H) 2.54 (td, $J = 14.0, 8.0$ Hz, 1 H); ^{13}C -NMR (125 MHz, CD_3OD) δ 141.4, 139.7, 137.4, 129.4, 129.3, 128.9, 128.9, 128.7, 128.5, 128.2, 126.1, 120.5, 119.4, 111.7, 111.6, 75.7, 74.9, 74.5, 74.3, 73.4, 47.3, 42.8, 41.9, 30.8; HRMS (ESI) m/z observed 517.22540 [$\text{C}_{31}\text{H}_{33}\text{ClN}_2\text{O}_3$ ($\text{M}+\text{H}$) $^+$ requires 517.22520].



(1S/R, 5R/S, 12R/S)-6,6-Bis((benzyloxy)methyl)-10-chloro-2-methyl-2,3,4,5,6,7-hexahydro-1H-5,1-ethanoazocino[4,3-b]indol-12-ol. (4.68a). (WLM8_43).

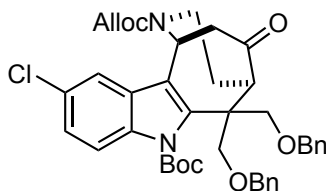
A mixture of **4.67a** (5.5 mg, 0.0106 mmol) and 37% aq formaldehyde solution (3 mg, 0.106 mmol, 8.5 μL) in CH_2Cl_2 (0.3 mL) was stirred for 5 min at room temperature whereupon sodium triacetoxyborohydride (11 mg, 0.0532 mmol) was added in one portion. Stirring was continued for 12 h at room temperature. The reaction was quenched with saturated aq Rochelle's salt (0.5 mL) and extracted with CH_2Cl_2 (3 x 5 mL). The combined organic extracts were washed with brine (5 mL), dried (Na_2SO_4), filtered, and concentrated *in vacuo* to afford a brown oil. Subsequent purification by RP HPLC H_2O : MeCN (10% MeCN \rightarrow 95% MeCN over 30 min) afforded 1.9 mg (34%) of **4.48a** as a white solid: ^1H -NMR (500 MHz, CD_3OD) δ 7.59 (d, $J = 1.5$ Hz, 1 H) 7.39 (dd, $J = 9.0, 0.5$ Hz, 1 H) 7.31-7.24 (comp, 5 H) 7.20-7.16 (comp, 5 H) 7.15 (dd, $J = 9.0, 2.0$ Hz, 1 H) 5.07 (dd, $J = 6.0, 1.5$ Hz, 1 H) 4.60 (d, $J = 11.5$ Hz, 1 H) 4.57 (d, $J = 12.0$ Hz, 1 H) 4.49

(app t, 2 H) 4.34 (td, $J = 8.5, 2.0$ Hz, 1 H) 4.18 (d, $J = 9.5$ Hz, 1 H) 3.99 (d, $J = 9.5$ Hz, 1 H) 3.96 (d, $J = 9.5$ Hz, 1 H) 3.80 (d, $J = 9.0$ Hz, 1 H) 3.05-2.99 (comp, 2 H) 2.88 (td, $J = 14.0, 4.0$ Hz, 1 H) 2.83 (s, 3 H) 2.75 (m, 1 H) 2.28 (dm, $J = 16.5$ Hz, 1 H) 2.08 (ddd, $J = 15.0, 8.5, 1.5$ Hz, 1 H) 1.93 (tm, $J =$ Hz, 1 H); ^{13}C -NMR (125 MHz, CD_3OD) δ 144.4, 139.4, 139.4, 135.5, 129.6, 129.4, 129.3, 129.0, 128.9, 128.8, 128.7, 127.3, 123.5, 117.4, 113.9, 104.5, 74.8, 74.6, 74.4, 74.3, 73.5, 60.4, 52.6, 49.9, 46.3, 45.8, 39.9, 28.6; HRMS (ESI) m/z observed 553.22200 [$\text{C}_{32}\text{H}_{35}\text{ClN}_2\text{O}_3$ ($\text{M}+\text{Na}$) $^+$ requires 553.22280].



(1S/R, 5R/S, 12R/S)-6,6-Bis((benzyloxy)methyl)-9-chloro-2-methyl-2,3,4,5,6,7-hexahydro-1H-5,1-ethanoazocino[4,3-b]indol-12-ol. (4.68b). (WLM8_90). A mixture of **4.67b** (44 mg, 0.0807 mmol) and 37% aq formaldehyde solution (24 mg, 0.807 mmol, 65 μL) in CH_2Cl_2 (0.8 mL) was stirred for 5 min at room temperature whereupon sodium triacetoxyborohydride (86 mg, 0.404 mmol) was added in one portion. Stirring was continued for 4 h at room temperature. The reaction was quenched with saturated aq Rochelle's salt (1.0 mL) and extracted with CH_2Cl_2 (3 x 10 mL). The combined organic extracts were washed with brine (15 mL), dried (Na_2SO_4), filtered, and concentrated *in vacuo* to afford 27 mg (60%) of **4.68b** as a white solid: ^1H -NMR (500 MHz, CD_3OD) δ 7.46 (d, $J = 8.5$ Hz, 1 H) 7.36 (dd, $J = 4.0, 0.5$ Hz, 1 H) 7.33-7.25 (comp, 5 H) 7.20-7.15 (comp, 5 H) 7.02 (dd, $J = 8.0, 2.0$ Hz, 1 H) 4.62 (d, $J = 12.0$ Hz, 1 H) 4.58 (m, 1 H) 4.58 (d, $J = 12.0$ Hz, 1 H) 4.47 (app t, 2 H) 4.39 (td, $J = 9.0, 2.5$ Hz, 1 H) 4.17 (d, $J = 9.0$ Hz, 1 H) 4.00 (d, $J = 9.0$ Hz, 1 H) 3.96 (d, $J = 9.5$ Hz, 1 H) 3.70 (d, $J = 9.0$ Hz, 1 H) 2.91 (ddd, $J = 15.5, 9.5, 6.5$ Hz, 1 H) 2.67 (m, 1 H) 2.62 (dd, $J = 13.0, 4.0$ Hz, 1 H) 2.54 (s, 3

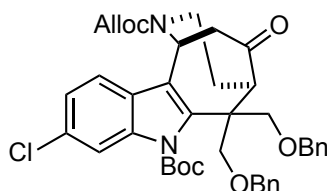
H) 2.44 (td, $J = 13.5, 3.5$ Hz, 1 H) 2.06 (m, 1 H) 1.94-1.83 (comp, 2 H); ^{13}C -NMR (125 MHz, CD_3OD) δ 142.1, 139.6, 139.6, 137.2, 129.4, 129.3, 128.9, 128.9, 128.7, 128.6, 128.3, 127.6, 121.1, 119.6, 111.9, 108.4, 75.3, 75.1, 74.6, 74.3, 73.4, 58.1, 52.2, 49.6, 46.5, 46.5, 41.4, 29.7; HRMS (ESI) m/z observed 553.22310 [$\text{C}_{32}\text{H}_{35}\text{ClN}_2\text{O}_3$ ($\text{M}+\text{Na}$) $^+$ requires 553.22280].



(1S/R, 5R/S)-2-Allyl 7-tert-butyl 6,6-bis((benzyloxy)methyl)-10-chloro-12-oxo-3,4,5,6-tetrahydro-1H-1,5-ethanoazocino[4,3-b]indole-2,7-dicarboxylate. (4.69a).

(WLM8_142). 4-dimethylaminopyridine (67 mg, 0.551 mmol) was added to a solution of **4.65a** (220 mg, 0.367 mmol) in a mixture of di-*tert*-butyl dicarbonate (1.0 mL) and toluene (0.8 mL), and the reaction was stirred for 5 h at room temperature. The reaction was partitioned between H_2O (15 mL) and Et_2O (15 mL). The layers were separated, and the organic layer was extracted with Et_2O (2 x 20 mL). The combined organic extracts were washed with brine (20 mL), dried (Na_2SO_4), and concentrated under reduced pressure. The resulting yellow oil was purified by flash chromatography eluting with Hexanes : EtOAc (10 : 1 \rightarrow 6 : 1) to give 174 mg (68%) of **4.69a** as a yellow foam: ^1H NMR (500 MHz, CD_3CN , 70 $^\circ\text{C}$) δ 7.77 (d, $J = 8.9$ Hz, 1H), 7.45 (d, $J = 2.1$ Hz, 1H), 7.30 (dd, $J = 8.9, 2.1$ Hz, 1H), 7.25 (comp, 6H), 7.18 (comp, 4H), 6.02 (br, $J = 24.8$ Hz, 1H), 5.76 (br, 1H), 5.18 (comp, 2H), 4.65 (comp, 2H), 4.51 (d, $J = 9.2$ Hz, 1H), 4.48 (d, $J = 11.7$ Hz, 1H), 4.43 (d, $J = 11.8$ Hz, 1H), 4.37 (d, $J = 11.7$ Hz, 1H), 4.30 (d, $J = 11.8$ Hz, 1H), 4.09 (d, $J = 9.7$ Hz, 1H), 3.77 (comp, 3H), 3.22 (dd, $J = 5.9, 3.1$ Hz, 1H), 3.07 (dd, $J = 18.4, 2.8$ Hz, 1H), 2.93 (dd, $J = 18.4, 4.7$ Hz, 1H), 2.89 – 2.76 (m, 1H), 2.14 (ddt, $J =$

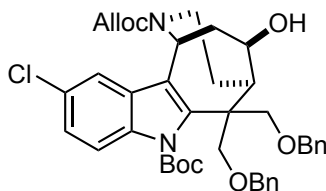
15.3, 5.8, 2.9 Hz, 1H), 1.78 – 1.69 (m, 1H), 1.64 (s, 9H); ^{13}C NMR (125 MHz, CD_3CN , 70 °C) δ 211.3, 156.0, 152.2, 140.8, 139.4, 139.2, 136.2, 134.8, 130.1, 129.5, 129.4, 129.1, 129.0, 128.8, 128.7, 128.7, 125.9, 123.3, 120.0, 118.7, 116.9, 87.1, 76.7, 74.6, 74.3, 74.3, 67.1, 64.9, 50.4, 48.1, 46.4, 41.2, 29.9, 28.6; HRMS (ESI) m/z observed 699.28300 [$\text{C}_{40}\text{H}_{43}\text{ClN}_2\text{O}_7$ ($\text{M}+\text{H}$) $^+$ requires 699.28320].



(1S/R, 5R/S)-2-Allyl 7-tert-butyl 6,6-bis((benzyloxy)methyl)-9-chloro-12-oxo-3,4,5,6-tetrahydro-1H-1,5-ethanoazocino[4,3-b]indole-2,7-dicarboxylate. (4.69b).

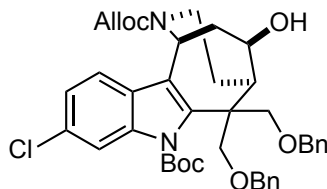
(WLM8_196). 4-dimethylaminopyridine (43 mg, 0.351 mmol) was added to a solution of **4.65b** (140 mg, 0.234 mmol) in a mixture of di-*tert*-butyl dicarbonate (0.5 mL) and toluene (0.4 mL), and the reaction was stirred for 3 h at room temperature. The reaction was partitioned between H_2O (15 mL) and Et_2O (25 mL). The layers were separated, and the organic layer was extracted with Et_2O (2 x 25 mL). The combined organic extracts were washed with brine (40 mL), dried (Na_2SO_4), and concentrated under reduced pressure. The resulting yellow oil was purified by flash chromatography eluting with Hexanes : EtOAc (4 : 1) to give 128 mg (78%) of **4.69b** as a yellow foam: ^1H -NMR (500 MHz, CD_3CN , 70 °C) δ 7.83 (d, J = 2.0 Hz, 1 H) 7.42 (d, J = 8.0 Hz, 1 H) 7.27-7.21 (comp, 7H) 7.18-7.15 (comp, 4 H) 5.97 (br, 1 H) 5.77 (br, 1 H) 5.28 (br, 1 H) 5.20 (br, 1 H) 4.61 (br, 2 H) 4.50 (d, J = 9.5 Hz, 1 H) 4.47 (d, J = 11.5 Hz, 1 H) 4.42 (d, J = 11.5 Hz, 1 H) 4.36 (d, J = 11.5 Hz, 1 H) 4.29 (d, J = 11.5 Hz, 1 H) 4.09 (d, J = 10.0 Hz, 1 H) 3.79-3.74 (m, 1 H) 3.76 (d, J = 9.0 Hz, 1 H) 3.73 (d, J = 9.5 Hz, 1 H) 3.20 (dd, J = 6.0, 3.0 Hz, 1 H) 3.06 (dd, J = 18.5, 2.5 Hz, 1 H) 2.93 (dd, J = 18.5, 4.5 Hz, 1 H) 2.81 (m, 1 H) 2.13

(dm, $J = 15.0$ Hz, 1 H) 1.72 (tm, $J = 12.5$ Hz, 1 H) 1.64 (s, 9 H); ^{13}C -NMR (125 MHz, CD_3CN , 70 °C) δ 211.4, 156.0, 152.1, 140.1, 139.4, 139.3, 138.0, 134.8, 131.4, 129.5, 129.4, 129.1, 128.9, 128.8, 128.7, 127.6, 124.0, 120.5, 120.4, 115.6, 87.3, 76.6, 74.7, 74.3, 74.3, 67.1, 65.1, 50.4, 48.0, 46.5, 41.1, 29.9, 28.6; HRMS (ESI) m/z observed 721.26490 [$\text{C}_{40}\text{H}_{43}\text{ClN}_2\text{O}_7$ ($\text{M}+\text{Na}$) $^+$ requires 721.26510].



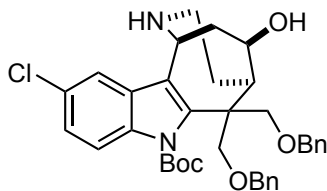
(1*S*/*R*, 5*R*/*S*, 12*R*/*S*)-2-Allyl 7-*tert*-butyl 6,6-bis((benzyloxy)methyl)-10-chloro-12-hydroxy-3,4,5,6-tetrahydro-1*H*-5,1-ethanoazocino[4,3-*b*]indole-2,7-dicarboxylate. (4.70a). (WLM8_144). Lithium aluminum hydride (79 μL of a 1M solution in THF, 0.079 mmol) was added to a solution of **4.69a** (55 mg, 0.079 mmol) in dry THF (0.8 mL) and the reaction was stirred for 2 h at 0 °C until starting material was consumed by TLC. Excess lithium aluminum hydride was quenched with saturated aq Rochelle's Salt (1.0 ml) and stirred for 15 min. The reaction mixture was extracted with CH_2Cl_2 (3 x 10 mL), and the combined organic extracts were washed with brine (15 mL), dried (Na_2SO_4), and concentrated under reduced pressure. The resulting yellow oil was purified by flash chromatography eluting with Hexanes : EtOAc (4:1 \rightarrow 1:1) to give 34 mg (62%) of **4.70a** as a white solid: ^1H -NMR (500 MHz, CD_3CN , 70 °C) δ 7.73 (d, $J = 9.0$ Hz, 1 H) 7.35 (d, $J = 1.5$ Hz, 1 H) 7.31-7.20 (comp, 9 H) 7.17-7.12 (comp, 2 H) 6.01 (br, 1 H) 5.55 (d, 1 H) 5.22 (br, 2 H) 4.64 (br, 2 H) 4.55 (d, $J = 12.0$ Hz, 1 H) 4.52-4.49 (comp, 3 H) 4.46 (d, $J = 12.0$ Hz, 1 H) 4.40 (d, $J = 12.0$ Hz, 1 H) 4.25 (d, $J = 9.5$ Hz, 1 H) 4.22 (br, 1 H) 3.75 (br, 1 H) 3.70 (d, $J = 9.5$ Hz, 1 H) 3.64 (d, $J = 5.0$ Hz, 1 H) 2.89 (ddd, $J = 14.0, 8.0, 6.5$ Hz, 1 H) 2.82 (m, 1 H) 2.50 (m, 1 H) 2.07-2.02 (comp, 2 H) 1.81-1.74 (m, 1 H) 1.61 (s, 9 H);

^{13}C -NMR (125 MHz, CD_3CN , 70 °C) δ 156.3, 152.3, 141.6, 139.7, 139.5, 136.2, 135.1, 130.0, 129.5, 129.4, 129.1, 128.9, 128.8, 128.6, 128.4, 125.5, 122.5, 118.4, 116.8, 86.6, 78.1, 75.8, 75.6, 74.2, 74.0, 66.8, 54.8, 51.2, 48.4, 42.0, 39.9, 32.0, 28.6; HRMS (ESI) m/z observed 723.28040 [$\text{C}_{40}\text{H}_{45}\text{ClN}_2\text{O}_7$ ($\text{M}+\text{Na}$) $^+$ requires 723.28080].



(1S/R, 5R/S, 12R/S)-2-Allyl 7-tert-butyl 6,6-bis((benzyloxy)methyl)-9-chloro-12-hydroxy-3,4,5,6-tetrahydro-1H-5,1-ethanoazocino[4,3-b]indole-2,7-dicarboxylate. (4.70b). (WLM8_197). Lithium aluminum hydride (183 μL of a 1M solution in THF, 0.183 mmol) was added to a solution of **4.69b** (128 mg, 0.183 mmol) in dry THF (1.8 mL) and the reaction was stirred for 2 h at 0 °C until starting material was consumed by TLC. Excess lithium aluminum hydride was quenched with saturated aq Rochelle's Salt (0.25 mL) and stirred for 15 min. The reaction mixture was extracted with CH_2Cl_2 (3 x 25 mL), and the combined organic extracts were washed with brine (40 mL), dried (Na_2SO_4), and concentrated under reduced pressure. The resulting yellow oil was purified by flash chromatography eluting with Hexanes : EtOAc (3 : 1 \rightarrow 2 : 1) to give 80 mg (63%) of **4.70b** as a white solid: ^1H -NMR (500 MHz, CD_3CN , 70 °C) δ 7.98 (d, J = 1.5 Hz, 1 H) 7.34 (d, J = 8.5 Hz, 1 H) 7.31-7.25 (comp, 5 H) 7.23-7.19 (comp, 4 H) 7.14-7.12 (comp, 2 H) 6.00 (br, 1 H) 5.58 (br, 1 H) 5.21 (br, 2 H) 4.63 (br, 2 H) 4.56-4.49 (comp, 3 H) 4.46 (d, J = 11.5 Hz, 1 H) 4.40 (d, J = 12.0 Hz, 1 H) 4.26 (d, J = 10.0 Hz, 1 H) 4.22 (dd, J = 17.5, 9.5 Hz, 1 H) 3.72 (br, 1 H) 3.69 (d, J = 10.0 Hz, 1 H) 3.63 (d, J = 6.5 Hz, 1 H) 2.88 (m, 1 H) 2.82 (app t, 1 H) 2.48 (br, 1 H) 2.03 (m, 1 H) 1.81-1.73 (comp, 2 H) 1.62 (s, 9 H); ^{13}C -NMR (125 MHz, CD_3CN , 70 °C) δ 156.3, 152.2, 139.7,

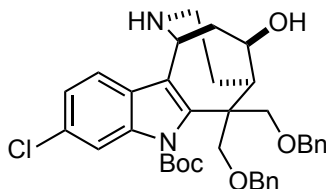
139.5, 138.1, 135.1, 131.1, 129.7, 129.5, 129.4, 129.1, 128.8, 128.6, 128.4, 127.4, 123.7, 123.0, 120.9, 120.2, 115.4, 86.7, 78.2, 75.8, 75.5, 74.2, 74.0, 66.8, 54.9, 51.2, 48.5, 42.0, 32.1, 28.7; HRMS (ESI) m/z observed 723.28060 [$C_{40}H_{45}ClN_2O_7$ ($M+Na$)⁺ requires 723.28080].



(1S/R, 5R/S, 12R/S)-tert-Butyl 6,6-bis((benzyloxy)methyl)-10-chloro-12-hydroxy-3,4,5,6-tetrahydro-1H-5,1-ethanoazocino[4,3-b]indole-7(2H)-carboxylate.

(4.71a). (WLM8_145). A round bottom flask charged with $Pd_2(dba)_3$ (1.6 mg, 0.00178 mmol) and 1,4-bis(diphenylphosphino)butane (1.5 mg, 0.00356 mmol) was placed under vacuum and backfilled with N_2 three times. A second round bottom flask was charged with **4.70a** (12.5 mg, 0.0178 mmol) and 1,3-dimethylbarbituric acid (28 mg, 0.178 mmol) and placed under vacuum and backfilled with N_2 three times. THF (0.2 mL) was then added to both flasks, and the mixtures were stirred at room temperature under N_2 for 5 min. An aliquot of the Pd/ligand mixture (20 μ L) was added via syringe to the flask containing **4.70a**, and stirring was continued at room temperature until **4.70a** was gone by TLC. The reaction was quenched with saturated aq $NaHCO_3$ (0.1 mL) and stirred at room temperature for 15 min. The reaction mixture was diluted with H_2O (0.5 mL) extracted with CH_2Cl_2 (3 x 10 mL). The combined organic extracts were washed with brine (10 mL), dried (Na_2SO_4), filtered, and concentrated *in vacuo* to afford a brown oil. Subsequent purification by flash chromatography eluting with CH_2Cl_2 : MeOH (98 : 2) containing 1% NEt_3 provided 9 mg (82%) of **4.71a** as a white solid: 1H -NMR (500 MHz, CD_3OD) δ 7.71 (d, J = 8.5 Hz, 1 H) 7.61 (d, J = 2.0 Hz, 1 H) 7.27-7.22 (comp, 6 H) 7.16-

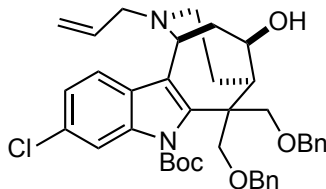
7.13 (comp, 3 H) 7.09-7.07 (comp, 2 H) 4.75 (d, $J = 6.0$ Hz, 1 H) 4.55-4.38 (comp, 7 H) 4.32 (d, $J = 10.0$ Hz, 1 H) 3.65 (d, $J = 9.5$ Hz, 1 H) 2.84 (m, 1 H) 2.77 (ddd, $J = 14.0, 9.0, 7.0$ Hz, 1 H) 2.59 (dd, $J = 13.5, 5.5$ Hz, 1 H) 2.46 (td, $J = 13.5, 4.0$ Hz, 1 H) 2.12 (dd, $J = 13.0, 10.0$ Hz, 1 H) 2.02 (dm, $J = 14.5$ Hz, 1 H) 1.76 (m, 1 H) 1.54 (s, 9 H); ^{13}C -NMR (125 MHz, CD_3OD) δ 152.3, 141.3, 139.6, 139.5, 136.3, 129.9, 129.3, 129.1, 129.0, 128.8, 128.6, 128.2, 127.7, 125.3, 118.7, 116.4, 86.0, 78.1, 75.6, 75.1, 74.2, 73.6, 54.6, 51.1, 44.1, 42.3, 41.4, 31.8, 28.2; HRMS (ESI) m/z observed 639.25890 [$\text{C}_{36}\text{H}_{41}\text{ClN}_2\text{O}_5$ ($\text{M}+\text{Na}$) $^+$ requires 639.25960].



***tert*-Butyl (1*S/R*, 5*R/S*, 12*R/S*)-6,6-bis((benzyloxy)methyl)-9-chloro-12-hydroxy-1,2,3,4,5,6-hexahydro-7*H*-5,1-ethanoazocino[4,3-*b*]indole-7-carboxylate.**

(4.71b). (WLM8_198). A round bottom flask charged with $\text{Pd}_2(\text{dba})_3$ (3.4 mg, 0.00371 mmol) and 1,4-bis(diphenylphosphino)butane (3.2 mg, 0.00741 mmol) was placed under vacuum and backfilled with N_2 three times. A second round bottom flask was charged with **4.70b** (26 mg, 0.0371 mmol) and 1,3-dimethylbarbituric acid (58 mg, 0.371 mmol) and placed under vacuum and backfilled with N_2 three times. THF (0.35 mL) was then added to both flasks, and the mixtures were stirred at room temperature under N_2 for 5 min. An aliquot of the Pd/ligand mixture (35 μL) was added via syringe to the flask containing **4.70b**, and stirring was continued at room temperature until **4.70b** was gone by TLC. The reaction was quenched with saturated aq NaHCO_3 (1.0 mL) and stirred at room temperature for 15 min. The reaction mixture was diluted with H_2O (5.0 mL) extracted with CH_2Cl_2 (3 x 10 mL). The combined organic extracts were washed with brine (10 mL), dried (Na_2SO_4), filtered, and concentrated *in vacuo* to afford a brown oil.

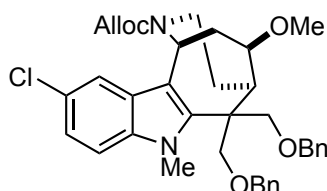
Subsequent purification by RPHPLC eluting with MeCN : H₂O (10% MeCN → 90% MeCN over 45 min) containing 0.1% TFA provided 18.4 mg (81%) of **4.71b** as a white solid and 1.5 mg (6%) of **4.71c** as a white solid: ¹H-NMR (500 MHz, CD₃OD) δ 7.78 (dd, *J* = 1.8, 0.5 Hz, 1H), 7.60 (d, *J* = 8.5 Hz, 1H), 7.29 (dd, *J* = 8.5, 1.8 Hz, 1H), 7.24 (comp, 5H), 7.16 (comp, 3H), 7.07 (comp, *J* = 6.7, 2.8, 1.3 Hz, 2H), 5.29 (dd, *J* = 6.8, 1.1 Hz, 1H), 4.52 (comp, 4H), 4.43 (comp, 3H), 4.37 (td, *J* = 9.1, 1.6 Hz, 1H), 3.67 (d, *J* = 9.9 Hz, 1H), 2.93 (comp, 3H), 2.69 (td, *J* = 13.7, 4.5 Hz, 1H), 2.31 (ddd, *J* = 15.0, 9.5, 1.3 Hz, 1H), 2.20 (dt, *J* = 15.8, 5.1 Hz, 1H), 1.97 – 1.86 (m, 1H), 1.60 (s, 9H); ¹³C-NMR (125 MHz, CD₃OD) δ 151.7, 142.7, 139.5, 139.1, 137.9, 131.8, 129.3, 129.2, 129.1, 128.7, 128.5, 127.8, 126.3, 124.0, 120.1, 116.4, 115.3, 87.1, 78.0, 74.5, 74.3, 74.1, 73.7, 53.9, 51.3, 49.0, 42.0, 38.6, 29.2, 28.2; HRMS (ESI) *m/z* observed 617.27830 [C₃₆H₄₁ClN₂O₅ (M+H)⁺ requires 617.27770].



***tert*-Butyl (1*S/R*, 5*R/S*, 12*R/S*)-2-allyl-6,6-bis((benzyloxy)methyl)-9-chloro-12-hydroxy-1,2,3,4,5,6-hexahydro-7*H*-5,1-ethanoazocino[4,3-*b*]indole-7-carboxylate.**

(4.71c). (WLM8_198). ¹H-NMR (500 MHz, CD₃OD) δ 7.74 (s, 1H), 7.60 (d, *J* = 8.6 Hz, 1H), 7.20 (comp, 11H), 6.00 (ddd, *J* = 17.2, 11.9, 5.5 Hz, 1H), 5.57 (d, *J* = 10.4 Hz, 1H), 5.48 (d, *J* = 17.1 Hz, 1H), 5.27 (d, *J* = 6.1 Hz, 1H), 4.46 (comp, 8H), 3.98 (dd, *J* = 13.7, 6.4 Hz, 1H), 3.66 (d, *J* = 10.1 Hz, 1H), 3.45 (dd, *J* = 13.3, 7.7 Hz, 1H), 3.10 (dd, *J* = 13.2, 5.5 Hz, 1H), 3.06 – 2.95 (m, 1H), 2.96 – 2.85 (m, 1H), 2.79 (td, *J* = 14.4, 3.6 Hz, 1H), 2.26 (comp, 2H), 2.01 – 1.81 (m, 1H), 1.61 (s, 9H); ¹³C-NMR (125 MHz, CD₃OD) δ 151.6, 143.5, 139.3, 138.9, 137.9, 131.7, 129.3, 129.3, 129.1, 128.7, 128.7, 128.4, 128.1,

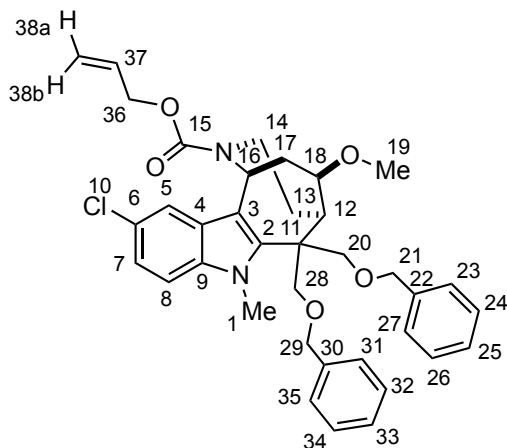
126.3, 124.4, 119.9, 115.5, 113.8, 87.4, 77.6, 74.5, 74.1, 74.1, 73.8, 62.1, 58.5, 53.1, 51.3, 50.6, 38.9, 29.3, 28.2; HRMS (ESI) m/z observed 657.30850 [$C_{39}H_{45}ClN_2O_5$ (M+H) $^+$ requires 657.30900].



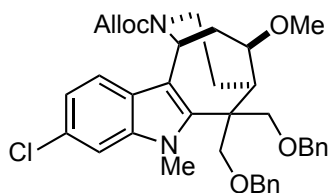
(1*S/R*, 5*R/S*, 12*R/S*)-allyl 6,6-bis((benzyloxy)methyl)-10-chloro-12-methoxy-7-methyl-3,4,5,6-tetrahydro-1*H*-5,1-ethanoazocino[4,3-*b*]indole-2(7*H*)-carboxylate.

(4.72a). (WLM7_294_2). A mixture of **4.66a** (20 mg, 0.033 mmol) and 60% NaH dispersion in mineral oil (13 mg, 0.33 mmol) in DMF (0.3 mL) at 0 °C under N₂ was stirred for five min and methyl *p*-toluenesulfonate (31 mg, 0.17 mmol) was added in one portion. The reaction was allowed to warm slowly to room temperature overnight. The reaction was quenched with saturated aq NH₄Cl (0.5 mL), diluted with H₂O (0.5 mL), and extracted with CH₂Cl₂ (3 x 10 mL). The combined organic extracts were washed with brine (10 mL), dried (Na₂SO₄), filtered, and concentrated *in vacuo* to afford a clear oil. Purification by flash chromatography eluting with Hexanes : EtOAc (6 : 1) to provide 21 mg (quant) of **4.72a** as a clear oil: ¹H-NMR (500 MHz, CD₃CN, 70 °C) δ 7.33-7.22 (comp, 10 H) 7.19-7.12 (comp, 2 H) 7.11 (dd, *J* = 9.0, 2.0 Hz, 1 H) 6.03 (br, 1 H) 5.58 (d, *J* = 6.5 Hz, 1 H) 5.36 (br, 1 H) 5.22 (br, 1 H) 4.65 (br, 2 H) 4.52-4.47 (comp, 3 H) 4.41 (d, *J* = 12.0 Hz, 1 H) 4.38 (d, *J* = 10.5 Hz, 1 H) 3.98-3.92 (comp, 3 H) 3.82-3.75 (m, 1 H) 3.82 (s, 3 H) 3.77 (t, *J* = 8.5 Hz, 1 H) 3.31 (s, 3 H) 3.02-2.97 (comp, 2 H) 2.77 (m, 1 H) 2.15 (dm, *J* = 14.5 Hz, 1 H) 1.78-1.70 (m, 2 H); ¹³C-NMR (125 MHz, CD₃CN, 70 °C) δ 156.3, 142.7, 140.1, 139.5, 137.5, 135.2, 129.5, 129.5, 129.0, 128.9, 128.8, 128.7, 128.5, 126.0, 122.8, 117.6, 117.4, 115.3, 111.8, 86.3, 77.9, 75.1, 74.2, 74.1, 66.7, 57.5, 50.8,

48.4, 47.1, 42.1, 34.0, 32.6; HRMS (ESI) m/z observed 651.25910 [$C_{37}H_{41}ClN_2O_5$ ($M+Na$)⁺ requires 651.25960].

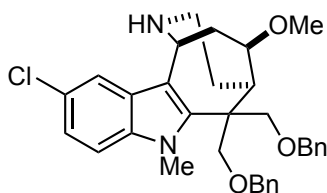


Assignments: 1H -NMR (500 MHz, CD_3CN , 70 °C) δ 7.33-7.22 (comp, 10 H) 7.19-7.12 (comp, 2 H) 7.11 (dd, J = 9.0, 2.0 Hz, 1 H) 6.03 (br, 1 H, C37-H) 5.58 (d, J = 6.5 Hz, 1 H, C16-H) 5.36 (br, 1 H, C38-H) 5.22 (br, 1 H, C38-H) 4.65 (br, 2 H, C36-H₂) 4.52-4.47 (comp, 3 H, C20-H₂ or C28-H₂) 4.41 (d, J = 12.0 Hz, 1 H, C20-H or C28-H) 4.38 (d, J = 10.5 Hz, 1 H, C21-H or C29-H) 3.98-3.92 (comp, 3 H, C21-H₂ or C29-H₂) 3.82-3.75 (m, 1 H, C14-H) 3.82 (s, 3 H, C1-H₃) 3.77 (t, J = 8.5 Hz, 1 H, C18-H) 3.31 (s, 3 H, C19-H₃) 3.02-2.97 (comp, 2 H, C12-H, C17-H) 2.77 (m, 1 H, C14-H) 2.15 (dm, J = 14.5 Hz, 1 H, C13-H) 1.78-1.70 (m, 2 H, C13-H, C17-H); ^{13}C -NMR (125 MHz, CD_3CN , 70 °C) δ 156.3 (C15), 142.7, 140.1, 139.5, 137.5, 135.2, 129.5, 129.5, 129.0, 128.9, 128.8, 128.7, 128.5, 126.0, 122.8 (C7), 117.6 (C5), 117.4, 115.3, 111.8 (C8), 86.3 (C18), 77.9 (C20 or C28), 75.1 (C20 or C28), 74.2 (C21 or C29), 74.1 (C21 or C29), 66.7 (C36), 57.5 (C19), 50.8 (C11), 48.4 (C16), 47.1 (C12), 42.1 (C17), 34.0 (C1), 32.6 (C13).



(1*S/R*, 5*R/S*, 12*R/S*)-allyl 6,6-bis((benzyloxy)methyl)-9-chloro-12-methoxy-7-methyl-3,4,5,6-tetrahydro-1*H*-5,1-ethanoazocino[4,3-*b*]indole-2(7*H*)-carboxylate.

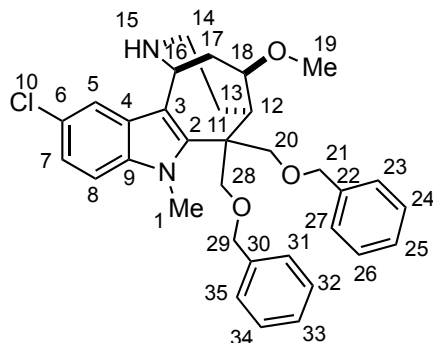
(4.72b). (WLM8_85). A mixture of **4.66b** (481 mg, 0.80 mmol) and 60% NaH dispersion in mineral oil (160 mg, 4.0 mmol) in DMF (8.0 mL) at 0 °C under N₂ was stirred for five min and methyl *p*-toluenesulfonate (447 mg, 2.4 mmol) was added in one portion. The reaction was allowed to warm slowly to room temperature overnight. The reaction was quenched with saturated aq NH₄Cl (5.0 mL), diluted with H₂O (20 mL), and extracted with EtOAc (3 x 40 mL). The combined organic extracts were washed with brine (50 mL), dried (Na₂SO₄), filtered, and concentrated *in vacuo* to afford a clear oil. Purification by flash chromatography eluting with hexanes : EtOAc (4 : 1 to 2 : 1) to provide 473 mg (94%) of **4.72b** as a clear oil: ¹H-NMR (500 MHz, CD₃CN, 70 °C) δ 7.34-7.19 (comp, 11 H) 7.18 (dd, *J* = 7.0, 2.0 Hz, 1 H) 7.02 (dd, *J* = 8.5, 1.5 Hz, 1 H) 6.02 (br, 1 H) 5.61 (d, *J* = 6.5 Hz, 1 H) 5.34 (br, 1 H) 5.22 (br, 1 H) 4.64 (br, 2 H) 4.51 (d, *J* = 12.0 Hz, 1 H) 4.49 (app t, *J* = 12.0 Hz, 2 H) 4.41 (d, *J* = 11.5 Hz, 1 H) 4.37 (d, *J* = 10.5 Hz, 1 H) 3.97 (d, *J* = 9.5 Hz, 1 H) 3.94 (d, *J* = 9.5 Hz, 1 H) 3.92 (d, *J* = 10.5 Hz, 1 H) 3.80 (s, 3 H) 3.77 (t, *J* = 10.0 Hz, 2 H) 3.30 (s, 3 H) 3.03-2.97 (comp, 2 H) 2.78 (m, 1 H) (dm, *J* = 14.5 Hz, 1 H) 1.80-1.70 (comp, 2 H); ¹³C-NMR (125 MHz, CD₃CN, 70 °C) δ 156.3, 142.0, 140.1, 139.4, 139.4, 135.2, 129.5, 129.5, 129.0, 128.9, 128.8, 128.7, 128.5, 126.2, 120.8, 119.5, 117.4, 115.8, 110.4, 86.3, 77.9, 75.1, 74.2, 74.0, 66.6, 57.5, 50.7, 48.4, 47.1, 42.1, 38.8, 34.0, 32.7; HRMS (ESI) *m/z* observed 651.25980 [C₃₇H₄₁ClN₂O₅ (M+Na)⁺ requires 651.25960].



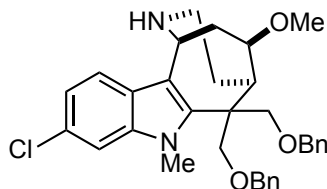
(1*S/R*, 5*R/S*, 12*R/S*)-6,6-bis((benzyloxy)methyl)-10-chloro-12-methoxy-7-methyl-2,3,4,5,6,7-hexahydro-1*H*-5,1-ethanoazocino[4,3-*b*]indole. (4.73a).

(WLM8_70). A round bottom flask charged with Pd₂(dba)₃ (1.1 mg, 0.00121 mmol) and 1,4-bis(diphenylphosphino)butane (1.0 mg, 0.00242 mmol) was placed under vacuum and backfilled with N₂ three times. A second round bottom flask was charged with **4.72a** (76 mg, 0.121 mmol) and 1,3-dimethylbarbituric acid (189 mg, 0.121 mmol) and placed under vacuum and backfilled with N₂ three times. THF (0.6 mL) was then added to both flasks, and the mixtures were stirred at room temperature under N₂ for 5 min. The Pd/ligand mixture was added via syringe to the flask containing **4.72a**, and stirring was continued at room temperature until **4.72a** was gone by TLC. The reaction was quenched with saturated aq NaHCO₃ (1.0 mL) and stirred at room temperature for 15 min. The reaction mixture was diluted with H₂O (5.0 mL) extracted with CH₂Cl₂ (3 x 15 mL). The combined organic extracts were washed with brine (15 mL), dried (Na₂SO₄), filtered, and concentrated *in vacuo* to afford a brown oil. Subsequent purification by flash chromatography eluting with CH₂Cl₂ : MeOH (98 : 2) containing 1% NEt₃ provided 58 mg (88%) of **4.73a** as a white solid: ¹H-NMR (600 MHz, CD₃OD) δ 7.56 (d, *J* = 1.8 Hz, 1 H) 7.36 (d, *J* = 9.0 Hz, 1 H) 7.31-7.30 (comp, 3 H) 7.28-7.26 (m, 1 H) 7.21-7.20 (comp, 3 H) 7.18 (dd, *J* = 10.8, 2.4 Hz, 1 H) 7.12-7.10 (comp, 2 H) 5.21 (dd, *J* = 6.0, 1.5 Hz, 1 H) 4.55 (d, *J* = 12.0 Hz, 1 H) 4.51 (comp, 2 H) 4.48 (d, *J* = 10.8 Hz, 1 H) 4.41 (d, *J* = 12.0 Hz, 1 H) 4.01 (d, *J* = 9.0 Hz, 1 H) 3.88 (d, *J* = 9.0 Hz, 1 H) 3.86 (d, *J* = 10.8 Hz, 1 H) 3.85 (td, *J* = 7.8, 1.8 Hz, 1 H) 3.80 (s, 3 H) 3.39 (s, 3 H) 3.16 (m, 1 H) 3.00-2.91 (comp, 3 H) 2.38 (dm, *J* = 15.6 Hz, 1 H) 2.09 (dd, *J* = 14.4, 9.0 Hz, 1 H) 1.86 (m, 1 H);

^{13}C -NMR (150 MHz, CD_3OD) δ 143.3, 139.6, 138.9, 137.6, 129.4, 129.4, 128.9, 128.9, 128.8, 128.7, 128.0, 127.0, 123.7, 117.7, 111.8, 109.3, 85.2, 78.6, 74.2, 74.2, 73.9, 57.9, 50.6, 49.6, 45.6, 41.9, 38.2, 33.4, 29.3; HRMS (ESI) m/z observed 567.23740 [$\text{C}_{33}\text{H}_{37}\text{ClN}_2\text{O}_3$ ($\text{M}+\text{Na}$) $^+$ requires 567.23850].



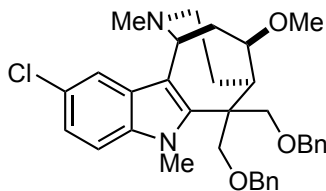
Assignments: ^1H -NMR (600 MHz, CD_3OD) δ 7.56 (d, $J = 1.8$ Hz, 1 H, C5-H) 7.36 (d, $J = 9.0$ Hz, 1 H, C8-H) 7.31-7.30 (comp, 3 H) 7.28-7.26 (m, 1 H) 7.21-7.20 (comp, 3 H) 7.18 (dd, $J = 10.8, 2.4$ Hz, 1 H, C7-H) 7.12-7.10 (comp, 2 H) 5.21 (dd, $J = 6.0, 1.5$ Hz, 1 H, C16-H) 4.55 (d, $J = 12.0$ Hz, 1 H, C21-H or C29-H) 4.51 (comp, 2 H, C21-H₂ or C29-H₂) 4.48 (d, $J = 10.8$ Hz, 1 H, C20-H or C28-H) 4.41 (d, $J = 12.0$ Hz, 1 H, C21-H or C29-H) 4.01 (d, $J = 9.0$ Hz, 1 H, C20-H or C28-H) 3.88 (d, $J = 9.0$ Hz, 1 H, C20-H or C28-H) 3.86 (d, $J = 10.8$ Hz, 1 H, C20-H or C28-H) 3.85 (td, $J = 7.8, 1.8$ Hz, 1 H, C18-H) 3.80 (s, 3 H, C1-H₃) 3.39 (s, 3 H, C19-H₃) 3.16 (m, 1 H, C12-H) 3.00-2.91 (comp, 3 H, C14-H₂, C17-H) 2.38 (dm, $J = 15.6$ Hz, 1 H, C13-H) 2.09 (dd, $J = 14.4, 9.0$ Hz, 1 H, C17-H) 1.86 (m, 1 H, C13-H); ^{13}C -NMR (150 MHz, CD_3OD) δ 143.3 (C2), 139.6 (C22 or C30), 138.9 (C22 or C30), 137.6 (C9), 129.4, 129.4, 128.9, 128.9, 128.8, 128.7, 128.0 (C4), 127.0 (C6), 123.7 (C7), 117.7 (C5), 111.8 (C8), 109.3 (C3), 85.2 (C18), 78.6 (C20 or C28), 74.2 (C21 or C29), 74.2 (C20 or C28), 73.9 (C21 or C29), 57.9 (C19), 50.6 (C11), 49.6 (C16), 45.6 (C12), 41.9 (C14), 38.2 (C17), 33.4 (C1), 29.3 (C13).



(1*S/R*, 5*R/S*, 12*R/S*)-6,6-bis((benzyloxy)methyl)-9-chloro-12-methoxy-7-methyl-2,3,4,5,6,7-hexahydro-1*H*-5,1-ethanoazocino[4,3-*b*]indole. (4.73b).

(WLM8_89). A round bottom flask charged with Pd₂(dba)₃ (1.6 mg, 0.00175 mmol) and 1,4-bis(diphenylphosphino)butane (1.5 mg, 0.0035 mmol) was placed under vacuum and backfilled with N₂ three times. A second round bottom flask was charged with **4.72b** (110 mg, 0.175 mmol) and 1,3-dimethylbarbituric acid (273 mg, 1.75 mmol) and placed under vacuum and backfilled with N₂ three times. THF (0.8 mL) was then added to both flasks, and the mixtures were stirred at room temperature under N₂ for 5 min. The Pd/ligand mixture was added via syringe to the flask containing **4.72b**, and stirring was continued at room temperature until **4.72b** was gone by TLC. The reaction was quenched with saturated aq NaHCO₃ (20 mL) and stirred at room temperature for 15 min. The reaction mixture was diluted with H₂O (20 mL) extracted with CH₂Cl₂ (3 x 20 mL). The combined organic extracts were washed with brine (30 mL), dried (Na₂SO₄), filtered, and concentrated *in vacuo* to afford a brown oil. Subsequent purification by flash chromatography eluting with CH₂Cl₂ : MeOH (99 : 1) containing 1% NEt₃ provided 63 mg (66%) of **4.73b** as a white solid: ¹H-NMR (500 MHz, CD₃CN) δ 7.40 (d, *J* = 9.0 Hz, 1 H) 7.32-7.16 (comp, 11 H) 6.97 (dd, *J* = 8.5, 2.0 Hz, 1 H) 4.57 (d, *J* = 6.0 Hz, 1 H) 4.48 (d, *J* = 12.0 Hz, 1 H) 4.46 (comp, 2 H) 4.37 (d, *J* = 12.0 Hz, 1 H) 4.34 (d, *J* = 10.5 Hz, 1 H) 3.96 (td, 1 H) 3.91 (d, *J* = 9.0 Hz, 1 H) 3.86 (d, *J* = 7.0 Hz, 1 H) 3.84 (d, *J* = 6.0 Hz, 1 H) 3.76 (s, 3 H) 3.29 (s, 3 H) 2.90 (m, 1 H) 2.68 (ddd, *J* = 13.0, 8.5, 6.5 Hz, 1 H) 2.51-2.48 (comp, 2 H) 2.10 (dm, 14.0 Hz, 1 H) (ddd, *J* = 13.5, 8.5, 1.0 Hz, 1 H) 1.61 (m, 1 H);

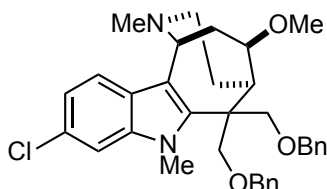
^{13}C -NMR (125 MHz, CD_3CN) δ 140.7, 139.8, 139.3, 139.0, 129.2, 129.2, 128.7, 128.6, 128.5, 128.4, 127.5, 126.0, 119.8, 119.6, 116.6, 109.8, 84.5, 78.1, 75.1, 73.8, 73.5, 57.2, 50.1, 48.0, 46.5, 42.6, 42.1, 33.4, 33.3; HRMS (ESI) m/z observed 567.23900 [$\text{C}_{33}\text{H}_{37}\text{ClN}_2\text{O}_3$ ($\text{M}+\text{Na}$) $^+$ requires 567.23850].



(1*S*/*R*, 5*R*/*S*, 12*R*/*S*)-6,6-bis((benzyloxy)methyl)-10-chloro-12-methoxy-2,7-dimethyl-2,3,4,5,6,7-hexahydro-1*H*-5,1-ethanoazocino[4,3-*b*]indole. (4.74a).

(WLM8_71). A mixture of **4.73a** (58 mg, 0.106 mmol) and 37% aq formaldehyde solution (32 mg, 1.06 mmol, 86 μL) in CH_2Cl_2 (1.0 mL) was stirred for 5 min at room temperature and sodium triacetoxyborohydride (113 mg, 0.532 mmol) was added in one portion. Stirring was continued for 4 h at room temperature. The reaction was quenched with saturated aq Rochelle's salt (0.5 mL) and extracted with CH_2Cl_2 (3 x 20 mL). The combined organic extracts were washed with brine (15 mL), dried (Na_2SO_4), filtered, and concentrated *in vacuo* to afford a brown oil. Subsequent purification by flash chromatography eluting with CH_2Cl_2 : MeOH (98 : 2) containing 1% NEt_3 afforded 56 mg (94%) of **4.74a** as a white solid: ^1H -NMR (500 MHz, CD_3OD) δ 7.45 (d, J = 2.0 Hz, 1 H) 7.29-7.18 (comp, 9 H) 7.15-7.13 (comp, 2 H) 7.06 (dd, J = 9.0, 2.0 Hz, 1 H) 4.49 (d, J = 7.0 Hz, 1 H) 4.48 (app t, 2 H) 4.34-4.31 (comp, 2 H) 4.28 (d, J = 5.0 Hz, 1 H) 3.91 (d, J = 9.0 Hz, 1 H) 3.89 (td, J = 9.0, 2.0 Hz, 1 H) 3.83 (d, J = 10.5 Hz, 1 H) 3.77 (d, J = 9.0 Hz, 1 H) 3.72 (s, 3 H) 3.32 (s, 3 H) 2.95 (m, 1 H) 2.82 (ddd, J = 14.0, 9.0, 6.5 Hz, 1 H) 2.41 (td, J = 13.0, 4.0 Hz, 1 H) 2.35 (s, 3 H) 2.32 (dd, J = 13.0, 5.0 Hz, 1 H) 2.14 (dm, J = 14.5 Hz, 1 H) 1.77-1.71 (comp, 2 H); ^{13}C -NMR (125 MHz, CD_3OD) δ 141.7, 139.8,

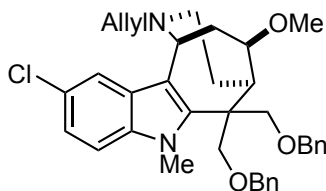
139.2, 137.5, 130.3, 129.3, 129.3, 128.7, 128.7, 128.6, 128.6, 126.0, 122.5, 118.3, 112.7, 111.2, 86.5, 78.6, 75.0, 74.1, 73.8, 57.4, 56.7, 52.5, 50.5, 47.8, 45.8, 40.5, 33.3, 31.7; HRMS (ESI) m/z observed 559.27250 [$C_{34}H_{39}ClN_2O_3$ (M+H) $^+$ requires 559.27220].



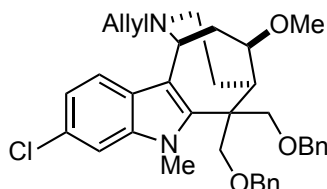
(1S/R, 5R/S, 12R/S)-6,6-bis((benzyloxy)methyl)-9-chloro-12-methoxy-2,7-dimethyl-2,3,4,5,6,7-hexahydro-1H-5,1-ethanoazocino[4,3-*b*]indole. (4.74b).

(WLM8_90). A mixture of **4.73b** (44 mg, 0.0807 mmol) and 37% aq formaldehyde solution (24 mg, 0.807 mmol, 65 μ L) in CH_2Cl_2 (0.8 mL) was stirred for 5 min at room temperature and sodium triacetoxyborohydride (86 mg, 0.404 mmol) was added in one portion. Stirring was continued for 4 h at room temperature. The reaction was quenched with saturated aq Rochelle's salt (0.5 mL) and extracted with CH_2Cl_2 (3 x 15 mL). The combined organic extracts were washed with brine (15 mL), dried (Na_2SO_4), filtered, and concentrated *in vacuo* to afford 27 mg (60%) of **4.74b** as a white solid: 1H -NMR (500 MHz, CD_3CN) δ 7.42 (d, J = 6.5 Hz, 1 H) 7.32-7.16 (comp, 11H) 7.00 (dd, J = 8.5, 2.0 Hz, 1 H) 4.48-4.43 (comp, 3 H) 4.37 (d, J = 7.0 Hz, 1 H) 4.35 (d, J = 8.5 Hz, 1 H) 4.32 (d, J = 5.5 Hz, 1 H) 3.92 (td, J = 10.0, 1.5 Hz, 1 H) 3.92 (d, J = 9.0 Hz, 1 H) 3.80 (d, J = 10.0 Hz, 2 H) 3.75 (s, 3 H) 3.29 (s, 3 H) 2.92 (m, 1 H) 2.83 (ddd, J = 13.5, 9.0, 6.5 Hz, 1 H) 2.38 (dd, J = 6.5, 1.5 Hz, 1 H) 2.35 (s, 3 H) 2.31 (td, J = 13.0, 4.0 Hz, 1 H) 2.11 (dm, J = 6.5 Hz, 1 H) 1.80 (m, 1 H) 1.69 (ddd, J = 13.5, 9.0, 1.5 Hz, 1 H); ^{13}C -NMR (500 MHz, CD_3CN) δ 141.0, 139.7, 139.0, 138.8, 129.3, 129.2, 128.9, 128.6, 128.6, 128.4, 127.7, 127.5, 120.3, 120.1, 113.3, 109.8, 85.9, 78.5, 74.9, 73.9, 73.4, 57.3, 56.4, 52.0, 50.0, 47.5,

45.6, 40.2, 33.5, 31.4; HRMS (ESI) m/z observed 559.27230 [$C_{34}H_{39}ClN_2O_3$ ($M+H$)⁺ requires 559.27220].

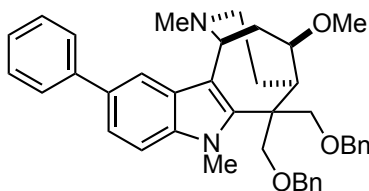


(1S/R, 5R/S, 12R/S)-2-Allyl-6,6-bis((benzyloxy)methyl)-10-chloro-12-methoxy-7-methyl-2,3,4,5,6,7-hexahydro-1H-5,1-ethanoazocino[4,3-b]indole. (4.75a). (WLM8_190). A round bottom flask charged with $Pd(PPh_3)_4$ (1.1 mg, 0.000935 mmol) and **4.72a** (12 mg, 0.19 mmol) was placed under vacuum and backfilled with N_2 three times. THF (0.2 mL) was added and the mixture was stirred at room temperature over night. The reaction mixture was diluted with H_2O (5.0 mL) and extracted with CH_2Cl_2 (3 x 15 mL). The combined organic extracts were washed with brine (10 mL), dried (Na_2SO_4), filtered, and concentrated *in vacuo* to afford a brown oil. Subsequent purification by RP HPLC H_2O : MeCN (10% MeCN \rightarrow 95% MeCN over 60 min) provided 4.9 mg (44%) of **4.75a** as a white solid: 1H -NMR (500 MHz, CD_3CN) δ 7.52 (d, J = 2.0 Hz, 1H), 7.32 (comp, 10H), 7.20 (dd, J = 8.8, 2.0 Hz, 1H), 7.18 – 7.12 (m, 2H), 6.11 (ddt, J = 17.2, 10.6, 6.8 Hz, 1H), 5.49 (d, J = 10.5 Hz, 1H), 5.39 (d, J = 17.2 Hz, 1H), 4.97 (d, J = 6.0 Hz, 1H), 4.49 (comp, 3H), 4.40 (d, J = 11.7 Hz, 1H), 4.00 (comp, J = 9.2 Hz, 2H), 3.83 (comp, 6H), 3.46 – 3.34 (m, 1H), 3.32 (s, 3H), 3.14 (comp, 3H), 2.90 – 2.76 (m, 1H), 2.37 – 2.28 (m, 1H), 2.11 – 2.04 (m, 1H), 2.05 – 1.97 (m, 1H); ^{13}C NMR (125 MHz, CD_3CN) δ 144.0, 139.5, 138.7, 137.0, 129.6, 129.4, 129.3, 129.0, 129.0, 128.8, 128.7, 128.5, 126.7, 124.5, 123.2, 117.5, 112.2, 107.9, 84.3, 78.5, 74.2, 74.0, 73.5, 61.2, 57.8, 57.6, 55.3, 50.2, 44.6, 37.6, 33.8, 28.8; HRMS (ESI) m/z observed 585.28740 [$C_{36}H_{41}ClN_2O_3$ ($M+H$)⁺ requires 585.28780].



(1*S/R*, 5*R/S*, 12*R/S*)-2-Allyl-6,6-bis((benzyloxy)methyl)-9-chloro-12-methoxy-7-methyl-2,3,4,5,6,7-hexahydro-1*H*-5,1-ethanoazocino[4,3-*b*]indole. (4.75b).

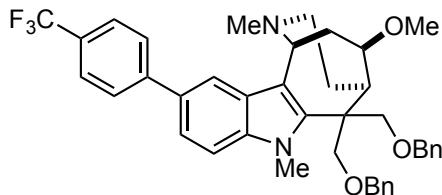
(WLM8_88). A round bottom flask charged with Pd(PPh₃)₄ (1.2 mg, 0.00098 mmol) and **4.72b** (31 mg, 0.049 mmol) was placed under vacuum and backfilled with N₂ three times. THF (0.5 mL) was added and the mixture was stirred at room temperature over night. The reaction mixture was diluted with H₂O (5.0 mL) and extracted with CH₂Cl₂ (3 x 10 mL). The combined organic extracts were washed with brine (10 mL), dried (Na₂SO₄), filtered, and concentrated *in vacuo* to afford a brown oil. Subsequent purification by PTLC eluting with CH₂Cl₂ : MeOH (99 : 1) containing 1% NEt₃ provided 8.1 mg (28%) of **4.75b** as a white solid: ¹H-NMR (500 MHz, CD₃CD) δ 7.45-7.44 (comp, 2 H) 7.36-7.23 (comp, 8 H) 7.15-7.12 (comp, 3 H) 6.06 (m, 1 H) 5.47 (d, *J* = 10.0 Hz, 1 H) 5.39 (d, *J* = 18.0 Hz, 1 H) 5.01 (d, *J* = 5.0 Hz, 1 H) 4.51-4.44 (comp, 4 H) 4.39 (d, *J* = 11.5 Hz, 1 H) 3.99 (d, *J* = 9.0 Hz, 1 H) 3.96 (td, *J* = 9.0, 2.0 Hz, 1 H) 3.83 (d, *J* = 9.0 Hz, 1 H) 3.79 (s, 3 H) 3.79-3.77 (comp, 2 H) 3.36 (m, 1 H) 3.32 (s, 3 H) 3.16-3.07 (comp, 3 H) 2.78 (m, 1H) 2.31 (dm, *J* = 16.0 Hz, 1 H) 2.02-1.97 (comp, 2 H); ¹³C-NMR (500 MHz, CD₃CD) δ 143.4, 139.5, 139.0, 138.6, 129.4, 129.3, 129.2, 129.0, 128.8, 128.8, 128.7, 128.5, 126.6, 124.9, 121.7, 119.4, 110.7, 108.2, 84.2, 78.4, 74.1, 74.0, 73.5, 61.3, 57.9, 57.8, 50.2, 50.1, 44.6, 37.6, 33.8, 28.8; HRMS (ESI) *m/z* observed 585.28800 [C₃₆H₄₁ClN₂O₃ (M+H)⁺ requires 585.28780].



(1*S/R*, 5*R/S*, 12*R/S*)-6,6-Bis((benzyloxy)methyl)-12-methoxy-2,7-dimethyl-10-phenyl-2,3,4,5,6,7-hexahydro-1*H*-5,1-ethanoazocino[4,3-*b*]indole. (4.76a).

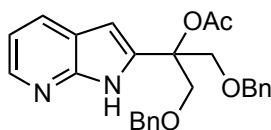
(WLM8_205). A screw top vial charged with Pd(OAc)₂ (3.5 mg, 0.0156 mmol) and SPhos (16 mg, 0.0390 mmol) was placed under vacuum and backfilled with N₂ three times, and toluene (0.1 mL) was added to the reaction vial. A second screw top vial charged with K₃PO₄ (7.6 mg, 0.0358 mmol), phenylboronic acid (4.4 mg, 0.0358 mmol), and **4.74a** (10 mg, 0.0179 mmol) was placed under vacuum and backfilled with N₂ three times, and toluene (0.15 mL) was added to the second reaction vial. Both vials were stirred for 30 min, and an aliquot (5.7 μL) of the Pd/ligand mixture was added to the vial containing **4.74a**. The reaction was heated to 100 °C for 24 h. The reaction mixture was cooled to rt, diluted with H₂O (0.5 mL), and extracted with CH₂Cl₂ (3 x 5 mL). The combined organic extracts were washed with brine (10 mL), dried (Na₂SO₄), filtered, and concentrated *in vacuo* to afford a black oil. Subsequent purification by flash chromatography eluting with Hexanes : EtOAc (1 : 1 → 100% EtOAc) containing 1% NEt₃ followed by further purification via RPHPLC eluting with MeCN : H₂O (10% MeCN → 90% MeCN over 60 min) containing 0.1% TFA afforded 3.5 mg (33%) of **4.76a** as a white solid: ¹H-NMR (600 MHz, CD₃CN) δ 7.77 – 7.73 (m, 1H), 7.67 (comp, 2H), 7.51 (dd, *J* = 8.6, 1.7 Hz, 1H), 7.44 (comp, 2H), 7.31 (comp, 10H), 7.17 (comp, 2H), 5.07 (d, *J* = 6.0 Hz, 1H), 4.50 (comp, 4H), 4.41 (d, *J* = 11.7 Hz, 1H), 4.03 (d, *J* = 9.1 Hz, 1H), 3.97 (td, *J* = 9.0, 1.5 Hz, 1H), 3.88 (d, *J* = 9.1 Hz, 1H), 3.85 (s, 3H), 3.80 (d, *J* = 10.8 Hz, 1H), 3.33 (s, 3H), 3.17 (ddd, *J* = 15.2, 9.3, 6.2 Hz, 1H), 3.13 – 3.06 (m, 1H), 3.01 (comp, 2H), 2.76 (s, 3H), 2.32 – 2.25 (m, 1H), 2.01 (comp, 2H); ¹³C-NMR (150

MHz, CD₃CN) δ 141.8, 141.8, 138.6, 137.7, 137.2, 133.6, 128.8, 128.4, 128.3, 128.0, 127.8, 127.6, 127.5, 127.5, 127.1, 126.6, 121.8, 115.4, 110.1, 110.0, 83.4, 77.6, 73.3, 73.0, 72.4, 58.2, 56.8, 51.5, 49.1, 45.1, 43.5, 36.4, 32.6, 28.1; HRMS (ESI) m/z observed 601.34170 [C₄₀H₄₄N₂O₃ (M+H)⁺ requires 601.34250].



(1*S*/R, 5*R*/S, 12*R*/S)-6,6-Bis((benzyloxy)methyl)-12-methoxy-2,7-dimethyl-10-(4-(trifluoromethyl)phenyl)-2,3,4,5,6,7-hexahydro-1*H*-5,1-ethanoazocino[4,3-*b*]indole. (4.76b). (WLM8_206). A screw top vial charged with Pd(OAc)₂ (3.5 mg, 0.0156 mmol) and SPhos (16 mg, 0.0390 mmol) was placed under vacuum and backfilled with N₂ three times, and toluene (0.1 mL) was added to the reaction vial. A second screw top vial charged with K₃PO₄ (5.6 mg, 0.0264 mmol), 4-(trifluoromethyl)phenylboronic acid (5.0 mg, 0.0264 mmol), and **4.74a** (7.4 mg, 0.0132 mmol) was placed under vacuum and backfilled with N₂ three times, and toluene (0.13 mL) was added to the second reaction vial. Both vials were stirred for 30 min, and an aliquot (4.3 μ L) of the Pd/ligand mixture was added to the vial containing **4.74a**. The reaction was heated to 100 °C for 24 h. The reaction mixture was cooled to rt, diluted with H₂O (0.5 mL), and extracted with CH₂Cl₂ (3 x 5 mL). The combined organic extracts were washed with brine (10 mL), dried (Na₂SO₄), filtered, and concentrated *in vacuo* to afford a black oil. Subsequent purification by flash chromatography eluting with Hexanes : EtOAc (1 : 1 \rightarrow 100% EtOAc) containing 1% NEt₃ followed by further purification via RPHPLC eluting with MeCN : H₂O (10% MeCN \rightarrow 90% MeCN over 60 min) containing 0.1% TFA afforded 1.5 mg (17%) of **4.76b** as a white solid: ¹H-NMR (500 MHz, CD₃OD) δ 7.88 (comp,

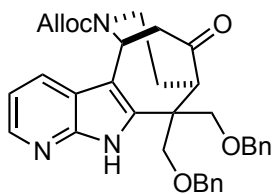
3H), 7.73 (d, $J = 8.1$ Hz, 2H), 7.61 (dd, $J = 8.6, 1.7$ Hz, 1H), 7.56 (d, $J = 8.7$ Hz, 1H), 7.26 (comp, 10H), 5.30 (d, $J = 5.8$ Hz, 1H), 4.58 (d, $J = 11.6$ Hz, 1H), 4.53 (comp, 3H), 4.43 (d, $J = 11.7$ Hz, 1H), 4.08 (d, $J = 7.0$ Hz, 1H), 3.88 (comp, 6H), 3.43 (s, 3H), 3.29 – 3.21 (m, 1H), 3.14 (comp, 3H), 2.89 (s, 3H), 2.47 – 2.30 (m, 1H), 2.15 (dd, $J = 15.1, 8.5$ Hz, 1H), 2.02 – 1.85 (m, 1H); HRMS (ESI) m/z observed 669.32930 [$C_{41}H_{43}F_3N_2O_3$ (M+H)⁺ requires 669.32990].



1,3-Bis(benzyloxy)-2-(1*H*-pyrrolo[2,3-*b*]pyridin-2-yl)propan-2-yl acetate.

(4.78). (WLM8_131). A solution of *n*-BuLi (1.86 mL of 2.5 M solution in hexanes, 4.66 mmol) was added dropwise to a solution of **4.77** (500 mg, 4.23 mmol) in dry THF (18 mL) at -78 °C. The reaction was stirred for 30 min, and dried CO₂ gas (passed through a short column of anhydrous CaSO₄) was bubbled through the reaction for 15 min. The reaction was stirred for 15 min, the bath was removed, and the reaction was stirred for 1 h at room temperature. Excess CO₂ was removed via freeze-pump-thaw (3 cycles), and the reaction was evacuated for 30 sec, and then sparged with N₂ for 30 min. The reaction was cooled to -78 °C, whereupon *t*-BuLi (2.59 mL of 1.8 M solution in pentane, 4.66 mmol) was added dropwise. The reaction was stirred for 2 h and transferred via cannula to a solution of **3.17** (1.26 g, 4.66 mmol) in dry THF (18 mL) at -78 °C. The reaction was stirred for 3.5 h, freshly distilled acetic anhydride (1.295 g, 12.69 mmol, 1.2 mL) was added dropwise, and the reaction was allowed to warm to room temperature over 7 h. Saturated aq NaHCO₃ (10 mL) was added, and the reaction was stirred for 30 min, whereupon brine (20 mL) and CH₂Cl₂ (40 mL) were added. The layers were separated, and the aqueous layer was extracted with CH₂Cl₂ (2 x 40 mL). The combined organic

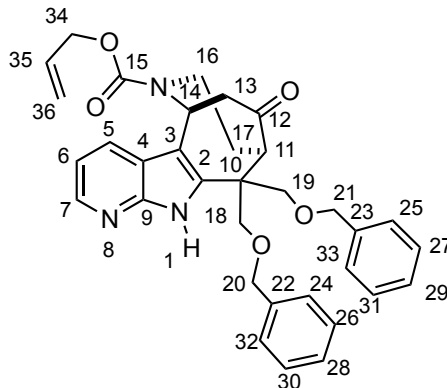
layers were dried (Na₂SO₄), filtered, and concentrated under reduced pressure. The resulting yellow oil was purified by flash chromatography eluting with Hexanes : EtOAc (4 : 1 → 2 : 1 → 100% EtOAc) containing 1% NEt₃ to give 767 mg (42%) of **4.78** as a white solid: ¹H-NMR (500 MHz, CD₂Cl₂) δ 12.92 (br, 1 H) 8.42 (td, *J* = 3.0, 1.5 Hz, 1 H) 8.00 (dd, *J* = 8.0, 1.0 Hz, 1 H) 7.14 (dd, *J* = 4.0, 2.0 Hz, 1 H) 7.33-7.26 (comp, 10 H) 6.55 (d, *J* = 2.0 Hz, 1 H) 4.63 (app s, 4 H) 4.40 (d, *J* = 9.0 Hz, 2 H) 4.35 (d, *J* = 9.0 Hz, 2 H) 2.05 (s, 3 H); ¹³C-NMR (125 MHz, CD₂Cl₂) δ 169.8, 149.2, 142.6, 138.7, 138.4, 129.3, 128.6, 128.1, 128.0, 121.1, 116.1, 98.6, 80.8, 74.0, 70.5, 22.0; HRMS (ESI) *m/z* observed 431.19710 [C₂₆H₂₆N₂O₄ (M+H)⁺ requires 431.19650].



Allyl (5*S*/*R*, 9*R*/*S*)-10,10-bis((benzyloxy)methyl)-12-oxo-5,7,8,9,10,11-hexahydro-6*H*-5,9-ethanopyrido[3',2':4,5]pyrrolo[3,2-*c*]azocine-6-carboxylate.

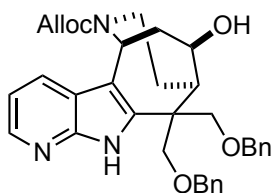
(4.79). (WLMX_258). A solution of TMS-OTf (83 mg, 0.372 mmol, 67 μL) in dry CH₂Cl₂ (0.3 mL) was added dropwise to a solution of **3.10** (29 mg, 0.0818 mmol), **4.78** (32 mg, 0.0734 mmol), and 2,6-di(*tert*-butyl)-4-methylpyridine (92 mg, 0.446 mmol) in dry CH₂Cl₂ (0.5 mL) at −78 °C. The reaction was stirred for 3 h at −78 °C, whereupon a solution of TBAF•3H₂O (152 mg, 0.483 mmol) in CH₂Cl₂ (0.5 mL) was added dropwise. The bath was removed, and the reaction was stirred at room temperature for 1 h. Saturated aq NaHCO₃ (0.5 mL) was added, and the layers were separated. The aqueous layer was extracted with CH₂Cl₂ (3 x 10 mL). The combined organic extracts were washed with brine (15 mL), dried (Na₂SO₄), filtered, and concentrated under reduced pressure. The resultant yellow oil was purified by flash chromatography eluting with

Hexanes : EtOAc (4 : 1 \rightarrow 1 : 1) containing 1% NEt₃ to afford 33 mg (78 %) of **4.79** as a yellow foam: ¹H-NMR (500 MHz, CD₃CN, 70 °C) δ 9.89 (br, 1H), 8.29 (dd, J = 4.7, 1.5 Hz, 1H), 7.90 (dd, J = 8.0, 1.3 Hz, 1H), 7.40 (comp, 5H), 7.29 (comp, 3H), 7.26 – 7.18 (m, 2H), 7.14 (dd, J = 7.9, 4.7 Hz, 1H), 6.05 (br, 1H), 5.86 (t, J = 3.6 Hz, 1H), 5.36 (d, J = 17.5 Hz, 1H), 5.26 (d, J = 10.7 Hz, 1H), 4.67 (comp, 4H), 4.45 (d, J = 11.9 Hz, 1H), 4.40 (d, J = 11.8 Hz, 1H), 4.10 (dd, J = 9.4, 1.4 Hz, 1H), 3.98 (d, J = 14.8 Hz, 1H), 3.88 (d, J = 9.4 Hz, 1H), 3.84 (d, J = 9.4 Hz, 1H), 3.75 (d, J = 9.4 Hz, 1H), 3.18 (dd, J = 5.9, 2.9 Hz, 1H), 3.10 (comp, 2H), 2.95 (dd, J = 18.7, 3.0 Hz, 1H), 2.18 – 2.08 (m, 1H), 1.85 (dddd, J = 15.6, 13.2, 4.8, 2.9 Hz, 1H). ¹³C-NMR (125 MHz, CD₃CN, 70 °C) δ 211.9, 156.5, 149.7, 145.3, 140.6, 139.9, 139.8, 135.3, 130.2, 129.9, 129.6, 129.5, 129.4, 129.3, 127.4, 120.6, 118.2, 117.8, 110.6, 76.6, 75.2, 74.9, 74.0, 67.5, 59.1, 50.6, 47.3, 46.5, 41.4, 29.4. HRMS (ESI) m/z observed 566.26440 [C₃₄H₃₅N₃O₅ (M+H)⁺ requires 566.26490].



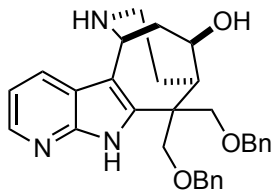
Assignments: ¹H-NMR (500 MHz, CD₃CN, 70 °C) δ 9.89 (br, 1H, N1-H), 8.29 (dd, J = 4.7, 1.5 Hz, 1H, C7-H), 7.90 (dd, J = 8.0, 1.3 Hz, 1H, C5-H), 7.40 (comp, 5H, C24-H, C25-H, C26-H, C27-H, C28-H, C29-H, C30-H, C31-H, C32-H, or C33-H), 7.29 (comp, 3H, C24-H, C25-H, C26-H, C27-H, C28-H, C29-H, C30-H, C31-H, C32-H, or C33-H), 7.26 – 7.18 (m, 2H, C24-H, C25-H, C26-H, C27-H, C28-H, C29-H, C30-H, C31-H, C32-H, or C33-H), 7.14 (dd, J = 7.9, 4.7 Hz, 1H, C6-H), 6.05 (br, 1H, C35-H),

5.86 (t, $J = 3.6$ Hz, 1H, C14-H), 5.36 (d, $J = 17.5$ Hz, 1H, C36-H), 5.26 (d, $J = 10.7$ Hz, 1H, C36-H), 4.67 (comp, 4H, C34-H₂ and C20-H₂ or C21-H₂), 4.45 (d, $J = 11.9$ Hz, 1H, C20-H or C21-H), 4.40 (d, $J = 11.8$ Hz, 1H, C20-H or C21-H), 4.10 (dd, $J = 9.4, 1.4$ Hz, 1H, C18-H or C19-H), 3.98 (d, $J = 14.8$ Hz, 1H, C16-H), 3.88 (d, $J = 9.4$ Hz, 1H, C18-H or C19-H), 3.84 (d, $J = 9.4$ Hz, 1H, C18-H or C19-H), 3.75 (d, $J = 9.4$ Hz, 1H, C18-H or C19-H), 3.18 (dd, $J = 5.9, 2.9$ Hz, 1H, C11-H), 3.10 (comp, 2H, C13-H and C16-H), 2.95 (dd, $J = 18.7, 3.0$ Hz, 1H, C13-H), 2.18 – 2.08 (m, 1H, C17-H), 1.85 (dddd, $J = 15.6, 13.2, 4.8, 2.9$ Hz, 1H, C17-H). ¹³C-NMR (125 MHz, CD₃CN, 70 °C) δ 211.9 (C12), 156.5 (C15), 149.7 (C9), 145.3 (C7), 140.6 (C2), 139.9 (C22 or C23), 139.8 (C22 or C23), 135.3 (C35), 130.2 (C26 and C30 or C27 and C31), 129.9 (C26 and C30 or C27 and C31), 129.6 (C25 and C33 or C24 and C32), 129.5 (C28 or C29), 129.4 (C25 and C33 or C24 and C32), 129.3 (C28 or C29), 127.4 (C5), 120.6 (C4), 118.2 (C36), 117.8 (C6), 110.6 (C3), 76.6 (C), 75.2 (C), 74.9 (C), 74.0 (C), 67.5 (C34), 59.1 (C11), 50.6 (C13), 47.3 (C10), 46.5 (C14), 41.4 (C16), 29.4 (C17).



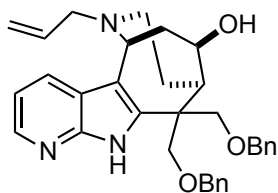
Allyl (5*S*/*R*, 9*R*/*S*, 12*R*/*S*)-10,10-bis((benzyloxy)methyl)-12-hydroxy-5,7,8,9,10,11-hexahydro-6*H*-9,5-ethanopyrido[3',2':4,5]pyrrolo[3,2-*c*]azocine-6-carboxylate. (4.82). (WLM8_269). Lithium borohydride (24 mg, 1.092 mmol) was added to a solution of **4.79** (155 mg, 0.273 mmol) in dry MeOH (2.7 mL) at 0 °C. After 4 h, saturated aq Rochelle's salt (1.0 mL) was added, and the reaction was stirred for 5 min. the reaction mixture was extracted with CH₂Cl₂ (3 x 20 mL), washed with brine (30 mL), dried (Na₂SO₄), filtered, and concentrated under reduced pressure. Subsequent

purification by flash chromatography eluting with Hexanes : EtOAc (2:1 → 1:1) afforded 50 mg (32%) of **4.82** as a white solid: ^1H -NMR (500 MHz, CD_3CN , 70 °C) δ 9.72 (br, 1H), 8.20 (dd, J = 4.7, 0.9 Hz, 1H), 7.77 (dd, J = 7.9, 1.0 Hz, 1H), 7.33 (comp, 13H), 7.05 (ddd, J = 7.8, 4.7, 0.7 Hz, 1H), 6.03 (br, 1H), 5.58 (d, J = 6.6 Hz, 1H), 5.35 (d, J = 17.9 Hz, 1H), 5.24 (d, J = 8.2 Hz, 1H), 4.64 (comp, 4H), 4.52 (d, J = 12.2 Hz, 1H), 4.50 (d, J = 12.1 Hz, 1H), 4.29 (t, J = 9.3 Hz, 1H), 4.13 (d, J = 9.1 Hz, 1H), 4.10 (d, J = 9.6 Hz, 1H), 4.04 (d, J = 9.5 Hz, 1H), 3.83 (d, J = 16.2 Hz, 1H), 3.76 (d, J = 9.2 Hz, 1H), 2.99 (dt, J = 14.8, 7.5 Hz, 1H), 2.72 (t, J = 14.2 Hz, 1H), 2.62 (m, 1H), 1.89 (comp, 2H), 1.84 – 1.73 (m, 1H); ^{13}C -NMR (125 MHz, CD_3CN , 70 °C) δ 156.3, 149.2, 144.2, 139.8, 139.7, 135.2, 129.7, 129.5, 129.1, 129.0, 128.9, 128.7, 126.5, 119.8, 117.4, 117.1, 112.4, 76.0, 74.7, 74.5, 74.3, 74.3, 66.7, 48.4, 48.2, 48.1, 41.7, 41.7, 31.3; HRMS (ESI) m/z observed 568.28020 [$\text{C}_{34}\text{H}_{37}\text{N}_3\text{O}_5$ ($\text{M}+\text{H}$) $^+$ requires 568.28060].



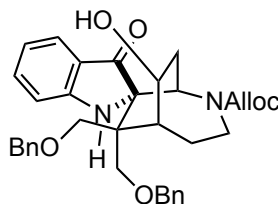
(5*S*/*R*, 9*R*/*S*, 12*R*/*S*)-10,10-Bis((benzyloxy)methyl)-6,7,8,9,10,11-hexahydro-5*H*-9,5-ethanopyrido[3',2':4,5]pyrrolo[3,2-*c*]azocin-12-ol. (4.83a). (WLM8_271). A round bottom flask charged with $\text{Pd}_2(\text{dba})_3$ (2.4 mg, 0.00264 mmol) and 1,4-bis(diphenylphosphino)butane (2.3 mg, 0.00528 mmol) was placed under vacuum and backfilled with N_2 three times. A second round bottom flask was charged with **4.82** (15 mg, 0.0264 mmol) and 1,3-dimethylbarbituric acid (21 mg, 0.132 mmol) and placed under vacuum and backfilled with N_2 three times. THF (.25 mL) was then added to both flasks, and the mixtures were stirred at room temperature under N_2 for 5 min. An aliquot of the Pd/ligand mixture (25 μL) was added via syringe to the flask containing **4.82**, and

stirring was continued at room temperature until **4.82** was gone by TLC. The reaction was quenched with saturated aq NaHCO₃ (0.5 mL) and stirred at room temperature for 15 min. The reaction mixture was diluted with H₂O (0.5 mL) extracted with CH₂Cl₂ (3 x 10 mL). The combined organic extracts were washed with brine (10 mL), dried (Na₂SO₄), filtered, and concentrated *in vacuo* to afford a brown oil. Subsequent purification by RPHPLC eluting with MeCN : H₂O (10% MeCN → 90% MeCN) containing 0.1% TFA provided 4.9 mg (38%) of **4.83a** as a white solid and 1.6 mg (12%) of **4.83b**: ¹H-NMR (500 MHz, CD₃OD) δ 8.27 (br, 1H), 8.06 (dd, *J* = 8.0, 1.4 Hz, 1H), 7.27 (comp, 11H), 5.22 (dd, *J* = 6.5, 1.6 Hz, 1H), 4.63 (d, *J* = 11.6 Hz, 1H), 4.59 (d, *J* = 11.5 Hz, 1H), 4.53 (d, *J* = 12.1 Hz, 1H), 4.49 (d, *J* = 12.0 Hz, 1H), 4.41 (td, *J* = 8.9, 2.3 Hz, 1H), 4.19 (d, *J* = 9.4 Hz, 1H), 4.05 (d, *J* = 9.4 Hz, 1H), 4.02 (d, *J* = 9.4 Hz, 1H), 3.91 (d, *J* = 9.4 Hz, 1H), 2.99 (comp, 2H), 2.82 (comp, 2H), 2.34 – 2.26 (m, 1H), 2.13 (ddd, *J* = 15.0, 8.6, 1.6 Hz, 1H), 1.99 – 1.86 (m, 1H); ¹³C-NMR (126 MHz, CD₃OD) δ 143.9, 143.1, 139.3, 139.3, 135.6, 129.4, 129.3, 129.0, 128.9, 128.8, 128.7, 120.9, 117.4, 111.4, 106.7, 74.6, 74.5, 74.5, 74.4, 74.0, 54.8, 49.3, 47.3, 41.6, 40.1, 28.3; HRMS (ESI) *m/z* observed 506.24100 [C₃₀H₃₃N₃O₃ (M+Na)⁺ requires 506.24100].



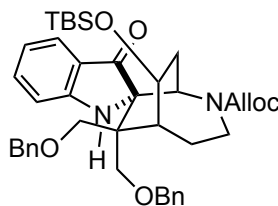
(5S,9R,12R)-6-Allyl-10,10-bis((benzyloxy)methyl)-6,7,8,9,10,11-hexahydro-5H-9,5-ethanopyrido[3',2':4,5]pyrrolo[3,2-c]azocin-12-ol. (4.83b). (WLM8_271). ¹H-NMR (600 MHz, CD₃OD) δ 8.29 (br, 1H), 8.02 (d, *J* = 8.2 Hz, 1H), 7.25 (comp, 11H), 6.02 (td, *J* = 17.1, 7.0 Hz, 1H), 5.58 (d, *J* = 10.3 Hz, 1H), 5.51 (d, *J* = 17.1 Hz, 1H), 5.18 (d, *J* = 5.9 Hz, 1H), 4.61 (d, *J* = 11.6 Hz, 1H), 4.58 (d, *J* = 11.5 Hz, 1H), 4.52 (d, *J* = 12.2

Hz, 1H), 4.49 (d, $J = 12.1$ Hz, 1H), 4.38 (t, $J = 8.7$ Hz, 1H), 4.19 (d, $J = 9.5$ Hz, 1H), 4.05 (d, $J = 9.3$ Hz, 1H), 4.02 (d, $J = 9.5$ Hz, 1H), 3.93 (dd, $J = 14.3, 7.4$ Hz, 1H), 3.90 (d, $J = 9.5$ Hz, 1H), 3.45 (dd, $J = 13.6, 7.3$ Hz, 1H), 3.20 – 3.11 (m, 1H), 3.01 (ddd, $J = 15.2, 9.2, 6.0$ Hz, 1H), 2.92 – 2.82 (m, 1H), 2.82 – 2.75 (m, 1H), 2.35 (d, $J = 16.0$ Hz, 1H), 2.14 (dd, $J = 15.3, 8.0$ Hz, 1H), 1.94 (t, $J = 15.3$ Hz, 1H); ^{13}C -NMR (150 MHz, CD_3OD) δ 144.5, 144.0, 139.3, 139.2, 136.1, 129.4, 129.3, 129.0, 129.0, 128.9, 128.7, 128.5, 127.6, 126.2, 125.8, 117.9, 104.2, 74.8, 74.7, 74.4, 74.3, 74.0, 61.6, 58.8, 50.2, 49.7, 46.5, 40.2, 28.4; HRMS (ESI) m/z observed 524.29020 [$\text{C}_{33}\text{H}_{37}\text{N}_3\text{O}_3$ ($\text{M}+\text{H}$) $^+$ requires 524.29080].

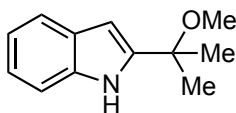


Allyl (1R/S, 5R/S, 6S/R, 8R/S)-7,7-bis((benzyloxy)methyl)-8-hydroxy-3'-oxo-4-azaspiro[bicyclo[3.2.2]nonane-6,2'-indoline]-4-carboxylate (4.86a). (WLM8_86). 70% *meta*-chloroperoxyacetic acid (5 mg, 0.0194 mmol) was added to a solution of **4.12** (10 mg, 0.0176 mmol) and NaHCO_3 (3 mg, 0.0352 mmol) in CH_2Cl_2 (0.3 mL) at rt. After 45 min, the reaction was quenched with saturated aq NaHCO_3 (2.5 mL) and extracted with CH_2Cl_2 (3 x 5 mL). The combined organic extracts were washed with brine (10 mL), dried (Na_2SO_4), filtered and concentrated *in vacuo* to afford a yellow solid. Subsequent purification by flash chromatography eluting with Hexanes : EtOAc (1 : 1) afforded 8 mg (80%) of **4.86a** as a bright yellow solid: ^1H -NMR (500 MHz, CD_3CN , 70 $^\circ\text{C}$) δ 7.42 (comp, 2H), 7.31 (comp, 5H), 7.18 (comp, 3H), 7.02 (comp, 2H), 6.80 (dt, $J = 8.3, 0.8$ Hz, 1H), 6.71 (ddd, $J = 7.9, 7.0, 0.9$ Hz, 1H), 5.85 (br, 1H), 5.69 (s, 1H), 5.19 (d, $J = 17.0$ Hz, 1H), 5.13 (d, $J = 10.8$ Hz, 1H), 4.50 (comp, 3H), 4.46 (d, $J = 12.0$ Hz, 1H), 4.26

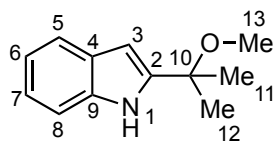
(comp, 3H), 4.20 (d, J = 11.8 Hz, 1H), 4.15 – 4.12 (m, 1H), 4.11 (d, J = 7.2 Hz, 1H), 4.08 (d, J = 7.0 Hz, 1H), 3.85 (d, J = 9.4 Hz, 1H), 3.72 (d, J = 9.3 Hz, 1H), 3.69 (d, J = 9.4 Hz, 1H), 3.14 (ddd, J = 14.2, 12.6, 5.6 Hz, 1H), 2.55 (dt, J = 16.3, 4.2 Hz, 1H), 2.36 (ddd, J = 16.3, 9.9, 2.3 Hz, 1H), 2.31 – 2.20 (m, 1H), 2.18 (d, J = 7.3 Hz, 1H), 1.73 – 1.64 (m, 1H); ^{13}C -NMR (125 MHz, CD_3CN , 70 °C) δ 203.5, 161.2, 157.7, 140.3, 140.0, 137.9, 134.5, 129.4, 129.1, 128.7, 128.6, 128.5, 128.2, 125.1, 121.6, 119.0, 117.8, 113.3, 74.3, 73.2, 72.2, 72.1, 71.7, 68.0, 67.3, 56.9, 48.8, 42.2, 41.6, 31.1, 26.9.



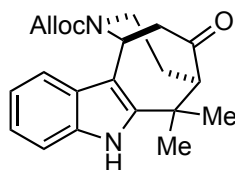
Allyl (1*R*/S, 5*R*/S, 6*S*/R, 8*R*/S)-7,7-bis((benzyloxy)methyl)-8-((*tert*-butyldimethylsilyl)oxy)-3'-oxo-4-azaspiro[bicyclo[3.2.2]nonane-6,2'-indoline]-4-carboxylate. (4.86b). (WLM8_261). 70% *meta*-chloroperoxyacetic acid (5.5 mg, 0.0226 mmol) was added to a solution of **4.13** (14 mg, 0.0206 mmol) in toluene (0.2 mL) at rt. After 45 min, the reaction was quenched with saturated aq NaHCO_3 (2.5 mL) and extracted with CH_2Cl_2 (3 x 5 mL). The combined organic extracts were washed with brine (10 mL), dried (Na_2SO_4), filtered and concentrated *in vacuo* to afford a yellow solid. Subsequent purification by flash chromatography eluting with Hexanes : EtOAc (10 : 1 \rightarrow 4 : 1) afforded 11 mg (77%) of **4.86b** as a bright yellow solid: M.p. 130-135 °C (decomp).



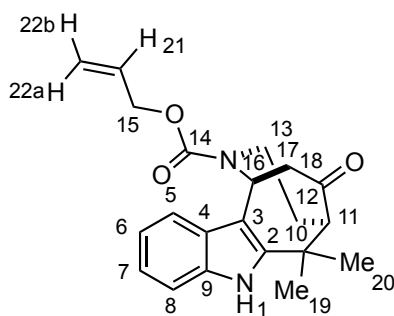
2-(2-methoxypropan-2-yl)-1H-indole. (4.102). (WLM8_42). Silica gel imbedded with oxalic acid (570 mg silica prepared via dissolving 1 mmol oxalic acid onto 4 g silica gel) was added to a solution of **4.99** (250 mg, 1.43 mmol) in MeOH (14.3 mL) at room temperature. After 1.5 h, the solvent was removed, and the reaction was diluted with CH₂Cl₂ (25 mL). The solution was washed with water (25 mL), brine (25 mL), dried (Na₂SO₄), and concentrated under reduced pressure to afford a yellow oil. Subsequent purification by flash chromatography eluting with Hexanes : EtOAc (4 : 1) provided 203 mg (75%) of **4.102** as a white solid and 58 mg (23%) of **4.99** as a white solid: ¹H-NMR (400 MHz, CD₃CN) δ 9.32 (br, 1 H) 7.53 (dd, *J* = 7.2, 2.0 Hz, 1 H) 7.40 (dd, *J* = 7.2, 2.0 Hz, 1 H) 7.13 (td, *J* = 7.2, 1.2 Hz, 1 H) 7.04 (td, *J* = 7.2, 1.2 Hz, 1 H) 6.36 (dd, *J* = 2.2, 1.0 Hz, 1 H) 3.03 (s, 3 H) 1.59 (s, 6 H); ¹³C-NMR (100 MHz, CD₃CN) δ 144.2, 137.4, 129.0, 122.4, 121.0, 120.2, 111.9, 100.4, 74.3, 51.0, 26.9. HRMS (CI) *m/z* observed 189.1154 [C₁₂H₁₅NO (M)⁺ requires 189.1154].



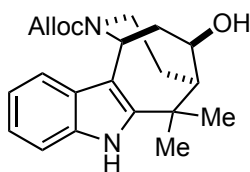
Assignments: ¹H-NMR (400 MHz, CD₃CN) δ 9.32 (br, 1 H, N1-H) 7.53 (dd, *J* = 7.2, 2.0 Hz, 1 H, C5-H) 7.40 (dd, *J* = 7.2, 2.0 Hz, 1 H, C8-H) 7.13 (td, *J* = 7.2, 1.2 Hz, 1 H, C7-H) 7.04 (td, *J* = 7.2, 1.2 Hz, 1 H, C6-H) 6.36 (dd, *J* = 2.2, 1.0 Hz, 1 H, C3-H) 3.03 (s, 3 H, C13-H₃) 1.59 (s, 6 H, C11-H₃ and C12-H₃); ¹³C-NMR (100 MHz, CD₃CN) δ 144.2, 137.4, 129.0, 122.4 (C7), 121.0 (C5), 120.2 (C6), 111.9 (C8), 100.4 (C3), 74.3 (C10), 51.0 (C13), 26.9 (C11 and C12).



(1*S/R*, 5*R/S*)-Allyl 6,6-dimethyl-12-oxo-3,4,5,6-tetrahydro-1*H*-1,5-ethanoazocino[4,3-*b*]indole-2(7*H*)-carboxylate. (**4.96**). (WLM8_61). A solution of TMS-OTf (141 mg, 0.634 mmol, 115 μ L) in dry CH₂Cl₂ (1.0 mL) was added dropwise to a solution of **4.99** (50 mg, 0.264 mmol), **3.10** (102 mg, 0.291 mmol), and 2,6-di(*tert*-butyl)-4-methylpyridine (190 mg, 0.924 mmol) in a dry CH₂Cl₂ (1.0 mL) and MeCN (0.4 mL) mixture at -78 °C. The reaction was stirred for 4 h at -78 °C, whereupon a solution of TBAF•3H₂O (333 mg, 1.06 mmol) in CH₂Cl₂ (1.0 mL) was added dropwise. The bath was removed, and the reaction was stirred at room temperature for 1 h. Saturated aq NaHCO₃ (5 mL) was added, and the layers were separated. The aqueous layer was extracted with CH₂Cl₂ (3 x 10). The combined organic extracts were washed with brine (20 mL), dried (Na₂SO₄), filtered, and concentrated under reduced pressure. The resultant yellow oil was purified by flash chromatography eluting with Hexanes : EtOAc (5 : 1 to 3 : 1 to 1 : 1) containing 1% NEt₃ to provide 40 mg (43%) of **4.96** as a yellow foam: ¹H-NMR (500 MHz, CD₃CN, 70 °C) δ 9.31 (br, 1 H) 7.45 (d, *J* = 8.0 Hz, 1 H) 7.37 (d, *J* = 8.0 Hz, 1 H) 7.13 (td, *J* = 7.0, 1.0 Hz, 1 H) 7.06 (td, *J* = 7.5, 1.0 Hz, 1 H) 6.00 (br, 1 H) 5.83 (t, *J* = 3.5 Hz, 1 H) 5.30 (br, 1 H) 5.22 (br, 1 H) 4.63 (br, 2 H) 3.96 (d, 14.5 Hz, 1 H) 3.02 (dd, *J* = 14.0, 4.0 Hz, 1 H) 3.05 (t, *J* = 14.5 Hz, 1 H) 2.82 (dd, *J* = 19.0, 3.5 Hz, 1 H) 2.68 (dd, *J* = 6.0, 3.0 Hz, 1 H) 2.14 (dm, *J* = 15.5 Hz, 1 H) 1.87 (tm, 1 H) 1.53 (s, 3 H) 1.35 (s, 3 H); ¹³C-NMR (125 MHz, CD₃CN, 70 °C) δ 213.2, 156.1, 144.8, 136.9, 134.9, 128.2, 123.0, 120.7, 118.6, 117.6, 111.9, 108.1, 66.9, 65.6, 50.0, 46.1, 40.4, 37.1, 32.2, 28.9, 28.1; HRMS (ESI) *m/z* observed 375.16770 [C₂₁H₂₄N₂O₃ (M+Na)⁺ requires 375.16790].

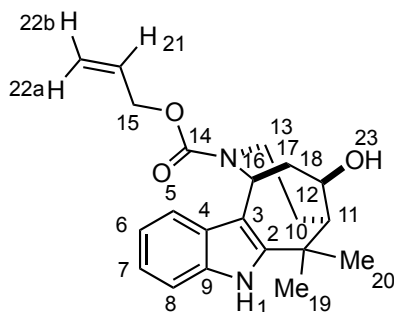


Assignments: $^1\text{H-NMR}$ (500 MHz, CD_3CN , 70 $^\circ\text{C}$) δ 9.31 (br, 1 H, N1-H) 7.45 (d, $J = 8.0$ Hz, 1 H, C5-H) 7.37 (d, $J = 8.0$ Hz, 1 H, C8-H) 7.13 (td, $J = 7.0, 1.0$ Hz, 1 H, C7-H) 7.06 (td, $J = 7.5, 1.0$ Hz, 1 H, C6-H) 6.00 (br, 1 H, C21-H) 5.83 (t, $J = 3.5$ Hz, 1 H, C16-H) 5.30 (br, 1 H, C22_a-H or C22_b-H) 5.22 (br, 1 H, C22_a-H or C22_b-H) 4.63 (br, 2 H, C15-H₂) 3.96 (d, 14.5 Hz, 1 H, C13-H) 3.02 (dd, $J = 14.0, 4.0$ Hz, 1 H, C17-H) 3.05 (t, $J = 14.5$ Hz, 1 H, C13-H) 2.82 (dd, $J = 19.0, 3.5$ Hz, 1 H, C17-H) 2.68 (dd, $J = 6.0, 3.0$ Hz, 1 H, C11-H) 2.14 (dm, $J = 15.5$ Hz, 1 H, C12-H) 1.87 (tm, 1 H, C12-H) 1.53 (s, 3 H, C19-H₃ or C20-H₃) 1.35 (s, 3 H, C19-H₃ or C20-H₃); $^{13}\text{C-NMR}$ (125 MHz, CD_3CN , 70 $^\circ\text{C}$) δ 213.2 (C18), 156.1 (C14), 144.8, 136.9, 134.9, 128.2, 123.0 (C7), 120.7 (C6), 118.6 (C5), 117.6, 111.9 (C8), 108.1 (C3), 66.9 (C15), 65.6 (C11), 50.0 (C17), 46.1 (C16), 40.4 (C13), 37.1 (C10), 32.2 (C19 or C20), 28.9 (C12), 28.1 (C19 or C20).



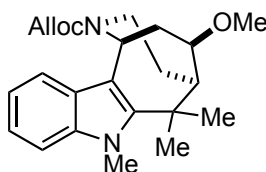
(1*S*/*R*, 5*R*/*S*, 12*R*/*S*)-allyl 12-hydroxy-6,6-dimethyl-3,4,5,6-tetrahydro-1*H*-5,1-ethanoazocino[4,3-*b*]indole-2(7*H*)-carboxylate. (4.103). (WLM7_300). Lithium borohydride (3.6 mg, 0.165 mmol) was added to a solution of **4.96** (29 mg, 0.0823 mmol) in dry MeOH (0.8 mL) at 0 $^\circ\text{C}$. After 14 h, saturated aq Rochelle's salt (0.5 mL) was added, and the reaction was stirred for 5 min. the reaction mixture was extracted with

CH₂Cl₂ (3 x 5), washed with brine (10 mL), dried (Na₂SO₄), filtered, and concentrated under reduced pressure. The resulting yellow oil was purified by flash chromatography eluting with Hexanes : EtOAc (1 : 1) to give 17 mg (93%) of **4.103** as a white solid: ¹H-NMR (500 MHz, CD₃CN, 70 °C) δ 9.12 (br, 1 H) 7.36-7.33 (comp, 2 H) 7.08 (td, *J* = 8.0, 1.0 Hz, 1 H) 7.02 (td, *J* = 8.0, 1.0 Hz, 1 H) 6.03 (br, 1 H) 5.57 (d, *J* = 6.5 Hz, 1 H) 5.36 (br, 1 H) 5.23 (br, 1 H) 4.66 (br, 2 H) 4.35 (app t, *J* = 9.0 Hz, 1 H) 3.80 (d, *J* = 7.5 Hz, 1 H) 3.00 (m, 1 H) 2.74-2.68 (comp, 2 H) 2.10 (m, 1 H) 1.97 (m, 1 H) 1.89 (m, 1 H) 1.77 (m, 1 H) 1.58 (s, 3 H) 1.50 (s, 3 H); ¹³C-NMR (500 MHz, CD₃CN, 70 °C) δ 156.5, 146.7, 136.8, 135.3, 128.0, 122.3, 120.5, 118.2, 117.3, 111.8, 111.0, 76.3, 66.6, 56.4, 48.4, 41.6, 41.2, 39.1, 32.2, 31.9, 31.4; HRMS (ESI) *m/z* observed 377.18350 [C₂₁H₂₆N₂O₃ (M+Na)⁺ requires 377.18360].

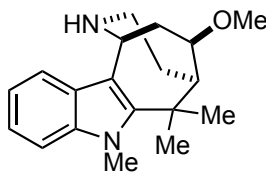


Assignments: ¹H-NMR (500 MHz, CD₃CN, 70 °C) δ 9.12 (br, 1 H, N1-H) 7.36-7.33 (comp, 2 H, C5-H and C8-H) 7.08 (td, *J* = 8.0, 1.0 Hz, 1 H, C7-H) 7.02 (td, *J* = 8.0, 1.0 Hz, 1 H, C6-H) 6.03 (br, 1 H, C21-H) 5.57 (d, *J* = 6.5 Hz, 1 H, C16-H) 5.36 (br, 1 H, C22-H) 5.23 (br, 1 H, C22-H) 4.66 (br, 2 H, C15-H₂) 4.35 (app t, *J* = 9.0 Hz, 1 H, C18-H) 3.80 (d, *J* = 7.5 Hz, 1 H, C13-H) 3.00 (m, 1 H, C17-H) 2.74-2.68 (comp, 2 H, C13-H and O23-H) 2.10 (m, 1 H, C11-H) 1.97 (m, 1 H, C12-H) 1.89 (m, 1 H, C17-H) 1.77 (m, 1 H, C12-H) 1.58 (s, 3 H, C19-H₃ or C20-H₃) 1.50 (s, 3 H, C19-H₃ or C20-H₃); ¹³C-NMR (500 MHz, CD₃CN, 70 °C) δ 156.5 (C14), 146.7, 136.8, 135.3, 128.0, 122.3 (C7), 120.5 (C6),

118.2 (C5), 117.3 (C22), 111.8 (C8), 111.0 (C3), 76.3 (C18), 66.6 (C15), 56.4 (C11), 48.4 (C16), 41.6 (C17) 41.2 (C13), 39.1 (C10), 32.2 (C12), 31.9 (C19 or C20), 31.4 (C19 or C20).

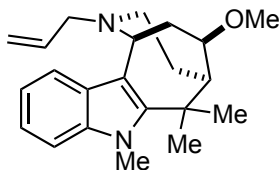


Allynol (1*S/R*, 5*R/S*, 12*R/S*)-12-methoxy-6,6,7-trimethyl-1,3,4,5,6,7-hexahydro-2*H*-5,1-ethanoazocino[4,3-*b*]indole-2-carboxylate. (4.104). (WLM8_54). A mixture of **4.103** (27 mg, 0.0762 mmol) and 60% NaH dispersion in mineral oil (30.5 mg, 0.762 mmol) in DMF (0.75 mL) at 0 °C under N₂ was stirred for five min and methyl *p*-toluenesulfonate (71 mg, 0.381 mmol) was added in one portion. The reaction was allowed to warm slowly to room temperature overnight. The reaction was quenched with saturated aq NH₄Cl (0.5 mL), diluted with H₂O (5.0 mL), and extracted with CH₂Cl₂ (3 x 10 mL). The combined organic extracts were washed with brine (10 mL), dried (Na₂SO₄), filtered, and concentrated *in vacuo* to afford a clear oil. Purification by flash chromatography eluting with Hexanes : EtOAc (4 : 1) to provide 22 mg (76%) of **4.104** as a clear oil: ¹H-NMR (500 MHz, CD₃CN, 70 °C) δ 7.37 (d, *J* = 7.9 Hz, 1H), 7.34 (d, *J* = 8.1 Hz, 1H), 7.17 (ddd, *J* = 8.2, 7.0, 1.2 Hz, 1H), 7.06 (ddd, *J* = 7.9, 7.0, 1.0 Hz, 1H), 6.05 (br, 1H), 5.64 (d, *J* = 6.7 Hz, 1H), 5.30 (comp, 2H), 4.67 (br, 2H), 3.89 (s, 3H), 3.83 (td, *J* = 9.3, 1.5 Hz, 2H), 3.34 (s, 3H), 3.03 (dt, *J* = 14.5, 7.6 Hz, 1H), 2.73 (br, 1H), 2.37 – 2.24 (m, 1H), 2.17 – 2.09 (m, 1H), 1.78 – 1.69 (m, 1H), 1.68 (s, 3H), 1.63 (s, 3H); ¹³C-NMR (125 MHz, CD₃CN, 70 °C) δ 156.3, 146.7, 139.3, 135.2, 127.6, 122.6, 120.6, 118.2, 117.4, 112.5, 110.2, 86.4, 66.6, 57.2, 54.3, 48.5, 41.2, 40.2, 34.1, 31.6, 29.0; HRMS (ESI) *m/z* observed 383.23250 [C₂₃H₃₀N₂O₃ (M+H)⁺ requires 383.23290].

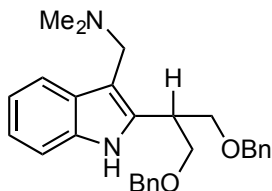


(1*S/R*, 5*R/S*, 12*R/S*)-12-Methoxy-6,6,7-trimethyl-2,3,4,5,6,7-hexahydro-1*H*-5,1-ethanoazocino[4,3-*b*]indole. (4.105). (WLM8_41). A round bottom flask charged with Pd₂(dba)₃ (1.2 mg, 0.0013 mmol) and 1,4-bis(diphenylphosphino)butane (1.1 mg, 0.0026 mmol) was placed under vacuum and backfilled with N₂ three times. A second round bottom flask was charged with **4.104** (5 mg, 0.013 mmol) and 1,3-dimethylbarbituric acid (20 mg, 0.13 mmol) and placed under vacuum and backfilled with N₂ three times. THF (0.1 mL) was then added to both flasks, and the mixtures were stirred at room temperature under N₂ for 5 min. An aliquot of the Pd/ligand mixture (10 μL) was added via syringe to the flask containing **4.104**, and stirring was continued at room temperature until **4.104** was gone by TLC. The reaction was quenched with saturated aq NaHCO₃ (0.1 mL) and stirred at room temperature for 15 min. The reaction mixture was diluted with H₂O (0.5 mL) extracted with CH₂Cl₂ (3 x 5 mL). The combined organic extracts were washed with brine (10 mL), dried (Na₂SO₄), filtered, and concentrated *in vacuo* to afford a brown oil. Subsequent purification by flash chromatography eluting with MeCN : H₂O (10% MeCN → 90% MeCN) containing 0.1% TFA provided 3 mg (77%) of **4.105** as a white solid: ¹H-NMR (600 MHz, CD₃OD) δ 7.54 (dt, *J* = 8.0, 1.0 Hz, 1H), 7.40 (dt, *J* = 8.3, 0.8 Hz, 1H), 7.22 (ddd, *J* = 8.3, 7.0, 1.1 Hz, 1H), 7.13 (ddd, *J* = 7.9, 7.0, 0.9 Hz, 1H), 5.26 (dd, *J* = 6.3, 1.8 Hz, 1H), 3.96 (comp, 4H), 3.41 (s, 3H), 3.03 (comp, 2H), 2.83 (td, *J* = 13.8, 3.6 Hz, 1H), 2.45 (comp, 2H), 2.16 (ddd, *J* = 14.9, 8.6, 1.8 Hz, 1H), 1.94 – 1.82 (m, 1H), 1.74 (s, 3H), 1.68 (s, 3H); ¹³C-NMR (151 MHz, CD₃OD) δ 147.6, 139.5, 127.1, 123.4, 121.3, 118.0, 110.3, 106.0, 85.0, 57.3,

52.5, 49.8, 40.8, 40.5, 38.0, 33.8, 30.9, 28.7, 28.5; HRMS (ESI) m/z observed 321.19320 [$C_{19}H_{26}N_2O$ ($M+Na$)⁺ requires 321.19370].

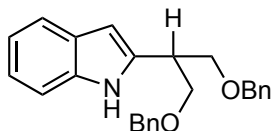


(1S, 5R/S, 12R/S)-2-Allyl-12-methoxy-6,6,7-trimethyl-2,3,4,5,6,7-hexahydro-1H-5,1-ethanoazocino[4,3-b]indole. (4.106). (WLM8_55). A round bottom flask charged with $Pd(PPh_3)_4$ (3.3 mg, 0.00288 mmol) and **4.104** (22 mg, 0.0575 mmol) was placed under vacuum and backfilled with N_2 three times. THF (0.5 mL) was added and the mixture was stirred at room temperature over night. The reaction mixture was diluted with H_2O (5.0 mL) and extracted with CH_2Cl_2 (3 x 10 mL). The combined organic extracts were washed with brine (10 mL), dried (Na_2SO_4), filtered, and concentrated *in vacuo* to afford a brown oil. Subsequent purification by RP HPLC H_2O : MeCN (10% MeCN \rightarrow 95% MeCN over 60 min) provided 5.3 mg (27%) of **4.106** as a white solid: 1H -NMR (600 MHz, $CDCl_3$) δ 7.49 (dt, $J = 7.9, 1.0$ Hz, 1H), 7.26 (dt, $J = 8.2, 0.9$ Hz, 1H), 7.18 (ddd, $J = 8.2, 7.0, 1.2$ Hz, 1H), 7.09 (ddd, $J = 8.0, 7.0, 1.0$ Hz, 1H), 6.13 – 5.95 (m, 1H), 5.31 (dq, $J = 17.4, 1.9$ Hz, 1H), 5.22 (dq, $J = 10.3, 1.6$ Hz, 1H), 4.41 (d, $J = 6.4$ Hz, 1H), 4.03 (td, $J = 9.0, 2.0$ Hz, 1H), 3.89 (s, 3H), 3.36 (s, 3H), 3.31 (dd, $J = 14.4, 6.5$ Hz, 1H), 3.06 (dd, $J = 13.9, 5.1$ Hz, 1H), 2.90 – 2.73 (m, 1H), 2.57 – 2.42 (m, 1H), 2.29 (td, $J = 13.0, 3.8$ Hz, 1H), 2.22 – 2.16 (m, 1H), 2.17 – 2.09 (m, 1H), 1.83 (ddd, $J = 13.5, 9.0, 1.5$ Hz, 2H), 1.64 (s, 3H), 1.58 (s, 3H); ^{13}C -NMR (150 MHz, $CDCl_3$) δ 144.9, 137.9, 137.7, 128.3, 121.2, 119.3, 118.3, 116.8, 109.9, 108.6, 85.6, 77.4, 77.2, 76.9, 62.1, 56.7, 56.1, 52.9, 49.2, 40.3, 39.3, 33.3, 31.5, 31.5, 28.7; HRMS (ESI) m/z observed 339.24340 [$C_{22}H_{30}N_2O$ ($M+H$)⁺ requires 339.24310].



1-(2-(1,3-bis(benzyloxy)propan-2-yl)-1H-indol-3-yl)-N,N-

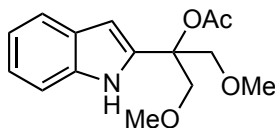
Dimethylmethanamine. (4.107). (WLM9_83). Zinc chloride (4.7 mg, 0.0343 mmol) was added to a solution of **4.108** (8.5 mg, 0.0229 mmol), 36% aq formaldehyde (2.1 mg, 0.0252 mmol, 2 μ L), and 40% aq dimethylamine (25.8 mg, 0.229 mmol, 26 μ L) in EtOH (0.23 mL). The reaction mixture was stirred at rt. After 36 h, the reaction was diluted with H₂O (5 mL) and extracted with CH₂Cl₂ (3 x 5 mL). The combined organic extracts were washed with brine (5 mL), dried (Na₂SO₄), filtered, and concentrated *in vacuo* to afford a brown oil. Subsequent purification by flash chromatography eluting with Hexanes : EtOAc (10 : 1 \rightarrow 100% EtOAc) containing 1% NEt₃ afforded 5 mg (51%) of **4.107** as a clear oil: ¹H-NMR (500 MHz, CD₃CN) δ 9.24 (br, 1H), 7.57 (ddt, J = 7.8, 1.4, 0.7 Hz, 1H), 7.31 (comp, 11H), 7.07 (ddd, J = 8.1, 7.0, 1.3 Hz, 1H), 7.00 (ddd, J = 8.0, 7.0, 1.1 Hz, 1H), 4.57 – 4.49 (comp, 4H), 3.80 (comp, 4H), 3.63 (p, J = 5.8 Hz, 1H), 3.51 (s, 2H), 2.14 (s, 6H); ¹³C-NMR (125 MHz, CD₃CN) δ 139.7, 137.8, 136.5, 129.5, 129.3, 128.6, 128.5, 121.9, 119.7, 119.6, 111.7, 110.2, 73.7, 70.9, 54.1, 45.5, 38.4; HRMS (ESI) m/z observed 429.25480 [C₂₈H₃₂N₂O₂ (M+H)⁺ requires 429.25370].



2-(1,3-bis(benzyloxy)propan-2-yl)-1H-Indole. (4.108). (WLM9_84).

Ammonium formate (80 mg, 1.26 mmol) was added to a solution of **3.11** (54 mg, 0.126

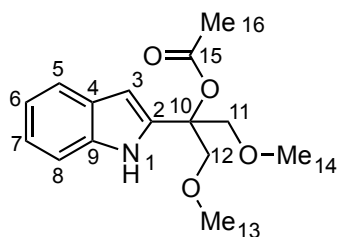
mmol) and 10% Pd/C (7.4 mg) in EtOH (0.65 mL) in a glass vial. The glass vial was sealed, and the reaction was stirred for 12 h at 80 °C. The reaction mixture was cooled to rt, diluted with EtOAc (10 mL), and filtered through a pad of Celite[®] that was subsequently washed with EtOAc (3 x 5 mL). The combined organic extracts were washed with H₂O (20 mL), brine (20 mL), dried (Na₂SO₄), filtered, and concentrated *in vacuo* to afford a brown oil that was subsequently purified by flash chromatography eluting with Hexanes : EtOAc (8 : 1) to afford 26 mg (55%) of **4.108** as a clear oil: ¹H-NMR (400 MHz, CDCl₃) δ 8.87 (br, 1H), 7.55 (dd, *J* = 7.8, 1.2 Hz, 1H), 7.33 (comp, 11H), 7.13 (ddd, *J* = 8.1, 7.0, 1.3 Hz, 1H), 7.07 (ddd, *J* = 8.1, 7.0, 1.1 Hz, 1H), 6.33 – 6.25 (m, 1H), 4.58 (comp, 4H), 3.87 (qd, *J* = 9.1, 5.7 Hz, 4H), 3.42 (p, *J* = 5.7 Hz, 1H); ¹³C-NMR (100 MHz, CDCl₃) δ 139.1, 138.2, 135.9, 128.6, 128.2, 127.9, 127.9, 121.3, 120.1, 119.6, 110.8, 99.6, 73.6, 70.6, 39.7; HRMS (ESI) *m/z* observed 394.17800 [C₂₅H₂₅NO₂ (M+Na)⁺ requires 394.17780].



2-(1*H*-indol-2-yl)-1,3-Dimethoxypropan-2-yl acetate. (4.118a).

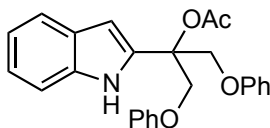
(WLM7_239_2). A solution of *n*-BuLi (3.94 mL of 2.5 M solution in hexanes, 9.86 mmol) was added dropwise to a solution of indole (**3.18**) (1.05 g, 8.96 mmol) in dry THF (25 mL) at –78 °C. The reaction was stirred for 30 min, and dried CO₂ gas (passed through a short column of anhydrous CaSO₄) was bubbled through the reaction for 15 min. The reaction was stirred for 15 min, the bath was removed, and the reaction was stirred for 1 h at room temperature. Excess CO₂ was removed via freeze-pump-thaw (3 cycles), and the reaction was evacuated for 30 sec, and then sparged with N₂ for 20 min. The reaction was cooled to –78 °C, whereupon *t*-BuLi (5.48 mL of 1.8 M solution in

pentane, 9.86 mmol) was added dropwise. The reaction was stirred for 80 min and transferred via cannula to a solution of **4.117** (1.16 g, 9.86 mmol) in dry THF (25 mL) at $-78\text{ }^{\circ}\text{C}$. The reaction was stirred for 2.5 h, freshly distilled acetic anhydride (2.75 g, 26.89 mmol, 2.54 mL) was added dropwise, and the reaction was allowed to warm to room temperature over 7 h. Saturated aq NaHCO_3 (25 mL) was added, and the reaction was stirred for 30 min, whereupon brine (50 mL) and Et_2O (50 mL) were added. The layers were separated, and the aqueous layer was extracted with Et_2O (2 x 50 mL). The combine organic layers were dried (Na_2SO_4), filtered, and concentrated under reduced pressure. The resulting yellow oil was purified by flash chromatography eluting with Hexanes : EtOAc (10:1 to 8:1 to 5:1 to 2:1) containing 1% NEt_3 to give 1.25 g (50%) of **4.118a** as a white solid: ^1H -NMR (600 MHz, CD_3CN) δ 9.44 (br, 1 H) 7.51 (dd, $J = 7.8, 1.2$ Hz, 1 H) 7.39 (dd, $J = 7.8, 1.2$ Hz, 1 H) 7.11 (td, $J = 7.2, 1.2$ Hz, 1 H) 7.02 (td, $J = 7.2, 1.2$ Hz, 1 H) 6.38 (dd, $J = 2.4, 0.6$ Hz, 1 H) 4.01 (d, $J = 9.6$ Hz, 2 H) 3.98 (d, $J = 9.6$ Hz, 2 H) 3.35 (s, 6 H) 2.03 (s, 3 H); ^{13}C -NMR (150 MHz, CD_3CN) δ 170.5, 138.1, 136.9, 128.7, 122.6, 121.1, 120.4, 112.1, 100.4, 81.3, 73.7, 59.8, 22.1; HRMS (CI) m/z observed 277.1314 [$\text{C}_{15}\text{H}_{19}\text{NO}_4$ (M) $^+$ requires 277.1314].



Assignments: ^1H -NMR (600 MHz, CD_3CN) δ 9.44 (br, 1 H, N1-H) 7.51 (dd, $J = 7.8, 1.2$ Hz, 1 H, C5-H) 7.39 (dd, $J = 7.8, 1.2$ Hz, 1 H, C8-H) 7.11 (td, $J = 7.2, 1.2$ Hz, 1 H, C7-H) 7.02 (td, $J = 7.2, 1.2$ Hz, 1 H, C6-H) 6.38 (dd, $J = 2.4, 0.6$ Hz, 1 H, C3-H) 4.01 (d, $J = 9.6$ Hz, 2 H, C11-H $_2$ or C12-H $_2$) 3.98 (d, $J = 9.6$ Hz, 2 H, C11-H $_2$ or C12-H $_2$) 3.35

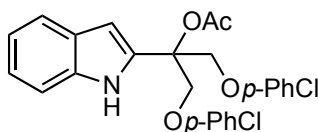
(s, 6 H, C13-H₃ and C14-H₃) 2.03 (s, 3 H, C16-H₃); ¹³C-NMR (150 MHz, CD₃CN) δ 170.5 (C15), 138.1, 136.9, 128.7, 122.6 (C7), 121.1 (C5), 120.4 (C6), 112.1 (C8), 100.4 (C3), 81.3 (C10), 73.7 (C11 and C12), 59.8 (C13 and C14), 22.1 (C16).



2-(1*H*-indol-2-yl)-1,3-Diphenoxypropan-2-yl acetate. (4.118b). (WLM8_107).

A solution of *n*-BuLi (1.88 mL of 2.5 M solution in hexanes, 4.695 mmol) was added dropwise to a solution of indole (**3.18**) (500 mg, 4.268 mmol) in dry THF (20 mL) at -78°C . The reaction was stirred for 30 min, and dried CO₂ gas (passed through a short column of anhydrous CaSO₄) was bubbled through the reaction for 15 min. The reaction was stirred for 15 min, the bath was removed, and the reaction was stirred for 1 h at room temperature. Excess CO₂ was removed via freeze-pump-thaw (3 cycles), and the reaction was evacuated for 30 sec, and then sparged with N₂ for 20 min. The reaction was cooled to -78°C , whereupon *t*-BuLi (2.61 mL of 1.8 M solution in pentane, 4.695 mmol) was added dropwise. The reaction was stirred for 80 min and transferred via cannula to a solution of **4.115a** (1.14 g, 4.695 mmol) in dry THF (20 mL) at -78°C . The reaction was stirred for 2.5 h, freshly distilled acetic anhydride (1.31 g, 12.8 mmol, 1.21 mL) was added dropwise, and the reaction was allowed to warm to room temperature over 7 h. Saturated aq NaHCO₃ (30 mL) was added, and the reaction was stirred for 30 min, whereupon brine (50 mL) and Et₂O (50 mL) were added. The layers were separated, and the aqueous layer was extracted with Et₂O (2 x 50 mL). The combined organic layers were dried (Na₂SO₄), filtered, and concentrated under reduced pressure. The resulting yellow oil was purified by flash chromatography eluting with Hexanes : EtOAc (8 : 1) containing 1% NEt₃ to give 1.245 g (73%) of **4.118b** as a white solid: ¹H-NMR (500

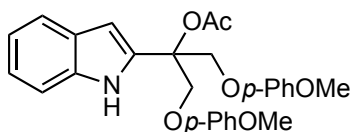
MHz, CD₃CN) δ 9.67 (br, 1 H) 7.55 (d, J = 8.5 Hz, 1 H) 7.43 (dd, J = 8.0, 1.0 Hz, 1 H) 7.29-7.24 (comp, 4 H) 7.15 (dt, J = 7.0, 1.5 Hz, 1 H) 7.05 (dt, J = 7.0, 1.0 Hz, 1 H) 6.98-6.93 (comp, 6 H) 6.59 (dd, J = 2.0, 0.5 Hz, 1 H) 4.80 (d, J = 10.0 Hz, 2 H) 4.77 (d, J = 10.0 Hz, 2 H) 2.07 (s, 3 H); ¹³C-NMR (500 MHz, CD₃CN) δ 170.6, 159.5, 137.1, 136.8, 130.5, 128.7, 123.0, 122.3, 121.3, 120.6, 115.8, 112.2, 101.0, 80.7, 69.2, 22.0; HRMS (ESI) m/z observed 424.15170 [C₂₅H₂₃NO₄ (M+Na)⁺ requires 424.15190].



1,3-Bis(4-chlorophenoxy)-2-(1H-indol-2-yl)propan-2-yl acetate. (4.118c).

(WLM8_122). A solution of *n*-BuLi (1.94 mL of 2.5 M solution in hexanes, 4.977 mmol) was added dropwise to a solution of indole (**3.18**) (530 mg, 4.524 mmol) in dry THF (23 mL) at -78 °C. The reaction was stirred for 30 min, and dried CO₂ gas (passed through a short column of anhydrous CaSO₄) was bubbled through the reaction for 15 min. The reaction was stirred for 15 min, the bath was removed, and the reaction was stirred for 1 h at room temperature. Excess CO₂ was removed via freeze-pump-thaw (3 cycles), and the reaction was evacuated for 30 sec, and then sparged with N₂ for 20 min. The reaction was cooled to -78 °C, whereupon *t*-BuLi (2.77 mL of 1.8 M solution in pentane, 4.977 mmol) was added dropwise. The reaction was stirred for 80 min and transferred via cannula to a solution of **4.115b** (1.55 g, 4.977 mmol) in dry THF (23 mL) at -78 °C. The reaction was stirred for 2.5 h, freshly distilled acetic anhydride (1.385 g, 13.57 mmol, 1.28 mL) was added dropwise, and the reaction was allowed to warm to room temperature over 7 h. Saturated aq NaHCO₃ (40 mL) was added, and the reaction was stirred for 30 min, whereupon brine (40 mL) and Et₂O (60 mL) were added. The

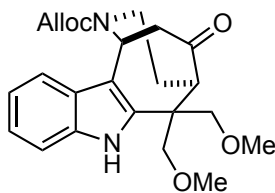
layers were separated, and the aqueous layer was extracted with Et₂O (2 x 60 mL). The combined organic layers were dried (Na₂SO₄), filtered, and concentrated under reduced pressure. The resulting yellow oil was purified by flash chromatography eluting with Hexanes : EtOAc (4 : 1) containing 1% NEt₃ to give 413 mg (19%) of **4.118c** as a white solid: ¹H-NMR (500 MHz, CD₃CN) δ 9.63 (br, 1 H) 7.54 (dd, *J* = 8.0, 1.0 Hz, 1 H) 7.42 (dd, *J* = 8.0, 1.0 Hz, 1 H) 7.24 (d, *J* = 9.0 Hz, 4 H) 7.15 (td, *J* = Hz, 1 H) 7.05 (td, *J* = 7.5, 1.0 Hz, 1 H) 6.93 (d, *J* = 9.0 Hz, 4 H) 6.57 (dd, *J* = 2.5, 1.0 Hz, 1 H); ¹³C-NMR (125 MHz, CD₃CN) δ 171.2, 158.9, 137.7, 137.0, 130.9, 129.3, 127.3, 123.7, 122.0, 121.3, 118.1, 112.8, 101.7, 81.1, 70.3, 22.6; HRMS (ESI) *m/z* observed 492.07400 [C₂₅H₂₁Cl₂NO₄ (M+Na)⁺ requires 492.07400].



2-(1*H*-indol-2-yl)-1,3-Bis(4-methoxyphenoxy)propan-2-yl acetate. (4.118d).

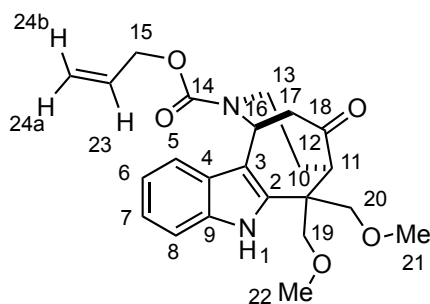
(WLM8_175). A solution of *n*-BuLi (3.76 mL of 2.5 M solution in hexanes, 9.390 mmol) was added dropwise to a solution of indole (**3.18**) (1.00 g, 8.536 mmol) in dry THF (25 mL) at −78 °C. The reaction was stirred for 30 min, and dried CO₂ gas (passed through a short column of anhydrous CaSO₄) was bubbled through the reaction for 15 min. The reaction was stirred for 15 min, the bath was removed, and the reaction was stirred for 1 h at room temperature. Excess CO₂ was removed via freeze-pump-thaw (3 cycles), and the reaction was evacuated for 30 sec, and then sparged with N₂ for 20 min. The reaction was cooled to −78 °C, whereupon *t*-BuLi (5.22 mL of 1.8 M solution in pentane, 9.390 mmol) was added dropwise. The reaction was stirred for 80 min and transferred via cannula to a solution of **4.115c** (2.84 g, 9.390 mmol) in dry THF (25 mL)

at $-78\text{ }^{\circ}\text{C}$. The reaction was stirred for 2.5 h, freshly distilled acetic anhydride (2.61 g, 25.61 mmol, 2.42 mL) was added dropwise, and the reaction was allowed to warm to room temperature over 7 h. Saturated aq NaHCO_3 (50 mL) was added, and the reaction was stirred for 30 min, whereupon brine (50 mL) and Et_2O (50 mL) were added. The layers were separated, and the aqueous layer was extracted with Et_2O (2 x 50 mL). The combined organic layers were dried (Na_2SO_4), filtered, and concentrated under reduced pressure. The resulting yellow oil was purified by flash chromatography eluting with Hexanes : EtOAc (9:1 \rightarrow 4:1 \rightarrow 3:2) containing 1% NEt_3 to give 3.071 g (78%) of **4.118d** as a white solid: ^1H -NMR (600 MHz, CD_3CN) δ 9.72 (br, 1 H) 7.61 (d, $J = 8.4$ Hz, 1 H) 7.49 (d, $J = 8.4$ Hz, 1 H) 7.20 (td, $J = 6.6, 1.2$ Hz, 1 H) 7.10 (td, $J = 6.6, 1.2$ Hz, 1 H) 6.94 (d, $J = 9.0$ Hz, 4 H) 6.86 (d, $J = 9.0$ Hz, 4 H) 6.64 (d, $J = 2.4$ Hz, 1 H) 4.79 (d, $J = 9.6$ Hz, 2 H) 4.76 (d, $J = 10.2$ Hz, 1 H) 3.73 (s, 6 H) 2.11 (s, 3 H); ^{13}C -NMR (150 MHz, CD_3CN) δ 170.7, 155.3, 153.6, 137.1, 136.9, 128.7, 123.0, 121.4, 120.6, 117.0, 115.6, 112.2, 101.1, 80.9, 70.1, 56.2, 22.1; HRMS (ESI) m/z observed 484.17230 [$\text{C}_{27}\text{H}_{27}\text{NO}_6$ ($\text{M}+\text{Na}$) $^+$ requires 484.17310].



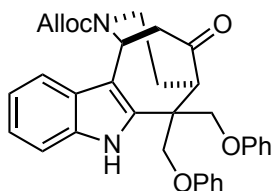
(1S/R, 5R/S)-Allyl 6,6-bis(methoxymethyl)-12-oxo-3,4,5,6-tetrahydro-1H-1,5-ethanoazocino[4,3-b]indole-2(7H)-carboxylate. (4.119a). (WLM8_44). A solution of TMS-OTf (867 mg, 3.9 mmol, 0.71 mL) in dry CH_2Cl_2 (3.9 mL) was added dropwise to a solution of **4.118a** (900 mg, 3.25 mmol), **3.10** (1.25 g, 3.57 mmol), and 2,6-di(*tert*-butyl)-4-methylpyridine (1.35 g, 6.5 mmol) in dry CH_2Cl_2 (12.0 mL) at $-78\text{ }^{\circ}\text{C}$. The reaction was stirred for 3 h at $-78\text{ }^{\circ}\text{C}$, whereupon a solution of TBAF $\cdot 3\text{H}_2\text{O}$ (3.08 g, 9.75 mmol)

in CH₂Cl₂ (12.0 mL) was added dropwise. The bath was removed, and the reaction was stirred at room temperature for 1 h. Saturated aq NaHCO₃ (5 mL) was added, and the layers were separated. The aqueous layer was extracted with CH₂Cl₂ (3 x 50 mL). The combined organic extracts were washed with brine (100 mL), dried (Na₂SO₄), filtered, and concentrated under reduced pressure. The resultant yellow oil was purified by flash chromatography eluting with Hexanes : EtOAc (4:1 → 3:1 → 1:1) containing 1% NEt₃ to provide 1.08 g (81%) of **4.119a** as a yellow foam: ¹H-NMR (500 MHz, CD₃CN, 70 °C) δ 9.56 (br, 1 H) 7.49 (d, *J* = 7.5 Hz, 1 H) 7.43 (d, *J* = 8.0 Hz, 1 H) 7.15 (td, *J* = 7.5, 1.0 Hz, 1 H) 7.08 (td, 7.5, 1.0 Hz, 1 H) 6.01 (br, 1 H) 5.87 (app t, *J* = 3.5 Hz, 1 H) 5.33 (br, 1 H) 5.22 (d, *J* = 8.0 Hz, 1 H) 4.64 (br, 2 H) 4.00-3.96 (m, 1 H) 3.85 (d, *J* = 9.5 Hz, 1 H) 3.65 (d, *J* = 9.0 Hz, 1 H) 3.60 (d, *J* = 9.0 Hz, 1 H) 3.51 (d, *J* = 9.0 Hz, 1 H) 3.40 (s, 3 H) 3.18 (s, 3 H) 3.11-3.02 (comp, 3 H) 2.92 (dd, *J* = 8.5, 3.0 Hz, 1 H) 2.04 (dm, *J* = 15.5 Hz, 1 H) 1.79 (tdd, *J* = 14.5, 4.5, 2.5 Hz, 1 H); ¹³C-NMR (125 MHz, CD₃CN, 70 °C) δ 211.7, 156.1, 139.6, 136.8, 134.9, 127.9, 123.2, 120.8, 118.6, 117.7, 112.3, 110.8, 78.2, 75.9, 66.9, 59.9, 59.4, 58.5, 46.3, 46.2, 40.8, 28.9; HRMS (ESI) *m/z* observed 435.18930 [C₂₃H₂₈N₂O₅ (M+Na)⁺ requires 435.18900].



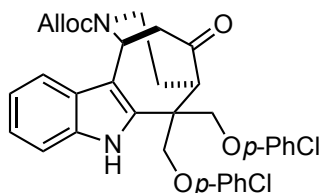
Assignments: ¹H-NMR (500 MHz, CD₃CN, 70 °C) δ 9.56 (br, 1 H, N1-H) 7.49 (d, *J* = 7.5 Hz, 1 H, C5-H) 7.43 (d, *J* = 8.0 Hz, 1 H, C8-H) 7.15 (td, *J* = 7.5, 1.0 Hz, 1 H, C7-H) 7.08 (td, 7.5, 1.0 Hz, 1 H, C6-H) 6.01 (br, 1 H, C23-H) 5.87 (app t, *J* = 3.5 Hz, 1

H, C16-H) 5.33 (br, 1 H, C24-H or C25-H) 5.22 (d, $J = 8.0$ Hz, 1 H, C24-H or C25-H) 4.64 (br, 2 H, C15-H₂) 4.00-3.96 (m, 1 H, C13-H) 3.85 (d, $J = 9.5$ Hz, 1 H, C19-H or C20-H) 3.65 (d, $J = 9.0$ Hz, 1 H, C19-H or C20-H) 3.60 (d, $J = 9.0$ Hz, 1 H, C19-H or C20-H) 3.51 (d, $J = 9.0$ Hz, 1 H, C19-H or C20-H) 3.40 (s, 3 H, C21-H₃ or C22-H₃) 3.18 (s, 3 H, C21-H₃ or C22-H₃) 3.11-3.02 (comp, 3 H, C11-H, C13-H, and C17-H) 2.92 (dd, $J = 8.5, 3.0$ Hz, 1 H, C17-H) 2.04 (dm, $J = 15.5$ Hz, 1 H, C12-H) 1.79 (tdd, $J = 14.5, 4.5, 2.5$ Hz, 1 H, C12-H); ¹³C-NMR (125 MHz, CD₃CN, 70 °C) δ 211.7 (C18), 156.1 (C14), 139.6, 136.8, 134.9, 127.9, 123.2 (C7), 120.8 (C6), 118.6 (C5), 117.7, 112.3 (C8), 110.8 (C3), 78.2 (C19 or C20), 75.9 (C19 or C20), 66.9 (C15), 59.9 (C21 or C22), 59.4 (C21 or C22), 58.5 (C11), 50.2 (C17), 46.3 (C10), 46.2 (C16), 40.8 (C13), 28.9 (C12).



(1S/R, 5R/S)-Allyl 12-oxo-6,6-bis(phenoxymethyl)-3,4,5,6-tetrahydro-1H-1,5-ethanoazocino[4,3-b]indole-2(7H)-carboxylate. (4.119b). (WLM8_117). A solution of TMS-OTf (373 mg, 1.54 mmol, 0.304 mL) in dry CH₂Cl₂ (1.0 mL) was added dropwise to a solution of **4.118b** (562 mg, 1.40 mmol), **3.10** (541 mg, 1.54 mmol), and 2,6-di(*tert*-butyl)-4-methylpyridine (575 mg, 2.80 mmol) in dry CH₂Cl₂ (6.0 mL) at -78 °C. The reaction was stirred for 3 h at -78 °C, whereupon a solution of TBAF•3H₂O (1.325 mg, 4.20 mmol) in CH₂Cl₂ (7.0 mL) was added dropwise. The bath was removed, and the reaction was stirred at room temperature for 1 h. Saturated aq NaHCO₃ (10 mL) was added, and the layers were separated. The aqueous layer was extracted with CH₂Cl₂ (3 x 30 mL). The combined organic extracts were washed with brine (20 mL), dried (Na₂SO₄), filtered, and concentrated under reduced pressure. The resultant yellow oil was purified

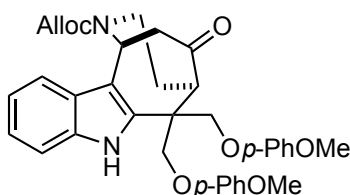
by flash chromatography eluting with Hexanes : EtOAc (4 : 1) containing 1% NEt₃ to afford 562 mg (75%) of **4.118b** as a yellow foam: ¹H-NMR (500 MHz, CD₃CN, 70 °C) δ 9.67 (br, 1 H) 7.55 (d, *J* = 8.0 Hz, 1 H) 7.45 (dm, *J* = 8.5 Hz, 1 H) 7.34-7.30 (comp, 2 H) 7.24-7.17 (comp, 3 H) 7.11 (td, *J* = 7.5, 1.0 Hz, 1 H) 7.08 (dm, *J* = 9.0 Hz, 2 H) 7.00 (dt, *J* = 7.0, 1.0 Hz, 1 H) 6.92 (dt, *J* = 7.5, 1.0 Hz, 1 H) 6.86 (dm, *J* = 8.0 Hz, 2 H) 6.01 (br, 1 H) 5.97 (t, *J* = 3.5 Hz, 1 H) 5.35 (br, 1 H) 5.22 (br, 1 H) 4.68-4.66 (comp, 3 H) 4.40 (d, *J* = 9.5 Hz, 1 H) 4.37 (d, *J* = 9.0 Hz, 1 H) 4.29 (d, *J* = 9.5 Hz, 1 H) 4.05 (m, 1 H) 3.41 (dd, *J* = 6.0, 2.5 Hz, 1 H) 3.20 (dd, *J* = 19.0, 4.0 Hz, 1 H) 3.20 (m, 1 H) 3.09 (dd, *J* = 19.0, 3.0 Hz, 1 H) 2.20 (dm, *J* = 15.5 Hz, 1 H) 1.96-1.88 (comp, 2 H); ¹³C-NMR (125 MHz, CD₃CN, 70 °C) δ 211.6, 159.9, 159.7, 156.1, 137.8, 137.1, 134.9, 130.8, 130.7, 127.9, 123.6, 122.9, 122.6, 121.0, 118.9, 117.7, 116.5, 116.1, 112.4, 111.7, 73.8, 71.3, 67.0, 58.2, 50.4, 46.2, 46.2, 41.0, 29.0; HRMS (ESI) *m/z* observed 559.22140 [C₃₃H₃₂N₂O₅ (M+Na)⁺ requires 559.22030].



(1S/R, 5R/S)-Allyl 6,6-bis((4-chlorophenoxy)methyl)-12-oxo-3,4,5,6-tetrahydro-1H-1,5-ethanoazocino[4,3-b]indole-2(7H)-carboxylate. (4.119c).

(WLM8_132). A solution of TMS-OTf (72 mg, 0.324 mmol, 59 μL) in dry CH₂Cl₂ (0.4 mL) was added dropwise to a solution of **4.118c** (127 mg, 0.27 mmol), **3.10** (104 mg, 0.297 mmol), and 2,6-di(*tert*-butyl)-4-methylpyridine (111 mg, 0.54 mmol) in dry CH₂Cl₂ (1.0 mL) at −78 °C. The reaction was stirred for 3 h at −78 °C, whereupon a solution of TBAF•3H₂O (256 mg, 0.81 mmol) in CH₂Cl₂ (2.0 mL) was added dropwise. The bath was removed, and the reaction was stirred at room temperature for 1 h.

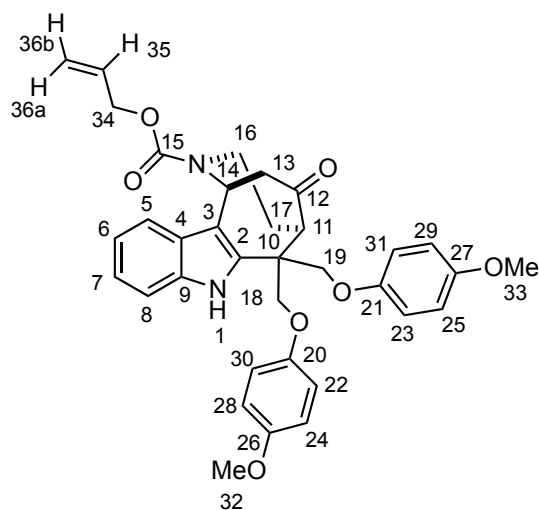
Saturated aq NaHCO₃ (2.0 mL) was added, and the layers were separated. The aqueous layer was extracted with CH₂Cl₂ (3 x 15 mL). The combined organic extracts were washed with brine (25 mL), dried (Na₂SO₄), filtered, and concentrated under reduced pressure. The resultant yellow oil was purified by flash chromatography eluting with Hexanes : EtOAc (10 : 1 → 4 : 1) containing 1% NEt₃ to afford 73 mg (44%) of **4.119c** as a yellow foam: ¹H-NMR (500 MHz, CD₃CN, 70 °C) δ 9.63 (br, 1 H) 7.54 (d, *J* = 7.5 Hz, 1 H) 7.45 (d, *J* = 8.5 Hz, 1 H) 7.31 (d, *J* = 9.5 Hz, 2 H) 7.22-7.17 (comp, 3 H) 7.11 (t, *J* = 7.5 Hz, 1 H) 7.05 (d, *J* = 9.0 Hz, 2 H) 6.83 (d, *J* = 9.0 Hz, 2 H) 6.02 (br, 1 H) 5.95 (app t, 1 H) 5.33 (br, 1 H) 5.22 (br, 1 H) 4.63 (br, 2 H) 4.62 (d, *J* = 9.5 Hz, 1 H) 4.37 (d, *J* = 10.0 Hz, 1 H) 4.26 (d, *J* = 9.5 Hz, 1 H) 4.26 (d, *J* = 9.5 Hz, 1 H) 4.03 (app d, *J* = 15.5 Hz, 1 H) 3.37 (dd, *J* = 5.5, 3.0 Hz, 1 H) 3.22-3.14 (m, 1 H) 3.18 (dd, *J* = 19.0, 4.0 Hz, 1 H) 3.05 (dd, *J* = 19.0, 3.0 Hz, 1 H) 2.17 (dm, *J* = 15.5 Hz, 1 H) 1.91-1.88 (m, 1 H); ¹³C-NMR (125 MHz, CD₃CN, 70 °C) δ 211.6, 158.6, 158.4, 156.1, 137.3, 137.1 134.9, 130.5, 130.5, 127.8, 127.4, 127.1, 123.7, 121.0, 118.9, 118.2, 117.7, 112.4, 111.8, 74.0, 71.5, 67.0, 58.0, 50.3, 46.1, 46.1, 41.0, 28.8; HRMS (ESI) *m/z* observed 627.10000 [C₃₃H₃₀Cl₂N₂O₅ (M+Na)⁺ requires 627.10000].



Allyl (1*S/R*, 5*R/S*)-6,6-bis((4-methoxyphenoxy)methyl)-12-oxo-1,3,4,5,6,7-hexahydro-2*H*-1,5-ethanoazocino[4,3-*b*]indole-2-carboxylate. (4.119d).

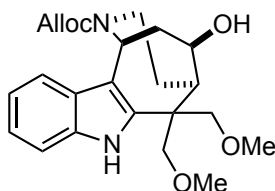
(WLM8_199). A solution of TMS-OTf (115 mg, 0.517 mmol, 94 μL) in dry CH₂Cl₂ (0.5 mL) was added dropwise to a solution of **3.10** (167 mg, 0.474 mmol), **4.118d** (199 mg, 0.431 mmol), and 2,6-di(*tert*-butyl)-4-methylpyridine (177 mg, 0.862 mmol) in dry

CH₂Cl₂ (2.2 mL) at -78 °C. The reaction was stirred for 3 h at -78 °C, whereupon a solution of TBAF•3H₂O (408 mg, 1.293 mmol) in CH₂Cl₂ (3.0 mL) was added dropwise. The bath was removed, and the reaction was stirred at room temperature for 1 h. Saturated aq NaHCO₃ (10 mL) was added, and the layers were separated. The aqueous layer was extracted with CH₂Cl₂ (3 x 20 mL). The combined organic extracts were washed with brine (25 mL), dried (Na₂SO₄), filtered, and concentrated under reduced pressure. The resultant yellow oil was purified by flash chromatography eluting with Hexanes : EtOAc (10 : 1 → 4 : 1 → 2 : 1) containing 1% NEt₃ to afford 178 mg (69 %) of **4.119d** as a yellow foam: ¹H-NMR (500 MHz, CD₃CN, 70 °C) δ 9.67 (br, 1 H), 7.54 (dd, *J* = 8.0, 1.0 Hz, 1 H), 7.45 (dt, *J* = 8.2, 1.0 Hz, 1 H), 7.17 (ddd, *J* = 8.2, 7.0, 1.2 Hz, 1 H), 7.11 (ddd, *J* = 8.0, 7.0, 1.1 Hz, 1 H), 7.02 (d, *J* = 9.2 Hz, 2 H), 6.88 (d, *J* = 9.2 Hz, 2 H), 6.78 (d, *J* = 0.6 Hz, 4 H), 6.02 (br, 1 H) 5.97 (t, *J* = 3.5 Hz, 1 H), 5.33 (d, *J* = 16.8 Hz, 1 H), 5.22 (d, *J* = 10.0 Hz, 1 H), 4.65 (br, 2 H), 4.59 (d, *J* = 9.5 Hz, 1 H), 4.32 (d, *J* = 9.6 Hz, 1 H), 4.29 (d, *J* = 9.3 Hz, 1 H), 4.21 (d, *J* = 9.3 Hz, 1 H), 4.03 (d, *J* = 14.6 Hz, 1 H), 3.74 (s, 3 H), 3.69 (s, 3 H), 3.37 (dd, *J* = 5.8, 2.7 Hz, 1 H), 3.19 (dd, *J* = 18.9, 4.3 Hz, 2 H), 3.07 (dd, *J* = 18.8, 3.2 Hz, 1 H), 2.18 (ddt, *J* = 15.7, 5.7, 2.8 Hz, 1 H), 1.89 (ddd, *J* = 15.8, 4.9, 2.6 Hz, 1 H). ¹³C-NMR (125 MHz, CD₃CN, 70 °C) δ 211.60, 156.14, 156.10, 155.90, 153.97, 153.84, 138.02, 137.04, 134.88, 127.84, 123.57, 120.97, 118.85, 117.70, 117.26, 116.17, 116.05, 112.38, 111.58, 74.64, 72.21, 67.02, 61.11, 58.14, 56.69, 56.62, 50.40, 46.22, 41.01, 28.96. HRMS (ESI) *m/z* observed 619.24180 [C₃₅H₃₆N₂O₇ (M+Na)⁺ requires 619.24150].



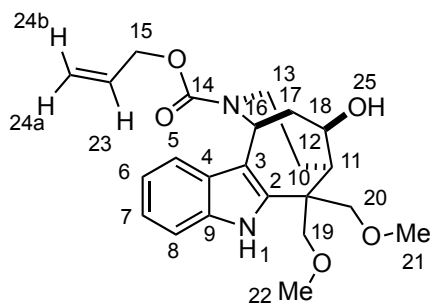
Assignment: ^1H -NMR (500 MHz, CD_3CN , 70 $^\circ\text{C}$) δ 9.67 (br, 1 H, N1-H), 7.54 (dd, $J = 8.0, 1.0$ Hz, 1 H, C5-H), 7.45 (dt, $J = 8.2, 1.0$ Hz, 1 H, C8-H), 7.17 (ddd, $J = 8.2, 7.0, 1.2$ Hz, 1 H, C7-H), 7.11 (ddd, $J = 8.0, 7.0, 1.1$ Hz, 1 H, C6-H), 7.02 (d, $J = 9.2$ Hz, 2 H, C22-H and C30-H or C23-H and C31-H), 6.88 (d, $J = 9.2$ Hz, 2 H, C22-H and C30-H or C23-H and C31-H), 6.78 (d, $J = 0.6$ Hz, 4 H, C24-H and C25-H and C28-H and C29-H), 6.02 (br, 1 H, C35-H) 5.97 (t, $J = 3.5$ Hz, 1 H, C14-H), 5.33 (d, $J = 16.8$ Hz, 1 H, C36-H), 5.22 (d, $J = 10.0$ Hz, 1 H, C36-H), 4.65 (br, 2 H, C34-H), 4.59 (d, $J = 9.5$ Hz, 1 H, C18-H or C19-H), 4.32 (d, $J = 9.6$ Hz, 1 H, C18-H or C19-H), 4.29 (d, $J = 9.3$ Hz, 1 H, C18-H or C19-H), 4.21 (d, $J = 9.3$ Hz, 1 H, C18-H or C19-H), 4.03 (d, $J = 14.6$ Hz, 1 H, C16), 3.74 (s, 3 H, C32-H₃ or C33-H₃), 3.69 (s, 3 H, C32-H₃ or C33-H₃), 3.37 (dd, $J = 5.8, 2.7$ Hz, 1 H, C11), 3.19 (dd, $J = 18.9, 4.3$ Hz, 2 H, C13-H and C16-H), 3.07 (dd, $J = 18.8, 3.2$ Hz, 1 H, C13-H), 2.18 (ddt, $J = 15.7, 5.7, 2.8$ Hz, 1 H, C17-H), 1.89 (ddd, $J = 15.8, 4.9, 2.6$ Hz, 1 H, C17-H). ^{13}C -NMR (125 MHz, CD_3CN , 70 $^\circ\text{C}$) δ 211.60 (C15), 156.14 (C20 or C21), 156.10 (C15), 155.90 (C20 or C21), 153.97 (C26 or C27), 153.84 (C26 or C27), 138.02 (C2 or C9), 137.04 (C2 or C9), 134.88 (C36), 127.84 (C4), 123.57 (C7), 120.97 (C6), 118.85 (C5), 117.70 (C30 and C22 or C31 and C23), 117.26 (C30 and C22 or C31 and C23), 116.17 (C24 and C28 or C25 and C29), 116.05 (C24 and C28 or

C25 and C29), 112.38 (C8), 111.58 (C3), 74.64 (C18 or C19), 72.21 (C18 or C19), 67.02 (C34), 61.11 (C10), 58.14 (C11), 56.69 (C32 or C33), 56.62 (C32 or C33), 50.40 (C13), 46.22 (C14), 41.01 (C16), 28.96 (C17).

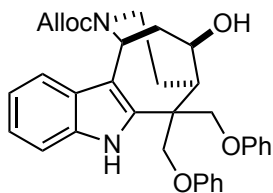


(1*S*/R, 5*R*/S, 12*R*/S)-Allyl 12-hydroxy-6,6-bis(methoxymethyl)-3,4,5,6-tetrahydro-1*H*-5,1-ethanoazocino[4,3-*b*]indole-2(7*H*)-carboxylate. (4.120a).

(WLM7_246_2). Lithium borohydride (29 mg, 1.31 mmol) was added to a solution of **4.119a** (108 mg, 0.262 mmol) in dry MeOH (1.3 mL) at 0 °C. After 14 h, saturated aq Rochelle's salt (1.0 mL) was added, and the reaction was stirred for 5 min. the reaction mixture was extracted with CH₂Cl₂ (3 x 5 mL), washed with brine (10 mL), dried (Na₂SO₄), filtered, and concentrated under reduced pressure. The resulting yellow oil was purified by flash chromatography eluting with Hexanes : EtOAc (1:1 to 100% EtOAc) to give 44 mg (40%) of **4.120a** as a white solid and 30 mg of recovered **4.119a**: ¹H-NMR (500 MHz, CD₃CN, 70 °C) δ 9.50 (br, 1 H) 7.39 (d, *J* = 8.5 Hz, 2 H) 7.11 (td, *J* = 7.0, 1.0 Hz, 1 H) 7.03 (td, *J* = 7.5, 0.5 Hz, 1 H) 6.03 (br, 1 H) 5.60 (d, *J* = 7.0 Hz, 1 H) 5.34 (br, 1 H) 5.23 (br, 1 H) 4.65 (br, 2 H) 4.26 (t, *J* = 9.0 Hz, 1 H) 3.89-3.81 (comp, 4 H) 3.54 (d, *J* = 9.0 Hz, 1 H) 3.45 (s, 3 H) 3.29 (s, 3 H) 3.00 (m, 1 H) 2.70 (m, 1 H) 2.50 (m, 1 H) 1.90-1.85 (comp, 2 H) 1.81-1.73 (m, 1 H); ¹³C-NMR (125 MHz, CD₃CN, 70 °C) δ 156.4, 141.1, 136.8, 135.3, 127.6, 122.7, 120.5, 117.4, 113.3, 112.2, 77.0, 76.4, 76.1, 66.6, 59.8, 59.4, 48.3, 48.2, 47.9, 41.6, 31.3; HRMS (ESI) *m/z* observed 437.20460 [C₂₃H₃₀N₂O₅ (M+Na)⁺ requires 437.20470].



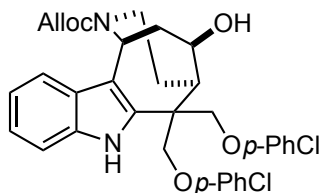
Assignments: $^1\text{H-NMR}$ (500 MHz, CD_3CN , 70 °C) δ 9.50 (br, 1 H, N1-H) 7.39 (d, J = 8.5 Hz, 2 H, C5-H and C8-H) 7.11 (td, J = 7.0, 1.0 Hz, 1 H, C7-H) 7.03 (td, J = 7.5, 0.5 Hz, 1 H, C6-H) 6.03 (br, 1 H, C23-H) 5.60 (d, J = 7.0 Hz, 1 H, C16-H) 5.34 (br, 1 H, C24a-H or C24b-H) 5.23 (br, 1 H, C24-H or C25-H) 4.65 (br, 2 H, C25-H₂) 4.26 (t, J = 9.0 Hz, 1 H, C18-H) 3.89-3.81 (comp, 4 H, C19-H, C20-H₂, and C13-H) 3.54 (d, J = 9.0 Hz, 1 H, C19-H) 3.45 (s, 3 H, C21-H₃ or C22-H₃) 3.29 (s, 3 H, C21-H₃ or C22-H₃) 3.00 (m, 1 H, C17-H) 2.70 (m, 1 H, C13-H) 2.50 (m, 1 H, C11-H) 1.90-1.85 (comp, 2 H, C12-H and C17-H) 1.81-1.73 (m, 1 H, C12-H); $^{13}\text{C-NMR}$ (125 MHz, CD_3CN , 70 °C) δ 156.4 (C14), 141.1, 136.8, 135.3, 127.6, 122.7 (C7), 120.5 (C6), 117.4, 113.3 (C3), 112.2 (C5 or C8), 77.0 (C19 or C20), 76.4 (C19 or C20), 76.1 (C18), 66.6 (C15), 59.8 (C21 or C22), 59.4 (C21 or C22), 48.3 (C16), 48.2 (C10), 47.9 (C11), 41.6 (C13), 31.3 (C12).



(1S/R, 5R/S, 12R/S)-Allyl 12-hydroxy-6,6-bis(phenoxymethyl)-3,4,5,6-tetrahydro-1H-5,1-ethanoazocino[4,3-*b*]indole-2(7H)-carboxylate. (4.120b).

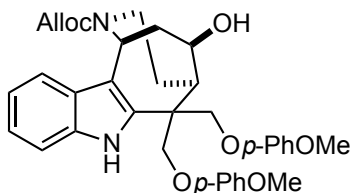
(WLM8_123). Lithium borohydride (24 mg, 1.07 mmol) was added to a solution of **4.119b** (287 mg, 0.535 mmol) in dry MeOH (5.4 mL) at 0 °C. After 12 h, saturated aq Rochelle's salt (5.0 mL) was added, and the reaction was stirred for 5 min. the reaction

mixture was extracted with CH₂Cl₂ (3 x 20 mL), washed with brine (25 mL), dried (Na₂SO₄), filtered, and concentrated under reduced pressure. The resulting yellow oil was purified by flash chromatography eluting with Hexanes : EtOAc (3:1 to 1:1) to give 108 mg (38%) of **4.120b** as a white solid and 158 mg (55%) of recovered **4.119b** as a white solid: ¹H-NMR (500 MHz, CD₃OD, 70° C) δ 9.57 (br, 1 H) 7.44 (d, *J* = 8.0 Hz, 1 H) 7.43 (d, *J* = 8.0 Hz, 1 H) 7.31- 7.28 (comp, 2 H) 7.24-7.20 (comp, 2 H) 7.14 (dt, *J* = 7.0, 1.0 Hz, 1 H) 7.08-7.04 (comp, 3 H) 6.97 (t, *J* = 7.0 Hz, 1 H) 6.94 (dd, *J* = 8.0, 1.0 Hz, 2 H) 6.89 (t, *J* = 7.0 Hz, 1 H) 6.04 (br, 1 H) 5.67 (d, *J* = 6.0 Hz, 1 H) 5.37 (br, 1 H) 5.23 (br, 1 H) 4.78 (d, *J* = 9.0 Hz, 1 H) 4.67 (br, 2 H) 4.65 (d, *J* = 8.5 Hz, 1 H) 4.55 (d, *J* = 8.5 Hz, 1 H) 4.45 (t, *J* = 8.0 Hz, 1 H) 4.34 (d, *J* = 8.5 Hz, 1 H) 3.88 (m, 1 H) 3.08 (m, 1 H) 3.01 (d, *J* = 1.0 Hz, 1 H) 2.91 (m, 1 H) 2.81 (m, 1 H) 2.00-1.84 (comp, 3 H). ¹³C-NMR (125 MHz, CD₃OD, 70 °C) δ 160.4, 160.2, 156.4, 139.5, 137.0, 135.2, 130.8, 130.6, 127.4, 123.0, 122.6, 122.2, 120.7, 118.5, 117.4, 116.5, 116.3, 114.0, 112.3, 75.9, 72.1, 71.4, 66.7, 48.4, 48.0, 47.6, 41.8, 31.2, 30.5. HRMS (ESI) *m/z* observed 561.23620 [C₃₃H₃₄N₂O₅ (M+Na)⁺ requires 561.23600].



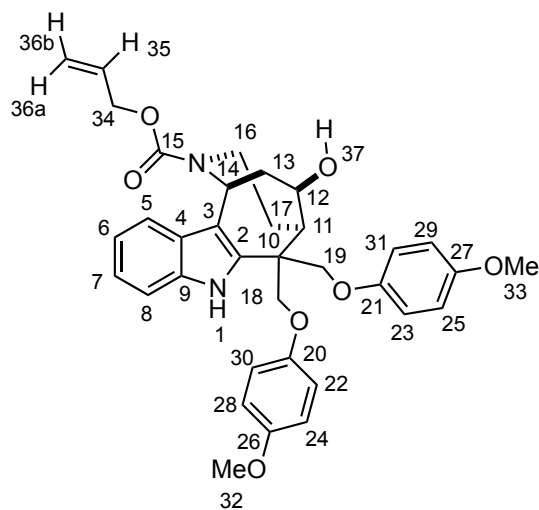
(1*S/R*, 5*R/S*, 12*R/S*)-Allyl 6,6-bis((4-chlorophenoxy)methyl)-12-hydroxy-3,4,5,6-tetrahydro-1*H*-5,1-ethanoazocino[4,3-*b*]indole-2(7*H*)-carboxylate. (4.120c). (WLM8_180). Lithium borohydride (10.2 mg, 0.469 mmol) was added to a solution of **4.119c** (71 mg, 0.117 mmol) in dry MeOH (2.4 mL) at 0 °C. After 12 h, saturated aq Rochelle's salt (3.0 mL) was added, and the reaction was stirred for 5 min. the reaction mixture was extracted with CH₂Cl₂ (3 x 15 mL), washed with brine (20 mL), dried

(Na₂SO₄), filtered, and concentrated under reduced pressure. The resulting yellow oil was purified by flash chromatography eluting with Hexanes : EtOAc (2 : 1 → 1:1) to give 55 mg (77%) of **4.120c** as a white solid: ¹H-NMR (500 MHz, (CD₃)₂SO, 70 °C) δ 10.88 (br, 1H), 7.42 (d, *J* = 8.7 Hz, 1H), 7.35 (d, *J* = 7.9 Hz, 1H), 7.31 (d, *J* = 9.0 Hz, 2H), 7.25 (d, *J* = 9.0 Hz, 2H), 7.12 – 7.07 (m, 1H), 7.07 (d, *J* = 9.0 Hz, 2H), 7.00 (td, *J* = 8.0, 0.9 Hz, 1H), 6.95 (d, *J* = 9.0 Hz, 2H), 6.22 (br, 1H), 5.56 (d, *J* = 6.5 Hz, 1H), 5.30 (br, 2H), 4.94 (d, *J* = 8.8 Hz, 2H), 4.62 (br, 2H), 4.53 (d, *J* = 9.6 Hz, 1H), 4.43 (dd, *J* = 9.7, 1.3 Hz, 1H), 4.35 (comp, 2H), 3.88 – 3.70 (m, 1H), 3.06 – 2.91 (m, 1H), 2.89 – 2.81 (m, 1H), 2.67 (d, *J* = 39.7 Hz, 1H), 1.84 (comp, 3H); ¹³C-NMR (125 MHz, (CD₃)₂SO, 70 °C) δ 157.4, 157.2, 135.1, 133.5, 128.9, 128.7, 125.4, 124.6, 124.1, 120.9, 118.7, 116.6, 116.4, 116.3, 111.4, 110.9, 73.2, 71.1, 68.9, 64.8, 46.3, 45.4. HRMS (ESI) *m/z* observed 629.15810 [C₃₃H₃₂Cl₂N₂O₅ (M+Na)⁺ requires 629.15800].



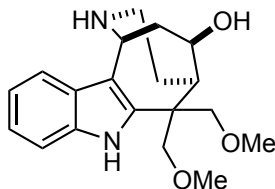
Allyl (1*S*/*R*, 5*R*/*S*)-12-hydroxy-6,6-bis((4-methoxyphenoxy)methyl)-1,3,4,5,6,7-hexahydro-2*H*-1,5-ethanoazocino[4,3-*b*]indole-2-carboxylate. (4.120d). (WLM8_200). Lithium borohydride (6.5 mg, 0.298 mmol) was added to a solution of **4.119d** (89 mg, 0.149 mmol) in dry MeOH (1.5 mL) at 0 °C. After 12 h, saturated aq Rochelle's salt (5 mL) was added, and the reaction was stirred for 5 min. the reaction mixture was extracted with CH₂Cl₂ (3 x 20 mL), washed with brine (25 mL), dried (Na₂SO₄), filtered, and concentrated under reduced pressure. The resulting yellow oil was purified by flash chromatography eluting with Hexanes : EtOAc (2 : 1 → 1 : 1) to give 70 mg (79 %) of **4.120d** as a white solid: ¹H-NMR (500 MHz, CD₃CN, 70 °C) δ 9.59 (br,

1H), 7.47 – 7.38 (m, 2H), 7.13 (td, $J = 7.4$, 1.2 Hz, 1H), 7.06 (td, $J = 7.3$, 0.9 Hz, 1H), 6.98 (d, $J = 9.2$ Hz, 2H), 6.89 – 6.82 (comp, 4H), 6.79 (d, $J = 9.2$ Hz, 2H), 6.04 (br, 1H), 5.67 (d, $J = 6.5$ Hz, 1H), 5.36 (br, 1H), 5.23 (br, 1H), 4.72 (d, $J = 9.3$ Hz, 1H), 4.67 (br, 2H), 4.58 (d, $J = 9.4$ Hz, 1H), 4.50 (d, $J = 9.4$ Hz, 1H), 4.43 (td, $J = 9.0$, 1.9 Hz, 1H), 4.26 (d, $J = 9.2$ Hz, 1H), 3.96 – 3.84 (m, 1H), 3.74 (s, 3H), 3.69 (s, 3H), 3.13 – 3.01 (m, 1H), 2.91 – 2.70 (comp, 2H), 2.04 – 1.96 (comp, 2H), 1.89 – 1.84 (m, 1H). ^{13}C -NMR (125 MHz, CD_3CN , 70 °C) δ 156.4, 155.9, 155.6, 154.5, 154.3, 139.7, 137.0, 135.2, 127.5, 123.0, 120.7, 118.5, 117.7, 117.4, 116.1, 116.0, 113.8, 112.2, 75.9, 73.0, 72.3, 66.7, 56.7, 56.6, 48.4, 48.1, 47.5, 41.8, 41.7, 31.2. HRMS (ESI) m/z observed 621.25690 [$\text{C}_{35}\text{H}_{38}\text{N}_2\text{O}_7$ ($\text{M}+\text{Na}$) $^+$ requires 621.25710].



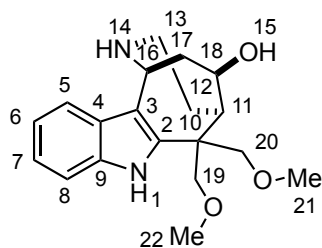
Assignments: ^1H -NMR (500 MHz, CD_3CN , 70 °C) δ 9.59 (br, 1H, N1-H), 7.47 – 7.38 (comp, 2H, C5-H and C8-H), 7.13 (td, $J = 7.4$, 1.2 Hz, 1H, C7-H) 7.06 (td, $J = 7.3$, 0.9 Hz, 1H, C6-H), 6.98 (d, $J = 9.2$ Hz, 2H, C22-H and C30-H or C23-H and C31-H), 6.89 – 6.82 (comp, 4H, C22-H, C23-H, C24-H, C25-H, C28-H, C29-H, C30-H, or C31-H), 6.79 (d, $J = 9.2$ Hz, 2H, C24-H and C28-H or C25-H and C29-H), 6.04 (br, 1H, C35-H), 5.67 (d, $J = 6.5$ Hz, 1H, C14-H), 5.36 (br, 1H, C36-H), 5.23 (br, 1H, C36-H), 4.72 (d,

$J = 9.3$ Hz, 1H, C18-H or C19-H), 4.67 (br, 2H, C34-H₂), 4.58 (d, $J = 9.4$ Hz, 1H, C18-H or C19-H), 4.50 (d, $J = 9.4$ Hz, 1H, C18-H or C19-H), 4.43 (td, $J = 9.0, 1.9$ Hz, 1H, C13-H), 4.26 (d, $J = 9.2$ Hz, 1H, C18-H or C19-H), 3.96 – 3.84 (m, 1H, C16-H), 3.74 (s, 3H, C32-H₃ or C33-H₃), 3.69 (s, 3H, C32-H₃ or C33-H₃), 3.13 – 3.01 (m, 1H, C13-H), 2.91 – 2.70 (comp, 2H, C11-H, C16-H), 2.04 – 1.96 (comp, 2H, C13-H and C17-H), 1.89 – 1.84 (m, 1H, C17-H). ¹³C-NMR (125 MHz, CD₃CN, 70 °C) δ 156.4 (C15), 155.9 (C20 or C21), 155.6 (C20 or C21), 154.5 (C26 or C27), 154.3 (C26 or C27), 139.7 (C35), 137.0 (C9), 135.2 (C2), 127.5 (C4), 123.0 (C7), 120.7 (C6), 118.5 (C5), 117.7 (C30 and C22 or C31 and C23), 117.4 (C30 and C22 or C31 and C23), 116.1 (C28 and C24 or C29 and C25), 116.0 (C28 and C24 or C29 and C25), 113.8 (C3), 112.2 (C8), 75.9 (C12), 73.0 (C18 or C19), 72.3 (C18 or C19), 66.7 (C34), 56.7 (C32 or C33), 56.6 (C32 or C33), 48.4 (C10), 48.1 (C14), 47.5 (C11), 41.8 (C13 or C16), 41.7 (C13 or C16), 31.2 (C17).



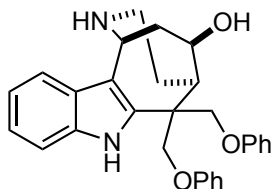
(1S/R, 5R/S, 12R/S)-6,6-bis(methoxymethyl)-2,3,4,5,6,7-hexahydro-1H-5,1-ethanoazocino[4,3-*b*]indol-12-ol. (4.121a). (WLM7_251_2). A round bottom flask charged with Pd₂(dba)₃ (1.0 mg, 0.00106 mmol) and 1,4-bis(diphenylphosphino)butane (0.9 mg, 0.00212 mmol) was placed under vacuum and backfilled with N₂ three times. A second round bottom flask was charged with **4.120a** (44 mg, 0.106 mmol) and 1,3-dimethylbarbituric acid (165 mg, 1.06 mmol) and placed under vacuum and backfilled with N₂ three times. THF (0.5 mL) was then added to both flasks, and the mixtures were stirred at room temperature under N₂ for 5 min. The Pd/ligand mixture was added via syringe to the flask containing **4.120a**, and stirring was continued at room temperature

until **4.120a** was gone by TLC. The reaction was quenched with saturated aq NaHCO₃ (0.3 mL) and stirred at room temperature for 15 min. The reaction mixture was diluted with H₂O (3.0 mL) extracted with CH₂Cl₂ (3 x 5 mL). The combined organic extracts were washed with brine (10 mL), dried (Na₂SO₄), filtered, and concentrated *in vacuo* to afford a brown oil. Subsequent purification by flash chromatography eluting with CH₂Cl₂/MeOH (100% CH₂Cl₂ to 95:5) containing 1% NEt₃ to provide 23 mg (66%) of **4.121a** as a white solid: ¹H-NMR (500 MHz, CD₃OD) δ 10.67 (br, 1 H) 7.53 (d, *J* = 8.0 Hz, 1 H) 7.39 (d, *J* = 8.0 Hz, 1 H) 7.13 (td, *J* = 8.0, 1.0 Hz, 1 H) 7.07 (td, *J* = 8.0, 1.0 Hz, 1 H) 5.21 (d, *J* = 5.0 Hz, 1 H) 4.42 (td, *J* = 9.0, 2.0 Hz, 1 H) 3.98 (d, *J* = 9.5 Hz, 1 H) 3.87 (d, *J* = 9.5 Hz, 1 H) 3.83 (d, *J* = 9.5 Hz, 1 H) 3.67 (d, *J* = 9.5 Hz, 1 H) 3.41 (s, 3 H) 3.30 (s, 3 H) 3.04-2.97 (comp, 2 H) 2.84 (td, *J* = 9.0, 4.0 Hz, 1 H) 2.72 (m, 1 H) 2.26 (dm, *J* = 15.0 Hz, 1 H) 2.16 (ddd, *J* = 15.0, 4.0, 1.0 Hz, 1 H) 1.92 (tm, 1 H); ¹³C-NMR (125 MHz, CD₃OD) δ 141.9, 137.1, 127.0, 123.1, 120.8, 117.9, 112.2, 106.8, 77.3, 76.4, 74.8, 59.4, 59.2, 49.8, 49.6, 46.9, 41.5, 40.4, 28.3; HRMS (ESI) *m/z* observed 353.18360 [C₁₉H₂₆N₂O₃ (M+Na)⁺ requires 353.18360].



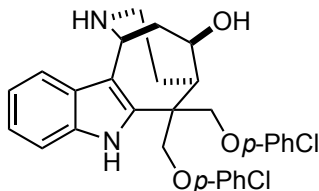
Assignments: ¹H-NMR (500 MHz, CD₃OD) δ 10.67 (br, 1 H, N1-H) 7.53 (d, *J* = 8.0 Hz, 1 H, C5-H) 7.39 (d, *J* = 8.0 Hz, 1 H, C8-H) 7.13 (td, *J* = 8.0, 1.0 Hz, 1 H, C7-H) 7.07 (td, *J* = 8.0, 1.0 Hz, 1 H, C6-H) 5.21 (d, *J* = 5.0 Hz, 1 H, C16-H) 4.42 (td, *J* = 9.0, 2.0 Hz, 1 H, C18-H) 3.98 (d, *J* = 9.5 Hz, 1 H, C19-H or C20-H) 3.87 (d, *J* = 9.5 Hz, 1 H, C19-H or C20-H) 3.83 (d, *J* = 9.5 Hz, 1 H, C19-H or C20-H) 3.67 (d, *J* = 9.5 Hz, 1 H,

C19-H or C20-H) 3.41 (s, 3 H, C21-H₃ or C22-H₃) 3.30 (s, 3 H, C22-H₃ or C22-H₃) 3.04-2.97 (comp, 2 H, C13-H and C17-H) 2.84 (td, *J* = 9.0, 4.0 Hz, 1 H, C13-H) 2.72 (m, 1 H, C11-H) 2.26 (dm, *J* = 15.0 Hz, 1 H, C12-H) 2.16 (ddd, *J* = 15.0, 4.0, 1.0 Hz, 1 H, C17-H) 1.92 (tm, 1 H, C12-H); ¹³C-NMR (125 MHz, CD₃OD) δ 141.9, 137.1, 127.0, 123.1 (C7), 120.8 (C6), 117.9 (C5), 112.2 (C8), 106.8 (C3), 77.3 (C19 or C20), 76.4 (C19 or C20), 74.8 (C18), 59.4 (C21 or C22), 59.2 (C21 or C22), 49.8 (C16), 49.6 (C10), 46.9 (C11), 41.5 (C13), 40.4 (C17), 28.3 (C12).



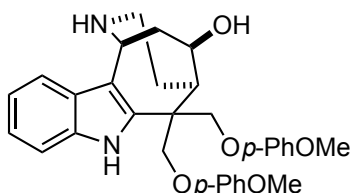
(1*S/R*, 5*R/S*, 12*R/S*)-6,6-Bis(phenoxymethyl)-2,3,4,5,6,7-hexahydro-1*H*-5,1-ethanoazocino[4,3-*b*]indol-12-ol. (4.121b). (WLM8_126). A round bottom flask charged with Pd₂(dba)₃ (2.7 mg, 0.00297 mmol) and 1,4-bis(diphenylphosphino)butane (2.5 mg, 0.00594 mmol) was placed under vacuum and backfilled with N₂ three times. A second round bottom flask was charged with **4.120b** (16 mg, 0.0297 mmol) and 1,3-dimethylbarbituric acid (46 mg, 0.297 mmol) and placed under vacuum and backfilled with N₂ three times. THF (0.3 mL) was then added to both flasks, and the mixtures were stirred at room temperature under N₂ for 5 min. The Pd/ligand mixture (30 μL) was added via syringe to the flask containing **4.120b**, and stirring was continued at room temperature until **4.120b** was gone by TLC. The reaction was quenched with saturated aq NaHCO₃ (0.5 mL) and stirred at room temperature for 15 min. The reaction mixture was diluted with H₂O (2.0 mL) extracted with CH₂Cl₂ (3 x 10 mL). The combined organic extracts were washed with brine (15 mL), dried (Na₂SO₄), filtered, and concentrated *in vacuo* to afford a brown oil. Subsequent purification by flash chromatography eluting

with CH₂Cl₂ : MeOH (96 : 4 → 90 : 10) containing 1% NEt₃ provided 11.5 mg (85%) of **4.121b** as a white solid: ¹H-NMR (500 MHz, CD₃OD) δ 7.56 (dt, *J* = 7.9, 1.0 Hz, 1H), 7.41 (dt, *J* = 8.1, 0.9 Hz, 1H), 7.27 (d, *J* = 7.1 Hz, 1H), 7.25 (d, *J* = 7.7 Hz, 1H), 7.19 (d, *J* = 7.1 Hz, 1H), 7.17 (d, *J* = 7.5 Hz, 1H), 7.12 (dd, *J* = 7.1, 1.2 Hz, 1H), 7.05 (td, *J* = 7.8, 0.9 Hz, 1H), 7.00 (comp, 2H), 6.96 – 6.91 (m, 3H), 6.91 – 6.80 (m, 1H), 5.00 (dd, *J* = 6.7, 1.4 Hz, 1H), 4.94 (d, *J* = 9.5 Hz, 1H), 4.63 (dd, *J* = 9.0, 2.2 Hz, 1H), 4.57 (comp, 2H), 4.35 (d, *J* = 9.4 Hz, 1H), 3.00 (comp, 2H), 2.84 (comp, 2H), 2.16 (comp, 2H), 1.99 – 1.88 (m, 1H); ¹³C-NMR (125 MHz, CD₃OD) δ 160.4, 160.2, 139.6, 137.3, 130.5, 130.3, 127.2, 122.8, 122.3, 122.0, 120.4, 118.3, 116.1, 116.0, 112.0, 110.5, 75.4, 72.9, 70.8, 48.8, 48.3, 47.2, 42.1, 41.9, 30.0; HRMS (ESI) *m/z* observed 477.21490 [C₂₉H₃₀N₂O₃ (M+Na)⁺ requires 477.21490].



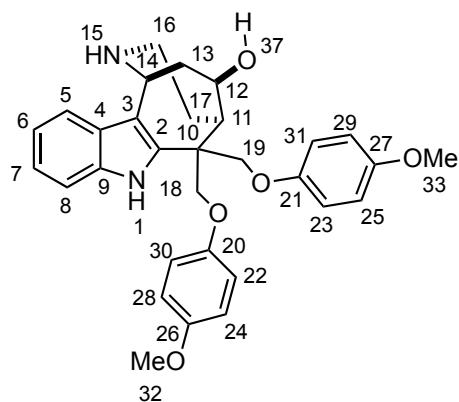
(1S/R, 5R/S, 12R/S)-6,6-Bis((4-chlorophenoxy)methyl)-2,3,4,5,6,7-hexahydro-1H-5,1-ethanoazocino[4,3-*b*]indol-12-ol. (4.121c). (WLM8_137). A 1 mL vial charged with Pd₂(dba)₃ (1.8 mg, 0.00198 mmol) and 1,4-bis(diphenylphosphino)butane (1.7 mg, 0.00396 mmol) was placed under vacuum and backfilled with N₂ three times. A second round bottom flask was charged with **4.120c** (12 mg, 0.0198 mmol) and 1,3-dimethylbarbituric acid (31 mg, 0.198 mmol) and placed under vacuum and backfilled with N₂ three times. THF (0.2 mL) was then added to both flasks, and the mixtures were stirred at room temperature under N₂ for 5 min. An aliquot of the Pd/ligand mixture (20 μL) was added via syringe to the flask containing **4.120c**, and stirring was continued at room temperature until **4.120c** was gone by TLC. The reaction was quenched with

saturated aq NaHCO₃ (0.2 mL) and stirred at room temperature for 15 min. The reaction mixture was diluted with H₂O (1.0 mL) extracted with CH₂Cl₂ (3 x 10 mL). The combined organic extracts were washed with brine (10 mL), dried (Na₂SO₄), filtered, and concentrated *in vacuo* to afford a brown oil. Subsequent purification by flash chromatography eluting with CH₂Cl₂ : MeOH (95 : 5) containing 1% NEt₃ provided 6 mg (58%) of **4.121c** as a white solid: ¹H-NMR (500 MHz, CD₃OD) δ 7.59 (d, *J* = 8.0 Hz, 1 H) 7.42 (d, *J* = 8.0 Hz, 1 H) 7.25 (d, *J* = 9.0 Hz, 2 H) 7.19-7.15 (comp, 3 H) 7.11 (td, *J* = 7.5 Hz, 1 H) 6.97 (d, *J* = 9.0 Hz, 2 H) 6.90 (d, *J* = 9.0 Hz, 2 H) 5.31 (d, *J* = 5.5 Hz, 1 H) 4.87 (d, *J* = 10.0 Hz, 1 H) 4.57-4.52 (comp, 3 H) 4.46 (d, *J* = 9.5 Hz, 1 H) 3.11-3.04 (comp, 3 H) 2.97 (td, *J* = 13.5, 4.0 Hz, 1 H) 2.31 (dm, *J* = 16.0 Hz, 1 H) 2.27 (dd, *J* = 15.0, 10.0 Hz, 1 H) 2.04 (tm, *J* = 17.0 Hz, 1 H); ¹³C-NMR (125 MHz, CD₃OD) δ 158.9, 158.7, 140.1, 137.4, 130.5, 130.2, 127.4, 127.0, 127.0, 123.5, 121.0, 118.2, 117.5, 117.5, 112.3, 107.6, 74.6, 73.1, 71.6, 49.8, 49.6, 47.0, 41.6, 40.3, 28.1; HRMS (ESI) *m/z* observed 545.13820 [C₂₉H₂₈Cl₂N₂O₃ (M+Na)⁺ requires 545.13690].

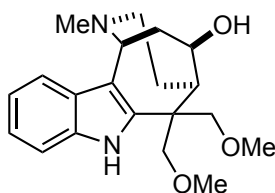


(1*S/R*, 5*R/S*)-6,6-Bis((4-methoxyphenoxy)methyl)-2,3,4,5,6,7-hexahydro-1*H*-1,5-ethanoazocino[4,3-*b*]indol-12-ol. (4.121d). (WLM9_80). A round bottom flask charged with Pd₂(dba)₃ (3.4 mg, 0.00367 mmol) and 1,4-bis(diphenylphosphino)butane (3.1 mg, 0.00734 mmol) was placed under vacuum and backfilled with N₂ three times. A second round bottom flask was charged with **4.120d** (22 mg, 0.367 mmol) and 1,3-dimethylbarbituric acid (57 mg, 0.367 mmol) and placed under vacuum and backfilled with N₂ three times. THF (0.3 mL) was then added to both flasks, and the mixtures were

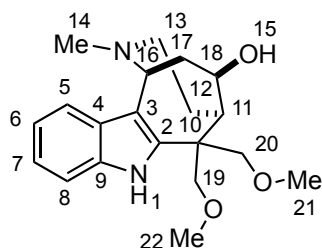
stirred at room temperature under N₂ for 5 min. A 30 μ L aliquot of the Pd/ligand mixture was added via syringe to the flask containing **4.120d**, and stirring was continued at room temperature until **4.120d** was gone by TLC. The reaction was quenched with saturated aq NaHCO₃ (5 mL) and stirred at room temperature for 15 min. The reaction mixture was diluted with H₂O (5 mL) and extracted with CH₂Cl₂ (3 x 10 mL). The combined organic extracts were washed with brine (10 mL), dried (Na₂SO₄), filtered, and concentrated *in vacuo* to afford a brown oil. Subsequent purification by flash chromatography eluting with CH₂Cl₂ : MeOH (95 : 5 \rightarrow 90 : 10) containing 1% NEt₃ followed by RP HPLC H₂O : MeCN (75 : 25 \rightarrow 90 : 10 over 30 min) provided 11.5 mg (61%) of **4.121d** as a white solid. ¹H-NMR (500 MHz, CD₃OD) δ 7.58 (d, *J* = 7.9 Hz, 1H), 7.43 (dt, *J* = 8.1, 0.9 Hz, 1H), 7.14 (td, *J* = 7.7, 1.0 Hz, 1H), 7.08 (td, *J* = 7.4, 1.1 Hz, 1H), 6.96 (d, *J* = 9.0 Hz, 2H), 6.88 (d, *J* = 9.1 Hz, 2H), 6.85 (d, *J* = 9.0 Hz, 2H), 6.77 (d, *J* = 9.1 Hz, 2H), 5.06 (d, *J* = 6.3 Hz, 1H), 4.90 (d, *J* = 9.7 Hz, 1H), 4.66 – 4.58 (m, 1H), 4.52 (app s, 2H), 4.30 (d, *J* = 9.4 Hz, 1H), 3.75 (s, 3H), 3.71 (s, 3H), 3.07 – 2.96 (comp, 2H), 2.96 – 2.78 (comp, 2H), 2.28 – 2.15 (comp, 2H), 2.01 – 1.92 (m, 1H). ¹³C-NMR (125 MHz, CD₃OD) δ 154.3, 154.1, 153.1, 152.9, 138.4, 135.8, 125.7, 121.4, 118.9, 116.8, 115.8, 115.6, 114.2, 114.0, 110.6, 73.8, 72.4, 70.2, 54.6, 54.5, 48.1, 45.9, 45.5, 40.3, 40.3, 28.2. HRMS (ESI) *m/z* observed 537.23570 [C₃₁H₃₄N₂O₅ (M⁺ Na)⁺ requires 537.23600].



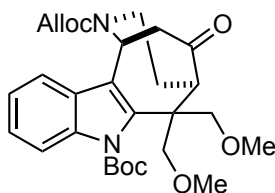
Assignments: ^1H -NMR (500 MHz, CD_3OD) δ 7.58 (d, $J = 7.9$ Hz, 1H, C5-H), 7.43 (dt, $J = 8.1, 0.9$ Hz, 1H, C8-H), 7.14 (td, $J = 7.7, 1.0$ Hz, 1H, C7-H), 7.08 (td, $J = 7.4, 1.1$ Hz, 1H, C6-H), 6.96 (d, $J = 9.0$ Hz, 2H, C22-H and C30-H or C23-H and C31-H), 6.88 (d, $J = 9.1$ Hz, 2H, C22-H and C30-H or C23-H and C31-H), 6.85 (d, $J = 9.0$ Hz, 2H, C24-H and C28-H or C25-H and C29-H), 6.77 (d, $J = 9.1$ Hz, 2H, C24-H and C28-H or C25-H and C29-H), 5.06 (d, $J = 6.3$ Hz, 1H, C14-H), 4.90 (d, $J = 9.7$ Hz, 1H, C18-H or C19-H), 4.63 (td, $J = 9.0, 1.8$ Hz, 1H, C12-H), 4.52 (app s, 2H, C18-H and C19-H), 4.30 (d, $J = 9.4$ Hz, 1H, C18-H or C19-H), 3.75 (s, 3H, C32-H₃ or C33-H₃), 3.71 (s, 3H, C32-H₃ or C33-H₃), 3.07 – 2.96 (comp, 2H, C11-H and C13-H), 2.96 – 2.78 (comp, 2H, C16-H₂), 2.28 – 2.15 (comp, 2H, C13-H and C17-H), 2.01 – 1.92 (m, 1H, C17-H). ^{13}C -NMR (125 MHz, CD_3OD) δ 154.3 (C20 or C21), 154.1 (C20 or C21), 153.1 (C26 or C27), 152.9 (C26 or C27), 138.4 (C9), 135.8 (C2), 125.7 (C4), 121.4 (C7), 118.9 (C6), 116.8 (C5), 115.8 (C22 and C30 or C23 and C31), 115.6 (C22 and C30 or C23 and C31), 114.2 (C24 and C28 or C25 and C29), 114.0 (C24 and C28 or C25 and C29), 110.6 (C8), 108.4 (C3), 73.8 (C12), 72.4 (C18 or C19), 70.2 (C18 or C19), 54.6 (C32 or C33), 54.5 (C32 or C33), 48.1 (C14), 45.9 (C10), 45.5 (C11), 40.3 (C13 or C16), 40.3 (C13 or C16), 28.2 (C17).



(1S/R, 5R/S, 12R/S)-6,6-Bis(methoxymethyl)-2-methyl-2,3,4,5,6,7-hexahydro-1H-5,1-ethanoazocino[4,3-b]indol-12-ol. (4.122a). (WLM7_265_2). A mixture of **4.121a** (4.0 mg, 0.012 mmol) and 37% aq formaldehyde solution (3.6 mg, 0.12 mmol, 10 μ L) in CH_2Cl_2 (0.3 mL) was stirred for 5 min at room temperature whereupon sodium triacetoxyborohydride (10 mg, 0.048 mmol) was added in one portion. Stirring was continued for 14 h at room temperature. The reaction was quenched with saturated aq Rochelle's salt (0.5 mL) and extracted with CH_2Cl_2 (3 x 2 mL). The combined organic extracts were washed with brine (3 mL), dried (Na_2SO_4), filtered, and concentrated *in vacuo* to afford a brown oil. Subsequent purification by RP HPLC $\text{H}_2\text{O}/\text{MeCN}$ (90 : 10 to 5 : 95 over 30 min) afforded 4.0 mg (95%) of **4.122a** as a white solid. ^1H -NMR (500 MHz, CD_3OD) δ 10.82 (br, 1 H) 7.55 (d, J = 8.0 Hz, 1 H) 7.42 (d, J = 8.0 Hz, 1 H) 7.15 (td, J = 7.0, 1.0 Hz, 1 H) 7.11 (td, J = 7.0, 1.0 Hz, 1 H) 5.12 (d, J = 5.0 Hz, 1 H) 4.37 (td, J = 9.5, 3.0 Hz, 1 H) 3.96 (d, J = 9.0 Hz, 1 H) 3.88 (d, J = 9.0 Hz, 1 H) 3.84 (d, J = 9.0 Hz, 1 H) 3.70 (d, J = 9.0 Hz, 1 H) 3.40 (s, 3 H) 3.30 (s, 3 H) 3.12-3.05 (comp, 2 H) 2.95 (td, J = 13.5, 4.0 Hz, 1 H) 2.86 (s, 3 H) 2.70 (m, 1 H) 2.28 (dm, 16.0 Hz, 1 H) 2.15 (ddd, J = 15.0, 8.0, 2.0 Hz, 1 H) 1.96 (tm, 1 H); ^{13}C -NMR (125 MHz, CD_3OD) δ 142.6, 137.1, 128.4, 123.2, 121.4, 117.8, 112.5, 104.5, 77.4, 76.6, 74.6, 60.6, 59.4, 59.2, 52.6, 49.7, 46.3, 45.8, 40.1, 28.7; HRMS (ESI) m/z observed 345.21710 [$\text{C}_{20}\text{H}_{28}\text{N}_2\text{O}_3$ ($\text{M}+\text{H}$) $^+$ requires 345.21730].



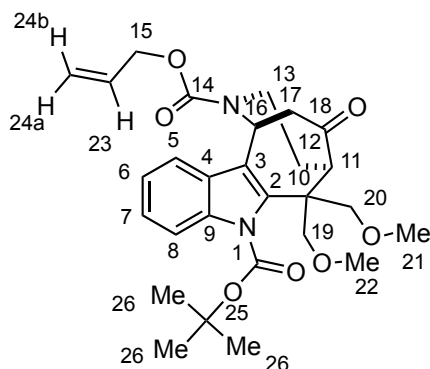
Assignments: ^1H -NMR (500 MHz, CD_3OD) δ 10.82 (br, 1 H, N1-H) 7.55 (d, J = 8.0 Hz, 1 H, C5-H) 7.42 (d, J = 8.0 Hz, 1 H, C8-H) 7.15 (td, J = 7.0, 1.0 Hz, 1 H, C7-H) 7.11 (td, J = 7.0, 1.0 Hz, 1 H, C6-H) 5.12 (d, J = 5.0 Hz, 1 H, C16-H) 4.37 (td, J = 9.5, 3.0 Hz, 1 H, C18-H) 3.96 (d, J = 9.0 Hz, 1 H, C19-H or C20-H) 3.88 (d, J = 9.0 Hz, 1 H, C19-H or C20-H) 3.84 (d, J = 9.0 Hz, 1 H, C19-H or C20-H) 3.70 (d, J = 9.0 Hz, 1 H, C19-H or C20-H) 3.40 (s, 3 H, C21-H₃ or C22-H₃) 3.30 (s, 3 H, C21-H₃ or C22-H₃) 3.12-3.05 (comp, 2 H, C13-H and C17-H) 2.95 (td, J = 13.5, 4.0 Hz, 1 H, C13-H) 2.86 (s, 3 H, C14-H₃) 2.70 (m, 1 H, C11-H) 2.28 (dm, 16.0 Hz, 1 H, C12-H) 2.15 (ddd, J = 15.0, 8.0, 2.0 Hz, 1 H, C17-H) 1.96 (tm, 1 H, C12-H); ^{13}C -NMR (125 MHz, CD_3OD) δ 142.6, 137.1, 128.4, 123.2 (C7), 121.4 (C6), 117.8 (C5), 112.5 (C8), 104.5 (C3), 77.4 (C19 or C20), 76.6 (C19 or C20), 74.6 (C18), 60.6 (C16), 59.4 (C21 or C22), 59.2 (C21 or C22), 52.6 (C13), 49.7 (C10), 46.3 (C11), 45.8 (C14), 40.1 (C17), 28.7 (C12).



(1*S*/R, 5*R*/S)-2-Allyl 7-*tert*-butyl 6,6-bis(methoxymethyl)-12-oxo-3,4,5,6-tetrahydro-1*H*-1,5-ethanoazocino[4,3-*b*]indole-2,7-dicarboxylate. (4.123a).

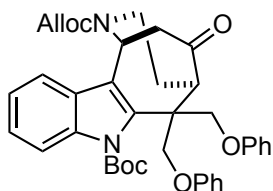
(WLM7_259_2). 4-dimethylaminopyridine (136 mg, 1.12 mmol) was added to a solution of **4.119a** (307 mg, 0.744 mmol) in a mixture of di-*tert*-butyl dicarbonate (1.5 ml) and toluene (2.5 mL), and the reaction was stirred for 3 h at room temperature. The reaction

was partitioned between H₂O (25.0 mL) and Et₂O (25.0 mL). The layers were separated, and the organic layer was extracted with Et₂O (2 x 25 mL). The combined organic extracts were washed with brine (40 mL), dried (Na₂SO₄), and concentrated under reduced pressure. The resulting yellow oil was purified by flash chromatography eluting with Hexanes : EtOAc (10 : 1 → 4 : 1 → 100% EtOAc) containing 1% NEt₃ to give 232 mg (63%) of **4.123a** as a yellow foam and 94 mg (31%) of unreacted starting material **4.119a**: ¹H-NMR (500 MHz, CD₃CN, 70 °C) δ 7.84 (dd, *J* = 9.0, 1.0 Hz, 1 H) 7.53 (d, *J* = 8.0 Hz, 1 H) 7.38 (td, *J* = 7.5, 1.0 Hz, 1 H) 7.29 (td, *J* = 7.5, 1.0 Hz, 1 H) 6.15 (br, 1 H) 5.89 (br, 1 H) 5.27 (br, 2 H) 4.69 (br, 2 H) 4.42 (d, *J* = 9.0 Hz, 1 H) 4.00 (d, *J* = 9.5 Hz, 1 H) 3.95-3.92 (m, 1 H) 3.60 (d, *J* = 9.5 Hz, 1 H) 3.60 (d, *J* = 9.5 Hz, 1 H) 3.32 (s, 3 H) 3.17 (s, 3 H) 3.16-3.11 (comp, 2 H) 3.03 (dd, *J* = 13.5, 4.5 Hz, 1 H) 2.88 (m, 1 H) 2.18 (dm, *J* = 15.0 Hz, 1 H) 1.83-1.76 (m, 1 H) 1.79 (s, 9 H); ¹³C-NMR (125 MHz, CD₃CN, 70 °C) δ 211.4, 156.0, 152.8, 139.0, 137.7, 134.8, 128.7, 125.9, 123.5, 120.1, 119.1, 115.1, 109.6, 86.6, 84.2, 78.7, 76.7, 67.0, 64.7, 59.5, 58.9, 49.9, 49.0, 46.5, 43.7, 41.1, 30.0, 28.7; HRMS (ESI) *m/z* observed 535.24110 [C₂₀H₂₈N₂O₃ (M+Na)⁺ requires 535.24150].



Assignments: ¹H-NMR (500 MHz, CD₃CN, 70 °C) δ 7.84 (dd, *J* = 9.0, 1.0 Hz, 1 H, C8-H) 7.53 (d, *J* = 8.0 Hz, 1 H, C5-H) 7.38 (td, *J* = 7.5, 1.0 Hz, 1 H, C7-H) 7.29 (td, *J* = 7.5, 1.0 Hz, 1 H, C6-H) 6.15 (br, 1 H, C23-H) 5.89 (br, 1 H, C16-H) 5.27 (br, 2 H,

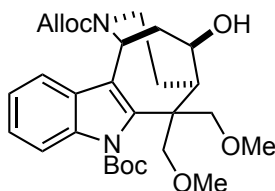
C24_a-H and C24_b-H) 4.69 (br, 2 H, C15-H₂) 4.42 (d, $J = 9.0$ Hz, 1 H, C19-H or C20-H) 4.00 (d, $J = 9.5$ Hz, 1 H, C19-H or C20-H) 3.95-3.92 (m, 1 H, C13-H) 3.60 (d, $J = 9.5$ Hz, 1 H, C19-H or C20-H) 3.60 (d, $J = 9.5$ Hz, 1 H, C19-H or C20-H) 3.32 (s, 3 H, C21-H₃ or C22-H₃) 3.17 (s, 3 H, C21-H₃ or C22-H₃) 3.16-3.11 (comp, 2 H, C11-H and C17-H) 3.03 (dd, $J = 13.5, 4.5$ Hz, 1 H, C17-H) 2.88 (m, 1 H, C13-H) 2.18 (dm, $J = 15.0$ Hz, 1 H, C12-H) 1.83-1.76 (m, 1 H, C12-H) 1.79 (s, 9 H, C26-H₃); ¹³C-NMR (125 MHz, CD₃CN, 70 °C) δ 211.4 (C18), 156.0 (C14), 152.8 (C1), 139.0, 137.7, 134.8, 128.7, 125.9 (C7), 123.5 (C6), 120.1, 119.1 (C5), 115.1 (C8), 109.6 (C3), 86.6 (C25), 78.7 (C19 or C20), 76.7 (C19 or C20), 67.0 (C15), 64.7 (C11), 59.5 (C21 or C22), 58.9 (C21 or C22), 49.9 (C13), 46.5 (C16), 43.7 (C10), 41.1 (C13), 30.0 (C12), 28.7 (C26).



(1S/R, 5R/S)-2-allyl 7-tert-butyl 12-oxo-6,6-bis(phenoxy)methyl-3,4,5,6-tetrahydro-1H-1,5-ethanoazocino[4,3-b]indole-2,7-dicarboxylate. (4.123b).

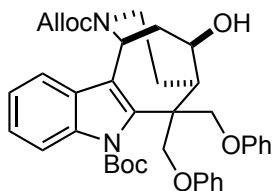
(WLM8_120). 4-dimethylaminopyridine (54 mg, 0.442 mmol) was added to a solution of **4.119b** (158 mg, 0.294 mmol) in a mixture of di-*tert*-butyl dicarbonate (0.6 mL) and toluene (0.4 mL), and the reaction was stirred for 5 h at room temperature. The reaction was partitioned between H₂O (10 mL) and Et₂O (25 mL). The layers were separated, and the organic layer was extracted with Et₂O (2 x 25 mL). The combined organic extracts were washed with brine (25 mL), dried (Na₂SO₄), and concentrated under reduced pressure. The resulting yellow oil was purified by flash chromatography eluting with Hexanes : EtOAc (4 : 1) to give 75 mg (40%) of **4.123b** as a yellow foam and 73 mg (46%) of recovered starting material: ¹H-NMR (500 MHz, CD₃CN, 70 °C) δ 7.82 (d, $J =$

8.0 Hz, 1 H) 7.57 (d, $J = 7.5$ Hz, 1 H) 7.37 (td, $J = 7.0, 1.5$ Hz, 1 H) 7.31-7.22 (comp, 5 H) 6.99-6.92 (comp, 2 H) 6.87-6.81 (comp, 4 H) 5.99 (comp, 2 H) 5.43-5.20 (comp, 2 H) 4.95 (d, $J = 9.0$ Hz, 1 H) 4.74 (d, $J = 10.0$ Hz, 1 H) 4.65 (comp, 2 H) 4.51 (d, $J = 9.0$ Hz, 1 H) 4.38 (d, $J = 10.0$ Hz, 1 H) 3.97 (d, $J = 13.0$ Hz, 1 H) 3.44 (dd, $J = 6.0, 3.0$ Hz, 1 H) 2.95 (dd, $J = 18.5, 2.0$ Hz, 1 H) 3.13 (dd, $J = 18.5, 5.0$ Hz, 1 H) 3.09 (m, 1 H) 2.16 (dm, $J = 15.5$ Hz, 1 H) 1.84 (tm, $J = 14.0$ Hz, 1 H) 1.45 (s, 9 H); ^{13}C -NMR (500 MHz, CD_3CN , 70 °C) δ 211.3, 159.6, 159.5, 156.1, 152.9, 137.8, 137.8, 134.8, 130.7, 130.7, 128.8, 126.4, 123.8, 122.7, 122.6, 121.2, 119.4, 116.0, 115.9, 115.6, 86.8, 74.2, 72.7, 67.1, 65.1, 49.4, 48.5, 46.5, 41.2, 30.1, 28.4; HRMS (ESI) m/z observed 659.27270 [$\text{C}_{38}\text{H}_{40}\text{N}_2\text{O}_7$ ($\text{M}+\text{Na}$) $^+$ requires 659.27280].



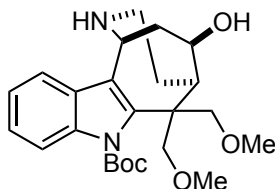
(1*S/R*, 5*R/S*, 12*R/S*)-2-allyl 7-*tert*-butyl 12-hydroxy-6,6-bis(methoxymethyl)-3,4,5,6-tetrahydro-1*H*-5,1-ethanoazocino[4,3-*b*]indole-2,7-dicarboxylate. (4.124a).
(WLM7_289_2). Lithium aluminum hydride (7.3 mg, 0.191 mmol) was added to a solution of **4.123a** (24.5 mg, 0.0478 mmol) in dry THF (0.5 mL) and the reaction was stirred for 2 h at 0 °C until starting material was consumed by TLC. Excess lithium aluminum hydride was quenched with saturated aq Rochelle's Salt (0.3 ml) and stirred for 15 min. The reaction mixture was extracted with CH_2Cl_2 (3 x 10 mL), and the combined organic extracts were washed with brine (20 mL), dried (Na_2SO_4), and concentrated under reduced pressure. The resulting yellow oil was purified by flash chromatography eluting with CH_2Cl_2 : MeOH (100% $\text{CH}_2\text{Cl}_2 \rightarrow 96 : 3$) to give 14 mg (57%) of **4.123a** as a white solid: ^1H -NMR (500 MHz, CD_3CN , 70 °C) δ 7.75 (d, $J = 8.0$

Hz, 1 H) 7.37 (d, $J = 8.0$ Hz, 1 H) 7.29 (td, $J = 8.0, 1.0$ Hz, 1 H) 7.19 (td, $J = 7.5, 0.5$ Hz, 1 H) 6.02 (br, 1 H) 5.60 (br, 1 H) 5.36 (br, 1 H) 5.25 (br, 1 H) 4.67 (br, 2 H) 4.27 (s, 2 H) 4.22 (m, 1 H) 4.06 (d, $J = 12.0$ Hz, 1 H) 3.81 (br, 1 H) 3.60 (d, $J = 7.0$ Hz, 1 H) 4.47 (d, $J = 10.0$ Hz, 1 H) 3.30 (s, 3 H) 3.23 (s, 3 H) 2.92 (m, 1 H) 2.72 (m, 1 H) 2.50 (br, 1 H) 1.97 (comp, 2 H) 1.84-1.76 (m, 1 H) 1.73 (s, 9 H); ^{13}C -NMR (125 MHz, CD_3CN) δ 156.3, 152.8, 137.4, 135.1, 128.5, 125.6, 123.3, 122.7, 122.6, 118.3, 115.0, 86.1, 80.2, 77.5, 75.8, 59.3, 59.1, 54.5, 50.7, 42.0, 28.7; HRMS (ESI) m/z observed 537.25690 [$\text{C}_{28}\text{H}_{38}\text{N}_2\text{O}_7$ ($\text{M}+\text{Na}$) $^+$ requires 537.25710].



(1*S/R*, 5*R/S*, 12*R/S*)-2-Allyl 7-*tert*-butyl 12-hydroxy-6,6-bis(phenoxyethyl)-3,4,5,6-tetrahydro-1*H*-5,1-ethanoazocino[4,3-*b*]indole-2,7-dicarboxylate. (4.124b). (WLM8_124). Lithium aluminum hydride (132 μL of a 1M solution in THF, 0.132 mmol) was added to a solution of **4.123b** (42 mg, 0.066 mmol) in dry THF (0.65 mL) and the reaction was stirred for 2 h at 0 $^\circ\text{C}$ until starting material was consumed by TLC. Excess lithium aluminum hydride was quenched with saturated aq Rochelle's Salt (1.0 ml) and stirred for 15 min. The reaction mixture was extracted with CH_2Cl_2 (3 x 10 mL), and the combined organic extracts were washed with brine (20 mL), dried (Na_2SO_4), and concentrated under reduced pressure. The resulting yellow oil was purified by flash chromatography eluting with Hexanes : EtOAc (4 : 1 \rightarrow 2 : 1) to give 26 mg (62%) of **4.124b** as a yellow foam: ^1H -NMR (500 MHz, $(\text{CD}_3)_2\text{SO}$, 70 $^\circ\text{C}$) δ 7.75 (dt, $J = 8.4, 0.8$ Hz, 1H), 7.43 (d, $J = 7.4$ Hz, 1H), 7.35 (ddd, $J = 8.4, 7.1, 1.3$ Hz, 1H), 7.27 (comp, 5H), 6.95 (comp, 4H), 6.74 (d, $J = 8.5$ Hz, 2H), 5.99 (br, 1H), 5.66 (d, $J = 6.2$ Hz, 1H), 5.51 –

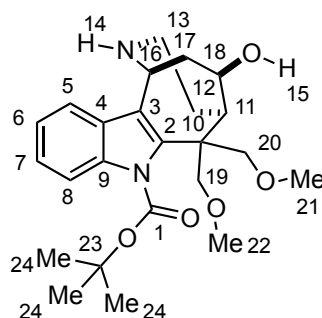
5.18 (m, 2H), 5.15 (d, $J = 8.1$ Hz, 1H), 4.90 (comp, 2H), 4.66 (comp, $J = 3.7$ Hz, 2H), 4.25 (comp, 2H), 3.82 (d, $J = 14.2$ Hz, 1H), 3.10 – 3.04 (m, 1H), 2.99 – 2.84 (m, 1H), 2.82 – 2.62 (m, 1H), 2.14 – 1.97 (m, 1H), 1.95 – 1.85 (m, 1H), 1.85 – 1.73 (m, 1H), 1.33 (s, 9H); ^{13}C -NMR (125 MHz, CD_3CN , 70 °C) δ 159.3, 158.5, 155.4, 151.8, 137.8 136.8, 134.1, 129.6, 129.6, 127.5, 124.9, 122.4, 122.4, 121.2, 121.0, 118.1, 115.2, 114.9, 114.4, 85.143, 75.3, 74.7, 71.1, 65.8, 53.1, 49.4, 47.5, 41.1, 29.5, 27.3; HRMS (ESI) m/z observed 661.28840 [$\text{C}_{38}\text{H}_{42}\text{N}_2\text{O}_7$ ($\text{M}+\text{Na}$) $^+$ requires 661.28840].



(1S/R, 5R/S, 12R/S)-tert-Butyl 12-hydroxy-6,6-bis(methoxymethyl)-3,4,5,6-tetrahydro-1H-5,1-ethanoazocino[4,3-b]indole-7(2H)-carboxylate. (4.125a).

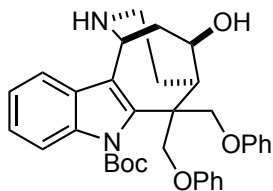
(WLM7_290_2). A round bottom flask charged with $\text{Pd}_2(\text{dba})_3$ (0.5 mg, 0.000534 mmol) and 1,4-bis(diphenylphosphino)butane (0.5 mg, 0.00107 mmol) was placed under vacuum and backfilled with N_2 three times. A second round bottom flask was charged with **4.124a** (5.5 mg, 0.0107 mmol) and 1,3-dimethylbarbituric acid (17 mg, 0.107 mmol) and placed under vacuum and backfilled with N_2 three times. THF (0.2 mL) was then added to both flasks, and the mixtures were stirred at room temperature under N_2 for 5 min. The Pd/ligand mixture was added via syringe to the flask containing **4.124a**, and stirring was continued at room temperature until **4.124a** was gone by TLC. The reaction was quenched with saturated aq NaHCO_3 (0.5 mL) and stirred at room temperature for 15 min. The reaction mixture was diluted with H_2O (1.0 mL) extracted with CH_2Cl_2 (3 x 5 mL). The combined organic extracts were washed with brine (5 mL), dried (Na_2SO_4), filtered, and concentrated *in vacuo* to afford a brown oil. Subsequent purification by RP

HPLC H₂O/MeCN (10% MeCN to 95% MeCN over 30 min) to provide 4.5 mg (98%) of **4.125a** as a white solid: ¹H-NMR (600 MHz, CD₃OD) δ 7.73 (d, *J* = 8.2 Hz, 1 H) 7.59 (d, *J* = 7.8 Hz, 1 H) 7.33 (td, *J* = 7.8, 1.2 Hz, 1 H) (td, *J* = 7.8, 0.6 Hz, 1 H) 5.30 (d, *J* = 6.0 Hz, 1 H) 4.41 (d, *J* = 8.4 Hz, 1 H) 4.39 (td, *J* = 9.0, 1.2 Hz, 1 H) 4.28 (d, *J* = 10.2 Hz, 1 H) 4.15 (d, *J* = 8.4 Hz, 1 H) 3.41 (d, *J* = 10.2 Hz, 1 H) 3.30 (s, 3 H) 3.24 (s, 3 H) 3.01 (dd, *J* = 13.2, 5.4 Hz, 1 H) 2.95 (m, 1 H) 2.91 (m, 1 H) 2.71 (td, *J* = 13.8, 4.8 Hz, 1 H) 2.28-2.02 (comp, 2 H) 1.95 (m, 1 H) 1.75 (s, 9 H); ¹³C-NMR (150 MHz, CD₃OD) δ 152.5, 141.4, 137.7, 127.5, 125.9, 123.4, 118.7, 115.9, 115.0, 86.4, 80.4, 76.4, 74.5, 59.1, 58.7, 53.1, 50.9, 49.6, 42.0, 38.6, 29.1, 28.4; HRMS (ESI) *m/z* observed 431.25580 [C₂₄H₃₄N₂O₅ (M+H)⁺ requires 431.25400].



Assignments: ¹H-NMR (600 MHz, CD₃OD) δ 7.73 (d, *J* = 8.2 Hz, 1 H, C5-H) 7.59 (d, *J* = 7.8 Hz, 1 H, C8-H) 7.33 (td, *J* = 7.8, 1.2 Hz, 1 H, C7-H) (td, *J* = 7.8, 0.6 Hz, 1 H, C6-H) 5.30 (d, *J* = 6.0 Hz, 1 H, C16-H) 4.41 (d, *J* = 8.4 Hz, 1 H, C19-H or C20-H) 4.39 (td, *J* = 9.0, 1.2 Hz, 1 H, C18-H) 4.28 (d, *J* = 10.2 Hz, 1 H, C19-H or C20-H) 4.15 (d, *J* = 8.4 Hz, 1 H, C19-H or C20-H) 3.41 (d, *J* = 10.2 Hz, 1 H, O15-H) 3.30 (s, 3 H, C21-H₃ or C22-H₃) 3.24 (s, 3 H, C21-H₃ or C22-H₃) 3.01 (dd, *J* = 13.2, 5.4 Hz, 1 H, C13-H) 2.95 (m, 1 H, C17-H) 2.91 (m, 1 H, C11-H) 2.71 (td, *J* = 13.8, 4.8 Hz, 1 H, C13-H) 2.28-2.02 (comp, 2 H, C12-H and C17-H) 1.95 (m, 1 H, C12-H) 1.75 (s, 9 H, C24-H₃);

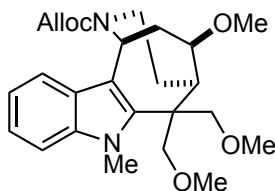
^{13}C -NMR (150 MHz, CD_3OD) δ 152.5 (C1), 141.4, 137.7, 127.5, 125.9 (C7), 123.4 (C6), 118.7 (C8), 115.9 (C3), 115.0 (C5), 86.4 (C23), 80.4 (C19 or C20), 76.4 (C19 or C20), 74.5 (C18), 59.1 (C21 or C22), 58.7 (C21 or C22), 53.1 (C11), 50.9 (C10), 49.6 (C16), 42.0 (C13), 38.6 (C17), 29.1 (C12), 28.4 (C24).



(1S/R, 5R/S, 12R/S)-tert-Butyl 12-hydroxy-6,6-bis(phenoxyethyl)-3,4,5,6-tetrahydro-1H-5,1-ethanoazocino[4,3-b]indole-7(2H)-carboxylate. (4.125b).

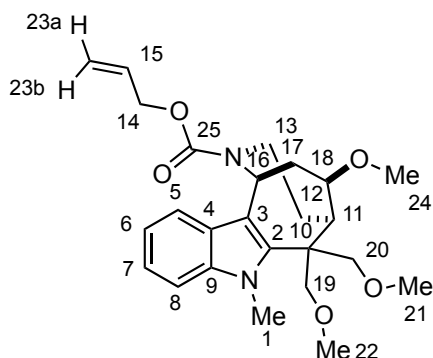
(WLM8_125). A round bottom flask charged with $\text{Pd}_2(\text{dba})_3$ (1.2 mg, 0.00133 mmol) and 1,4-bis(diphenylphosphino)butane (1.2 mg, 0.0027 mmol) was placed under vacuum and backfilled with N_2 three times. A second round bottom flask was charged with **4.124b** (17 mg, 0.027 mmol) and 1,3-dimethylbarbituric acid (42 mg, 0.27 mmol) and placed under vacuum and backfilled with N_2 three times. THF (0.2 mL) was then added to both flasks, and the mixtures were stirred at room temperature under N_2 for 5 min. The Pd/ligand mixture was added via syringe to the flask containing **4.124b**, and stirring was continued at room temperature until **4.124b** was gone by TLC. The reaction was quenched with saturated aq NaHCO_3 (0.5 mL) and stirred at room temperature for 15 min. The reaction mixture was diluted with H_2O (2.0 mL) extracted with CH_2Cl_2 (3 x 5 mL). The combined organic extracts were washed with brine (10 mL), dried (Na_2SO_4), filtered, and concentrated *in vacuo* to afford a brown oil. Subsequent purification by preparative TLC eluting with CH_2Cl_2 : MeOH (98 : 2) containing 1% NEt_3 provided 5.0 mg (34%) of **4.125b** as a white solid: ^1H -NMR (600 MHz, CD_3OD) δ 7.74 (d, J = 8.4 Hz, 1 H) 7.63 (d, J = 7.8 Hz, 1 H) 7.29 (td, J = 7.8, 1.2 Hz, 1 H) 7.27-7.20 (comp, 5 H) (dm, J = Hz, 2 H)

6.89 (tm, $J = 7.2$ Hz, 2 H) 6.72 (dm, $J = 7.8$ Hz, 2 H) 5.32 (d, $J = 8.4$ Hz, 1 H) 4.95 (d, $J = 9.6$ Hz, 1 H) 4.83 (m, 1 H) 4.80 (d, $J = 8.4$ Hz, 1 H) 4.59 (td, $J = 9.6, 1.2$ Hz, 1 H) 4.24 (d, $J = 9.6$ Hz, 1 H) 3.10 (m, 1 H) 2.83 (m, 1 H) 2.67 (dd, $J = 9.6, 2.4$ Hz, 2 H) (ddd, $J = 13.8, 9.6, 1.2$ Hz, 1 H) 2.01 (dm, $J = 14.4$ Hz, 1 H) 1.83 (m, 1 H) 1.30 (s, 9 H); ^{13}C -NMR (150 MHz, CD_3OD) δ 160.4, 159.6, 152.9, 138.3, 137.9, 130.4, 130.3, 128.5, 125.4, 122.9, 122.6, 122.0, 121.6, 119.2, 116.0, 115.5, 115.0, 85.5, 76.3, 75.5, 71.6, 53.8, 50.3, 48.3, 42.5, 41.4, 31.9, 28.0; HRMS (ESI) m/z observed 577.26740 [$\text{C}_{34}\text{H}_{38}\text{N}_2\text{O}_5$ ($\text{M}+\text{Na}$) $^+$ requires 577.26730].



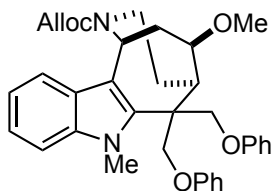
(1S/R, 5R/S, 12R/S)-Allyl 12-methoxy-6,6-bis(methoxymethyl)-7-methyl-3,4,5,6-tetrahydro-1H-5,1-ethanoazocino[4,3-b]indole-2(7H)-carboxylate. (4.126a). (WLM7_263_2). A mixture of **4.120a** (46 mg, 0.11 mmol) and 60% NaH dispersion in mineral oil (22 mg, 0.56 mmol) in DMF (1.1 mL) at 0 °C under N_2 was stirred for five min and methyl *p*-toluenesulfonate (207 mg, 1.11 mmol) was added in one portion. The reaction was allowed to warm slowly to room temperature overnight. The reaction was quenched with saturated aq NH_4Cl (1.0 mL), diluted with H_2O (5 mL), and extracted with EtOAc (3 x 15 mL). The combined organic extracts were washed with brine (25 mL), dried (Na_2SO_4), filtered, and concentrated *in vacuo* to afford a clear oil. Purification by flash chromatography eluting with Hexanes : EtOAc (4 : 1 to 2 : 1) to provide 48 mg (quant) of **4.126a** as a clear oil: ^1H -NMR (500 MHz, CD_3CN) δ 7.37 (d, $J = 8.0$ Hz, 1 H) 7.33 (d, $J = 8.0$ Hz, 1 H) 7.17 (td, $J = 8.0, 1.0$ Hz, 1 H) 7.05 (td, $J = 8.0, 1.5$ Hz, 1 H) 6.04 (br, 1 H) 5.65 (d, $J = 7.0$ Hz, 1 H) 5.25 (br, 1 H) 5.23 (br, 1 H) 4.66 (br, 2 H) 4.25 (d, $J =$

10.5 Hz, 1 H) 3.89 (s, 3 H) 3.80 (comp, 3 H) 3.76 (td, $J = 9.0, 1.0$ Hz, 1 H) 3.66 (d, $J = 10.5$ Hz, 1 H) 3.34 (s, 3 H) 3.28 (s, 3 H) 3.27 (s, 3 H) 3.02 (m, 1 H) 2.92 (m, 1 H) 2.81 (m, 1 H) 2.08 (dm, $J = 14.5$ Hz, 1 H) 1.81 (app t, $J = 12.5$ Hz, 1 H) 1.73 (m, 1 H); ^{13}C -NMR (125 MHz, CD_3CN) δ 156.3, 140.8, 138.9, 135.3, 127.5, 122.8, 120.5, 117.3, 115.4, 110.3, 86.4, 80.5, 77.4, 66.6, 61.1, 59.0, 59.0, 57.3, 50.4, 48.5, 46.7, 42.1, 33.5; HRMS (ESI) m/z observed 465.23580 [$\text{C}_{25}\text{H}_{34}\text{N}_2\text{O}_5$ ($\text{M}+\text{Na}$) $^+$ requires 465.23600].



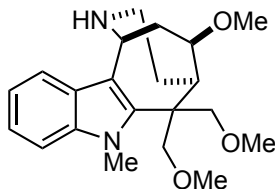
Assignments: ^1H -NMR (500 MHz, CD_3CN) δ 7.37 (d, $J = 8.0$ Hz, 1 H, C5-H) 7.33 (d, $J = 8.0$ Hz, 1 H, C8-H) 7.17 (td, $J = 8.0, 1.0$ Hz, 1 H, C7-H) 7.05 (td, $J = 8.0, 1.5$ Hz, 1 H, C6-H) 6.04 (br, 1 H, C15-H) 5.65 (d, $J = 7.0$ Hz, 1 H, C16-H) 5.25 (br, 1 H, C23-H) 5.23 (br, 1 H, C23-H) 4.66 (br, 2 H, C14-H₂) 4.25 (d, $J = 10.5$ Hz, 1 H, C19-H or C20-H) 3.89 (s, 3 H, C1-H₃) 3.80 (comp, 3 H, C19-H, C20-H, and C13-H) 3.76 (td, $J = 9.0, 1.0$ Hz, 1 H, C18-H) 3.66 (d, $J = 10.5$ Hz, 1 H, C19-H or C20-H) 3.34 (s, 3 H, C24-H₃) 3.28 (s, 3 H, C21-H₃ or C22-H₃) 3.27 (s, 3 H, C21-H or C22-H₃) 3.02 (m, 1 H, C17-H) 2.92 (m, 1 H, C11-H) 2.81 (m, 1 H, C13-H) 2.08 (dm, $J = 14.5$ Hz, 1 H, C12-H) 1.81 (app t, $J = 12.5$ Hz, 1 H, C17-H) 1.73 (m, 1 H, C12-H); ^{13}C -NMR (125 MHz, CD_3CN) δ 156.3 (C25), 140.8, 138.9, 135.3, 127.5, 122.8 (C7), 120.5 (C6), 118.2 (5), 117.3, 115.4 (C3), 110.3 (C8), 86.4 (C18), 80.5 (C19 or C20), 77.4 (C19 or C20), 66.6 (C14), 61.1

(C17), 59.0 (C21 or C22), 59.0 (C21 or C22), 57.3 (C24), 50.4 (C10), 48.5 (C16), 46.7 (C11), 42.1 (C13), 33.5 (C1) 32.7 (C12).



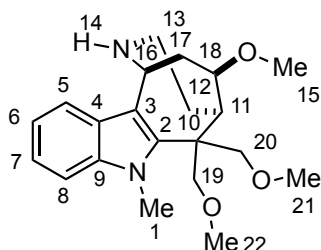
(1S/R, 5R/S, 12R/S)-Allyl 12-methoxy-7-methyl-6,6-bis(phenoxyethyl)-3,4,5,6-tetrahydro-1H-5,1-ethanoazocino[4,3-b]indole-2(7H)-carboxylate. (4.126b). (WLM8_189). A mixture of **4.120b** (39 mg, 0.0725 mmol) and 60% NaH dispersion in mineral oil (29 mg, 0.725 mmol) in dry DMF (0.7 mL) at 0 °C under N₂ was stirred for five min and methyl *p*-toluenesulfonate (67 mg, 0.362 mmol) was added in one portion. The reaction was allowed to warm slowly to room temperature overnight. The reaction was quenched with saturated aq NH₄Cl (0.5 mL), diluted with H₂O (2.0 mL), and extracted with CH₂Cl₂ (3 x 15 mL). The combined organic extracts were washed with brine (10 mL), dried (Na₂SO₄), filtered, and concentrated *in vacuo* to afford a clear oil. Purification by flash chromatography eluting with Hexanes : EtOAc (10 : 1) to provide 45.5 mg (99%) of **4.126b** as a clear oil: ¹H-NMR (500 MHz, CD₃CD) δ 7.64 (d, *J* = 8.0 Hz, 1 H) 7.47 (d, *J* = 8.0 Hz, 1 H) 7.31-7.21 (comp, 6 H) 6.97-6.92 (comp, 4 H) 6.88 (d, *J* = 8.5 Hz, 1 H) 6.15 (m, 1 H) 5.64-5.59 (comp, 2 H) 5.35 (d, *J* = 6.0 Hz, 1 H) 5.19 (d, *J* = 11.0 Hz, 1 H) 4.73 (d, *J* = 9.0 Hz, 1 H) 4.53 (d, *J* = 11.0 Hz, 1 H) 4.42 (d, *J* = 9.0 Hz, 1 H) 4.07 (dd, *J* = 13.5, 6.5 Hz, 1 H) 3.95 (td, *J* = 7.5 Hz, 1 H) 3.92 (s, 3 H) 3.61 (dd, *J* = 14.0, 8.0 Hz, 1 H) 3.43 (m, 1 H) 3.34-3.26 (m, 1 H) 3.21-3.12 (comp, 2 H) 3.18 (s, 3 H) 2.41 (dm, *J* = 15.5 Hz, 1 H) 2.24 (dd, *J* = 15.0, 8.0 Hz, 1 H) 2.05 (m, 1 H); ¹³C-NMR (500 MHz, CD₃CD) δ 159.7, 159.1, 141.0, 139.5, 130.8, 130.5, 128.9, 128.4, 125.9, 124.1, 122.8, 122.1, 122.0, 118.1, 115.5, 115.5, 111.0, 108.4, 84.7, 76.4, 71.6, 61.7, 59.1, 57.9,

50.5, 50.0, 44.7, 38.4, 33.3, 29.3; HRMS (ESI) m/z observed 589.26750 [$C_{35}H_{38}N_2O_5$ ($M+Na$)⁺ requires 589.26730].

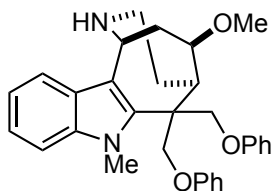


(1*S/R*, 5*R/S*, 12*R/S*)-12-Methoxy-6,6-bis(methoxymethyl)-7-methyl-2,3,4,5,6,7-hexahydro-1*H*-5,1-ethanoazocino[4,3-*b*]indole. (4.127a). (WLM7_269_2). A round bottom flask charged with $Pd_2(dba)_3$ (0.6 mg, 0.00066 mmol) and 1,4-bis(diphenylphosphino)butane (0.55 mg, 0.00131 mmol) was placed under vacuum and backfilled with N_2 three times. A second round bottom flask was charged with **4.126a** (29 mg, 0.066 mmol) and 1,3-dimethylbarbituric acid (103 mg, 0.66 mmol) and placed under vacuum and backfilled with N_2 three times. THF (0.3 mL) was then added to both flasks, and the mixtures were stirred at room temperature under N_2 for 5 min. The Pd/ligand mixture was added via syringe to the flask containing **4.126a**, and stirring was continued at room temperature until **4.126a** was gone by TLC. The reaction was quenched with saturated aq $NaHCO_3$ (0.5 mL) and stirred at room temperature for 15 min. The reaction mixture was diluted with H_2O (0.5 mL) extracted with CH_2Cl_2 (3 x 5 mL). The combined organic extracts were washed with brine (10 mL), dried (Na_2SO_4), filtered, and concentrated *in vacuo* to afford a brown oil. Subsequent purification by flash chromatography eluting with CH_2Cl_2 : MeOH (100% CH_2Cl_2 to 100 : 1) containing 1% NEt_3 to provide 20 mg (85%) of **4.127a** as a white solid: 1H -NMR (500 MHz, CD_3OD) δ 7.54 (d, J = 8.0 Hz, 1 H) 7.39 (d, J = 8.0 Hz, 1 H) 7.22 (td, J = 7.5, 1.0 Hz, 1 H) 7.11 (td, J = 7.5, 1.0 Hz, 1 H) 5.26 (dd, J = 6.5, 1.0 Hz, 1 H) 4.38 (d, J = 11.0 Hz, 1 H) 3.92 (s, 3 H) 3.87 (td, J = 9.0, 2.0 Hz, 1 H) 3.85 (d, J = 9.0 Hz, 1 H) 3.76 (d, J = 9.0 Hz, 1 H) 3.62

(d, $J = 11.0$ Hz, 1 H) 3.43 (s, 3 H) 3.30 (s, 3 H) 3.29 (s, 3 H) 3.11 (m, 1 H) 3.04-2.98 (comp, 3 H) 3.34 (dm, $J = 15.5$ Hz, 1 H) 2.10 (ddd, $J = 15.0, 9.0, 2.0$ Hz, 1 H) 1.94-1.86 (m, 1 H); ^{13}C -NMR (125 MHz, CD_3OD) δ 141.5, 139.2, 127.0, 123.5, 121.1, 118.0, 110.4, 109.4, 85.3, 81.2, 76.5, 58.8, 58.8, 57.7, 50.3, 49.6, 45.3, 41.9, 38.4, 33.0, 29.4; HRMS (ESI) m/z observed 381.21510 [$\text{C}_{21}\text{H}_{30}\text{N}_2\text{O}_3$ ($\text{M}+\text{Na}$) $^+$ requires 381.21490].

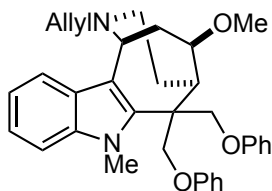


Assignments: ^1H -NMR (500 MHz, CD_3OD) δ 7.54 (d, $J = 8.0$ Hz, 1 H, C5-H) 7.39 (d, $J = 8.0$ Hz, 1 H, C8-H) 7.22 (td, $J = 7.5, 1.0$ Hz, 1 H, C7-H) 7.11 (td, $J = 7.5, 1.0$ Hz, 1 H, C6-H) 5.26 (dd, $J = 6.5, 1.0$ Hz, 1 H, C16-H) 4.38 (d, $J = 11.0$ Hz, 1 H, C19-H or C20-H) 3.92 (s, 3 H, C1-H₃) 3.87 (td, $J = 9.0, 2.0$ Hz, 1 H, C18-H) 3.85 (d, $J = 9.0$ Hz, 1 H, C19-H or C20-H) 3.76 (d, $J = 9.0$ Hz, 1 H, C19-H or C20-H) 3.62 (d, $J = 11.0$ Hz, 1 H, C19-H or C20-H) 3.43 (s, 3 H, C15-H₃) 3.30 (s, 3 H, C21-H₃ or C22-H₃) 3.29 (s, 3 H, C21-H₃ or C22-H₃) 3.11 (m, 1 H, C11-H) 3.04-2.98 (comp, 3 H, C13-H₂, C17-H) 3.34 (dm, $J = 15.5$ Hz, 1 H, C12-H) 2.10 (ddd, $J = 15.0, 9.0, 2.0$ Hz, 1 H, C17-H) 1.94-1.86 (m, 1 H, C12-H); ^{13}C -NMR (125 MHz, CD_3OD) δ 141.5, 139.2, 127.0, 123.5 (C7), 121.1 (C6), 118.0 (C5), 110.4 (C8), 109.4 (C3), 85.3 (C18), 81.2 (C19 or C20), 76.5 (C19 or C20), 58.8 (C21 or C22), 58.8 (C21 or C22), 57.7 (C15), 50.3 (C10), 49.6 (C16), 45.3 (C11), 41.9 (C13), 38.4 (C17), 33.0 (C1), 29.4 (C12).



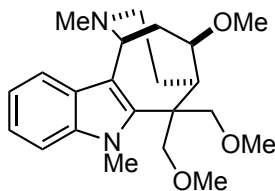
(1S/R, 5R/S, 12R/S)-12-Methoxy-7-methyl-6,6-bis(phenoxymethyl)-2,3,4,5,6,7-hexahydro-1H-5,1-ethanoazocino[4,3-b]indole (4.127b). (WLM8_191). A round bottom flask charged with $\text{Pd}_2(\text{dba})_3$ (0.73 mg, 0.000794 mmol) and 1,4-bis(diphenylphosphino)butane (0.68 mg, 0.00159 mmol) was placed under vacuum and backfilled with N_2 three times. A second round bottom flask was charged with **4.126b** (45 mg, 0.0794 mmol) and 1,3-dimethylbarbituric acid (124 mg, 0.794 mmol) and placed under vacuum and backfilled with N_2 three times. THF (0.4 mL) was then added to both flasks, and the mixtures were stirred at room temperature under N_2 for 5 min. The Pd/ligand mixture was added via syringe to the flask containing **4.126b**, and stirring was continued at room temperature until **4.126b** was gone by TLC. The reaction was quenched with saturated aq NaHCO_3 (0.5 mL) and stirred at room temperature for 15 min. The reaction mixture was diluted with H_2O (5 mL) extracted with CH_2Cl_2 (3 x 10 mL). The combined organic extracts were washed with brine (10 mL), dried (Na_2SO_4), filtered, and concentrated *in vacuo* to afford a brown oil. Subsequent purification by flash chromatography eluting with CH_2Cl_2 : MeOH (99 : 1) containing 1% NEt_3 followed by RP HPLC eluting with H_2O : MeCN (10% MeCN \rightarrow 90% MeCN over 60 min) provided 25 mg (66%) of **4.127b** as a white solid and 7.5 mg (18%) of **4.127c** as a white solid: ^1H -NMR (500 MHz, CD_3OD) δ 7.65 (d, J = 9.0 Hz, 1 H) 7.40 (d, J = 9.0 Hz, 1 H) 7.28-7.24 (comp, 5 H) 7.17 (dt, J = 7.5, 1.0 Hz, 1 H) 6.96-6.91 (comp, 4 H) 6.82 (dd, J = 8.5, 1.0 Hz, 1 H) 5.39 (d, J = 5.5 Hz, 1 H) 5.14 (d, J = 10.5 Hz, 1 H) 4.70 (d, J = 9.0 Hz, 1 H) 4.53 (d, J = 11.0 Hz, 1 H) 4.42 (d, J = 9.0 Hz, 1 H) 3.94 (dt, J = 9.0, 1.5 Hz, 1 H) 3.87 (s, 3 H) 3.41 (m, 1 H) 3.25 (dt, J = 14.0, 4.0 Hz) 3.18 (s, 3 H) 3.15-3.06 (comp, 2 H) 2.36

(dm, $J = 16.0$ Hz, 1 H) 2.20 (ddd, $J = 14.0, 8.5, 2.0$ Hz, 1 H) 2.00 (tm, 1 H). ^{13}C -NMR (125 MHz, CD_3OD) δ 159.8, 159.1, 140.1, 139.5, 130.8, 130.5, 127.1, 123.9, 122.7, 122.1, 121.4, 118.4, 115.6, 115.4, 110.5, 110.4, 85.0, 76.2, 71.7, 57.8, 49.9, 45.3, 41.8, 38.5, 33.1, 29.2. HRMS (ESI) m/z observed 505.24660 [$\text{C}_{31}\text{H}_{34}\text{N}_2\text{O}_3$ ($\text{M}+\text{Na}$) $^+$ requires 505.24620].



(1*S/R*, 5*R/S*, 12*R/S*)-2-Allyl-12-methoxy-7-methyl-6,6-bis(phenoxyethyl)-2,3,4,5,6,7-hexahydro-1*H*-5,1-ethanoazocino[4,3-*b*]indole. (4.127c). (WLM8_143). A round bottom flask charged with $\text{Pd}(\text{PPh}_3)_4$ (0.12 mg, 0.000106 mmol) and **4.126b** (6 mg, 0.0106 mmol) was placed under vacuum and backfilled with N_2 three times. THF (0.1 mL) was added and the mixture was stirred at room temperature over night. The reaction mixture was diluted with H_2O (1.0 mL) and extracted with CH_2Cl_2 (3 x 5 mL). The combined organic extracts were washed with brine (5 mL), dried (Na_2SO_4), filtered, and concentrated *in vacuo* to afford a brown oil. Subsequent purification by RP HPLC $\text{H}_2\text{O} : \text{MeCN}$ (10% MeCN \rightarrow 95% MeCN over 60 min) provided 3 mg (55%) of **4.127c** as a white solid: ^1H -NMR (500 MHz, CD_3OD) δ 7.65 (d, $J = 7.9$ Hz, 1H), 7.48 (d, $J = 8.3$ Hz, 1H), 7.28 (comp, 6H), 6.96 (comp, 4H), 6.89 (d, $J = 8.1$ Hz, 2H), 6.15 (ddd, $J = 17.1, 10.3, 5.6$ Hz, 1H), 5.64 (d, $J = 6.6$ Hz, 1H), 5.61 (d, $J = 13.3$ Hz, 1H), 5.36 (d, $J = 5.9$ Hz, 1H), 5.24 – 5.17 (m, 1H), 4.73 (dd, $J = 9.1, 1.4$ Hz, 1H), 4.54 (d, $J = 11.0$ Hz, 1H), 4.43 (d, $J = 9.0$ Hz, 1H), 4.08 (dd, $J = 13.6, 6.6$ Hz, 1H), 4.00 – 3.93 (m, 1H), 3.92 (s, 3H), 3.62 (dd, $J = 14.0, 7.5$ Hz, 1H), 3.47 – 3.42 (m, 1H), 3.30 – 3.26 (m, 1H), 3.19 (comp, 5H), 2.42 (d, $J = 16.8$ Hz, 1H), 2.25 (dd, $J = 15.2, 8.4$ Hz, 1H), 2.13 – 2.00 (m, 1H); ^{13}C -

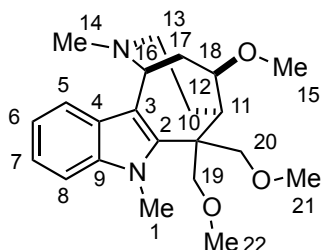
NMR (125 MHz, CD₃OD) δ 159.7, 159.1, 141.0, 139.5, 130.8, 130.5, 128.9, 128.4, 125.9, 124.1, 122.8, 122.1, 122.0, 118.1, 115.5, 115.5, 111.0, 108.4, 84.7, 76.4, 71.6, 61.7, 59.1, 57.9, 50.5, 50.0, 44.7, 38.4, 33.3, 29.3; HRMS (ESI) m/z observed 523.29600 [C₃₄H₃₈N₂O₃ (M+H)⁺ requires 523.29550].



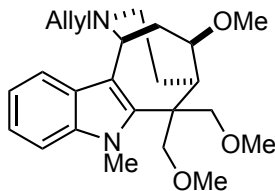
(1S/R, 5R/S, 12R/S)-12-Methoxy-6,6-bis(methoxymethyl)-2,7-dimethyl-2,3,4,5,6,7-hexahydro-1H-5,1-ethanoazocino[4,3-b]indole. (4.128a). (WLM7_281_2).

A mixture of **4.127a** (6.3 mg, 0.018 mmol) and 37% aq formaldehyde solution (14 mg, 0.18 mmol, 14 μ L) in CH₂Cl₂ (0.2 mL) was stirred for 5 min at room temperature whereupon sodium triacetoxyborohydride (19 mg, 0.088 mmol) was added in one portion. Stirring was continued for 4 h at room temperature. The reaction was quenched with saturated aq Rochelle's salt (0.5 mL) and extracted with CH₂Cl₂ (3 x 5 mL). The combined organic extracts were washed with brine (5 mL), dried (Na₂SO₄), filtered, and concentrated *in vacuo* to afford 6.5 mg (quant) of **4.128a** as a white solid: ¹H-NMR (500 MHz, CDCl₃) δ 7.45 (d, J = 8.0 Hz, 1 H) 7.35 (d, J = 8.0 Hz, 1 H) 7.26 (td, J = 8.0, 1.0 Hz, 1 H) 7.17 (td, J = 8.0, 1.0 Hz, 1 H) 4.72 (d, J = 5.0 Hz, 1 H) 4.31 (d, J = 10.5 Hz, 1 H) 4.20 (t, J = 9.0 Hz, 1 H) 3.91 (s, 3 H) 3.86 (d, J = 9.0 Hz, 1 H) 3.66 (d, J = 9.0 Hz, 1 H) 3.57 (d, J = 10.5 Hz, 1 H) 3.41 (s, 3 H) 3.41-3.39 (m, 1 H) 3.28 (s, 6 H) 2.98 (m, 1 H) 2.90 (m, 1 H) 2.86 (m, 1 H) 2.72 (s, 3 H) 2.30-2.22 (m, 1 H) 2.15-2.11 (m, 1 H) 1.95 (dd, J = 13.0, 8.5 Hz, 1 H); ¹³C-NMR (125 MHz, CDCl₃) δ 140.3, 137.6, 127.1, 122.2, 120.3, 117.1, 109.4, 108.1, 83.6, 80.5, 76.0, 58.6, 58.4, 57.9, 57.1, 51.4, 49.0, 46.1, 44.2, 37.3,

32.5, 28.8; HRMS (ESI) m/z observed 372.24830 [$C_{22}H_{32}N_2O_3$ (M+H) $^+$ requires 372.24860].

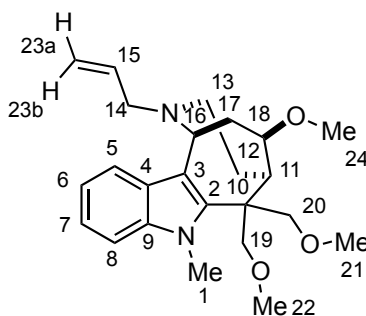


Assignments: 1H -NMR (500 MHz, $CDCl_3$) δ 7.45 (d, $J = 8.0$ Hz, 1 H, C5-H) 7.35 (d, $J = 8.0$ Hz, 1 H, C8-H) 7.26 (td, $J = 8.0, 1.0$ Hz, 1 H, C7-H) 7.17 (td, $J = 8.0, 1.0$ Hz, 1 H, C6-H) 4.72 (d, $J = 5.0$ Hz, 1 H, C16-H) 4.31 (d, $J = 10.5$ Hz, 1 H, C19-H or C20-H) 4.20 (t, $J = 9.0$ Hz, 1 H, C18-H) 3.91 (s, 3 H, C1-H₃) 3.86 (d, $J = 9.0$ Hz, 1 H, C19-H or C20-H) 3.66 (d, $J = 9.0$ Hz, 1 H, C19-H or C20-H) 3.57 (d, $J = 10.5$ Hz, 1 H, C19-H or C20-H) 3.41 (s, 3 H, C15-H₃) 3.41-3.39 (m, 1 H, C17-H) 3.28 (s, 6 H, C21-H₃ and C22-H₃) 2.98 (m, 1 H, C11-H) 2.90 (m, 1 H, C13-H) 2.86 (m, 1 H, C13-H) 2.72 (s, 3 H, C14-H₃) 2.30-2.22 (m, 1 H, C12-H) 2.15-2.11 (m, 1 H, C12-H) 1.95 (dd, $J = 13.0, 8.5$ Hz, 1 H, C17-H); ^{13}C -NMR (125 MHz, $CDCl_3$) δ 140.3, 137.6, 127.1, 122.2 (C7), 120.3 (C6), 117.1 (C5), 109.4 (C8), 108.1 (C3), 83.6 (C18), 80.5 (C19 or C20), 76.0 (C19 or C20), 58.6 (C21 or C22), 58.4 (C21 or C22), 57.9 (C16), 57.1 (C15), 51.4 (C13), 49.0 (C10), 46.1 (C14), 44.2 (C11), 37.3 (C17), 32.5 (C1), 28.8 (C12).



(1*S*/*R*, 5*R*/*S*, 12*R*/*S*)-2-Allyl-12-methoxy-6,6-bis(methoxymethyl)-7-methyl-2,3,4,5,6,7-hexahydro-1*H*-5,1-ethanoazocino[4,3-*b*]indole. (4.129). (WLM7_271_2). A

round bottom flask charged with $\text{Pd}(\text{PPh}_3)_4$ (0.5 mg, 0.00407 mmol) and **4.127a** (18 mg, 0.0407 mmol) was placed under vacuum and backfilled with N_2 three times. THF (0.4 mL) was added and the mixture was stirred at room temperature over night. The reaction mixture was diluted with H_2O (2.0 mL) and extracted with CH_2Cl_2 (3 x 5 mL). The combined organic extracts were washed with brine (10 mL), dried (Na_2SO_4), filtered, and concentrated *in vacuo* to afford a brown oil. Subsequent purification by flash chromatography eluting with Hexanes : EtOAc (1 : 1) containing 1% NEt_3 to provide 14.5 mg (90%) of **4.129** as a white solid: ^1H -NMR (500 MHz, CDCl_3) δ 7.50 (d, $J = 7.5$ Hz, 1 H) 7.29 (d, $J = 8.0$ Hz, 1 H) 7.19 (td, $J = 8.0, 1.0$ Hz, 1 H) 7.07 (td, $J = 8.0, 1.0$ Hz, 1 H) 6.06 (m, 1 H) (dd, $J = 7.0, 1.0$ Hz, 1 H) 5.22 (dd, $J = 10.0, 1.0$ Hz, 1 H) 4.46 (d, $J = 6.0$ Hz, 1 H) 4.23 (d, $J = 10.5$ Hz, 1 H) 4.00 (td, $J = 9.0, 1.5$ Hz, 1 H) 3.89 (s, 3 H) 3.79 (d, $J = 9.0$ Hz, 1 H) 3.64 (d, $J = 9.0$ Hz, 1 H) 3.61 (d, $J = 10.5$ Hz, 1 H) 3.39 (s, 3 H) 3.36-3.25 (m, 1 H) 3.29 (s, 3 H) 3.27 (s, 3 H) 3.07 (dd, $J = 14.0, 5.5$ Hz, 1 H) 2.88 (m, 1 H) 2.82 (m, 1 H) 2.52 (dd, $J = 12.0, 6.0$ Hz, 1 H) 2.11-2.06 (m, 1 H) 1.86-1.79 (m, 1 H) 1.81 (ddd, $J = 13.5, 4.5, 1.0$ Hz, 1 H); ^{13}C -NMR (125 MHz, CDCl_3) 138.5, 137.3, 128.1, 121.3, 119.0, 118.1, 108.7, 85.3, 80.4, 76.5, 61.9, 58.5, 58.3, 56.7, 52.7, 50.0, 48.8, 44.8, 40.4, 32.3, 31.3; HRMS (ESI) m/z observed 399.26430 [$\text{C}_{24}\text{H}_{34}\text{N}_2\text{O}_3$ ($\text{M}+\text{H}$) $^+$ requires 399.26420].



Assignments: ^1H -NMR (500 MHz, CDCl_3) δ 7.50 (d, $J = 7.5$ Hz, 1 H, C5-H) 7.29 (d, $J = 8.0$ Hz, 1 H, C8-H) 7.19 (td, $J = 8.0, 1.0$ Hz, 1 H, C7-H) 7.07 (td, $J = 8.0, 1.0$ Hz, 1 H, C6-H) 6.06 (m, 1 H, C15-H) (dd, $J = 17.0, 1.5$ Hz, 1 H, C23_a-H) 5.22 (dd, $J = 10.0, 1.0$ Hz, 1 H, C23_b-H) 4.46 (d, $J = 6.0$ Hz, 1 H, C16-H) 4.23 (d, $J = 10.5$ Hz, 1 H, C19-H or C20-H) 4.00 (td, $J = 9.0, 1.5$ Hz, 1 H, C18-H) 3.89 (s, 3 H, C1-H₃) 3.79 (d, $J = 9.0$ Hz, 1 H, C19-H or C20-H) 3.64 (d, $J = 9.0$ Hz, 1 H, C19-H or C20-H) 3.61 (d, $J = 10.5$ Hz, 1 H, C19-H or C20-H) 3.39 (s, 3 H, C24-H₃) 3.36-3.25 (m, 1 H, C14-H) 3.29 (s, 3 H, C21-H₃) 3.27 (s, 3 H, C22-H₃) 3.07 (dd, $J = 14.0, 5.5$ Hz, 1 H, C14-H₃) 2.88 (m, 1 H, C11-H) 2.82 (m, 1 H, C17-H) 2.52 (dd, $J = 12.0, 6.0$ Hz, 1 H, C13-H) 2.11-2.06 (m, 1 H, C13-H) 1.86-1.79 (m, 1 H, C12-H or C17-H) 1.81 (ddd, $J = 13.5, 4.5, 1.0$ Hz, 1 H, C12-H or C17-H); ^{13}C -NMR (125 MHz, CDCl_3) 138.5, 137.3, 128.1, 121.3 (C7), 119.0 (C6), 118.1 (C5), 108.7 (C8), 85.3 (C18), 80.4 (C19 or C20), 76.5 (C19 or C20), 61.9 (C14), 58.5 (C21 or C22), 58.3 (C21 or C22), 56.7 (C24), 52.7 (C16), 50.0 (C13), 48.8 (C10), 44.8 (C11), 40.4 (C17), 32.3 (C1), 31.3 (C12).

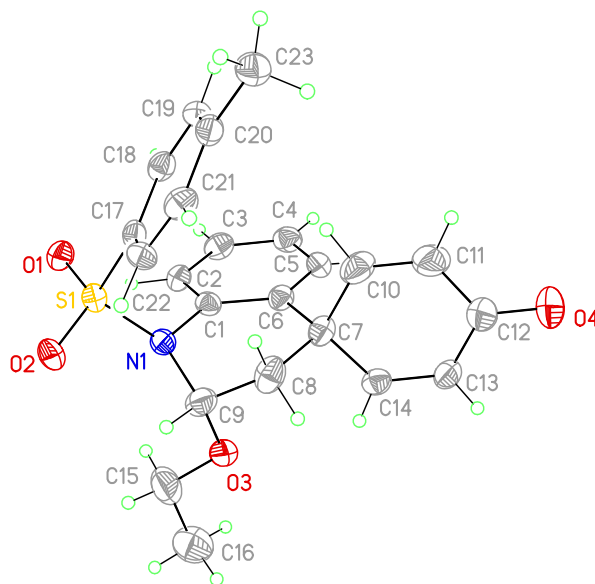
Chapter 6: Crystallography Data

Note: All crystallography data was collected by Dr. Vincent Lynch at the University of Texas at Austin.

6.1 CRYSTALLOGRAPHY DATA FOR COMPOUND 2.14

View of **2.14** showing the atom labeling scheme. Displacement ellipsoids are scaled to the 50% probability level.

Figure 6.1. X-ray Structure of **2.14**



X-ray Experimental for $C_{23}H_{23}NO_4S$: Crystals grew as highly intergrown clusters by slow cooling in MeOH. The data crystal was cut from a cluster of crystals and had approximate dimensions; 0.15 x 0.08 x 0.06 mm. The data were collected on a Rigaku SCX-Mini diffractometer with a Mercury CCD using a graphite monochromator with $MoK\alpha$ radiation ($\lambda = 0.71075 \text{ \AA}$). A total of 1080 frames of data were collected using ω -scans with a scan range of 0.5° and a counting time of 30 seconds per frame. The data

were collected at 153 K using a Rigaku XStream low temperature device. Details of crystal data, data collection and structure refinement are listed in Table 6.1. Data reduction were performed using the Rigaku Americas Corporation's Crystal Clear version 1.40.³⁰¹ The structure was solved by direct methods using SIR97³⁰² and refined by full-matrix least-squares on F^2 with anisotropic displacement parameters for the non-H atoms using SHELXL-97.³⁰³ Structure analysis was aided by use of the programs PLATON98³⁰⁴ and WinGX.³⁰⁵ The hydrogen atoms on carbon were calculated in ideal positions with isotropic displacement parameters set to 1.2xUeq of the attached atom (1.5xUeq for methyl hydrogen atoms). The function, $\sum w(|F_o|^2 - |F_c|^2)^2$, was minimized, where $w = 1/[(\sigma(F_o))^2 + (0.0657*P)^2 + (0.5409*P)]$ and $P = (|F_o|^2 + 2|F_c|^2)/3$. $R_w(F^2)$ refined to 0.178, with $R(F)$ equal to 0.0751 and a goodness of fit, S , = 1.06. Definitions used for calculating $R(F)$, $R_w(F^2)$ and the goodness of fit, S , are given below.³⁰⁶ The data were checked for secondary extinction effects but no correction was necessary. Neutral atom scattering factors and values used to calculate the linear absorption coefficient are from the International Tables for X-ray Crystallography (1992).³⁰⁷ All figures were generated using SHELXTL/PC.³⁰⁸ Tables of positional and thermal parameters, bond lengths and angles, torsion angles and figures are found elsewhere.

Table 6.1. Crystal Data and Structure Refinement for **2.14**.

Empirical formula	C ₂₃ H ₂₃ N O ₄ S
Formula weight	409.48
Temperature	153(2) K
Wavelength	0.71075 Å
Crystal system	Monoclinic
Space group	P2 ₁ /c
Unit cell dimensions	a = 13.644(3) Å α = 90°. b = 11.362(3) Å β = 106.798(5)°. c = 13.569(3) Å γ = 90°.
Volume	2013.7(8) Å ³
Z	4
Density (calculated)	1.351 Mg/m ³
Absorption coefficient	0.191 mm ⁻¹
F(000)	864
Crystal size	0.15 x 0.08 x 0.06 mm
Theta range for data collection	2.38 to 25.00°.
Index ranges	-16 ≤ h ≤ 16, -13 ≤ k ≤ 13, -16 ≤ l ≤ 16
Reflections collected	17158
Independent reflections	3544 [R(int) = 0.1577]
Completeness to theta = 25.00°	99.9 %
Absorption correction	None
Refinement method	Full-matrix least-squares on F ²
Data / restraints / parameters	3544 / 174 / 264
Goodness-of-fit on F ²	1.057
Final R indices	[I > 2σ(I)] R ₁ = 0.0751, wR ₂ = 0.1512
R indices (all data)	R ₁ = 0.1310, wR ₂ = 0.1777
Largest diff. peak and hole	0.316 and -0.370 e.Å ⁻³

Table 6.2. Atomic Coordinates ($\times 10^4$) and Equivalent Isotropic Displacement Parameters ($\text{\AA}^2 \times 10^3$) for **2.14**

U(eq) is defined as one third of the trace of the orthogonalized U^{ij} tensor.

	x	y	z	U(eq)
C1	7215(3)	744(3)	9295(3)	24(1)
C2	6658(3)	-105(4)	8613(3)	28(1)
C3	6984(3)	-454(4)	7783(3)	31(1)
C4	7872(3)	10(4)	7633(3)	31(1)
C5	8431(3)	830(4)	8328(3)	29(1)
C6	8116(3)	1221(4)	9166(3)	25(1)
C7	8798(3)	2093(4)	9927(3)	28(1)
C8	8385(3)	2369(4)	10860(4)	36(1)
C9	7728(3)	1388(4)	11091(3)	34(1)
C10	8810(4)	3226(4)	9348(4)	40(1)
C11	9655(4)	3698(4)	9219(4)	49(1)
C12	10664(4)	3157(4)	9624(4)	42(1)
C13	10687(3)	2049(4)	10177(3)	33(1)
C14	9848(3)	1570(4)	10319(3)	28(1)
C15	7856(4)	-571(5)	11758(5)	62(2)
C16	8617(4)	-1434(4)	12306(4)	55(2)
C17	5889(3)	3161(4)	9543(3)	25(1)
C18	5789(3)	3344(4)	8508(3)	27(1)
C19	5927(3)	4473(4)	8172(3)	26(1)
C20	6194(3)	5414(4)	8863(3)	27(1)

Table 6.2., cont.

C21	6297(3)	5206(4)	9899(3)	30(1)
C22	6134(3)	4093(4)	10246(3)	27(1)
C23	6356(3)	6629(4)	8494(4)	36(1)
N1	6877(2)	1075(3)	10175(2)	25(1)
O1	5024(2)	1120(3)	9188(2)	31(1)
O2	5602(2)	1826(3)	10995(2)	33(1)
O3	8360(2)	399(3)	11426(2)	34(1)
O4	11444(3)	3608(3)	9502(3)	59(1)
S1	5754(1)	1735(1)	9988(1)	27(1)

Table 6.3. Bond lengths [\AA] and angles [$^\circ$] for **2.14**.

Lengths:

C1-C6	1.401(6)
C1-C2	1.399(6)
C1-N1	1.448(5)
C2-C3	1.382(6)
C2-H2	0.95
C3-C4	1.390(6)
C3-H3	0.95
C4-C5	1.386(6)
C4-H4	0.95
C5-C6	1.399(6)
C5-H5	0.95
C6-C7	1.535(6)
C7-C14	1.499(6)
C7-C10	1.510(6)
C7-C8	1.559(6)
C8-C9	1.519(6)
C8-H8A	0.99
C8-H8B	0.99
C9-O3	1.410(5)
C9-N1	1.478(5)
C9-H9	1.00
C10-C11	1.328(7)

Table 6.3., cont.

C10-H10	0.95
C11-C12	1.463(7)
C11-H11	0.95
C12-O4	1.235(5)
C12-C13	1.461(6)
C13-C14	1.331(6)
C13-H13	0.95
C14-H14	0.95
C15-O3	1.438(6)
C15-C16	1.465(7)
C15-H15A	0.99
C15-H15B	0.99
C16-H16A	0.98
C16-H16B	0.98
C16-H16C	0.98
C17-C18	1.388(6)
C17-C22	1.400(6)
C17-S1	1.757(4)
C18-C19	1.392(6)
C18-H18	0.95
C19-C20	1.400(6)
C19-H19	0.95
C20-C21	1.391(6)

Table 6.3., cont.

C20-C23	1.507(6)
C21-C22	1.390(6)
C21-H21	0.95
C22-H22	0.95
C23-H23A	0.98
C23-H23B	0.98
C23-H23C	0.98
N1-S1	1.658(3)
O1-S1	1.426(3)
O2-S1	1.444(3)

Angles:

C6-C1-C2	120.8(4)
C6-C1-N1	120.2(4)
C2-C1-N1	118.9(4)
C3-C2-C1	119.8(4)
C3-C2-H2	120.1
C1-C2-H2	120.1
C2-C3-C4	120.6(4)
C2-C3-H3	119.7
C4-C3-H3	119.7
C5-C4-C3	119.1(4)
C5-C4-H4	120.4
C3-C4-H4	120.4

Table 6.3., cont.

C4-C5-C6	121.9(4)
C4-C5-H5	119.0
C6-C5-H5	119.0
C1-C6-C5	117.8(4)
C1-C6-C7	123.3(4)
C5-C6-C7	118.9(4)
C14-C7-C10	111.7(4)
C14-C7-C6	108.3(3)
C10-C7-C6	107.2(4)
C14-C7-C8	108.9(3)
C10-C7-C8	108.2(4)
C6-C7-C8	112.6(3)
C9-C8-C7	113.2(4)
C9-C8-H8A	108.9
C7-C8-H8A	108.9
C9-C8-H8B	108.9
C7-C8-H8B	108.9
H8A-C8-H8B	107.8
O3-C9-N1	109.7(3)
O3-C9-C8	108.0(3)
N1-C9-C8	111.7(4)
O3-C9-H9	109.1
N1-C9-H9	109.1

Table 6.3., cont.

C8-C9-H9	109.1
C11-C10-C7	123.6(4)
C11-C10-H10	118.2
C7-C10-H10	118.2
C10-C11-C12	122.6(5)
C10-C11-H11	118.7
C12-C11-H11	118.7
O4-C12-C11	122.0(5)
O4-C12-C13	122.4(5)
C11-C12-C13	115.7(4)
C14-C13-C12	122.4(4)
C14-C13-H13	118.8
C12-C13-H13	118.8
C13-C14-C7	124.1(4)
C13-C14-H14	118.0
C7-C14-H14	118.0
O3-C15-C16	109.9(4)
O3-C15-H15A	109.7
C16-C15-H15A	109.7
O3-C15-H15B	109.7
C16-C15-H15B	109.7
H15A-C15-H15B	108.2
C15-C16-H16A	109.5

Table 6.3., cont.

C15-C16-H16B	109.5
H16A-C16-H16B	109.5
C15-C16-H16C	109.5
H16A-C16-H16C	109.5
H16B-C16-H16C	109.5
C18-C17-C22	120.7(4)
C18-C17-S1	119.8(3)
C22-C17-S1	119.5(3)
C17-C18-C19	119.1(4)
C17-C18-H18	120.4
C19-C18-H18	120.4
C18-C19-C20	121.2(4)
C18-C19-H19	119.4
C20-C19-H19	119.4
C21-C20-C19	118.5(4)
C21-C20-C23	120.6(4)
C19-C20-C23	120.8(4)
C20-C21-C22	121.2(4)
C20-C21-H21	119.4
C22-C21-H21	119.4
C21-C22-C17	119.2(4)
C21-C22-H22	120.4
C17-C22-H22	120.4

Table 6.3., cont.

C20-C23-H23A	109.5
C20-C23-H23B	109.5
H23A-C23-H23B	109.5
C20-C23-H23C	109.5
H23A-C23-H23C	109.5
H23B-C23-H23C	109.5
C1-N1-C9	113.3(3)
C1-N1-S1	119.4(3)
C9-N1-S1	119.1(3)
C9-O3-C15	114.1(3)
O1-S1-O2	119.70(18)
O1-S1-N1	107.81(17)
O2-S1-N1	105.46(17)
O1-S1-C17	108.03(19)
O2-S1-C17	108.51(19)
N1-S1-C17	106.63(18)

Table 6.4. Anisotropic Displacement parameters ($\text{\AA}^2 \times 10^3$) for **2.14**

The anisotropic displacement factor exponent takes the form: $-2\pi^2[h^2 a^{*2} U^{11} + \dots + 2 h k a^* b^* U^{12}]$.

	U^{11}	U^{22}	U^{33}	U^{23}	U^{13}	U^{12}
C1	26(2)	23(2)	23(2)	3(2)	9(2)	4(2)
C2	22(2)	32(2)	28(3)	1(2)	4(2)	-3(2)
C3	31(2)	30(2)	27(3)	-6(2)	3(2)	0(2)
C4	33(2)	37(3)	24(3)	0(2)	9(2)	5(2)
C5	26(2)	35(3)	28(3)	7(2)	11(2)	1(2)
C6	23(2)	27(2)	25(2)	1(2)	6(2)	3(2)
C7	23(2)	26(2)	35(3)	-1(2)	7(2)	1(2)
C8	29(2)	40(3)	40(3)	-11(2)	10(2)	1(2)
C9	29(2)	45(3)	25(3)	-2(2)	5(2)	7(2)
C10	32(3)	30(3)	50(3)	6(2)	-1(2)	1(2)
C11	48(3)	39(3)	51(3)	17(2)	-1(2)	-7(3)
C12	36(3)	49(3)	39(3)	3(2)	7(2)	-10(2)
C13	24(2)	44(3)	28(3)	-1(2)	4(2)	-2(2)
C14	28(2)	31(2)	24(2)	-2(2)	5(2)	3(2)
C15	48(3)	72(4)	74(4)	38(3)	32(3)	10(3)
C16	66(4)	46(3)	53(4)	3(3)	19(3)	6(3)
C17	19(2)	28(2)	31(3)	2(2)	10(2)	1(2)
C18	23(2)	32(2)	23(2)	-6(2)	5(2)	-1(2)

Table 6.4., cont.

C19	25(2)	30(2)	20(2)	2(2)	5(2)	0(2)
C20	23(2)	27(2)	32(3)	2(2)	9(2)	1(2)
C21	28(2)	30(2)	30(3)	-4(2)	5(2)	3(2)
C22	30(2)	34(3)	18(2)	0(2)	9(2)	0(2)
C23	36(3)	33(3)	38(3)	7(2)	12(2)	4(2)
N1	24(2)	32(2)	20(2)	-2(2)	9(2)	1(2)
O1	24(2)	35(2)	33(2)	1(1)	5(1)	-5(1)
O2	33(2)	45(2)	28(2)	4(1)	18(1)	3(2)
O3	28(2)	45(2)	29(2)	8(1)	9(1)	5(2)
O4	40(2)	72(3)	64(3)	11(2)	12(2)	-24(2)
S1	24(1)	30(1)	28(1)	3(1)	11(1)	-1(1)

Table 6.5. Hydrogen coordinates ($\times 10^4$) and isotropic displacement parameters ($\text{\AA}^2 \times 10^3$) for **2.14**.

	x	y	z	U(eq)
H2	6059	-440	8720	33
H3	6596	-1017	7312	37
H4	8093	-231	7061	37
H5	9045	1134	8232	35
H8A	8972	2509	11477	44
H8B	7975	3101	10716	44
H9	7440	1648	11655	40
H10	8179	3623	9061	48
H11	9601	4416	8848	59
H13	11323	1656	10445	39
H14	9918	853	10693	34
H15A	7371	-947	11154	74
H15B	7463	-280	12218	74
H16A	8965	-1770	11832	82
H16B	8275	-2064	12575	82
H16C	9121	-1047	12879	82
H18	5628	2707	8034	32
H19	5839	4606	7461	31
H21	6483	5836	10377	36
H22	6188	3966	10952	32
H23A	5949	7198	8752	54
H23B	6142	6643	7740	54
H23C	7083	6837	8751	54

Table 6.6. Torsion angles [$^{\circ}$] for **2.14**.

C6-C1-C2-C3	-1.9(6)
N1-C1-C2-C3	-178.3(4)
C1-C2-C3-C4	1.5(6)
C2-C3-C4-C5	0.1(6)
C3-C4-C5-C6	-1.3(6)
C2-C1-C6-C5	0.7(6)
N1-C1-C6-C5	177.1(3)
C2-C1-C6-C7	-175.9(4)
N1-C1-C6-C7	0.5(6)
C4-C5-C6-C1	0.9(6)
C4-C5-C6-C7	177.6(4)
C1-C6-C7-C14	121.4(4)
C5-C6-C7-C14	-55.2(5)
C1-C6-C7-C10	-118.0(4)
C5-C6-C7-C10	65.5(5)
C1-C6-C7-C8	0.9(6)
C5-C6-C7-C8	-175.6(4)
C14-C7-C8-C9	-94.5(4)
C10-C7-C8-C9	143.9(4)
C6-C7-C8-C9	25.6(5)
C7-C8-C9-O3	66.3(5)
C7-C8-C9-N1	-54.5(5)
C14-C7-C10-C11	-0.7(7)

Table 6.6., cont.

C6-C7-C10-C11	-119.2(5)
C8-C7-C10-C11	119.1(5)
C7-C10-C11-C12	0.3(8)
C10-C11-C12-O4	-179.7(5)
C10-C11-C12-C13	0.6(8)
O4-C12-C13-C14	179.2(5)
C11-C12-C13-C14	-1.1(7)
C12-C13-C14-C7	0.7(7)
C10-C7-C14-C13	0.2(6)
C6-C7-C14-C13	118.0(5)
C8-C7-C14-C13	-119.2(5)
C22-C17-C18-C19	-0.5(6)
S1-C17-C18-C19	-178.1(3)
C17-C18-C19-C20	1.9(6)
C18-C19-C20-C21	-1.4(6)
C18-C19-C20-C23	179.2(4)
C19-C20-C21-C22	-0.4(6)
C23-C20-C21-C22	179.0(4)
C20-C21-C22-C17	1.8(6)
C18-C17-C22-C21	-1.3(6)
S1-C17-C22-C21	176.3(3)
C6-C1-N1-C9	-29.3(5)
C2-C1-N1-C9	147.1(4)

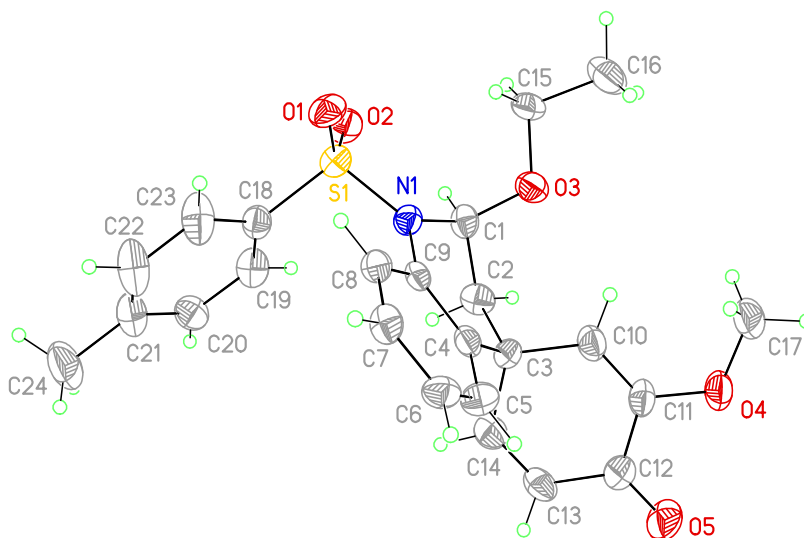
Table 6.6., cont.

C6-C1-N1-S1	119.0(4)
C2-C1-N1-S1	-64.6(4)
O3-C9-N1-C1	-63.5(4)
C8-C9-N1-C1	56.2(5)
O3-C9-N1-S1	148.1(3)
C8-C9-N1-S1	-92.2(4)
N1-C9-O3-C15	-63.0(5)
C8-C9-O3-C15	175.0(4)
C16-C15-O3-C9	-167.0(4)
C1-N1-S1-O1	45.0(3)
C9-N1-S1-O1	-168.5(3)
C1-N1-S1-O2	174.0(3)
C9-N1-S1-O2	-39.6(4)
C1-N1-S1-C17	-70.8(3)
C9-N1-S1-C17	75.7(3)
C18-C17-S1-O1	-32.8(4)
C22-C17-S1-O1	149.6(3)
C18-C17-S1-O2	-164.0(3)
C22-C17-S1-O2	18.4(4)
C18-C17-S1-N1	82.9(3)
C22-C17-S1-N1	-94.8(3)

6.2 CRYSTALLOGRAPHIC DATA FOR 2.33G

View of **2.33g** showing the atom labeling scheme. Displacement ellipsoids are scaled to the 50% probability level.

Figure 6.2. X-ray Structure of **2.33g**



X-ray Experimental for C₂₄H₂₅NO₅S: Crystals grew as long colorless laths by slow cooling from MeOH. The data crystal was cut from a larger crystal and had approximate dimensions; 0.58 x 0.08 x 0.02 mm. The data were collected on a Rigaku SCX-Mini diffractometer with a Mercury 2 CCD using a graphite monochromator with MoK α radiation ($\lambda = 0.71075\text{\AA}$). A total of 360 frames of data were collected using ω -scans with a scan range of 1° and a counting time of 120 seconds per frame. The data

were collected at 163 K using a Rigaku XStream low temperature device. Details of crystal data, data collection and structure refinement are listed in Table 6.7. Data reduction were performed using the Rigaku Americas Corporation's Crystal Clear version 1.40.³⁰¹ The structure was solved by direct methods using SIR97³⁰² and refined by full-matrix least-squares on F^2 with anisotropic displacement parameters for the non-H atoms using SHELXL-97.³⁰³ Structure analysis was aided by use of the programs PLATON98³⁰⁴ and WinGX.³⁰⁵ The hydrogen atoms on carbon were calculated in ideal positions with isotropic displacement parameters set to 1.2xUeq of the attached atom (1.5xUeq for methyl hydrogen atoms). The function, $\sum w(|F_o|^2 - |F_c|^2)^2$, was minimized, where $w = 1/[(\sigma(F_o))^2 + (0.0542*P)^2 + (1.9824*P)]$ and $P = (|F_o|^2 + 2|F_c|^2)/3$. $R_w(F^2)$ refined to 0.223, with $R(F)$ equal to 0.0979 and a goodness of fit, S , = 1.15. Definitions used for calculating $R(F)$, $R_w(F^2)$ and the goodness of fit, S , are given below.³⁰⁶ The data were checked for secondary extinction effects but no correction was necessary. Neutral atom scattering factors and values used to calculate the linear absorption coefficient are from the International Tables for X-ray Crystallography (1992).³⁰⁷ All figures were generated using SHELXTL/PC.³⁰⁸ Tables of positional and thermal parameters, bond lengths and angles, torsion angles and figures are found elsewhere.

Table 6.7. Crystal data and structure refinement for **2.33g**

Empirical formula	C ₂₄ H ₂₅ N O ₅ S
Formula weight	439.51
Temperature	163(2) K
Wavelength	0.71073 Å
Crystal system	Monoclinic
Space group	P21/c
Unit cell dimensions	a = 12.624(6) Å α = 90°. b = 6.874(3) Å β = 101.420(13)°. c = 25.203(11) Å γ = 90°.
Volume	2143.8(17) Å ³
Z	4
Density (calculated)	1.362 Mg/m ³
Absorption coefficient	0.188 mm ⁻¹
F(000)	928
Crystal size	0.58 x 0.08 x 0.02 mm
Theta range for data collection	1.65 to 25.00°.
Index ranges	-15 ≤ h ≤ 15, -7 ≤ k ≤ 8, -29 ≤ l ≤ 29
Reflections collected	11784
Independent reflections	3758 [R(int) = 0.1360]
Completeness to theta = 25.00°	99.9 %
Absorption correction Semi-empirical from equivalents	
Max. and min. transmission	1.00 and 0.808
Refinement method	Full-matrix least-squares on F ²
Data / restraints / parameters	3758 / 0 / 283
Goodness-of-fit on F ²	1.152
Final R indices [I > 2σ(I)]	R1 = 0.0979, wR2 = 0.1819
R indices (all data)	R1 = 0.1799, wR2 = 0.2233
Largest diff. peak and hole	0.359 and -0.455 e.Å ⁻³

Table 6.8. Atomic coordinates ($\times 10^4$) and equivalent isotropic displacement parameters ($\text{\AA}^2 \times 10^3$) for **2.33g**.

U(eq) is defined as one third of the trace of the orthogonalized U^{ij} tensor.

	x	y	z	U(eq)
C1	3645(5)	9055(8)	496(2)	30(2)
C2	3353(5)	11031(9)	663(2)	35(2)
C3	2811(4)	11003(8)	1162(2)	29(1)
C4	3362(4)	9536(8)	1579(2)	29(1)
C5	3092(5)	9535(9)	2097(2)	34(2)
C6	3572(5)	8265(9)	2489(2)	35(2)
C7	4360(5)	6964(9)	2384(2)	32(2)
C8	4633(5)	6905(9)	1884(2)	28(1)
C9	4137(4)	8179(8)	1475(2)	26(1)
C10	1624(5)	10463(9)	1007(2)	36(2)
C11	821(5)	11663(9)	1071(3)	36(2)
C12	1016(5)	13652(9)	1296(3)	40(2)
C13	2154(5)	14209(9)	1462(3)	38(2)
C14	2951(5)	13004(9)	1407(2)	37(2)
C15	2871(5)	6153(9)	67(3)	40(2)
C16	1790(6)	5221(9)	-135(3)	52(2)
C17	-541(5)	9312(9)	726(3)	51(2)
C18	6577(5)	8420(9)	1248(2)	33(2)
C19	6704(5)	10327(10)	1136(3)	40(2)
C20	7556(5)	11416(9)	1437(2)	39(2)

Table 6.8., cont.

C21	8265(5)	10516(11)	1863(3)	45(2)
C22	8129(6)	8597(12)	1960(3)	61(2)
C23	7278(5)	7504(11)	1653(3)	54(2)
C24	9174(6)	11680(12)	2201(3)	64(2)
N1	4414(4)	8109(7)	946(2)	29(1)
O1	5605(3)	5119(6)	1016(2)	38(1)
O2	5560(3)	7482(6)	278(2)	40(1)
O3	2706(3)	7925(6)	332(2)	38(1)
O4	-253(3)	11237(6)	931(2)	45(1)
O5	285(4)	14719(6)	1352(2)	54(1)
S1	5532(1)	7104(2)	835(1)	34(1)

Table 6.9. Bond lengths [\AA] and angles [$^\circ$] for **2.33g**.

Lengths:

C1-O3	1.409(7)
C1-N1	1.488(7)
C1-C2	1.489(8)
C1-H1	1.00
C2-C3	1.546(8)
C2-H2A	0.99
C2-H2B	0.99
C3-C14	1.504(8)
C3-C10	1.518(8)
C3-C4	1.522(8)
C4-C5	1.412(8)
C4-C9	1.413(8)
C5-C6	1.368(8)
C5-H5	0.95
C6-C7	1.402(8)
C6-H6	0.95
C7-C8	1.370(8)
C7-H7	0.95
C8-C9	1.403(8)
C8-H8	0.95
C9-N1	1.445(7)
C10-C11	1.341(8)

Table 6.9., cont.

C10-H10	0.95
C11-O4	1.363(7)
C11-C12	1.482(9)
C12-O5	1.209(7)
C12-C13	1.465(8)
C13-C14	1.330(8)
C13-H13	0.95
C14-H14	0.95
C15-O3	1.424(7)
C15-C16	1.502(8)
C15-H15A	0.99
C15-H15B	0.99
C16-H16A	0.98
C16-H16B	0.98
C16-H16C	0.98
C17-O4	1.441(7)
C17-H17A	0.98
C17-H17B	0.98
C17-H17C	0.98
C18-C19	1.357(8)
C18-C23	1.365(8)
C18-S1	1.760(6)
C19-C20	1.403(8)
C19-H19	0.95

Table 6.9., cont.

C20-C21	1.398(9)
C20-H20	0.95
C21-C22	1.359(10)
C21-C24	1.516(9)
C22-C23	1.410(9)
C22-H22	0.95
C23-H23	0.95
C24-H24A	0.98
C24-H24B	0.98
C24-H24C	0.98
N1-S1	1.643(5)
O1-S1	1.436(4)
O2-S1	1.435(4)
<u>Angles:</u>	
O3-C1-N1	111.6(5)
O3-C1-C2	110.2(5)
N1-C1-C2	110.1(5)
O3-C1-H1	108.3
N1-C1-H1	108.3
C2-C1-H1	108.3
C1-C2-C3	113.1(5)
C1-C2-H2A	109.0
C3-C2-H2A	109.0

Table 6.9., cont.

C1-C2-H2B	109.0
C3-C2-H2B	109.0
H2A-C2-H2B	107.8
C14-C3-C10	111.1(5)
C14-C3-C4	108.7(5)
C10-C3-C4	108.0(5)
C14-C3-C2	106.8(5)
C10-C3-C2	111.5(5)
C4-C3-C2	110.8(5)
C5-C4-C9	118.4(5)
C5-C4-C3	118.5(5)
C9-C4-C3	123.1(5)
C6-C5-C4	121.0(6)
C6-C5-H5	119.5
C4-C5-H5	119.5
C5-C6-C7	119.9(6)
C5-C6-H6	120.0
C7-C6-H6	120.0
C8-C7-C6	120.7(6)
C8-C7-H7	119.7
C6-C7-H7	119.7
C7-C8-C9	120.0(5)
C7-C8-H8	120.0

Table 6.9., cont.

C9-C8-H8	120.0
C8-C9-C4	119.9(5)
C8-C9-N1	120.2(5)
C4-C9-N1	119.8(5)
C11-C10-C3	123.3(6)
C11-C10-H10	118.3
C3-C10-H10	118.3
C10-C11-O4	125.0(6)
C10-C11-C12	122.8(6)
O4-C11-C12	112.2(5)
O5-C12-C13	122.4(6)
O5-C12-C11	122.1(6)
C13-C12-C11	115.4(6)
C14-C13-C12	121.8(6)
C14-C13-H13	119.1
C12-C13-H13	119.1
C13-C14-C3	125.6(6)
C13-C14-H14	117.2
C3-C14-H14	117.2
O3-C15-C16	108.5(5)
O3-C15-H15A	110.0
C16-C15-H15A	110.0
O3-C15-H15B	110.0
C16-C15-H15B	110.0

Table 6.9., cont.

H15A-C15-H15B	108.4
C15-C16-H16A	109.5
C15-C16-H16B	109.5
H16A-C16-H16B	109.5
C15-C16-H16C	109.5
H16A-C16-H16C	109.5
H16B-C16-H16C	109.5
O4-C17-H17A	109.5
O4-C17-H17B	109.5
H17A-C17-H17B	109.5
O4-C17-H17C	109.5
H17A-C17-H17C	109.5
H17B-C17-H17C	109.5
C19-C18-C23	121.0(6)
C19-C18-S1	118.6(5)
C23-C18-S1	120.3(5)
C18-C19-C20	120.8(6)
C18-C19-H19	119.6
C20-C19-H19	119.6
C21-C20-C19	119.0(6)
C21-C20-H20	120.5
C19-C20-H20	120.5
C22-C21-C20	118.9(6)
C22-C21-C24	121.3(7)

Table 6.9., cont.

C20-C21-C24	119.8(7)
C21-C22-C23	121.8(7)
C21-C22-H22	119.1
C23-C22-H22	119.1
C18-C23-C22	118.4(7)
C18-C23-H23	120.8
C22-C23-H23	120.8
C21-C24-H24A	109.5
C21-C24-H24B	109.5
H24A-C24-H24B	109.5
C21-C24-H24C	109.5
H24A-C24-H24C	109.5
H24B-C24-H24C	109.5
C9-N1-C1	116.5(4)
C9-N1-S1	122.9(4)
C1-N1-S1	120.5(4)
C1-O3-C15	114.7(5)
C11-O4-C17	117.2(5)
O2-S1-O1	118.1(3)
O2-S1-N1	106.1(3)
O1-S1-N1	110.4(3)
O2-S1-C18	109.0(3)
O1-S1-C18	107.9(3)
N1-S1-C18	104.6(3)

Table 6.10. Anisotropic displacement parameters ($\text{\AA}^2 \times 10^3$) for **2.33g**

The anisotropic displacement factor exponent takes the form: $-2\pi^2 [h^2 a^{*2} U^{11} + \dots + 2 h k a^* b^* U^{12}]$

	U^{11}	U^{22}	U^{33}	U^{23}	U^{13}	U^{12}
C1	28(3)	30(3)	31(3)	7(3)	1(3)	1(3)
C2	44(4)	32(4)	28(4)	2(3)	5(3)	1(3)
C3	25(3)	28(3)	32(4)	-1(3)	5(3)	4(3)
C4	24(3)	26(3)	33(4)	-3(3)	-1(3)	-4(3)
C5	42(4)	38(4)	24(3)	2(3)	15(3)	1(3)
C6	42(4)	36(4)	28(4)	-5(3)	12(3)	-2(3)
C7	32(4)	30(3)	30(4)	11(3)	-2(3)	4(3)
C8	29(3)	31(3)	23(3)	2(3)	0(3)	4(3)
C9	21(3)	28(3)	30(3)	-6(3)	3(3)	-7(3)
C10	28(4)	38(4)	37(4)	0(3)	-2(3)	-1(3)
C11	22(3)	41(4)	43(4)	3(3)	2(3)	2(3)
C12	34(4)	40(4)	44(4)	-2(4)	7(3)	4(3)
C13	42(4)	28(4)	42(4)	-4(3)	-1(3)	-7(3)
C14	40(4)	35(4)	35(4)	0(3)	3(3)	-2(3)
C15	41(4)	26(3)	50(4)	-13(3)	1(3)	1(3)
C16	53(5)	36(4)	58(5)	-8(4)	-9(4)	-7(4)
C17	34(4)	39(4)	78(6)	-9(4)	7(4)	-9(3)
C18	27(3)	39(4)	32(4)	0(3)	6(3)	0(3)

Table 6.10., cont.

C19	37(4)	46(4)	37(4)	10(4)	7(3)	0(3)
C20	40(4)	34(4)	42(4)	0(3)	9(3)	-7(3)
C21	32(4)	63(5)	39(4)	6(4)	2(3)	-6(4)
C22	35(4)	81(6)	61(5)	19(5)	-6(4)	-9(4)
C23	36(4)	59(5)	62(5)	19(4)	-2(4)	-4(4)
C24	41(5)	84(6)	63(5)	-10(5)	-1(4)	-21(4)
N1	27(3)	31(3)	28(3)	-1(2)	4(2)	4(2)
O1	41(3)	23(2)	52(3)	3(2)	13(2)	6(2)
O2	42(3)	53(3)	26(2)	-1(2)	11(2)	5(2)
O3	38(3)	34(2)	37(2)	-7(2)	-2(2)	2(2)
O4	24(2)	43(3)	65(3)	-4(3)	2(2)	1(2)
O5	41(3)	36(3)	85(4)	-2(3)	10(3)	11(2)
S1	31(1)	35(1)	36(1)	-1(1)	9(1)	3(1)

Table 6.11. Hydrogen coordinates ($\times 10^4$) and isotropic displacement parameters ($\text{\AA}^2 \times 10^{-3}$) for **2.33g**

	x	y	z	U(eq)
H1	4010	9198	181	37
H2A	2856	11649	357	42
H2B	4016	11836	747	42
H5	2568	10430	2173	40
H6	3372	8265	2833	42
H7	4707	6113	2661	38
H8	5159	6002	1815	34
H10	1441	9211	857	43
H13	2328	15463	1612	46
H14	3669	13445	1535	45
H15A	3336	5270	323	48
H15B	3233	6416	-240	48
H16A	1458	4887	174	78
H16B	1885	4037	-337	78
H16C	1321	6131	-373	78
H17A	-291	9125	385	77
H17B	-1327	9159	662	77
H17C	-199	8344	991	77
H19	6210	10932	851	48
H20	7650	12744	1352	47
H22	8620	7975	2244	73

Table 6.11., cont.

H23	7196	6162	1726	64
H24A	9055	11781	2573	96
H24B	9190	12986	2047	96
H24C	9864	11026	2203	96

Table 6.12. Torsion angles [°] for **2.33g**

O3-C1-C2-C3	63.5(6)
N1-C1-C2-C3	-60.0(6)
C1-C2-C3-C14	158.9(5)
C1-C2-C3-C10	-79.7(6)
C1-C2-C3-C4	40.6(7)
C14-C3-C4-C5	52.8(7)
C10-C3-C4-C5	-67.8(7)
C2-C3-C4-C5	169.8(5)
C14-C3-C4-C9	-126.8(6)
C10-C3-C4-C9	112.6(6)
C2-C3-C4-C9	-9.8(8)
C9-C4-C5-C6	0.5(9)
C3-C4-C5-C6	-179.2(5)
C4-C5-C6-C7	1.2(9)
C5-C6-C7-C8	-2.0(9)
C6-C7-C8-C9	1.1(9)
C7-C8-C9-C4	0.6(8)
C7-C8-C9-N1	-179.3(5)
C5-C4-C9-C8	-1.4(8)
C3-C4-C9-C8	178.3(5)
C5-C4-C9-N1	178.6(5)
C3-C4-C9-N1	-1.8(8)
C14-C3-C10-C11	1.7(9)

Table 6.12., cont.

C4-C3-C10-C11	120.9(7)
C2-C3-C10-C11	-117.2(7)
C3-C10-C11-O4	179.3(5)
C3-C10-C11-C12	0.6(10)
C10-C11-C12-O5	-179.9(7)
O4-C11-C12-O5	1.2(9)
C10-C11-C12-C13	-1.9(10)
O4-C11-C12-C13	179.3(5)
O5-C12-C13-C14	178.6(7)
C11-C12-C13-C14	0.6(10)
C12-C13-C14-C3	2.1(11)
C10-C3-C14-C13	-3.1(9)
C4-C3-C14-C13	-121.8(7)
C2-C3-C14-C13	118.6(7)
C23-C18-C19-C20	-0.6(10)
S1-C18-C19-C20	-176.9(5)
C18-C19-C20-C21	-1.2(10)
C19-C20-C21-C22	2.3(10)
C19-C20-C21-C24	-178.5(6)
C20-C21-C22-C23	-1.6(12)
C24-C21-C22-C23	179.2(7)
C19-C18-C23-C22	1.3(10)
S1-C18-C23-C22	177.6(5)
C21-C22-C23-C18	-0.2(12)

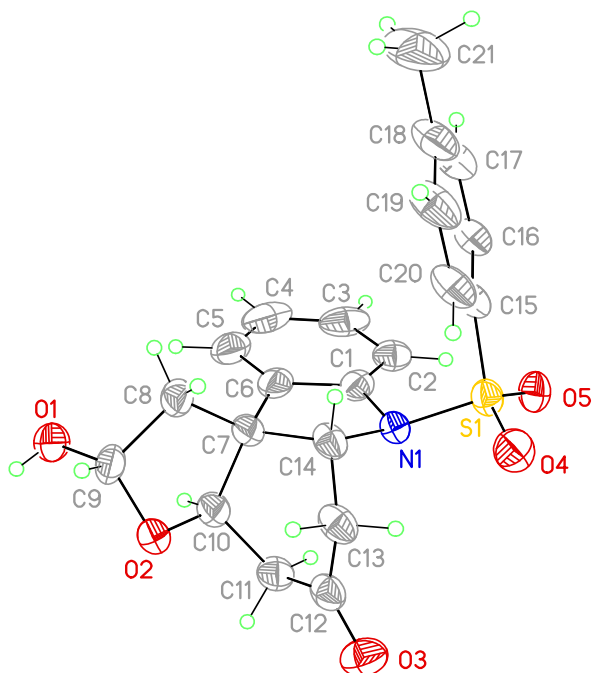
Table 6.12., cont.

C8-C9-N1-C1	162.4(5)
C4-C9-N1-C1	-17.5(7)
C8-C9-N1-S1	-19.3(7)
C4-C9-N1-S1	160.7(4)
O3-C1-N1-C9	-74.9(6)
C2-C1-N1-C9	47.9(6)
O3-C1-N1-S1	106.8(5)
C2-C1-N1-S1	-130.4(5)
N1-C1-O3-C15	-68.8(6)
C2-C1-O3-C15	168.5(5)
C16-C15-O3-C1	-174.1(5)
C10-C11-O4-C17	3.4(10)
C12-C11-O4-C17	-177.8(5)
C9-N1-S1-O2	-174.8(4)
C1-N1-S1-O2	3.4(5)
C9-N1-S1-O1	56.1(5)
C1-N1-S1-O1	-125.7(4)
C9-N1-S1-C18	-59.7(5)
C1-N1-S1-C18	118.5(4)
C19-C18-S1-O2	47.5(6)
C23-C18-S1-O2	-128.8(5)
C19-C18-S1-O1	176.8(5)
C23-C18-S1-O1	0.5(6)
C19-C18-S1-N1	-65.7(6)
C23-C18-S1-N1	118.0(6)

6.3 CRYSTALLOGRAPHY DATA FOR COMPOUND **2.81**

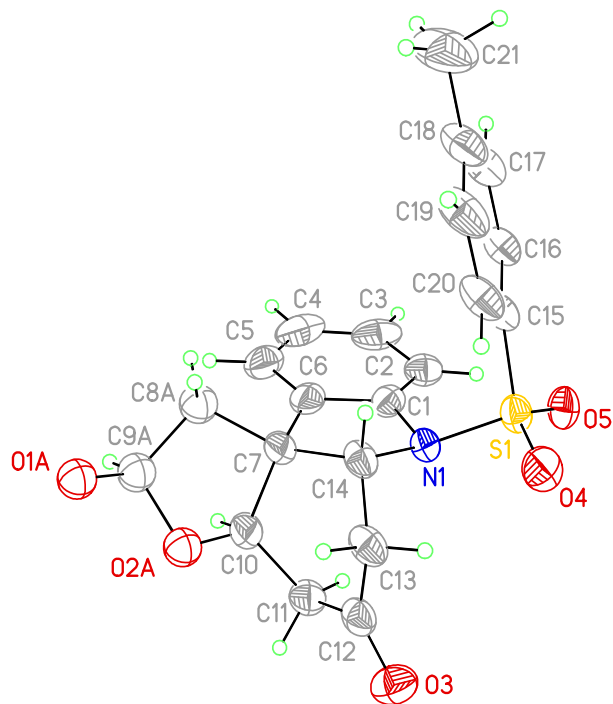
View of **2.81** showing the atom labeling scheme. Displacement ellipsoids are scaled to the 50% probability level. The diastereomer shown has an R, S, R configuration at C7, C9 and C14, respectively.

Figure 6.3. X-ray Structure of **2.81**



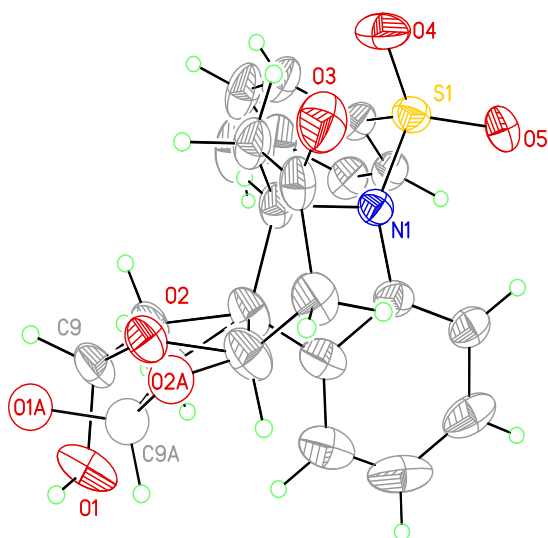
View of **2.81** showing the atom labeling scheme. Displacement ellipsoids are scaled to the 50% probability level. The diastereomer shown has an R, R, R configuration at C7, C9a and C14, respectively. The hydrogen atom on O9a was not included in the refinement model.

Figure 6.4. X-ray Structure of **2.81**



View of **2.81** showing the overlap of the two diastereomers found in the crystal. The diastereomers are present in a 4:1 ratio. The major component is composed of atoms O1, O2, C8 (not labeled) and C9.

Figure 6.5. X-ray Structure of **2.81**



X-ray Experimental for $C_{21}H_{21}NO_5S$: Crystals grew as colorless prisms by slow cooling from MeOH. The data crystal was cut from a cluster of crystals and had approximate dimensions; 0.24 x 0.22 x 0.20 mm. The data were collected on a Rigaku SCX-Mini diffractometer with a Mercury 2 CCD using a graphite monochromator with MoK α radiation ($\lambda = 0.71075\text{\AA}$). A total of 1080 frames of data were collected using ω -scans with a scan range of 0.5° and a counting time of 25 seconds per frame. The data were collected at 153 K using a Rigaku XStream low temperature device. Details of crystal data, data collection and structure refinement are listed in Table 6.13. Data reduction were performed using the Rigaku Americas Corporation's Crystal Clear version 1.40.³⁰¹ The structure was solved by direct methods using SIR97³⁰² and refined by full-matrix least-squares on F^2 with anisotropic displacement parameters for the non-H atoms using SHELXL-97.³⁰³ Structure analysis was aided by use of the programs PLATON98³⁰⁴ and WinGX.³⁰⁵ The hydrogen atoms on carbon were calculated in ideal positions with isotropic displacement parameters set to $1.2 \times U_{eq}$ of the attached atom

(1.5xUeq for methyl hydrogen atoms). The hydrogen atom on O9 was observed in a ΔF map and refined with an isotropic displacement parameter.

The crystal was a racemic twin. In addition, the molecule appeared to be disordered. The apparent disorder was due to the presence of a small amount of a different diastereomer at C9. The chiral carbon atoms in the molecule are C7, C9 and C14, which are R, S, R in the major component in the refinement model. Inversion at C9 yields the R, R, R diastereomer in a 4:1 ratio. This ratio was determined by refining the site occupancy factors for the two components. No hydrogen atom for the minor hydroxyl oxygen atom, O9a, was included in the final refinement model.

The function, $\sum w(|F_o|^2 - |F_c|^2)^2$, was minimized, where $w = 1/[(\sigma(F_o))^2 + (0.0589*P)^2 + (0.8331*P)]$ and $P = (|F_o|^2 + 2|F_c|^2)/3$. $R_w(F^2)$ refined to 0.140, with $R(F)$ equal to 0.0610 and a goodness of fit, S , = 1.10. Definitions used for calculating $R(F)$, $R_w(F^2)$ and the goodness of fit, S , are given below.³⁰⁶ The data were corrected for secondary extinction effects. The correction takes the form: $F_{corr} = kF_c/[1 + (4.9(8) \times 10^{-6}) * F_c^2 \lambda^3 / (\sin 2\theta)]^{0.25}$ where k is the overall scale factor. Neutral atom scattering factors and values used to calculate the linear absorption coefficient are from the International Tables for X-ray Crystallography (1992).³⁰⁷ All figures were generated using SHELXTL/PC.³⁰⁸ Tables of positional and thermal parameters, bond lengths and angles, torsion angles and figures are found elsewhere.

Table 6.13. Crystal data and structure refinement for **2.81**.

Empirical formula	C ₂₁ H ₂₁ N O ₅ S
Formula weight	399.45
Temperature	153(2) K
Wavelength	0.71075 Å
Crystal system	Tetragonal
Space group	P41212
Unit cell dimensions	a = 10.487(7) Å α = 90°. b = 10.487(7) Å β = 90°. c = 35.25(4) Å γ = 90°.
Volume	3877(6) Å ³
Z	8
Density (calculated)	1.369 Mg/m ³
Absorption coefficient	0.200 mm ⁻¹
F(000)	1680
Crystal size	0.24 x 0.22 x 0.20 mm
Theta range for data collection	2.26 to 27.50°.
Index ranges	-13 ≤ h ≤ 13, -13 ≤ k ≤ 13, -45 ≤ l ≤ 45
Reflections collected	38992
Independent reflections	4461 [R(int) = 0.1205]
Completeness to theta = 27.50°	99.9 %
Absorption correction Semi-empirical from equivalents	
Max. and min. transmission	1.00 and 0.774
Refinement method	Full-matrix least-squares on F ²
Data / restraints / parameters	4461 / 30 / 274
Goodness-of-fit on F ²	1.105
Final R indices [I > 2σ(I)]	R1 = 0.0610, wR2 = 0.1342
R indices (all data)	R1 = 0.0720, wR2 = 0.1398
Absolute structure parameter	0.50(11)
Extinction coefficient	4.9(8) × 10 ⁻⁶
Largest diff. peak and hole	0.209 and -0.280 e.Å ⁻³

Table 6.14. Atomic coordinates ($\times 10^4$) and equivalent isotropic displacement parameters ($\text{\AA}^2 \times 10^3$) for **2.81**

U(eq) is defined as one third of the trace of the orthogonalized U_{ij} tensor.

	x	y	z	U(eq)
C1	-474(3)	2892(3)	617(1)	33(1)
C2	-717(3)	1754(3)	426(1)	38(1)
C3	-1142(3)	1861(4)	53(1)	51(1)
C4	-1342(3)	3044(5)	-116(1)	61(1)
C5	-1135(3)	4155(4)	87(1)	52(1)
C6	-700(3)	4072(3)	453(1)	40(1)
C7	-503(3)	5135(3)	740(1)	40(1)
C10	-1816(3)	5625(3)	881(1)	44(1)
C11	-2368(3)	4906(3)	1216(1)	41(1)
C12	-1473(3)	4821(3)	1544(1)	37(1)
C13	-69(3)	4935(3)	1451(1)	40(1)
C14	247(3)	4454(3)	1057(1)	34(1)
C15	2408(3)	2303(3)	890(1)	34(1)
C16	2554(3)	1658(3)	552(1)	37(1)
C17	3582(3)	1926(3)	323(1)	46(1)
C18	4474(3)	2838(4)	423(1)	54(1)
C19	4314(3)	3475(3)	766(1)	56(1)
C20	3295(3)	3221(3)	1001(1)	43(1)
C21	5600(4)	3106(5)	172(2)	85(2)
N1	-44(2)	3052(2)	1001(1)	29(1)
O1	-1365(3)	7812(4)	389(1)	54(1)

Table 6.14., cont.

O2	-1543(3)	6956(3)	1005(1)	37(1)
C8	190(4)	6381(4)	620(1)	39(1)
C9	-717(4)	7459(4)	722(1)	39(1)
O1A	-770(11)	8403(9)	608(3)	41
O2A	-1890(12)	6735(13)	873(3)	41
C8A	-170(16)	6246(14)	471(5)	41
C9A	-1249(14)	7183(11)	541(4)	41
O3	-1825(2)	4652(2)	1867(1)	50(1)
O4	1318(2)	2449(2)	1545(1)	50(1)
O5	582(2)	793(2)	1099(1)	42(1)
S1	1047(1)	2054(1)	1168(1)	34(1)

Table 6.15. Bond lengths [\AA] and angles [$^\circ$] for **2.81**

Lengths:

C1-C6	1.386(4)
C1-C2	1.394(4)
C1-N1	1.437(4)
C2-C3	1.392(5)
C2-H2	0.95
C3-C4	1.392(6)
C3-H3	0.95
C4-C5	1.383(6)
C4-H4	0.95
C5-C6	1.373(5)
C5-H5	0.95
C6-C7	1.519(5)
C7-C8A	1.541(18)
C7-C14	1.542(4)
C7-C10	1.551(4)
C7-C8	1.554(5)
C10-O2A	1.167(14)
C10-O2	1.491(5)
C10-C11	1.517(4)
C10-H10	1.00
C11-C12	1.490(5)
C11-H11A	0.99

Table 6.15., cont.

C11-H11B	0.99
C12-O3	1.213(4)
C12-C13	1.513(4)
C13-C14	1.515(4)
C13-H13A	0.99
C13-H13B	0.99
C14-N1	1.514(4)
C14-H14	1.00
C15-C16	1.380(4)
C15-C20	1.395(4)
C15-S1	1.751(3)
C16-C17	1.375(5)
C16-H16	0.95
C17-C18	1.384(5)
C17-H17	0.95
C18-C19	1.391(5)
C18-C21	1.501(5)
C19-C20	1.377(5)
C19-H19	0.95
C20-H20	0.95
C21-H21A	0.98
C21-H21B	0.98
C21-H21C	0.98

Table 6.15., Cont.

N1-S1	1.659(3)
O1-C9	1.405(5)
O1-H1O	0.72(5)
O2-C9	1.424(4)
C8-C9	1.520(5)
C8-H8A	0.99
C8-H8B	0.99
C9-H9A	1.00
O1A-C9A	1.394(10)
O1A-H1O	1.26(5)
O2A-C9A	1.428(10)
C8A-C9A	1.519(10)
C8A-H8AA	0.99
C8A-H8AB	0.99
C9A-H1O	1.43(5)
C9A-H9AA	1.00
O4-S1	1.420(3)
O5-S1	1.430(2)
<u>Angles:</u>	
C6-C1-C2	122.1(3)
C6-C1-N1	110.0(3)
C2-C1-N1	127.8(3)
C3-C2-C1	116.5(3)

Table 6.15., Cont.

C3-C2-H2	121.8
C1-C2-H2	121.8
C4-C3-C2	121.6(3)
C4-C3-H3	119.2
C2-C3-H3	119.2
C5-C4-C3	120.5(3)
C5-C4-H4	119.8
C3-C4-H4	119.8
C6-C5-C4	118.9(3)
C6-C5-H5	120.5
C4-C5-H5	120.5
C5-C6-C1	120.4(3)
C5-C6-C7	128.7(3)
C1-C6-C7	110.8(3)
C6-C7-C8A	100.2(7)
C6-C7-C14	102.2(2)
C8A-C7-C14	132.8(7)
C6-C7-C10	109.7(3)
C8A-C7-C10	98.5(5)
C14-C7-C10	111.9(3)
C6-C7-C8	120.1(3)
C14-C7-C8	110.3(3)
C10-C7-C8	102.9(3)

Table 6.15., Cont.

O2A-C10-C11	119.3(6)
O2-C10-C11	108.1(3)
O2A-C10-C7	112.5(6)
O2-C10-C7	103.5(3)
C11-C10-C7	115.1(3)
O2A-C10-H10	86.1
O2-C10-H10	110.0
C11-C10-H10	110.0
C7-C10-H10	110.0
C12-C11-C10	113.1(3)
C12-C11-H11A	108.9
C10-C11-H11A	108.9
C12-C11-H11B	108.9
C10-C11-H11B	108.9
H11A-C11-H11B	107.8
O3-C12-C11	123.1(3)
O3-C12-C13	120.8(3)
C11-C12-C13	116.1(3)
C12-C13-C14	112.6(3)
C12-C13-H13A	109.1
C14-C13-H13A	109.1
C12-C13-H13B	109.1
C14-C13-H13B	109.1

Table 6.15., Cont.

H13A-C13-H13B	107.8
N1-C14-C13	113.5(2)
N1-C14-C7	104.7(2)
C13-C14-C7	113.5(3)
N1-C14-H14	108.3
C13-C14-H14	108.3
C7-C14-H14	108.3
C16-C15-C20	120.3(3)
C16-C15-S1	120.1(2)
C20-C15-S1	119.4(2)
C17-C16-C15	119.6(3)
C17-C16-H16	120.2
C15-C16-H16	120.2
C16-C17-C18	121.4(3)
C16-C17-H17	119.3
C18-C17-H17	119.3
C17-C18-C19	118.1(3)
C17-C18-C21	120.7(4)
C19-C18-C21	121.1(4)
C20-C19-C18	121.5(3)
C20-C19-H19	119.2
C18-C19-H19	119.2
C19-C20-C15	118.9(3)

Table 6.15., Cont.

C19-C20-H20	120.5
C15-C20-H20	120.5
C18-C21-H21A	109.5
C18-C21-H21B	109.5
H21A-C21-H21B	109.5
C18-C21-H21C	109.5
H21A-C21-H21C	109.5
H21B-C21-H21C	109.5
C1-N1-C14	107.4(2)
C1-N1-S1	118.57(19)
C14-N1-S1	115.32(18)
C9-O1-H1O	114(4)
C9-O2-C10	105.0(3)
C9-C8-C7	105.6(3)
C9-C8-H8A	110.6
C7-C8-H8A	110.6
C9-C8-H8B	110.6
C7-C8-H8B	110.6
H8A-C8-H8B	108.8
O1-C9-O2	112.9(3)
O1-C9-C8	107.6(3)
O2-C9-C8	105.7(3)
O1-C9-H9A	110.2

Table 6.15., Cont.

O2-C9-H9A	110.2
C8-C9-H9A	110.2
C10-O2A-C9A	108.5(10)
C9A-C8A-C7	102.7(10)
C9A-C8A-H8AA	111.2
C7-C8A-H8AA	111.2
C9A-C8A-H8AB	111.2
C7-C8A-H8AB	111.2
H8AA-C8A-H8AB	109.1
O1A-C9A-O2A	109.5(10)
O1A-C9A-C8A	110.7(11)
O2A-C9A-C8A	105.7(11)
O1A-C9A-H9AA	110.3
O2A-C9A-H9AA	110.3
C8A-C9A-H9AA	110.3
O4-S1-O5	119.80(15)
O4-S1-N1	106.67(13)
O5-S1-N1	106.69(13)
O4-S1-C15	108.53(16)
O5-S1-C15	108.69(14)
N1-S1-C15	105.57(14)

Table 6.16. Anisotropic displacement parameters ($\text{\AA}^2 \times 10^3$) for **2.81**.

The anisotropic displacement factor exponent takes the form: $-2\pi^2 [h^2 a^{*2} U^{11} + \dots + 2 h k a^* b^* U^{12}]$

	U^{11}	U^{22}	U^{33}	U^{23}	U^{13}	U^{12}
C1	25(1)	42(2)	32(1)	5(1)	0(1)	0(1)
C2	29(2)	47(2)	37(2)	-4(1)	1(1)	-2(1)
C3	28(2)	88(3)	38(2)	-11(2)	4(1)	-9(2)
C4	31(2)	120(4)	32(2)	14(2)	2(1)	6(2)
C5	37(2)	76(3)	43(2)	19(2)	9(2)	12(2)
C6	26(2)	53(2)	40(2)	13(2)	7(1)	6(1)
C7	35(2)	34(2)	50(2)	10(1)	14(1)	9(1)
C10	37(2)	42(2)	54(2)	13(2)	12(2)	11(1)
C11	29(2)	43(2)	52(2)	7(2)	9(1)	3(1)
C12	39(2)	24(1)	49(2)	-2(1)	5(1)	-1(1)
C13	38(2)	28(2)	53(2)	-8(1)	0(1)	1(1)
C14	26(1)	27(1)	50(2)	1(1)	2(1)	0(1)
C15	27(1)	31(2)	42(2)	-8(1)	-6(1)	5(1)
C16	30(1)	35(2)	47(2)	-7(1)	-4(1)	5(1)
C17	39(2)	44(2)	55(2)	-10(2)	-2(2)	9(1)
C18	34(2)	45(2)	82(3)	-7(2)	8(2)	8(2)
C19	29(2)	39(2)	99(3)	-20(2)	-3(2)	0(1)
C20	29(2)	37(2)	63(2)	-15(2)	-8(1)	5(1)
C21	43(2)	80(3)	133(4)	-11(3)	33(3)	-8(2)
N1	28(1)	27(1)	31(1)	1(1)	-2(1)	3(1)

Table 6.16., Cont.

O1	57(2)	61(2)	45(2)	21(2)	6(2)	27(2)
O2	37(2)	31(1)	41(2)	3(1)	3(1)	6(1)
C8	33(2)	33(2)	52(2)	13(2)	5(2)	0(2)
C9	42(2)	32(2)	43(2)	15(2)	2(2)	2(2)
O3	54(2)	52(2)	46(1)	-3(1)	10(1)	-10(1)
O4	61(2)	59(2)	31(1)	-5(1)	-13(1)	16(1)
O5	51(1)	26(1)	48(1)	7(1)	-1(1)	-1(1)
S1	38(1)	32(1)	33(1)	0(1)	-6(1)	5(1)

Table 6.17. Hydrogen coordinates ($\times 10^4$) and isotropic displacement parameters ($\text{\AA}^2 \times 10^{-3}$) for **2.81**

	x	y	z	U(eq)
H2	-598	947	543	45
H3	-1298	1109	-90	62
H4	-1624	3089	-371	73
H5	-1291	4963	-26	62
H10	-2441	5631	667	53
H11A	-3159	5337	1300	49
H11B	-2598	4033	1134	49
H13A	429	4443	1639	47
H13B	190	5840	1471	47
H14	1178	4590	1011	41
H16	1948	1033	477	45
H17	3681	1476	91	55
H19	4922	4100	840	67
H20	3199	3665	1234	52
H21A	5899	3979	216	128
H21B	5348	3012	-94	128
H21C	6286	2504	230	128
H8A	1006	6473	759	47
H8B	370	6379	345	47
H9A	-229	8202	825	47
H1O	-1770(50)	8360(50)	412(13)	44(14)
H8AA	666	6625	536	41
H8AB	-154	5962	203	41
H9AA	-1846	7194	320	41

Table 6.18. Torsion angles [°] for **2.81**

C6-C1-C2-C3	3.0(4)
N1-C1-C2-C3	179.3(3)
C1-C2-C3-C4	-1.5(5)
C2-C3-C4-C5	-0.7(5)
C3-C4-C5-C6	1.5(5)
C4-C5-C6-C1	-0.1(5)
C4-C5-C6-C7	-174.6(3)
C2-C1-C6-C5	-2.3(4)
N1-C1-C6-C5	-179.2(3)
C2-C1-C6-C7	173.2(3)
N1-C1-C6-C7	-3.7(3)
C5-C6-C7-C8A	-30.7(7)
C1-C6-C7-C8A	154.3(6)
C5-C6-C7-C14	-168.9(3)
C1-C6-C7-C14	16.1(3)
C5-C6-C7-C10	72.2(4)
C1-C6-C7-C10	-102.7(3)
C5-C6-C7-C8	-46.5(5)
C1-C6-C7-C8	138.5(3)
C6-C7-C10-O2A	-131.6(7)
C8A-C7-C10-O2A	-27.5(10)
C14-C7-C10-O2A	115.7(8)
C8-C7-C10-O2A	-2.7(8)

Table 6.18., Cont.

C6-C7-C10-O2	-155.0(2)
C8A-C7-C10-O2	-50.9(7)
C14-C7-C10-O2	92.3(3)
C8-C7-C10-O2	-26.1(3)
C6-C7-C10-C11	87.3(4)
C8A-C7-C10-C11	-168.6(7)
C14-C7-C10-C11	-25.4(4)
C8-C7-C10-C11	-143.8(3)
O2A-C10-C11-C12	-84.9(9)
O2-C10-C11-C12	-61.7(3)
C7-C10-C11-C12	53.4(4)
C10-C11-C12-O3	156.7(3)
C10-C11-C12-C13	-24.3(4)
O3-C12-C13-C14	149.6(3)
C11-C12-C13-C14	-29.3(4)
C12-C13-C14-N1	-62.0(3)
C12-C13-C14-C7	57.4(3)
C6-C7-C14-N1	-21.5(3)
C8A-C7-C14-N1	-138.1(7)
C10-C7-C14-N1	95.8(3)
C8-C7-C14-N1	-150.3(3)
C6-C7-C14-C13	-145.8(2)
C8A-C7-C14-C13	97.7(8)

Table 6.18., Cont.

C10-C7-C14-C13	-28.5(4)
C8-C7-C14-C13	85.4(3)
C20-C15-C16-C17	0.0(5)
S1-C15-C16-C17	175.5(2)
C15-C16-C17-C18	-0.4(5)
C16-C17-C18-C19	0.6(5)
C16-C17-C18-C21	179.2(4)
C17-C18-C19-C20	-0.4(5)
C21-C18-C19-C20	-179.0(4)
C18-C19-C20-C15	0.0(5)
C16-C15-C20-C19	0.2(5)
S1-C15-C20-C19	-175.3(3)
C6-C1-N1-C14	-10.9(3)
C2-C1-N1-C14	172.4(3)
C6-C1-N1-S1	-143.8(2)
C2-C1-N1-S1	39.6(4)
C13-C14-N1-C1	144.8(3)
C7-C14-N1-C1	20.5(3)
C13-C14-N1-S1	-80.5(3)
C7-C14-N1-S1	155.16(18)
O2A-C10-O2-C9	-73.7(14)
C11-C10-O2-C9	164.0(3)
C7-C10-O2-C9	41.5(3)

Table 6.18., Cont.

C6-C7-C8-C9	125.4(3)
C8A-C7-C8-C9	85.5(12)
C14-C7-C8-C9	-116.3(3)
C10-C7-C8-C9	3.2(4)
C10-O2-C9-O1	77.6(4)
C10-O2-C9-C8	-39.7(4)
C7-C8-C9-O1	-98.7(4)
C7-C8-C9-O2	22.1(4)
O2-C10-O2A-C9A	109.9(18)
C11-C10-O2A-C9A	177.1(8)
C7-C10-O2A-C9A	37.8(12)
C6-C7-C8A-C9A	117.5(10)
C14-C7-C8A-C9A	-125.1(9)
C10-C7-C8A-C9A	5.6(11)
C8-C7-C8A-C9A	-96.8(15)
C10-O2A-C9A-O1A	-150.9(12)
C10-O2A-C9A-C8A	-31.6(15)
C7-C8A-C9A-O1A	130.7(12)
C7-C8A-C9A-O2A	12.1(14)
C1-N1-S1-O4	178.4(2)
C14-N1-S1-O4	49.1(2)
C1-N1-S1-O5	-52.4(2)
C14-N1-S1-O5	178.23(19)
C1-N1-S1-C15	63.1(2)

Table 6.18., Cont.

C14-N1-S1-C15	-66.2(2)
C16-C15-S1-O4	159.9(2)
C20-C15-S1-O4	-24.6(3)
C16-C15-S1-O5	28.1(3)
C20-C15-S1-O5	-156.4(2)
C16-C15-S1-N1	-86.1(3)
C20-C15-S1-N1	89.5(3)

Table 6.19. Hydrogen bonds for **2.81** [Å and °]

D-H...A	d(D-H)d(H...A)	d(D...A)	<(DHA)
O1-H1O...O3#1	0.72(5)2.14(5)2.840(5)		162(5)

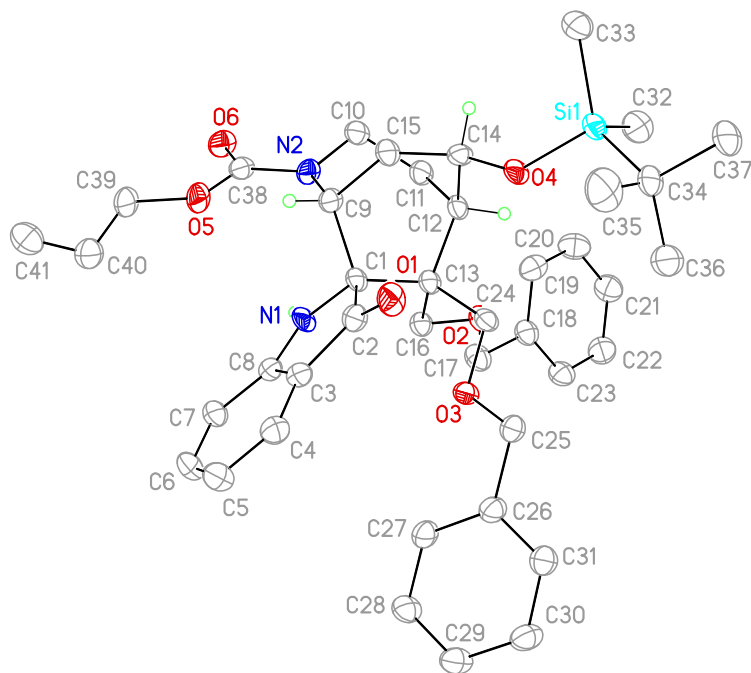
Symmetry transformations used to generate equivalent atoms:

#1 -x-1/2,y+1/2,-z+1/4

6.4 CRYSTALLOGRAPHY DATA FOR COMPOUND 4.86b

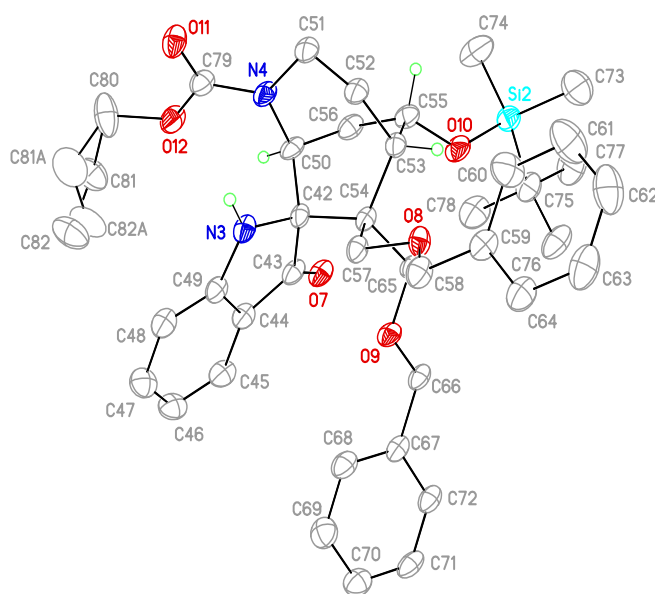
View of **4.86b** showing the atom labeling scheme. Displacement ellipsoids are scaled to the 50% probability level.

Figure 6.6. X-ray Structure of **4.86b**



View of **4.86b** showing the atom labeling scheme. Displacement ellipsoids are scaled to the 50% probability level.

Figure 6.7. X-ray Structure of **4.86b**



X-ray Experimental for complex $C_{41}H_{52}N_2O_6Si$: Crystals grew as long, colorless needles by cooling slowly in Hexanes. The data crystal had approximate dimensions; 0.41 x 0.03 x 0.02 mm. The data were collected on an Agilent Technologies SuperNova Dual Source diffractometer using a μ -focus Cu $K\alpha$ radiation source ($\lambda = 1.5418\text{\AA}$) with collimating mirror monochromators. A total of 1037 frames of data were collected using ω -scans with a scan range of 1° and a counting time of 16 seconds per frame with a detector offset of $\pm 40.8^\circ$ and 50 seconds per frame with a detector offset of $\pm 108.3^\circ$. The data were collected at 100 K using an Oxford Cryostream low temperature device. Details of crystal data, data collection and structure refinement are listed in Table 1. Data collection, unit cell refinement and data reduction were performed using Agilent

Technologies CrysAlisPro V 1.171.37.31.³⁰¹ The structure was solved by direct methods using SuperFlip³⁰² and refined by full-matrix least-squares on F^2 with anisotropic displacement parameters for the non-H atoms using SHELXL-2014/7.³⁰³ Structure analysis was aided by use of the programs PLATON98³⁰⁴ and WinGX.³⁰⁵ The hydrogen atoms were calculated in ideal positions with isotropic displacement parameters set to 1.2xUeq of the attached atom (1.5xUeq for methyl hydrogen atoms). The hydrogen atoms on nitrogen were observed in a ΔF map and refined with isotropic displacement parameters.

There are two molecules in the asymmetric unit. The ethylene group on one molecule was disordered about two positions. The disorder was modeled by assigning the variable x to the site occupancy for the atoms of one orientation, C81 and C82, and (1-x) the site occupancy for the atoms in the alternate orientation, C81a and C82a. The geometry for the two groups was restrained to be equivalent throughout the refinement process. A common isotropic displacement parameter was refined while refining the variable x. In this way, the site occupancy for the major component refined to 55(1)%.

The function, $\sum w(|F_o|^2 - |F_c|^2)^2$, was minimized, where $w = 1/[(\sigma(F_o))^2 + (0.0456 \cdot P)^2]$ and $P = (|F_o|^2 + 2|F_c|^2)/3$. $R_w(F^2)$ refined to 0.182, with $R(F)$ equal to 0.0697 and a goodness of fit, S , = 1.00. Definitions used for calculating $R(F)$, $R_w(F^2)$ and the goodness of fit, S , are given below.³⁰⁶ The data were checked for secondary extinction effects but no correction was necessary. Neutral atom scattering factors and values used to calculate the linear absorption coefficient are from the International Tables for X-ray Crystallography (1992).³⁰⁷ All figures were generated using SHELXTL/PC.³⁰⁸ Tables of positional and thermal parameters, bond lengths and angles, torsion angles and figures are found elsewhere.

Table 6.20. Crystal data and structure refinement for **4.86b**

Empirical formula	C ₄₁ H ₅₂ N ₂ O ₆ Si
Formula weight	696.93
Temperature	100(2) K
Wavelength	1.54184 Å
Crystal system	triclinic
Space group	P -1
Unit cell dimensions	a = 14.6462(12) Å α = 78.522(6)°. b = 17.2261(10) Å β = 66.733(7)°. c = 18.0845(13) Å γ = 67.941(7)°.
Volume	3877.9(6) Å ³
Z	4
Density (calculated)	1.194 Mg/m ³
Absorption coefficient	0.914 mm ⁻¹
F(000)	1496
Crystal size	0.410 x 0.030 x 0.020 mm ³
Theta range for data collection	2.664 to 74.239°.
Index ranges	-13 ≤ h ≤ 17, -14 ≤ k ≤ 21, -22 ≤ l ≤ 22
Reflections collected	23896
Independent reflections	15018 [R(int) = 0.0774]
Completeness to theta = 67.684°	98.8 %
Absorption correction	Semi-empirical from equivalents
Max. and min. transmission	1.00 and 0.647
Refinement method	Full-matrix least-squares on F ²
Data / restraints / parameters	15018 / 36 / 939
Goodness-of-fit on F ²	1.003
Final R indices	[I > 2σ(I)] R1 = 0.0697, wR2 = 0.1456
R indices (all data)	R1 = 0.1283, wR2 = 0.1820
Extinction coefficient	n/a
Largest diff. peak and hole	0.586 and -0.491 e.Å ⁻³

Table 6.21. Atomic coordinates ($\times 10^4$) and equivalent isotropic displacement parameters ($\text{\AA}^2 \times 10^3$) for **4.86b**

U(eq) is defined as one third of the trace of the orthogonalized U^{ij} tensor.

	x	y	z	U(eq)
C1	2214(3)	5973(2)	6750(2)	21(1)
C2	1013(3)	6262(2)	6854(2)	24(1)
C3	907(3)	5668(2)	6451(2)	25(1)
C4	12(3)	5616(2)	6380(2)	28(1)
C5	152(3)	4986(3)	5933(3)	34(1)
C6	1156(3)	4429(3)	5569(2)	32(1)
C7	2049(3)	4465(2)	5640(2)	28(1)
C8	1904(3)	5093(2)	6106(2)	23(1)
C9	2644(3)	6681(2)	6206(2)	22(1)
C10	4428(3)	6482(2)	6243(2)	26(1)
C11	4180(3)	6118(2)	7119(2)	26(1)
C12	2999(3)	6364(2)	7636(2)	23(1)
C13	2413(3)	5797(2)	7573(2)	22(1)
C14	2473(3)	7299(2)	7460(2)	24(1)
C15	2252(3)	7460(2)	6669(2)	25(1)
C16	3055(3)	4861(2)	7647(2)	24(1)
C17	3869(3)	3863(2)	8490(2)	31(1)
C18	4460(3)	3802(2)	9029(2)	28(1)
C19	5021(3)	4344(3)	8877(3)	34(1)
C20	5590(3)	4281(3)	9349(3)	40(1)

Table 6.21., Cont.

C21	5603(3)	3669(3)	9986(3)	37(1)
C22	5055(3)	3129(3)	10132(3)	37(1)
C23	4476(3)	3196(2)	9658(2)	31(1)
C24	1384(3)	5954(2)	8299(2)	25(1)
C25	-161(3)	5626(3)	8884(2)	30(1)
C26	-705(3)	5019(2)	8925(2)	27(1)
C27	-349(3)	4494(2)	8308(2)	29(1)
C28	-902(3)	3970(2)	8345(2)	29(1)
C29	-1805(3)	3975(2)	9000(2)	31(1)
C30	-2164(3)	4496(2)	9627(2)	31(1)
C31	-1608(3)	5015(2)	9579(2)	30(1)
C32	2244(4)	7744(3)	9318(3)	40(1)
C33	1569(3)	9254(2)	8236(3)	35(1)
C34	-99(3)	8442(3)	9436(2)	32(1)
C35	-804(3)	8758(3)	8920(3)	48(1)
C36	-236(4)	7616(3)	9904(3)	46(1)
C37	-441(4)	9097(3)	10039(3)	43(1)
C38	4310(3)	6126(2)	5065(2)	25(1)
C39	4075(3)	5864(3)	3919(2)	31(1)
C40	3230(4)	5746(3)	3747(3)	38(1)
C41	3011(4)	6071(3)	3093(3)	40(1)
C42	7427(3)	1065(2)	6592(2)	23(1)
C43	6918(3)	1744(2)	7231(2)	26(1)

Table 6.21., Cont.

C44	7733(3)	1664(2)	7547(2)	25(1)
C45	7684(3)	2078(2)	8158(2)	31(1)
C46	8594(3)	1875(3)	8326(2)	34(1)
C47	9517(3)	1271(3)	7899(3)	34(1)
C48	9575(3)	853(2)	7290(2)	29(1)
C49	8654(3)	1061(2)	7119(2)	24(1)
C50	7314(3)	1552(2)	5783(2)	25(1)
C51	8063(3)	461(2)	4767(2)	27(1)
C52	7693(3)	-187(2)	5421(2)	25(1)
C53	6680(3)	174(2)	6140(2)	23(1)
C54	6897(3)	348(2)	6858(2)	20(1)
C55	5922(3)	937(2)	5848(2)	27(1)
C56	6232(3)	1728(2)	5746(2)	29(1)
C57	7632(3)	-471(2)	7138(2)	23(1)
C58	7793(3)	-1891(2)	7542(2)	29(1)
C59	7465(3)	-2585(2)	7448(2)	26(1)
C60	7231(4)	-2584(3)	6772(3)	39(1)
C61	6960(4)	-3238(3)	6675(3)	51(1)
C62	6926(4)	-3900(3)	7253(3)	47(1)
C63	7157(4)	-3905(3)	7921(3)	43(1)
C64	7420(3)	-3249(3)	8021(3)	34(1)
C65	5856(3)	600(2)	7577(2)	24(1)
C66	5190(3)	983(2)	8912(2)	26(1)

Table 6.21., Cont.

C67	5480(3)	921(2)	9645(2)	24(1)
C68	6522(3)	706(3)	9580(2)	32(1)
C69	6762(3)	672(3)	10265(3)	36(1)
C70	5971(3)	851(3)	11004(2)	34(1)
C71	4925(3)	1065(2)	11074(2)	31(1)
C72	4693(3)	1090(2)	10397(2)	29(1)
C73	3466(5)	469(3)	6142(3)	60(2)
C74	3866(4)	2092(3)	5294(3)	51(1)
C75	2758(3)	1972(3)	7157(3)	36(1)
C76	2709(4)	1354(3)	7909(3)	48(1)
C77	1667(4)	2336(4)	7074(3)	58(1)
C78	3061(4)	2692(3)	7270(3)	48(1)
C79	9089(3)	1291(2)	4731(2)	28(1)
C80	9973(3)	2215(3)	4712(3)	48(1)
C81	9687(9)	2874(6)	5321(7)	46(2)
C82	10023(11)	2731(12)	5933(11)	55(3)
C81A	10239(11)	2587(9)	5168(9)	63(3)
C82A	9702(13)	2821(14)	5866(14)	54(4)
N1	2648(2)	5225(2)	6296(2)	23(1)
N2	3805(2)	6361(2)	5840(2)	24(1)
N3	8523(2)	763(2)	6532(2)	26(1)
N4	8174(3)	1121(2)	5080(2)	29(1)
O1	337(2)	6895(2)	7169(2)	30(1)

Table 6.21., Cont.

O2	3337(2)	4728(2)	8343(2)	27(1)
O3	872(2)	5388(2)	8313(2)	25(1)
O4	1507(2)	7642(2)	8097(2)	24(1)
O5	3615(2)	6170(2)	4724(2)	28(1)
O6	5253(2)	5900(2)	4713(2)	31(1)
O7	6048(2)	2271(2)	7372(2)	28(1)
O8	7194(2)	-1115(2)	7255(2)	24(1)
O9	6099(2)	596(2)	8266(2)	25(1)
O10	4879(2)	1078(2)	6406(2)	32(1)
O11	9868(2)	891(2)	4207(2)	32(1)
O12	9028(2)	1993(2)	5005(2)	35(1)
Si1	1312(1)	8264(1)	8766(1)	26(1)
Si2	3767(1)	1399(1)	6242(1)	29(1)

Table 6.22. Bond lengths [Å] and angles [°] for **4.86b**.

Bond Lengths:

C1-N1	1.459(4)
C1-C9	1.569(5)
C1-C13	1.579(5)
C1-C2	1.579(5)
C2-O1	1.218(4)
C2-C3	1.452(5)
C3-C8	1.393(5)
C3-C4	1.404(5)
C4-C5	1.386(5)
C4-H4	0.95
C5-C6	1.394(6)
C5-H5	0.95
C6-C7	1.387(5)
C6-H6	0.95
C7-C8	1.406(5)
C7-H7	0.95
C8-N1	1.368(5)
C9-N2	1.477(4)
C9-C15	1.523(5)
C9-H9	1.00
C10-N2	1.462(5)
C10-C11	1.535(5)

Table 6.22., Cont.

C10-H10A	0.99
C10-H10B	0.99
C11-C12	1.541(5)
C11-H11A	0.99
C11-H11B	0.99
C12-C14	1.532(5)
C12-C13	1.567(5)
C12-H12	1.00
C13-C24	1.529(5)
C13-C16	1.542(5)
C14-O4	1.425(4)
C14-C15	1.540(5)
C14-H14	1.00
C15-H15A	0.99
C15-H15B	0.99
C16-O2	1.424(4)
C16-H16A	0.99
C16-H16B	0.99
C17-O2	1.426(4)
C17-C18	1.506(5)
C17-H17A	0.99
C17-H17B	0.99
C18-C23	1.383(6)

Table 6.22., Cont.

C18-C19	1.385(6)
C19-C20	1.376(6)
C19-H19	0.95
C20-C21	1.398(6)
C20-H20	0.95
C21-C22	1.370(6)
C21-H21	0.95
C22-C23	1.389(6)
C22-H22	0.95
C23-H23	0.95
C24-O3	1.427(4)
C24-H24A	0.99
C24-H24B	0.99
C25-O3	1.412(4)
C25-C26	1.511(5)
C25-H25A	0.99
C25-H25B	0.99
C26-C31	1.383(5)
C26-C27	1.387(5)
C27-C28	1.398(5)
C27-H27	0.95
C28-C29	1.382(5)
C28-H28	0.95

Table 6.22., Cont.

C29-C30	1.395(5)
C29-H29	0.95
C30-C31	1.390(5)
C30-H30	0.95
C31-H31	0.95
C32-Si1	1.862(5)
C32-H32A	0.98
C32-H32B	0.98
C32-H32C	0.98
C33-Si1	1.875(4)
C33-H33A	0.98
C33-H33B	0.98
C33-H33C	0.98
C34-C37	1.532(5)
C34-C35	1.539(6)
C34-C36	1.544(6)
C34-Si1	1.877(4)
C35-H35A	0.98
C35-H35B	0.98
C35-H35C	0.98
C36-H36A	0.98
C36-H36B	0.98
C36-H36C	0.98

Table 6.22., Cont.

C37-H37A	0.98
C37-H37B	0.98
C37-H37C	0.98
C38-O6	1.210(4)
C38-O5	1.358(5)
C38-N2	1.364(5)
C39-O5	1.454(4)
C39-C40	1.480(6)
C39-H39A	0.99
C39-H39B	0.99
C40-C41	1.309(6)
C40-H40	0.95
C41-H41A	0.95
C41-H41B	0.95
C42-N3	1.455(5)
C42-C43	1.568(5)
C42-C50	1.572(5)
C42-C54	1.598(5)
C43-O7	1.217(5)
C43-C44	1.468(5)
C44-C49	1.393(5)
C44-C45	1.396(5)
C45-C46	1.386(6)

Table 6.22., Cont.

C45-H45	0.95
C46-C47	1.394(6)
C46-H46	0.95
C47-C48	1.393(5)
C47-H47	0.95
C48-C49	1.401(5)
C48-H48	0.95
C49-N3	1.370(5)
C50-N4	1.471(4)
C50-C56	1.523(5)
C50-H50	1.00
C51-N4	1.452(4)
C51-C52	1.536(5)
C51-H51A	0.99
C51-H51B	0.99
C52-C53	1.545(5)
C52-H52A	0.99
C52-H52B	0.99
C53-C55	1.526(5)
C53-C54	1.558(5)
C53-H53	1.00
C54-C65	1.538(4)
C54-C57	1.554(5)

Table 6.22., Cont.

C55-O10	1.419(4)
C55-C56	1.547(5)
C55-H55	1.00
C56-H56A	0.99
C56-H56B	0.99
C57-O8	1.422(4)
C57-H57A	0.99
C57-H57B	0.99
C58-O8	1.424(5)
C58-C59	1.504(5)
C58-H58A	0.99
C58-H58B	0.99
C59-C64	1.385(6)
C59-C60	1.395(6)
C60-C61	1.388(6)
C60-H60	0.95
C61-C62	1.387(7)
C61-H61	0.95
C62-C63	1.374(7)
C62-H62	0.95
C63-C64	1.387(6)
C63-H63	0.95
C64-H64	0.95

Table 6.22., Cont.

C65-O9	1.424(4)
C65-H65A	0.99
C65-H65B	0.99
C66-O9	1.413(4)
C66-C67	1.517(5)
C66-H66A	0.99
C66-H66B	0.99
C67-C68	1.389(5)
C67-C72	1.390(5)
C68-C69	1.401(6)
C68-H68	0.95
C69-C70	1.377(6)
C69-H69	0.95
C70-C71	1.393(6)
C70-H70	0.95
C71-C72	1.382(6)
C71-H71	0.95
C72-H72	0.95
C73-Si2	1.871(5)
C73-H73A	0.98
C73-H73B	0.98
C73-H73C	0.98
C74-Si2	1.873(5)

Table 6.22., Cont.

C74-H74A	0.98
C74-H74B	0.98
C74-H74C	0.98
C75-C78	1.538(6)
C75-C77	1.538(6)
C75-C76	1.547(6)
C75-Si2	1.876(4)
C76-H76A	0.98
C76-H76B	0.98
C76-H76C	0.98
C77-H77A	0.98
C77-H77B	0.98
C77-H77C	0.98
C78-H78A	0.98
C78-H78B	0.98
C78-H78C	0.98
C79-O11	1.220(5)
C79-N4	1.354(5)
C79-O12	1.356(5)
C80-C81A	1.376(14)
C80-O12	1.442(5)
C80-C81	1.566(11)
C80-H80C	0.9600

Table 6.22., Cont.

C80-H80D	0.9599
C80-H80A	0.9600
C80-H80B	0.9599
C81-C82	1.325(18)
C81-H81	0.95
C82-H82A	0.95
C82-H82B	0.95
C81A-C82A	1.25(3)
C81A-H81A	0.95
C82A-H82C	0.95
C82A-H82D	0.95
N1-H1N	0.90(4)
N3-H2N	0.87(4)
O4-Si1	1.644(2)
O10-Si2	1.638(3)
Bond Angles:	
N1-C1-C9	109.8(3)
N1-C1-C13	113.3(3)
C9-C1-C13	111.5(3)
N1-C1-C2	101.5(3)
C9-C1-C2	106.3(3)
C13-C1-C2	113.7(3)
O1-C2-C3	127.9(3)

Table 6.22., Cont.

O1-C2-C1	125.4(3)
C3-C2-C1	106.6(3)
C8-C3-C4	121.4(3)
C8-C3-C2	108.1(3)
C4-C3-C2	130.5(4)
C5-C4-C3	117.9(4)
C5-C4-H4	121.1
C3-C4-H4	121.1
C4-C5-C6	120.3(4)
C4-C5-H5	119.8
C6-C5-H5	119.8
C7-C6-C5	122.6(4)
C7-C6-H6	118.7
C5-C6-H6	118.7
C6-C7-C8	117.0(4)
C6-C7-H7	121.5
C8-C7-H7	121.5
N1-C8-C3	111.7(3)
N1-C8-C7	127.7(3)
C3-C8-C7	120.6(3)
N2-C9-C15	112.2(3)
N2-C9-C1	110.8(3)
C15-C9-C1	111.6(3)

Table 6.22., Cont.

N2-C9-H9	107.4
C15-C9-H9	107.4
C1-C9-H9	107.4
N2-C10-C11	113.3(3)
N2-C10-H10A	108.9
C11-C10-H10A	108.9
N2-C10-H10B	108.9
C11-C10-H10B	108.9
H10A-C10-H10B	107.7
C10-C11-C12	114.9(3)
C10-C11-H11A	108.6
C12-C11-H11A	108.6
C10-C11-H11B	108.6
C12-C11-H11B	108.6
H11A-C11-H11B	107.5
C14-C12-C11	108.7(3)
C14-C12-C13	113.2(3)
C11-C12-C13	115.3(3)
C14-C12-H12	106.4
C11-C12-H12	106.4
C13-C12-H12	106.4
C24-C13-C16	106.7(3)
C24-C13-C12	107.2(3)

Table 6.22., Cont.

C16-C13-C12	110.6(3)
C24-C13-C1	111.9(3)
C16-C13-C1	108.2(3)
C12-C13-C1	112.2(3)
O4-C14-C12	111.7(3)
O4-C14-C15	108.5(3)
C12-C14-C15	111.8(3)
O4-C14-H14	108.2
C12-C14-H14	108.2
C15-C14-H14	108.2
C9-C15-C14	114.7(3)
C9-C15-H15A	108.6
C14-C15-H15A	108.6
C9-C15-H15B	108.6
C14-C15-H15B	108.6
H15A-C15-H15B	107.6
O2-C16-C13	107.9(3)
O2-C16-H16A	110.1
C13-C16-H16A	110.1
O2-C16-H16B	110.1
C13-C16-H16B	110.1
H16A-C16-H16B	108.4
O2-C17-C18	108.2(3)

Table 6.22., Cont.

O2-C17-H17A	110.0
C18-C17-H17A	110.0
O2-C17-H17B	110.0
C18-C17-H17B	110.0
H17A-C17-H17B	108.4
C23-C18-C19	119.6(4)
C23-C18-C17	120.9(3)
C19-C18-C17	119.4(4)
C20-C19-C18	120.2(4)
C20-C19-H19	119.9
C18-C19-H19	119.9
C19-C20-C21	120.0(4)
C19-C20-H20	120.0
C21-C20-H20	120.0
C22-C21-C20	119.7(4)
C22-C21-H21	120.1
C20-C21-H21	120.1
C21-C22-C23	120.1(4)
C21-C22-H22	119.9
C23-C22-H22	119.9
C18-C23-C22	120.3(4)
C18-C23-H23	119.9
C22-C23-H23	119.9

Table 6.22., Cont.

O3-C24-C13	109.2(3)
O3-C24-H24A	109.8
C13-C24-H24A	109.8
O3-C24-H24B	109.8
C13-C24-H24B	109.8
H24A-C24-H24B	108.3
O3-C25-C26	110.5(3)
O3-C25-H25A	109.6
C26-C25-H25A	109.6
O3-C25-H25B	109.6
C26-C25-H25B	109.6
H25A-C25-H25B	108.1
C31-C26-C27	119.3(3)
C31-C26-C25	119.0(3)
C27-C26-C25	121.7(3)
C26-C27-C28	120.2(4)
C26-C27-H27	119.9
C28-C27-H27	119.9
C29-C28-C27	119.9(4)
C29-C28-H28	120.1
C27-C28-H28	120.1
C28-C29-C30	120.2(4)
C28-C29-H29	119.9

Table 6.22., Cont.

C30-C29-H29	119.9
C31-C30-C29	119.1(4)
C31-C30-H30	120.4
C29-C30-H30	120.4
C26-C31-C30	121.2(4)
C26-C31-H31	119.4
C30-C31-H31	119.4
Si1-C32-H32A	109.5
Si1-C32-H32B	109.5
H32A-C32-H32B	109.5
Si1-C32-H32C	109.5
H32A-C32-H32C	109.5
H32B-C32-H32C	109.5
Si1-C33-H33A	109.5
Si1-C33-H33B	109.5
H33A-C33-H33B	109.5
Si1-C33-H33C	109.5
H33A-C33-H33C	109.5
H33B-C33-H33C	109.5
C37-C34-C35	109.3(4)
C37-C34-C36	109.0(3)
C35-C34-C36	108.7(4)
C37-C34-Si1	109.9(3)

Table 6.22., Cont.

C35-C34-Si1	109.6(3)
C36-C34-Si1	110.3(3)
C34-C35-H35A	109.5
C34-C35-H35B	109.5
H35A-C35-H35B	109.5
C34-C35-H35C	109.5
H35A-C35-H35C	109.5
H35B-C35-H35C	109.5
C34-C36-H36A	109.5
C34-C36-H36B	109.5
H36A-C36-H36B	109.5
C34-C36-H36C	109.5
H36A-C36-H36C	109.5
H36B-C36-H36C	109.5
C34-C37-H37A	109.5
C34-C37-H37B	109.5
H37A-C37-H37B	109.5
C34-C37-H37C	109.5
H37A-C37-H37C	109.5
H37B-C37-H37C	109.5
O6-C38-O5	123.1(3)
O6-C38-N2	125.7(4)
O5-C38-N2	111.2(3)

Table 6.22., Cont.

O5-C39-C40	107.3(3)
O5-C39-H39A	110.2
C40-C39-H39A	110.2
O5-C39-H39B	110.2
C40-C39-H39B	110.2
H39A-C39-H39B	108.5
C41-C40-C39	122.7(4)
C41-C40-H40	118.7
C39-C40-H40	118.7
C40-C41-H41A	120.0
C40-C41-H41B	120.0
H41A-C41-H41B	120.0
N3-C42-C43	101.6(3)
N3-C42-C50	110.3(3)
C43-C42-C50	106.2(3)
N3-C42-C54	113.7(3)
C43-C42-C54	112.9(3)
C50-C42-C54	111.4(3)
O7-C43-C44	128.0(3)
O7-C43-C42	125.4(4)
C44-C43-C42	106.4(3)
C49-C44-C45	122.0(4)
C49-C44-C43	107.6(3)

Table 6.22., Cont.

C45-C44-C43	130.4(4)
C46-C45-C44	117.6(4)
C46-C45-H45	121.2
C44-C45-H45	121.2
C45-C46-C47	120.5(4)
C45-C46-H46	119.8
C47-C46-H46	119.8
C48-C47-C46	122.4(4)
C48-C47-H47	118.8
C46-C47-H47	118.8
C47-C48-C49	117.1(4)
C47-C48-H48	121.5
C49-C48-H48	121.5
N3-C49-C44	111.6(3)
N3-C49-C48	127.9(3)
C44-C49-C48	120.4(3)
N4-C50-C56	112.5(3)
N4-C50-C42	111.1(3)
C56-C50-C42	112.6(3)
N4-C50-H50	106.7
C56-C50-H50	106.7
C42-C50-H50	106.7
N4-C51-C52	113.5(3)

Table 6.22., Cont.

N4-C51-H51A	108.9
C52-C51-H51A	108.9
N4-C51-H51B	108.9
C52-C51-H51B	108.9
H51A-C51-H51B	107.7
C51-C52-C53	115.7(3)
C51-C52-H52A	108.3
C53-C52-H52A	108.3
C51-C52-H52B	108.3
C53-C52-H52B	108.3
H52A-C52-H52B	107.4
C55-C53-C52	109.9(3)
C55-C53-C54	113.3(3)
C52-C53-C54	113.3(3)
C55-C53-H53	106.6
C52-C53-H53	106.6
C54-C53-H53	106.6
C65-C54-C57	106.6(3)
C65-C54-C53	109.2(3)
C57-C54-C53	109.7(3)
C65-C54-C42	111.1(3)
C57-C54-C42	110.0(3)
C53-C54-C42	110.2(3)

Table 6.22., Cont.

O10-C55-C53	110.0(3)
O10-C55-C56	109.5(3)
C53-C55-C56	110.7(3)
O10-C55-H55	108.8
C53-C55-H55	108.8
C56-C55-H55	108.8
C50-C56-C55	114.5(3)
C50-C56-H56A	108.6
C55-C56-H56A	108.6
C50-C56-H56B	108.6
C55-C56-H56B	108.6
H56A-C56-H56B	107.6
O8-C57-C54	107.4(3)
O8-C57-H57A	110.2
C54-C57-H57A	110.2
O8-C57-H57B	110.2
C54-C57-H57B	110.2
H57A-C57-H57B	108.5
O8-C58-C59	109.1(3)
O8-C58-H58A	109.9
C59-C58-H58A	109.9
O8-C58-H58B	109.9
C59-C58-H58B	109.9

Table 6.22., Cont.

H58A-C58-H58B	108.3
C64-C59-C60	118.8(4)
C64-C59-C58	120.5(4)
C60-C59-C58	120.6(3)
C61-C60-C59	120.5(4)
C61-C60-H60	119.8
C59-C60-H60	119.8
C62-C61-C60	119.9(5)
C62-C61-H61	120.1
C60-C61-H61	120.1
C63-C62-C61	119.9(4)
C63-C62-H62	120.0
C61-C62-H62	120.0
C62-C63-C64	120.3(4)
C62-C63-H63	119.9
C64-C63-H63	119.9
C59-C64-C63	120.6(4)
C59-C64-H64	119.7
C63-C64-H64	119.7
O9-C65-C54	108.0(3)
O9-C65-H65A	110.1
C54-C65-H65A	110.1
O9-C65-H65B	110.1

Table 6.22., Cont.

C54-C65-H65B	110.1
H65A-C65-H65B	108.4
O9-C66-C67	109.6(3)
O9-C66-H66A	109.7
C67-C66-H66A	109.7
O9-C66-H66B	109.7
C67-C66-H66B	109.7
H66A-C66-H66B	108.2
C68-C67-C72	118.9(4)
C68-C67-C66	121.3(3)
C72-C67-C66	119.8(3)
C67-C68-C69	119.9(4)
C67-C68-H68	120.0
C69-C68-H68	120.0
C70-C69-C68	120.4(4)
C70-C69-H69	119.8
C68-C69-H69	119.8
C69-C70-C71	120.0(4)
C69-C70-H70	120.0
C71-C70-H70	120.0
C72-C71-C70	119.4(4)
C72-C71-H71	120.3
C70-C71-H71	120.3

Table 6.22., Cont.

C71-C72-C67	121.4(4)
C71-C72-H72	119.3
C67-C72-H72	119.3
Si2-C73-H73A	109.5
Si2-C73-H73B	109.5
H73A-C73-H73B	109.5
Si2-C73-H73C	109.5
H73A-C73-H73C	109.5
H73B-C73-H73C	109.5
Si2-C74-H74A	109.5
Si2-C74-H74B	109.5
H74A-C74-H74B	109.5
Si2-C74-H74C	109.5
H74A-C74-H74C	109.5
H74B-C74-H74C	109.5
C78-C75-C77	109.0(4)
C78-C75-C76	108.6(4)
C77-C75-C76	109.3(4)
C78-C75-Si2	110.4(3)
C77-C75-Si2	110.5(3)
C76-C75-Si2	109.0(3)
C75-C76-H76A	109.5
C75-C76-H76B	109.5

Table 6.22., Cont.

H76A-C76-H76B	109.5
C75-C76-H76C	109.5
H76A-C76-H76C	109.5
H76B-C76-H76C	109.5
C75-C77-H77A	109.5
C75-C77-H77B	109.5
H77A-C77-H77B	109.5
C75-C77-H77C	109.5
H77A-C77-H77C	109.5
H77B-C77-H77C	109.5
C75-C78-H78A	109.5
C75-C78-H78B	109.5
H78A-C78-H78B	109.5
C75-C78-H78C	109.5
H78A-C78-H78C	109.5
H78B-C78-H78C	109.5
O11-C79-N4	125.1(4)
O11-C79-O12	123.1(3)
N4-C79-O12	111.8(3)
C81A-C80-O12	123.6(8)
O12-C80-C81	101.6(5)
C81A-C80-H80C	106.3
O12-C80-H80C	106.5

Table 6.22., Cont.

C81-C80-H80C	133.6
C81A-C80-H80D	106.7
O12-C80-H80D	106.2
C81-C80-H80D	99.9
H80C-C80-H80D	106.6
C81A-C80-H80A	85.9
O12-C80-H80A	111.7
C81-C80-H80A	111.8
H80C-C80-H80A	22.6
H80D-C80-H80A	123.1
C81A-C80-H80B	112.0
O12-C80-H80B	111.1
C81-C80-H80B	111.0
H80C-C80-H80B	92.3
H80D-C80-H80B	14.3
H80A-C80-H80B	109.4
C82-C81-C80	125.6(12)
C82-C81-H81	117.2
C80-C81-H81	117.2
C81-C82-H82A	120.0
C81-C82-H82B	120.0
H82A-C82-H82B	120.0
C82A-C81A-C80	126.8(16)

Table 6.22., Cont.

C82A-C81A-H81A	116.6
C80-C81A-H81A	116.6
C81A-C82A-H82C	120.0
C81A-C82A-H82D	120.0
H82C-C82A-H82D	120.0
C8-N1-C1	112.0(3)
C8-N1-H1N	118(2)
C1-N1-H1N	126(2)
C38-N2-C10	117.5(3)
C38-N2-C9	122.0(3)
C10-N2-C9	118.9(3)
C49-N3-C42	111.8(3)
C49-N3-H2N	125(3)
C42-N3-H2N	121(3)
C79-N4-C51	118.3(3)
C79-N4-C50	122.6(3)
C51-N4-C50	119.0(3)
C16-O2-C17	111.5(3)
C25-O3-C24	109.7(3)
C14-O4-Si1	126.1(2)
C38-O5-C39	115.7(3)
C57-O8-C58	112.0(3)
C66-O9-C65	111.7(3)

Table 6.22., Cont.

C55-O10-Si2	129.7(2)
C79-O12-C80	117.1(3)
O4-Si1-C32	109.88(18)
O4-Si1-C33	109.37(16)
C32-Si1-C33	108.0(2)
O4-Si1-C34	103.72(15)
C32-Si1-C34	112.7(2)
C33-Si1-C34	113.10(19)
O10-Si2-C73	109.4(2)
O10-Si2-C74	110.16(19)
C73-Si2-C74	109.3(3)
O10-Si2-C75	104.80(17)
C73-Si2-C75	110.9(2)
C74-Si2-C75	112.2(2)

Table 6.23. Anisotropic displacement parameters ($\text{\AA}^2 \times 10^3$) for **4.86b**.

The anisotropic displacement factor exponent takes the form: $-2\pi^2 [h^2 a^{*2} U^{11} + \dots + 2 h k a^* b^* U^{12}]$

	U^{11}	U^{22}	U^{33}	U^{23}	U^{13}	U^{12}
C1	21(2)	18(2)	20(2)	-9(1)	-2(1)	-6(1)
C2	21(2)	26(2)	22(2)	-5(1)	-3(1)	-7(1)
C3	26(2)	26(2)	22(2)	-2(1)	-4(2)	-13(2)
C4	26(2)	32(2)	27(2)	-1(2)	-7(2)	-13(2)
C5	40(2)	33(2)	36(2)	-2(2)	-16(2)	-18(2)
C6	43(2)	30(2)	30(2)	-7(2)	-14(2)	-17(2)
C7	31(2)	27(2)	25(2)	-8(2)	-4(2)	-12(2)
C8	26(2)	24(2)	19(2)	-2(1)	-3(1)	-13(2)
C9	21(2)	19(2)	21(2)	-4(1)	-2(1)	-6(1)
C10	23(2)	26(2)	26(2)	-10(2)	1(2)	-10(1)
C11	23(2)	28(2)	24(2)	-7(2)	-2(1)	-10(2)
C12	23(2)	25(2)	20(2)	-9(1)	-2(1)	-9(1)
C13	21(2)	20(2)	21(2)	-9(1)	-1(1)	-6(1)
C14	23(2)	21(2)	24(2)	-6(1)	1(1)	-11(1)
C15	24(2)	22(2)	23(2)	-10(1)	0(1)	-6(1)
C16	23(2)	23(2)	23(2)	-6(1)	-4(1)	-7(1)
C17	35(2)	23(2)	35(2)	-5(2)	-14(2)	-6(2)
C18	28(2)	23(2)	30(2)	-8(2)	-6(2)	-5(2)

Table 6.23., Cont.

C19	31(2)	29(2)	35(2)	1(2)	-7(2)	-10(2)
C20	34(2)	39(2)	51(3)	0(2)	-17(2)	-16(2)
C21	35(2)	38(2)	42(2)	-2(2)	-18(2)	-12(2)
C22	43(2)	30(2)	37(2)	3(2)	-17(2)	-11(2)
C23	35(2)	21(2)	36(2)	-4(2)	-10(2)	-8(2)
C24	25(2)	25(2)	25(2)	-10(1)	-2(2)	-12(2)
C25	25(2)	34(2)	25(2)	-13(2)	6(2)	-14(2)
C26	28(2)	24(2)	26(2)	-4(2)	-2(2)	-11(2)
C27	27(2)	28(2)	24(2)	-7(2)	2(2)	-11(2)
C28	29(2)	22(2)	34(2)	-9(2)	-5(2)	-9(2)
C29	25(2)	26(2)	39(2)	-7(2)	-6(2)	-10(2)
C30	25(2)	26(2)	35(2)	-5(2)	1(2)	-11(2)
C31	26(2)	31(2)	29(2)	-10(2)	-2(2)	-9(2)
C32	46(3)	44(3)	38(2)	-2(2)	-17(2)	-20(2)
C33	39(2)	27(2)	36(2)	-7(2)	-6(2)	-13(2)
C34	30(2)	31(2)	27(2)	-15(2)	3(2)	-10(2)
C35	29(2)	57(3)	51(3)	-21(2)	-4(2)	-8(2)
C36	47(3)	38(2)	43(3)	-18(2)	9(2)	-21(2)
C37	43(2)	38(2)	38(2)	-22(2)	6(2)	-15(2)
C38	25(2)	18(2)	23(2)	-6(1)	2(2)	-8(1)
C39	35(2)	31(2)	21(2)	-9(2)	1(2)	-10(2)
C40	45(2)	37(2)	28(2)	-7(2)	-3(2)	-18(2)
C41	48(3)	31(2)	43(3)	-10(2)	-14(2)	-12(2)

Table 6.23., Cont.

C42	20(2)	26(2)	21(2)	-11(1)	3(1)	-11(1)
C43	29(2)	20(2)	22(2)	-6(1)	3(2)	-11(2)
C44	29(2)	18(2)	24(2)	-7(1)	-1(2)	-10(1)
C45	42(2)	22(2)	27(2)	-8(2)	-4(2)	-13(2)
C46	46(2)	29(2)	30(2)	-7(2)	-12(2)	-15(2)
C47	42(2)	29(2)	37(2)	-4(2)	-15(2)	-15(2)
C48	30(2)	23(2)	29(2)	-7(2)	-2(2)	-11(2)
C49	28(2)	19(2)	24(2)	-3(1)	-3(2)	-12(1)
C50	26(2)	23(2)	18(2)	-8(1)	3(1)	-7(1)
C51	25(2)	27(2)	25(2)	-12(2)	2(2)	-9(2)
C52	27(2)	22(2)	24(2)	-9(1)	-1(2)	-9(1)
C53	21(2)	24(2)	23(2)	-8(1)	-1(1)	-10(1)
C54	21(2)	17(2)	20(2)	-3(1)	-1(1)	-8(1)
C55	23(2)	30(2)	21(2)	-4(2)	-3(2)	-6(2)
C56	29(2)	24(2)	24(2)	-4(2)	-2(2)	-6(2)
C57	24(2)	20(2)	24(2)	-5(1)	-2(1)	-11(1)
C58	29(2)	24(2)	31(2)	-3(2)	-5(2)	-10(2)
C59	26(2)	18(2)	27(2)	-1(1)	-5(2)	-4(1)
C60	53(3)	27(2)	42(2)	-1(2)	-22(2)	-14(2)
C61	62(3)	35(3)	70(4)	-10(2)	-34(3)	-15(2)
C62	45(3)	27(2)	73(4)	-9(2)	-19(2)	-16(2)
C63	39(2)	31(2)	52(3)	2(2)	-6(2)	-16(2)
C64	36(2)	31(2)	32(2)	1(2)	-7(2)	-14(2)

Table 6.23., Cont.

C65	25(2)	24(2)	18(2)	-4(1)	0(1)	-9(1)
C66	22(2)	25(2)	21(2)	-6(1)	3(1)	-8(1)
C67	26(2)	16(2)	22(2)	-5(1)	1(1)	-7(1)
C68	31(2)	33(2)	24(2)	-5(2)	-1(2)	-11(2)
C69	30(2)	39(2)	36(2)	-8(2)	-6(2)	-10(2)
C70	41(2)	31(2)	28(2)	-6(2)	-7(2)	-12(2)
C71	40(2)	25(2)	21(2)	-5(2)	3(2)	-14(2)
C72	29(2)	26(2)	25(2)	-5(2)	1(2)	-11(2)
C73	81(4)	56(3)	56(3)	-13(3)	-19(3)	-38(3)
C74	38(2)	62(3)	34(3)	8(2)	-7(2)	-7(2)
C75	22(2)	37(2)	36(2)	-7(2)	-2(2)	-4(2)
C76	41(2)	43(3)	38(3)	-6(2)	7(2)	-12(2)
C77	28(2)	60(3)	69(4)	-2(3)	-8(2)	-7(2)
C78	49(3)	34(2)	46(3)	-15(2)	-2(2)	-8(2)
C79	28(2)	29(2)	24(2)	-4(2)	-4(2)	-9(2)
C80	32(2)	29(2)	85(4)	-14(2)	-19(2)	-11(2)
C81	53(5)	39(5)	55(5)	-11(4)	-26(5)	-14(4)
C82	58(8)	58(7)	58(6)	-7(5)	-40(6)	-6(7)
C81A	43(6)	68(7)	75(6)	-30(6)	-24(6)	-1(5)
C82A	39(7)	68(7)	56(7)	-18(6)	-37(7)	11(7)
N1	21(2)	22(2)	25(2)	-14(1)	-1(1)	-6(1)
N2	22(1)	24(2)	20(2)	-6(1)	2(1)	-7(1)
N3	22(2)	22(2)	26(2)	-14(1)	4(1)	-8(1)

Table 6.23., Cont.

N4	32(2)	29(2)	22(2)	-12(1)	4(1)	-16(1)
O1	21(1)	31(1)	29(1)	-12(1)	-2(1)	-2(1)
O2	31(1)	20(1)	29(1)	-6(1)	-11(1)	-5(1)
O3	20(1)	25(1)	27(1)	-11(1)	2(1)	-11(1)
O4	22(1)	22(1)	26(1)	-12(1)	2(1)	-8(1)
O5	27(1)	29(1)	20(1)	-10(1)	1(1)	-6(1)
O6	26(1)	27(1)	28(1)	-9(1)	4(1)	-7(1)
O7	28(1)	21(1)	26(1)	-9(1)	3(1)	-6(1)
O8	23(1)	18(1)	30(1)	-3(1)	-6(1)	-9(1)
O9	23(1)	26(1)	19(1)	-8(1)	1(1)	-6(1)
O10	18(1)	42(2)	25(1)	-4(1)	-1(1)	-6(1)
O11	23(1)	28(1)	39(2)	-11(1)	0(1)	-7(1)
O12	44(2)	34(2)	28(2)	-10(1)	1(1)	-25(1)
Si1	28(1)	23(1)	24(1)	-9(1)	-3(1)	-9(1)
Si2	24(1)	32(1)	27(1)	-6(1)	-4(1)	-8(1)

Table 6.24. Hydrogen coordinates ($\times 10^4$) and isotropic displacement parameters ($\text{\AA}^2 \times 10^{-3}$) for **4.86b**

	x	y	z	U(eq)
H4	-668	6000	6629	34
H5	-439	4933	5876	41
H6	1232	4008	5259	38
H7	2727	4082	5385	33
H9	2362	6845	5756	26
H10A	4296	7091	6236	32
H10B	5185	6215	5937	32
H11A	4539	6306	7377	31
H11B	4479	5498	7116	31
H12	2953	6301	8211	27
H14	2961	7603	7406	29
H15A	1483	7718	6794	30
H15B	2586	7870	6315	30
H16A	2630	4508	7702	28
H16B	3696	4709	7160	28
H17A	4365	3606	7974	37
H17B	3354	3561	8753	37
H19	5013	4761	8446	40
H20	5975	4653	9242	48
H21	5990	3629	10316	45

Table 6.24., Cont.

H22	5070	2707	10559	44
H23	4090	2825	9765	38
H24A	1533	5868	8803	30
H24B	920	6540	8260	30
H25A	-566	6198	8732	36
H25B	-136	5636	9421	36
H27	273	4490	7859	34
H28	-657	3612	7921	35
H29	-2183	3621	9024	37
H30	-2781	4496	10080	38
H31	-1852	5374	10002	36
H32A	2135	7217	9590	60
H32B	2118	8115	9720	60
H32C	2969	7627	8936	60
H33A	2310	9120	7884	53
H33B	1414	9638	8636	53
H33C	1119	9520	7912	53
H35A	-602	8332	8546	72
H35B	-717	9279	8614	72
H35C	-1541	8863	9272	72
H36A	-979	7714	10238	69
H36B	190	7419	10251	69
H36C	-6	7191	9522	69

Table 6.24., Cont.

H37A	-1151	9143	10424	65
H37B	-440	9642	9750	65
H37C	50	8925	10331	65
H39A	4656	5326	3894	37
H39B	4360	6275	3518	37
H40	2830	5421	4125	45
H41A	3401	6398	2707	48
H41B	2462	5980	3006	48
H45	7050	2486	8448	37
H46	8590	2149	8735	41
H47	10129	1140	8029	41
H48	10210	444	7002	35
H50	7388	2109	5769	30
H51A	8750	168	4366	33
H51B	7552	718	4485	33
H52A	8267	-513	5631	30
H52B	7577	-583	5166	30
H53	6330	-264	6344	28
H55	5953	827	5315	32
H56A	6216	2024	5220	34
H56B	5698	2110	6173	34
H57A	8348	-622	6725	28
H57B	7679	-393	7648	28

Table 6.24., Cont.

H58A	7671	-1865	8117	35
H58B	8553	-2001	7231	35
H60	7256	-2132	6374	46
H61	6798	-3232	6214	61
H62	6744	-4350	7188	56
H63	7136	-4360	8316	52
H64	7570	-3255	8488	41
H65A	5399	1166	7463	28
H65B	5478	197	7674	28
H66A	4660	704	9043	31
H66B	4880	1581	8754	31
H68	7071	582	9072	38
H69	7475	525	10220	44
H70	6138	828	11466	41
H71	4376	1194	11581	38
H72	3980	1224	10448	35
H73A	3993	186	5655	90
H73B	2765	655	6104	90
H73C	3481	79	6616	90
H74A	4049	2569	5337	77
H74B	3188	2298	5214	77
H74C	4412	1772	4834	77
H76A	3415	1085	7937	71

Table 6.24., Cont.

H76B	2442	925	7872	71
H76C	2237	1661	8395	71
H77A	1140	2593	7574	86
H77B	1486	1885	6971	86
H77C	1681	2762	6624	86
H78A	2526	2988	7748	72
H78B	3105	3085	6794	72
H78C	3745	2464	7340	72
H80C	10552	1709	4536	57
H80D	9955	2580	4237	57
H80A	10576	1739	4727	57
H80B	10100	2464	4172	57
H81	9234	3423	5246	55
H82A	10477	2191	6030	66
H82B	9809	3169	6274	66
H81A	10901	2674	4926	75
H82C	9034	2749	6136	65
H82D	9962	3072	6128	65
H1N	3330(30)	4990(20)	6000(20)	12(9)
H2N	8980(30)	330(30)	6250(20)	25(10)

Table 6.25. Torsion angles [°] for **4.86b**.

N1-C1-C2-O1	-176.3(4)
C9-C1-C2-O1	-61.5(5)
C13-C1-C2-O1	61.6(5)
N1-C1-C2-C3	-0.7(4)
C9-C1-C2-C3	114.1(3)
C13-C1-C2-C3	-122.8(3)
O1-C2-C3-C8	173.5(4)
C1-C2-C3-C8	-1.9(4)
O1-C2-C3-C4	-6.6(7)
C1-C2-C3-C4	177.9(4)
C8-C3-C4-C5	-1.9(6)
C2-C3-C4-C5	178.3(4)
C3-C4-C5-C6	-0.2(6)
C4-C5-C6-C7	1.0(6)
C5-C6-C7-C8	0.3(6)
C4-C3-C8-N1	-175.7(3)
C2-C3-C8-N1	4.2(4)
C4-C3-C8-C7	3.3(6)
C2-C3-C8-C7	-176.9(3)
C6-C7-C8-N1	176.4(4)
C6-C7-C8-C3	-2.4(6)
N1-C1-C9-N2	-51.5(4)

Table 6.25., Cont.

C13-C1-C9-N2	74.9(3)
C2-C1-C9-N2	-160.6(3)
N1-C1-C9-C15	-177.2(3)
C13-C1-C9-C15	-50.8(4)
C2-C1-C9-C15	73.7(4)
N2-C10-C11-C12	-48.9(4)
C10-C11-C12-C14	-43.0(4)
C10-C11-C12-C13	85.2(4)
C14-C12-C13-C24	-71.5(4)
C11-C12-C13-C24	162.6(3)
C14-C12-C13-C16	172.7(3)
C11-C12-C13-C16	46.8(4)
C14-C12-C13-C1	51.7(4)
C11-C12-C13-C1	-74.2(4)
N1-C1-C13-C24	-115.6(3)
C9-C1-C13-C24	119.9(3)
C2-C1-C13-C24	-0.4(4)
N1-C1-C13-C16	1.6(4)
C9-C1-C13-C16	-122.9(3)
C2-C1-C13-C16	116.9(3)
N1-C1-C13-C12	123.9(3)
C9-C1-C13-C12	-0.6(4)
C2-C1-C13-C12	-120.9(3)

Table 6.25., Cont.

C11-C12-C14-O4	-158.8(3)
C13-C12-C14-O4	71.8(4)
C11-C12-C14-C15	79.3(3)
C13-C12-C14-C15	-50.0(4)
N2-C9-C15-C14	-70.9(4)
C1-C9-C15-C14	54.1(4)
O4-C14-C15-C9	-126.7(3)
C12-C14-C15-C9	-3.0(4)
C24-C13-C16-O2	-66.2(3)
C12-C13-C16-O2	50.0(4)
C1-C13-C16-O2	173.3(3)
O2-C17-C18-C23	138.3(4)
O2-C17-C18-C19	-43.6(5)
C23-C18-C19-C20	0.0(6)
C17-C18-C19-C20	-178.1(4)
C18-C19-C20-C21	-0.1(7)
C19-C20-C21-C22	0.7(7)
C20-C21-C22-C23	-1.0(7)
C19-C18-C23-C22	-0.3(6)
C17-C18-C23-C22	177.8(4)
C21-C22-C23-C18	0.8(6)
C16-C13-C24-O3	-55.7(4)
C12-C13-C24-O3	-174.1(3)

Table 6.25., Cont.

C1-C13-C24-O3	62.5(4)
O3-C25-C26-C31	163.9(4)
O3-C25-C26-C27	-19.2(6)
C31-C26-C27-C28	0.4(6)
C25-C26-C27-C28	-176.6(4)
C26-C27-C28-C29	-0.1(6)
C27-C28-C29-C30	-0.4(6)
C28-C29-C30-C31	0.6(7)
C27-C26-C31-C30	-0.1(7)
C25-C26-C31-C30	177.0(4)
C29-C30-C31-C26	-0.4(7)
O5-C39-C40-C41	127.9(4)
N3-C42-C43-O7	166.2(3)
C50-C42-C43-O7	50.7(4)
C54-C42-C43-O7	-71.6(5)
N3-C42-C43-C44	-8.2(4)
C50-C42-C43-C44	-123.6(3)
C54-C42-C43-C44	114.0(3)
O7-C43-C44-C49	-170.1(4)
C42-C43-C44-C49	4.1(4)
O7-C43-C44-C45	9.9(7)
C42-C43-C44-C45	-175.9(4)
C49-C44-C45-C46	0.4(6)

Table 6.25., Cont.

C43-C44-C45-C46	-179.6(4)
C44-C45-C46-C47	-0.5(6)
C45-C46-C47-C48	0.4(6)
C46-C47-C48-C49	-0.2(6)
C45-C44-C49-N3	-177.8(3)
C43-C44-C49-N3	2.2(4)
C45-C44-C49-C48	-0.3(6)
C43-C44-C49-C48	179.8(3)
C47-C48-C49-N3	177.3(4)
C47-C48-C49-C44	0.2(5)
N3-C42-C50-N4	41.2(4)
C43-C42-C50-N4	150.6(3)
C54-C42-C50-N4	-86.1(3)
N3-C42-C50-C56	168.4(3)
C43-C42-C50-C56	-82.3(3)
C54-C42-C50-C56	41.1(4)
N4-C51-C52-C53	53.2(5)
C51-C52-C53-C55	35.5(4)
C51-C52-C53-C54	-92.3(4)
C55-C53-C54-C65	61.0(4)
C52-C53-C54-C65	-173.1(3)
C55-C53-C54-C57	177.5(3)
C52-C53-C54-C57	-56.6(4)

Table 6.25., Cont.

C55-C53-C54-C42	-61.3(4)
C52-C53-C54-C42	64.7(4)
N3-C42-C54-C65	128.3(3)
C43-C42-C54-C65	13.1(4)
C50-C42-C54-C65	-106.3(3)
N3-C42-C54-C57	10.4(4)
C43-C42-C54-C57	-104.8(3)
C50-C42-C54-C57	135.8(3)
N3-C42-C54-C53	-110.6(3)
C43-C42-C54-C53	134.2(3)
C50-C42-C54-C53	14.8(4)
C52-C53-C55-O10	158.0(3)
C54-C53-C55-O10	-74.2(4)
C52-C53-C55-C56	-80.8(4)
C54-C53-C55-C56	47.0(4)
N4-C50-C56-C55	69.1(4)
C42-C50-C56-C55	-57.3(4)
O10-C55-C56-C50	133.5(3)
C53-C55-C56-C50	12.0(4)
C65-C54-C57-O8	67.6(3)
C53-C54-C57-O8	-50.5(3)
C42-C54-C57-O8	-171.8(3)
O8-C58-C59-C64	-143.4(4)

Table 6.25., Cont.

O8-C58-C59-C60	38.4(5)
C64-C59-C60-C61	-0.2(7)
C58-C59-C60-C61	178.0(4)
C59-C60-C61-C62	-0.3(8)
C60-C61-C62-C63	0.3(8)
C61-C62-C63-C64	0.2(7)
C60-C59-C64-C63	0.7(6)
C58-C59-C64-C63	-177.5(4)
C62-C63-C64-C59	-0.7(7)
C57-C54-C65-O9	50.5(3)
C53-C54-C65-O9	168.9(3)
C42-C54-C65-O9	-69.4(4)
O9-C66-C67-C68	14.8(5)
O9-C66-C67-C72	-165.9(3)
C72-C67-C68-C69	-0.8(6)
C66-C67-C68-C69	178.5(3)
C67-C68-C69-C70	0.0(6)
C68-C69-C70-C71	0.1(6)
C69-C70-C71-C72	0.5(6)
C70-C71-C72-C67	-1.3(6)
C68-C67-C72-C71	1.4(6)
C66-C67-C72-C71	-177.9(3)
O12-C80-C81-C82	102.5(13)

Table 6.25., Cont.

O12-C80-C81A-C82A	-4(2)
C3-C8-N1-C1	-4.8(4)
C7-C8-N1-C1	176.3(4)
C9-C1-N1-C8	-109.0(3)
C13-C1-N1-C8	125.6(3)
C2-C1-N1-C8	3.3(4)
O6-C38-N2-C10	10.4(5)
O5-C38-N2-C10	-169.9(3)
O6-C38-N2-C9	176.0(3)
O5-C38-N2-C9	-4.4(5)
C11-C10-N2-C38	-137.6(3)
C11-C10-N2-C9	56.3(4)
C15-C9-N2-C38	-134.7(3)
C1-C9-N2-C38	100.0(4)
C15-C9-N2-C10	30.7(4)
C1-C9-N2-C10	-94.7(4)
C44-C49-N3-C42	-8.3(4)
C48-C49-N3-C42	174.4(4)
C43-C42-N3-C49	10.0(4)
C50-C42-N3-C49	122.3(3)
C54-C42-N3-C49	-111.7(3)
O11-C79-N4-C51	-5.7(6)
O12-C79-N4-C51	171.3(3)

Table 6.25., Cont.

O11-C79-N4-C50	171.4(4)
O12-C79-N4-C50	-11.5(6)
C52-C51-N4-C79	129.0(4)
C52-C51-N4-C50	-48.3(5)
C56-C50-N4-C79	142.3(4)
C42-C50-N4-C79	-90.4(4)
C56-C50-N4-C51	-40.6(5)
C42-C50-N4-C51	86.7(4)
C13-C16-O2-C17	175.7(3)
C18-C17-O2-C16	160.7(3)
C26-C25-O3-C24	-178.3(3)
C13-C24-O3-C25	-169.1(3)
C12-C14-O4-Si1	105.8(3)
C15-C14-O4-Si1	-130.5(3)
O6-C38-O5-C39	4.7(5)
N2-C38-O5-C39	-175.0(3)
C40-C39-O5-C38	164.8(3)
C54-C57-O8-C58	-177.9(3)
C59-C58-O8-C57	-165.5(3)
C67-C66-O9-C65	176.9(3)
C54-C65-O9-C66	167.8(3)
C53-C55-O10-Si2	-142.9(3)
C56-C55-O10-Si2	95.2(4)

Table 6.25., Cont.

O11-C79-O12-C80	-6.2(6)
N4-C79-O12-C80	176.7(4)
C81A-C80-O12-C79	-145.6(9)
C81-C80-O12-C79	-165.1(5)
C14-O4-Si1-C32	-57.3(3)
C14-O4-Si1-C33	61.0(3)
C14-O4-Si1-C34	-178.0(3)
C37-C34-Si1-O4	-173.5(3)
C35-C34-Si1-O4	-53.4(3)
C36-C34-Si1-O4	66.3(3)
C37-C34-Si1-C32	67.7(4)
C35-C34-Si1-C32	-172.2(3)
C36-C34-Si1-C32	-52.5(3)
C37-C34-Si1-C33	-55.1(4)
C35-C34-Si1-C33	65.0(3)
C36-C34-Si1-C33	-175.4(3)
C55-O10-Si2-C73	90.6(4)
C55-O10-Si2-C74	-29.5(4)
C55-O10-Si2-C75	-150.4(3)
C78-C75-Si2-O10	57.6(4)
C77-C75-Si2-O10	178.2(3)
C76-C75-Si2-O10	-61.6(3)
C78-C75-Si2-C73	175.5(4)

Table 6.25., Cont.

C77-C75-Si2-C73	-63.8(4)
C76-C75-Si2-C73	56.3(4)
C78-C75-Si2-C74	-61.9(4)
C77-C75-Si2-C74	58.7(4)
C76-C75-Si2-C74	178.8(3)

Table 6.26. Hydrogen bonds for **4.86b** [Å and °]

D-H...A	d(D-H)	d(H...A)	d(D...A)	<(DHA)
N1-H1N...O6#1	0.90(4)	2.15(4)	3.007(4)	160(3)
N3-H2N...O11#2	0.87(4)	2.21(4)	3.073(4)	168(4)

Symmetry transformations used to generate equivalent atoms:

#1 -x+1,-y+1,-z+1 #2 -x+2,-y,-z+1

References

- (1) Dewick, P. M. *Medicinal Natural Products: A Biosynthetic Approach*; Second. West Sussex, 2002.
- (2) Kodama, S.; Hamashima, Y.; Nishide, K.; Node, M. "Total synthesis of (–)-galanthamine by remote asymmetric induction." *Angew. Chem. Int. Ed.* 2004, 43, 2659–2661.
- (3) Node, M.; Kodama, S.; Hamashima, Y.; Baba, T.; Hamamichi, N.; Nishide, K. "An efficient synthesis of (±)-narwedine and (±)-galanthamine by an improved phenolic oxidative coupling." *Angew. Chem. Int. Ed.* 2001, 40, 3060–3062.
- (4) Bernhard Küenburg; Laszlo Czollner; Johannes Fröhlich, A.; Ulrich Jordis "Development of a Pilot Scale Process for the Anti-Alzheimer Drug (–)-Galanthamine Using Large-Scale Phenolic Oxidative Coupling and Crystallisation-Induced Chiral Conversion." *Org. Process Res. Dev.* 1999, 3, 425–431.
- (5) Czollner, L.; Frantsits, W.; Küenburg, B.; Hedenig, U.; Fröhlich, J.; Jordis, U. "New kilogram-synthesis of the anti-alzheimer drug (–)-galanthamine." *Tetrahedron Lett.* 1998, 39, 2087–2088.
- (6) Yasuyuki Kita; Mitsuhiro Arisawa; Michiyo Gyoten; Makiko Nakajima; Ryuji Hamada; Hirofumi Tohma, A.; Takada, T. "Oxidative Intramolecular Phenolic Coupling Reaction Induced by a Hypervalent Iodine(III) Reagent: Leading to Galanthamine-Type Amaryllidaceae Alkaloids." *J. Org. Chem.* 1998, 63, 6625–6633.

- (7) Shimizu, K.; Tomioka, K.; Yamada, S.; Koga, K. "Stereochemical studies. LIV. A biogenetic-type asymmetric synthesis of optically active galanthamine from L-tyrosine." *Chem. Pharm. Bull.* 1978, 26, 3765–3771.
- (8) Kametani, T.; Seino, C.; Yamaki, K.; Shibuya, S.; Fukumoto, K.; Kigasawa, K.; Satoh, F.; Hiiragi, M.; Hayasaka, T. "Studies on the syntheses of heterocyclic compounds. Part CCCLXXXVI. Alternative total syntheses of galanthamine and N -benzylgalanthamine iodide." *J. Chem. Soc.* 1971, 0, 1043–1047.
- (9) Barton, D. H. R.; Kirby, G. W. "153. Phenol oxidation and biosynthesis. Part V. The synthesis of galanthamine." *J. Chem. Soc.* 1962, 806–817.
- (10) Kametani, T.; Yamaki, K.; Yagi, H.; Fukomuto, K. "Modified total synthesis of (\pm)-galanthamine through phenol oxidation." *J. Chem. Soc. D* 1969, 0, 425–426.
- (11) Krikorian, D.; Tarpanov, V.; Parushev, S.; Mechkarova, P. "New Achievements in the Field of Intramolecular Phenolic Coupling Reactions, Using Hypervalent (III) Iodine Reagent: Synthesis of Galanthamine." *Synth. Commun.* 2000, 30, 2833–2846.
- (12) Kametani, T.; Shishido, K.; Hayashi, E.; Seino, C.; Kohno, T.; Shibuya, S.; Fukumoto, K. "Syntheses of heterocyclic compounds CCCXCVI. Alternative total synthesis of (+-)-galanthamine." *J. Org. Chem.* 1971, 36, 1295–1297.
- (13) Barton, D. H. R.; Kirby, G. W. "The Synthesis of Galanthamine." *Proc. Chem. Soc.* 1960, 392–393.
- (14) Chaplin, D. A.; Fraser, N.; Tiffin, P. D. "A concise, scaleable synthesis of narwedine." *Tetrahedron Lett.* 1997, 38, 7931–7932.
- (15) Shieh, W.-C.; Carlson, J. A. "Asymmetric Transformation of Either Enantiomer of Narwedine via Total Spontaneous Resolution Process, a Concise Solution to the Synthesis of (-)-Galanthamine." *J. Org. Chem.* 1994, 59, 5463–5465.

- (16) Vanderlaan, D. G.; Schwartz, M. A. "Synthesis and oxidative coupling of (.+-.)-3-oxoreticuline." *J. Org. Chem.* 1985, 50, 743–747.
- (17) Perry, N. B.; Blunt, J. W.; McCombs, J. D.; Munro, M. H. G. "Discorhabdin C, a highly cytotoxic pigment from a sponge of the genus *Latrunculia*." *J. Org. Chem.* 1986, 51, 5476–5478.
- (18) Thal, C.; Guillou, C.; Beunard, J.-L.; Gras, E.; Potier, P.; La Recherche Scientifique Cnrs, De, C. N. Total synthesis of galanthamine, analogues and derivatives thereof. WO2002102803A1, December 27, 2002.
- (19) Buechi, G.; Matsumoto, K. E.; Nishimura, H. "Total synthesis of (+/-)-vindorosine." *J. Am. Chem. Soc.* 1971, 93, 3299–3301.
- (20) Pereira, J.; Barlier, M.; Guillou, C. "Formal total syntheses of aspidosperma alkaloids via a novel and general synthetic pathway based on an intramolecular Heck cyclization." *Org. Lett.* 2007, 9, 3101–3103.
- (21) Du, J.-Y.; Zeng, C.; Han, X.-J.; Qu, H.; Zhao, X.-H.; An, X.-T.; Fan, C.-A. "Asymmetric total synthesis of Apocynaceae hydrocarbazole alkaloids (+)-deethylbophyllidine and (+)-limaspermidine." *J. Am. Chem. Soc.* 2015, 137, 4267–4273.
- (22) Kita, Y.; Tohma, H.; Inagaki, M.; Hatanaka, K.; Kikuchi, K.; Yakura, T. "Hypervalent iodine oxidation of O-silylated phenol derivatives to azacarbocyclic spirodienones; synthetic approach to the anticancer marine alkaloid, discorhabdin C." *Tetrahedron Lett.* 1991, 32, 2035–2038.
- (23) Kita, Y.; Yakura, T.; Tohma, H.; Kikuchi, K.; Tamura, Y. "A synthetic approach to discorhabdin alkaloids: Hypervalent iodine oxidation of -substituted phenol derivatives to azacarbocyclic spirodienones." *Tetrahedron Lett.* 1989, 30, 1119–1120.

- (24) Kita, Y.; Tohma, H.; Inagaki, M.; Hatanaka, K.; Yakura, T. "Total synthesis of discorhabdin C: a general aza spiro dienone formation from O-silylated phenol derivatives using a hypervalent iodine reagent." *J. Am. Chem. Soc.* 2002.
- (25) Tohma, H.; Harayama, Y.; Hashizume, M.; Iwata, M.; Kiyono, Y.; Egi, M.; Kita, Y. "The first total synthesis of discorhabdin A." *J. Am. Chem. Soc.* 2003, 125, 11235–11240.
- (26) Moisan, L.; Wagner, M.; Comesse, S.; Doris, E. "Ring expansions of a spirocyclohexadienone system." *Tetrahedron Lett.* 2006, 47, 9093–9094.
- (27) Yu, Z.; Ju, X.; Wang, J.; Yu, W. "Iodobenzene-Mediated Intramolecular Oxidative Coupling of Substituted 4-Hydroxyphenyl-N-phenylbenzamides for the Synthesis of Spirooxindoles." *Synthesis* 2011, 2011, 860–866.
- (28) Chabaud, L.; Hromjakova, T.; Rambla, M.; Retailleau, P.; Guillou, C. "Hypervalent iodine-mediated oxidative cyclisation of p-hydroxy acetanilides to 1,2-dispirodienones." *Chem. Commun.* 2013, 49, 11542–11544.
- (29) Hromjakova, T.; Retailleau, P.; Grimaud, L.; Gandon, V.; Chabaud, L.; Guillou, C. "Hypervalent-Iodine-Mediated Synthesis of 1,2-Dispirodienones: Experimental and Theoretical Investigations." *Eur. J. Org. Chem.* 2015, 2015, 7494–7503.
- (30) de Turiso, F. G.-L.; Curran, D. P. "Radical cyclization approach to spirocyclohexadienones." *Org. Lett.* 2005, 7, 151–154.
- (31) Lanza, T.; Leardini, R.; Minozzi, M.; Nanni, D.; Spagnolo, P.; Zanardi, G. "Approach to Spirocyclohexadienimines and Corresponding Dienones through Radical ipso Cyclization onto Aromatic Azides." *Angew. Chem. Int. Ed.* 2008, 120, 9581–9584.
- (32) Lanza, T.; Minozzi, M.; Monesi, A.; Nanni, D.; Spagnolo, P.; Zanardi, G. "Improved Radical Approach to N-Unsubstituted Indol-2-one and

- Dihydro-2-quinolinone Compounds Bearing Spirocyclic Cyclohexanone/Cyclohexadienone Rings.” *Adv. Synth. Catal.* 2010, 352, 2275–2280.
- (33) Chuang, C.-P.; Tsai, A.-I.; Tsai, M.-Y. “Free radical cyclization reactions of allylsulfonyl substituted N-aryl amide derivatives.” *Tetrahedron* 2013, 69, 3293–3301.
- (34) Nishiyama, S.; Cheng, J.-F.; Tao, X. L.; Yamamura, S. “Synthetic studies on novel sulfur-containing alkaloids, prianosins and discorhabdins: total synthesis of discorhabdin C.” *Tetrahedron Lett.* 1991, 32, 4151–4154.
- (35) Liang Tao, X.; Cheng, J.-F.; Nishiyama, S.; Yamamura, S. “Synthetic studies on tetrahydropyrroloquinoline-containing natural products: Syntheses of discorhabdin C, batzelline C and isobatzelline C.” *Tetrahedron* 1994, 50, 2017–2028.
- (36) Aubart, K. M.; Heathcock, C. H. “A Biomimetic Approach to the Discorhabdin Alkaloids: Total Syntheses of Discorhabdins C and E and Dethiadiscorhabdin D.” *J. Org. Chem.* 1999, 64, 16–22.
- (37) Knölker, H.-J.; Boese, R.; Hartmann, K. “Iron-Mediated Diastereoselective Spiroannellation to the Spiro[1,2,3,4-tetrahydroquinoline-4,1'-cyclohexane] System and a Novel Rearrangement to 2,3-Dihydroindole Derivatives.” *Angew. Chem. Int. Ed.* 1989, 28, 1678–1679.
- (38) Knölker, H. J.; Hartmann, K. “Transition Metal-Diene Complexes in Organic Synthesis; Part 8.1 Iron-Mediated Approach to the Discorhabdin and Prianosin Alkaloids.” *Synlett* 1991, 1991, 428–430.

- (39) Magnus, P.; Sane, N.; Fauber, B. P.; Lynch, V. "Concise syntheses of (-)-galanthamine and (+/-)-codeine via intramolecular alkylation of a phenol derivative." *J. Am. Chem. Soc.* 2009, 131, 16045–16047.
- (40) Winstein, S.; Baird, R. "The Formation of Dienones Through Ar1-Participation." *J. Am. Chem. Soc.* 1957, 79, 756–757.
- (41) Winstein, S.; Baird, R. "Isolation and Behavior of spiro[2,5]Octa-1,4-diene-3-one." *J. Am. Chem. Soc.* 1957, 79, 4238–4240.
- (42) Mandell, L.; Caine, D.; Kilpatrick, G. E. "The Synthesis of Dienones Related to Santonin and ψ -Santonin via Aryl Participation." *J. Am. Chem. Soc.* 1961, 83, 4457–4460.
- (43) Masamune, S. "Synthesis of 4a,6-Ethano-5,6,7,8-tetrahydro-2(4a)-naphthalenone." *J. Am. Chem. Soc.* 1961, 83, 1009–1010.
- (44) Masamune, S. "Total Syntheses of Diterpenes and Diterpene Alkaloids. II. 1A Tetracyclic Common Intermediate." *J. Am. Chem. Soc.* 1964, 86, 288–289.
- (45) Masamune, S. "Total Syntheses of Diterpenes and Diterpene Alkaloids. III. 1Kaurene." *J. Am. Chem. Soc.* 1964, 86, 289–290.
- (46) Masamune, S. "Total Syntheses of Diterpenes and Diterpene Alkaloids. IV. 1Garryine." *J. Am. Chem. Soc.* 1964, 86, 290–291.
- (47) Masamune, S. "Total Syntheses of Diterpenes and Diterpene Alkaloids. V. 1Atisine." *J. Am. Chem. Soc.* 1964, 86, 291–292.
- (48) Marshall, J.; Brady, S. "The Total Synthesis of (\pm)-Hinesol." *J. Org. Chem.* 1970, 35, 4068–4077.
- (49) Murphy, W. S.; Wattanasin, S. "Anionic cyclization of phenols." *Chem. Soc. Rev.* 1983, 12, 213–250.

- (50) Kublak, G. G.; Confalone, P. N. "The preparation of the AZA-spirobicyclic system of discorhabdin C via an intramolecular phenolate alkylation." *Tetrahedron Lett.* 1990, 31, 3845–3848.
- (51) Ghavimi, B.; Magnus, P. "Total Synthesis of 8,14-Dihydromorphinandienone Alkaloids." *Org. Lett.* 2014, 16, 1708–1711.
- (52) He, L.; Zhang, Y.-H.; Guan, H.-Y.; Zhang, J.-X.; Sun, Q.-Y.; Hao, X.-J. "Cepharatines A-D, hasubanan-type alkaloids from *Stephania cepharantha*." *J. Nat. Prod.* 2011, 74, 181–184.
- (53) Magnus, P.; Seipp, C. "Concise Synthesis of the Hasubanan Alkaloid (\pm)-Cepharatine A Using a Suzuki Coupling Reaction To Effect o,p-Phenolic Coupling." *Org. Lett.* 2013, 15, 4870–4871.
- (54) Chuang, K. V.; Navarro, R.; Reisman, S. E. "Short, Enantioselective Total Syntheses of (–)-8-Demethoxyrunanine and (–)-Cepharatines A, C, and D." *Angew. Chem. Int. Ed.* 2011, 50, 9447–9451.
- (55) Magnus, P.; Marks, K. D.; Meis, A. "New strategy for the synthesis of proaporphine and homoproaporphine-type alkaloids from a common intermediate." *Tetrahedron* 2015, 71, 3872–3877.
- (56) Meis, A. Unpublished Results.
- (57) Hodges, T. R. "The study of a codeine bromohydrin rearrangement and investigation of a phenolic alkylation strategy." Masters thesis, University of Texas at Austin, 2013.
- (58) Denton, R. M.; Scragg, J. T. "A strategy for the synthesis of the fargenone/fargenin family of natural products: synthesis of the tricyclic core." *Org. Biomol. Chem.* 2012, 10, 5629–5635.

- (59) Fauber, B. D. "Studies directed toward the syntheses of the biologically active alkaloids (-)-galanthamine and (-)-lemonomycin." Ph. D. dissertation, University of Texas at Austin, 2006.
- (60) Barber, H. J. "35. Some sulphonyl derivatives of amidines and imino-ethers." J. Chem. Soc. 1943, 101–104.
- (61) Russell Bowman, W.; Coghlan, D. R. "A facile method for the N-alkylation of α -amino esters." Tetrahedron 1997, 53, 15787–15798.
- (62) González-Rosende, M. E.; Castillo, E.; Asíns, B.; Mamouni, R.; Sepúlveda-Arques, J. "Transamidation reactions of 2-(2-sulfonylguanidino)acetamides." Tetrahedron 2007, 63, 8709–8714.
- (63) Kleb, V. K. G. "Neue Umlagerung vom Typ der Smiles-Reaktion." Angew. Chem. 1968, 80, 284–285.
- (64) Ono, M.; Araya, I.; Tamura, S. "Amidines. V. Smiles rearrangement of N1-(p-nitrobenzenesulfonyl)-N1,N2-diarylacetamidines." Chem. Pharm. Bull. 1990, 38, 1373–1378.
- (65) Sandoval, A.; Miramontes, L.; Rosenkranz, G.; Djerassi, C. "The Dienone—Phenol Rearrangement." J. Am. Chem. Soc. 1951, 73, 990–991.
- (66) Woodward, R. B.; Singh, T. "Synthesis and Rearrangement of Cyclohexadienones." J. Am. Chem. Soc. 1950, 72, 494–500.
- (67) Fenton, S. W.; Arnold, R. T.; Fritz, H. E. "The Dienone-Phenol Rearrangement. IV 1." J. Am. Chem. Soc. 1955, 77, 5983–5986.
- (68) Arnold, R. T.; Buckley, J. S., Jr; Richter, J. "The Dienone—Phenol Rearrangement." J. Am. Chem. Soc. 1947, 69, 2322–2325.
- (69) Wasserman, H. H.; Tremper, A. W. " β -lactams from azetidine carboxylic acids by peracid reaction with iminium salts." Tetrahedron Lett. 1977, 18, 1449–1450.

- (70) Grieco, P. A.; Oguri, T.; Yokoyama, Y. "One-step conversion of protected lactols into lactones." *Tetrahedron Lett.* 1978, 19, 419–420.
- (71) Staub, G. M.; Gloer, J. B.; Wicklow, D. T.; Dowd, P. F. "Aspernomine: a cytotoxic antiinsectan metabolite with a novel ring system from the sclerotia of *Aspergillus nomius*." *J. Am. Chem. Soc.* 1992, 114, 1015–1017.
- (72) Ding, L.; Maier, A.; Fiebig, H.-H.; Lin, W.-H.; Hertweck, C. "A family of multicyclic indolosesquiterpenes from a bacterial endophyte." *Org. Biomol. Chem.* 2011, 9, 4029–4031.
- (73) Yahua Liu; William W McWhorter, A., Jr; Hadden, C. E. "Novel Rearrangement of a 2-Aryl-3-alkyl-3H-indol-3-ol to a 1,4,5,6-Tetrahydro-2,6-methano-1-benzazocin-3(2H)-one with Implications for the Biosynthesis of Aspernomine." *Org. Lett.* 2003, 5, 333–335.
- (74) Ho, G. A.; Nouri, D. H.; Tantillo, D. J. "Carbocation rearrangements in aspernomine biosynthesis." *Tetrahedron Lett.* 2009, 50, 1578–1581.
- (75) Sun, Y.; Chen, P.; Zhang, D.; Baunach, M.; Hertweck, C.; Li, A. "Bioinspired Total Synthesis of Sespenine." *Angew. Chem. Int. Ed.* 2014, 53, 9012–9016.
- (76) Zhang, J.; Wei, C.; Li, C.-J. "Cu(I)Br mediated coupling of alkynes with N-acylimine and N-acyliminium ions in water." *Tetrahedron Lett.* 2002, 43, 5731–5733.
- (77) Maity, P.; Srinivas, H. D.; Watson, M. P. "Copper-Catalyzed Enantioselective Additions to Oxocarbenium Ions: Alkynylation of Isochroman Acetals." *J. Am. Chem. Soc.* 2011, 133, 17142–17145.
- (78) Luche, J.-L. "Lanthanides in organic chemistry. 1. Selective 1,2 reductions of conjugated ketones." *J. Am. Chem. Soc.* 1978, 100, 2226–2227.

- (79) Hioki, H.; Izawa, T.; Yoshizuka, M.; Kunitake, R.; Itô, S. "Intramolecular amidoalkylation of chiral imines and iminium ions: Stereoselective synthesis of anti-1,2- and -1,3-aminoalcohols." *Tetrahedron Lett.* 1995, 36, 2289–2292.
- (80) Tomita, D.; Yamatsugu, K.; Kanai, M.; Shibasaki, M. "Enantioselective Synthesis of SM-130686 Based on the Development of Asymmetric Cu(I)F Catalysis To Access 2-Oxindoles Containing a Tetrasubstituted Carbon." *J. Am. Chem. Soc.* 2009, 131, 6946–6948.
- (81) Seiji Suga; Yasuhisa Kageyama; Govindarajulu Babu; Kenichiro Itami, A.; Yoshida, J.-I. "Cationic Carbohydroxylation of Alkenes and Alkynes Using the Cation Pool Method." *Org. Lett.* 2004, 6, 2709–2711.
- (82) Burke, S. D.; Murtiashaw, C. W.; Dike, M. S.; Strickland, S. M. S.; Saunders, J. O. "Vinylsilane-mediated spiroannulation. Synthesis of spiro[4.5]decadienones." *J. Org. Chem.* 1981, 46, 2400–2402.
- (83) Candeias, N. R.; Montalbano, F.; Cal, P. M. S. D.; Gois, P. M. P. "Boronic Acids and Esters in the Petasis-Borono Mannich Multicomponent Reaction." *Chem. Rev.* 2010, 110, 6169–6193.
- (84) Robert A Batey; D Bruce MacKay, A.; Santhakumar, V. "Alkenyl and Aryl Boronates Mild Nucleophiles for the Stereoselective Formation of Functionalized N-Heterocycles." *J. Am. Chem. Soc.* 1999, 121, 5075–5076.
- (85) Vo, C.-V. T.; Mitchell, T. A.; Bode, J. W. "Expanded substrate scope and improved reactivity of ether-forming cross-coupling reactions of organotrifluoroborates and acetals." *J. Am. Chem. Soc.* 2011, 133, 14082–14089.
- (86) Åhman, J.; Somfai, P. "Carbon-carbon bond formation via N-tosyliminium ions." *Tetrahedron* 1992, 48, 9537–9544.

- (87) Koulocheri, S. D.; Pitsinos, E. N.; Haroutounian, S. A. "A Convenient Route to Alkaloid Lipids: Application for the Synthesis of a Leptophylline A Analogue." *Synthesis* 2002, 2002, 0111–0115.
- (88) Yang, C.-F.; Xu, Y.-M.; Liao, L.-X.; Zhou, W.-S. "Asymmetric total synthesis of (+)-desoxoprosophylline." *Tetrahedron Lett.* 1998, 39, 9227–9228.
- (89) Muthusamy, S.; Gangadurai, C.; Krishnamurthi, J.; Suresh, E. "Stereoselective synthesis of piperidinone and quinolinone systems via ring opening reactions using TiCl_4 /silyl reagents." *Tetrahedron* 2011, 67, 4212–4220.
- (90) Kobayashi, S.; Ishitani, H. "Catalytic Enantioselective Addition to Imines." *Chem. Rev.* 1999, 99, 1069–1094.
- (91) Dai, L. X.; Lin, Y. R.; Hou, X. L.; Zhou, Y. G. "Stereoselective reactions with imines." *Pure Appl. Chem.* 1999, 71, 1033–1040.
- (92) Čapka, M.; Hetflejš, J. "Ligand effects in the nickel catalysed addition of trichlorosilane to 1,3-butadiene." *Collect. Czech. Chem. Commun.* 1975, 40, 2073–2083.
- (93) Yu, W.; Mei, Y.; Kang, Y.; Hua, Z.; Jin, Z. "Improved procedure for the oxidative cleavage of olefins by OsO_4 - NaIO_4 ." *Org. Lett.* 2004, 6, 3217–3219.
- (94) Rossi, L.; Pecunioso, A. "Regiospecific procedure for the preparation of silyl enol ethers from α -(N-alkoxycarbonylamino)ketones." *Tetrahedron Lett.* 1994, 35, 5285–5288.
- (95) Knezevic, C. E. "Developement of Poly(ADP-Ribose) Glycohydrolase Inhibitors and Tetracyclic Indoles as Anticancer Compounds." Ph. D. dissertation, University of Illinois at Urbana-Champaign, 2014.

- (96) Parkinson, E. I. "Deoxynyboquinones as NQO1-Targeted Anticancer Compounds and Deoxynybomycins as Potent and Selective Antibiotics." Ph. D. dissertation, University of Illinois at Urbana-Champaign, 2015.
- (97) American Cancer Society Cancer Facts & Figures 2015; Atlanta, Ga, 2015; pp. 1–56.
- (98) Demain, A. L.; Vaishnav, P. "Natural products for cancer chemotherapy." *Microb. Biotechnol.* 2011, 4, 687–699.
- (99) World Health Organization WHO Model List of Essential Medicines; 2015; pp. 1–55.
- (100) Granger, B. A.; Jewett, I. T.; Butler, J. D.; Hua, B.; Knezevic, C. E.; Parkinson, E. I.; Hergenrother, P. J.; Martin, S. F. "Synthesis of (±)-actinophyllic acid and analogs: applications of cascade reactions and diverted total synthesis." *J. Am. Chem. Soc.* 2013, 135, 12984–12986.
- (101) Njardarson, J. T.; Gaul, C.; Shan, D.; Huang, X.-Y.; Danishefsky, S. J. "Discovery of potent cell migration inhibitors through total synthesis: lessons from structure-activity studies of (+)-migrastatin." *J. Am. Chem. Soc.* 2004, 126, 1038–1040.
- (102) Rivkin, A.; Chou, T. C.; Danishefsky, S. J. "On the Remarkable Antitumor Properties of Fludelone: How We Got There." *Angew. Chem. Int. Ed.* 2005, 44, 2838–2850.
- (103) Oskarsson, T.; Nagorny, P.; Krauss, I. J.; Perez, L.; Mandal, M.; Yang, G.; Ouerfelli, O.; Xiao, D.; Moore, M. A. S.; Massagué, J.; Danishefsky, S. J. "Diverted Total Synthesis Leads to the Generation of Promising Cell-Migration Inhibitors for Treatment of Tumor Metastasis: In vivo and Mechanistic Studies on the Migrastatin Core Ether Analog." *J. Am. Chem. Soc.* 2010, 132, 3224–3228.

- (104) Fürstner, A. "From Total Synthesis to Diverted Total Synthesis: Case Studies in the Amphidinolide Series." *Isr. J. Chem.* 2011, 51, 329–345.
- (105) Fürstner, A.; Kirk, D.; Fenster, M. D. B.; Aïssa, C.; De Souza, D.; Müller, O. "Diverted total synthesis: preparation of a focused library of latrunculin analogues and evaluation of their actin-binding properties." *Proc. Nat. Acad. Sci.* 2005, 102, 8103–8108.
- (106) Fuwa, H.; Kainuma, N.; Tachibana, K.; Tsukano, C.; Satake, M.; Sasaki, M. "Diverted Total Synthesis and Biological Evaluation of Gambierol Analogues: Elucidation of Crucial Structural Elements for Potent Toxicity." *Chem. Eur. J.* 2004, 10, 4894–4909.
- (107) Chany, A. C.; Casarotto, V.; Schmitt, M.; Tarnus, C.; Guenin Macé, L.; Demangel, C.; Mirguet, O.; Eustache, J.; Blanchard, N. "A Diverted Total Synthesis of Mycolactone Analogues: An Insight into Buruli Ulcer Toxins." *Chem. Eur. J.* 2011, 17, 14413–14419.
- (108) Li, C.; Dong, T.; Li, Q.; Lei, X. "Probing the Anticancer Mechanism of (–)-Ainsliatrimmer A through Diverted Total Synthesis and Bioorthogonal Ligation." *Angew. Chem. Int. Ed.* 2014, 53, 12111–12115.
- (109) Du, C.; Li, L.; Li, Y.; Xie, Z. "Construction of Two Vicinal Quaternary Carbons by Asymmetric Allylic Alkylation: Total Synthesis of Hyperolactone C and (–)-Biyouyanagin A." *Angew. Chem. Int. Ed.* 2009, 48, 7853–7856.
- (110) Szpilman, A. M.; Carreira, E. M. "Probing the Biology of Natural Products: Molecular Editing by Diverted Total Synthesis." *Angew. Chem. Int. Ed.* 2010.
- (111) Carroll, A. R.; Hyde, E.; Smith, J.; Quinn, R. J.; Guymer, G.; Forster, P. I. "Actinophyllic acid, a potent indole alkaloid inhibitor of the coupled enzyme

- assay carboxypeptidase u/hippuricase from the leaves of *Alstonia actinophylla* (Apocynaceae)." *J. Org. Chem.* 2005, 70, 1096–1099.
- (112) Leurs, J.; Nerme, V.; Sim, Y.; Hendriks, D. "Carboxypeptidase U (TAFIa) prevents lysis from proceeding into the propagation phase through a threshold-dependent mechanism." *J. Thromb. Haemost.* 2004, 2, 416–423.
- (113) Willemse, J. L.; Hendriks, D. F. "Measurement of Procarboxypeptidase U (TAFI) in Human Plasma: A Laboratory Challenge." *Clin. Chem.* 2006, 52, 30–36.
- (114) Bouma, B. N.; Mosnier, L. O. "Thrombin Activatable Fibrinolysis Inhibitor (TAFI) at the Interface between Coagulation and Fibrinolysis." *Pathophysiol. Haemos. Thromb.* 2003, 33, 375–381.
- (115) Dubis, J.; Witkiewicz, W. "The Role of Thrombin-Activatable Fibrinolysis Inhibitor in the Pathophysiology of Hemostasis." *Adv. Clin. Exp. Med.* 2010, 19, 379–387.
- (116) Hataji, O.; Taguchi, O.; Gabazza, E. C.; Yuda, H.; D'Alessandro-Gabazza, C. N.; Fujimoto, H.; Nishii, Y.; Hayashi, T.; Suzuki, K.; Adachi, Y. "Increased circulating levels of thrombin-activatable fibrinolysis inhibitor in lung cancer patients." *Am. J. Hematol.* 2004, 76, 214–219.
- (117) Kwaan, H. C.; McMahon, B. The Role of Plasminogen-Plasmin System in Cancer. In *Coagulation in Cancer*; Springer US, 2009; pp. 43–66.
- (118) Hanahan, D.; Weinberg, R. A. "The hallmarks of cancer." *Cell* 2000, 100, 57–70.
- (119) Reijerkerk, A.; Voest, E. E.; Gebbink, M. F. "No grip, no growth: the conceptual basis of excessive proteolysis in the treatment of cancer." *Eur. J. Cancer* 2000, 36, 1695–1705.
- (120) Granger, B. A. "Development of multicomponent assembly processes and their application to the synthesis of novel heterocyclic scaffolds and the total synthesis

- of actinophyllic acid : application of an iminium ion mediated cascade." Ph. D. dissertation, University of Texas at Austin, 2013.
- (121) Jewett, I. T. "Development of iminium ion cascade methodologies and their application to the synthesis of complex molecules." Ph. D. dissertation, University of Texas at Austin, 2010.
- (122) Granger, B. A.; Jewett, I. T.; Butler, J. D.; Martin, S. F. "Concise total synthesis of (\pm)-actinophyllic acid." *Tetrahedron* 2014, 70, 4094–4104.
- (123) O'Brien, J.; Wilson, I.; Orton, T.; Pognan, F. "Investigation of the Alamar Blue (resazurin) fluorescent dye for the assessment of mammalian cell cytotoxicity." *FEBS J.* 2000, 267, 5421–5426.
- (124) Gleeson, M. P.; Hersey, A.; Montanari, D.; Overington, J. "Probing the links between in vitro potency, ADMET and physicochemical parameters." *Nat. Rev. Drug Discov.* 2011, 10, 197–208.
- (125) Hann, M. M. "Molecular obesity, potency and other addictions in drug discovery." *Med. Chem. Commun.* 2011, 2, 349–355.
- (126) Holbeck, S. L.; Collins, J. M.; Doroshow, J. H. "Analysis of Food and Drug Administration–Approved Anticancer Agents in the NCI60 Panel of Human Tumor Cell Lines." *Mol. Cancer. Ther.* 2010, 9, 1451–1460.
- (127) Wong, C. C.; Cheng, K.-W.; Rigas, B. "Preclinical Predictors of Anticancer Drug Efficacy: Critical Assessment with Emphasis on Whether Nanomolar Potency Should Be Required of Candidate Agents." *J. Pharmacol. Exp. Ther.* 2012, 341, 572–578.
- (128) Hill, A. V. "The Possible Effects of the Aggregation of the Molecules of Haemoglobin on its Dissociation Curves." *J. Physiol.* 1910, 40, iv–vii.

- (129) Fallahi-Sichani, M.; Honarnejad, S.; Heiser, L. M.; Gray, J. W.; Sorger, P. K. "Metrics other than potency reveal systematic variation in responses to cancer drugs." *Nat. Chem. Biol.* 2013, 9, 708–714.
- (130) Vainstein, V.; Eide, C. A.; O'Hare, T.; Shukron, O.; Druker, B. J. "Integrating in vitro sensitivity and dose-response slope is predictive of clinical response to ABL kinase inhibitors in chronic myeloid leukemia." *Blood* 2013, 122, 3331–3334.
- (131) Sampah, M. E. S.; Shen, L.; Jilek, B. L.; Siliciano, R. F. "Dose–response curve slope is a missing dimension in the analysis of HIV-1 drug resistance." *Proc. Nat. Acad. Sci.* 2011, 108, 7613–7618.
- (132) Mestres, J.; Gregori-Puigjané, E.; Valverde, S.; Solé, R. V. "The topology of drug-target interaction networks: implicit dependence on drug properties and target families." *Mol. Biosyst.* 2009, 5, 1051–1057.
- (133) Peters, J.-U. "Polypharmacology – Foe or Friend?." *J. Med. Chem.* 2013, 56, 8955–8971.
- (134) Anighoro, A.; Bajorath, J.; Rastelli, G. "Polypharmacology: Challenges and Opportunities in Drug Discovery." *J. Med. Chem.* 2014, 57, 7874–7887.
- (135) Reddy, A. S.; Zhang, S. "Polypharmacology: drug discovery for the future." *Expert Rev. Clin. Pharm.* 2014, 6, 41–47.
- (136) Bair, J. S.; Palchaudhuri, R.; Hergenrother, P. J. "Chemistry and biology of deoxynyboquinone, a potent inducer of cancer cell death." *J. Am. Chem. Soc.* 2010, 132, 5469–5478.
- (137) Wictome, M.; Henderson, I.; Lee, A. G.; East, J. M. "Mechanism of inhibition of the calcium pump of sarcoplasmic reticulum by thapsigargin." *Biochem. J.* 1992, 283, 525–529.

- (138) Bonvini, P.; Zorzi, E.; Basso, G.; Rosolen, A. "Bortezomib-mediated 26S proteasome inhibition causes cell-cycle arrest and induces apoptosis in CD-30+ anaplastic large cell lymphoma." *Leukemia* 2007.
- (139) Rüegg, U. T.; Gillian, B. "Staurosporine, K-252 and UCN-01: potent but nonspecific inhibitors of protein kinases." *Trends Pharmacol. Sci.* 1989, 10, 218–220.
- (140) Wolan, D. W.; Zorn, J. A.; Gray, D. C.; Wells, J. A. "Small-Molecule Activators of a Proenzyme." *Science* 2009, 326, 853–858.
- (141) Coleman, M. D. "Dapsone toxicity: Some current perspectives." *Vascul. Pharmacol.* 1995, 26, 1461–1467.
- (142) Salauze, D.; Decouvelaere, D. "In vitro assessment of the haemolytic potential of candidate drugs." *Comp. Haematol. Int.* 1994, 4, 34–36.
- (143) Cho, W.-S.; Duffin, R.; Bradley, M.; Megson, I. L.; MacNee, W.; Lee, J. K.; Jeong, J.; Donaldson, K. "Predictive value of in vitro assays depends on the mechanism of toxicity of metal oxide nanoparticles." *Part. Fibre Toxicol.* 2013, 10, 1.
- (144) Lee, H. Y. Mice Work for 1257 and 1258.
- (145) Pulaski, B. A.; Ostrand-Rosenberg, S. *Mouse 4T1 Breast Tumor Model*; John Wiley & Sons, Inc.: Hoboken, NJ, USA, 2001.
- (146) Weaver, B. A. "How Taxol/paclitaxel kills cancer cells." *Mol. Biol. Cell* 2014, 25, 2677–2681.
- (147) Brito, D. A.; Yang, Z.; Rieder, C. L. "Microtubules do not promote mitotic slippage when the spindle assembly checkpoint cannot be satisfied." *J. Cell Biol.* 2008, 182, 623–629.

- (148) Pommier, Y. "Topoisomerase I inhibitors: camptothecins and beyond." *Nat. Rev. Cancer* 2006, 6, 789–802.
- (149) Gardner, S. N. "A Mechanistic, Predictive Model of Dose-Response Curves for Cell Cycle Phase-specific and -nonspecific Drugs." *Cancer Res.* 2000, 60, 1417–1425.
- (150) Alagkiozidis, I.; Facciabene, A.; Tsiatas, M.; Carpenito, C.; Benencia, F.; Adams, S.; Jonak, Z.; June, C. H.; Powell, D. J.; Coukos, G. "Time-dependent cytotoxic drugs selectively cooperate with IL-18 for cancer chemo-immunotherapy." *J. Transl. Med.* 2011, 9, 1.
- (151) Hoskins, P.; Eisenhauer, E.; Beare, S.; Roy, M.; Drouin, P.; Stuart, G.; Bryson, P.; Grimshaw, R.; Capstick, V.; Zee, B. "Randomized phase II study of two schedules of topotecan in previously treated patients with ovarian cancer: a National Cancer Institute of Canada Clinical Trials Group study." *J. Clin. Oncol.* 1998, 16, 2233–2237.
- (152) Un, F. "G1 arrest induction represents a critical determinant for cisplatin cytotoxicity in G1 checkpoint-retaining human cancers." *Anti-Cancer Drugs* 2007, 18, 411–417.
- (153) Sax, J. K.; El-Deiry, W. S. "p53 downstream targets and chemosensitivity." *Cell Death Differ.* 2003, 10, 413–417.
- (154) Weinberg, R. A. *The Biology of Cancer*; Garland Science: New York, 2007.
- (155) Jordan, M. A.; Thrower, D.; Wilson, L. "Effects of vinblastine, podophyllotoxin and nocodazole on mitotic spindles. Implications for the role of microtubule dynamics in mitosis." *J. Cell. Sci.* 1992, 102 (Pt 3), 401–416.

- (156) Suzuki, T.; Fujikura, K.; Higashiyama, T.; Takata, K. "DNA Staining for Fluorescence and Laser Confocal Microscopy." *J. Histochem. Cytochem.* 1997, 45, 49–53.
- (157) Ouyang, L.; Shi, Z.; Zhao, S.; Wang, F. T.; Zhou, T. T.; Liu, B.; Bao, J. K. "Programmed cell death pathways in cancer: a review of apoptosis, autophagy and programmed necrosis." *Cell Prolif.* 2012, 45, 487–498.
- (158) Elmore, S. "Apoptosis: a review of programmed cell death." *Toxicol. Pathol.* 2007, 35, 495–516.
- (159) Hongmei, Z. Extrinsic and Intrinsic Apoptosis Signal Pathway Review; InTech, 2012.
- (160) Caserta, T. M.; Smith, A. N.; Gultice, A. D.; Reedy, M. A.; Brown, T. L. "Q-VD-OPh, a broad spectrum caspase inhibitor with potent antiapoptotic properties." *Apoptosis* 2003, 8, 345–352.
- (161) Wolvetang, E. J.; Johnson, K. L.; Krauer, K.; Ralph, S. J.; Linnane, A. W. "Mitochondrial respiratory chain inhibitors induce apoptosis." *FEBS Lett.* 1994, 339, 40–44.
- (162) Bakker, E. P.; Van Den Heuvel, E. J.; Van Dam, K. "The binding of uncouplers of oxidative phosphorylation to rat-liver mitochondria." *BBA-Bioenergetics* 1974, 333, 12–21.
- (163) García-Rivas, G. de J.; Carvajal, K.; Correa, F.; Zazueta, C. "Ru360, a specific mitochondrial calcium uptake inhibitor, improves cardiac post-ischaemic functional recovery in rats in vivo." *Br. J. Pharmacol.* 2006, 149, 829–837.
- (164) Komarov, P. G.; Komarova, E. A.; Kondratov, R. V.; Christov-Tselkov, K.; Coon, J. S.; Chernov, M. V.; Gudkov, A. V. "A chemical inhibitor of p53 that

- protects mice from the side effects of cancer therapy.” *Science* 1999, 285, 1733–1737.
- (165) Bourdon, J.-C.; Surget, S.; Khoury, M. P. “Uncovering the role of p53 splice variants in human malignancy: a clinical perspective.” *Onco Targets Ther.* 2013, Volume 7, 57–68.
- (166) Strom, E.; Sathe, S.; Komarov, P. G.; Chernova, O. B.; Pavlovskaya, I.; Shyshynova, I.; Bosykh, D. A.; Burdelya, L. G.; Macklis, R. M.; Skaliter, R.; Komarova, E. A.; Gudkov, A. V. “Small-molecule inhibitor of p53 binding to mitochondria protects mice from gamma radiation.” *Nat. Chem. Biol.* 2006, 2, 474–479.
- (167) Becattini, B.; Sareth, S.; Zhai, D.; Crowell, K. J.; Leone, M.; Reed, J. C.; Pellecchia, M. “Targeting Apoptosis via Chemical Design.” *Chem. Biol.* 2004, 11, 1107–1117.
- (168) Chen, Y. N.; Aihara, M.; Araie, M.; Matsuyama, S. “Neuroprotective Effects of Bax-inhibiting Peptides on Hypoxic Damages in Purified Cultured Retinal Ganglion Cells.” *Invest. Ophthalmol. Vis. Sci.* 2005, 46, 1314–1314.
- (169) Peixoto, P. M.; Ryu, S.-Y.; Bombrun, A.; Antonsson, B.; Kinnally, K. W. “MAC inhibitors suppress mitochondrial apoptosis.” *Biochem. J.* 2009, 423, 381–387.
- (170) Ferraro, E.; Fuoco, C.; Strappazon, F.; Cecconi, F. Apoptosome Structure and Regulation. In *Apoptosome*; Springer Netherlands, 2010; pp. 27–39.
- (171) Lademann, U.; Cain, K.; Gyrd-Hansen, M.; Brown, D.; Peters, D.; Jäättelä, M. “Diarylurea Compounds Inhibit Caspase Activation by Preventing the Formation of the Active 700-Kilodalton Apoptosome Complex.” *Mol. Cell. Biol.* 2003, 23, 7829–7837.

- (172) Degterev, A.; Huang, Z.; Boyce, M.; Li, Y.; Jagtap, P.; Mizushima, N.; Cuny, G. D.; Mitchison, T. J.; Moskowitz, M. A.; Yuan, J. "Chemical inhibitor of nonapoptotic cell death with therapeutic potential for ischemic brain injury." *Nat. Chem. Biol.* 2005, 1, 112–119.
- (173) Bennett, B. L.; Sasaki, D. T.; Murray, B. W.; O'Leary, E. C.; Sakata, S. T.; Xu, W.; Leisten, J. C.; Motiwala, A.; Pierce, S.; Satoh, Y.; Bhagwat, S. S.; Manning, A. M.; Anderson, D. W. "SP600125, an anthrapyrazolone inhibitor of Jun N-terminal kinase." *Proc. Nat. Acad. Sci.* 2001, 98, 13681–13686.
- (174) Huang, Y.; Wang, K. K. W. "The calpain family and human disease." *Trends Mol. Med.* 2001, 7, 355–362.
- (175) Tsujinaka, T.; Kajiwar, Y.; Kambayashi, J.; Sakon, M.; Higuchi, N.; Tanaka, T.; Mori, T. "Synthesis of a new cell penetrating calpain inhibitor (calpeptin)." *Biochem. Biophys. Res. Commun.* 1988, 153, 1201–1208.
- (176) Dong, X.-X.; Wang, Y.; Qin, Z.-H. "Molecular mechanisms of excitotoxicity and their relevance to pathogenesis of neurodegenerative diseases." *Acta Pharmacol. Sin.* 2009, 30, 379–387.
- (177) Wong, E. H.; Kemp, J. A.; Priestley, T.; Knight, A. R.; Woodruff, G. N.; Iversen, L. L. "The anticonvulsant MK-801 is a potent N-methyl-D-aspartate antagonist.." *Proc. Nat. Acad. Sci.* 1986, 83, 7104–7108.
- (178) Heeres, J. T.; Hergenrother, P. J. "Poly(ADP-ribose) makes a date with death." *Curr. Opin. Chem. Biol.* 2007, 11, 644–653.
- (179) Vanderbist, F.; Maes, P.; Nève, J. "In vitro comparative assessment of the antioxidant activity of nacystelyn against three reactive oxygen species." *Arzneimittelforschung* 1996, 46, 783–788.

- (180) Taylor, C. W.; Tovey, S. C. "IP(3) receptors: toward understanding their activation." *Cold Spring Harb. Perspect. Biol.* 2010, 2, a004010.
- (181) Choe, C.-U.; Ehrlich, B. E. "The inositol 1,4,5-trisphosphate receptor (IP3R) and its regulators: sometimes good and sometimes bad teamwork." *Sci. Signal.* 2006, 2006, re15.
- (182) Prentki, M.; Deeney, J. T.; Matschinsky, F. M.; Joseph, S. K. "Neomycin: a specific drug to study the inositol-phospholipid signalling system?." *FEBS Lett.* 1986, 197, 285–288.
- (183) Clarke, H. J.; Chambers, J. E.; Liniker, E.; Marciniak, S. J. "Endoplasmic Reticulum Stress in Malignancy." *Cancer Cell* 2014, 25, 563–573.
- (184) Wang, G.; Yang, Z. Q.; Zhang, K. "Endoplasmic reticulum stress response in cancer: molecular mechanism and therapeutic potential." *Am J Transl Res* 2010.
- (185) Zhang, L.; Wang, A. "Virus-induced ER stress and the unfolded protein response." *Front. Plant Sci.* 2012, 3.
- (186) Katayama, T.; Imaizumi, K.; Manabe, T.; Hitomi, J.; Kudo, T.; Tohyama, M. "Induction of neuronal death by ER stress in Alzheimer's disease." *J. Chem. Neuroanat.* 2004, 28, 67–78.
- (187) Imaizumi, K.; Miyoshi, K.; Katayama, T.; Yoneda, T.; Taniguchi, M.; Kudo, T.; Tohyama, M. "The unfolded protein response and Alzheimer's disease." *Biochim. Biophys. Acta* 2001, 1536, 85–96.
- (188) Roussel, B. D.; Kruppa, A. J.; Miranda, E.; Crowther, D. C.; Lomas, D. A.; Marciniak, S. J. "Endoplasmic reticulum dysfunction in neurological disease." *Lancet Neurol.* 2013, 12, 105–118.
- (189) Hetz, C.; Chevet, E.; Harding, H. P. "Targeting the unfolded protein response in disease." *Nat. Rev. Drug Discov.* 2013, 12, 703–719.

- (190) Schröder, M.; Kaufman, R. J. "ER stress and the unfolded protein response." *Mutation Research/Fundamental and Molecular Mechanisms of Mutagenesis* 2005, 569, 29–63.
- (191) Papandreou, I.; Denko, N. C.; Olson, M.; Van Melckebeke, H.; Lust, S.; Tam, A.; Solow-Cordero, D. E.; Bouley, D. M.; Offner, F.; Niwa, M.; Koong, A. C. "Identification of an Ire1alpha endonuclease specific inhibitor with cytotoxic activity against human multiple myeloma." *Blood* 2011, 117, 1311–1314.
- (192) Axten, J. M.; Medina, J. R.; Feng, Y.; Shu, A.; Romeril, S. P.; Grant, S. W.; Li, W. H. H.; Heerding, D. A.; Minthorn, E.; Mencken, T.; Atkins, C.; Liu, Q.; Rabindran, S.; Kumar, R.; Hong, X.; Goetz, A.; Stanley, T.; Taylor, J. D.; Sigethy, S. D.; Tomberlin, G. H.; Hassell, A. M.; Kahler, K. M.; Shewchuk, L. M.; Gampe, R. T. "Discovery of 7-Methyl-5-(1-{[3-(trifluoromethyl)phenyl]acetyl}-2,3-dihydro-1H-indol-5-yl)-7H-pyrrolo[2,3-d]pyrimidin-4-amine (GSK2606414), a Potent and Selective First-in-Class Inhibitor of Protein Kinase R (PKR)-like Endoplasmic Reticulum Kinase (PERK)." *J. Med. Chem.* 2012.
- (193) de Almeida, S. F.; Picarote, G.; Fleming, J. V.; Carmo-Fonseca, M.; Azevedo, J. E.; de Sousa, M. "Chemical Chaperones Reduce Endoplasmic Reticulum Stress and Prevent Mutant HFE Aggregate Formation." *J. Biol. Chem.* 2007, 282, 27905–27912.
- (194) Schneider-Poetsch, T.; Ju, J.; Eyler, D. E.; Dang, Y.; Bhat, S.; Merrick, W. C.; Green, R.; Ben Shen; Liu, J. O. "Inhibition of eukaryotic translation elongation by cycloheximide and lactimidomycin." *Nat. Chem. Biol.* 2010, 6, 209–217.

- (195) Zucchi, R.; Ronca-Testoni, S. "The Sarcoplasmic Reticulum Ca^{2+} Channel/Ryanodine Receptor: Modulation by Endogenous Effectors, Drugs and Disease States." *Pharmacol. Rev.* 1997, 49, 1–52.
- (196) El-Hayek, R.; Parness, J.; Valdivia, H. H.; Coronado, R.; Hogan, K. "Dantrolene and azumolene inhibit [3H] PN200-110 binding to porcine skeletal muscle dihydropyridine receptors." *Biochem. Biophys. Res. Commun.* 1992, 187, 894–900.
- (197) Berisha, S. Z.; Hsu, J.; Robinet, P.; Smith, J. D. "Transcriptome Analysis of Genes Regulated by Cholesterol Loading in Two Strains of Mouse Macrophages Associates Lysosome Pathway and ER Stress Response with Atherosclerosis Susceptibility." *PLOS ONE* 2013, 8, e65003.
- (198) Boyce, M.; Bryant, K. F.; Jousse, C.; Long, K.; Harding, H. P.; Scheuner, D.; Kaufman, R. J.; Ma, D.; Coen, D. M.; Ron, D.; Yuan, J. "A selective inhibitor of eIF2 α dephosphorylation protects cells from ER stress." *Science* 2005, 307, 935–939.
- (199) Wu, L.; Luo, N.; Zhao, H.-R.; Gao, Q.; Lu, J.; Pan, Y.; Shi, J.-P.; Tian, Y.-Y.; Zhang, Y.-D. "Salubrinal protects against rotenone-induced SH-SY5Y cell death via ATF4-parkin pathway." *Brain Res.* 2014, 1549, 52–62.
- (200) Sokka, A.-L.; Putkonen, N.; Mudo, G.; Pryazhnikov, E.; Reijonen, S.; Khiroug, L.; Belluardo, N.; Lindholm, D.; Korhonen, L. "Endoplasmic reticulum stress inhibition protects against excitotoxic neuronal injury in the rat brain." *J. Neurosci.* 2007, 27, 901–908.
- (201) Drexler, H. C. A. "Synergistic Apoptosis Induction in Leukemic Cells by the Phosphatase Inhibitor Salubrinal and Proteasome Inhibitors." *PLOS ONE* 2009, 4, e4161.

- (202) Palchaudhuri, R.; Hergenrother, P. J. "Transcript Profiling and RNA Interference as Tools To Identify Small Molecule Mechanisms and Therapeutic Potential." *ACS Chem. Biol.* 2010, 6, 21–33.
- (203) Reich, N. C. "A death-promoting role for ISG54/IFIT2." *J. Interferon Cytokine Res.* 2013, 33, 199–205.
- (204) Zhou, X.; Michal, J. J.; Zhang, L.; Ding, B.; Lunney, J. K.; Liu, B.; Jiang, Z. "Interferon Induced IFITFamily Genes in Host Antiviral Defense." *Int. J. Biol. Sci.* 2013, 9, 200–208.
- (205) Arachchige Don, A. S.; Dallapiazza, R. F.; Bennin, D. A.; Cowan, C. E.; Brake, T.; Horne, M. C. "Cyclin G2 is a centrosome-associated nucleocytoplasmic shuttling protein that influences microtubule stability and induces a p53-dependent cell cycle arrest.." *Exp. Cell Res.* 2006, 312, 4181–4204.
- (206) Lamb, J.; Crawford, E. D.; Peck, D.; Modell, J. W.; Blat, I. C.; Wrobel, M. J.; Lerner, J.; Brunet, J.-P.; Subramanian, A.; Ross, K. N.; Reich, M.; Hieronymus, H.; Wei, G.; Armstrong, S. A.; Haggarty, S. J.; Clemons, P. A.; Wei, R.; Carr, S. A.; Lander, E. S.; Golub, T. R. "The Connectivity Map: Using Gene-Expression Signatures to Connect Small Molecules, Genes, and Disease." *Science* 2006, 313, 1929–1935.
- (207) Weinsberg, F.; Bickmeyer, U.; Wiegand, H. "Effects of tetrandrine on calcium channel currents of bovine chromaffin cells." *Neuropharmacol.* 1994, 33, 885–890.
- (208) Lamers, J. M. J.; Cysouw, K. J.; Verdouw, P. D. "Slow calcium channel blockers and calmodulin: Effect of felodipine, nifedipine, prenylamine and bepridil on cardiac sarcolemmal calcium pumping atpase." *Biochem. Pharmacol.* 1985, 34, 3837–3843.

- (209) Qiu, W.; Su, M.; Xie, F.; Ai, J.; Ren, Y.; Zhang, J.; Guan, R.; He, W.; Gong, Y.; Guo, Y. "Tetrandrine blocks autophagic flux and induces apoptosis via energetic impairment in cancer cells." *Cell Death Dis.* 2014, 5, e1123.
- (210) Reynolds, I. J.; Gould, R. J.; Snyder, S. H. "Loperamide: blockade of calcium channels as a mechanism for antidiarrheal effects." *J. Pharmacol. Exp. Ther.* 1984, 231, 628–632.
- (211) Wu, J.; Dougherty, J. J.; Nichols, R. A. "Dopamine receptor regulation of Ca²⁺ levels in individual isolated nerve terminals from rat striatum: comparison of presynaptic D1-like and D2-like receptors." *J. Neurochem.* 2006, 98, 481–494.
- (212) Suhara, T.; Inoue, O.; Kobayashi, K. "Effect of desipramine on dopamine receptor binding in vivo." *Life Sci.* 1990, 47, 2119–2126.
- (213) Azzam, M. E.; Algranati, I. D. "Mechanism of Puromycin Action: Fate of Ribosomes after Release of Nascent Protein Chains from Polysomes." *Proc. Nat. Acad. Sci.* 1973, 70, 3866–3869.
- (214) Lawson, B.; Brewer, J. W.; Hendershot, L. M. "Geldanamycin, an hsp90/GRP94-binding drug, induces increased transcription of endoplasmic reticulum (ER) chaperones via the ER stress pathway." *J. Cell. Physio.* 1998, 174, 170–179.
- (215) Hondeghem, L. M.; Dujardin, K.; Hoffmann, P.; Dumotier, B.; De Clerck, F. "Drug-Induced QTC Prolongation Dangerously Underestimates Proarrhythmic Potential: Lessons From Terfenadine." *J. Cardiovasc. Pharmacol.* 2011, 57, 589.
- (216) Liu, J. D.; Wang, Y. J.; Chen, C. H.; Yu, C. F.; Chen, L. C.; Lin, J. K.; Liang, Y. C.; Lin, S. Y.; Ho, Y. S. "Molecular mechanisms of G0/G1 cell-cycle arrest and apoptosis induced by terfenadine in human cancer cells." *Mol. Carcinog.* 2003, 37, 39–50.

- (217) Jangi, S.-M.; Ruiz-Larrea, M. B.; Nicolau-Galmés, F.; Andollo, N.; Arroyo-Berdugo, Y.; Ortega-Martínez, I.; Díaz-Pérez, J. L.; Boyano, M. D. "Terfenadine-induced apoptosis in human melanoma cells is mediated through Ca²⁺ homeostasis modulation and tyrosine kinase activity, independently of H1 histamine receptors." *Carcinogenesis* 2008, 29, 500–509.
- (218) Kiviluoto, S.; Vervliet, T.; Ivanova, H.; Decuypere, J.-P.; De Smedt, H.; Missiaen, L.; Bultynck, G.; Parys, J. B. "Regulation of inositol 1,4,5-trisphosphate receptors during endoplasmic reticulum stress." *BBA-Mol. Cell Res.* 2013, 1833, 1612–1624.
- (219) Raina, K.; Noblin, D. J.; Serebrenik, Y. V.; Adams, A.; Zhao, C.; Crews, C. M. "Targeted protein destabilization reveals an estrogen-mediated ER stress response." *Nat. Chem. Biol.* 2014, 10, 957–962.
- (220) Leslie, B. J.; Hergenrother, P. J. "Identification of the cellular targets of bioactive small organic molecules using affinity reagents." *Chem. Soc. Rev.* 2008, 37, 1347–1360.
- (221) Ziegler, S.; Pries, V.; Hedberg, C.; Waldmann, H. "Target identification for small bioactive molecules: finding the needle in the haystack." *Angew. Chem. Int. Ed.* 2013, 52, 2744–2792.
- (222) Schenone, M.; Dančík, V.; Wagner, B. K.; Clemons, P. A. "Target identification and mechanism of action in chemical biology and drug discovery." *Nat. Chem. Biol.* 2013, 9, 232–240.
- (223) Sumranjit, J.; Chung, S. "Recent Advances in Target Characterization and Identification by Photoaffinity Probes." *Molecules* 2013, 18, 10425–10451.
- (224) Reizelman, A.; Wigchert, S. C. M.; del-Bianco, C.; Zwanenburg, B. "Synthesis and bioactivity of labelled germination stimulants for the isolation and

- identification of the strigolactone receptor.” *Org. Biomol. Chem.* 2003, 1, 950–959.
- (225) Kitahata, N.; Nakano, T.; Kuchitsu, K.; Yoshida, S.; Asami, T. “Biotin-labeled abscisic acid as a probe for investigating abscisic acid binding sites on plasma membranes of barley aleurone protoplasts.” *Bioorg. Med. Chem.* 2005, 13, 3351–3358.
- (226) Randell C Clevenger; Joseph M Raibel; Angela M Peck, A.; Blagg, B. S. J. “Biotinylated Geldanamycin.” *J. Org. Chem.* 2004, 69, 4375–4380.
- (227) James M Nyangulu, 1.; Marek M Galka; Ashok Jadhav, 2.; Yuanzhu Gai; Cindy M Graham, 3.; Ken M Nelson; Adrian J Cutler; David C Taylor; Gary M Banowetz, 4. A.; Abrams, S. R. “An Affinity Probe for Isolation of Abscisic Acid-Binding Proteins.” *J. Am. Chem. Soc.* 2005.
- (228) Toshiyuki Kan; Yoichi Kita; Yuichi Morohashi; Yusuke Tominari; Shinnosuke Hosoda; Taisuke Tomita; Hideaki Natsugari; Takeshi Iwatsubo, A.; Tohru Fukuyama “Convenient Synthesis of Photoaffinity Probes and Evaluation of Their Labeling Abilities.” *Org. Lett.* 2007, 9, 2055–2058.
- (229) Shin, K. D.; Lee, M.-Y.; Shin, D.-S.; Lee, S.; Son, K.-H.; Koh, S.; Paik, Y.-K.; Kwon, B.-M.; Han, D. C. “Blocking Tumor Cell Migration and Invasion with Biphenyl Isoxazole Derivative KRIBB3, a Synthetic Molecule That Inhibits Hsp27 Phosphorylation.” *J. Biol. Chem.* 2005, 280, 41439–41448.
- (230) Wang, G.; Shang, L.; Burgett, A. W. G.; Harran, P. G.; Wang, X. “Diazonamide toxins reveal an unexpected function for ornithine δ -amino transferase in mitotic cell division.” *Proc. Nat. Acad. Sci.* 2007, 104, 2068–2073.

- (231) Weerapana, E.; Speers, A. E.; Cravatt, B. F. "Tandem orthogonal proteolysis-activity-based protein profiling (TOP-ABPP)—a general method for mapping sites of probe modification in proteomes." *Nat. Protoc.* 2007, 2, 1414–1425.
- (232) Shin-ichi Sato; Youngjoo Kwon; Shinji Kamisuki; Neeta Srivastava; Qian Mao; Yoshinori Kawazoe, A.; Motonari Uesugi "Polyproline-Rod Approach to Isolating Protein Targets of Bioactive Small Molecules: Isolation of a New Target of Indomethacin." *J. Am. Chem. Soc.* 2007, 129, 873–880.
- (233) Emami, K. H.; Nguyen, C.; Ma, H.; Kim, D. H.; Jeong, K. W.; Eguchi, M.; Moon, R. T.; Teo, J.-L.; Oh, S. W.; Kim, H. Y.; Moon, S. H.; Ha, J. R.; Kahn, M. "A small molecule inhibitor of β -catenin/cyclic AMP response element-binding protein transcription." *Proc. Nat. Acad. Sci.* 2004, 101, 12682–12687.
- (234) Statsuk, A. V.; Bai, R.; Baryza, J. L.; Verma, V. A.; Hamel, E.; Wender, P. A.; Kozmin, S. A. "Actin is the primary cellular receptor of bistramide A." *Nat. Chem. Biol.* 2005, 1, 383–388.
- (235) Fujii, T.; Manabe, Y.; Sugimoto, T.; Ueda, M. "Detection of 210kDa receptor protein for a leaf-movement factor by using novel photoaffinity probes." *Tetrahedron* 2005, 61, 7874–7893.
- (236) Meng, L.; Mohan, R.; Kwok, B. H. B.; Elofsson, M.; Sin, N.; Crews, C. M. "Epoxomicin, a potent and selective proteasome inhibitor, exhibits in vivo antiinflammatory activity." *Proc. Nat. Acad. Sci.* 1999, 96, 10403–10408.
- (237) Kwok, B. H. B.; Koh, B.; Ndubuisi, M. I.; Elofsson, M.; Crews, C. M. "The anti-inflammatory natural product parthenolide from the medicinal herb Feverfew directly binds to and inhibits I κ B kinase." *Chem. Biol.* 2001, 8, 759–766.
- (238) Wulff, J. E.; Siegrist, R.; Myers, A. G. "The natural product avrainvillamide binds to the oncoprotein nucleophosmin." *J. Am. Chem. Soc.* 2007, 129, 14444–14451.

- (239) Falsey, R. R.; Marron, M. T.; Gunaherath, G. M. K. B.; Shirahatti, N.; Mahadevan, D.; Gunatilaka, A. A. L.; Whitesell, L. "Actin microfilament aggregation induced by withaferin A is mediated by annexin II." *Nat. Chem. Biol.* 2006, 2, 33–38.
- (240) Sin, N.; Meng, L.; Wang, M. Q. W.; Wen, J. J.; Bornmann, W. G.; Crews, C. M. "The anti-angiogenic agent fumagillin covalently binds and inhibits the methionine aminopeptidase, MetAP-2." *Proc. Nat. Acad. Sci.* 1997, 94, 6099–6103.
- (241) Ismail, H. M.; Barton, V.; Phanchana, M.; Charoensutthivarakul, S.; Wong, M. H. L.; Hemingway, J.; Biagini, G. A.; O'Neill, P. M.; Ward, S. A. "Artemisinin activity-based probes identify multiple molecular targets within the asexual stage of the malaria parasites *Plasmodium falciparum* 3D7." *Proc. Nat. Acad. Sci.* 2016, 113, 2080–2085.
- (242) Green, N. M. Avidin. In *Advances in Protein Chemistry Volume 29; Advances in Protein Chemistry*; Elsevier, 1975; Vol. 29, pp. 85–133.
- (243) Fu, Y.; Mi, L.; Sanda, M.; Silverstein, S.; Aggarwal, M.; Wang, D.; Gupta, P.; Goldman, R.; Appella, D. H.; Chung, F.-L. "A click chemistry approach to identify protein targets of cancer chemopreventive phenethyl isothiocyanate." *RSC Adv.* 2013, 4, 3920–3923.
- (244) Speers, A. E.; Cravatt, B. F. "A Tandem Orthogonal Proteolysis Strategy for High-Content Chemical Proteomics." *J. Am. Chem. Soc.* 2005, 127, 10018–10019.
- (245) Qian Wang; Timothy R Chan; Robert Hilgraf; Valery V Fokin; K Barry Sharpless, A.; Finn, M. G. "Bioconjugation by Copper(I)-Catalyzed Azide-Alkyne [3 + 2] Cycloaddition." *J. Am. Chem. Soc.* 2003, 125, 3192–3193.

- (246) Vila, A.; Tallman, K. A.; Jacobs, A. T.; Liebler, D. C.; Porter, N. A.; Marnett, L. J. "Identification of Protein Targets of 4-Hydroxynonenal Using Click Chemistry for ex Vivo Biotinylation of Azido and Alkynyl Derivatives." *Chem. Res. Toxicol.* 2008, 21, 432–444.
- (247) Finn, F. M.; Titus, G.; Horstman, D.; Hofmann, K. "Avidin-biotin affinity chromatography: application to the isolation of human placental insulin receptor." *Proc. Nat. Acad. Sci.* 1984, 81, 7328–7332.
- (248) Campos, M.; Fadden, P.; Alms, G.; Qian, Z.; Haystead, T. A. J. "Identification of Protein Phosphatase-1-binding Proteins by Microcystin-Biotin Affinity Chromatography." *J. Biol. Chem.* 1996, 271, 28478–28484.
- (249) Chockalingam, P. S.; Jurado, L. A.; Jarrett, H. W. "DNA Affinity Chromatography." *Mol. Biotechnol.* 2001, 19, 189–200.
- (250) Lee, W.-C.; Lee, K. H. "Applications of affinity chromatography in proteomics." *Anal. Biochem.* 2004, 324, 1–10.
- (251) Peters, E. C.; Gray, N. S. "Chemical proteomics identifies unanticipated targets of clinical kinase inhibitors." *ACS Chem. Biol.* 2007, 2, 661–664.
- (252) Dorman, G.; Prestwich, G. D. "Benzophenone Photophores in Biochemistry." *Biochemistry* 1994, 33, 5661–5673.
- (253) Dormán, G.; Prestwich, G. D. "Using photolabile ligands in drug discovery and development." *Trends Biotechnol.* 2000, 18, 64–77.
- (254) Fleming, S. A. "Chemical reagents in photoaffinity labeling." *Tetrahedron* 1995, 51, 12479–12520.
- (255) Dubinsky, L.; Krom, B. P.; Meijler, M. M. "Diazirine based photoaffinity labeling." *Bioorg. Med. Chem.* 2012, 20, 554–570.

- (256) Zill, A.; Rutz, A. L.; Kohman, R. E.; Alkilany, A. M.; Murphy, C. J.; Kong, H.; Zimmerman, S. C. "Clickable polyglycerol hyperbranched polymers and their application to gold nanoparticles and acid-labile nanocarriers." *Chem. Commun.* 2011, 47, 1279–1281.
- (257) Li, Z.; Hao, P.; Li, L.; Tan, C. Y. J.; Cheng, X.; Chen, G. Y. J.; Sze, S. K.; Shen, H.-M.; Yao, S. Q. "Design and synthesis of minimalist terminal alkyne-containing diazirine photo-crosslinkers and their incorporation into kinase inhibitors for cell- and tissue-based proteome profiling." *Angew. Chem. Int. Ed.* 2013, 52, 8551–8556.
- (258) Tsaytler, P.; Harding, H. P.; Ron, D.; Bertolotti, A. "Selective Inhibition of a Regulatory Subunit of Protein Phosphatase 1 Restores Proteostasis." *Science* 2011, 332, 91–94.
- (259) NASH, D. T. "Clinical Trial with Guanabenz, a New Antihypertensive Agent." *J. Clin. Pharmacol. N. D.* 1973, 13, 416–421.
- (260) Munshi, S.; Dahl, R. "Cytoprotective small molecule modulators of endoplasmic reticulum stress." *Bioorg. Med. Chem.* 2016, 24, 2382–2388.
- (261) Walker, S. D.; Barder, T. E.; Martinelli, J. R.; Buchwald, S. L. "A Rationally Designed Universal Catalyst for Suzuki–Miyaura Coupling Processes." *Angew. Chem. Int. Ed.* 2004, 43, 1871–1876.
- (262) Zhongxing Zhang; Zhong Yang; Henry Wong; Juliang Zhu; Nicholas A Meanwell; John F Kadow, A.; Wang, T. "An Effective Procedure for the Acylation of Azaindoles at C-3." *J. Org. Chem.* 2002, 67, 6226–6227.
- (263) Johansson, H.; Boesgaard, M. W.; Nørskov-Lauritsen, L.; Larsen, I.; Kuhne, S.; Gloriam, D. E.; Bräuner-Osborne, H.; Pedersen, D. S. "Selective Allosteric

- Antagonists for the G Protein-Coupled Receptor GPRC6A Based on the 2-Phenylindole Privileged Structure Scaffold.” *J. Med. Chem.* 2015, 58, 8938–8951.
- (264) Fu, T.-H.; Bonaparte, A.; Martin, S. F. “Synthesis of β -heteroaryl propionates via trapping of carbocations with π -nucleophiles.” *Tetrahedron Lett.* 2009, 50, 3253–3257.
- (265) Bergman, J.; Norrby, P.-O.; Tilstam, U.; Venemalm, L. “Structure elucidation of some products obtained by acid-catalyzed condensation of indole with acetone.” *Tetrahedron* 1989, 45, 5549–5564.
- (266) Dai, H. G.; Li, J. T.; Li, T. S. “Efficient and Practical Synthesis of Mannich Bases Related to Gramine Mediated by Zinc Chloride.” *Synth. Commun.* 2006, 36, 1829–1835.
- (267) Piantadosi, C.; Hall, I. H.; Wyrick, S. D.; Ishaq, K. S. “Hypocholesterolemic activity of 1,3-bis(substituted phenoxy)-2-propanones.” *J. Med. Chem.* 2002, 19, 222–229.
- (268) Hidetsura Cho; Susumu Katoh; Shinsuke Sayama; Kengo Murakami; Hiroyuki Nakanishi; Yasuyuki Kajimoto; Hiroshi Ueno; Hisashi Kawasaki; Kazuo Aisaka, A.; Uchida, I. “Synthesis and Selective Coronary Vasodilatory Activity of 3,4-Dihydro-2,2-bis(methoxymethyl)-2H-1-benzopyran-3-ol Derivatives: Novel Potassium Channel Openers.” *J. Med. Chem.* 1996, 39, 3797–3805.
- (269) Naredla, R. R.; Klumpp, D. A. “Contemporary Carbocation Chemistry: Applications in Organic Synthesis.” *Chem. Rev.* 2013, 113, 6905–6948.
- (270) Nitsch, D.; Huber, S. M.; Pöthig, A.; Narayanan, A.; Olah, G. A.; Prakash, G. K. S.; Bach, T. “Chiral Propargylic Cations as Intermediates in S_N1 -Type Reactions: Substitution Pattern, Nuclear Magnetic Resonance Studies, and Origin of the Diastereoselectivity.” *J. Am. Chem. Soc.* 2014, 136, 2851–2857.

- (271) Stadler, D.; Mühlthau, F.; Rubenbauer, P.; Herdtweck, E.; Bach, T. "Diastereoselective Friedel-Crafts Alkylation Reactions Employing Chiral Cation Precursors with Polar α -Substituents." *Synlett* 2006, 2006, 2573–2576.
- (272) Rubenbauer, P.; Bach, T. "Gold(III) Chloride-Catalyzed Diastereoselective Alkylation Reactions with Chiral Benzylic Acetates." *Adv. Synth. Catal.* 2008, 350, 1125–1130.
- (273) Stadler, D.; Bach, T. "Concise Stereoselective Synthesis of (–)-Podophyllotoxin by an Intermolecular Iron(III)-Catalyzed Friedel–Crafts Alkylation." *Angew. Chem. Int. Ed.* 2008, 47, 7557–7559.
- (274) Chung, J. Y. L.; Steinhuebel, D.; Krska, S. W.; Hartner, F. W.; Cai, C.; Rosen, J.; Mancheno, D. E.; Pei, T.; DiMichele, L.; Ball, R. G.; Chen, C.-Y.; Tan, L.; Alorati, A. D.; Brewer, S. E.; Scott, J. P. "Asymmetric Synthesis of a Glucagon Receptor Antagonist via Friedel–Crafts Alkylation of Indole with Chiral α -Phenyl Benzyl Cation." *Org. Process Res. Dev.* 2012, 16, 1832-1845.
- (275) Chung, J. Y. L.; Mancheno, D.; Dormer, P. G.; Variankaval, N.; Ball, R. G.; Tsou, N. N. "Diastereoselective Friedel–Crafts Alkylation of Indoles with Chiral α -Phenyl Benzylic Cations. Asymmetric Synthesis of Anti-1,1,2-Triarylalkanes." *Org. Lett.* 2008, 10, 3037-3040.
- (276) Stadler, D.; Goeppert, A.; Rasul, G.; Olah, G. A.; Prakash, G. K. S.; Bach, T. "Chiral benzylic carbocations: low-temperature NMR studies and theoretical calculations.." *J. Org. Chem.* 2009, 74, 312–318.
- (277) Surendra, K.; Corey, E. J. "Highly Enantioselective Proton-Initiated Polycyclization of Polyenes." *J. Am. Chem. Soc.* 2012, 134, 11992–11994.
- (278) Wang, S.-G.; Han, L.; Zeng, M.; Sun, F.-L.; Zhang, W.; You, S.-L. "Enantioselective synthesis of fluorene derivatives by chiral N-triflyl

- phosphoramidate catalyzed double Friedel–Crafts alkylation reaction.” *Org. Biomol. Chem.* 2012, 10, 3202–3209.
- (279) Wilcke, D.; Herdtweck, E.; Bach, T. “Enantioselective Brønsted Acid Catalysis in the Friedel-Crafts Reaction of Indoles with Secondary ortho-Hydroxybenzylic Alcohols.” *Synlett* 2011, 2011, 1235–1238.
- (280) Rueping, M.; Uria, U.; Lin, M.-Y.; Atodiresei, I. “Chiral Organic Contact Ion Pairs in Metal-Free Catalytic Asymmetric Allylic Substitutions.” *J. Am. Chem. Soc.* 2011, 133, 3732–3735.
- (281) Guo, Q.-X.; Peng, Y.-G.; Zhang, J.-W.; Song, L.; Feng, Z.; Gong, L.-Z. “Highly Enantioselective Alkylation Reaction of Enamides by Brønsted-Acid Catalysis.” *Org. Lett.* 2009, 11, 4620–4623.
- (282) Bergonzini, G.; Vera, S.; Melchiorre, P. “Cooperative Organocatalysis for the Asymmetric γ Alkylation of α -Branched Enals.” *Angew. Chem. Int. Ed.* 2010, 49, 9685–9688.
- (283) Trifonidou, M.; Kokotos, C. G. “Enantioselective Organocatalytic α -Alkylation of Ketones by S_N1 -Type Reaction of Alcohols.” *Eur. J. Org. Chem.* 2012, 2012, 1563–1568.
- (284) Zhang, L.; Cui, L.; Li, X.; Li, J.; Luo, S.; Cheng, J. P. “Asymmetric S_N1 α -Alkylation of Cyclic Ketones Catalyzed by Functionalized Chiral Ionic Liquid (FCIL) Organocatalysts.” *Chem. Eur. J.* 2010, 16, 2045–2049.
- (285) Zhang, L.; Cui, L.; Li, X.; Li, J.; Luo, S.; Cheng, J. P. “Functionalized Chiral Ionic Liquid Catalyzed Asymmetric S_N1 α -Alkylation of Ketones and Aldehydes.” *Eur. J. Org. Chem.* 2010, 2010, 4876–4885.

- (286) Brown, A. R.; Kuo, W.-H.; Jacobsen, E. N. "Enantioselective Catalytic α -Alkylation of Aldehydes via an SN1 Pathway." *J. Am. Chem. Soc.* 2010, 132, 9286–9288.
- (287) Ford, D. D.; Lehnher, D.; Kennedy, C. R.; Jacobsen, E. N. "Anion-Abstraction Catalysis: The Cooperative Mechanism of α -Chloroether Activation by Dual Hydrogen-Bond Donors." *ACS Catal.* 2016, 6, 4616–4620.
- (288) Corey, E. J.; Lee, D.-H. "The E/Z geometry of the enolate component determines face selection of the aldehyde component in chiral diazaborolidine-directed enantioselective aldol coupling." *Tetrahedron Lett.* 1993, 34, 1737–1740.
- (289) Masamune, S.; Sato, T.; Kim, B.; Wollmann, T. A. "Organoboron compounds in organic synthesis. 4. Asymmetric aldol reactions." *J. Am. Chem. Soc.* 1986.
- (290) Reetz, M. T.; Kunisch, F.; Heitmann, P. "Chiral Lewis acids for enantioselective C-C bond formation." *Tetrahedron Lett.* 1986, 27, 4721–4724.
- (291) Corey, E. J.; Imwinkelried, R.; Pikul, S.; Bin Xiang, Y. "Practical enantioselective Diels-Alder and aldol reactions using a new chiral controller system." *J. Am. Chem. Soc.* 1989, 111, 5493–5495.
- (292) Corey, E. J.; Kim, S. S. "Versatile chiral reagent for the highly enantioselective synthesis of either anti or syn ester aldols." *J. Am. Chem. Soc.* 1990, 112, 4976–4977.
- (293) Abbott, J. "Preparation of Crystalline (Diisopinocampheyl)borane." *Org. Synth.* 2015, 92, 26–37.
- (294) Evans, D. A.; Nelson, J. V.; Vogel, E.; Taber, T. R. "Stereoselective aldol condensations via boron enolates." *J. Am. Chem. Soc.* 1981, 103, 3099–3111.

- (295) Paterson, I.; Lister, M. A.; McClure, C. K. "Enantioselective aldol condensations: The use of ketone boron enolates with chiral ligands attached to boron." *Tetrahedron Lett.* 1986, 27, 4787–4790.
- (296) Paterson, I.; Goodman, J. M.; Lister, M. A.; Schumann, R. C.; McClure, C. K.; Norcross, R. D. "Enantio- and diastereoselective aldol reactions of achiral ethyl and methyl ketones with aldehydes: the use of enol diisopinocampheylborinates." *Tetrahedron* 1990, 46, 4663–4684.
- (297) Meyers, A. I.; Yamamoto, Y. "Enantioselective aldol reactions with high threo or erythro selectivity using boron azaenolates." *J. Am. Chem. Soc.* 1981, 103, 4278–4279.
- (298) Blumberg, S.; Martin, S. F. "4-(Phenylazo)diphenylamine (PDA): a universal indicator for the colorimetric titration of strong bases, Lewis acids, and hydride reducing agents." *Tetrahedron Lett.* 2015, 56, 3674–3678.
- (299) Brown, H. C.; Kanner, B. "2,6-Di-*t*-Butylpyridine—an Unusual Pyridine Base." *J. Am. Chem. Soc.* 1953, 75, 3865–3865.
- (300) Still, W. C.; Kahn, M.; Mitra, A. "Rapid chromatographic technique for preparative separations with moderate resolution." *J. Org. Chem.* 1978, 43, 2923–2925.
- (301) CrystalClear 1.40 (2008). Rigaku Americas Corporation, The Woodlands, TX.
- (302) SIR97. (1999). A program for crystal structure solution. Altomare, A., Burla, M. C., Camalli, M., Cascarano, G. L., Giacovazzo, C., Guagliardi, A., Moliterni, A. G. G., Polidori, G. and Spagna, R. *J. Appl. Cryst.* 32, 115–119.
- (303) Sheldrick, G. M. (2008). SHELXL97. Program for the Refinement of Crystal Structures. *Acta Cryst.*, A64, 112–122.

- (304) Spek, A. L. (1998). PLATON, A Multipurpose Crystallographic Tool. Utrecht University, The Netherlands.
- (305) WinGX 1.64. (1999). An Integrated System of Windows Programs for the Solution, Refinement and Analysis of Single Crystal X-ray Diffraction Data. Farrugia, L. J. J. Appl. Cryst. 32. 837-838.
- (306) $R_w(F^2) = \{ \sum w(|F_o|^2 - |F_c|^2)^2 / \sum w(|F_o|^4) \}^{1/2}$ where w is the weight given each reflection.
- (307) $R(F) = \sum (|F_o| - |F_c|) / \sum |F_o|$ for reflections with $F_o > 4(\sigma(F_o))$. $S = [\sum w(|F_o|^2 - |F_c|^2)^2 / (n - p)]^{1/2}$, where n is the number of reflections and p is the number of refined parameters.
- (308) International Tables for X-ray Crystallography (1992). Vol. C, Tables 4.2.6.8 and 6.1.1.4, A. J. C. Wilson, editor, Boston: Kluwer Academic Press.